Design, Synthesis and Evaluation of Bioactivable Organic Donors of Sulfur Dioxide (SO₂)

A THESIS SUBMITTED IN PARTIAL FULFILLMENT OF THE REQUIREMENTS OF THE DEGREE OF

Doctor of Philosophy

By

Kundansingh A. Pardeshi

ID: 20113148

IISER PUNE

INDIAN INSTITUTE OF SCIENCE EDUCATION AND RESEARCH, PUNE-411008

2018

Dedicated to…

My **Parents**

And

Beloved **Family**

Dr. Harinath Chakrapani
Associate Professor
Department of Chemistry,
IISER Pune

CERTIFICATE

Certified that, the work incorporated in the thesis entitled, "**Design**, **Synthesis and Evaluation Bioactivable Organic Donors of Sulfur Dioxide (SO$_2$)"** submitted by **Kundansingh A. Pardeshi** was carried out by the candidate, under my supervision. The work presented here or any part of it has not been included in any other thesis submitted previously for the award of any degree or diploma from any other University or institution.

Date: 13. June. 2018   **Dr. Harinath Chakrapani**

Pune (MH), India   **Research Advisor**

DECLARATION

I declare that this written submission represents my ideas in my own words and where others' ideas have been included; I have adequately cited and referenced the original sources. I also declare that I have adhered to all principles of academic honesty and integrity and have not misrepresented or fabricated or falsified any idea/data/fact/source in my submission. I understand that violation of the above will be cause for disciplinary action by the Institute and can also evoke penal action from the sources which have thus not been properly cited or from whom proper permission has not been taken when needed.

Date: 13. June. 2018   **Kundansingh A. Pardeshi**

Pune (MH), India.   **ID: 20113148**

Table of Contents

Chapter 4. Nitroreductase Activated Specific Theranostic Prodrugs Therapy for Bacteria

General Remarks

- ^{1}H NMR spectra were recorded on JEOL ECX 400 MHz spectrometer using tetramethylsilane (TMS) as an internal standard. Chemical shifts are expressed in ppm units downfield to TMS.

- ^{13}C NMR spectra were recorded on JEOL ECX 100 MHz spectrometer.

- Mass spectra were obtained using an HRMS-ESI-Q-Time of Flight LC-MS (Synapt G2, Waters) or MALDI TOF/TOF Analyser (Applied Biosystems 4800 Plus).

- FT-IR spectra were obtained using NICOLET 6700 FT-IR spectrophotometer as KBr disc or Bruker Alpha-FT-IR spectrometer and reported in cm^{-1}.

- All reactions were monitored by Thin-Layer Chromatography carried out on precoated Merck silica plates (F254, 0.25 mm thickness); compounds were visualized by UV light.

- All reactions were carried out under nitrogen or argon atmosphere with dry freshly prepared solvents under anhydrous conditions and yields refer to chromatographically homogenous materials unless otherwise stated.

- Silica gel (60-120) and (100-200) mesh were used for column chromatography.

- Materials were obtained from commercial suppliers and were used without further purification.

- Purification of some of the compounds was performed Prep HPLC

- HPLC analysis data was obtained using Agilent Technologies 1260 Infinity, C18 (5 μm, 4.6×250 mm).

- Sulfur dioxide was detected using Metrohm Ion Chromatography.

- Spectrophotometric and fluorimetric measurements were performed using Thermo Scientific Varioscan microwell plate reader.

Abbreviations

Ar – Aryl

ACN – Acetonitrile

AcOH – Acetic acid

au – Arbitrary unit

bs – Broad singlet

Bn – benzyl

Bu – Butyl

t-Bu – tertiary-butyl

$CDCl_3$ – Chloroform-D

$CHCl_3$ – Chloroform

Calcd – Calculated

Cat – Catalytic

Compd – Compound

d – Doublet

dd – Doublet of doublet

dt – Doublet of triplet

δ – Delta (in PPM)

DEAD – Diethyl azodicarboxylate

DIAD – Di-isopropyl azodicarboxylate

DCM – Dichloromethane

DMAP – *N*, *N*-Dimethylaminopyridine

DMF – *N*, *N'*-Dimethylformamide

DMSO – Dimethyl Sulfoxide

DNA – Deoxyribonucleic acid

DNs – 2,4-dinitrophynylsulfonyl

E. coli – Escherichia coli

E. feacalis – Enterococcus faecalis

ES – E*sterase*

ESI – Electron spray ionization

EtOAc – Ethyl acetate

eq. – Equivalents

g – Gram

µg – microgram

GSH – Glutathione

h – Hour

HCl – Hydrochloric acid

H_2SO_4 – Sulfuric acid

H_2O – Water

HPLC – High-Performance Liquid Chromatography

HRMS – High-Resolution Mass Spectrometry

Hz – Hertz

IC_{50} – Half-maximal inhibitory concentration

IR – Infrared

J – Coupling constant

µL – Microliter

LB – Luria-Bertani

λ_{ex} – Excitation wavelength

λ_{em} – Emission wavelength

MSSA – Methicillin-sensitive Staphylococcus aureus

MRSA – Methicillin-resistant Staphylococcus aureus

m – Multiplet

Me – Methyl

mg – milligram

MIC – Minimum inhibitory concentration

min – Minutes

MHz – Megahertz

mol – mole (s)

mL – milliliter

mM – Millimolar

mmol – millimoles

mp – Melting point

MALDI-TOF – Matrix-Assisted Laser Desorption Ionization-Time of Flight

Mtb – Mycobacterium tuberculosis

MTT – 3-(4,5-Dimethylthiazol-2-yl)-2,5-Diphenyltetrazolium Bromide

μM – Micromolar

μmol– Micromolar

NADPH – Reduced nicotinamide-adenine-dinucleotide phosphate

Na_2SO_3 – Sodium sulfite

$NaHSO_3$ – Sodium bisulfite

Na_2SO_4 – Sodium sulfate

NBS – *N*-Chlorosuccinimide

NCS – *N*-Bromosuccinimide

NMR – Nuclear Magnetic Resonances

Nm – nanometer(s)

Nu – Nucleophile

NO – Nitric oxide

NTR – Nitroreductase

OD – Optical density

PBS – Phosphate Buffered Saline

pH – Potential of hydrogen

NBS – *N*-Chlorosuccinimide

PE – Petroleum ether

Pr – propyl

*i*Pr – isopropyl

Py–Pyridine

ppm – Parts per million

% – Percent

q – quartet

ROS – Reactive Oxygen Species

RNS – Reactive Nitrogen Species

RSS – Reactive Sulfur Species

Redox – Reduction-Oxidation

rt – Room temperature

s – Singlet

t – Triplet

t – Time

THF – Tetrahydrofuran

TLC – Thin Layer Chromatography

TMS – Tetramethylsilane

TRIS – Tris (hydroxymethyl)aminomethane

UV – Ultraviolet

vis – visible

v/v – volume by volume

Zn – Zinc

Acknowledgment

Well, the Ph.D. has been a long wonderful journey with all the ingredients of the life. I would like to carry all the positivity from this journey, for which many people have contributed directly or indirectly. Therefore, it is giving me immense pleasure to acknowledge all those people who are the part of this wonderful experience.

First and foremost I would like to sincerely thank and express my gratitude towards my research advisor Dr. Harinath Chakrapani without his support my Ph.D. would have been incomplete. It is not possible and will be unfair to him to describe his contribution in a few sentences. However, I feel that I was lucky to get a chance to work with him. He is one of the most hardworking person I came to know. He supported immensely in particular for independent critical thinking, designing experiments, given the freedom to choose and proceed with our ideas as well. He has given valuable suggestions and contributed immensely to the improvement of my language (communication, presentation, and writing) with whom he has mastery and expected same from us. He has given me the most required trust, belief, and support throughout my doctoral work at a personal and professional level to the best of his capacity. This has helped me to develop overall as a student and as an individual. He has looked after our the safety requirement in the lab strictly to provide a safe environment to conduct research. Apart from doing science is exceedingly organized. He has sound administrative skills. He is also a wonderful cricketer too and it was a nice experience to play cricket along with him.

Also, I would like to sincerely thank our director Prof. J. B. Udgaonkar for his wonderful initiatives and continuous efforts for the betterment of the IISER Pune. I would like to sincerely thank Prof. K. N. Ganesh, former Director IISER-Pune for his immense, untiring efforts (which I have witnessed during my Ph.D.) to build IISER literally from scratch and to provide us the research facilities at the global standards. Also, It gives me immense pleasure to express my gratitude towards all the faculty members in the department of chemistry for providing their research facilities, interactive scientific discussions and teaching me various courses.

I am very grateful to my former research advisory committee member Dr. Sayamsen Gupta, current research advisory members Dr. S. K. Asha from National Chemical Laboratory, Pune, and Dr. Pinaki Talukdar from IISER, Pune for their valuable suggestions and feedback during RAC evaluations. I would like to thank Prof. M. Jayakannan, Dr. S.G. Vatson and their students for helping me to carry out fluorescence and UV experiments. Dr. R.G. Bhat, Dr. Shabana Khan for looking after our safety in the Department of Chemistry. Also, I would like to sincerely thank

Prof. S. Hotha and his group we together enjoyed various outings. I sincerely thank Dr. S.G. Srivatsan for having played cricket with us. It was a great experience and fun to watch him for his amazing all-round cricketing skills.

I would like to thank our collaborators, Dr. Radha Rangarajan, Vitas Pharma, Hyderabad and Dr. Sidharth Chopra from CDRI, Lucknow for putting the hard work to provide us a valuable antibacterial data.

Words would not be sufficient to describe the deepest gratitude I feel towards my lab mates for their love, help, support, suggestions, criticism and memorable moments given throughout my life at IISER. I take this opportunity to say my sincere thank to all my hardworking seniors. They were the great strength of motivation. I had a really good rapport with all of them and they were the best of the seniors I could have ever imagined. Dr. Satish Malwal has excellent synthetic skills. He always used to generate really good quality of analytical data. These qualities of Satish helped me as well. I felt really comfortable in the company of Dr. A. T. Dharmaraja (Dharam Paaji) he is has been one of the most hardworking, humble guys with whom I shared ideas, food, jokes, played cricket and what not. I have learned so many things from him especially instrument handling. Dr. Kavita Sharma (Builder/Pelhalwaan) was a very positive, balanced light-hearted, and supportive person I came to know. She used to be a wonderful organizer. She has helped me in so many ways especially taught me to do mammalian cell culture and to conduct assays associated with it. Dr. Vinayak (Bhau) used to be prepared really well especially with literature before the start of any new project or experiment. Dr. Vinayak and we had a lot of fruitful discussions on do's and don'ts in the Ph.D. I extend my sincere gratitude to all my present hardworking lab mates. They are all very good students of science. On a lighter note, I will be exaggerating few of their special qualities. In Ravikumar (Ra), I had a nice and humble company after all the seniors were left. We shared food together. He has contributed nicely in one of my projects. Also, he has wonderful cricketing skills especially in the fielding and if spectators are around the ground he dives as well. Amogh Kulkarni (AK-47) is a talented singer and drama artist. He has given very good performances in various dramas. He has a special quality of chewing the food for infinity. Preeti Chauhan (PC) has wonderful communication skills and has done awesome proofreading of my thesis. She is also a really good organizer and flag bearer of feminism. She has a special skill to stretch a particular word for a light year. I had a really good company with Ajay Sharma (AJ), we together explored different cuisines in several places. He has a beautiful quality of having balanced emotions in every situation he faces. He is also a wonderful organizer and famous for his great jokes which

Abstract

Sulfur dioxide (SO_2) is colorless, pungent gas and has long been considered as a toxic pollutant but recently has been emerged as a possible mediator of cellular signaling. SO_2 is widely used as a food preservative and as an antibacterial agent in winemaking. SO_2 is produced endogenously by metabolism of sulfur-containing amino acids and by oxidation of H_2S. In aqueous media, SO_2 gets hydrated forms sulfite and bisulfite. In order to study the physiological roles of SO_2, typically inorganic or organic sources of SO_2 are used. To investigate precisely several untapped roles of SO_2 in a biological system, tools that generate SO_2 inside a cell in a reliable and controllable manner are needed. Hitherto, few chemical tools have been known to generate SO_2 and they all have certain limitations that we proposed to address. Our lab for the very first time previously has reported thiol activated SO_2 donors and their biological activity against *Mycobacterium tuberculosis* (*Mtb*). Structural modifications for thiol activated SO_2 donors led us to a new set of compounds that were excellent inhibitors of *Staphylococcus aureus* (*S.aureus*). Together, we have developed chemical tools for SO_2 donation based on diverse activation mechanisms with potential applications as antibacterials. Next, we describe efforts towards the new and improved SO_2 donors. First, we designed and synthesized a series of esterase-sensitive SO_2 donors. These compounds undergo self-immolation to generate SO_2 upon exposure to esterase, an enzyme that is widely prevalent in cells. Using this design as a prototype, we next directed the delivery of SO_2 to bacteria using the bacterial enzyme nitroreductase. The strategy was adapted to co-deliver SO_2 and a clinically used antibiotic. In this strategy, we presented the design and synthesis of a nitroreductase stimuli specific fluoroquinolone conjugated novel class of prodrugs. In this approach, we synthesized theranostic prodrug of ciprofloxacin as therapeutic with coumarin fluorophore for real-time monitoring for drug release.

Chapter 1: Introduction

1.1. Reactive Species

Biological reactive species derived from N, O and S are small reactive molecule that play major roles in cellular functionality and growth. These species are termed as reactive oxygen species (ROS), reactive nitrogen species (RNS) and reactive sulfur species (RSS). These species are produced endogenously and are freely diffusible across cell membranes. At elevated concentrations, these reactive species are hazardous to cells and can cause cell death by damaging macromolecules such as DNA, proteins, and lipids. However, at moderate concentrations, they have a profound effect in a vast array of cellular processes such as cell signaling, metabolism, and maintenance of redox homeostasis. These species are among the primary immune response mechanism to counter various infectious pathogens.[1–7]
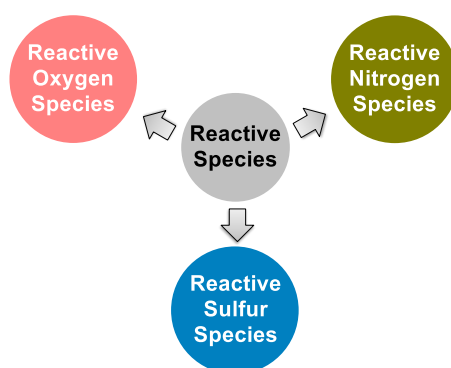
Figure 1.1. Reactive species in the biological systems

1.2. Reactive Sulfur Species

It has been more than 15 years since Jacob and co-workers have coined the term RSS. Similar to ROS and RNS, RSS is sulfur (S) centered small reactive molecules and are capable of performing oxidation or reduction under a physiological condition. Although both ROS and RNS have been extensively studied, reactive sulfur species have received much lesser attention. Traditionally, sulfur has been considered an important constituent of a cellular antioxidant system and proteins. Unlike nitrogen and oxygen, sulfur exists in higher multiple oxidation states. The various oxidation states of the sulfur range between -2 and +6, as a part of the RSS system, which is involved in various physiological processes. RSS include sulfide or thiols, thiyl radical, persulfides, polysulfides, sulfenic acid, sulfur dioxide (SO_2) and its hydrated forms bisulfite, sulfites (HSO_3/SO_3^{2-}), persulfite, and sulfate (SO_4^{2-}). The majority of RSS is generated upon the reaction between the sulfur of sulfhydryl group (-SH) with ROS

and RNS *e.g.* L-cysteine undergoes oxidation with ROS to produce sulfenic acid, which on subsequent oxidation by ROS generates sulfinic acid and sulfonic acid (Scheme 1.1).[7,8,9,10] The sulfenic acid may be reduced into a disulfide by reaction with thiols and may further oxidize to thiosulfinate and thiosulfonate by ROS (Scheme 1.1). Furthermore, ROS can also react with the thiol to form thiyl radical. This radical species can undergo oxidation with oxygen to produce sulfoxyl radical (Scheme 1.1). Sulfoxyl radical may further undergo oxidation in presence of O_2 to generate sulfonyl peroxyl radical. Further, the sulfoxyl radical, on reduction, produces sulfinyl radical in the presence of sulfinic acid. Thiol residues of cysteine can also react with NO to form nitrosothiol. These aforementioned chemically reactive forms of thiols are categorized into reactive sulfur species. Reactive sulfur species such as H_2S and SO_2 are generated from catabolism of L-cysteine by enzymatic pathways (Scheme 1.2).[8–10]
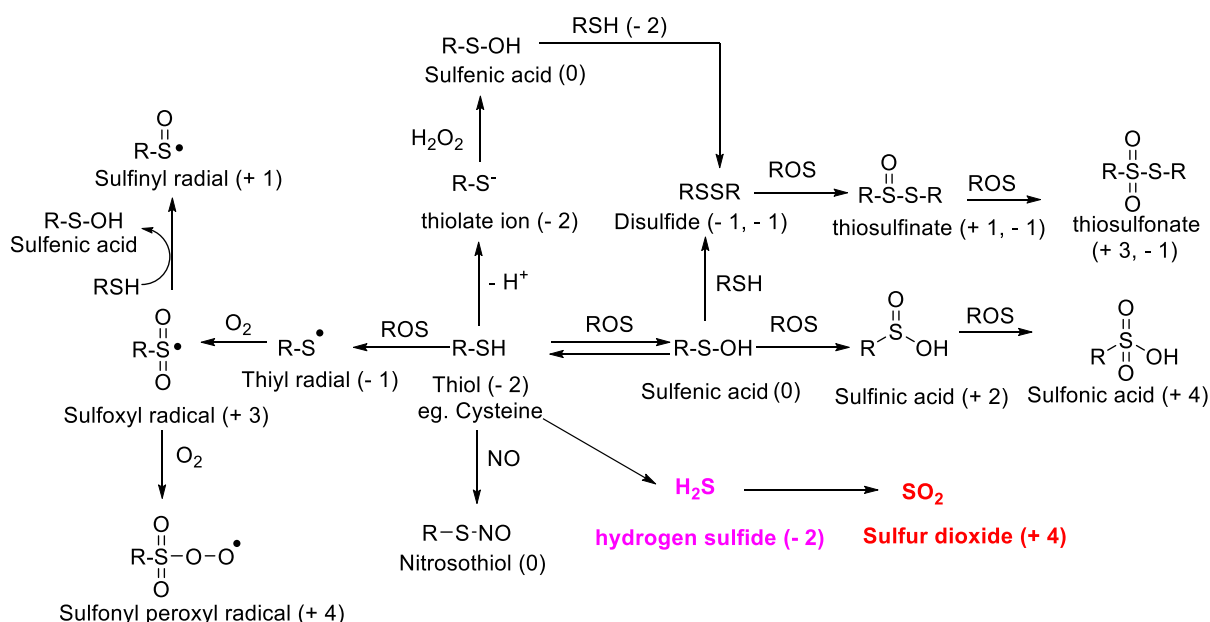
Scheme 1.1. Reactive sulfur species from a thiol in the presence of ROS and RNS

1.3. Biosynthesis of sulfur dioxide (SO₂) from L-cysteine

The gasotransmitter family consists of members such as NO, CO, and H_2S. They all participate in diverse physiological and pathophysiological processes. One of the oxidized products of H_2S is sulfur dioxide (SO_2) which has recently been found to mediate several cellular processes. SO_2 is synthesized inside a cell from the catabolism of L-cysteine. Biosynthesis of SO_2 involves its generation from H_2S, which is endogenously produced from

L-cysteine by cystathionine β-synthase (CBS) and cystathionine γ-lyase (CSE). H_2S, upon oxidation, generates thiosulfite, which in the presence of enzymes such as thiosulfate sulfurtransferase (TST) or glutathione-dependent thiosulfate reductase (GST) is oxidized to generate SO_2. Sulfur dioxide gets hydrated to form sulfite (SO_3^{2-}/HSO_3^-), which may undergo further oxidation in presence of O_2, by the enzyme molybdopterin dependent sulfite oxidase (SO) to generate sulfate (SO_4^{2-}).
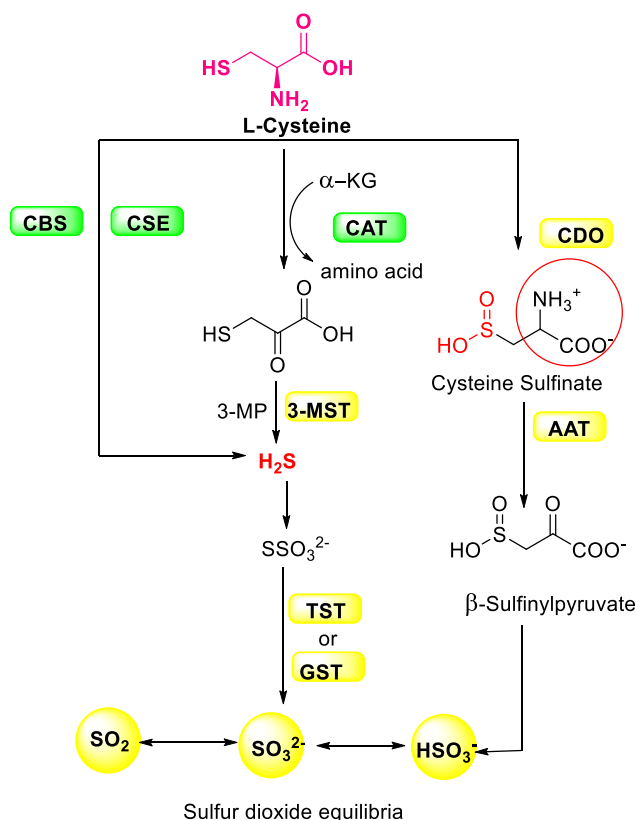
Scheme 1.2. Biosynthesis of sulfur dioxide (SO_2) from L-cysteine

SO_2 is also produced when L-cysteine gets oxidized to L-cysteine sulfinate by the enzyme cysteine dioxygenase (CDO). L-cysteine sulfinate is subsequently transaminated to produce β-sulfinyl pyruvate by the enzyme aspartate aminotransferase (AAT). β-sulfinyl pyruvate spontaneously decomposes to generate pyruvate and SO_2. In addition, L-cysteine, in the presence of α-ketoglutarate (α-KG) is converted into 3-mercaptopyruvate (3-MP) by cysteine aminotransferase (CAT) and 3-MP in the presence of 3-mercaptopyruvate sulfurtransferase (3-MST) to produce H_2S which is further oxidized to SO_2.[7,11–16]

The above is depicted in the Scheme 1.2.

1.4. Roles of Sulfur Dioxide (SO₂)

1.4.1. Environmental aspects and side effects of exogenous SO₂

Sulfur dioxide is a colorless gas and has a distinct pungent odor. Traditionally, SO_2 is considered a common corrosive air pollutant and contributor to acid rain. Sulfur dioxide is added to the atmosphere primarily because of industrialization, volcanic eruptions and the burning of fossil fuels. It readily dissolves in water and establishes an equilibrium with its hydrated forms (sulfite and bisulfite). Sulfur dioxide has an irritating effect on the mucosa of the nose, throat, and lungs[17,18] Asthmatic patients are hypersensitive towards the exposure of SO_2. Bronchoconstriction in asthmatic condition leads to the inflammation of the airway which is responsible for the breathing problem in the patients. However, the mechanism involved is not fully understood.[19] Also, sulfites do not have a significant effect on double-stranded DNA (dsDNA). However, documented studies suggest that a single strand of DNA (ssDNA) is more prone to undergo mutation with sulfite. In ssDNA, nucleophilic attack of sulfite on cytosine, followed by deamination generates uracil, which is present only in RNA.[19] Sulfite is also known to break disulfide bond in proteins to form $S\text{-}SO_3^{2-}$ and a thiol. Sulfite can form S-sulfonate with free thiol residues in proteins such as L-cysteine, glutathione. Sulfite in the presence of transition metal ions forms a series of highly reactive and lethal sulfoxyl radicals, such as $SO_3^{\bullet-}$, $SO_4^{\bullet-}$, $SO_5^{\bullet-}$. These sulfoxy radicals can cause oxidative damage to macromolecules. Proteins and DNA can be scissored in the presence of reactive sulfoxyl radicals whereas cellular membranes *i.e.* lipids undergo peroxidation.[20–29]
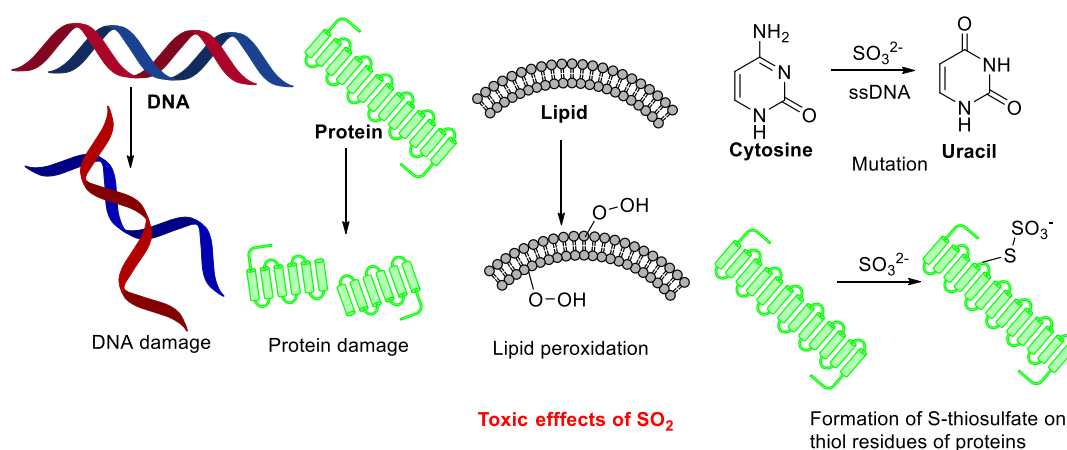

Figure 1.2. Toxic effects of SO₂

1.4.2. Sulfur dioxide in the food industry

In the previous section, we have described some of the potential toxic effects of sulfur dioxide. However, SO_2 has also been one of the most widely used food preservatives for centuries, especially in low pH foods such as beverages and fermented drinks, for example, wine. In the food industry, SO_2 is added in either the gaseous or liquid state or as a stable inorganic salt, called a sulfinating agent. The sulfinating agents include sulfites and bisulfites of Na^+ and Ca^{2+}, metabisulfites, and sometimes sodium thiosulfite and potassium bisulfite. These agents in aqueous solution form a pH- and temperature-dependent equilibrium mixture of SO_2, sulfite, and bisulfite. Also, when SO_2 is added to food products, it may exist in the free form or it may bond reversibly to compounds such as aldehydes, ketones or aldehyde based sugars. Therefore, SO_2 content in the food industry is a combination of both bound and unbound SO_2. Sulfur dioxide in bound form does not perform any function.[30–32] The broad goals achieved by the addition of SO_2 are outlined as follows.

1.4.2.1. Role of SO_2 as an antioxidant

SO_2 can act as an antioxidant by various modes of action. Sulfites rapidly react with dissolved molecular O_2 or H_2O_2 to form sulfate. Thus, SO_2 plays an important role as an antioxidant by scavenging of both O_2 and H_2O_2. Sulfite reduces quinone back to its phenolic form. Sulfite irreversibly inhibits polyphenol oxidases (tyrosinases) by damaging its active site. This enzyme catalyzes the oxidation of phenolic compounds to quinones which are responsible for the development of a brown color in freshly cut fruits or juices. Thus, sulfites are also known as antibrowning agents. SO_2 is also considered an inhibitor of Maillard reaction (between sugar and amines), whose end product is acrylamide, which is a potential carcinogen.

1.4.2.2. Antimycobacterial and yeast selectivity in wines

SO_2 is considered an antibiotic in its molecular form, which depends on the pH and temperature of the system. SO_2 is used predominantly in the wine industry as it plays multiple roles such as antioxidant and an antimicrobial, and it also has selectivity among yeasts and its addition does not alter the taste. As an antimicrobial, it inhibits several strains of lactic acid bacteria (LAB) and to a lesser extent, acetic acid bacteria. The LAB consists of mainly three different genera, namely *Oenococcus*, *Pediococcus,* and *Lactobacillus*. These bacteria produce acetic acid and other off-flavor compounds. This spoilage of wine gives a foul taste. However, SO_2 does not inhibit *Saccharomyces cerevisiae* which is commonly used in the

fermentation of sugar to make wine whereas *Brettanomyces* gets inhibited by SO_2. *Brettanomyces* causes the unpleasant smell of wine due to the generation of several unwanted compounds from the ethyl phenol family.

1.4.3. Role of sulfur dioxide in organic synthesis

Sulfur dioxide can be compressed into a liquid, which can be used as an excellent solvent for many chemicals reactions. Also, it is used extensively in organic synthesis. It is somewhat difficult to handle as a gas. However, recent efforts to make surrogate sulfur dioxide donors for organic synthesis have been reviewed elsewhere. An example is DABSO, which is an adduct of 1,4-diazabicyclo[2.2.2]octane (DABCO) and sulfur dioxide. This is used to generate SO_2 *in situ*.[33–36]
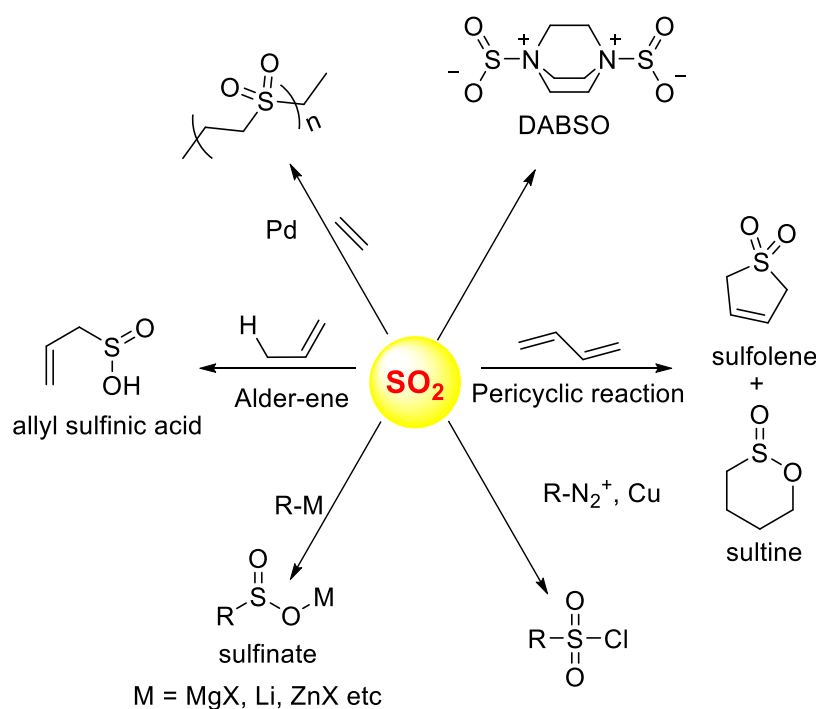
Figure1.3. Selected synthetic transformations of sulfur dioxide

1.4.4. Chemical biology of endogenous SO_2

Nitric oxide (NO), carbon monoxide (CO) and hydrogen sulfide (H_2S) are gaseous environmental pollutants but are also synthesized endogenously and have been shown to perform diverse physiological and pathophysiological functions inside a cell. These gaseous molecules are classified as cell signaling molecules or gasotransmitters. The major role

performed by all these three gases is to regulate the vascular homeostasis and central nervous system functions[37]
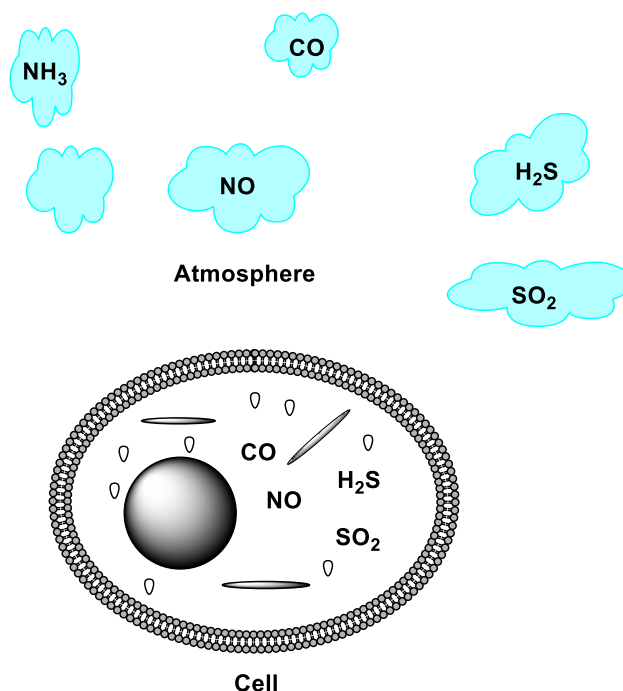
Figure 1.4. Common air pollutants are biologically active molecules and are synthesized in cells

SO_2 is found to be generated endogenously and performs similar functions as that of cell signaling molecules. SO_2 could be the potential fourth gaseous molecule in the family gasotransmitters. SO_2 is being looked upon as a potential entrant in the gasotransmitter family, and multiple reports suggesting its participation in diverse physiological and pathophysiological functions have surfaced in the past few years. SO_2 has shown significant vasodilatory effects. Meng and co-workers have investigated the effect of SO_2 on male Wistar rats. The blood pressure of rats upon exposure to SO_2 was observed to lower in a dose-dependent manner in comparison to control rats.[38] A similar study was conducted on SHRs (spontaneously hypertensive rats). The blood pressure of control SHRs from 180 mmHg was lowered significantly in the presence of sulfite to 138 mmHg.[39] Recently, Ming Xian and co-workers used an aortic ring model and found vasorelaxation in a dose-dependent manner with SO_2 solution.[40] Meng and co-workers performed a study of SO_2 on the perfused rat hearts which generated considerable negative inotropic effects.[41,42] In a recently conducted study on adipose tissue to monitor endogenous generation of SO_2 and its roles, it was suggested that

SO_2 is synthesized endogenously and inhibits inflammation. Therefore, SO_2 may play a vital role in inflammation-related diseases, such as obesity and insulin resistance.[43]

Thus, looking at all these different reports on SO_2, it deserves extensive attention. All reports need to be further validated to fully understand SO_2 biology and to establish SO_2 as the fourth gasotransmitter in the family.

1.5. Controlled generation of SO_2

To understand the chemical biology of SO_2 within cells, promising SO_2 donors need to be cell permeable. Also, the generation of SO_2 in a controlled manner with endogenous activation is highly desirable. Usually, to study the chemical biology of SO_2, it is either employed in gaseous form or predominantly in the form of inorganic salts (sulfinating agents) as a surrogate for SO_2. These salts have poor bioavailability, being a charged molecular species, and are required at higher concentrations to elicit a response in physiological and pathophysiological processes and this may compromise the final interpretations regarding SO_2.[42,44] Therefore, new and efficient SO_2 donors are highly anticipated to study the precise role of SO_2 in chemical biology and to assess its unique therapeutic potential. Few existing organic donors of SO_2 discussed herein have been shown to produce SO_2 under biologically relevant conditions.

1.5.1. Thiol activated SO_2 donors as antimycobacterial agents

The first report of sulfur dioxide donors in the literature describing anti-bacterial effects was from our laboratory in 2012. The authors used a 2,4-dinitrophenylsulfonamide as the major functional group for generating sulfur dioxide. This functional group has been used as a protective group in organic synthesis previously and is deprotected by thiols. Since cellular thiols occur in large concentrations, Malwal and co-workers demonstrated the suitability of this series of compounds as sources of sulfur dioxide (Scheme 1.3). They found that the rate of sulfur dioxide generation was dependent on the nature of the amine in the sulfonamide. The more basic the amine was, the faster was the sulfur dioxide generation. Thus, simple structural modifications that affected the basicity of the amine formed the basis for modulating SO_2 release rates.[45,46]
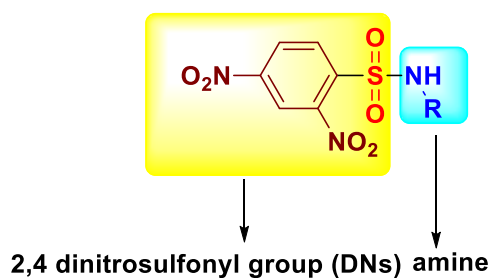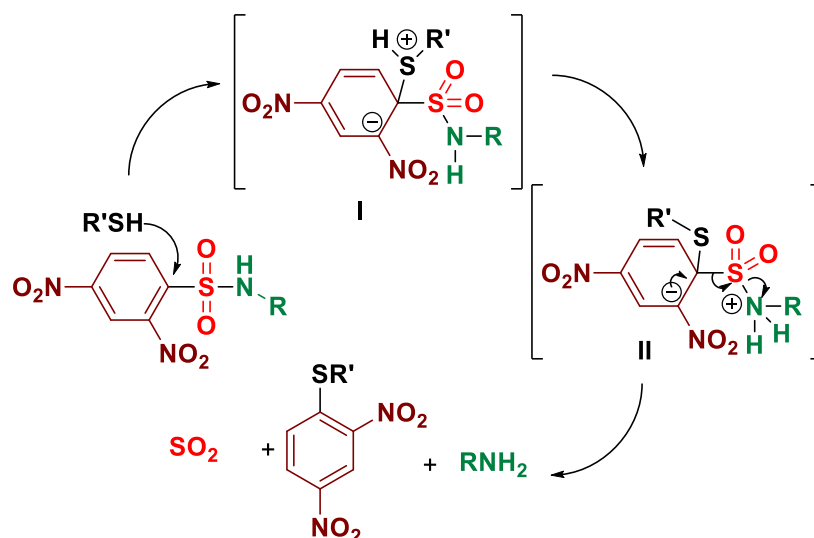
Figure 1.5. DNs protected scaffold for SO$_2$ generation
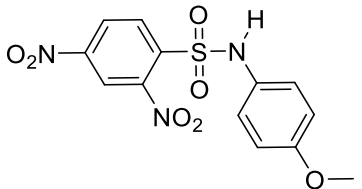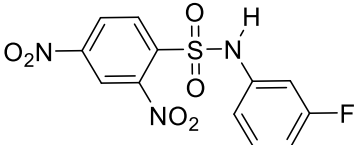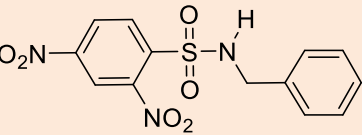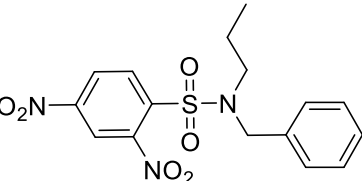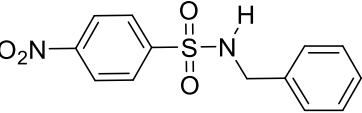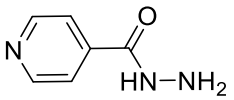

Scheme 1.3. Thiol activated SO$_2$ generation

The authors evaluated the potential for these compounds to inhibit bacterial growth and found that, among closely related compounds, the propensity to inhibit mycobacterial growth was dependent on the rate of sulfur dioxide generation. The lead compound was found to have low micromolar inhibitory potency against *Mycobacterium tuberculosis*, the causative agent of tuberculosis, a disease that affects millions each year. A recent study on the effects of sulfur dioxide on tuberculosis occurrence in human populations was conducted. The authors found protective effects of this gas when patients were exposed to low-level ambient sulfur dioxide.[47]

The 2,4-dinitroaryl sulfonamides were evaluated for broad-spectrum anti-bacterial activity and it was found that the benzylamine lead derivative, which had potent anti-mycobacterial activity, had no inhibitory activity against other Gram-positive as well as Gram-negative bacteria. Next, our group did a series of structural modifications that led to improved anti-bacterial properties, but only against Gram-positive pathogens.

The structural modifications resulted in compounds with good inhibitory activity against drug-resistant strains of *Staphylococcus aureus* and have been discussed in detail in Chapter 2.

Table 1.1. Correlation of inhibitory activity of SO₂ donor and the yield of SO₂ against *Mtb*

Compound	SO$_2$ yield (µM)	MIC (µM)
O$_2$N— ... S with O, O, N–H, and O— (para methoxy phenyl), NO$_2$	79.5	4.4
O$_2$N— ... S with O, O, N–H, phenyl–F (meta fluoro), NO$_2$	24	73
O$_2$N— ... S with O, O, N–H, benzyl, NO$_2$ **1a, lead compound**	100	0.15
O$_2$N— ... S with O, O, N–(propyl)benzyl, NO$_2$	88	8.25
O$_2$N— ... S with O, O, N–H, benzyl (para nitro)	0	>100
pyridine C(=O), HN–NH$_2$ **Isoniazid**	0	0.37

1.5.2. Sulfur dioxide generation by inter- and intramolecular "click and release"

Sulfones have been reported to undergo cycloreversion to generate sulfur dioxide, typically at elevated temperatures. This strategy has been modified by Binghe Wang and co-workers to generate a highly reactive sulfone intermediate *in situ*. The strategy followed was a "click and release" where a cycloaddition between a strained alkyne and a diene was conducted (Scheme 1.4). This reaction was carried out with two independent reactants. Thiophene dioxides as a diene, bearing electron withdrawing groups were synthesized for click reaction

with an alkyne, to tune the release of SO_2. They have also studied the real-time release of SO_2. However, the bimolecular click and release of SO_2 strategy may not be very good in order to study SO_2 in a biological system. Therefore, the follow-up report by Binghe Wang and co-workers had an intramolecular reaction (Scheme 1.4). In order to incorporate diene and alkyne in the same molecule, one of the free acid groups of the thiophene dioxide scaffold was derivatized selectively to accommodate the alkyne. Electron density was modulated on or adjacent to the alkyne group by using different alkyl substituents to have the tunable release of SO_2. The observed half-lives ranged from minutes to days. Intramolecular "click and release" donors of SO_2, when studied against super-coiled plasmid DNA, showed significant DNA damage, similar to positive control. Also, the compounds were found to be cell permeable by the latent SO_2 probe in the RAW 264.7 cells.[48,49]

.
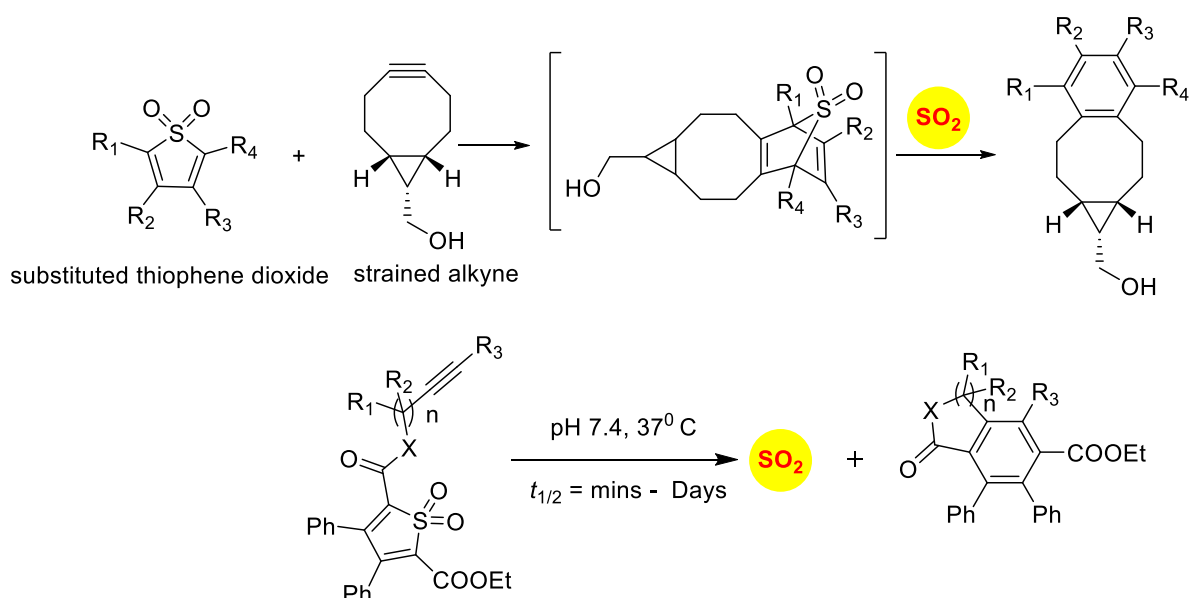
Scheme 1.4. Click and release strategies for sulfur dioxide generation

These inter- and intramolecular "click and release" strategies for the generation of SO_2 by Binghe Wang and co-workers (Scheme 1.4) have the unique advantage of having a wide range of rates of SO_2 generation. However, in the case of intermolecular "click and release" SO_2 donors, both reactants should be in proximity to generate SO_2 and that will be a complicated task to achieve in biological systems. These "click and release" SO_2 donors are more akin to spontaneous donors of SO_2. Intramolecular "click and release" SO_2 donor have both the alkyne and diene in the same molecule and in solution, they can react and generate sulfur dioxide. All these are the major limitations associated with these "click and release"

SO$_2$ donors. Therefore, the incorporation of a trigger will help in controlling the delivery of SO$_2$.

1.5.3. Esterase activated sulfur dioxide generation inspired by modified Julia olefination

Binghe Wang and co-workers recently reported a sulfone that undergoes Julia olefination reaction as SO$_2$ donors (Scheme 1.5).[50] They modified the substrate such that it would be triggered by esterases to generate an olefin and sulfur dioxide, similar to modified Julia olefination, which is also referred to as Julia-Kocienski olefination. The authors also show that the half-life of the release of sulfur dioxide ranges from minutes to hours and that could be modulated by employing different esters. The donor was found to permeate cells and generate sulfur dioxide. SO$_2$ was monitored intracellularly using a latent fluorophore for sulfite.

This donor may find wide use for cellular studies to investigate the chemical biology of sulfur dioxide.
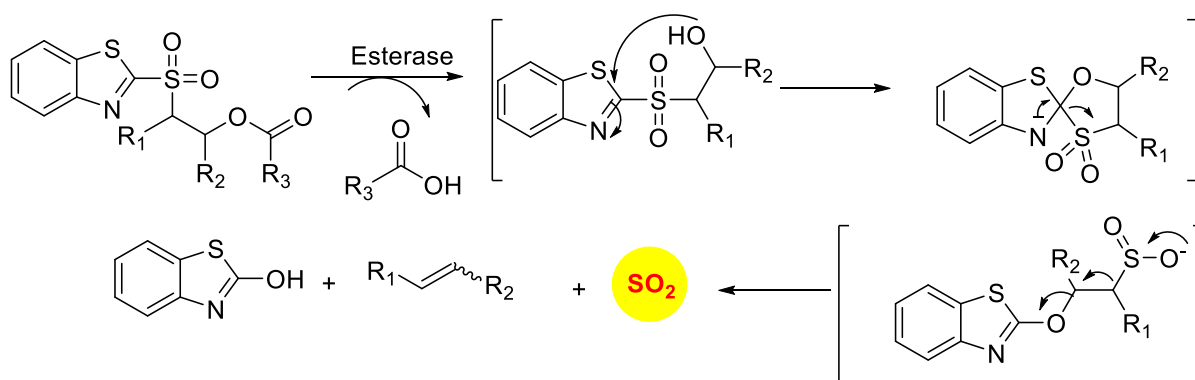
Scheme 1.5. Esterase activated sulfur dioxide generation

However, this method is associated with a few limitations, such as these molecules being hydrophobic. Further, it is necessary to have alkyl groups on a carbon atom α to a sulfone group as α-hydrogen atoms are labile. Also, these chemical scaffolds do not allow accommodation of drug candidates, which could be a potential application for the donor. Thus, this enzyme based method to generate SO$_2$ lacks versatility for broader applications.

1.5.4. Photoactivated sulfur dioxide generation from sulfones

Sulfones can also generate sulfur dioxide after exposure to light. Malwal and co-workers have demonstrated that benzosulfones can be irradiated with UV light to produce sulfur dioxide in a pH 7.4 buffer (Figure 1.6). The observed SO_2 yield of substituted benzosulfones upon photolysis was found to be favored by electron donating groups. While this method allows for triggerable sulfur dioxide generation, the wavelength and intensity of light used is not entirely compatible with biological studies. Uchida and co-workers have reported a closed ring isomer of diarylethene bearing a sulfone group as a masked SO_2 donor. In the presence of visible light, the closed ring isomer is converted into its open ring form, but does not generate SO_2 and is also found to be stable at 70 °C. However, upon exposure to UV light, both the isomers exist in an equilibrium and the open ring form efficiently generates SO_2 (Figure 1.6).[45,51]
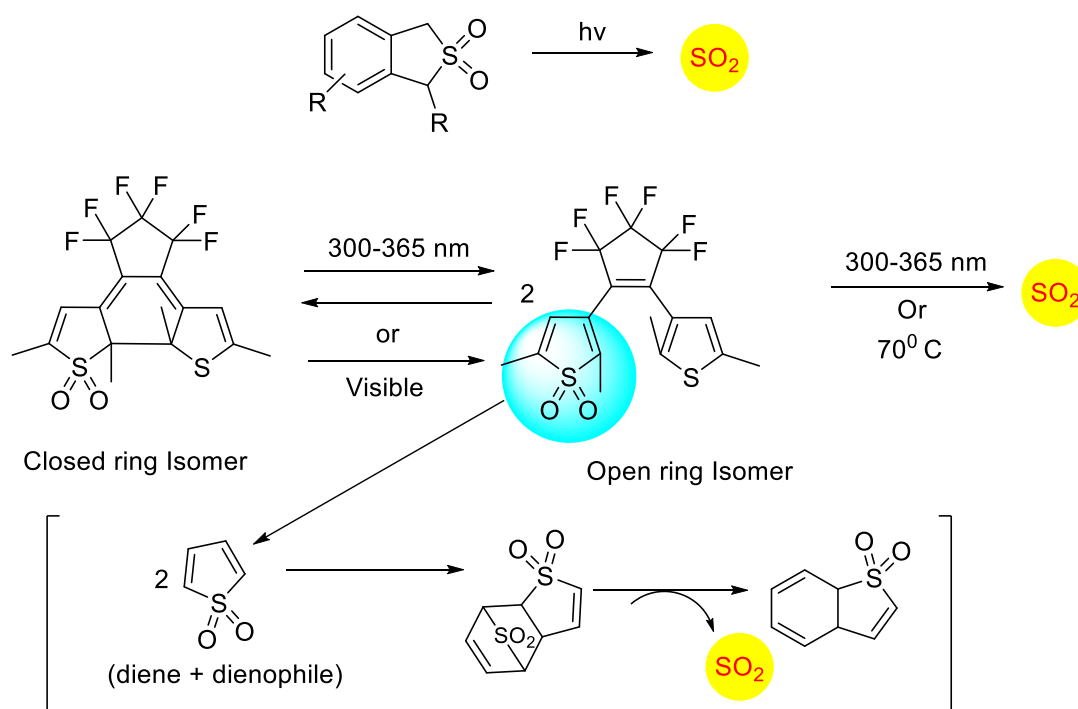

Figure 1.6. Photolabile SO_2 donors

1.5.5. Sulfinates as Sulfur dioxide donors

Sulfinates are also candidates for the sulfur dioxide generation. A cycloreversion strategy was reported by Malwal and co-workers. Here, benzosultines were synthesized and these compounds were found to undergo a retro Diels-Alder reaction with a thermal stimulus and produce SO_2 at physiological pH (Figure 1.7a). A

Hammett relationship study was carried out and the dependence of the rates of SO_2 release on substituents in the sulfinate ester was determined. A moderate electronic effect (σ = -0.6) was found and the range of half-lives for the SO_2 generation was found to be 10 to 68 min. A detailed computational investigation of the release mechanism was carried out and was found to be consistent with experimental data. This study showed that modulating the electronic environment around the sulfinate functional group may have an effect on the release of sulfur dioxide. DNA damage study for one of these SO_2 donors was performed over pBR322 plasmid DNA. Significant DNA damage due to the sulfinates was observed when used in the presence of Cu(II), similar to the case of the positive control of sulfite and Cu(II). A major limitation associated with these SO_2 donors is that SO_2 generation does not have a trigger for controlled generation.[40,52]
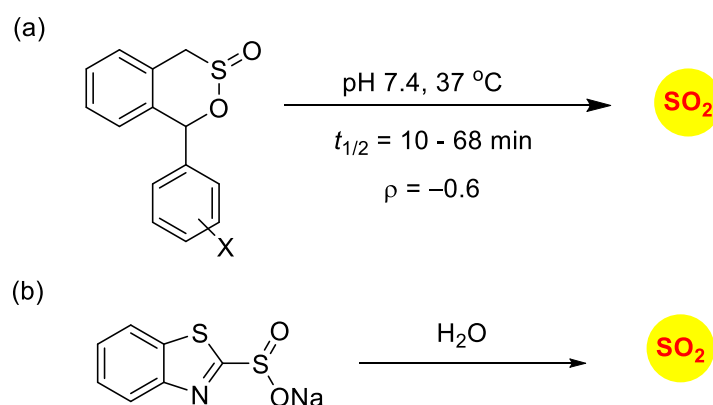

Figure 1.7. Sulfinate based SO_2 donors

Ming Xian and co-workers have developed a benzothiazole sulfinate salt, a new sulfinate ester-based donor that undergoes pH-dependent hydrolysis in a buffer, to produce sulfur dioxide (Figure 1.7b). Being a salt, it has excellent water solubility similar to that of inorganic salts such as sulfites. Benzothiazole sulfinate, when tested for the generation of SO_2 at physiological pH, generated SO_2 in a diminished yield. Half-lives were found to be 7.5 min at pH = 4, 75 min at pH = 5, 12.5 days at pH = 6, and 13 days at pH = 7.4. So, at a lower pH, this compound was found to release SO_2 more efficiently. They studied this donor's vasorelaxation properties as compared to the authentic SO_2 gas solutions and found that the donor compared well with SO_2 in this respect. Limitations associated with this benzothiazole sulfinate are that being a salt, it may have reduced cellular permeability similar to inorganic sulfites. Controlled generation of SO_2 in the case of benzothiazole sulfinate is not possible

due to the absence of a trigger. Also, the generation of SO_2 in this donor was found to be pH-dependent and was efficient primarily at lower pHs. Therefore this donor may not have utility.

1.6. Proposal

All the aforementioned reported SO_2 donors were associated with limitations because of the challenges they possessed due to the availability of limited chemical tools to incorporate SO_2. Benign, reliable and efficient delivery of SO_2, with the use of a trigger, in cellular models possesses several challenges. It is desirable to have SO_2 donors that are cell permeable and bioactivatable (Figure 1.8). Again, the previously reported donors did not allow having a chemical tool to incorporate site-specific delivery and release of SO_2. These donors lacked in versatility to use different triggers in the same model and therefore, cannot be employed as multifaceted donors. Therefore, there is a necessity to have universal SO_2 donors which will fulfill the aforementioned characteristic requirements of an ideal SO_2 donor.
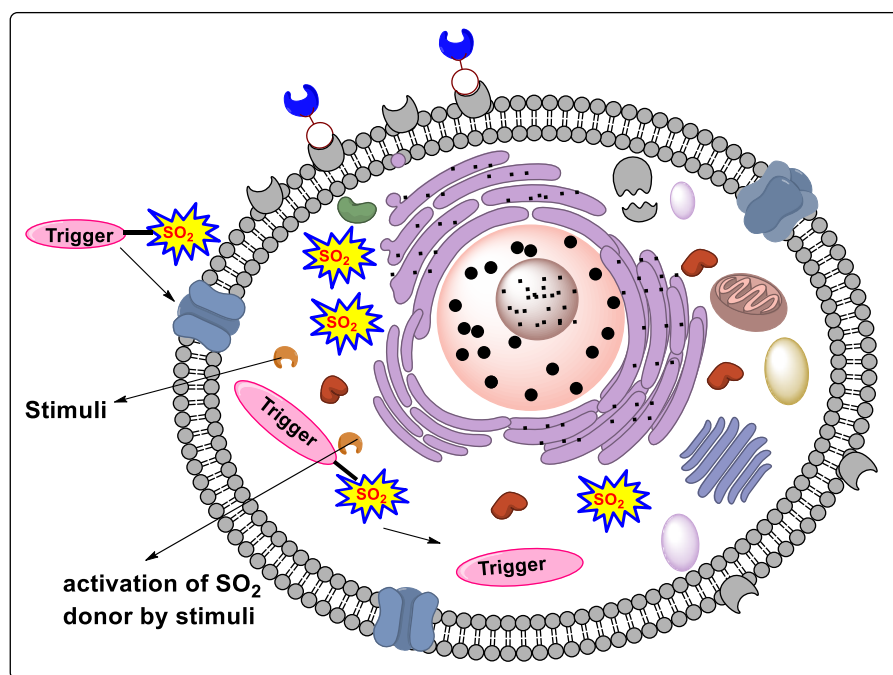

Figure 1.8. Characteristic features of the anticipated ideal SO_2 donor in a representative cell

1.7. General Design of SO₂ Donors

Sulfur dioxide is a small, angular, triatomic molecule. Therefore, for a molecule to act as an SO_2 donor, it would need, in principle, to be placed appropriately in a chemical scaffold. Various modes of activation, such as physical, chemical, photochemical, bio-activation *etc.*

should facilitate SO_2 generation. In all the currently used strategies for SO_2 generation, sulfones and sulfinic groups are bonded to various atoms such as N or O or C. Similar use of sulfones or sulfinic group as a starting point should also facilitate the SO_2 generation with a suitable trigger (Scheme 1.6). There various types of enzymes that are present in nearly all organisms. Benign enzyme based triggers, preferably from the host system, would be advantageous.
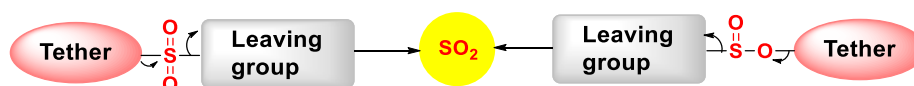

Scheme 1.6. General sulfone and sulfinate based methods of SO_2 donors

1.8. Hypothesis

The enzyme esterase is most commonly used for the delivery of prodrugs. Similarly, we hypothesized that esterase (ES) triggered SO_2 generation can be achieved within cells reliably. The existing general organic donors of SO_2 have either the sulfinate or sulfone moiety in their chemical scaffold. So, we decided to incorporate either sulfinate or sulfone in our new proposed design of esterase trigger based SO_2 generation. Therefore, we considered the chemistry associated with the decomposition of carbonates, which have been extensively used for drug delivery.[53,54] Carbonate prodrugs operate by the generation of carbon dioxide (CO_2), which presumably is an irreversible reaction. An appropriately placed trigger and the subsequent self-immolation can produce CO_2 from a carbonate (Scheme 1.7.1). The key bond that breaks is the C−O bond shown by an arrow, for which the estimated bond dissociation energy (BDE) is 68 kcal mol^{-1}.[55] Similarly, we envisaged that the cleavage of the C−S bond in sulfonates (shown by an arrow) will similarly trigger the generation of SO_2 and an alcohol (Scheme 1.7.2). The BDE of this bond is estimated to be 57 kcal mol^{-1}, which is comparable with the C−O bond.[56] Such a method may have broad relevance as a tool to study SO_2 biology as well as a methodology for co-delivery of an alcohol-based drug. Furthermore, the nature of the leaving group, *i.e.*, the alcohol, may determine the SO_2 generation capability.
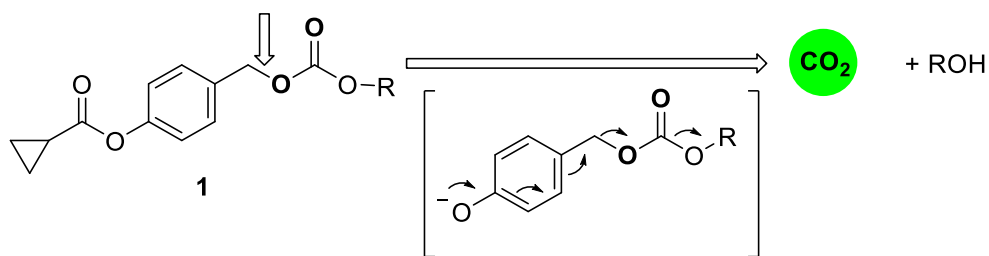
Scheme 1.7.1. Proposed ester hydrolysis of carbonate to generate CO_2 and an alcohol
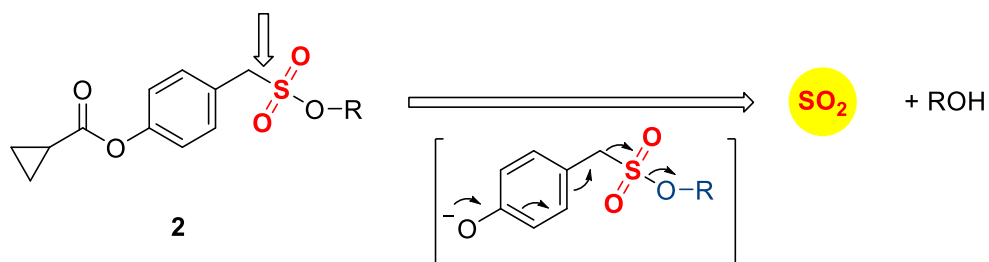
Scheme 1.7.2. Proposed ester hydrolysis of sulfonates to generate SO_2 and an alcohol

1.9. Proof of concept

We propose to synthesize a compound having both SO_2 and a fluorophore. Upon enzymatic activation, this compound is expected to undergo a self-immolation reaction to release a fluorescent compound called umbelliferone, which may be detected easily (Scheme 1.8).
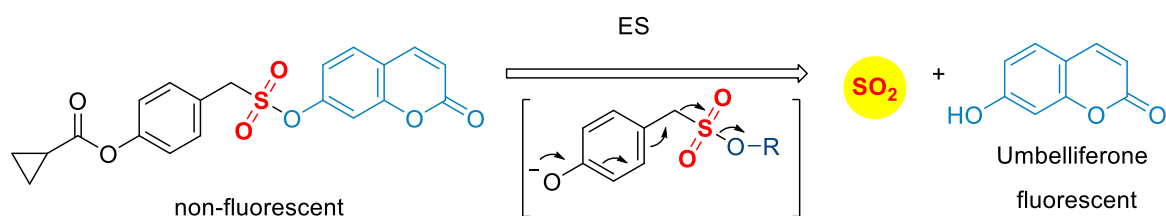
Scheme 1.8. Esterase activated self-immolative donors

1.10. Bacterial enzyme Nitroreductase-activated theranostic agents

If the esterase based SO_2 donor strategy is successful, then other triggers can be employed to make it a versatile strategy for broader applications. These should present an opportunity to incorporate a drug molecule into the available SO_2 donors with suitable linkers. Esterases are present in nearly all cells. Therefore, incorporation of the drug molecule and SO_2 donor along with specific enzymatic triggers would be advantageous. A specific trigger should protect the host from all the offset side effects. A potential application of enzyme-activated SO_2 donors

could be SO$_2$-conjugated theranostic prodrugs. The enzyme nitroreductase can be chosen as a specific enzymatic stimulus (Figure 1.9).

Theranostics is a rapidly emerging field with a vast potential, due to its applications of therapeutic and diagnostic applications on a single platform. In the case of any infectious disease, diagnostics is an important aspect, in order to cure the disease at an early stage of infection, by which morbidity and mortality will be greatly reduced. No secondary assays should be required in order to image a delivered drug. Thus far, there are a limited number of reports available for small molecule theranostics for bacteria.[57–63]
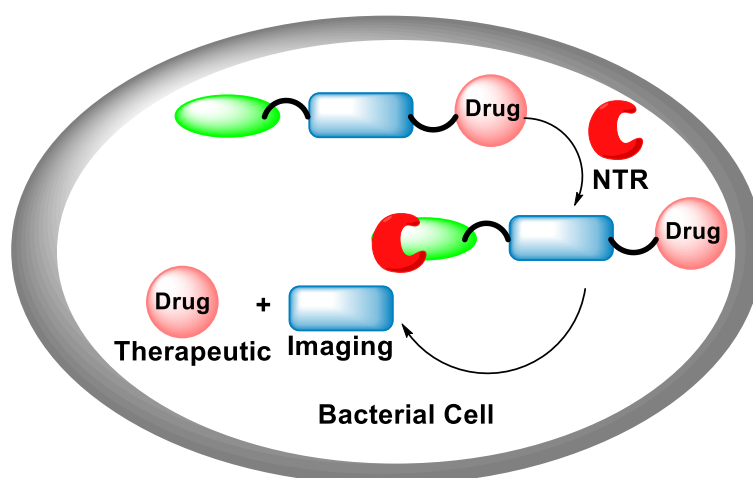

Figure 1.9. Proposed design for an NTR activated theranostic prodrug in bacteria

1.10. References

1   B. Halliwell, *Plant Physiol.*, 2006, **141**, 312–322.

2   C. C. Winterbourn, A. J. Kettle and M. B. Hampton, *Annu. Rev. Biochem.*, 2016, **85**, 765–792.

3   P. Sharma, A. B. Jha, R. S. Dubey and M. Pessarakli, *J. Bot.*, 2012, **2012**, 1–26.

4   G. Giles, M. Nasim, W. Ali and C. Jacob, *Antioxidants*, 2017, **6**, 38.

5   M. Chaki, R. Valderrama, A. M. Fernández-Ocaña, A. Carreras, M. V. Gómez-Rodríguez, J. R. Pedrajas, J. C. Begara-Morales, B. Sánchez-Calvo, F. Luque, M. Leterrier, F. J. Corpas and J. B. Barroso, *J. Exp. Bot.*, 2011, **62**, 1803–1813.

6   M. H. Stipanuk, *Annu. Rev. Nutr.*, 2004, **24**, 539–577.

7   X. B. Wang, H. F. Jin, C. S. Tang and J. B. Du, *Clin. Exp. Pharmacol. Physiol.*, 2010, **37**, 745–752.

8   T. V. Mishanina, M. Libiad and R. Banerjee, *Nat. Chem. Biol.*, 2015, **11**, 457–464.

9   G. GIles, K. Tasker and C. Jacob, 2001, **31**, 1279–1283.

10   M. C. H. Gruhlke and A. J. Slusarenko, *Plant Physiol. Biochem.*, 2012, **59**, 98–107.

11   K. R. Olson, E. R. DeLeon, Y. Gao, K. Hurley, V. Sadauskas, C. Batz and G. F. Stoy, *AJP Regul. Integr. Comp. Physiol.*, 2013, **305**, R592–R603.

12   T. M. Hildebrandt and M. K. Grieshaber, *FEBS J.*, 2008, **275**, 3352–3361.

13   C. Antoniou, A. Savvides, A. Christou and V. Fotopoulos, *Curr. Opin. Plant Biol.*, 2016, **33**, 101–107.

14   Y. Huang, C. Tang, J. Du and H. Jin, *Oxid. Med. Cell. Longev.*, , DOI:10.1155/2016/8961951.

15   J. Liu, W. Yu, Y. Liu, S. Chen, Y. Huang, X. Li, C. Liu, Y. Zhang, Z. Li, J. Du, C. Tang, J. Du and H. Jin, *Sci. Rep.*, 2016, **6**, 1–9.

16   X. B. Wang, J. B. Du and H. Cui, *Life Sci.*, 2014, **98**, 63–67.

17   A. Technical Committe, *ASBC Methods Anal.*, 2011, 598–606.

18   H. Vally and N. L. A. Misso, 2012, **5**, 16–23.

19   A. L. Reno, E. G. Brooks and B. T. Ameredes, 2015, **9**, 13–25.

20   E. Heydari-bafrooei and B. Rezaei, , DOI:10.1021/ac302693j.

21   R. G. M. Moreno, M. H. G. Medeiros and N. Coichev, 2005, 1101–1107.

22   T. Lindahl, *Nature*, 1993, **362**, 709–715.

23   N. Sang, *Toxicol. Res. (Camb).*, 2016, **6**, 7–16.

24   M. Bonini and R. Mason, *Environ. Health Perspect.*, 2010, **118**, 970–5.

25   Z. Meng, G. Qin and B. Zhang, 2005, **155**, 150–155.

26   Z. Meng, G. Qin, B. Zhang and J. Bai, 2018, **19**, 465–468.

27   H. Laggner, M. Hermann, B. Sturm and B. M. K. Gmeiner, 2005, **579**, 6486–6492.

28   M. T. Baker, D. Ph, M. S. Gregerson and M. Naguib, 2004, 1235–1241.

29   D. A. Keller and D. B. Menzel, *Chem. Biol. Interact.*, 1989, **70**, 145–156.

30   A. L. Coşkun, M. Türkyilmaz, Ö. T. Aksu, B. E. Koç, O. Yemiş and M. Özkan, *Food Chem.*, 2013, **141**, 3670–3680.

31   K. Prabhakar and E. N. Mallika, in *Encyclopedia of Food Microbiology*, Elsevier, 2014, pp. 108–112.

32   R. F. Guerrero and E. Cantos-Villar, *Trends Food Sci. Technol.*, 2015, **42**, 27–43.

33   P. Vogel, M. Turks, L. Bouchez, D. Markovic, a Varela-Alvarez and J. a Sordo, *Acc. Chem. Res.*, 2007, **40**, 931–942.

34   P. Bisseret and N. Blanchard, *Org. Biomol. Chem.*, 2013, **11**, 5393.

35   A. O. Ferreira, H. C. Polonini, S. L. Silva, F. B. Patrício, M. A. F. Brandão and N. R. B. Raposo, *J. Pharm. Biomed. Anal.*, 2016, **118**, 105–112.

36   B. Schnyder and W. J. Pichler, *J. Allergy Clin. Immunol.*, 2013, **131**, 256–257.e5.

37 L. Li and P. K. Moore, *Biochem. Soc. Trans.*, 2007, **35**, 1138–1141.

38 Z. Meng, H. Geng, J. Bai and G. Yan, *Inhal. Toxicol.*, 2008, **15**, 951–959.

39 W. Lu, Y. Sun, C. Tang, T. Ochs, J. Qi, J. Du and H. Jin, *Exp. Biol. Med.*, 2012, **237**, 867–872.

40 J. J. Day, Z. Yang, W. Chen, A. Pacheco and M. Xian, *ACS Chem. Biol.*, 2016, **11**, 1647–1651.

41 L.-S. Wang, L. Wang, L. Wang, G. Wang, Z.-H. Li and J.-J. Wang, *Environ. Toxicol.*, 2009, **24**, 296–303.

42 Q. Yao, Y. Huang, A. D. Liu, M. Zhu, J. Liu, H. Yan, Q. Zhang, B. Geng, Y. Gao, S. Du, P. Huang, C. Tang, J. Du and H. Jin, *Am. J. Physiol. - Regul. Integr. Comp. Physiol.*, 2016, **310**, R1073–R1080.

43 H. Zhang, Y. Huang, D. Bu, S. Chen, C. Tang, G. Wang, J. Du and H. Jin, *Sci. Rep.*, 2016, **6**, 1–10.

44 M. Belén García-Alonso, J. Pena-Egido and C. García-Moreno, *J. Agric. Food Chem.*, 2001, **49**, 423–429.

45 S. R. Malwal and H. Chakrapani, *Org. Biomol. Chem.*, 2015, **13**, 2399–2406.

46 S. R. Malwal, D. Sriram, P. Yogeeswari, V. B. Konkimalla and H. Chakrapani, *J. Med. Chem.*, 2012, **55**, 553–557.

47 E. Ge, M. Fan, H. Qiu, H. Hu, L. Tian, X. Wang, G. Xu and X. Wei, *Environ. Pollut.*, 2017, **228**, 408–415.

48 W. Wang, X. Ji, Z. Du and B. Wang, *Chem. Commun.*, 2017, **53**, 1370–1373.

49 X. Ji, E. M. El-labbad, K. Ji, D. S. Lasheen, R. A. T. Serya, K. A. Abouzid and B. Wang, *Org. Lett.*, 2017, **19**, 818–821.

50 W. Wang and B. Wang, *Chem. Commun.*, 2017, **53**, 10124–10127.

51 R. Kodama, K. Sumaru, K. Morishita, T. Kanamori, K. Hyodo, T. Kamitanaka, M. Morimoto, S. Yokojima, S. Nakamura and K. Uchida, *Chem. Commun.*, 2015, **51**, 1736–1738.

52   S. R. Malwal, M. Gudem, A. Hazra and H. Chakrapani, *Org. Lett.*, 2013, **15**, 1116–1119.

53   Y. Yang, H. Aloysius, D. Inoyama, Y. Chen and L. Hu, *Acta Pharm. Sin. B*, 2011, **1**, 143–159.

54   D. D. N'Da and J. C. Breytenbach, *J. Pharm. Pharmacol.*, 2009, **61**, 721–731.

55   S. J. Blanksby and G. B. Ellison, *Acc. Chem. Res.*, 2003, **36**, 255–263.

56   H.-Z. Yu, F. Fu, L. Zhang, Y. Fu, Z.-M. Dang and J. Shi, *Phys. Chem. Chem. Phys.*, 2014, **16**, 20964–20970.

57   O. S. Wolfbeis, *Chem. Soc. Rev.*, 2015, **44**, 4743–4768.

58   M. Thakur, S. Pandey, A. Mewada, V. Patil, M. Khade, E. Goshi and M. Sharon, *J. Drug Deliv.*, 2014, **2014**, 282193.

59   Z. Zhao, R. Yan, X. Yi, J. Li, J. Rao, Z. Guo, Y. Yang, W. Li, Y. Q. Li and C. Chen, *ACS Nano*, 2017, **11**, 4428–4438.

60   Y. Kong, H. Yao, H. Ren, S. Subbian, S. Cirillo, J. Sacchettini, J. Rao and J. Cirillo, *Proc. Natl. Acad. Sci.*, 2010, 107, 12239–12244.

61   P. Panizzi, M. Nahrendorf, J. L. Figueiredo, J. Panizzi, B. Marinelli, Y. Iwamoto, E. Keliher, A. A. Maddur, P. Waterman, H. K. Kroh, F. Leuschner, E. Aikawa, F. K. Swirski, M. J. Pittet, T. M. Hackeng, P. Fuentes-Prior, O. Schneewind, P. E. Bock and R. Weissleder, *Nat. Med.*, 2011, **17**, 1142–1147.

62   Z. Zhang, M. Taylor, C. Collins, S. Haworth, Z. Shi, Z. Yuan, X. He, Z. Cao and Y. C. Park, *ACS Appl. Mater. Interfaces*, 2018, **10**, 1534–1543.

63   R. Weinstain, E. Segal, R. Satchi-Fainaro and D. Shabat, *Chem. Commun.*, 2010, **46**, 553–555.

Chapter 2. Thiol Activated SO₂ Donors as *MRSA* Inhibitors

2.1. Introduction

As described in the previous chapter, in order to find the therapeutic potential of SO_2, our group exploited the unique antibacterial property of SO_2 against *Mycobacterium tuberculosis*.[1] These compounds get activated with thiol stimulus to generate SO_2. The activities of these SO_2 donors were correlated with the amount of SO_2 generated from them. Lead compound *N*-Benzyl-2,4-dinitrobenzenesulfonamide (**1a**) showed a potency (minimum inhibitory concentration (MIC) = 0.15 μM) for inhibiting *Mycobacterium tuberculosis* (*Mtb*) higher than the clinically used agent isoniazid (MIC = 0.37 μM). However, these SO_2 donors were found to be inactive when tested for their broad-spectrum antibacterial activity. Therefore, in order to further evaluate the therapeutic potential of these SO_2 donors against other bacterial species, we planned to synthesize a library of 2,4-Dinitrobenzenesulfonamides. To start the synthesis, we planned to choose **1a** as a prototype to synthesize its analogs that can generate one or two moles of SO_2 per donor molecule. We planned to modulate **1a** systematically to study structure-activity relationship. Herein, we propose a hypothesis that organic sources of SO_2 might be capable of inhibiting the growth of other bacteria.

2.2. Result and Discussion

2.2.1. Synthesis and characterization

2.2.1.1. Synthesis of *N*-alkyl substituted analogs of 1a

In order to test our hypothesis, we synthesized *N*-alkyl substituted analogs of **1a**, which was the lead compound in our previous study on *Mtb*. The precursor benzyl sulfonamides were prepared by following a reported procedure. Derivatives of *N*-benzyl DNs (2,4-dinitrophenyl sulfonamide) compounds were synthesized by the treatment of the parent sulfonamides with an alkyl halide in the presence of potassium carbonate to afford the corresponding products in moderate to good yields (Table 2.1).

DNsCl: 2,4-Dinitro sulfonylchloride;
Py: Pyridine

R_1 = H (**1a**),
R_1 = 4-OMe (**2a**)
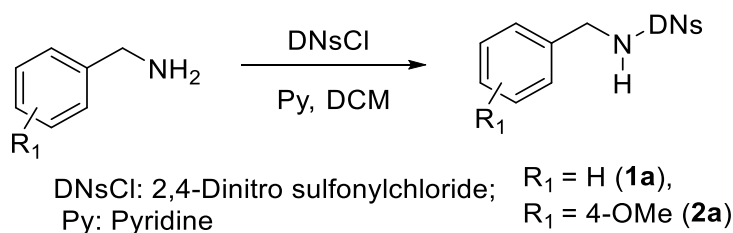
Scheme 2.1. Synthesis of benzyl sulfonamides precursors

Table 2.1. Synthesis of *N*-alkyl substituted benzyl-DNs derivative

R$_1$ = H (**1a**),
R$_1$ = 4-OMe (**2a**)   R$_2$X = alkyl halide
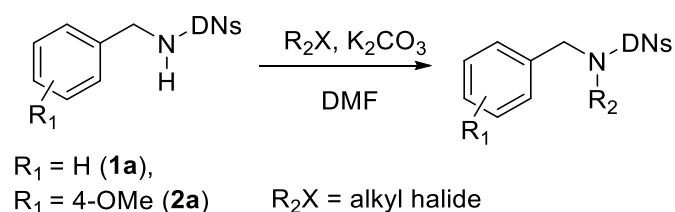
Entry	R$_1$	R$_2$	Compound	% Yield
1	H	Me	**1b**	86
2	H	Propargyl	**1c**	64
3	H	(CH$_2$)$_3$OH	**1d**	75
4	4-OMe	Propargyl	**2b**	48

2.2.2. Determination of SO$_2$ yield by Ion Chromatography

The sulfur dioxide yields from the synthesized *N*-alkyl substituted benzyl sulfonamides were evaluated by ion chromatography, following a reported protocol.[1] Under physiological conditions, SO$_2$ exists in an equilibrium with sulfite and bisulfite ions (Figure 2.1). The ability of thiol activated sulfur dioxide donors to produce SO$_2$ under physiological conditions was evaluated by monitoring sulfite using ion chromatography coupled with conductivity detection. The eluent used was 1 mM NaHCO$_3$/3.2 mM Na$_2$CO$_3$. Sulfite formation from SO$_2$ donors was monitored at 30 min time point. All *N*-alkyl benzyl sulfonamides produced >80 % of SO$_2$ (Table 2.2).
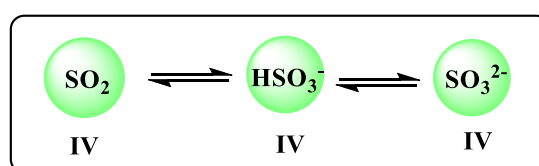
Figure 2.1. The equilibrium between SO$_2$, bisulfite, and sulfite-all the species have common oxidation state (IV)

2.2.3. Calculation of partition coefficient (clogP) values

clogP values are a measure of hydrophilicity/hydrophobicity of a compound and thus, an approximate measure of absorption and permeability of compounds. clogP values were calculated using Chembio ultra software 15.0.

2.2.4. Minimum inhibitory concentration determination (MIC)

The MIC assay is used to determine the inhibitory potential of a compound against bacterial pathogens. Compound **1a** was found to be inactive against Gram-positive Methicillin-sensitive *Staphylococcus aureus* (*MSSA)* bacteria. *MSSA* is pathogenic and commonly causes skin infections. *N*-alkyl substituted analogs of **1a** were found to be good antibacterial agents against *MSSA* (Table 2.2). Substitution of sulfonamido hydrogen (NH) from **1a** by an alkyl group significantly improved the antibacterial property of **1a** without significantly affecting the SO_2 yield and clogP value. Therefore, the antibacterial data we obtained for these substituted SO_2 donors of **1a** (Table 2.2) encouraged us to synthesize a new library of SO_2 donors for an understanding of the structure-activity relationship.

Table 2.2. Compounds with SO_2 yield, clogP, and antimicrobial activity

Entry	Compd	% SO_2	clogP	MIC (µg/mL) *MSSA*
1	**1a**	100	2.86	>16
2	**1b**	100	2.41	8
3	**1c**	100	3.01	4
4	**1d**	87	2.19	16
5	**2b**	84	2.78	8

MIC Values were provided by Vitas pharma, Hyderabad

2.2.1.2. Synthesis of aniline-DNs compounds

In order to understand the structure-activity relationship, a library of aniline-DNs analogs was synthesized. When these SO_2 donors were subjected to SO_2 analysis, **3d**, **4a,** and **5a** were found to be efficient donors of SO_2 (Table 2.3). These compounds were tested for antibacterial activity. We found 2-OMe aniline-DNs (**4a**, 8µg/mL) and 3-OMe aniline-DNs (**5a**, 16 µg/mL) to be good antibacterial agents against *MSSA*. Hence, based on their SO_2 yield and antibacterial activity, we proceeded to synthesize further *N*-alkyl substituted analogs of **4a** and **5a** (Table 2.3).

Table 2.3. Synthesis of DNs analogs of aniline

Entry	R	Compd	% Yield	% SO$_2$	clogP	MIC (µg/mL) *MSSA*
1	4-CN	**3b**	35	5	2.28	>16
2	4-F	**3c**	58	55	2.92	16
3	4-OMe	**3d**	52	80	2.69	>16
4	2-OMe	**4a**	45	86	2.69	8
5	3-OMe	**5a**	70	76	2.69	16

MIC Values were provided by Vitas pharma, Hyderabad

2.2.1.3. Synthesis of *N*-alkyl substituted analogs of 4a and 5a

N-alkyl substituted analogs
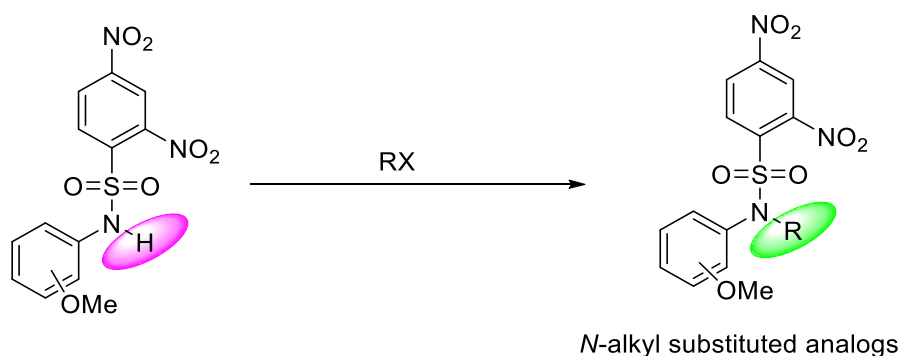
Figure 2.2. Proposed synthesis of *N*-alkyl Substituted aniline-DNs analogs

N-alkyl substitution increased the activity of **1a** significantly. Therefore, we synthesized a library of *N*-alkyl substituted analogs of **4a** and **5a** (Table 2.4) in a good to moderate yield. All the compounds, when subjected to SO$_2$ analysis, gave a good SO$_2$ yield. On alkyl substitution, we found several potent compounds against *MSSA*. Although all the synthesized compounds (Table 2.4) produced SO$_2$ in a good yield, compounds with clogP < 3 have shown good antibacterial activity as well. We found the *N*-propargyl substituted derivatives to have very good inhibitory potency (Table 2.2 **1c, 2b** and Table 2.4, **4g**, **5e**) among all the tested compounds. Therefore, our efforts served the purpose of making several compounds with structural modification, in order to study structure-activity relationship. Along with sulfur

dioxide, propargyl as *N*-alkyl substituent played an important role as an antibacterial agent in our screening against *MSSA*.

Table 2.4. Synthesis *N*-alkyl substituted analogs of **4a** and **5a**
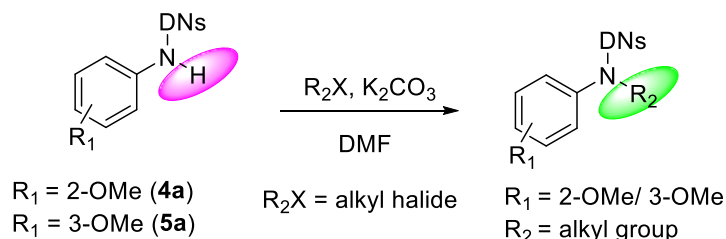
Entry	R	R_2	Compd	% Yield	% SO_2	clogP	MIC (μg/mL) *MSSA*
1	2-OMe	Me	**4b**	92	77	2.05	16
2	2-OMe	Et	**4c**	79	86	2.58	8
3	2-OMe	^{n}Pr	**4d**	83	quant	3.11	>32
4	2-OMe	^{n}Bu	**4e**	80	quant	3.64	>32
5	2-OMe	Allyl	**4f**	76	83	2.83	8
6	2-OMe	Propargyl	**4g**	90	91	2.47	4
7	2-OMe	Bn	**4h**	76	96	3.82	>32
8	3-OMe	Me	**5b**	81	97	2.12	8
9	3-OMe	Et	**5c**	50	98	2.65	8
10	3-OMe	Allyl	**5d**	76	99	2.90	8
11	3-OMe	Propargyl	**5e**	83	89	2.54	4

MIC Values were provided by Vitas pharma, Hyderabad

2.2.1.4. Synthesis of *N*-alkyl substituted analogs of propargyl DNs

N-propargyl substituted SO_2 donors in the previous series showed enhanced antibacterial activity (Table 2.2 **1c, 2b** and Table 2.4, **4g**, **5e**). Therefore, we synthesized *N*-alkyl substituted analogs of propargyl DNs (Table 2.5, **8a-8c**). When these donors were analyzed for SO_2, they produced > 95 % sulfur dioxide. Since the antibacterial property of several SO_2 donors was very good, therefore, they were further tested for broad-spectrum antibacterial activity.

Table 2.5. Synthesis DNs analogs of propargyl

RX = Alkyl halide
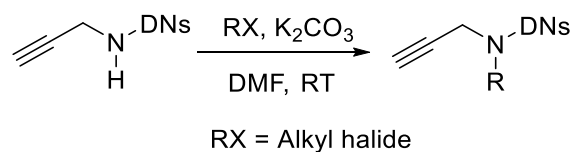
Entry	R	Compd	% Yield	% SO_2	clogP	MIC (µg/mL) MSSA
1	Me	**8a**	64	quant	1.24	8
2	Et	**8b**	85	97	1.77	16
3	3-OMeBn	**8c**	78	95	2.30	16

MIC values were provided by Vitas pharma, Hyderabad

2.2.5. Broad-spectrum antibacterial activity

In the quest for lead optimization, several SO_2 donors were identified as good *MSSA* inhibitors. Next, these compounds were tested for their broad-spectrum antibacterial activity. Potent sulfur dioxide donors found in the previous study were screened against the resistant strain of *MSSA, i.e., MRSA (Methicillin-resistant Staphylococcus aureus)*, Gram-negative *Escherichia coli* (*E. coli*) bacteria and Gram-positive *Enterococcus faecalis* (*E. faecalis*) bacteria. Majority of the strains of *E. coli* are harmless. Some of them cause diarrhea, urinary tract infections, pneumonia, and other infections. *E. faecalis* is a *Streptococcus* bacterium and causes several life-threatening infections in humans. Majority of our SO_2 donors were found to be active against *MRSA* and *E. faecalis* (Table 2.6), while none of them were found to be active against *E. coli* (Table 2.6). All *N*-alkyl substituted compounds obtained from **5a** were found to be significant inhibitors of *MRSA* and *E. faecalis*. **5e** was found to be one of the most potent compounds among the SO_2 donors, screened for broad-spectrum activity.

Table 2.6. Broad-spectrum antibacterial activity of the SO$_2$ donors

Entry	Compd	MIC^a (µg/mL) MRSA	MIC^b (µg/mL) E. faecalis	MIC^c (µg/mL) E. coli
1	**1c**	4	16	>32
2	**1d**	8	32	>32
3	**2b**	8	16	>32
4	**4a**	8	16	>32
5	**4b**	16	16	>32
6	**4c**	8	>32	>32
7	**4d**	>32	>32	>32
8	**4e**	>32	>32	>32
9	**4f**	4	>32	>32
10	**4g**	8	8	>32
11	**4h**	>32	>32	>32
12	**5a**	32	>32	>32
13	**5b**	4	8	>32
14	**5c**	8	8	>32
15	**5d**	8	16	>32
16	**5e**	4	8	>32
17	**8a**	8	>32	>32
18	**8b**	16	>32	>32
19	Linezolid	1	2	-
20	Ciprofloxacin	0.25	-	≤ 0.00075
21	Vancomycin	2	-	-
22	Tobramycin	>32	-	-

MIC values were provided by Vitas pharma, Hyderabad

2.2.6. The activity of lead compound 5e against clinically isolated resistant strains

Compound **5e** showed very good antibacterial activity against Gram-positive pathogens. Therefore, the compound **5e** was tested to inhibit the growth of various strains of *MRSA*, which were patient-derived. We found excellent inhibitory potency with several strains being

inhibited at concentrations of 2 µg/mL (Table 2.7). For example, the MIC of **5e** against *MRSA* 7386, which was resistant to meropenem and tobramycin, was 2 µg/mL and was comparable to commercially used clinical agents like vancomycin, ciprofloxacin, and linezolid. These drugs are among the very few drugs available to treat the infections caused by these bacteria and are, therefore, termed 'drugs of last resort'.

Table 2.7. MIC (µg/mL) of **5e** determined against patient-derived *MRSA* strains

Comp	MRSA 7419	B19506	MRSA K-1	MRSA 7425	MRSA 7386
5e	4	2	4	2	2
Vancomycin	1	1	1	1	2
Linezolid	2	4	2	4	2
Ciprofoxacin	>4	32	0.5	>4	>4
Meropenem	16	1	0.5	4	>32
Tobramycin	>32	>32	8	1	>32

MIC values were provided by Vitas Pharma, Hyderabad

2.2.7. Cell permeability of 5e and depletion

Our hypothesis was that the antibacterial activity of SO_2 prodrugs is mediated by the compound's entry into cells, followed by thiol attack at the 2,4-dinitrosulfonyl group to generate SO_2 intracellularly. Therefore, intracellular generation of oxidative reactive sulfur species occurs, which can possibly induce oxidative stress and perturb redox equilibrium. In addition, thiols are primary responders to oxidative stress and are converted to disulfides. Depletion of free thiols might, thus, occur as a response to enhanced oxidative species as well. A monobromobimane (mBBr) protocol was used to assess levels of free thiols within cells. Here, the weakly fluorescent mBBr reacts with thiols and is converted to a highly fluorescent adduct.[2,3] Hence, increased fluorescence response in this assay is an indicator of free thiol levels inside cells and vice versa. *MRSA* cells were treated with increasing concentration of compound **5e** and we found a decrease in fluorescence in a dose-dependent manner, compared to the untreated control indicating that **5e** is capable of depleting thiols in bacteria (Figure 2.3).
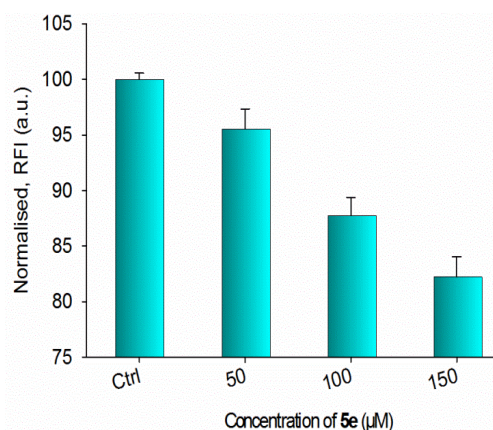
Figure 2.3. Intracellular thiol depletion in *S. aureus* upon dose-dependent treatment of **5e**. Fluorescence measured after 60 min of incubation at 37 °C using monobromobimane (mBBr) based fluorescence assay

2.2.8 Estimation of intracellular oxidative species using DCFH2-DA assay

Thiols attack at 2,4-dinitrosulfonyl group and SO_2 is generated intracellularly. SO_2 is known to generate oxidative species which results in biomacromolecular damage.[4–7] We tested the ability of **5e** to produce oxidative species intracellularly, using 7-dichlorodihydrofluorescein-diacetate (DCFH2-DA) assay.[8,9] We found increased fluorescence levels intracellularly in *S. aureus* upon incubation with **5e** (Figure 2.4).
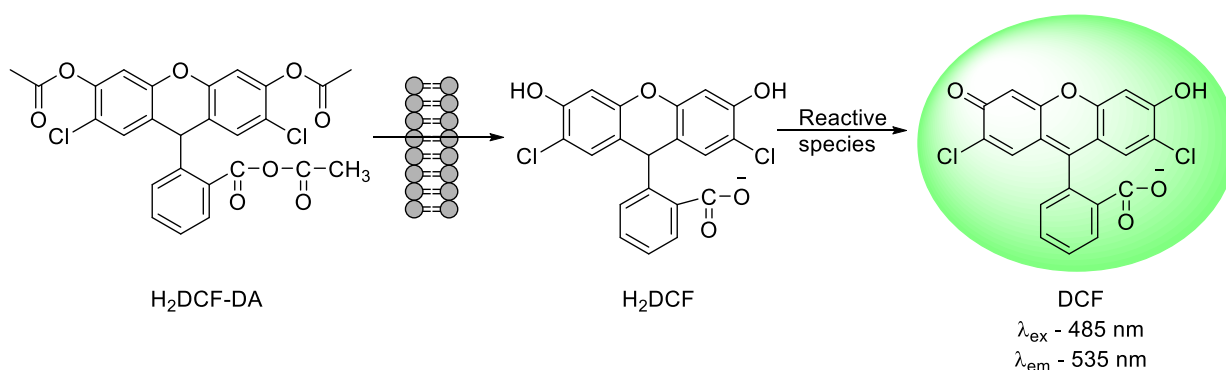
Figure 2.4. Oxidation of non-fluorescent H2DCF-DA by reactive species to a fluorescent dye, DCF

This result is indicative of production of oxidative species and perhaps, induction of oxidative stress is a mechanism of action.[9–14] The obtained result was consistent with the thiol depletion assay described previously.
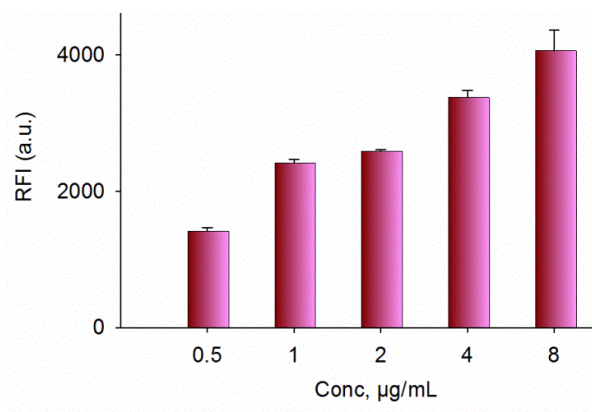
Figure 2.5. The dichlorofluorescein-diacetate (DCFH$_2$-DA) fluorescence assay was used to estimate the levels of oxidative species generated intracellularly in *S. aureus* upon exposure to **5e**

2.2.9. Click reaction with cell lysate

We set about determining the cell permeability of **5e**, as we have expected the penetration of **5e** into a bacterial cell. Therefore, we hypothesized **5e** to either to get activated by thiol attack and to generate SO$_2$ and amine or to remain unchanged.
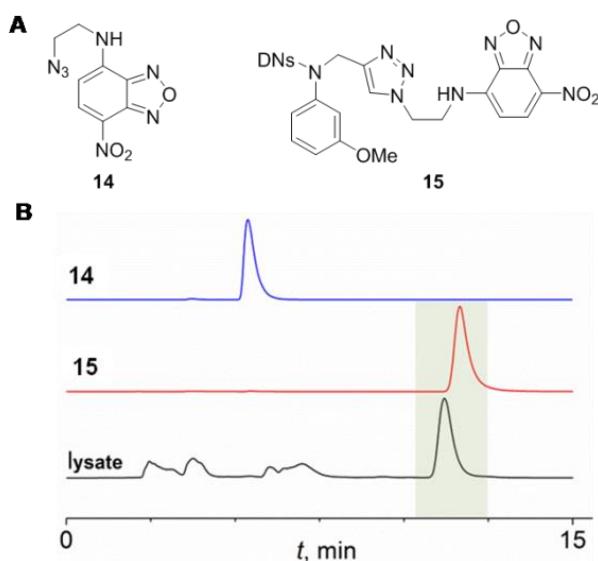
Figure 2.6. (a) Compounds **14** and **15**. (b) high-performance liquid chromatography (HPLC) traces recorded for **14** and **15**. *MRSA* cells were incubated with **5e** (200 µM) for 3 h. The bacterial cells were centrifuged and the resulting pellet was washed twice with PBS (pH 7.4, 50 mM)

In the case of thiol attack on **5e**, propargylamine should be generated and needs to be detected. However, it is difficult to monitor by HPLC. In order to do that, a fluorescent azide

was synthesized (**14**) to exploit the presence of propargyl group in **5e**. HPLC is utilized principally to have the advantage of characterizing decomposed and undecomposed products more accurately. A copper-catalyzed 1,3-dipolar cycloaddition reaction or "click" reaction was performed with cell lysate of *MRSA* (prior to that *MRSA* whole cells were pretreated with **5e**). This click reaction was monitored by HPLC with a fluorescence detector; thus, we evaluated evidence for the permeability **5e** in *MRSA* (Figure 2.6). In this experiment, we ideally expect to observe the propargylamine click adduct with the fluorescent azide, which, we did not find. Nevertheless, the results of this experiment together with the previous experiments supported that **5e** was able to permeate the cells.

2.2.10. Cytotoxicity assay

The ability of **5e** to inhibit A549 lung carcinoma cells was tested and the GI_{50} was found to be 27 µM. Selectivity index (GI_{50}/MIC) of **5e** was found to be 5.2, which was encouraging.

Lead compound **5e** showed similar or better antibacterial activity compared to commercially used antibiotics, and hence, we proposed to enhance the SO_2 payload in order to further increase efficacy.

2.2.11. The hypothesis for the synthesis of double SO₂ donors

Sulfur dioxide donors reported in the previous study showed significant antibacterial activity. To take this further, we explored the possibility of enhancement in the efficacy of existing thiol activated sulfur dioxide donors to bring about an increment in the SO_2 payload.
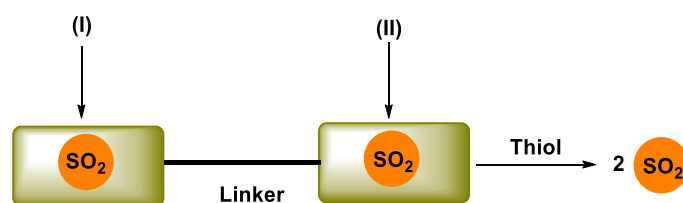
Figure 2.7. Proposed design for thiol activated double SO_2 donor

2.2.1.6. Synthesis of double sulfur dioxide donors using Mitsunobu reaction

In order to synthesize SO_2 donors with increased SO_2 payload, we designed several synthetic routes. However, we succeeded in synthesizing the molecules for an enhanced payload of SO_2 by the Mitsunobu reaction method. The Mitsunobu reaction was successfully conducted on SO_2 donor **1d** with several other SO_2 donor nucleophiles in order to synthesize double SO_2 donors (**9a-9i**, Table 2.8). We faced challenges in purification with this synthetic scheme, due

to the co-elution of the reduced azodicarboxylate along with the desired product through silica gel column chromatography. Therefore, further purification resulted in a diminished synthetic yield for these compounds (Table 2.8), which could be improved by using a suitable purification protocol. Also, attempts to purify double SO_2 donor of propargyl DNs were unsuccessful. Compounds **12a**-**12c** which contained a single nitro group on the aryl sulfonamide ring were synthesized from benzylamine.

Table 2.8. Synthesis of double SO_2 donors
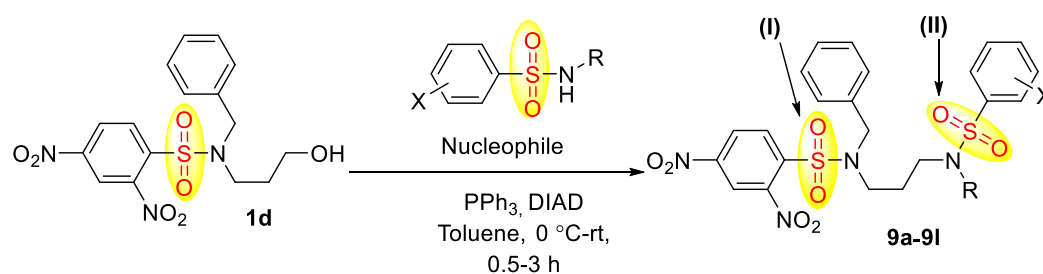
Entry	R	X	Nucleophile	Product	% Yield
1	PhCH$_2$	2,4-dinitro	**1a**	**9a**	15
2	2-OMePhCH$_2$	2,4-dinitro	**10a**	**9b**	14
3	4-OMePhCH$_2$	2,4-dinitro	**2a**	**9c**	15
4	2,4-DimethoxyPhCH$_2$	2,4-dinitro	**11a**	**9d**	19
5	Ph	2,4-dinitro	**3a**	**9e**	17
6	2-FPh	2,4-dinitro	**3e**	**9f**	14
7	2-OMePh	2,4-dinitro	**4a**	**9g**	14
8	3-OMePh	2,4-dinitro	**5a**	**9h**	15
9	4-OMePh	2,4-dinitro	**3d**	**9i**	10
10	PhCH$_2$	2-nitro	**12a**	**9j**	29
11	PhCH$_2$	3-nitro	**12b**	**9k**	36
12	PhCH$_2$	4-nitro	**12c**	**9l**	20

Upon synthesis of double SO_2 donors, we tested their ability of two-fold SO_2 generation from a single molecule and also, their antibacterial property.

Next, **12a-12c** were used as nucleophiles in the Mitsunobu reaction with **1d** to give **9j-9l** in moderate yields. When these double SO_2 donors were subjected to SO_2 analysis among the bis(2,4-dinitrophenylsulfonamides), **9a-9i** gave nearly two moles of SO_2 per mole of compound (Table 2.8, entries 1-9). As expected we found that **9j-9l** to give one mole of SO_2 per mole of compound (Table 2.8, entries 10-12), consistent with previous observations that both nitro groups were necessary for decomposition.[1]

2.2.12 Antibacterial activity of bis(SO₂ generator) against *MSSA*

We validated our hypothesis of two moles of SO_2 generation per molecule from the thiol activated SO_2 donors (Table 2.9, **9a-9i**). Next, these double SO_2 donors **9a-9i** and compounds **9j-9l** were tested for their antibacterial activity against *MSSA*.

Table 2.9. Antibacterial activity of double SO_2 donors

Entry	R	% SO₂ Yield	clogP	MIC (µg/mL), *MSSA*
1	**9a**	77	5.41	>16
2	**9b**	100	5.33	>32
3	**9c**	Quant	5.33	>32
4	**9d**	99	5.06	>16
5	**9e**	87	4.96	>16
6	**9f**	98	5.01	>32
7	**9g**	100	5.08	>32
8	**9h**	101	5.08	>32
9	**9i**	101	5.42	>32
10	**9j**	45	5.67	>32
11	**9k**	51	5.85	>32
12	**9l**	47	5.85	>16
13	Vancomycin			0.5-1

MIC values were provided by Vitas pharma, Hyderabad

They were all found to be inactive. Although some of these molecules **9a-9i** produce two moles of SO_2 per molecule, their clogP values were relatively large (approximate logP $\geq$ 5), which indicates that cell permeability would have been a major factor for these compounds to get into the bacterial cell. Thus, ineffectiveness as an antibacterial agent can be attributed to their lack of cell permeability. Therefore, an increase in the payload of SO_2 increased the hydrophobicity, which possibly hampered the prospects of the SO_2 donor to be more efficacious.

2.2.13 Thiol depletion Assay

In order to check permeability of double SO_2 donors, a thiol depletion assay was performed as earlier. Double SO_2 donor **9d** and compound **8b** with poor inhibitory activity against *MRSA* showed an enhanced fluorescence signal, indicating their diminished capacity to deplete thiols, whereas **5e** depleted thiol significantly (Figure 2.8). In this experiment, we used a known thiol-reactive compound, *N*-ethylmaleimide (NEM), as the positive control and we found a diminished fluorescence that is consistent with decreased thiol levels. These data indicate that the capacity of the compound to permeate cells to deplete free thiols played a significant role in the observed inhibitory potency.
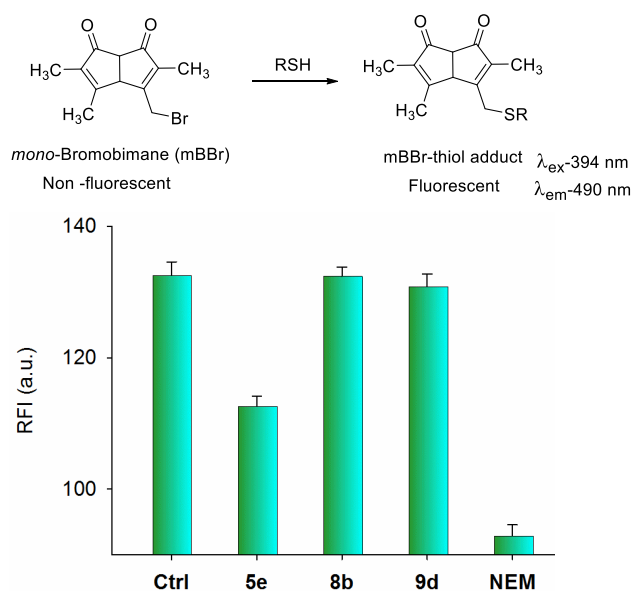
Figure 2.8. Intracellular thiol depletion in *S. aureus* upon treatment with the compounds measured after 30 min of incubation at 37 °C using monobromobimane (mBBr) based fluorescence assay

2.3 Summary

In this chapter, we have designed and systematically synthesized structurally modified *N*-alkyl substituted analogs of thiol activated prodrugs of sulfur dioxide. These SO$_2$ donors were found to be potent inhibitors of *MSSA*. Also, these donors were found to be excellent inhibitors of infectious bacteria, such as *MRSA* and *E. faecalis*. Antibacterial activity of **5e** was found to be comparable with clinically used antibiotics against patient-derived strains of *MRSA*. The various assays that we have conducted on sulfur dioxide donors indicate that cell permeability plays a major role and thus, determines the efficacy of compounds. Therefore, the double SO$_2$ donors with increased hydrophobicity were found to be inactive. Our results are consistent with previously published reports that *S. aureus* is sensitive to redox active species, such as reactive oxygen species and reactive nitrogen species.[15–17] We were the first to report that *MRSA* is sensitive to sulfur dioxide, a reactive sulfur species (RSS).

2.4. Experimental section

2.4.1. MIC

To determine MIC, the microbroth dilution technique, as recommended by the National Committee for Clinical Laboratory Standards (CLSI), was used. For this, a fixed bacterial inoculum (5×10^5 CFU/mL) was added into a series of test wells in a microtitre plate that contained various concentrations of the compound under test. Following a period of incubation (37 °C, 18-20 h), the wells were examined for growth. The lowest concentration of antibiotic that inhibited the growth of the organism, as detected visually, was designated as the MIC.

2.4.2. Thiol depletion assay

10 mM stock solutions of compounds **5e**, *NEM*, **8b**, **9d**, and mBBr were independently prepared in Dimethyl sulfoxide (DMSO). An overnight grown culture of *MRSA* in cation adjusted Mueller Hinton broth (CA-MHB) was harvested by centrifugation, washed twice with PBS and re-suspended in CA-MHB. *MRSA* culture (1 mL, OD$_{600}$ 1) was incubated at a different concentration of **5e** in the dose-dependent assay. Similarly, in the cell permeability assay for double SO$_2$ donors, compound **5e**, *N*-ethylmaleimide and other SO$_2$ donors (**8b**, **9d**) were incubated for 30 min, then, centrifuged at 10,000 rpm for 5 min. The obtained

bacterial pellet was washed twice with PBS and re-suspended in fresh 1 mL PBS (pH 8, 25 mM). mBBR (100 µM) was added to the compound-treated bacterial solution, incubated for 60/75 min and depletion of cellular thiols was estimated by measuring fluorescence emission at 490 nm (λ_{ex} 394 nm) using a Thermo Varioskan microwell plate reader. An untreated bacterial control was included as a negative control. The experiment was carried out twice in four replicates each.[2,3,18]

2.4.3. Estimation of intracellular oxidative species using DCFH2-DA.

An overnight culture of *MSSA* 29213 was diluted 1:100 with fresh Cation Adjusted Mueller Hinton broth (CA-MHB) and allowed to grow until an OD_{625} of 0.3 was reached. This culture was split into multiple tubes of 2 mL each. To each tube, 20 µL of DMSO stocks of **5e** was added, such that a series of final concentrations ranging from 0.5 µg/mL to 8 µg/mL was obtained in triplicate. The culture tubes with compounds were incubated for 1 h and normalized to an OD_{625} of 1.0, followed by centrifugation of 1 mL of the normalized culture, washing twice with PBS and re-suspending in 500 µL of PBS. This was further diluted 1:10 to 135µL of the diluted culture; 15 µL of 100 µM dichloro-dihydro-fluorescein diacetate (DCFH2-DA) was added per well of a 96-well black plate. The plate was incubated for 2 h at 37 °C. Fluorescence was measured at an excitation wavelength of 485 nm and an emission wavelength of 535 nm. Fluorescence intensity of treated versus untreated cells was compared.

2.4.4. Click reaction with cell lysate.

MRSA 33591 was grown overnight in CA-MHB. These cells were centrifuged for 10 min at 4,000 rpm, 4 °C. The resulting bacterial pellet was washed twice with PBS and re-suspended in fresh PBS. *MRSA* culture (1 mL, OD_{600} of 0.5) was incubated with **5e** (200 µM) for 3 h. Then, it was centrifuged at 10,000 rpm at 4 °C for 10 min and washed twice with PBS to remove excess compound. Cells were lysed by re-suspension of bacterial pellet in PBS (25 mM, pH 7.4) and THF (1:1, v/v, to a final volume of 1 mL). A 10 mM stock solution of **14** and tris[(1-benzyl-1H-1,2,3-triazol-4-yl) methyl]amine (TBTA) were prepared in DMSO. 100 mM stock solutions of $CuSO_4.5H_2O$ and sodium ascorbate were prepared in water. The reaction mixture with a final concentration of **14** (100 µM), TBTA (200 µM), sodium ascorbate (1 mM) and $CuSO_4.5H_2O$ (1 mM) was done in 1 mL of cell lysate and was incubated at 37 °C for 30 min. The reaction mixture was centrifuged, filtered (0.22 µm) and

injected (50 µL) in an Agilent HPLC attached with a fluorescence detector. Fluorescence emission was measured at 535 nm (λ_{ex} 455 nm). The column used was Zorbax SB C-18 reversed phase column (250 mm × 4.6 mm, 5 µm), the mobile phase was isocratic 50% acetonitrile: dI water at flow rate of 1 mL/min.

2.4.5. Cytotoxicity Assay[19]

To test the effect of **5e** on the growth of mammalian cells, a cytotoxicity assay was performed as per published protocols. In brief, 10,000 A549 (lung cell carcinoma) cells were seeded in a 96-well plate and grown for 24 h at 37 °C in a humidified atmosphere of 5% CO_2 and 95% air in F12K medium supplemented with 10% heat-inactivated fetal bovine serum, 1.5 g sodium bicarbonate/L, 100 µg/mL of penicillin and 10 µg/mL of streptomycin. The next day, cells were washed with PBS and different concentrations of **5e** were added in serum-free media in triplicate. Following 72 h of incubation, MTT (3-(4, 5-Dimethyl-2-thiazolyl)-2, 5-diphenyl-2H-tetrazolium bromide) was added to a final concentration of 1 mg/mL for 5 h. At the end of the incubation period, the media were removed by gently inverting the plate. DMSO was added to the wells to solubilize the formazan crystals and absorbance was read at 595 nm in a plate reader. The absorbance of treated vs. untreated cells was compared. % survival vs. concentration of **5e** was plotted to determine the GI_{50} concentration.

2.4.6. Synthetic procedures

Compounds **1a**[20], **1b**[20], **2a**[20], **3a**[20,] **3b**[1], **3c**[1], **3d**[20], **4a**[20], **12a**[20], **12b**[21], **12c**[20] and **14**[22] were prepared following reported protocols and the spectral data that we obtained were consistent with reported values. Unless otherwise specified, the following general procedures were used for the synthesis of intermediates and products presented in this study.

2.4.6.1. General Procedure for the Synthesis of 2,4-Dinitrobenzenesulfonamides (A).[1,20]

To a solution of 2,4-Dinitrobenzenesulfonyl chloride (DNsCl) in DCM (25-50 mL), the amine (1.2 eq), and pyridine (1.2-2 eq) were added sequentially at −78 °C and was stirred for 0.5 – 2 h at 0 °C. To the reaction mixture, dI water (50-100 mL) was added and was extracted with DCM (2 x 25 mL). The organic layers were collected and washed with brine (50-

100mL), dried over anhydrous Na₂SO₄, filtered and were concentrated under reduced pressure. The residue was purified by silica gel column using pet ether/EtOAc or DCM/Methanol as the eluent.

2.4.6.2. General Procedure for the synthesis of N- alkyl substituted 2,4-dinitrobenzenesulfonamides (B).[1]

To a solution of 2, 4-dinitrobenzenesulfonamide in DMF (5-15 mL), K₂CO₃ (3-4 eq) was added. A brown solution was formed. The reaction mixture was treated with the corresponding alkyl halide (3-6 eq) and was stirred at rt for 0.5-6 h. To the reaction mixture dI water (50-100mL) was added and was extracted with DCM (2 x 30 mL) or EtOAc (2 x 30 mL). The combined organic fraction was dried over anhydrous Na₂SO₄, filtered and was concentrated under reduced pressure. The crude product was purified by silica gel chromatography using a mixture of pet ether/ EtOAc or DCM/Methanol as the eluent.

2.4.6.3. General Procedure for Mitsunobu Reaction (C)[23,24]

The alcohol (**1d**) and the corresponding nucleophile 1-2 eq (synthesized by reaction of a primary amine with DNsCl as given in general procedure) were dissolved in toluene (20 mL) at 0 °C, treated with Triphenylphosphine (3-6 eq) and Diisopropyl azodicarboxylate (DIAD) (3-6 eq) and stirred for 0.5-3 h at rt. To the reaction mixture, dI water (50-100mL) was added and was extracted with EtOAc (2 x 30 mL). The organic layers were collected, dried over Na₂SO₄, filtered and were concentrated under reduced pressure. The crude product was purified by a silica gel column using mixtures of pet ether/ EtOAc. Due to the co-elution of reduced DIAD along with the desired product, the crude was further washed with pet ether, *n*-pentane, and diethyl ether. This last step in the purification contributes to a diminished yield of the desired product which can be optimized using a suitable purification protocol.

2.4.6.4 Experimental data

N-benzyl-2,4-dinitro-*N*-(prop-2-yn-1-yl)benzenesulfonamide (1c).
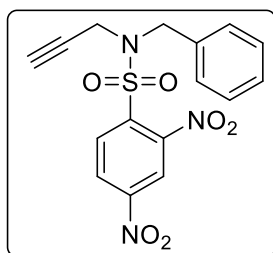
Synthesized by following general procedure B: Starting from **1a** (150 mg, 0.52 mmol), K₂CO₃ (215 mg, 1.56 mmol) and propargyl bromide (444 mg, 2.6 mmol), **1c** was isolated as a pale yellow solid (125 mg, 63%): mp 126-127 °C; ^{1}H NMR (DMSO-d₆): δ 9.02 (d, *J* = 2.3 Hz, 1H), 8.61 (dd, *J* = 8.7, 2.3 Hz, 1H), 8.42 (d, *J* = 8.7 Hz, 1H), 7.41-7.30 (m, 5H), 4.56 (s, 2H), 4.03 (d, *J* = 2.3 Hz, 2H), 3.26 (t, *J* = 2.4 Hz, 1H); ^{13}C NMR (100

MHz, DMSO-d_6): δ 150.7, 148.2, 136.3, 135.0, 132.8, 129.3, 128.8, 127.4, 120.6, 120.5, 79.9, 76.7, 51.0, 36.9; FTIR (ν_{max}, cm^{-1}): 3279, 3082, 2121, 1608, 1561, 1531, 1364; HRMS (ESI) calcd for [C$_{16}$H$_{13}$N$_3$O$_6$S + H]$^+$: 376.0603, found: 376.0620.

N-benzyl-*N*-(3-hydroxypropyl)-2,4-dinitrobenzenesulfonamide (1d).
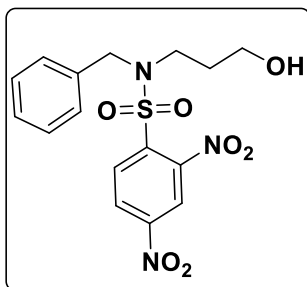
Synthesized by following general procedure B: Starting from **1e** (2.5 g, 8.2 mmol), K$_2$CO$_3$ (3.4 g, 24 mmol) and benzyl bromide (2.1 g, 12.2 mmol), **1d** was isolated as a pale yellow solid (1.2 g, 50%): mp 108-110 °C; ^{1}H NMR (DMSO-d_6): δ 8.99 (d, *J* = 2.2 Hz, 1H), 8.55 (dd, *J* = 8.7, 2.2 Hz, 1H), 8.32 (d, *J* = 8.7 Hz, 1H), 7.38-7.29 (m, 5H), 4.54 (s, 2H), 4.40 (t, *J* = 4.9 Hz, 1H), 3.29 (t, *J* = 7.5 Hz, 2H), 3.23 (q, *J* = 5.2 Hz, 2H), 1.48 (quintet, *J* = 6.1 Hz, 2H); ^{13}C NMR (100 MHz, DMSO-d_6): δ 150.5, 147.9, 137.4, 136.5, 132.3, 129.2, 128.45, 128.37, 127.5, 120.6, 58.3, 51.4, 45.7, 31.2; FTIR (ν_{max}, cm^{-1}): 3577, 3103, 1543, 1350; HRMS (ESI) calcd for C$_{16}$H$_{17}$N$_3$O$_7$S [M + Na]$^+$: 418.0684, found: 418.069.

N-(3-hydroxypropyl)-2,4-dinitrobenzenesulfonamide (1e).
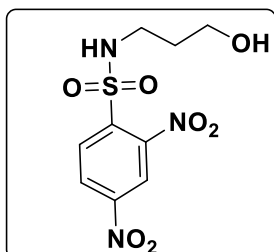
Synthesized by following general procedure A: Starting from DNsCl (12 g, 45 mmol), 3-Amino-propanol (5 g, 67 mmol), product was isolated as yellow solid (3 g, 21% yield): mp 126-128 °C; ^{1}H NMR (DMSO-d_6): δ 8.89 (d, *J* = 2.2 Hz, 1H), 8.65 (dd, *J* = 8.7, 2.2 Hz, 1H), 8.42 (t, *J* = 5.5 Hz, 1H), 8.23 (d, *J* = 8.7 Hz, 1H), 4.46 (t, *J* = 5.0 Hz, 1H), 3.37 (q, *J* = 5.1 Hz, 2H), 2.99 (q, *J* = 6.5 Hz, 2H), 1.57 (quintet, *J* = 6.8 Hz, 2H)); FTIR (ν_{max}, cm^{-1}): 3342, 3117, 1605, 1556, 1535, 1462, 1413, 1358, 1254, 1179, 1099; ^{13}C NMR(100 MHz, DMSO-d_6): δ 150.1, 148.2, 138.2, 131.7, 127.8, 120.6, 58.3, 40.7, 32.8; MALDI-TOF C$_9$H$_{11}$N$_3$O$_7$S [M + Na]$^+$: 328.0215. Found: 328.0922.

***N*-(4-methoxybenzyl)-2,4-dinitro-*N*-(prop-2-yn-yl)benzenesulfonamide (2b).**
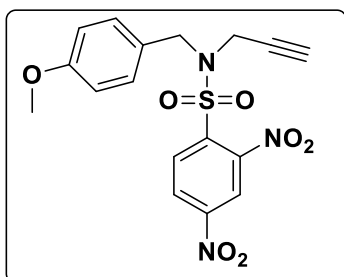
Synthesized by following general procedure B: Starting from **2a** (300 mg, 0.95 mmol), K$_2$CO$_3$ (339 mg, 2.85 mmol) and propargyl bromide (339 mg, 2.85 mmol), **2b** was isolated as a pale yellow solid (250 mg, 75%): mp 115-116 °C; ^{1}H NMR (CDCl$_3$): δ 8.49-8.47 (m, 2H), 8.26 (d, *J* = 8.6, 1H), 7.27-7.25

(m, 2H), 6.86 (d, J = 1.8 Hz, 2H), 4.55 (s, 2H), 4.04 (d, J = 2.4 Hz, 2H), 3.80 (s, 3H), 2.21 (t, J = 2.4 Hz, 1H); ^{13}C NMR(100 MHz, DMSO-d$_6$): δ 159.8, 150.6, 148.1, 136.3, 132.7, 130.3, 127.3, 126.5, 120.4, 114.7, 77.7, 76.7, 55.6, 50.4, 36.5; FTIR (ν_{max}, cm^{-1}): 3269, 3105, 1612, 1550, 1508, 1367, 1170; HRMS (ESI) calcd for C$_{17}$H$_{15}$N$_3$O$_7$S [M + H]$^+$: 406.0709, found: 406.0699.

N-(2-fluorophenyl)-2,4-dinitrobenzenesulfonamide (3e).
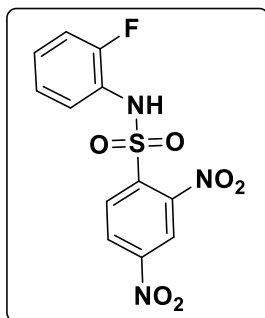
Synthesized by following general procedure A: Starting from DNsCl (400 mg, 1.5 mmol), 2-Fluoro aniline (250 mg, 2.25 mmol) **3e** was isolated as white solid (246 mg, 48% yield),: mp 165-167 °C; ^{1}H NMR (CDCl$_3$): δ 8.73 (d, J = 2.2 Hz, 1H), 8.42 (dd, J = 8.6, 2.2 Hz, 1H), 8.06 (d, J = 8.6 Hz, 1H), 7.76-7.61 (m, 2H), 7.25-7.18 (m, 2H), 7.01 (S, 1H); ^{13}C NMR(100 MHz, CDCl$_3$): δ 156.8, 154.3, 150.2, 138.1, 132.9, 128.8, 127.0, 125.2, 122.5, 121.18, 116.1, 115.9; FTIR (ν_{max}, cm^{-1}): 3342, 3117, 1556, 1462, 1413, 1358, 1254, 1179, 1095; HRMS (ESI) calcd for C$_{12}$H$_8$FN$_3$O$_6$S [M + Na]$^+$: 364.0015, found: 364.0019.

### *N*-(2-methoxyphenyl)-*N*-methyl-2,4-dinitrobenzenesulfonamide (4b).
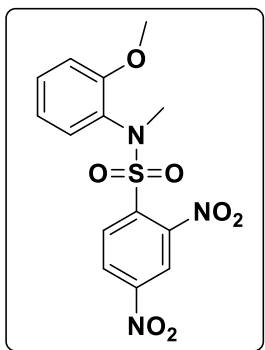
Synthesized by following general procedure B: Starting from **4a** (200 mg, 0.56 mmol), K$_2$CO$_3$ (312 mg, 2.26 mmol) and methyl iodide (401 mg, 2.83 mmol), **4b** was isolated as a white solid (190 mg, 92%): mp 160-162 °C; ^{1}H NMR (CDCl$_3$): δ 8.43 (d, J = 2.2 Hz, 1H), 8.32 (dd, J = 8.7, 2.2 Hz, 1H), 7.84 (d, J = 8.7 Hz, 1H), 7.37 (m, 2H), 7.00 (m, 1H), 6.83 (d, J = 8.7 Hz, 1H), 3.44 (s, 3H), 3.38 (s, 3H); ^{13}C NMR (100 MHz, CDCl$_3$): δ 156.0, 149.4, 148.0, 138.6, 133.0, 132.1, 130.9, 127.0, 125.1, 121.4, 119.0, 112.0, 55.0, 39.0; FTIR (ν_{max}, cm^{-1}): 3107, 1599, 1557, 1361, 1176, 1026; HRMS (ESI) calcd for C$_{14}$H$_{13}$N$_3$O$_7$S [M + H]$^+$: 368.0552, found: 368.0547.

N-ethyl-*N*-(2-methoxyphenyl)-2,4-dinitrobenzenesulfonamide (4c).
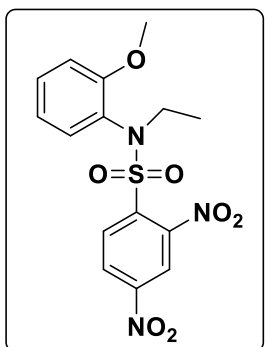
Synthesized by following general procedure B: Starting from **4a** (200 mg, 0.56 mmol), K$_2$CO$_3$ (312 mg, 2.26 mmol) and ethyl bromide (308 mg, 2.83 mmol), **4c** was isolated as a white solid (170 mg, 79%): mp 144-146 °C; ^{1}H NMR (CDCl$_3$): δ 8.42 (d, J = 2.1 Hz, 1H), 8.30 (dd, J

= 8.7, 2.0 Hz, 1H), 7.82 (d, J = 8.7 Hz, 1H), 7.36 (m, 2H), 7.01 (m, 1H), 6.82 (d, J = 8.3 Hz, 1H), 3.81 (br, 2H), 3.40 (s, 3H), 1.12 (t, J = 7.1 Hz, 3H); ^{13}C NMR (100 MHz, CDCl$_3$): δ 156.1, 149.3, 148.0, 139.0, 134.0, 133.0, 130.9, 125.0, 124.2, 121.1, 119.0, 111.9, 55.0, 46.2, 14.6; FTIR (ν_{max}, cm^{-1}): 3102, 1600, 1537, 1367, 1152, 1065; HRMS (ESI) calcd for C$_{15}$H$_{15}$N$_3$O$_7$S [M + H]$^+$: 382.0709, found: 382.0700.

N-(2-methoxyphenyl)-2,4-dinitro-*N*-propylbenzenesulfonamide (4d).
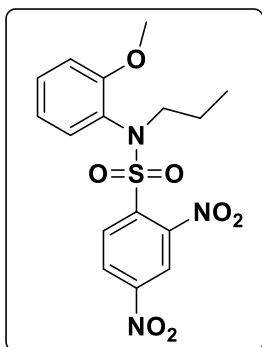
Synthesized by following general procedure B: Starting from **4a** (200 mg, 0.56 mmol), K$_2$CO$_3$ (312 mg, 2.26 mmol) and *n*-propyl iodide (476 mg, 2.83 mmol),.**4d** was isolated as a white solid (184 mg, 83%): mp 118-120 °C; ^{1}H NMR (CDCl$_3$): δ 8.39 (d, J = 2.2 Hz, 1H), 8.26 (dd, J = 8.7, 2.2 Hz, 1H), 7.76 (d, J = 8.7 Hz, 1H), 7.37-7.32 (m, 2H), 6.99 (m, 1H), 6.78 (dd, J = 8.7, 1.1 Hz, 1H), 3.69 (s, 2H), 3.35 (s, 3H), 1.45 (sextet, J = 8.7 Hz, 2H), 0.92 (t, J = 7.4 Hz, 3H); ^{13}C NMR (100 MHz, CDCl$_3$): δ 156.0, 149.2, 147.9, 139.0, 133.9, 133.0, 130.9, 124.9, 124.5, 121.2, 118.9, 111.8, 54.9, 52.7, 22.1, 11.0; FTIR (ν_{max}, cm^{-1}): 3096, 1601, 1556, 1535, 1368, 1180, 1017; HRMS (ESI) calcd for C$_{16}$H$_{17}$N$_3$O$_7$S [M + H]$^+$: 396.0865, found: 396.0868.

N-butyl-*N*-(2-methoxyphenyl)-2,4-dinitrobenzenesulfonamide (4e).
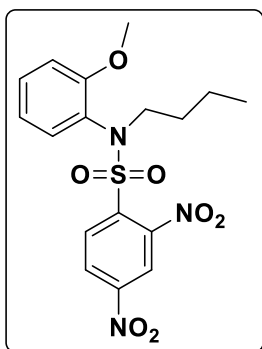
Synthesized by following general procedure B: Starting from **4a** (200 mg, 0.56 mmol), K$_2$CO$_3$ (312 mg, 2.26 mmol) and *n*-butyl bromide (387 mg, 2.83 mmol), **4e** was isolated as a white solid (184 mg, 80%): mp 152-153 °C; ^{1}H NMR (CDCl$_3$): δ 8.41 (d, J = 2.2 Hz, 1H), 8.28 (dd, J = 2.2, 8.7 Hz, 1H), 7.77 (d, J = 8.7 Hz, 1H), 7.39-7.37 (m, 2H), 7.01 (m, 1H), 6.80 (m, 1H), 3.74 (br, 2H), 3.37 (s, 3H), 1.41(m, 4H), 0.89 (t, J = 7.28 Hz, 3H); ^{13}C NMR (100 MHz, CDCl$_3$): δ 156.0, 149.2, 147.9, 138.9, 133.9, 133.0, 130.9, 124.9, 124.5, 121.2, 118.9, 111.8, 54.9, 50.8, 30.9, 19.7, 13.7; FTIR (ν_{max}, cm^{-1}): 3096, 1602, 1557, 1535, 1496, 1370, 1175, 1014; HRMS (ESI) calcd for C$_{17}$H$_{19}$N$_3$O$_7$S [M + H]$^+$: 410.1022, found: 410.1013.

N-allyl-*N*-(2-methoxyphenyl)-2,4-dinitrobenzenesulfonamide (4f).
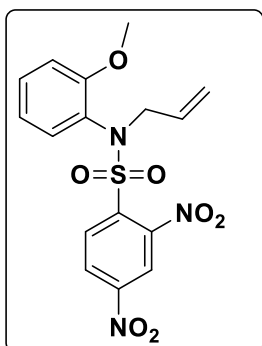
Synthesized by following general procedure B: Starting from **4a** (200 mg, 0.56 mmol), allyl bromide (342 mg, 76% yield), **4f** was isolated as

white solid: mp 144 °C; ^{1}H NMR (CDCl$_3$): δ 8.44 (s, 1H), 8.29 (d, J = 8.7 Hz, 1H), 7.80 (d, J = 8.7 Hz, 1H), 7.37-7.30 (m, 2H), 6.99 (m, J = 7.6 Hz, 1H), 6.80 (d, J = 8.3 Hz, 1H), 5.85-5.75 (m, 1H), 5.09 (s, 1H), 5.06 (d, J = 5.3 Hz, 1H), 4.36 (b, 2H), 3.40 (s, 3H); ^{13}C NMR(100 MHz, CDCl$_3$): 156.0, 149.3, 147.9, 138.8, 134.0, 132.8, 131.1, 130.9, 125.0, 124.4, 121.1, 119.4, 119.0, 111.7, 54.9, 53.9; FTIR (ν_{max}, cm^{-1}): 1608, 1550, 1532, 1370, 1170, 1042; HRMS (ESI) calcd for C$_{15}$H$_{15}$N$_3$O$_7$S [M + H]$^+$: 394.0709, found: 394.0715.

N-(2-methoxyphenyl)-2,4-dinitro-*N*-(prop-2-yn-1-yl)benzenesulfonamide (4g).
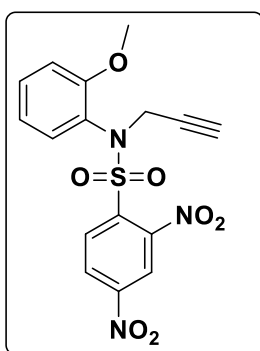
Synthesized by following general procedure B: Starting from **4a** (600 mg, 1.7 mmol), K$_2$CO$_3$ (937 mg, 6.8 mmol) and propargyl bromide (1.26 g, 8.5 mmol), **4g** was isolated as a pale yellow solid (600 mg, 90%): mp 160-162 °C; ^{1}H NMR (CDCl$_3$): δ 8.49 (d, J = 2.2 Hz, 1H), 8.31 (dd, J = 8.7, 2.2 Hz, 1H), 7.83 (d, J = 8.7 Hz, 1H), 7.46 (dd, J = 7.8, 1.6 Hz, 1H), 7.42-7.37 (m, 1H), 7.05-7.01 (m, 1H), 6.82 (d, J = 8.2 Hz, 1H), 4.61 (s, 2H), 3.42 (s, 3H), 2.24 (t, J = 2.6 Hz, 1H); ^{13}C NMR (100 MHz, CDCl$_3$): δ 156.0, 149.5, 147.9, 138.7, 134.0, 133.2, 131.4, 125.4, 124.0, 121.3, 119.3, 111.8, 77.9, 74.0, 55.1, 41.2; FTIR (ν_{max}, cm^{-1}): 3279, 3107, 2123, 1605, 1556, 1536, 1371, 1260, 1170, 1042; HRMS (ESI) calcd for C$_{16}$H$_{13}$N$_3$O$_7$S [M + H]$^+$: 392.0552, found: 392.0554.

N-benzyl-*N*-(2-methoxyphenyl)-2,4-dinitrobenzenesulfonamide (4h).
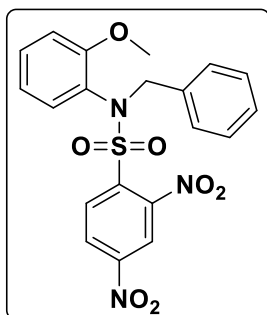
Synthesized by following general procedure B: Starting from **4a** (200 mg, 0.56 mmol), K$_2$CO$_3$ (231 mg, 1.68 mmol) and benzylbromide (280 mg, 1.68 mmol), **4h** was isolated as a pale yellow solid (190 mg, 76%): mp 152-153 °C; ^{1}H NMR (DMSO-d$_6$): δ 8.98 (m, 1H), 8.55-8.53 (m, 1H), 8.03-8.00 (m, 1H), 7.34-7.20 (m, 6H), 6.98 (m, 1H), 6.95-6.92 (m, 1H), 6.84-6.80 (m, 1H), 4.90 (br, 2H), 3.34 (br, 3H); ^{13}C NMR (100 MHz, DMSO-d$_6$): δ 156.4, 150.4, 145.4, 143.9, 147.8, 136.8, 136.3, 133.6, 132.9, 131.3, 128.92, 128.87, 128.3, 126.7, 124.5, 120.9, 120.0, 113.0, 55.6, 54.4; FTIR (ν_{max}, cm^{-1}): 1612, 1550, 1508, 1367, 1299, 1170, 1020; HRMS (ESI) calcd for C$_{20}$H$_{17}$N$_3$O$_7$S [M + H]$^+$: 443.0865, found: 444.0871

N-(3-methoxyphenyl)-2,4-dinitrobenzenesulfonamide (5a).
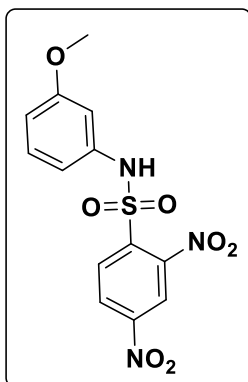
Synthesized by following general procedure A: Starting from DNsCl (1.5 g, 5.63 mmol), pyridine (540 μL, 6.77 mmol) and *meta*-anisidine (832 mg, 6.77 mmol), **5a** was isolated as pale yellow solid (1.40g, 70%): mp 172-174 °C; ^{1}H NMR (CDCl$_3$): δ 8.65 (d, J = 2.1 Hz, 1H), 8.38-8.37 (m, 1H), 8.08 (d, J = 8.5 Hz, 1H), 7.24 (br, 1H), 7.16 (m, 1H), 6.80-6.79 (m, 1H), 6.75-6.71 (m, 2H), 3.76 (s, 3H); ^{13}C NMR (100 MHz, CDCl$_3$): δ 160.5, 150.1, 149.5 137.6, 135.7, 133.7, 130.6, 126.9, 120.7, 115.1, 112.6, 109.4, 55.5; FTIR (v_{max}, cm^{-1}): 3312, 3108, 1611, 1442, 1402, 1273, 1035; HRMS (ESI) calcd for C$_{13}$H$_{11}$N$_3$O$_7$S [M + H]$^+$: 354.0396, found: 354.0396.

N-(3-methoxyphenyl)-N-methyl-2,4-dinitrobenzenesulfonamide (5b).
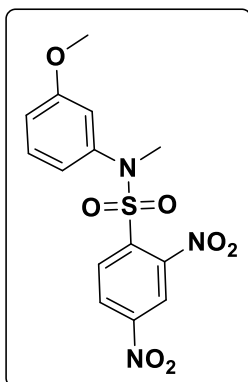
Synthesized by following general procedure B: Starting from **5a** (200 mg, 0.56 mmol), K$_2$CO$_3$ (312 mg, 2.26 mmol) and methyl iodide (401 mg, 2.83 mmol), **5b** was isolated as a white solid (168 mg, 81%): mp 124-126 °C; ^{1}H NMR (CDCl$_3$): δ 8.44 (m,1H), 8.32-8.29 (m,1H), 7.75 (m, 1H), 7.24 (m, 1H), 6.90-6.88 (m, 1H), 6.82 (m, 1H), 6.75 (m, 1H), 3.79 (s, 3H), 3.42 (s, 3H); ^{13}C NMR (100 MHz, CDCl$_3$): δ 160.4, 149.7, 148.3, 140.6, 136.7, 133.5, 130.2, 125.4, 119.3, 119.2, 114.1, 113.8, 55.5, 39.8; FTIR (v_{max}, cm^{-1}): 3097, 1667, 1557, 1536, 1369, 1174, 1069; HRMS (ESI) calcd for C$_{14}$H$_{13}$N$_3$O$_7$S [M + H]$^+$: 368.0552, found: 368.0562.

N-ethyl-N-(3-methoxyphenyl)-2,4-dinitrobenzenesulfonamide (5c).
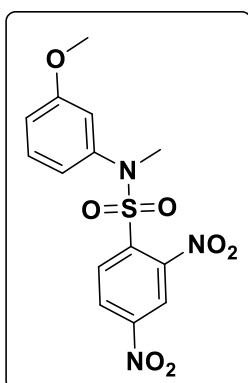
Synthesized by following general procedure B: Starting from **5a** (200 mg, 0.56 mmol), K$_2$CO$_3$ (312 mg, 2.26 mmol) and ethylbromide (308 mg, 2.83 mmol), **5c** was isolated as a white solid (108 mg, 50%): mp 126-128 °C; ^{1}H NMR (CDCl$_3$): δ 8.45 (d, J = 2.0 Hz, 1H), 8.29 (dd, J = 8.7, 2.1 Hz, 1H), 7.76 (d, J = 8.7 Hz, 1H), 7.25-7.23 (m, 1H), 6.91 (m, 1H), 6.79 (m, 1H), 6.73 (d, J = 7.9 Hz, 1H), 3.87 (q, J = 7.1 Hz, 2H), 3.79 (s, 3H), 1.17 (t, J = 7.1 Hz, 3H); ^{13}C NMR (100 MHz, CDCl$_3$): δ 160.3, 149.5, 148.0, 137.9, 137.6, 133.6, 130.2, 125.3, 121.2, 119.3, 115.7, 114.3, 55.5, 47.8, 14.5; FTIR (v_{max}, cm^{-1}): 1596, 1553, 1535, 1373, 1350, 1041; HRMS (ESI) calcd for C$_{15}$H$_{15}$N$_3$O$_7$S [M + H]$^+$: 382.0709, found: 382.0716.

N-allyl-N-(3-methoxyphenyl)-2,4-dinitrobenzenesulfonamide (5d).
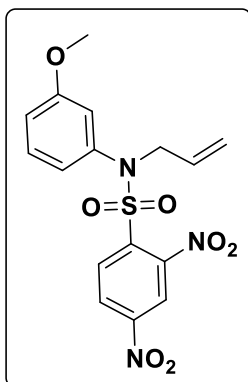
Synthesized by following general procedure B: Starting from **5a** (200 mg, 0.56 mmol), K_2CO_3 (312 mg, 2.26 mmol) and allyl bromide (342 mg, 2.83 mmol), **5d** was isolated as a white solid (170 mg, 76%): mp 110-112 °C; ^{1}H NMR (CDCl$_3$): δ 8.44 (d, J = 2.2 Hz, 1H), 8.26 (dd, J = 2.2, 8.7 Hz, 1H), 7.77 (d, J = 8.7 Hz, 1H), 7.21 (m, 1H), 6.88-6.86 (m, 1H), 6.77 (m, J = 8.2 Hz, 1H), 6.72-6.69 (m, 1H), 5.86-5.76 (m, 1H), 5.17-5.15 (m, 1H), 5.13 (s, 1H), 4.39 (d, J = 5.37 Hz, 2H), 3.77(s, 3H);

^{13}C NMR (100 MHz, CDCl$_3$): δ 160.3, 149.7, 148.0, 138.2, 137.7, 133.8, 132.7, 130.2, 125.5, 121.2, 119.9, 119.5, 115.8, 114.4, 55.6, 55.5; FTIR (ν_{max}, cm^{-1}): 3099, 1604, 1553, 1531, 1377, 1349, 1178; HRMS (ESI) calcd for $C_{16}H_{15}N_3O_7S$ [M + H]$^+$: 394.0709, found: 394.0716.

N-(3-methoxyphenyl)-2,4-dinitro-N-(prop-2-yn-1-yl)benzenesulfonamide (5e).
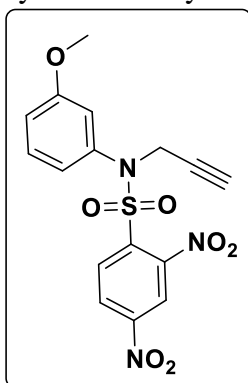
Synthesized by following general procedure B: Starting from **5a** (200 mg, 0.56 mmol), K_2CO_3 (231 mg, 1.68 mmol) and propargyl bromide (420 mg, 2.5 mmol), **5e** was isolated as a pale yellow solid (184 mg, 83%): mp 111-113 °C; ^{1}H NMR (CDCl$_3$): δ 8.48 (d, J = 2.1 Hz, 1H), 8.33 (dd, J = 2.2, 8.7 Hz, 1H), 7.91 (d, J = 8.7 Hz, 1H), 7.27-7.23 (m, 1H), 6.94 (dd, J = 2.4, 8.4 Hz, 1H), 6.89 (m, J = 2.0 Hz, 1H) 6.82-6.80 (m, 1H), 4.60 (d, J = 2.5 Hz, 2H), 3.79 (s, 3H), 2.31 (t, J = 2.4 Hz, 1H); ^{13}C NMR(100 MHz, CDCl$_3$): δ 160.4, 149.9, 148.0, 138.2, 137.7, 133.8, 130.3, 125.7, 121.1, 119.7, 115.6, 115.0, 77.8, 74.5, 55.6, 42.8; FTIR (ν_{max}, cm^{-1}): 3293, 3099, 2123, 1603, 1555, 1537, 1366, 1171; HRMS (ESI) calcd for $C_{16}H_{13}N_3O_7S$ [M + H]$^+$: 392.0552, found: 392.0555

2,4-dinitro-N-(prop-2-yn-1-yl)benzenesulfonamide (8).
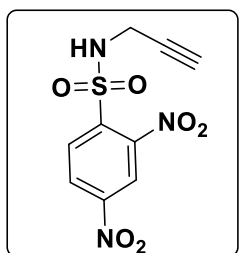
Synthesized by following general procedure A: Starting from DNsCl (2 g, 7.51 mmol), pyridine (700 μl, 9mmol) and propargyl amine (523 mg, 6.77 mmol), **8** was isolated as pale yellow solid (716mg, 33%): mp 163-165 °C; ^{1}H NMR (DMSO- d$_6$): δ 8.96 (s, 1H), 8.90 (d, J = 2.3 Hz, 1H), 8.66 (dd, J = 8.7, 2.3 Hz, 1H), 8.30 (d, J = 8.7, Hz, 1H), 3.89 (d, 2.5 Hz, 2H), 3.08 (m, 1H); ^{13}C NMR(100 MHz, DMSO-d$_6$): δ 150.3, 148.1, 138.4, 132.4, 127.6,

120.5, 79.1, 76.1, 32.6; FTIR (ν_{max}, cm^{-1}): 3339, 3296, 3106, 2225, 1611, 1559, 1540, 1411, 1164; HRMS (ESI) calcd for $C_9H_7N_3O_6S$ [M + H]$^+$: 286.0134, found: 286.0131.

N-methyl-2,4-dinitro-*N*-(prop-2-yn-1-yl)benzenesulfonamide (8a).
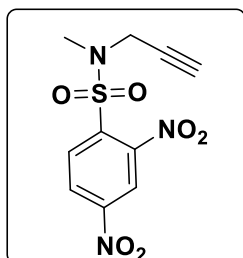
Synthesized by following general procedure B: Starting from **8** (150 mg, 0.52 mmol), K$_2$CO$_3$ (215 mg, 1.56 mmol) and methyl iodide (369 mg, 2.6 mmol), **8a** was isolated as pale yellow solid (100 mg, 64%): mp 126-127 °C; ^{1}H NMR (CDCl$_3$): δ 8.50 (dd, *J* = 2.3, 8.7 Hz, 1H), 8.47 (d, *J* = 2.0 Hz, 1H), 8.27 (d, *J* = 8.6 Hz, 1H), 4.20 (d, *J* = 2.3 Hz, 2H), 3.06 (s, 3H), 2.24 (t, *J* = 2.4 Hz, 1H); ^{13}C NMR(100 MHz, CDCl$_3$): δ 150.0, 148.5, 137.5, 132.8, 126.1, 119.8, 76.0, 74.8, 40.0, 34.8; FTIR (ν_{max}, cm^{-1}): 3260, 3110, 2118, 1606, 1555, 1536, 1422, 1338, 1164; HRMS (ESI) calcd for $C_{10}H_9N_3O_6S$ [M + H]$^+$: 300.0290, found: 300.0300

N-ethyl-2,4-dinitro-*N*-(prop-2-yn-1-yl)benzenesulfonamide (8b).
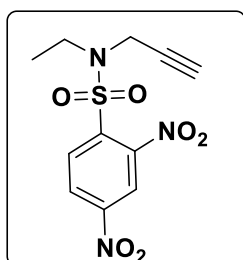
Synthesized by following general procedure B: Starting from **8** (150 mg, 0.52 mmol), K$_2$CO$_3$ (215 mg, 1.68 mmol) and ethyl bromide (283 mg, 2.6 mmol), **8b** was isolated as a pale yellow solid (140 mg, 85%): mp 129-130 °C; ^{1}H NMR (CDCl$_3$): δ 8.50 (dd, *J* = 2.2, 8.7 Hz, 1H), 8.47 (d, *J* = 2.0 Hz, 1H), 8.28 (d, *J* = 8.6 Hz, 1H), 4.25 (d, *J* = 2.4 Hz, 2H), 3.51 (q, *J* = 7.2 Hz, 2H), 2.22 (t, *J* = 2.4 Hz, 1H), 1.25 (t, *J* = 7.2 Hz, 3H); ^{13}C NMR (100 MHz, CDCl$_3$): δ 149.8, 138.5, 132.6, 126.1, 119.8, 76.4, 74.4, 42.3, 36.1, 13.3; FTIR (ν_{max}, cm^{-1}): 3254, 3109, 2116, 1605, 1535, 1462, 1353; HRMS (ESI) calcd for $C_{11}H_{11}N_3O_6S$ [M + H]$^+$: 314.0447, found: 314.0455.

N-(3-methoxybenzyl)-2,4-dinitro-*N*-(prop-2-yn-yl)benzenesulfonamide (8c).
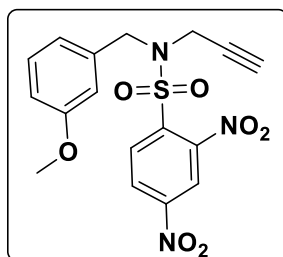
Synthesized following general procedure B: Starting from **10b** (300 mg, 0.82 mmol), K$_2$CO$_3$ (339mg, 2.46 mmol) and propargyl bromide (293 mg, 2.46 mmol), **8c** was isolated as a pale yellow solid (260 mg, 78%): mp 114-115 °C; ^{1}H NMR (CDCl$_3$): δ 8.50-8.46 (m, 1H), 8.26 (d, *J* = 8.6 Hz, 1H), 7.28-7.24 (m, 1H), 6.91 (d, *J* = 7.7 Hz, 1H), 6.87-6.84 (m, 2H), 4.58 (s, 2H), 4.09 (d, *J* = 2.5 Hz, 2H), 3.79 (s, 3H), 2.21 (t, *J* = 2.4 Hz, 1H), ^{13}C NMR(100 MHz, DMSO-d$_6$): 159.8, 150.5, 148.0, 136.4, 136.1, 132.7, 130.3, 127.2,

120.7, 120.4, 114.1, 113.9, 77.6, 76.6, 55.4, 50.8, 36.8; FTIR (ν_{max}, cm^{-1}): 3305, 3092, 2125, 1600, 1541, 1463, 1335, 1165, 1034; HRMS (ESI) calcd for $C_{17}H_{15}N_3O_7S$ [M + H]$^+$: 406.0709, found: 406.0713

N,N'-(propane-1,3-diyl)bis(N-benzyl-2,4-dinitrobenzenesulfonamide) (9a).
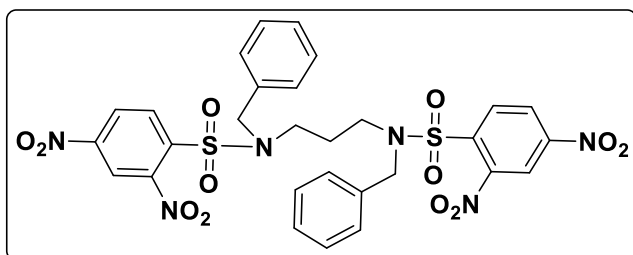
Synthesized by following general procedure C: Starting from **1d** (65 mg, 0.16 mmol), **1a** (110 mg, 0.33 mmol) **9a** was isolated as pale yellow solid (18 mg, 15%): mp 186-189 °C; ^{1}H NMR (400 MHz, DMSO-d$_6$): δ 8.95 (d, J = 2.2 Hz, 2H), 8.51 (dd, J = 8.7, 2.2 Hz, 2H), 8.21 (d, J = 8.7 Hz, 2H), 7.33-7.26 (m, 6H), 7.16-7.15 (m, 4H), 4.37 (s, 4H), 3.05 (t, J = 7.3 Hz, 4H), 1.42 (quintet, J = 6.7 Hz, 2H); ^{13}C NMR (100 MHz, DMSO- d$_6$): 150.4, 147.8, 143.3, 137.0, 136.0, 132.2, 129.2, 128.4, 127.5, 120.7, 51.4, 45.5, 26.5; FTIR (ν_{max}, cm^{-1}): 3104, 1561, 1371, 1166; HRMS (ESI) calcd for $C_{29}H_{26}N_6O_{12}S_2$ [M + K]$^+$: 753.0687, found: 753.0684.

N-benzyl-N-(3-(N-(2-methoxybenzyl)-2,4-dinitrophenylsulfonamido)propyl)-2,4-dinitrobezenesulfonamide (9b).
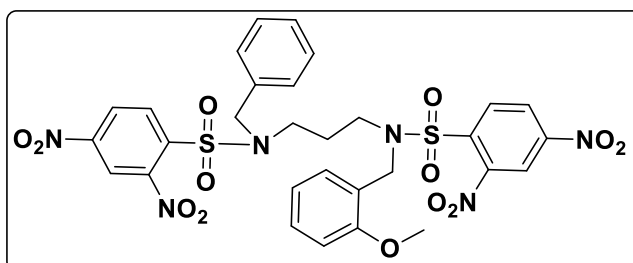
Synthesized by following general procedure C: Starting from **1d** (100 mg, 0.25 mmol), **10a** (92 mg, 0.25 mmol) **9b** was isolated as pale yellow solid (27 mg, 14 % yield): mp 81-83 °C; ^{1}H NMR (CDCl$_3$): δ 8.46 (d, J = 2.1 Hz, 1H), 8.41 (dd, J = 8.7, 2.2 Hz, 1H), 8.39 (d, J = 2.2 Hz, 1H), 8.27 (dd, J = 8.6, 2.1 Hz, 1H), 8.14 (d, J = 8.6 Hz, 1H), 7.90 (d, J = 8.7 Hz, 1H), 7.32-7.27 (m, 3H), 7.24-7.20 (m, 3H), 7.10-7.08 (m, 1H), 6.83-6.81 (m, 1H), 6.71 (d, J = 8.2 Hz, 1H), 4.46 (s, 2H), 4.37 (s, 2H), 3.69 (s, 3H), 3.22 (q, J = 7.1 Hz, 4H), 1.68 (quintet, J = 7.2 Hz, 2H); ^{13}C NMR (CDCl$_3$): δ 157.7, 154.3, 149.7, 149.3, 147.9, 147.7, 139.2, 138.7, 134.9, 134.8, 132.9, 132.6, 130.9, 130.1, 129.0, 128.4, 126.3, 125.9, 122.3, 120.7, 119.9, 119.5, 110.5, 55.3, 51.9, 46.8, 46.3, 45.5, 27.2; FTIR (ν_{max}, cm^{-1}): 1537, 1348, 1159; HRMS (ESI) CALCD FOR$C_{30}H_{28}N_6O_{13}S_2$ [M + K]$^+$: 783.0793, found: 783.0817.

N-benzyl-N-(3-(N-(4-methoxybenzyl)-2,4-dinitrophenylsulfonamido)propyl)-2,4-dinitrobezenesulfonamide (9c).
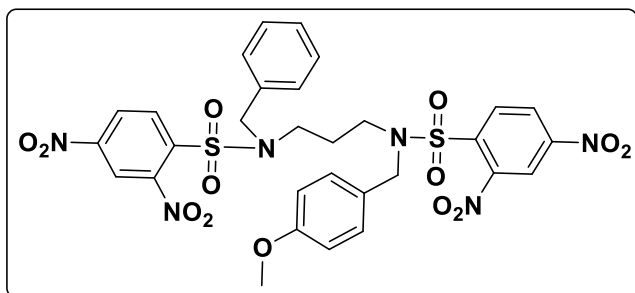
Synthesized by following general procedure C: Starting from **1d** (100 mg, 0.25 mmol), **2a** (92 mg, 0.25 mmol) **9c** was isolated as pale yellow solid (28 mg, 14 % yield): mp 78-80 °C; ^{1}H NMR (CDCl$_3$): δ 8.46-8.44 (m, 2H), 8.43-8.38 (m, 2H), 8.17-8.09 (m, 2H), 7.29-7.27 (m, 3H), 7.17-7.15 (m, 2H), 7.08-7.6 (m, 2H), 6.80-6.78 (m, 2H), 4.39 (s, 2H), 4.30 (s, 2H), 3.75 (s, 3H), 3.13-3.07 (m, 4H), 1.61-1.57 (m, 2H); ^{13}C NMR (CDCl$_3$): δ 159.8, 149.71, 149.67, 147.8, 138.6, 134.6, 132.8, 130.0, 129.0, 128.5, 128.4, 126.4, 126.3, 126.2, 119.85, 119.83, 114.3, 55.4, 51.7, 51.4, 45.4, 45.3, 26.9; FTIR (ν$_{max}$, cm^{-1}): 1539, 1348, 1160; HRMS (ESI) calcd for C$_{30}$H$_{28}$N$_6$O$_{13}$S$_2$ [M + K]$^+$: 783.0793, found: 783.0804.

_N_-benzyl-_N_-(3-(_N_-(2,4-dimethoxybenzyl)-2,4-dinitrophenylsulfonamido)propyl)-2,4-dinitrobezenesulfonamide (9d).
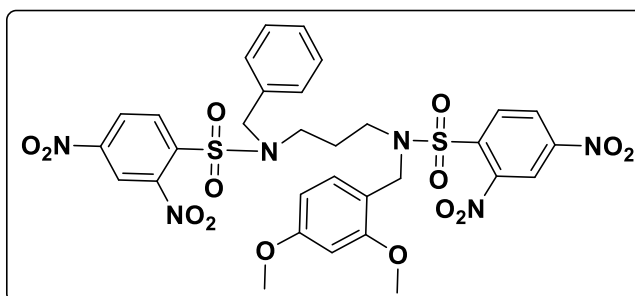
Synthesized by following general procedure C: Starting from **1d** (100 mg, 0.25 mmol), **11a** (100 mg, 0.25 mmol) **9d** was isolated as pale yellow solid (38 mg, 19 % yield): mp 73-74 °C; ^{1}H NMR (CDCl$_3$): δ 8.46 (d, _J_ = 2.1 Hz, 1H), 8.42-8.39 (m, 2H), 8.29 (dd, _J_ = 8.6, 2.2 Hz, 1H), 8.13 (d, _J_ = 8.6 Hz, 1H), 7.92 (d, _J_ = 8.6 Hz, 1H), 7.33-7.27 (m, 3H), 7.24-7.18 (m, 2H), 7.0 (d, _J_ = 8.3 Hz, 1H), 6.34 (dd, _J_ = 8.3, 2.2 Hz, 1H), 6.25 (d, _J_ = 2.1 Hz, 1H), 4.47 (s, 2H), 4.30 (s, 2H), 3.75 (s, 3H), 3.60 (s, 3H), 3.22 (t, _J_ = 7.4 Hz, 2H), 3.17 (t, _J_ = 7 Hz, 2H), 1.67 (quintet, _J_ = 7.2 Hz, 2H); ^{13}C NMR (CDCl$_3$): δ 161.5, 158.8, 149.7, 149.3, 147.9, 147.7, 139.3, 138.7, 134.9, 132.9, 132.6, 131.9, 129.0, 128.4, 126.3, 125.8, 119.9, 119.5, 114.6, 104.4, 98.3, 55.5, 55.2, 51.9, 46.5, 46.1, 45.5, 27.2; FTIR (ν$_{max}$, cm^{-1}): 1545, 1348, 1159; HRMS (ESI) calcd for C$_{31}$H$_{30}$N$_6$O$_{13}$S$_2$ [M + K]$^+$: 813.0898, found: 813.0897.

***N*-benzyl-*N*-(3-((2,4-dinitro-*N*-phenylphenyl)sulfonamido)propyl)-2,4-dinitrobenzenesulfonamide (9e).**
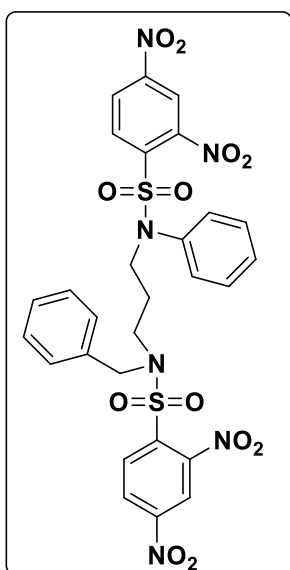
Synthesized by following general procedure C: Starting from **1d** (75 mg, 0.19 mmol), **3a** (73 mg, 0.23 mmol) **9e** was isolated as brown solid (24 mg, 17 % yield): mp 151-153°C; ^{1}H NMR (400 MHz, CDCl$_3$): δ 8.48 (d, J = 2.2 Hz, 1H), 8.45-8.42 (m, 2H), 8.23 (dd, J = 8.7, 2.2 Hz, 1H), 8.20 (d, J = 8.6 Hz, 1H), 7.60 (d, J = 8.6 Hz, 1H), 7.37-7.28 (m, 6H), 7.24-7.20 (m, 2H), 7.08-7.05 (m, 2H), 4.51 (s, 2H), 3.67 (t, J = 6.8 Hz, 2H), 3.37 (t, J = 7.5 Hz , 2H), 1.61 (quintet, J = 7.8 Hz, 2H); ^{13}C NMR (100 MHz, CDCl$_3$): δ 149.8, 149.7, 148.0, 138.8, 137.0, 136.7, 134.8, 133.8, 132.8, 130.0, 129.4, 129.3, 129.0, 128.4, 128.3, 126.3, 125.5, 120.0, 119.5, 119.9, 52.1, 50.3, 45.3, 27.3; FTIR (ν$_{max}$, cm^{-1}): 3101, 1545, 1356; HRMS (ESI) calcd for C$_{28}$H$_{24}$N$_6$O$_{12}$S$_2$ [M + K]$^+$: 739.0531, found: 739.0518.

***N*-benzyl-*N*-(3-((*N*-(2-fluorophenyl)-2,4-dinitrophenyl)sulfonamido)propyl)-2,4-dinitrobenzenesulfonamide (9f).**
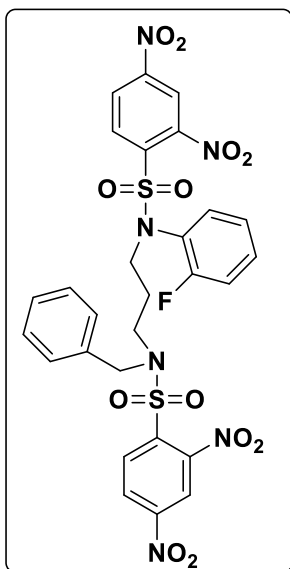
Synthesized by following general procedure C: Starting from **1d** (100 mg, 0.25 mmol), **3e** (116 mg, 0.34 mmol) **9f** was isolated as white solid (26 mg, 14 % yield): mp 151-153°C; ^{1}H NMR (400 MHz, DMSO-d$_6$): δ 8.97 (b, 2H), 8.54 (s, 1H), 8.52 (s, 1H), 8.29 (d, J = 8.5 Hz, 1H), 7.95 (d, Jν$_{max}$, cm^{-1}= 8.6 Hz, 1H), 7.50-7.45 (m, 1H), 7.28-7.19 (m, 7H), 7.13-7.09 (m, J = 7.1 Hz, 1H), 4.48 (s, 2H), 3.56-3.53 (m, 2H), 3.33-3.30 (b, 2H), 1.44-1.38 (m, 2H); ^{13}C NMR (100 MHz, DMSO-d$_6$): δ 150.8, 150.5, 147.9, 137.0, 136.3, 135.4, 132.7, 132.6, 132.1, 129.2, 128.4, 128.3, 127.6, 127.3, 125.8, 124.1, 124.0, 120.7, 120.5, 117.5, 117.3, 52.2, 49.4, 46.1, 27.4; FTIR (ν$_{max}$, cm^{-1}): 3105, 1546, 1357, 1166; HRMS (ESI) calcd for C$_{28}$H$_{23}$FN$_6$O$_{12}$S$_2$ [M + H]$^+$: 719.0878, found: 719.0874.

***N*-benzyl-*N*-(3-((*N*-(2-methoxyphenyl)-2,4-dinitrophenyl)sulfonamido)propyl)-2,4-dinitrobezenenesulfonamide (9g).**
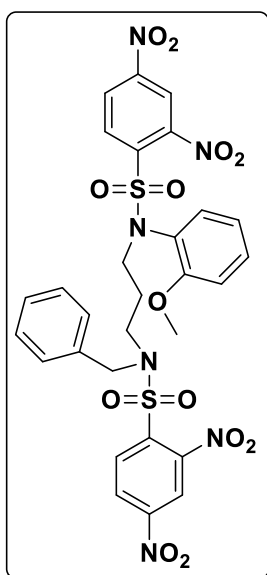
Synthesized following general procedure C: Starting from **1d** (100 mg, 0.25 mmol), **4a** (107 mg, 0.30 mmol) **9g** was isolated as white solid (65 mg, 35 % yield); mp 141-143 °C; ^{1}H NMR (CDCl$_3$): δ 8.46-8.40 (m, 3H), 8.26-8.24 (m, 1H), 8.19 (d, *J* = 8.6 Hz, 1H), 7.66 (d, *J* = 8.6 Hz, 1H), 7.39-7.35 (m, 1H), 7.31-7.28 (m, 3H), 7.23-7.20 (m, 2H), 7.19-7.17 (m, *J* = 7.6 Hz, 1H), 6.96 (t, *J* = 7.6 Hz, 1H), 6.77 (d, *J* = 8.3 Hz, 1H), 4.51 (s, 2H), 3.88-3.34(m, 4H), 3.32 (s, 3H), 1.60-1.55 (m, 2H); ^{13}C NMR (CDCl$_3$): δ 155.7, 149.7, 149.4, 147.9, 147.8, 138.8, 138.1, 134.9, 133.6, 133.2, 132.8, 131.3, 130.0, 128.4, 128.3, 126.4, 125.0, 124.0, 121.4, 119.9, 119.0, 112.0, 55.0, 52.1, 48.5, 45.5, 27.5; FTIR (v_{max}, cm^{-1}): 1545, 1356, 1163; HRMS (ESI) calcd for C$_{29}$H$_{26}$N$_6$O$_{13}$S$_2$ [M + H]$^+$: 731.1078, found: 731.1082

***N*-benzyl-*N*-(3-((*N*-(3-methoxyphenyl)-2,4-dinitrophenyl)sulfonamido)propyl)-2,4-dinitrobenzenesulfonamide (9h).**
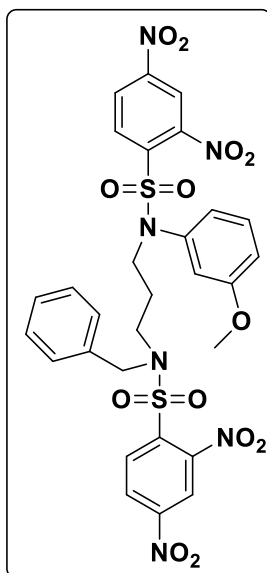
Synthesized following general procedure C: Starting from **1d** (75 mg, 0.19 mmol), **5a** (77 mg, 0.23 mmol), **9h** was isolated as a white solid (45 mg, 33 % yield): mp 108-110 °C; ^{1}H NMR (400 MHz, DMSO-d$_6$): δ 8.97 (d, *J* = 2.2 Hz, 1H), 8.94 (d, *J* = 2.1 Hz, 1H), 8.51-8.47 (m, 2H), 8.27 (d, *J* = 2.2 Hz, 1H), 7.83 (d, *J* = 8.7 Hz, 1H), 7.30-7.20 (m, 6H), 6.97-6.94 (m, 1H), 6.64 (b, 1H), 6.60-6.58 (m, 1H), 4.49 (s, 2H), 3.69 (s, 3H), 3.60 (t, *J* = 6.4 Hz, 2H), 3.31-3.26 (m, 2H), 1.40 (quintet, *J* = 7.6 Hz, 2H); ^{13}C NMR (100 MHz, DMSO-d$_6$): δ 160.2, 150.7, 150.4, 148.1, 148.0, 138.0, 137.0, 136.3, 135.1, 132.8, 132.1, 130.7, 129.1, 128.4, 127.5, 127.1, 121.3, 120.7, 120.5, 115.1, 115.0, 119.0, 55.9, 52.1, 49.4, 46.1, 27.2; FTIR (v_{max}, cm^{-1}): 3103, 1545, 1367, 1166; HRMS (ESI) calcd for C$_{29}$H$_{26}$N$_6$O$_{13}$S$_2$ [M + H]$^+$: 731.1078, found: 731.1082.

***N*-benzyl-*N*-((3-((*N*-(4-methoxyphenyl)-2,4-dinitrophenyl)sulfonamido)propyl)-2,4-dinitrobenzenesulfonamide (9i).**
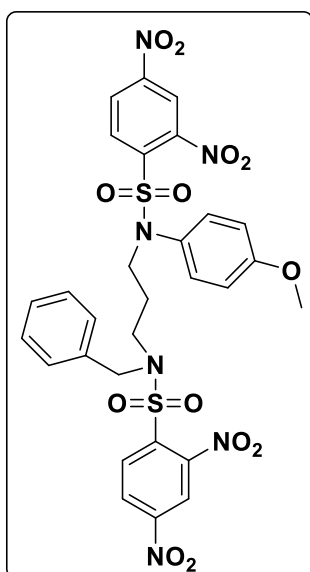
Synthesized following general procedure C: Starting from **1d** (75 mg, 0.19 mmol), **5a** (77 mg, 0.23 mmol), **9i** was isolated as white solid (45 mg, 33 % yield): mp 118-120 °C; ^{1}H NMR (400 MHz, DMSO-d$_6$): δ 8.99-8.98 (m, 1H), 8.95-8.94 (m, 1H), 8.54-8.51 (m, 1H), 8.49-8.46 (m, 1H), 8.29 (d, J = 8.6 Hz, 1H), 7.77 (d, J = 8.7 Hz, 1H), 7.32-7.30 (m, 5H), 6.91 (m, 4H), 4.5 (s, 2H), 3.77 (s, 3H), 3.56 (t, J = 6.0 Hz, 2H), 3.31-3.29 (m, 2H), 1.40 (quintet, J = 6.9 Hz, 2H); ^{13}C NMR (100 MHz, DMSO-d$_6$): δ 159.7, 150.6, 150.4, 148.02, 147.99, 147.9, 137.1, 136.3, 135.2, 132.8, 132.1, 130.8, 129.1, 129.0, 128.4, 127.5, 127.1, 120.7, 120.4, 115.1, 55.9, 52.1, 49.7, 46.1, 27.0; FTIR ($ν_{max}$, cm^{-1}): 3101, 1545, 1356, 1166; HRMS (ESI) calcd for $C_{29}H_{26}N_6O_{13}S_2$ [M + K]$^+$: 769.0636, found: 769.0654.

***N*-benzyl-*N*-((3-(N-benzyl-2-nitrophenyl)sulfonamido)propyl)-2,4-dinitrobenzenesulfonamide (9j).**
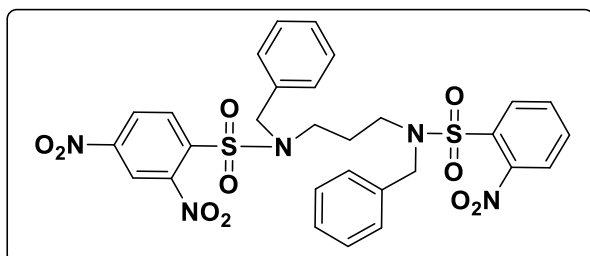
Synthesized by following general procedure C: Starting from **1d** (130 mg, 0.32 mmol), **12a** (136 mg, 0.46 mmol), **9j** was isolated as white solid (62mg, 27% yield): mp 159-167 °C; ^{1}H NMR (400 MHz, DMSO-d$_6$): δ 8.96 (d, J = 2.1 Hz, 1H), 8.51 (dd, J = 2.1, 8.6 Hz, 1H), 8.20 (d, J = 8.7 Hz, 1H), 7.98 (d, J = 7.8 Hz, 1H), 7.95 (d, J = 7.7 Hz, 1H), 7.91-7.87 (m, 1H), 7.82-7.78 (m, 1H), 7.33-7.27 (m, 6H), 7.15 (d, J = 6.9 Hz, 4H), 4.36 (s, 2H), 4.34 (s, 2H), 3.05-2.99 (m, 4H), 1.40 (quintet, J = 6.8 Hz, 2H); ^{13}C NMR (100 MHz, DMSO-d$_6$): δ 150.4, 147.9, 147.8, 137.1, 136.4, 136.0, 135.2, 133.0, 132.2, 132.1, 130.3, 129.2, 129.1, 128.44, 128.37, 128.3, 127.5, 124.9, 120.7, 51.4, 51.2, 45.4, 45.2, 26.5; FTIR ($ν_{max}$, cm^{-1}): 1544, 1358, 1169; HRMS (ESI) calcd for $C_{29}H_{27}N_5O_{10}S_2$ [M + K]$^+$: 708.0836, found: 708.0837.

***N*-benzyl-*N*-(3-((N-benzyl-3-nitrophenyl)sulfonamido)propyl)-2,4-dinitrobenzenesulfonamide (9k).**
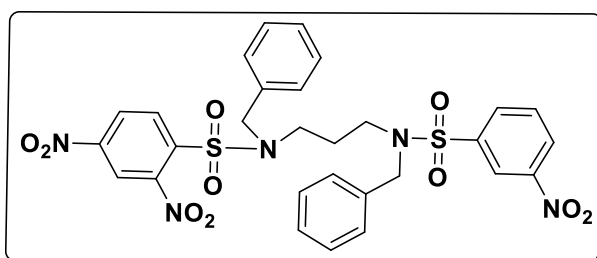
Synthesized by following general procedure C: Starting from **1d** (125 mg, 0.32 mmol), **12b** (138 mg, 0.47 mmol), **9k** was isolated as white solid (77 mg, 36 % yield): mp 140-142 °C; ^{1}H NMR (400 MHz, CDCl$_3$): δ 8.55 (b, 1H), 8.44-8.41 (m, 2H), 8.36 (dd, J = 1.9, 8.68 Hz, 1H), 8.07 (d, J = 7.8 Hz, 1H), 8.03 (d, J = 8.6 Hz, 1H), 7.75-7.71 (m, 1H), 7.32-7.22 (m, 6H), 7.19-7.08 (m, 4H), 4.35 (s, 2H), 4.25 (s, 2H), 3.17 (t, J = 7.2 Hz, 2H) , 3.05 (t, J = 7.3 Hz, 2H), 1.62-1.58 (m, 2H); ^{13}C NMR (100 MHz, DMSO-d$_6$): δ 150.4, 148.5, 147.8, 141.1, 137.1, 136.6, 136.1, 133.3, 132.2, 132.1, 129.2, 129.0, 128.5, 128.4, 128.2, 128.0, 127.5, 122.1, 120.7, 51.9, 51.5, 46.1, 45.7, 27.0; FTIR (v_{max}, cm^{-1}): 1543, 1356, 1169; HRMS (ESI) calcd for C$_{29}$H$_{27}$N$_5$O$_{10}$S$_2$ [M + K]$^+$: 708.0836, found: 708.0844.

***N*-benzyl-*N*-(3-((*N*-benzyl-4-nitrophenyl)sulfonamido)propyl)-2,4-dinitrobenzenesulfonamide (9l).**
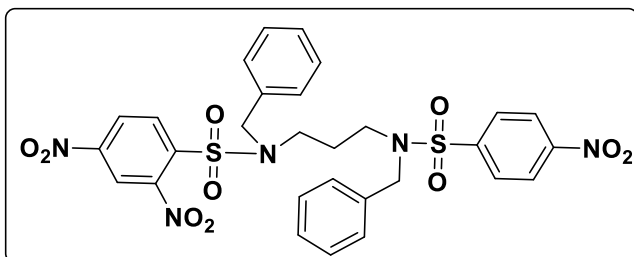
Synthesized by following general procedure C: Starting from **1d** (125 mg, 0.32 mmol), **12c** (138 mg, 0.47 mmol), **9l** was isolated as white solid (43 mg, 21 % yield): mp 171-173 °C; ^{1}H NMR (400 MHz, DMSO-d$_6$): δ 8.97 (d, J = 2.1 Hz ,1H), 8.51 (dd, J = 2.1, 8.6, Hz, 1H), 8.37 (d, J = 8.7 Hz, 2H), 8.21 (d, J = 8.6 Hz, 1H), 8.03 (d, J = 8.7 Hz, 2H), 7.32-7.26 (m, 6H), 7.18-7.14 (m, 4H), 4.35 (s, 2H), 4.23 (s, 2H), 3.03 (t, J = 7.4 Hz, 2H), 2.92 (t, J = 7.3 Hz, 2H), 1.35 (quintet, J = 7.0 Hz, 2H); ^{13}C NMR (100 MHz, DMSO-d$_6$): δ 150.4, 150.3, 147.8, 144.9, 137.0, 136.6, 136.0, 132.2, 129.2, 129.0, 128.9, 128.5, 128.43, 128.39, 128.2, 127.5, 125.2, 120.7, 51.9, 51.4, 46.0, 45.6, 26.9; FTIR (v_{max}, cm^{-1}): 1541, 1355, 1166; HRMS (ESI) calcd for C$_{29}$H$_{27}$N$_5$O$_{10}$S$_2$ [M + K]$^+$: 708.0836, found: 708.0850.

***N*-(2-methoxybenznyl)-2,4-dinitrobenzenesulfonamide (10a).**
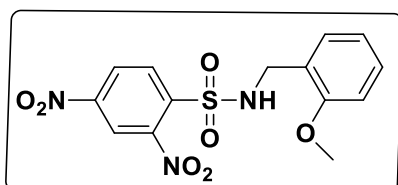
Synthesized by following general procedure A: Starting from DNsCl (400 mg, 1.5 mmol), 2-methoxbenzylamine

(226 mg, 1.65 mmol), **11a** was isolated as pale yellow solid (300 mg, 54% yield): mp 156-158 °C; ^{1}H NMR (CDCl$_3$): δ 8.50 (s, 1H), 8.22 (d, J = 8.6 Hz, 1H), 7.96 (d, J = 8.6, Hz, 1H), 7.12-7.06 (m, 2H), 6.75-6.72 (m, 1H), 6.54 (d, J = 8.2 Hz, 1H), 6.49-6.46 (m, 1H), 4.40 (d, J = 6.4 Hz, 2H), 3.70 (s, 3H); ^{13}C NMR(100 MHz, CDCl$_3$): δ 157.3, 148.2, 147.3, 140.1, 132.8, 130.5, 130.0, 126.5, 123.4, 120.2, 120.1, 109.9, 55.2, 45.5; FTIR (ν_{max}, cm^{-1}): 2921, 1535, 1430, 1154, 1094; HRMS (ESI) calcd for C$_{14}$H$_{13}$N$_3$O$_7$S [M + Na]$^+$: 390.0372, found: 390.0370.

N-(3-methoxybenznyl)-2,4-dinitrobenzenesulfonamide (10b).
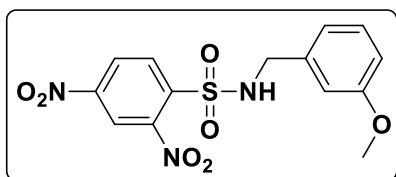
Synthesized by following general procedure A: Starting from DNsCl (400 mg, 1.5 mmol), 3-methoxybenzylamine (226 mg, 1.65 mmol), **11b** was isolated as yellow solid (264 mg, 48% yield): mp 111-113 °C; ^{1}H NMR (DMSO-d$_6$): δ 9.02 (s, 1H), 8.86 (d, J = 2.2 Hz, 1H), 8.49 (dd, J = 8.7, 2.2 Hz, 1H), 8.09 (d, J = 8.7 Hz, 1H), 7.15 (t, J = 7.8 Hz, 1H), 6.80 (d, J = 7.52 Hz, 1H), 6.77-6.73 (br, 2H), 4.18(br, 2H), 3.66 (s, 3H); ^{13}C NMR(100 MHz, DMSO-d$_6$): δ 159.7, 149.9, 147.8, 138.9, 138.6, 131.9, 129.9, 27.4, 120.4, 113.6, 113.4, 55.4, 46.8; FTIR (ν_{max}, cm^{-1}): 1532, 1343, 1159; HRMS (ESI) calcd for C$_{14}$H$_{13}$N$_3$O$_7$S [M + Na]$^+$: 390.0372, found: 390.0372.

N-(2,4-dimethoxybenznyl)-2,4-dinitrobenzenesulfonamide (11a).
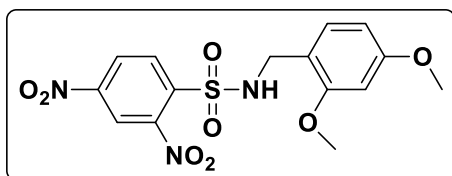
Synthesized by following general procedure A: Starting from DNsCl (400 mg, 1.5 mmol), 2,4 dimethoxybenzylamine (276 mg, 1.65 mmol), **12a** was isolated as pale yellow solid (250 mg, 42 % yield): mp 140-142 °C; ^{1}H NMR (CDCl$_3$): δ 8.51 (d, J = 2.2 Hz, 1H), 8.25 (dd, J = 8.6, 2.2 Hz, 1H), 7.98 (d, J = 8.6 Hz, 1H), 6.95 (d, J = 8.2 Hz, 1H), 6.41-6.38 (t, J = 6.4 Hz, 1H), 6.22 (dd, J = 8.2, 2.3Hz, 1H), 6.07 (d, J = 2.3 Hz, 2H), 4.31(d, J = 6.4 Hz, 2H), 3.68 (s, 3H), 3.65(s, 3H); ^{13}C NMR (100 MHz, CDCl$_3$): δ 161.4, 158.4, 149.3, 140.2, 133.03, 131.1, 126.5, 120.1, 116.2, 103.2, 98.1, 55.5, 55.3, 45.1; FTIR (ν_{max}, cm^{-1}): 1538, 1512, 1159, 1022; HRMS (ESI) calcd for C$_{15}$H$_{15}$N$_3$O$_8$S [M + Na]$^+$: 420.0478, found: 420.0478.

***N*-(3-methoxyphenyl)-2,4-dinitro-*N*-((1-(2-((7-nitrobenzo[c][1,2,5]oxadiazol-4-yl)amino)ethyl)-1H-1,2,3-triazol-4-yl)methyl)benzenesulfonamide (15).**
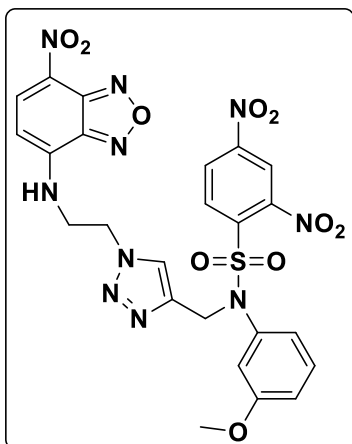
5e (100 mg, 0.25 mmol), and **14** (80 mg, 0.31 mmol) were dissolved in ACN (20 mL), sequentially treated with CuI (3eq) and di-isopropyl ethyl amine (DIPEA, 3eq). The RM was warmed to RT for 0.5 h. On completion, The RM was purified by silica gel chromatography using mixtures of DCM/ Methanol, **15** was isolated as a yellow solid (35%): mp 178-180 °C; ^{1}H NMR (DMSO-d_6): δ 9.39 (s, 1H), 8.99 (d, *J* = 2.3 Hz, 1H), 8.52 (dd, *J* = 2.3, 8.8 Hz, 1H), 8.42 (d, *J* = 9.0 Hz, 1H), 8.08 (s, 1H), 8.00 (d, *J* = 8.8 Hz, 1H), 7.13 (m, 1H), 6.83 (m, 1H), 6.70 (m, 1H), 6.67-6.65 (m, 1H), 6.29 (d, *J* = 8.0 Hz, 1H), 4.98 (s, 2H), 4.66 (t, *J* = 5.4 Hz, 2H), 3.93 (s, 2H), 3.61 (s, 3H); ^{13}C NMR(100 MHz, DMSO-d_6): δ 160.1, 150.7, 148.1, 145.3, 144.8, 142.6, 138.6, 138.2, 135.7, 132.9, 130.7, 127.3, 125.2, 121.5, 120.6, 120.5, 115.2, 114.7, 109.7, 55.8, 48.4, 47.7, 43.7; FTIR (ν_{max}, cm^{-1}): 3363, 1578, 1533, 1365, 1318, 1165; HRMS (ESI) calcd for $C_{24}H_{20}N_{10}O_{10}S$ [M + H]$^+$: 641.1163, found: 641.1168.

2.5 Spectral data

^{1}H NMR Spectrum (400 MHz, CDCl$_3$) of **1c**[1]
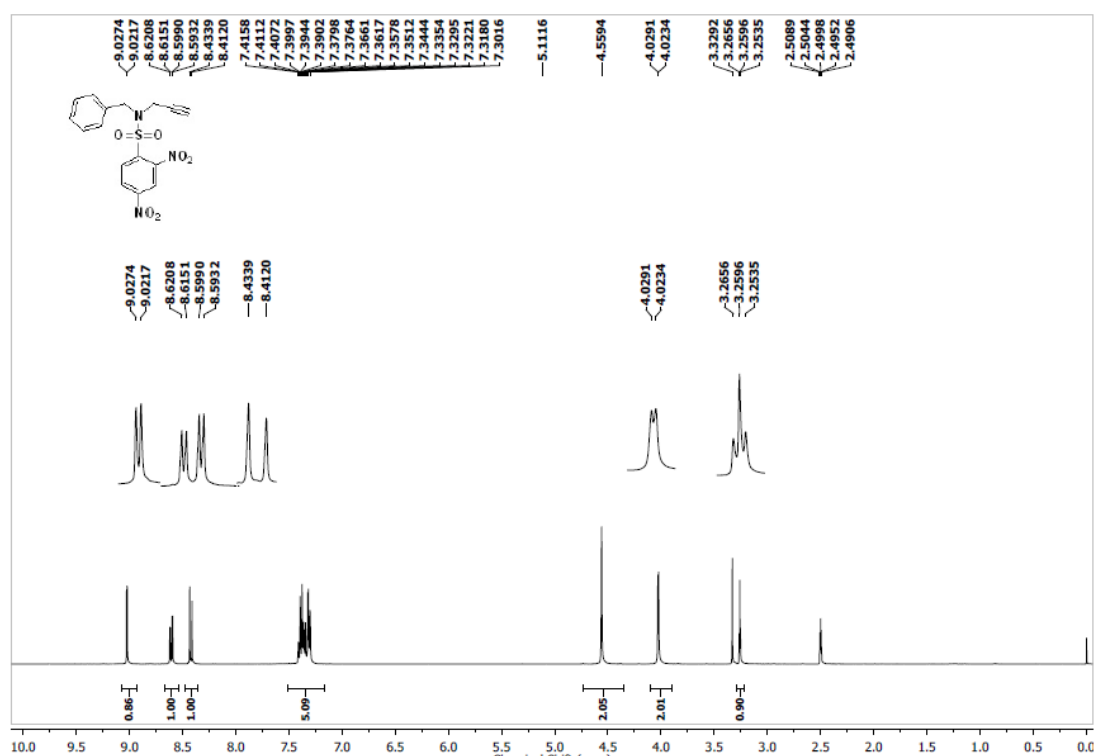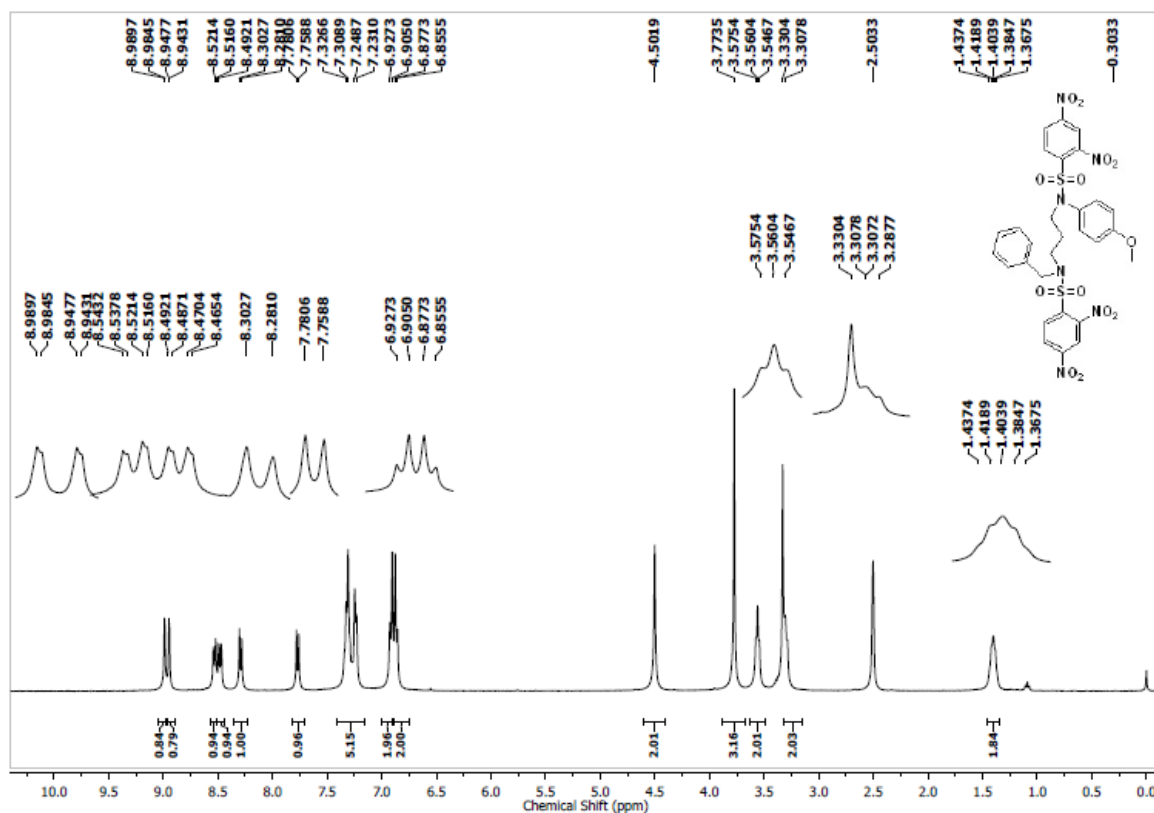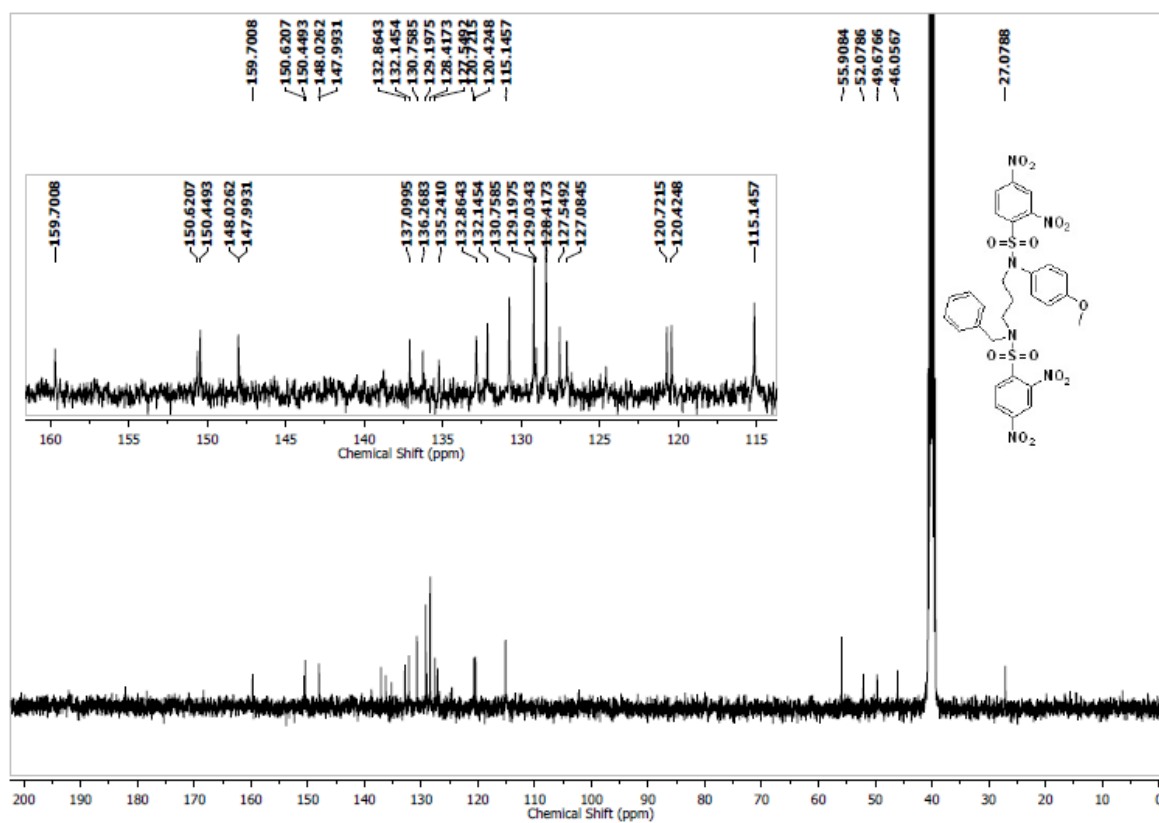

^{13}C NMR Spectrum (100 MHz, CDCl$_3$) of **1c**
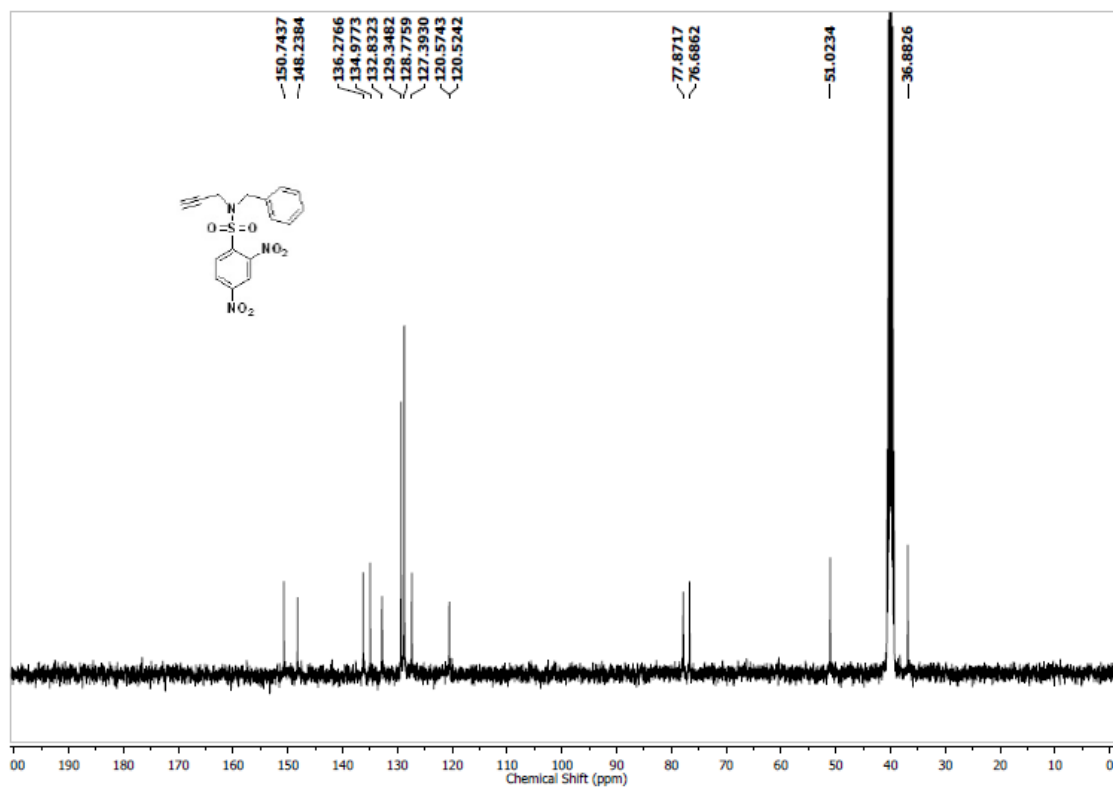
^{1}H NMR Spectrum (400 MHz, CDCl$_3$) of **1d**
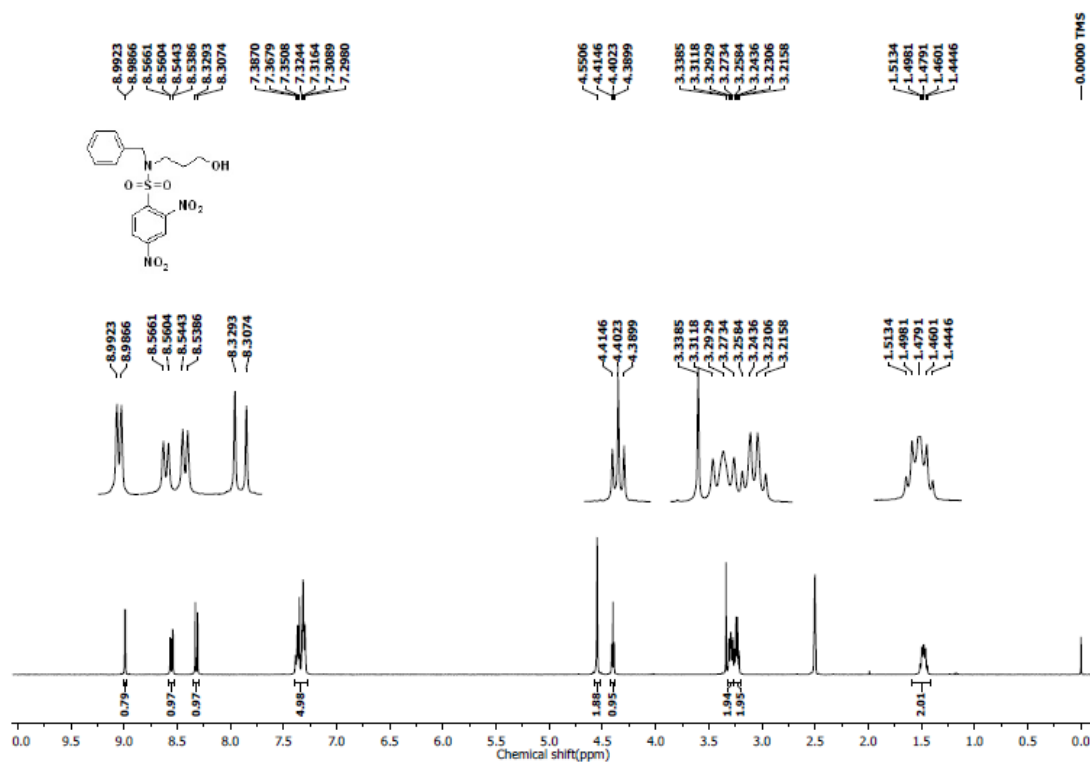
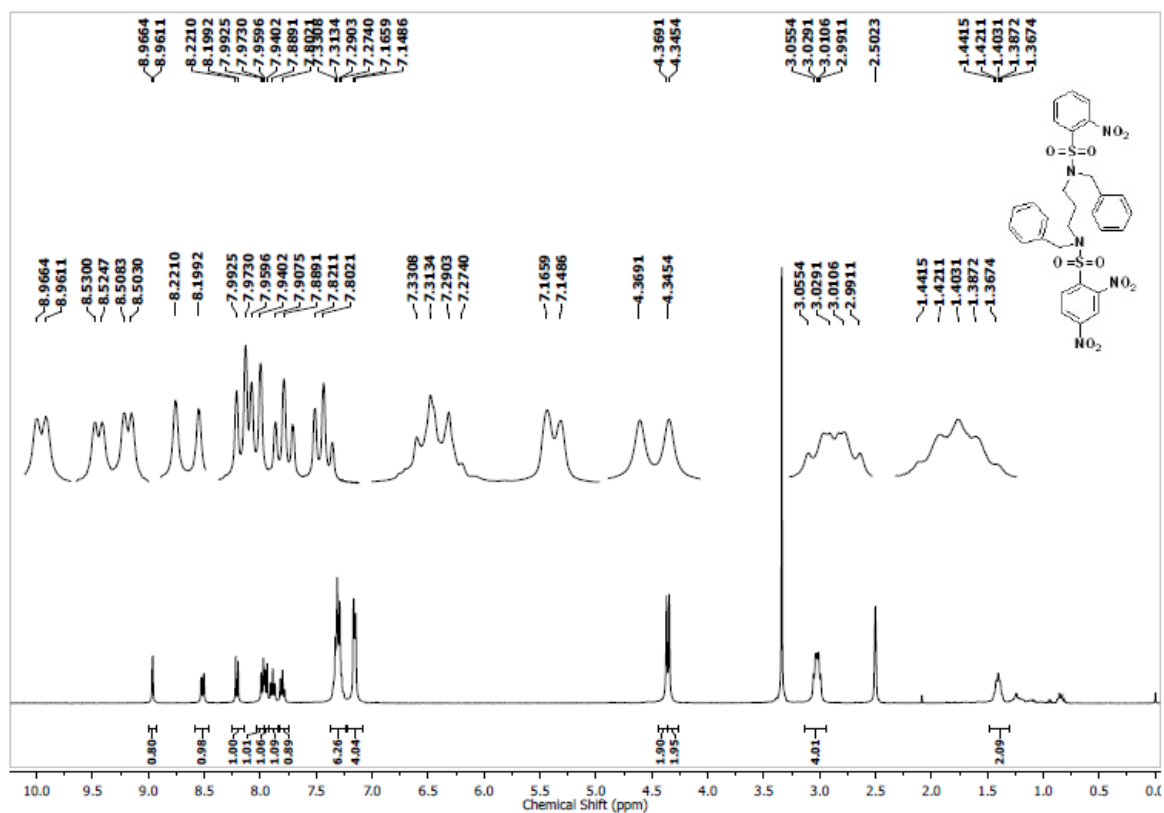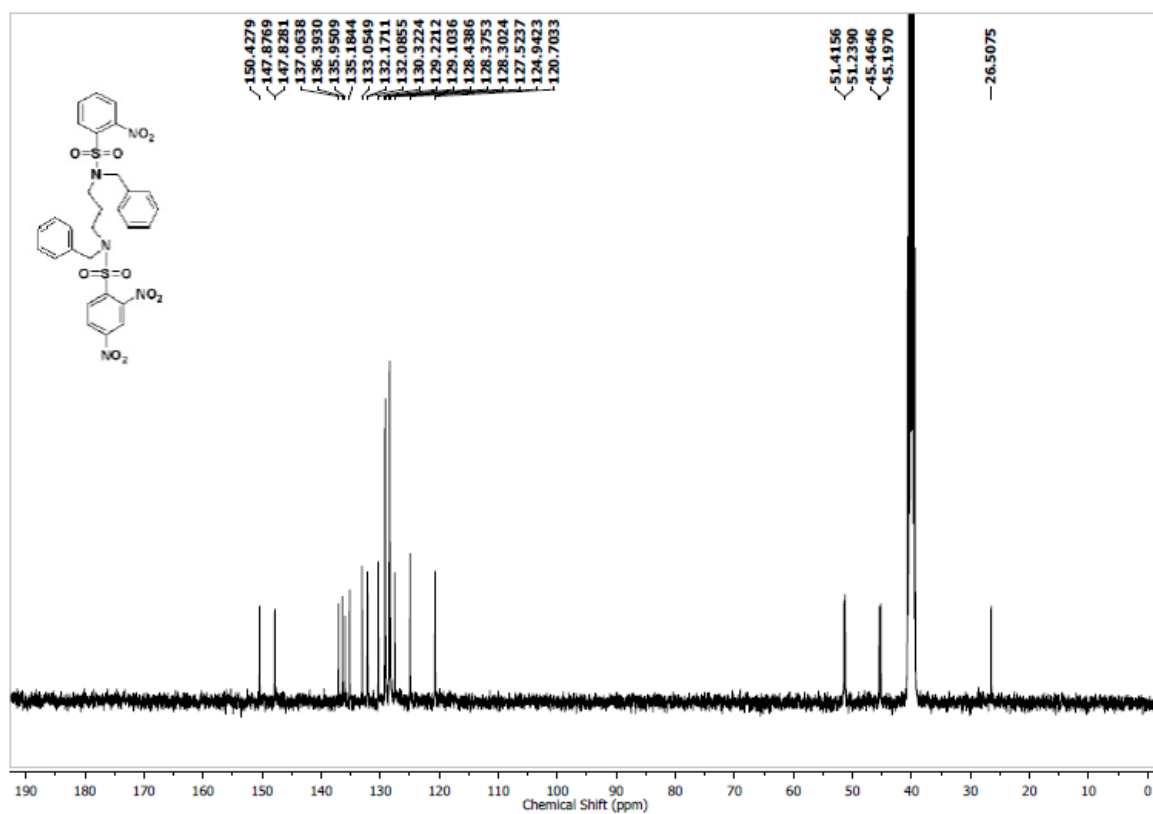^{13}C NMR Spectrum (100 MHz, CDCl$_3$) of **1d**
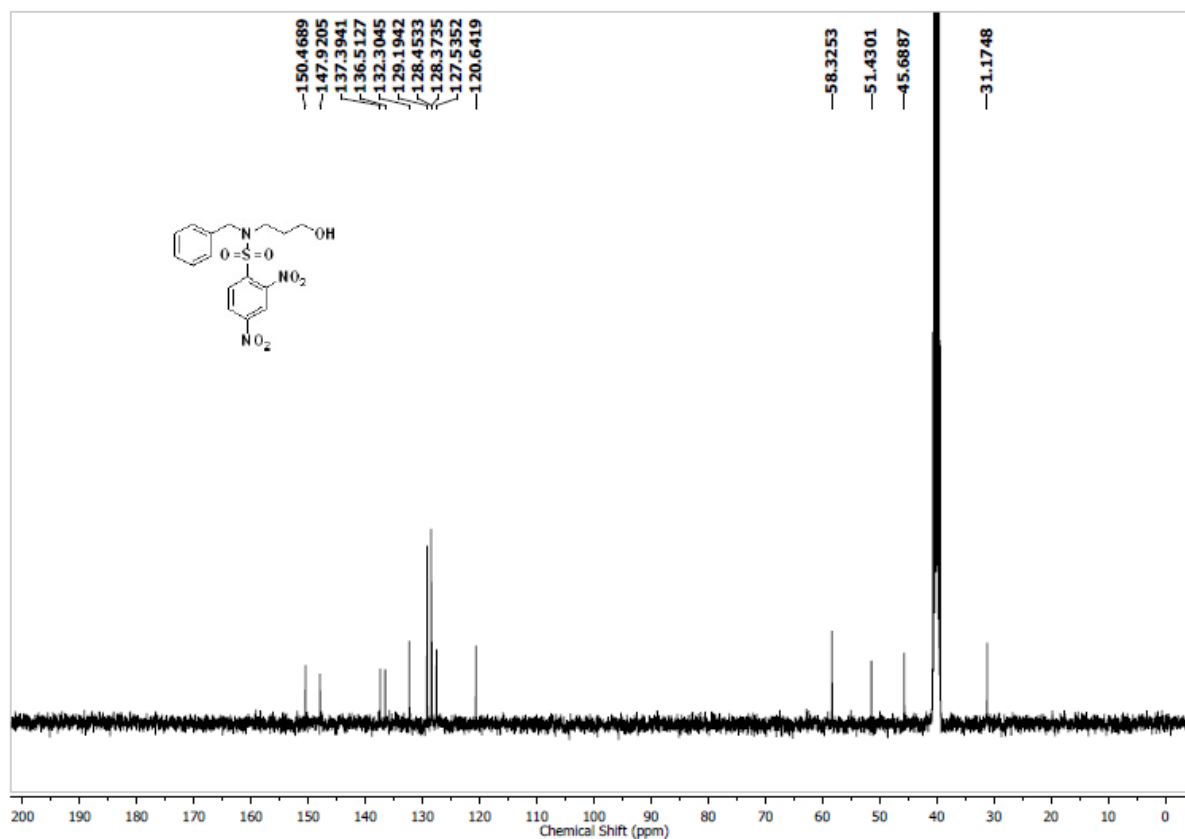
NMR Spectrum (400 MHz, CDCl₃) of **1e**
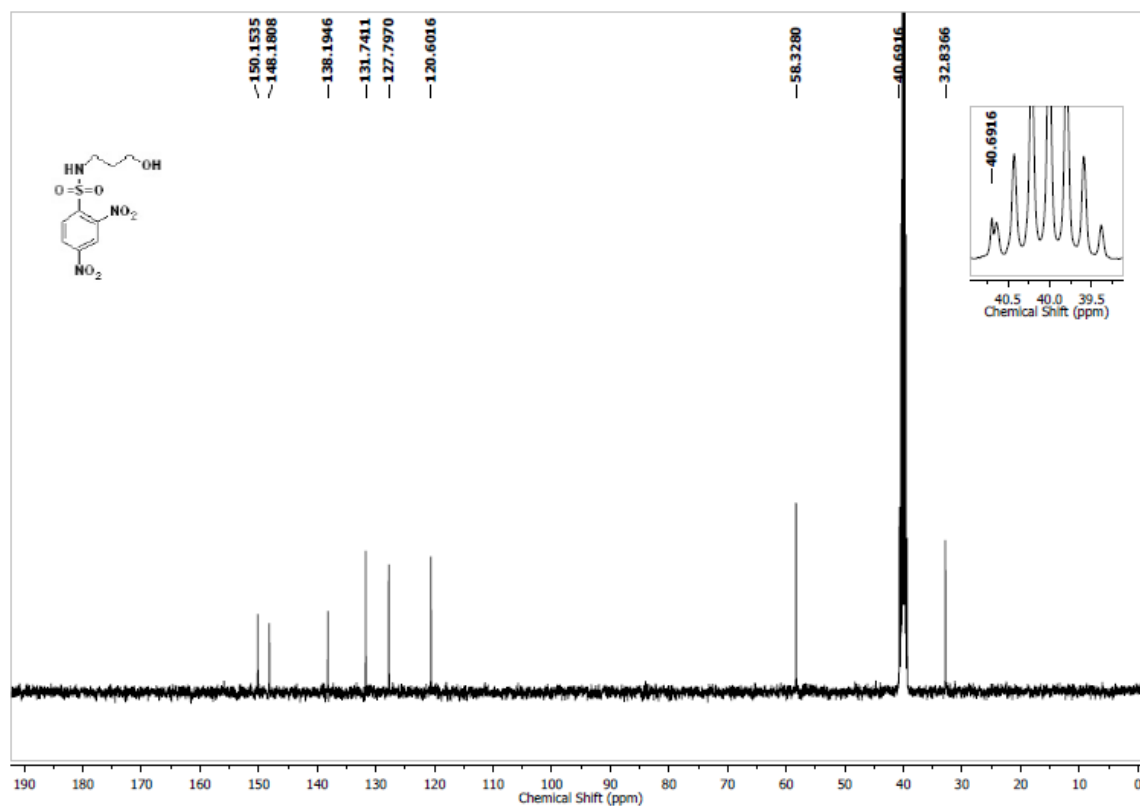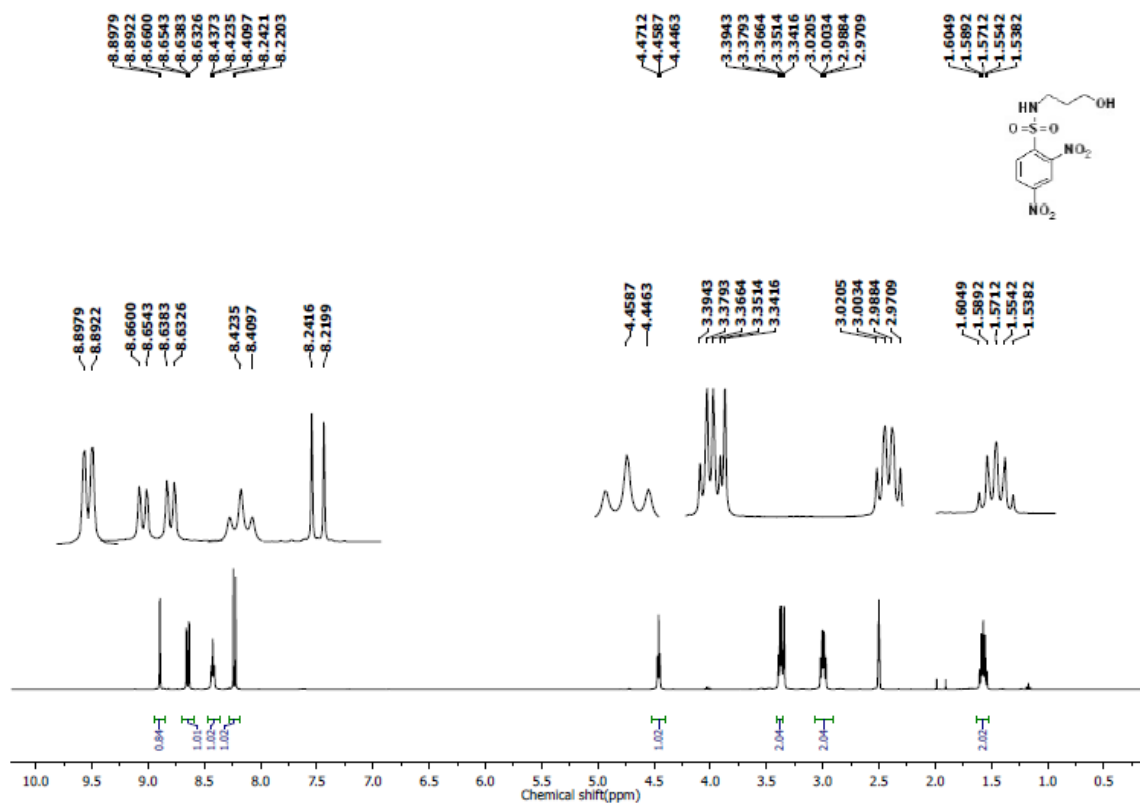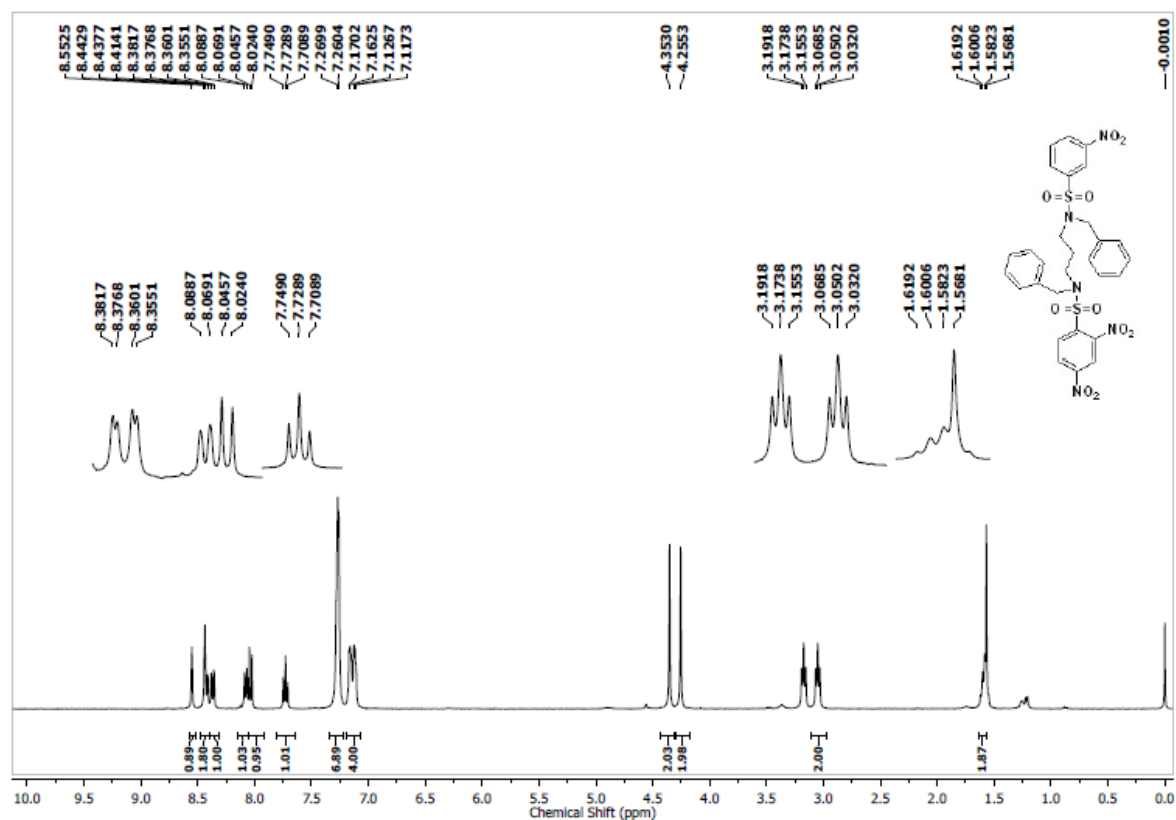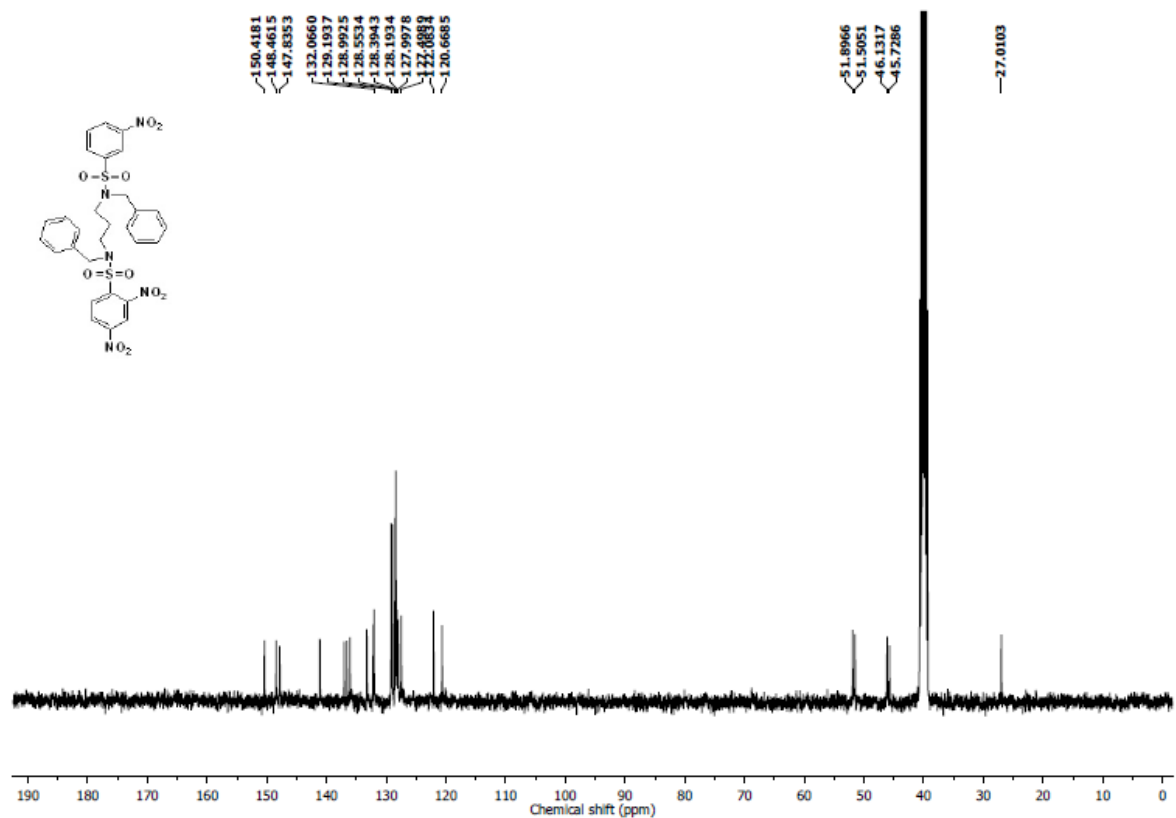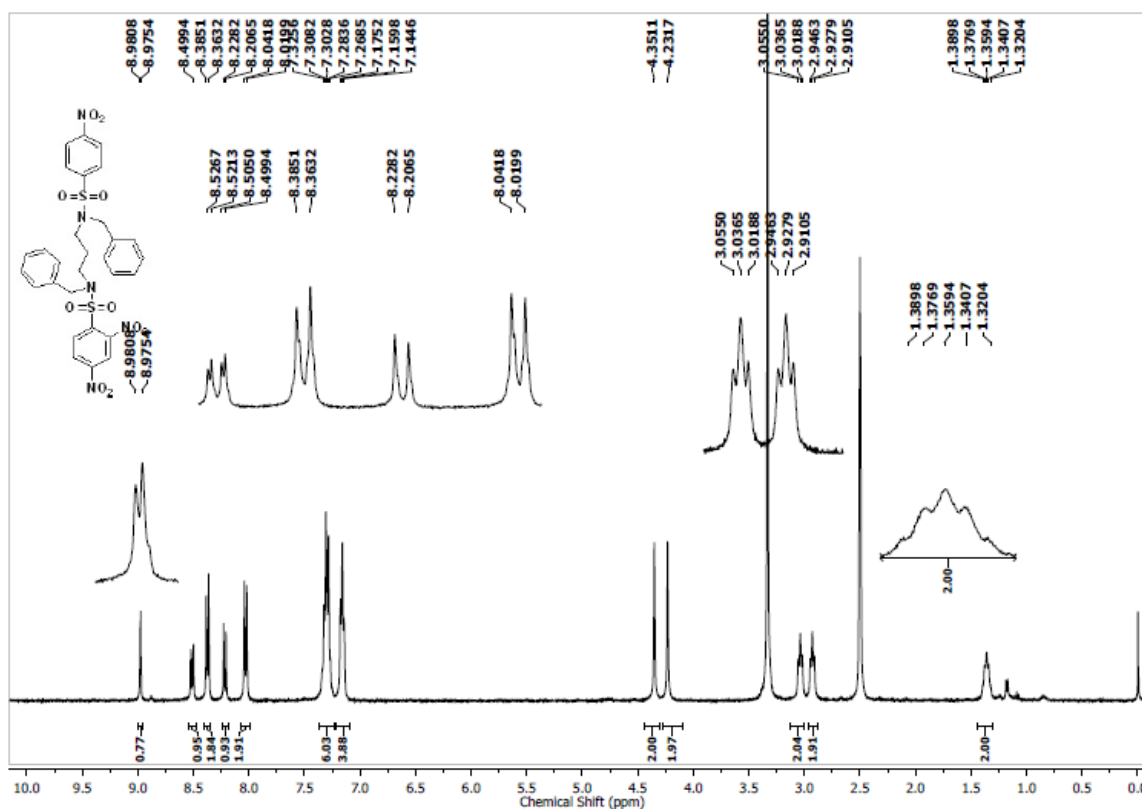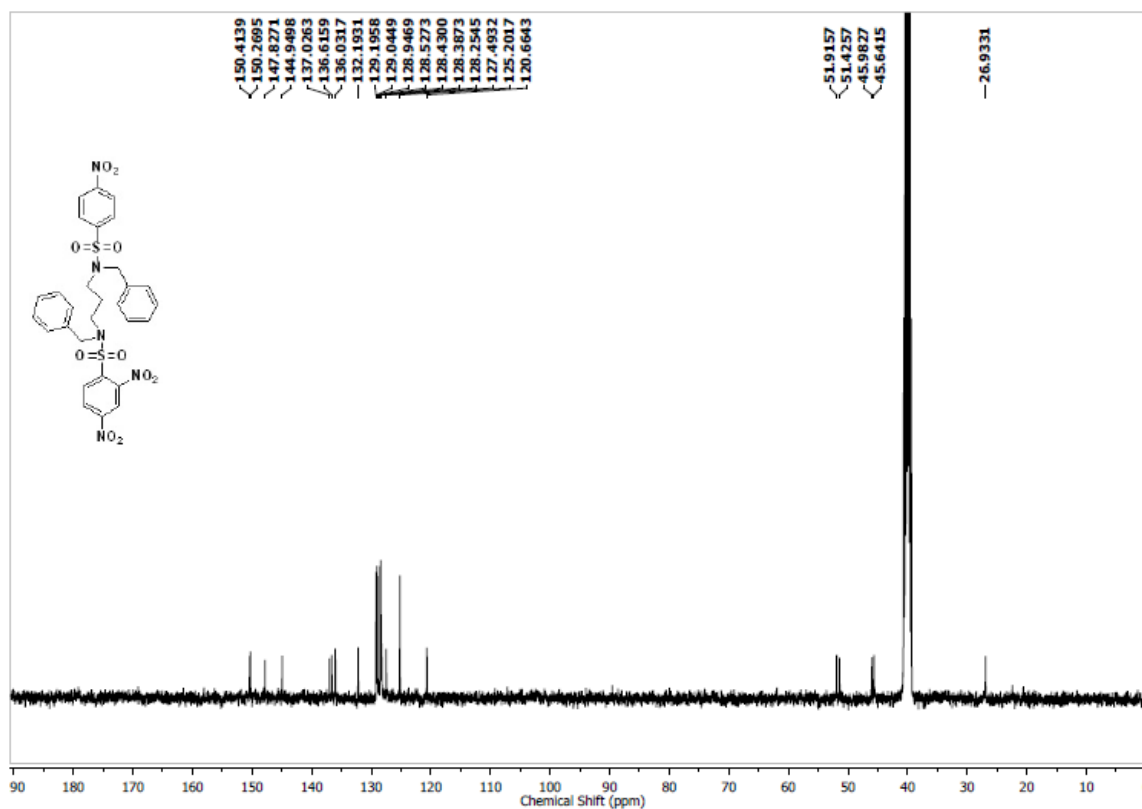
NMR Spectrum (400 MHz, CDCl$_3$) of **2b**
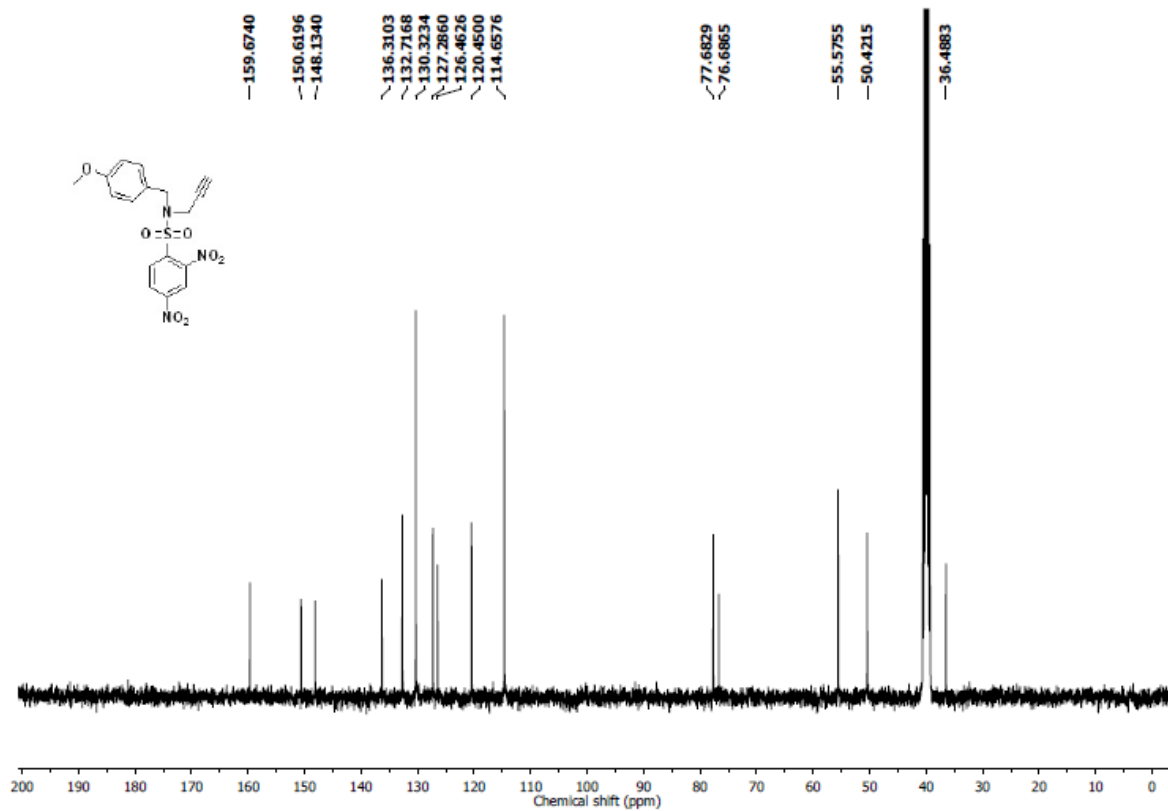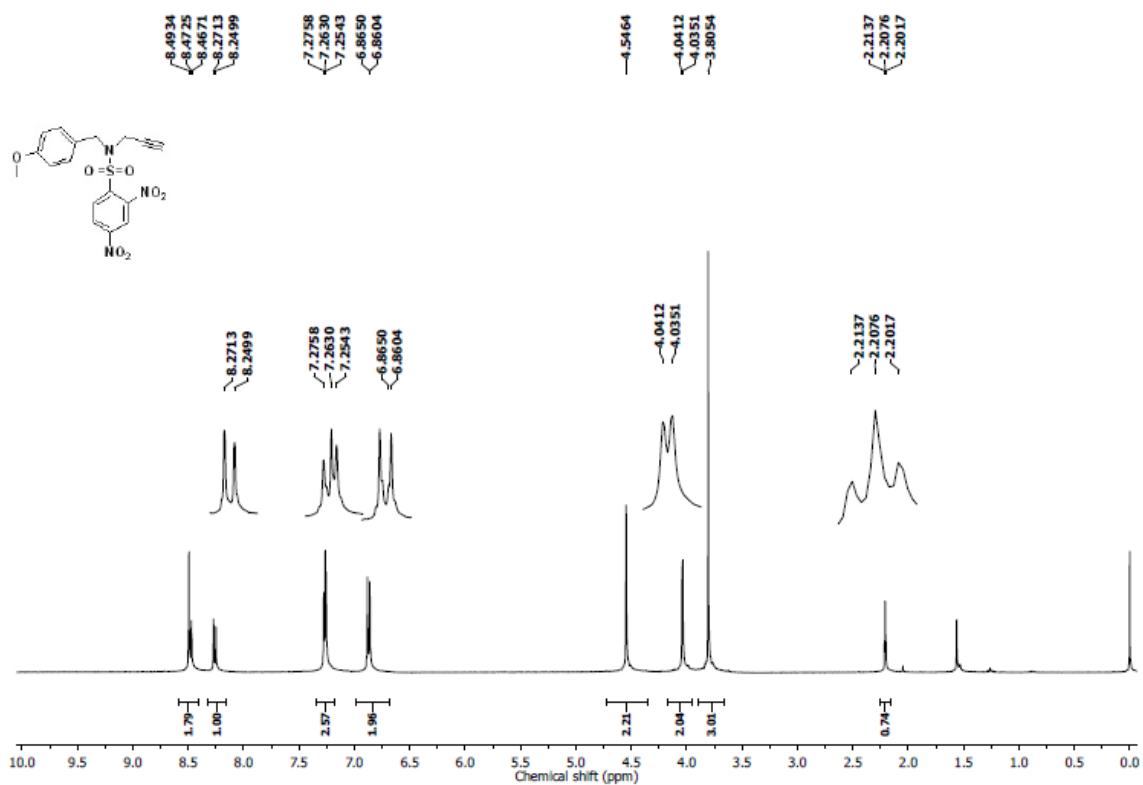
NMR Spectrum (400 MHz, CDCl₃) of **3e**
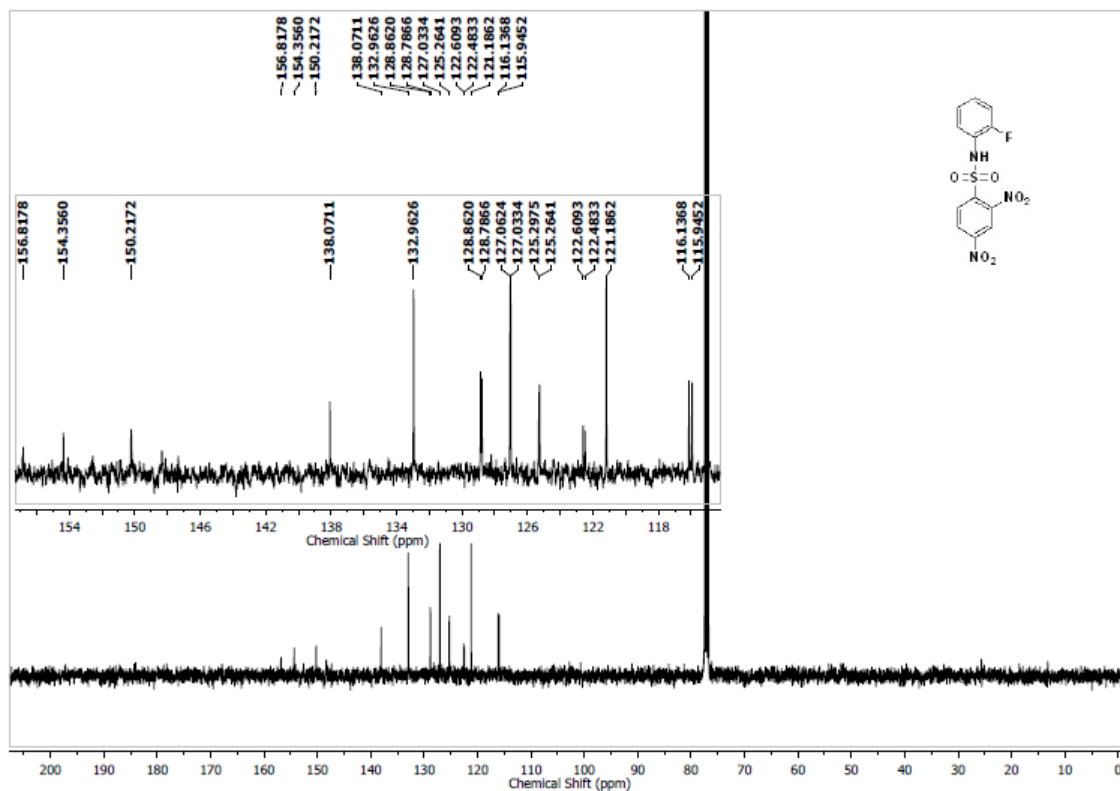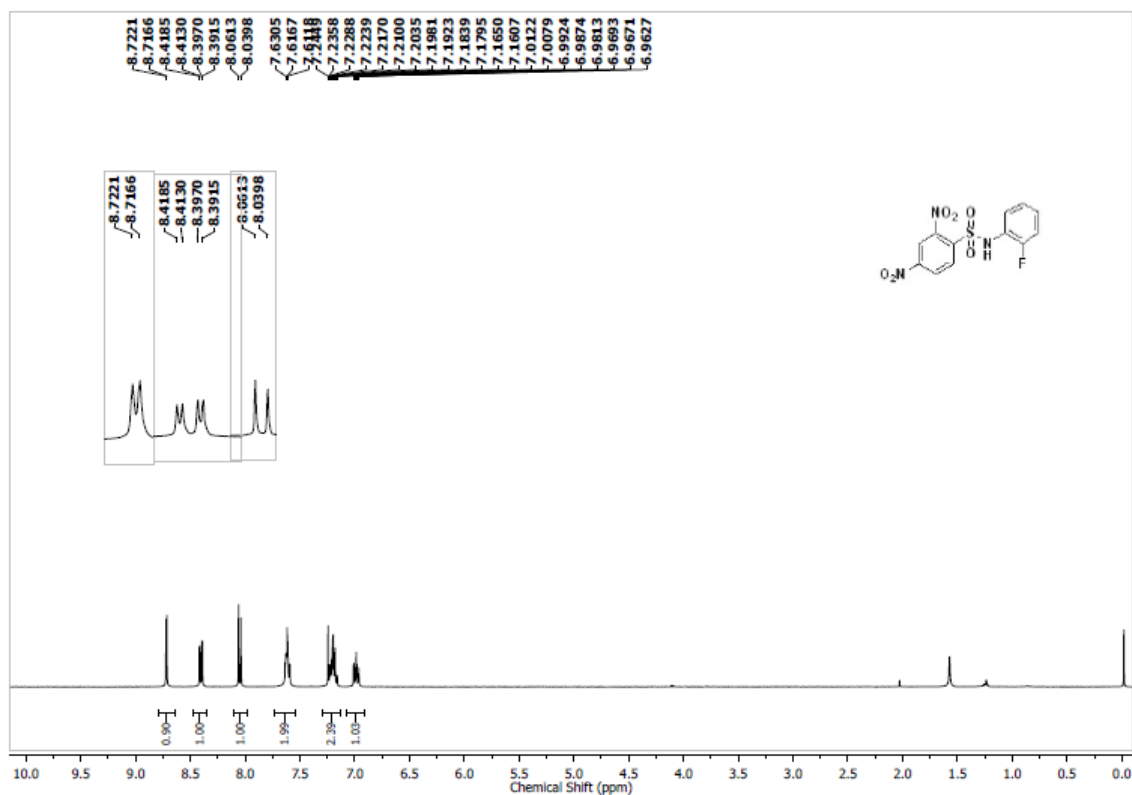
NMR Spectrum (400 MHz, CDCl₃) of **4b**
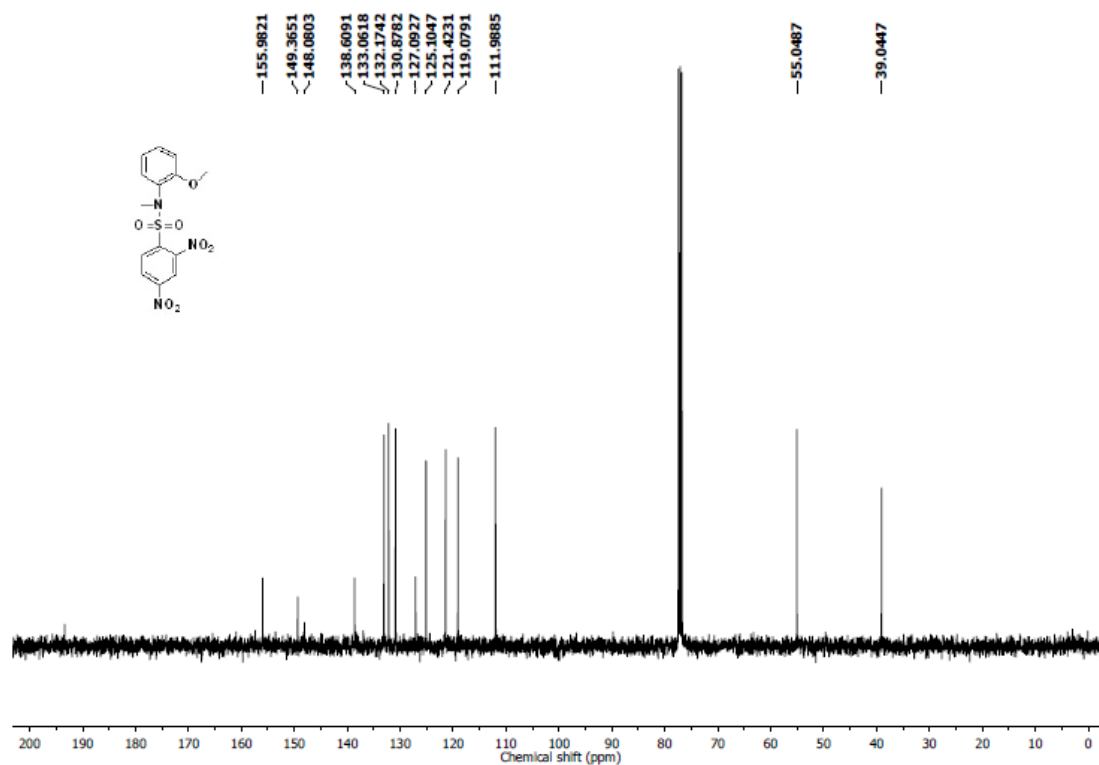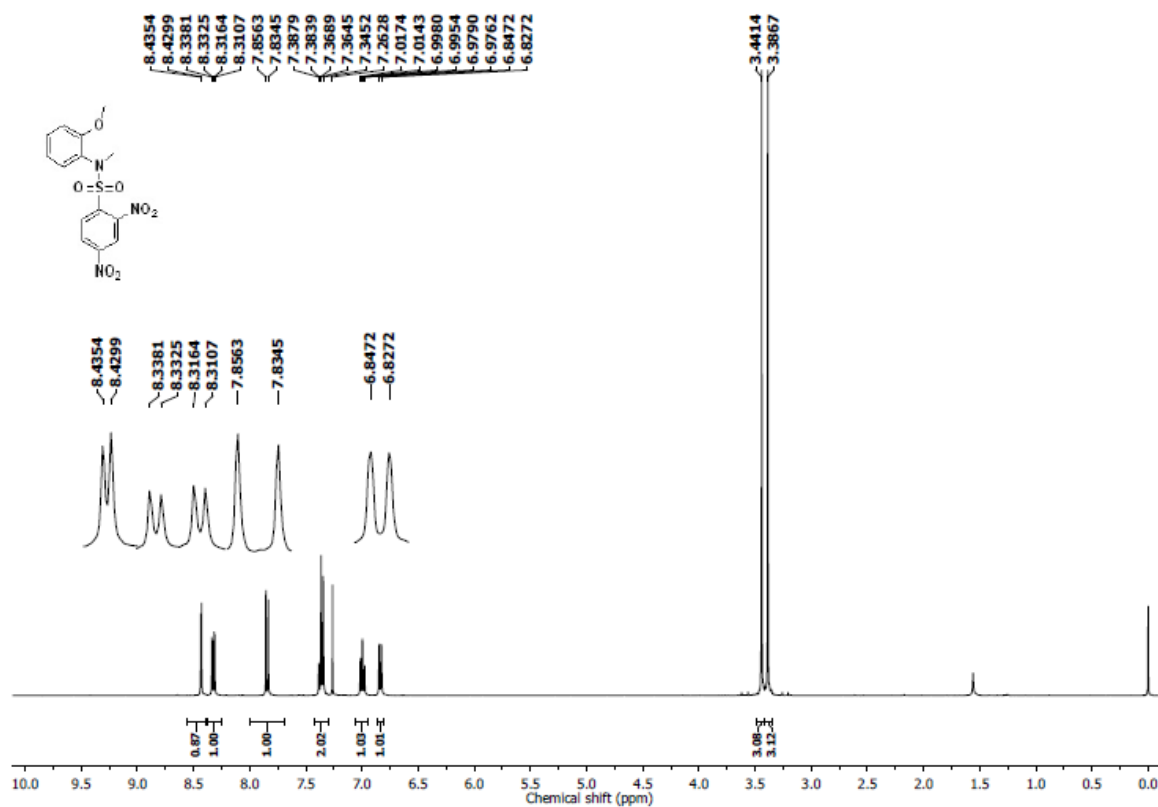
NMR Spectrum (400 MHz, CDCl₃) of **4c.**
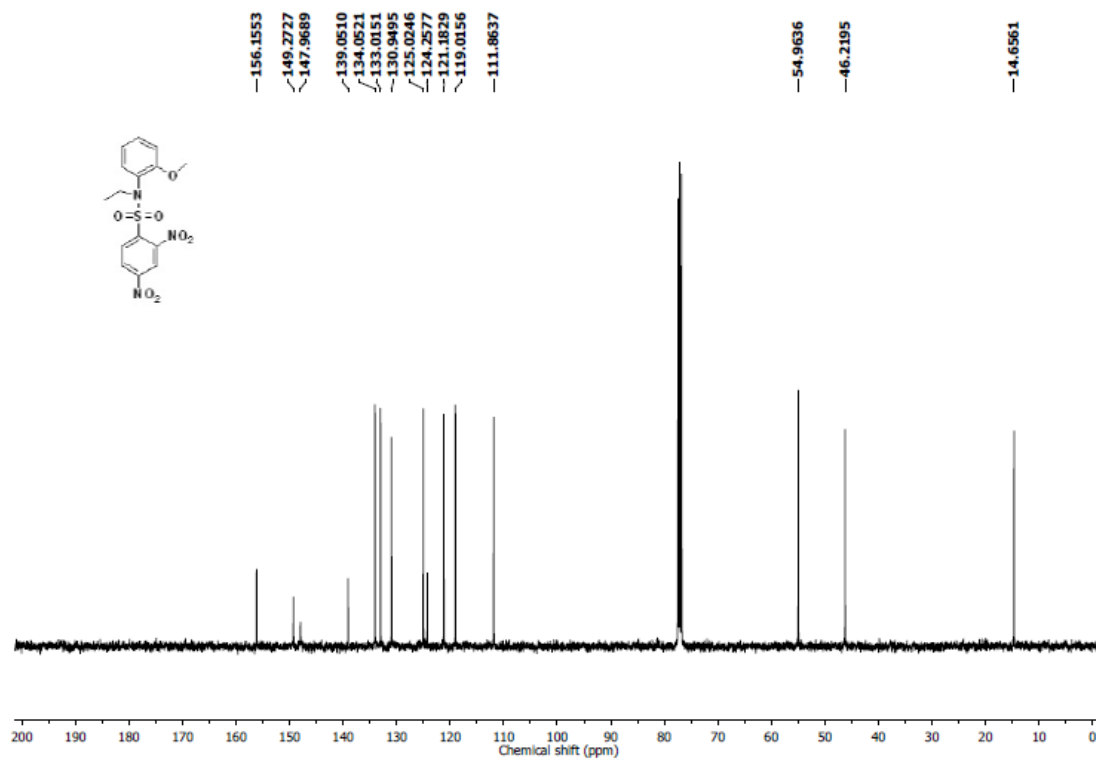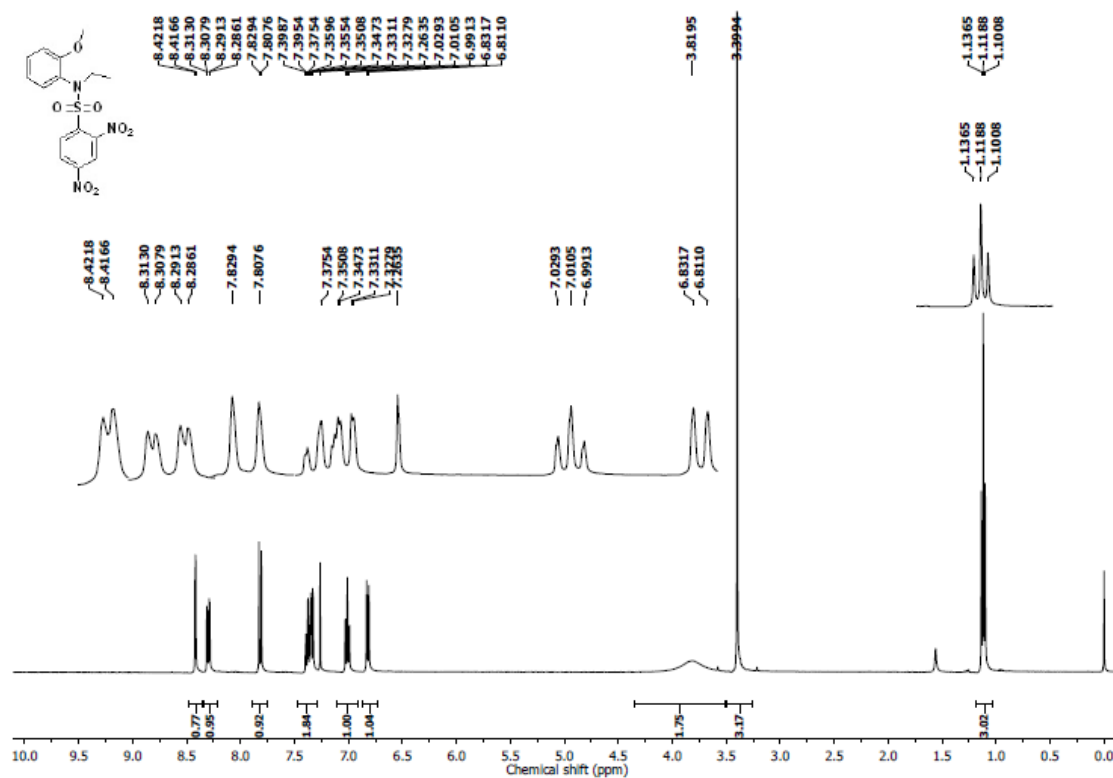
NMR Spectrum (400 MHz, CDCl$_3$) of **4d**
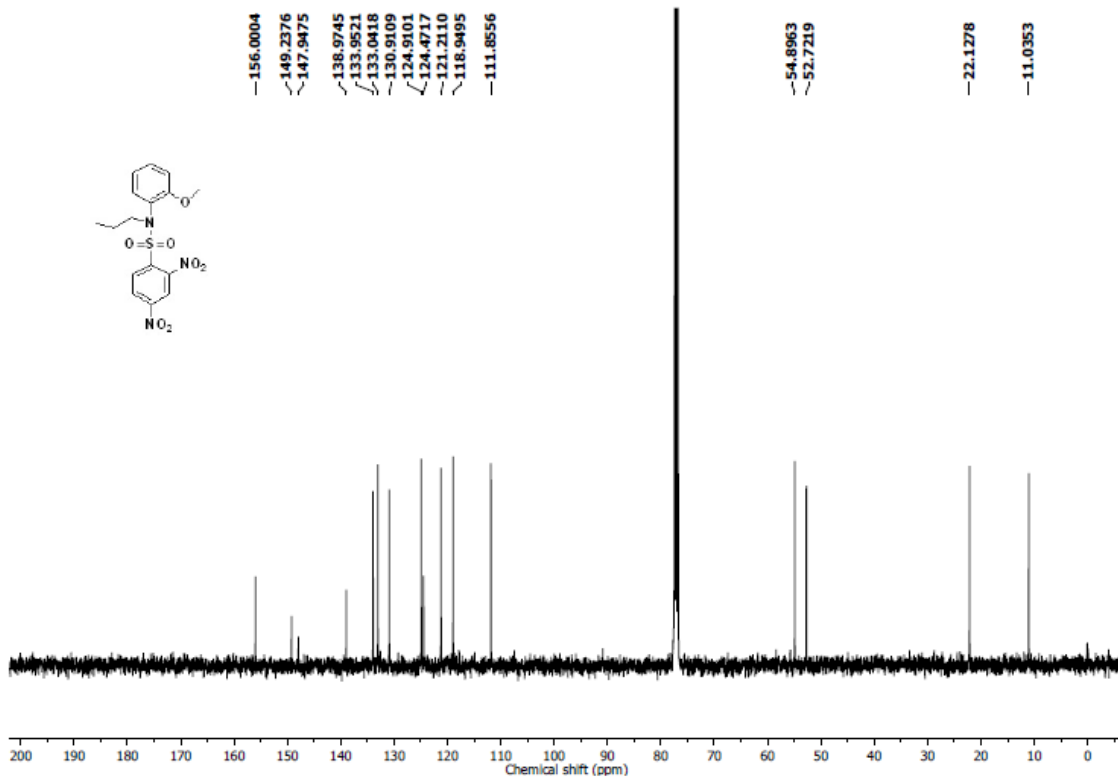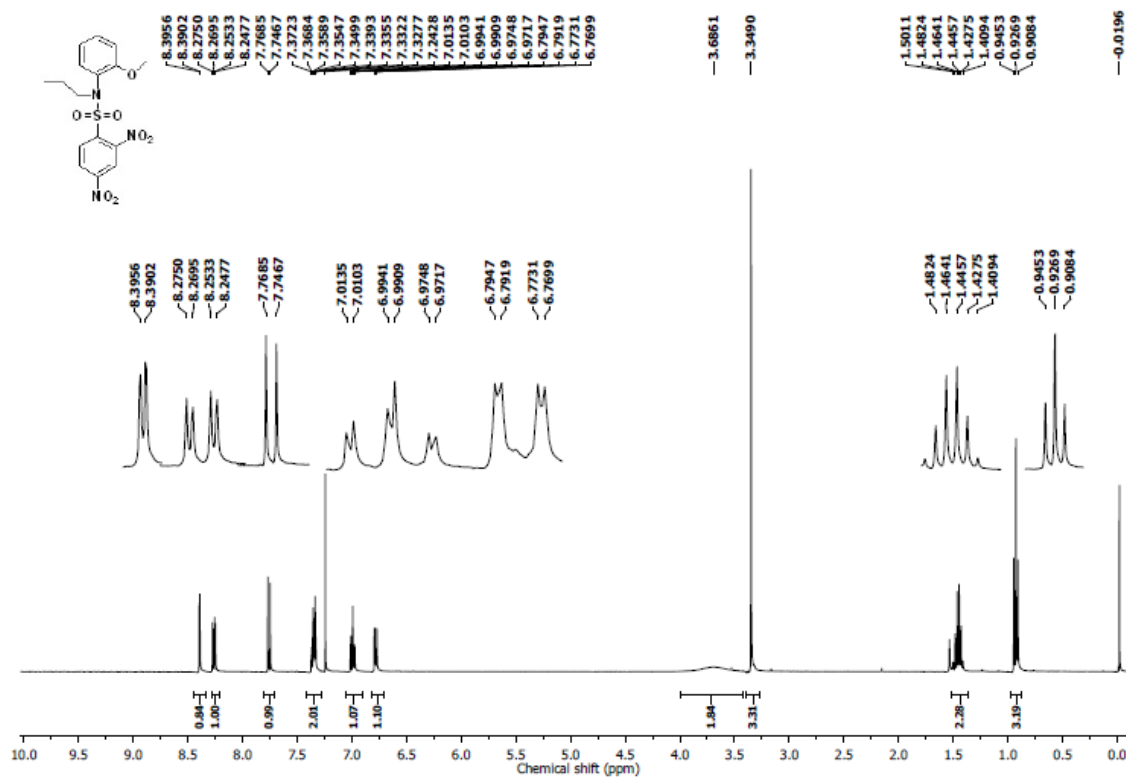
NMR Spectrum (400 MHz, CDCl$_3$) of **4e**
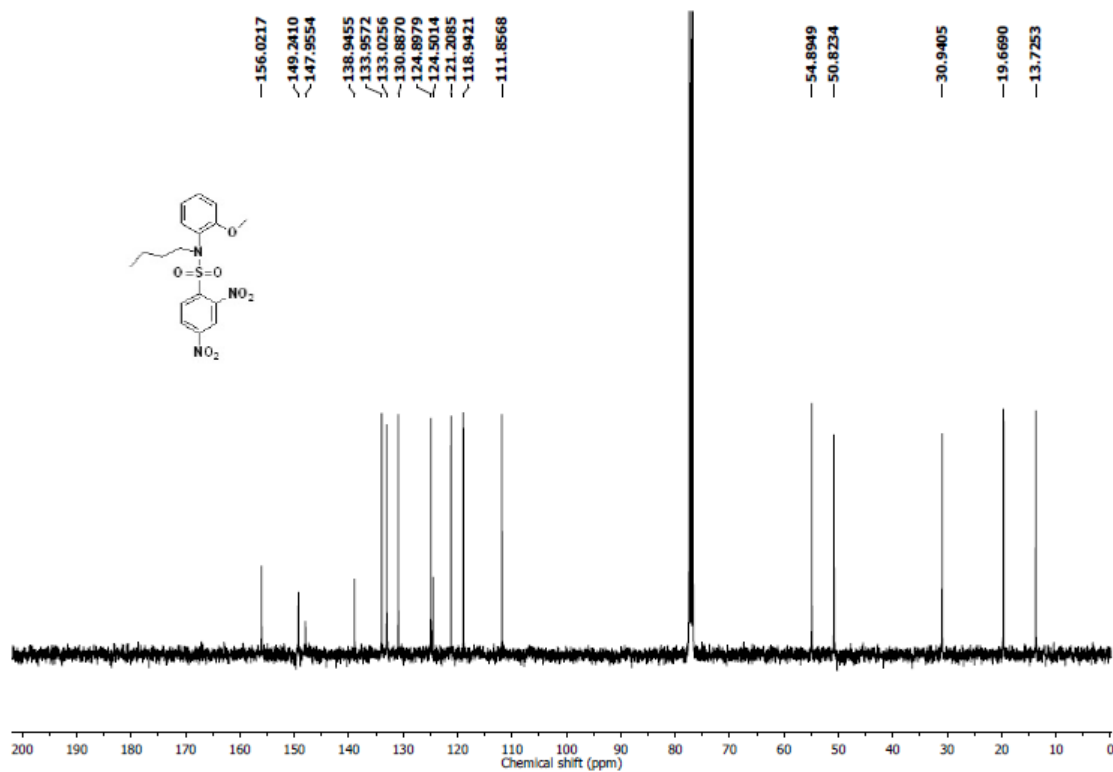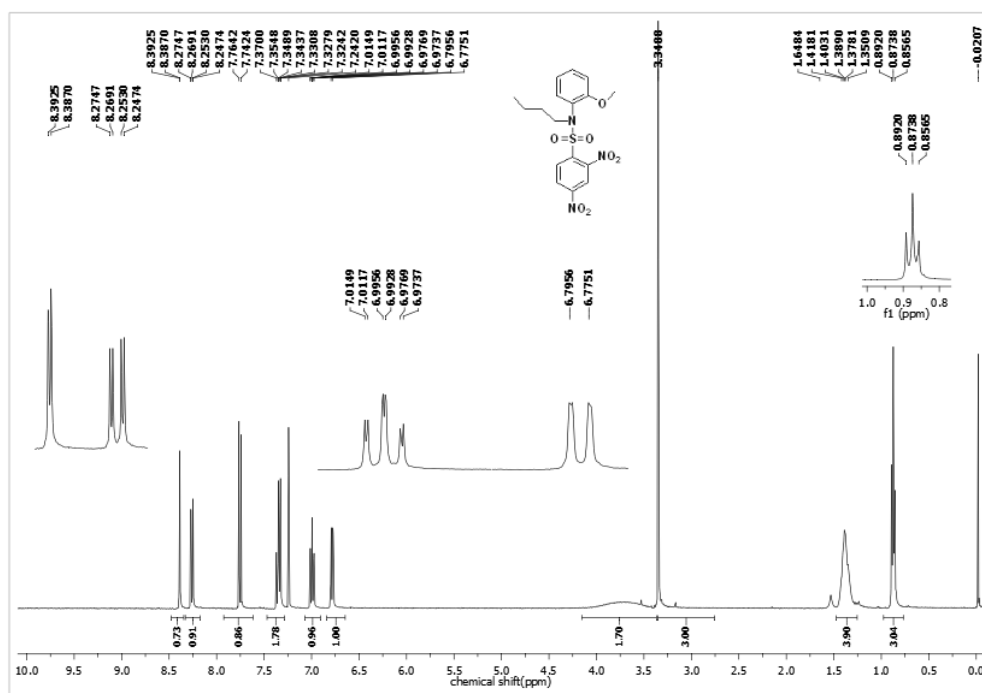
NMR Spectrum (400 MHz, CDCl₃) of **4f**
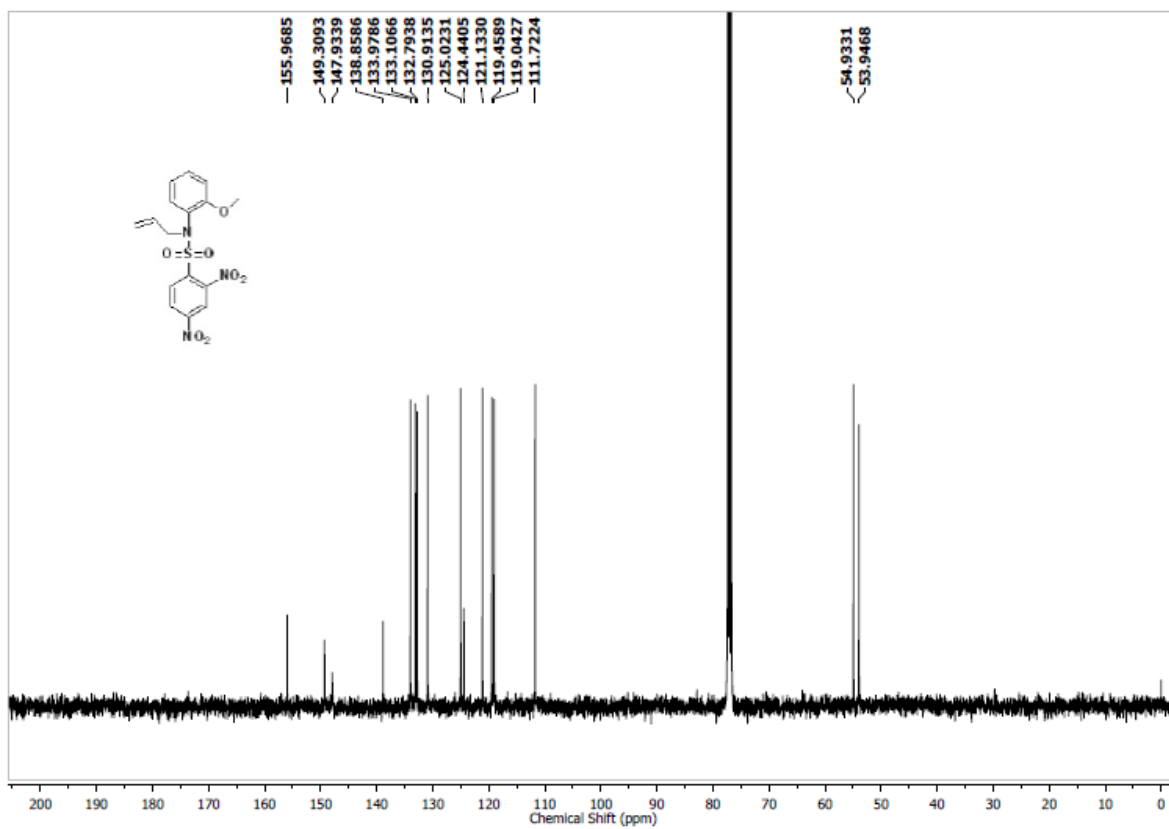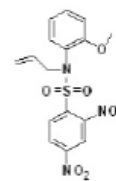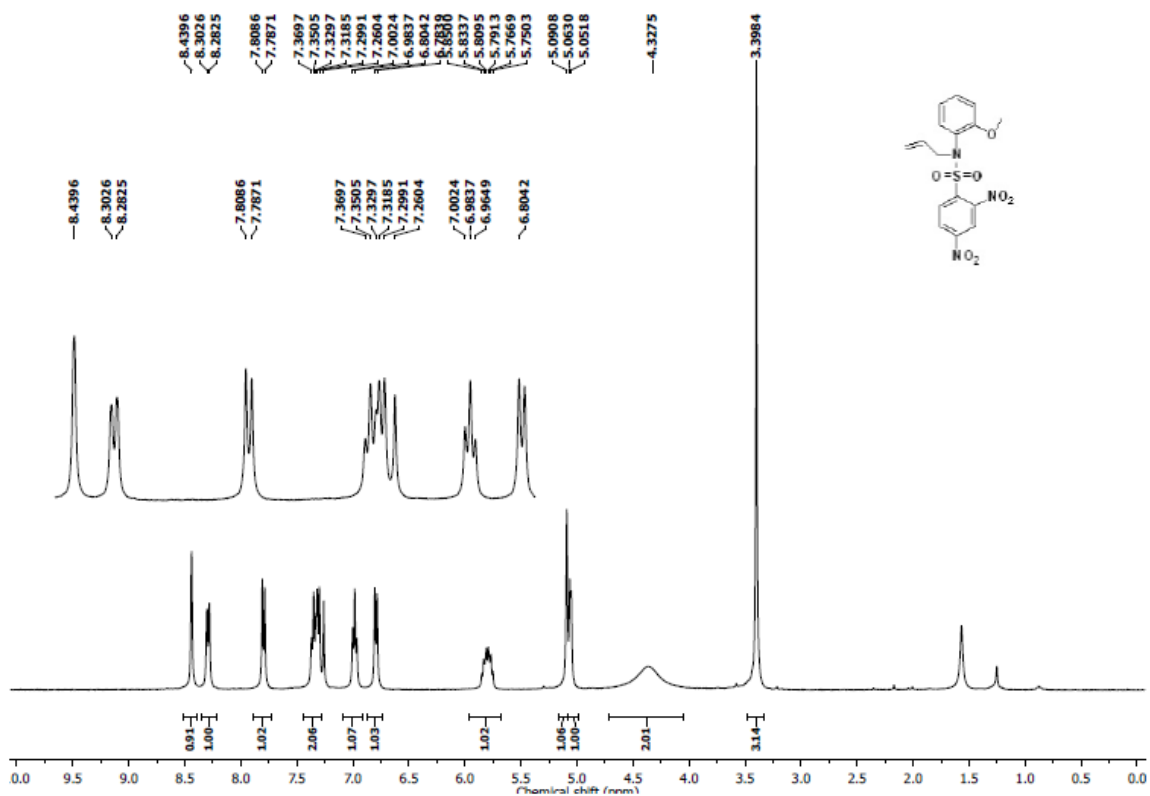
¹H NMR Spectrum (400 MHz, CDCl₃) of **4g**
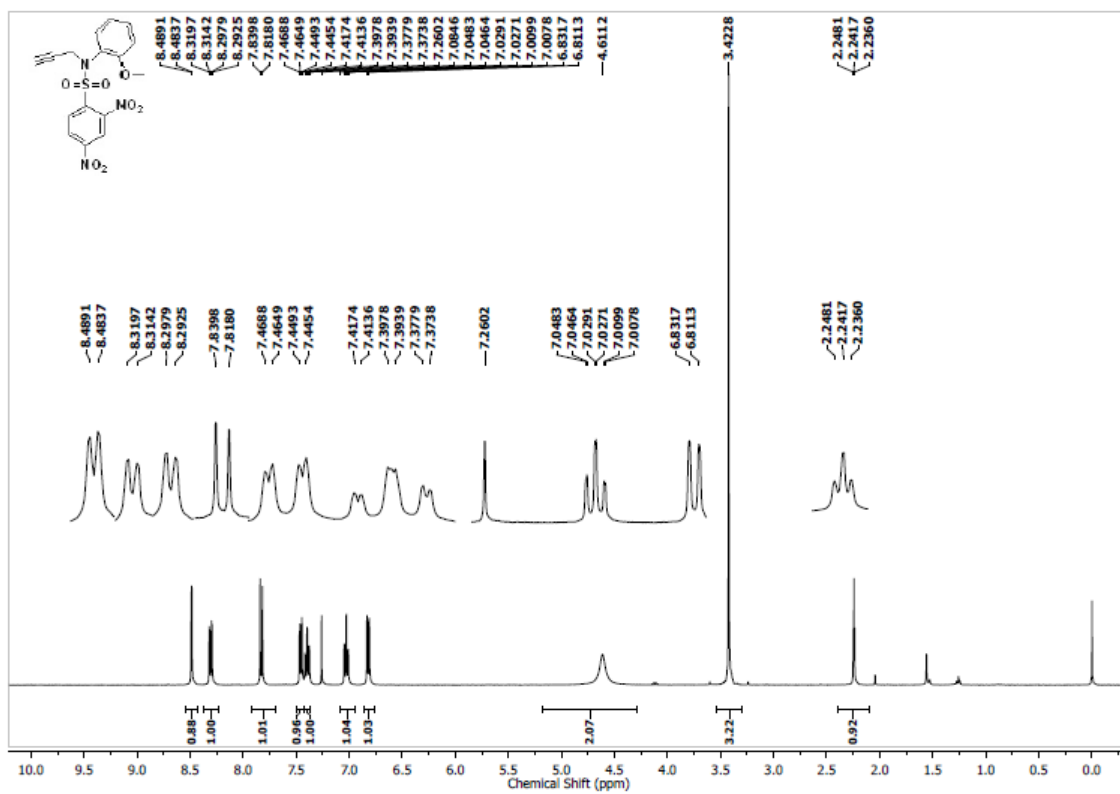
¹³C NMR Spectrum (100 MHz, CDCl₃) of **4g**
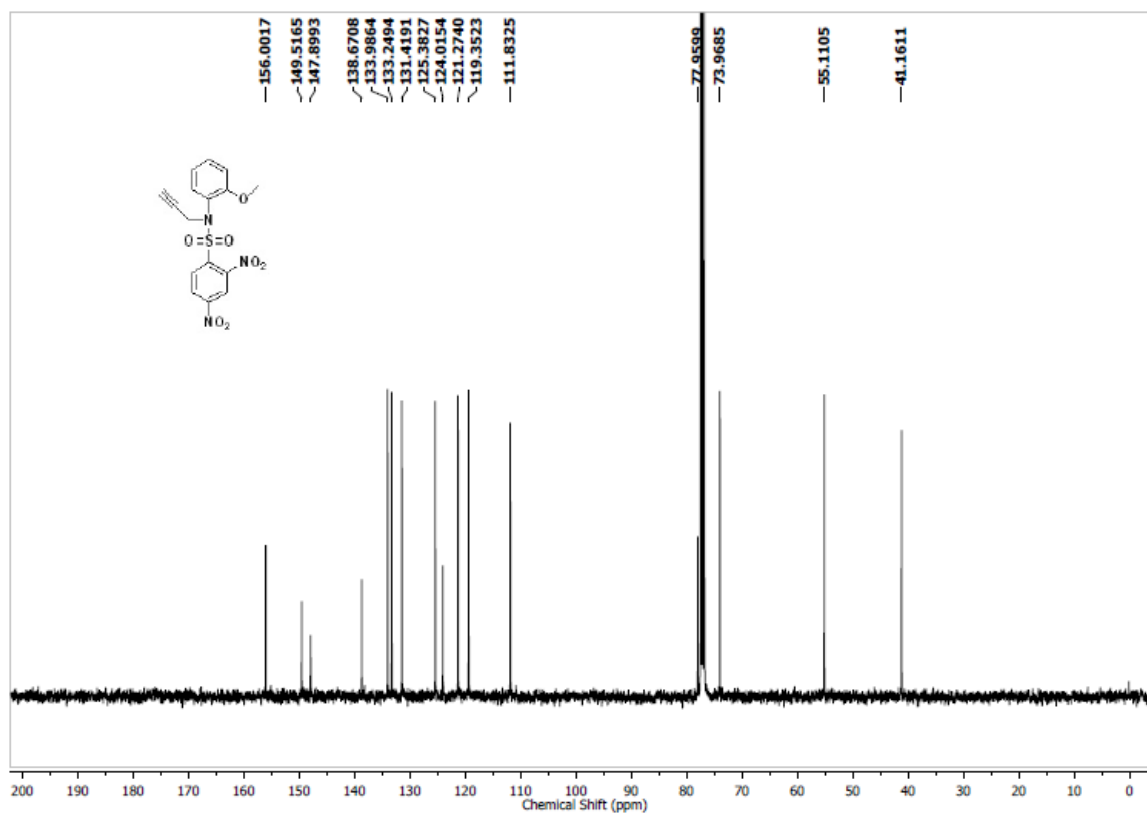
^{1}H NMR Spectrum (400 MHz, CDCl$_3$) of **4h**
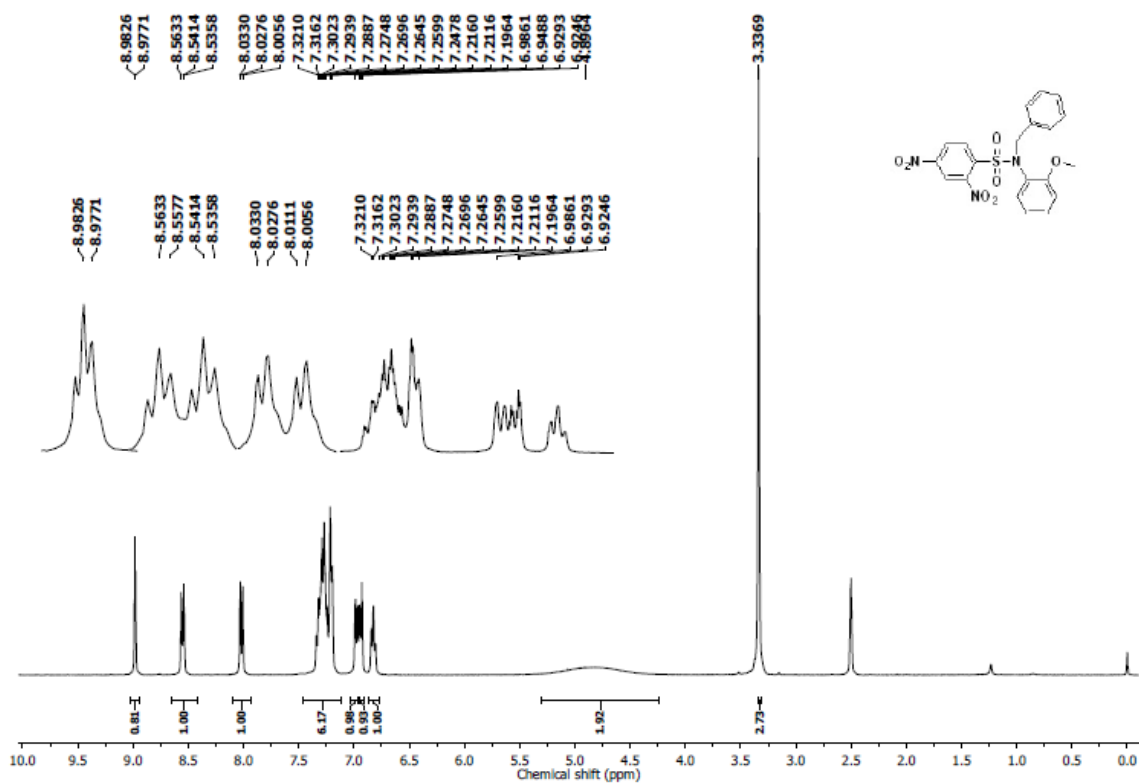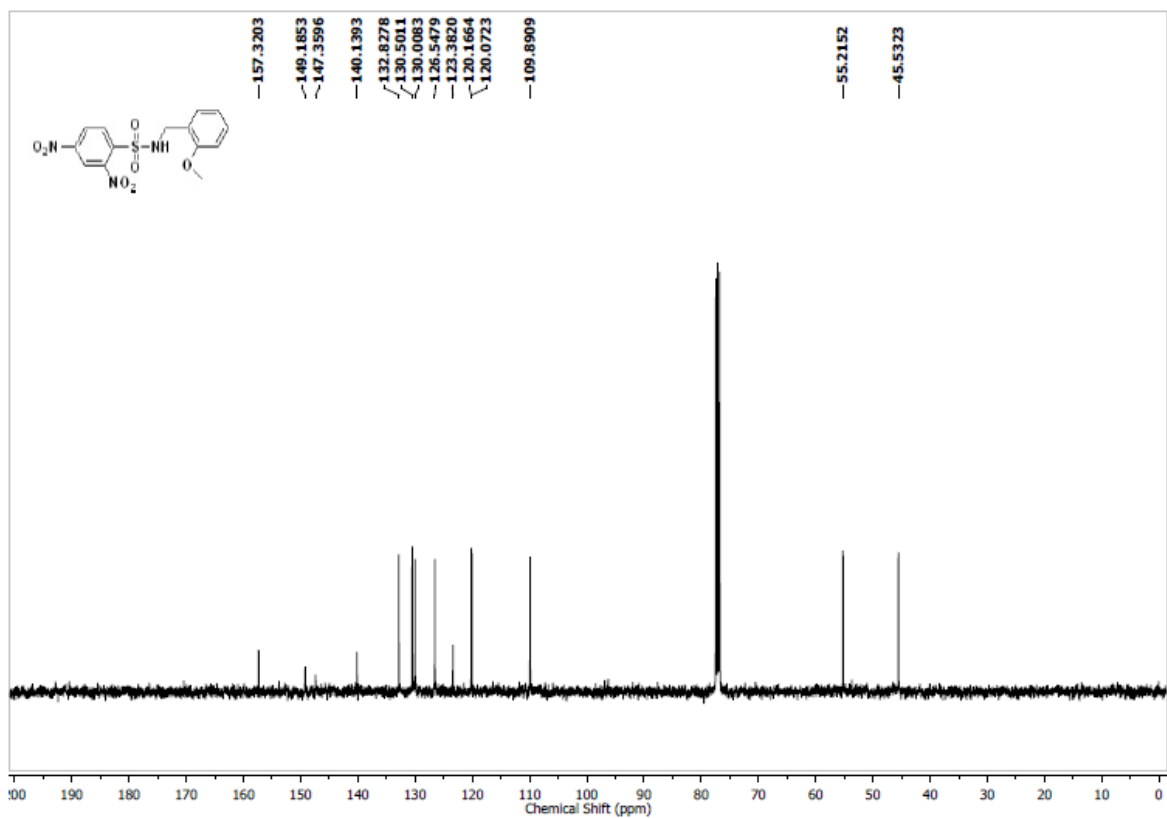

^{13}C NMR Spectrum (100 MHz, CDCl$_3$) of **4h**
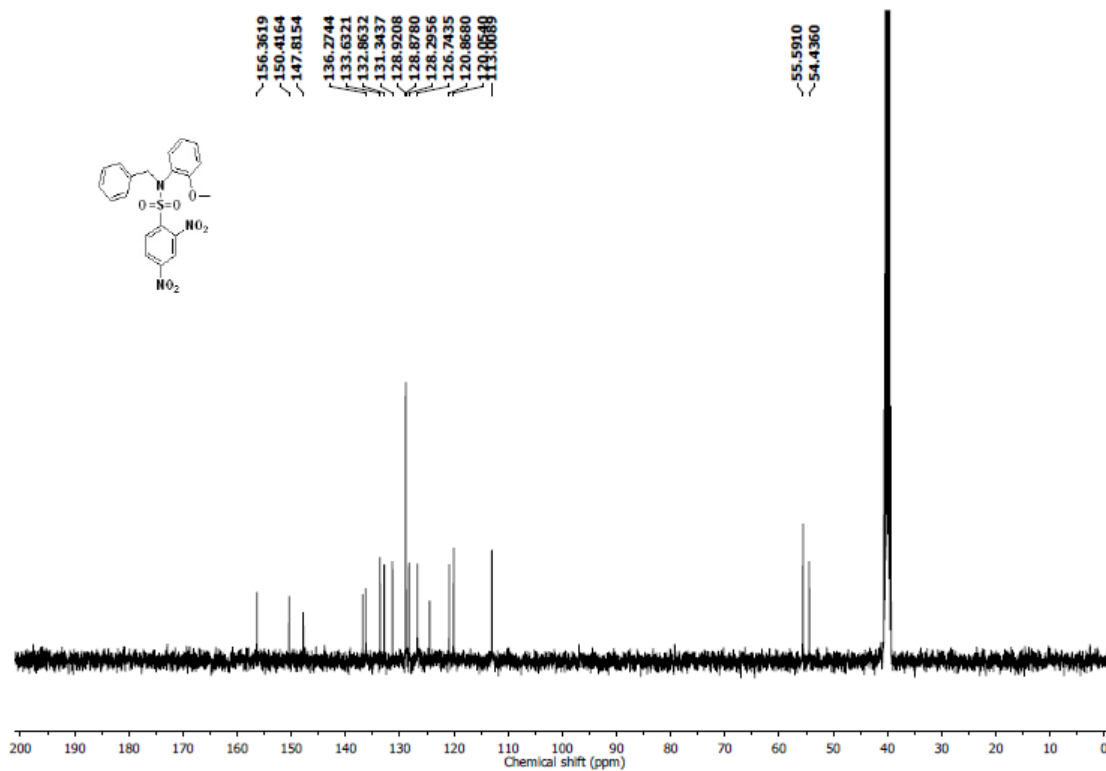
1H NMR Spectrum (400 MHz, CDCl$_3$) of **5a**
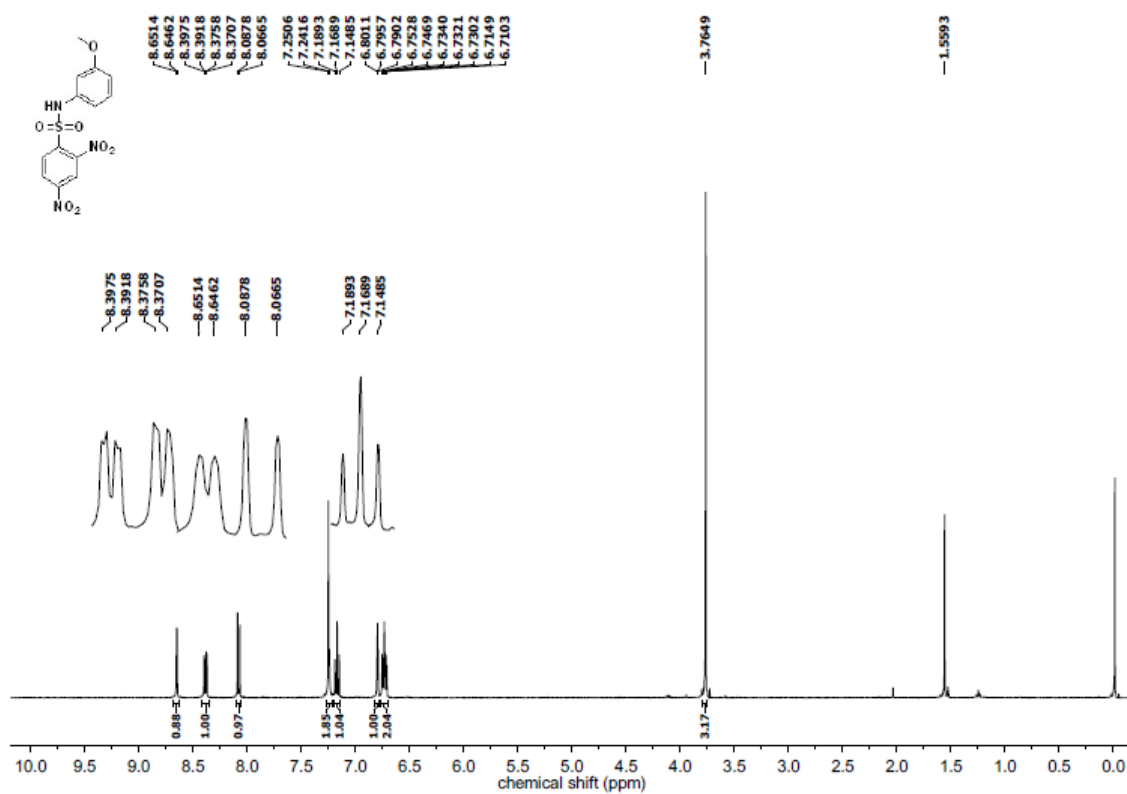
^{13}C NMR Spectrum (100 MHz, CDCl$_3$) of **5a**
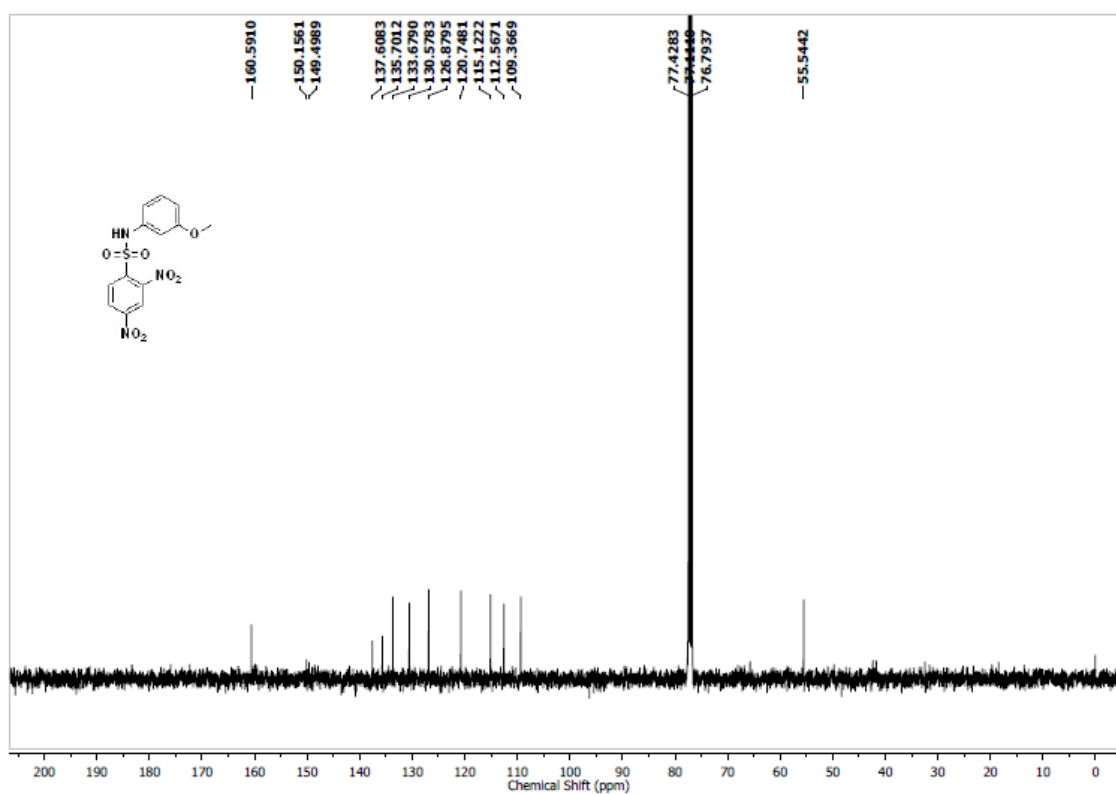
^{1}H NMR Spectrum (400 MHz, CDCl$_3$) of **5b**
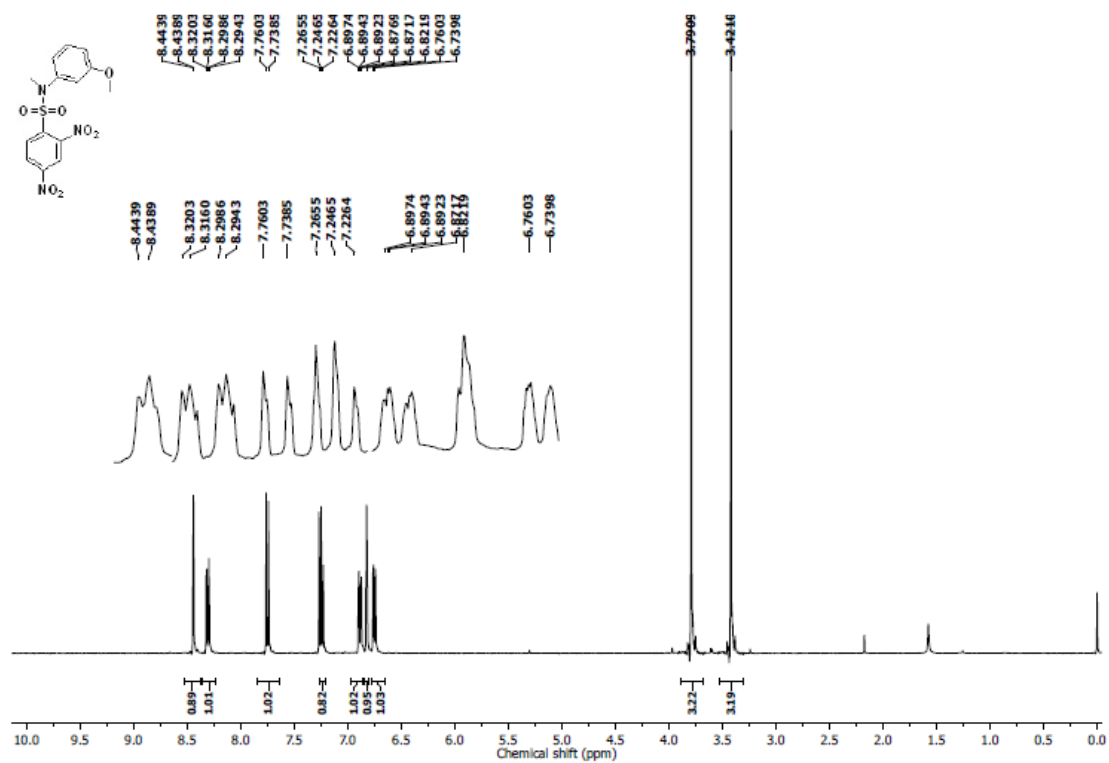
^{13}C NMR Spectrum (100 MHz, CDCl$_3$) of **5b**
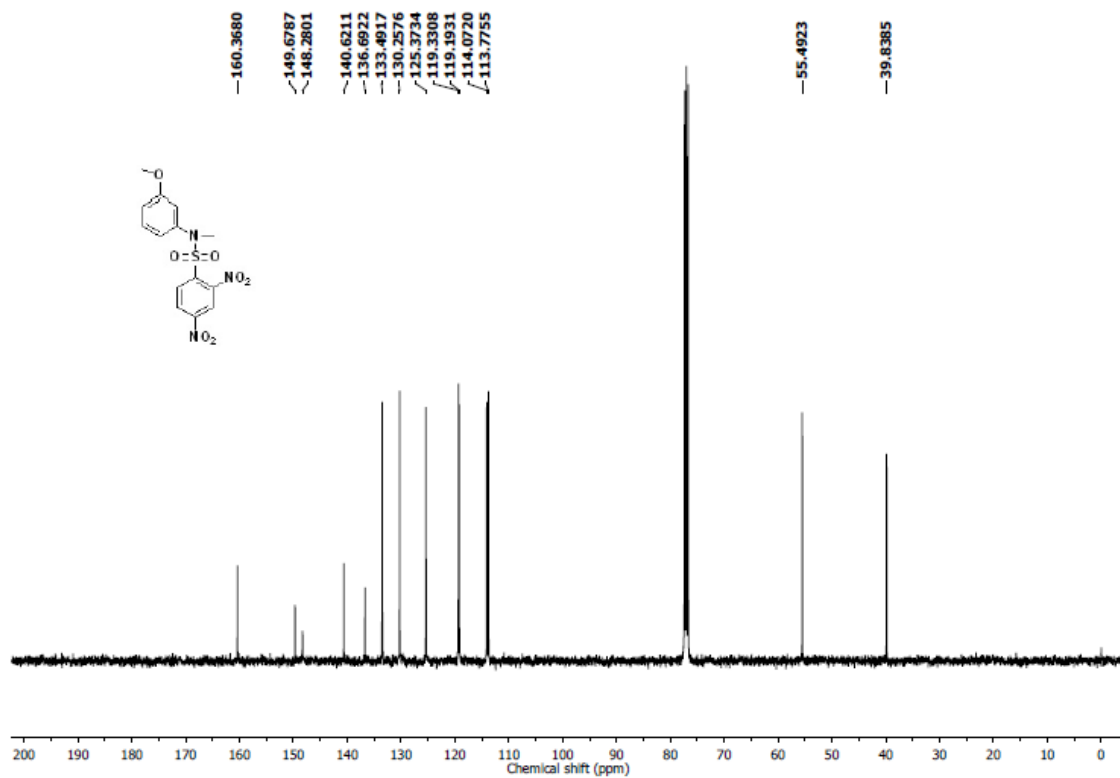
^{1}H NMR Spectrum (400 MHz, CDCl$_3$) of **5c**
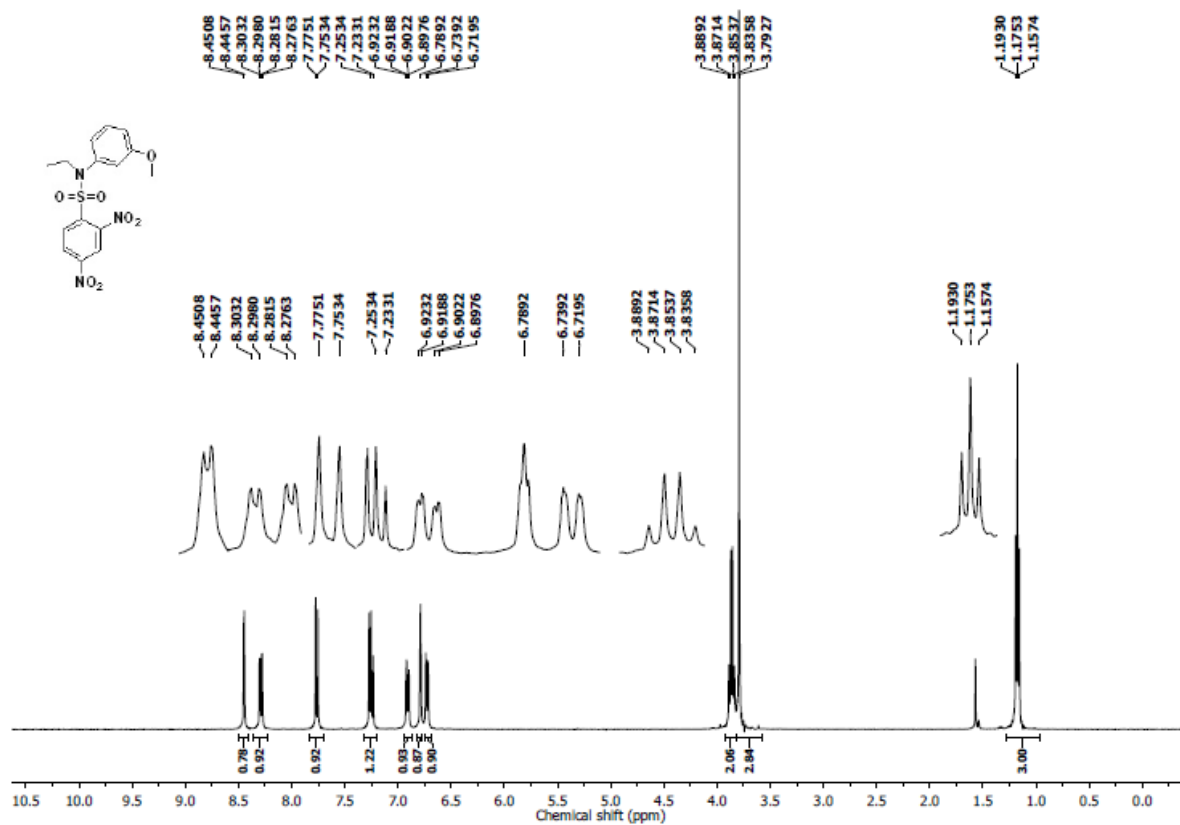
^{13}C NMR Spectrum (100 MHz, CDCl$_3$) of **5c**
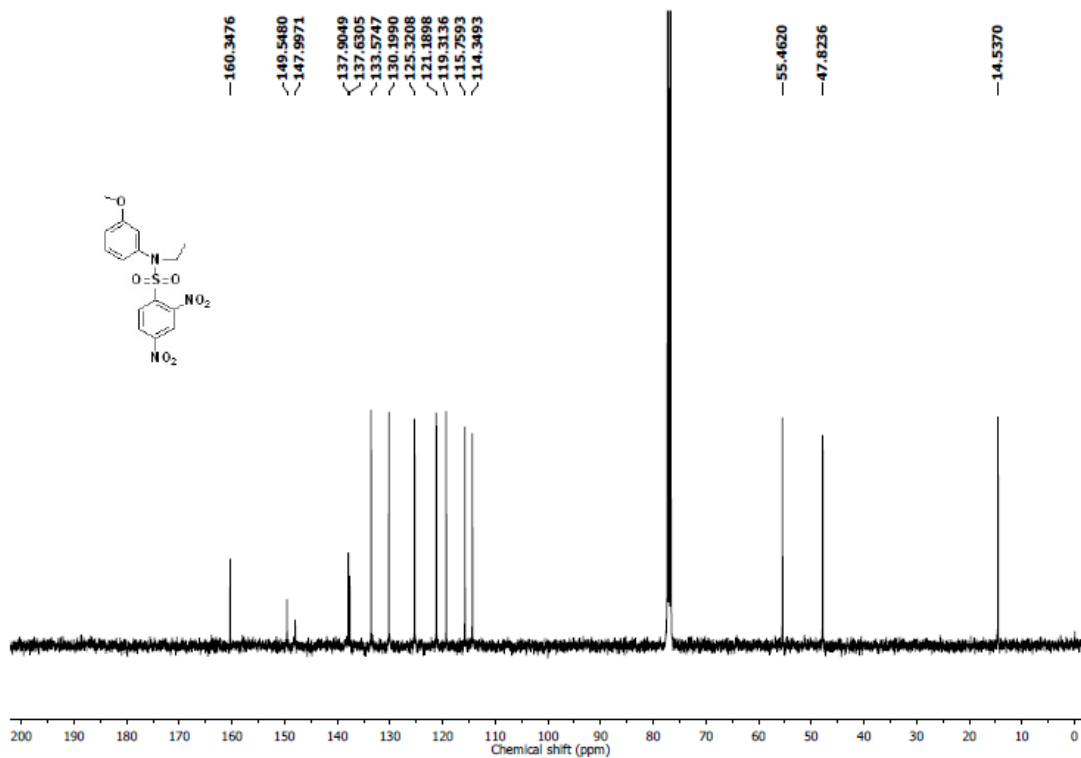
^{1}H NMR Spectrum (400 MHz, CDCl$_3$) of **5d**
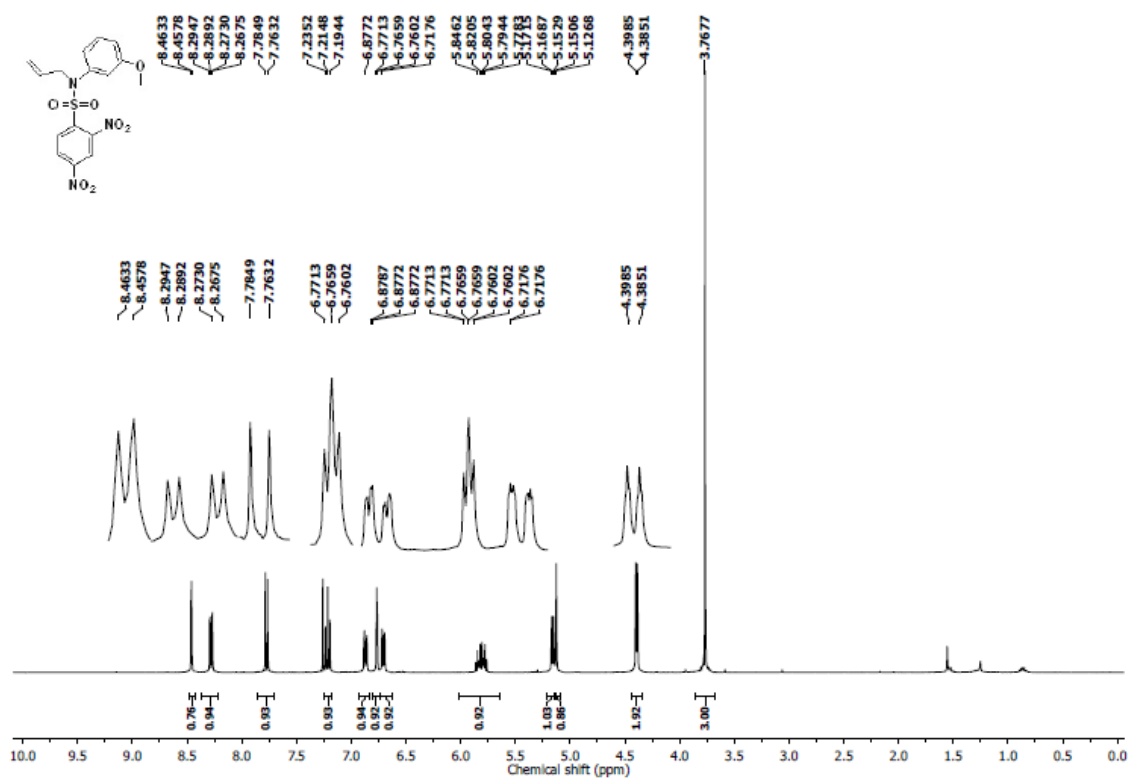
^{13}C NMR Spectrum (100 MHz, CDCl$_3$) of **5d**
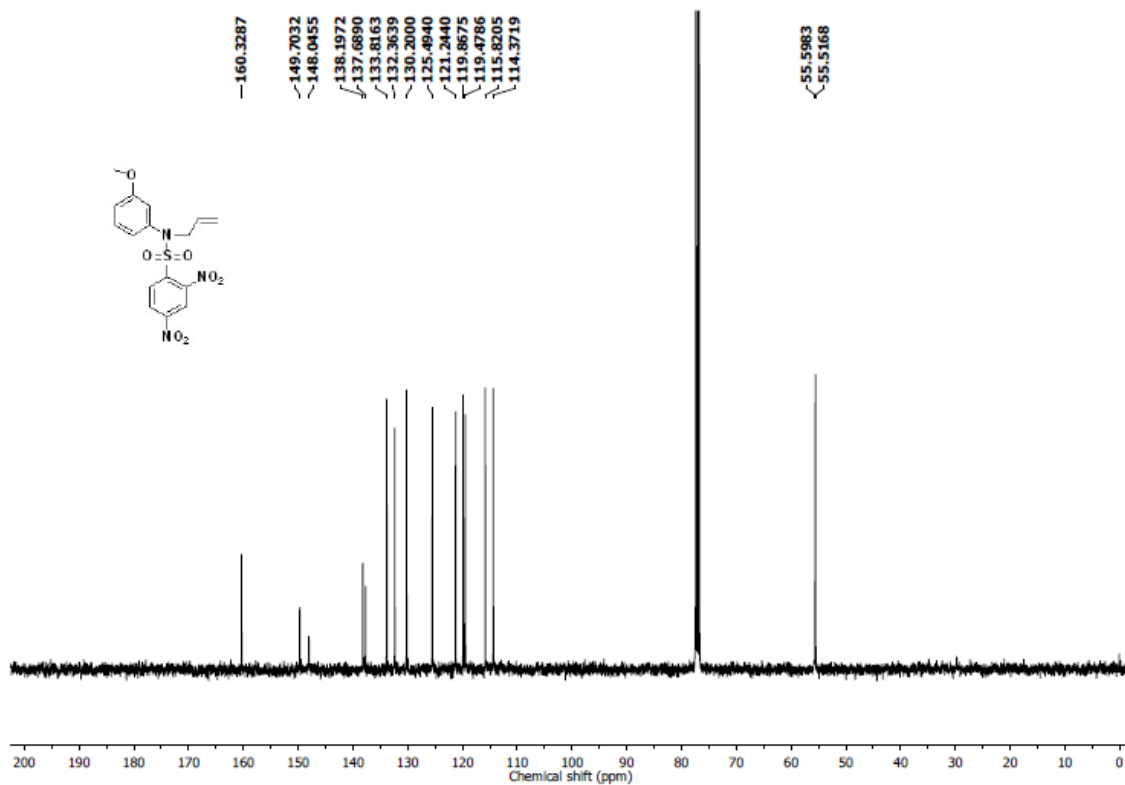
^{1}H NMR Spectrum (400 MHz, CDCl$_3$) of **5e**
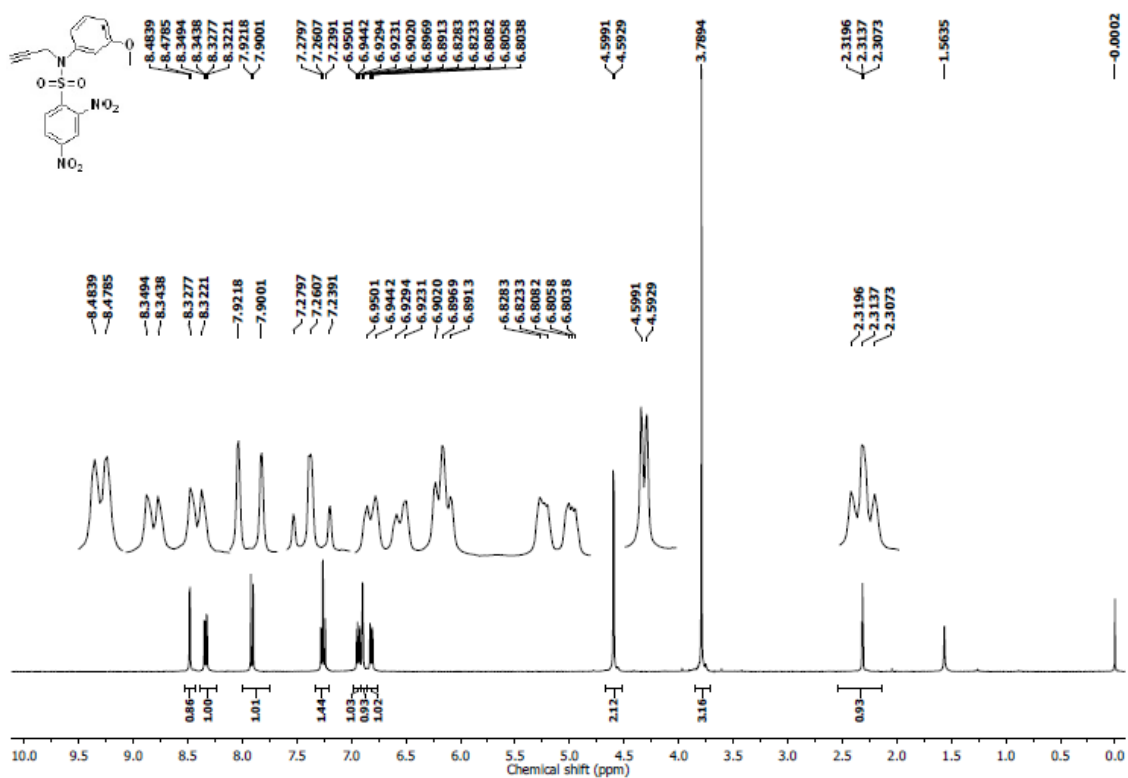
^{13}C NMR Spectrum (100 MHz, CDCl$_3$) of **5e**
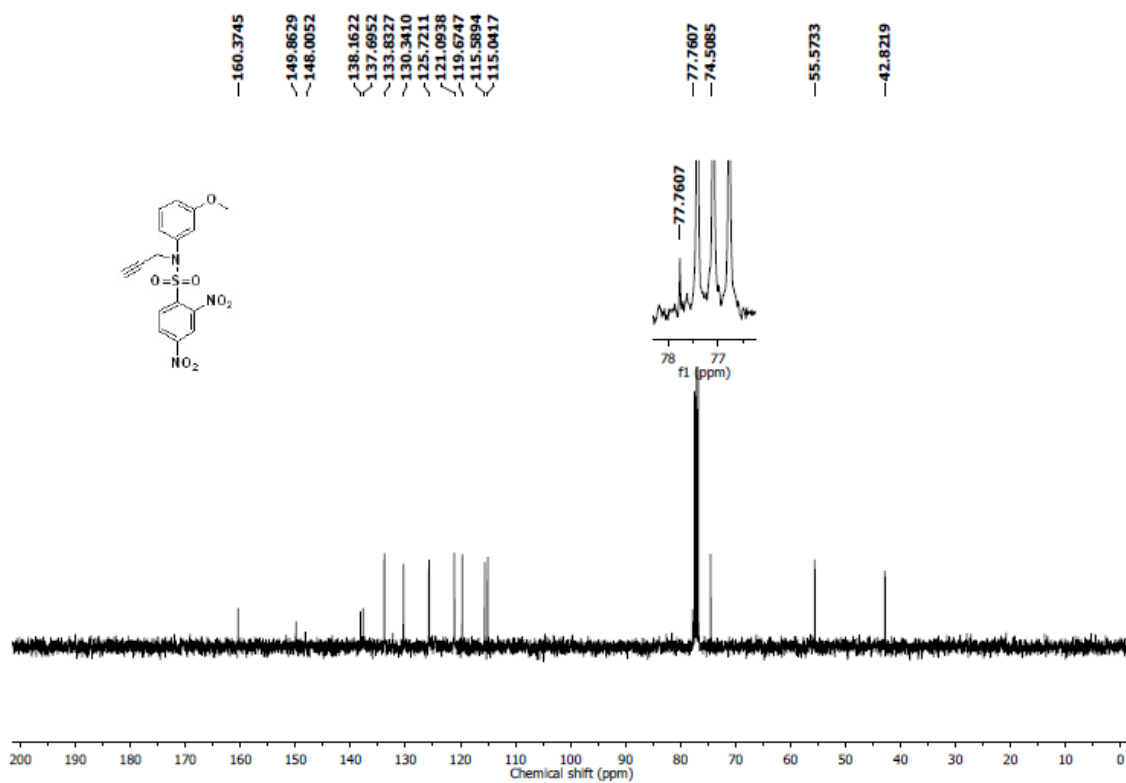
^{1}H NMR Spectrum (400 MHz, CDCl$_3$) of **8a**
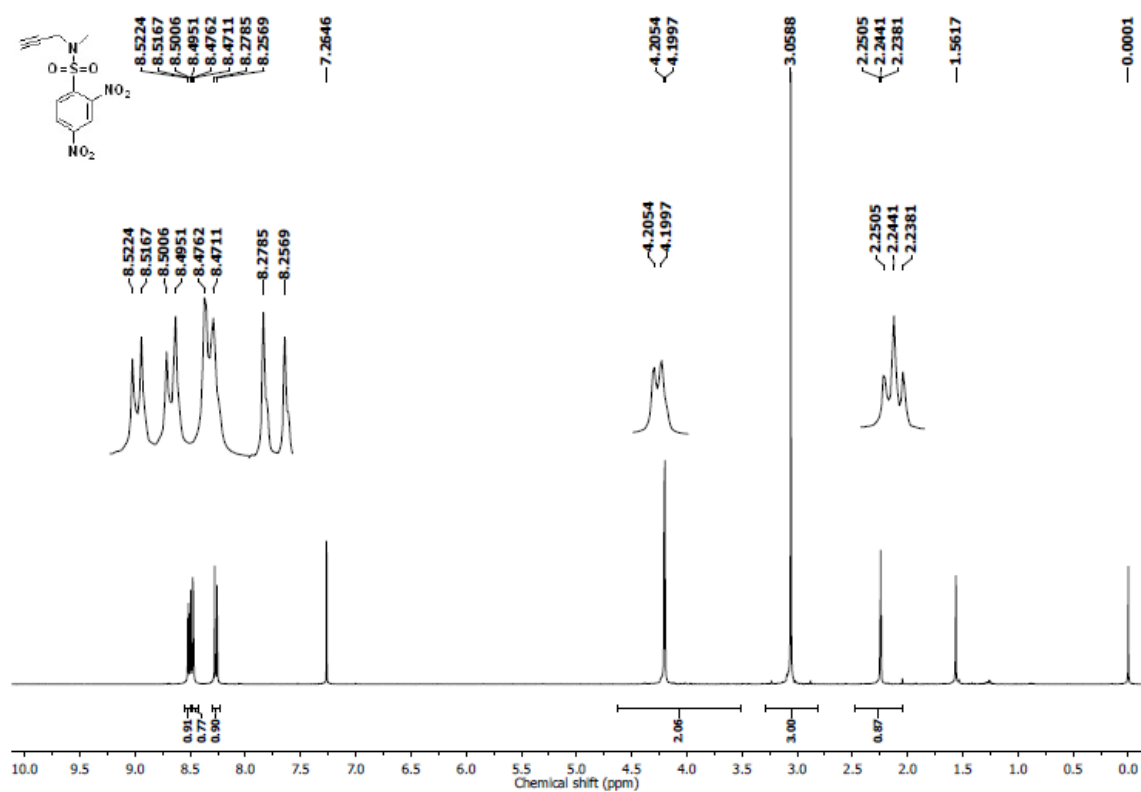
^{13}C NMR Spectrum (400 MHz, CDCl$_3$) of **8a**
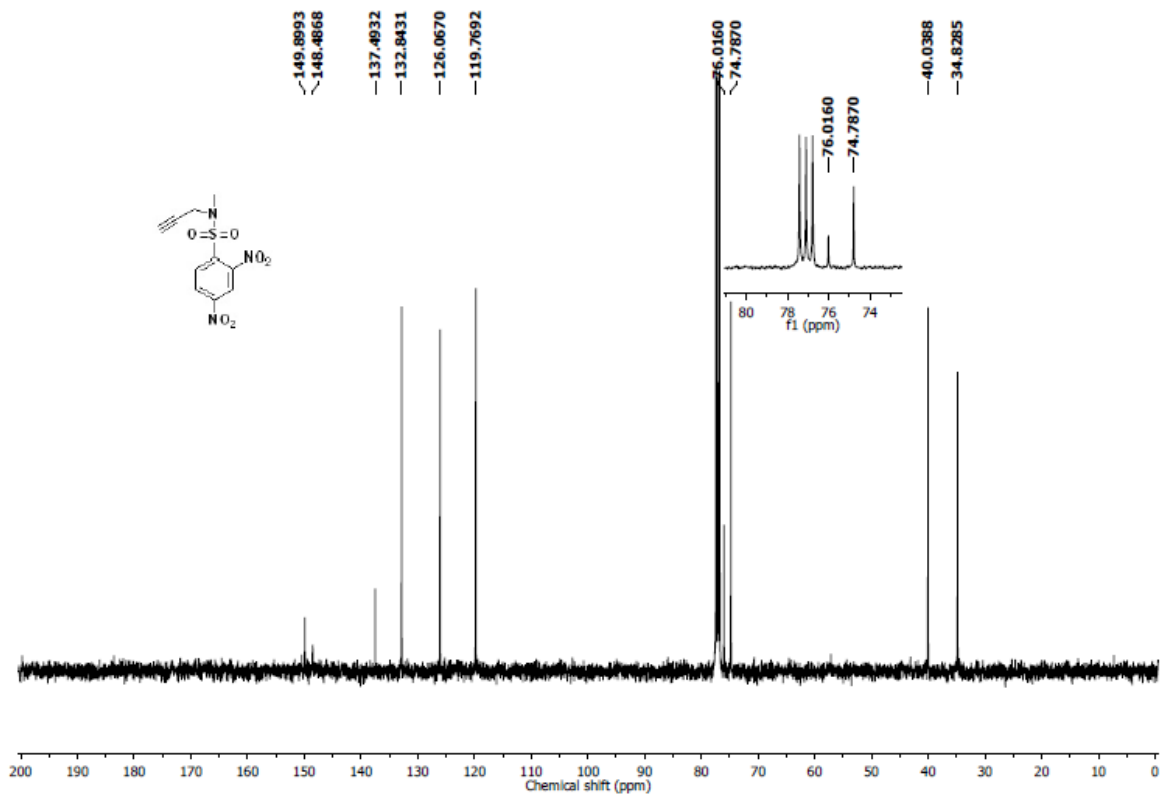
^{1}H NMR Spectrum (400 MHz, CDCl$_3$) of **8b**
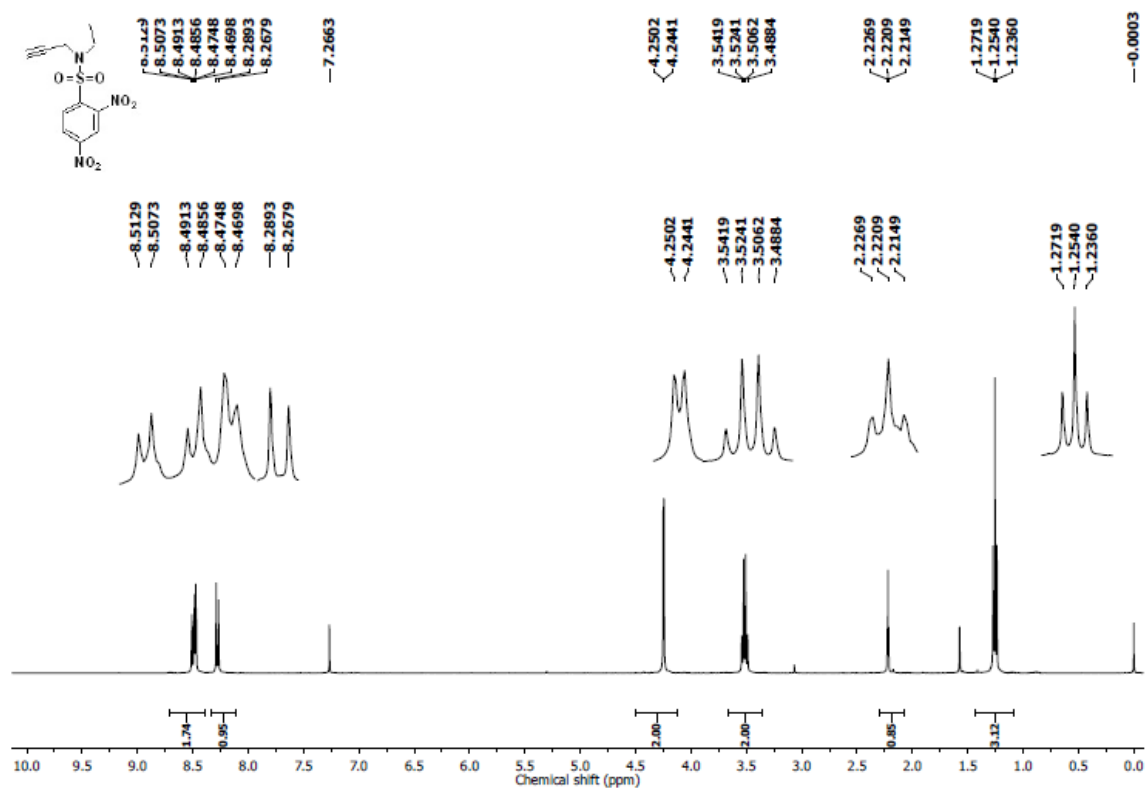
^{13}C NMR Spectrum (100 MHz, CDCl$_3$) of **8b**
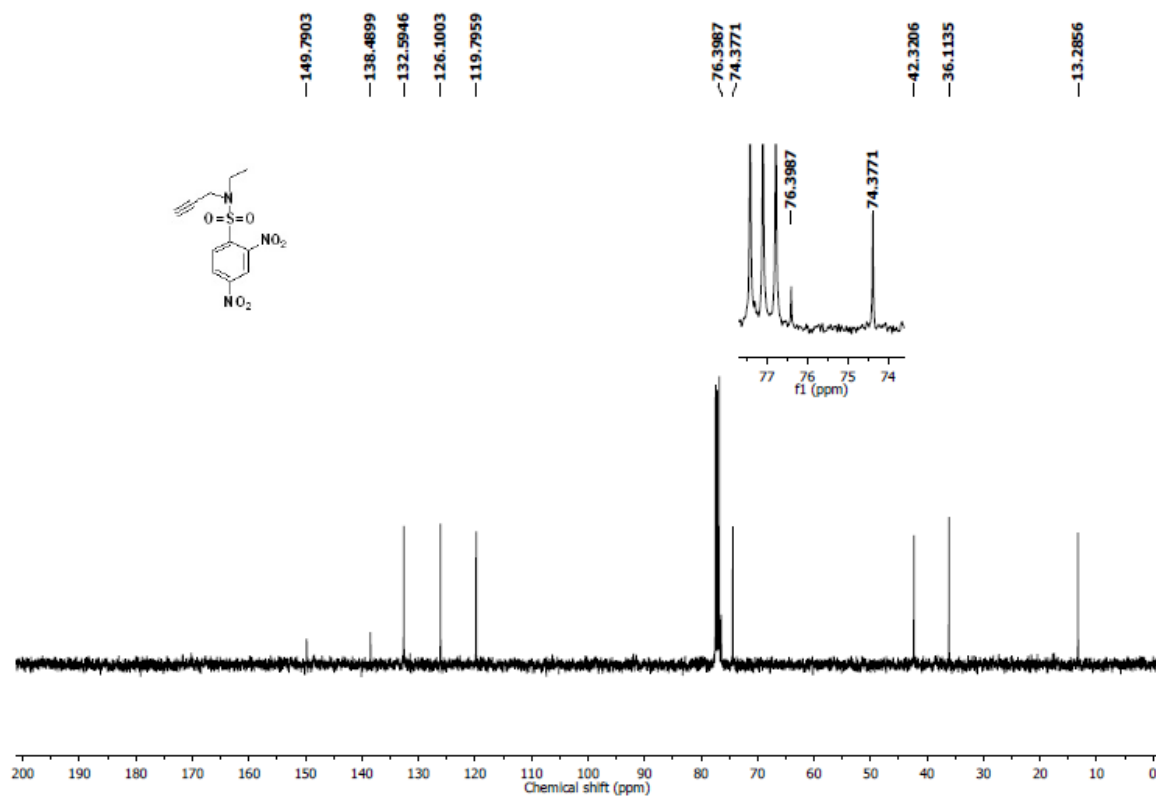
^{1}H NMR Spectrum (400 MHz, CDCl$_3$) of **8c**
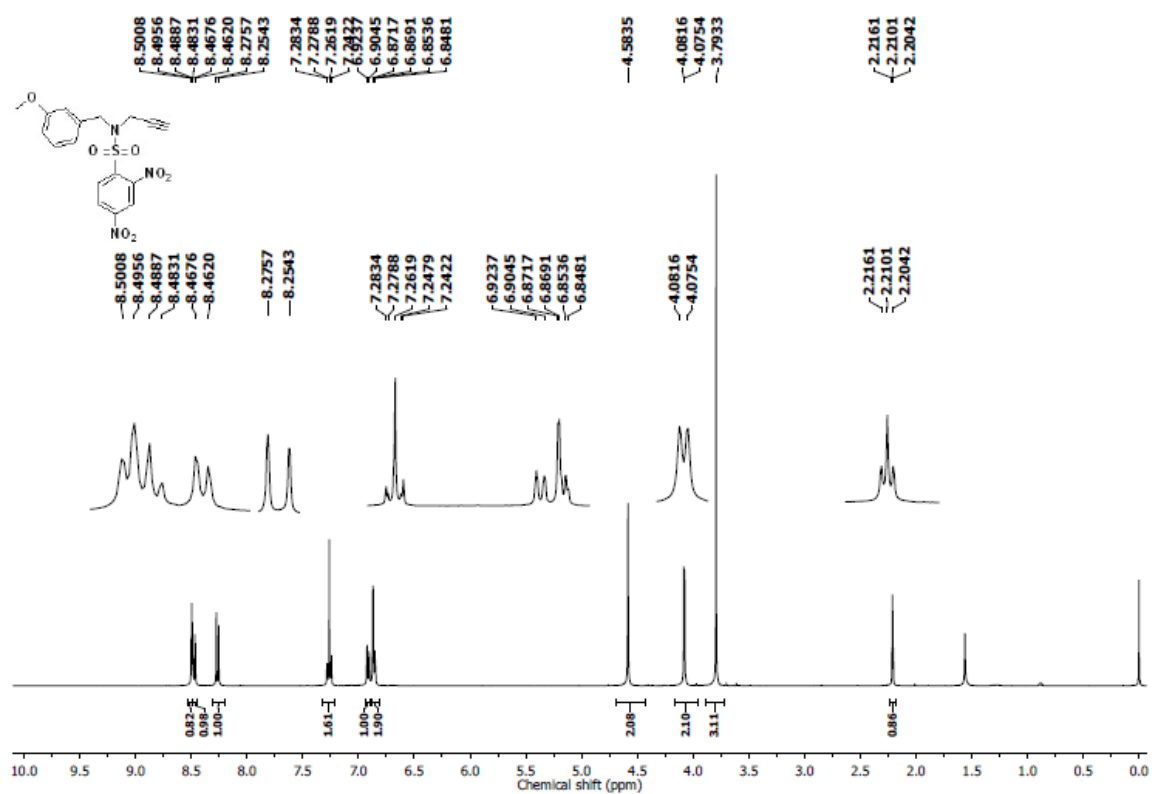
^{13}C NMR Spectrum (400 MHz, CDCl$_3$) of **8c**
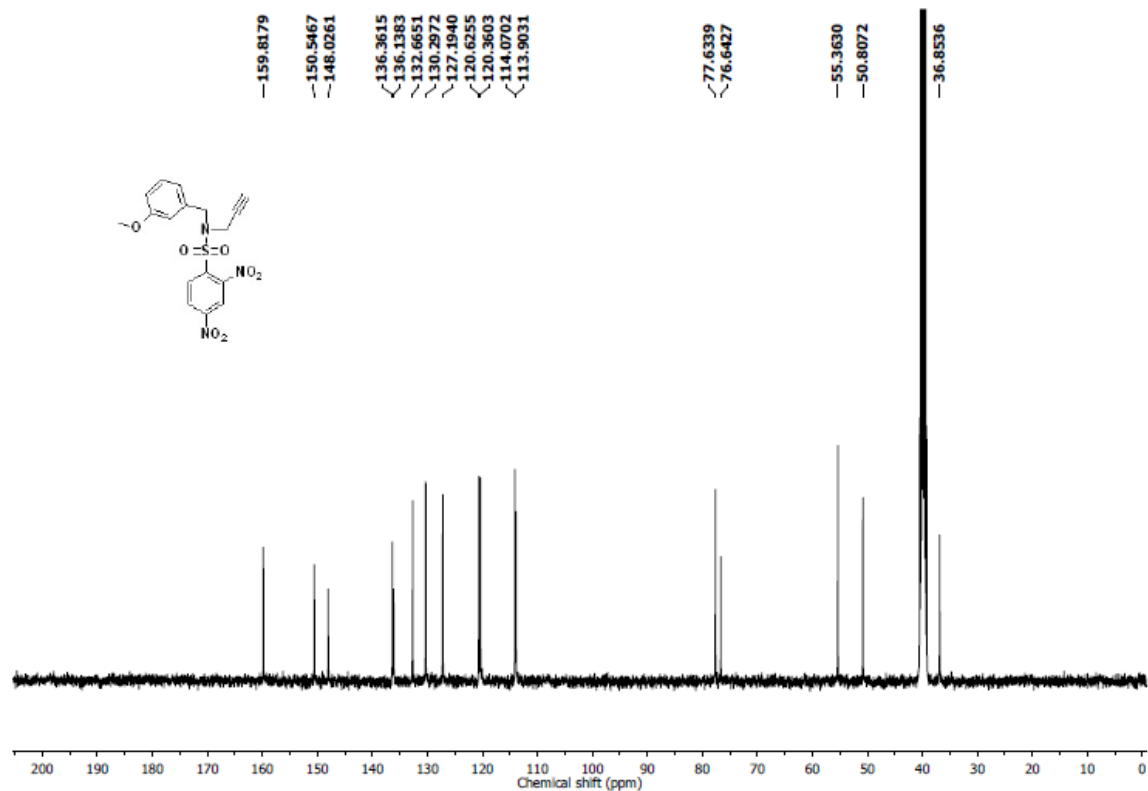
¹H NMR Spectrum (400 MHz, DMSO-d₆) of **9a**
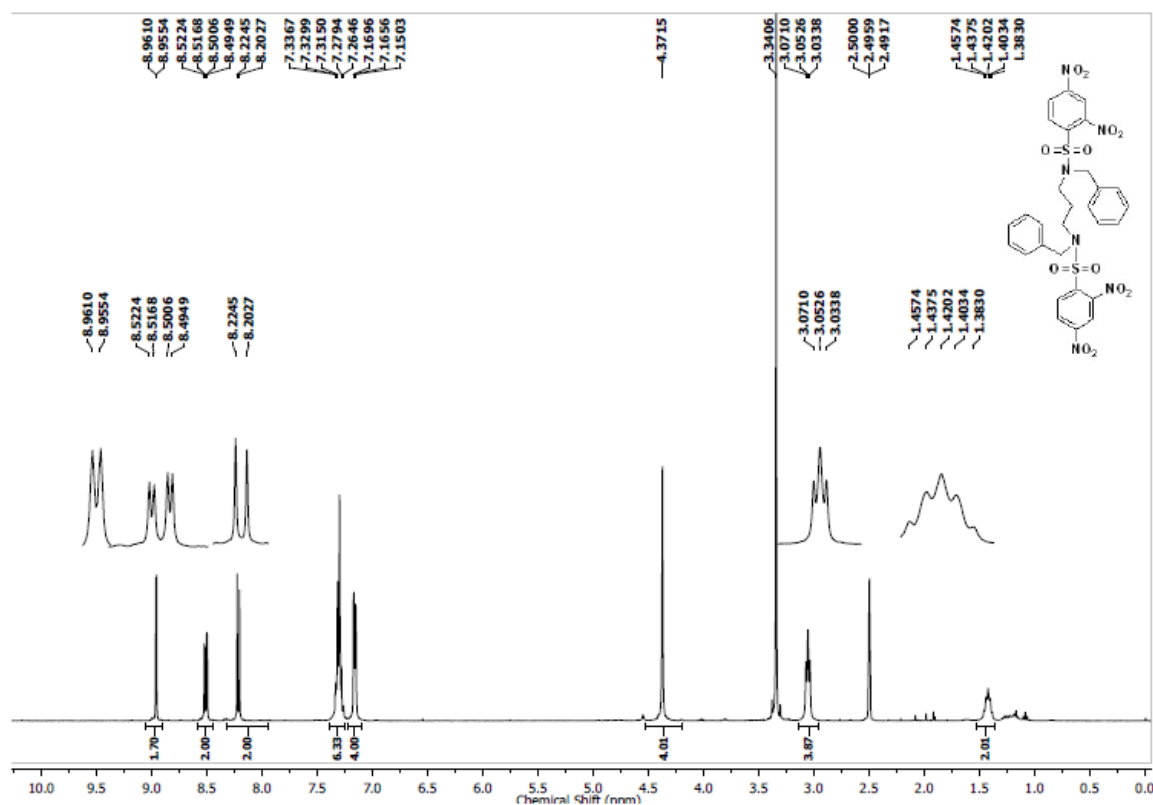
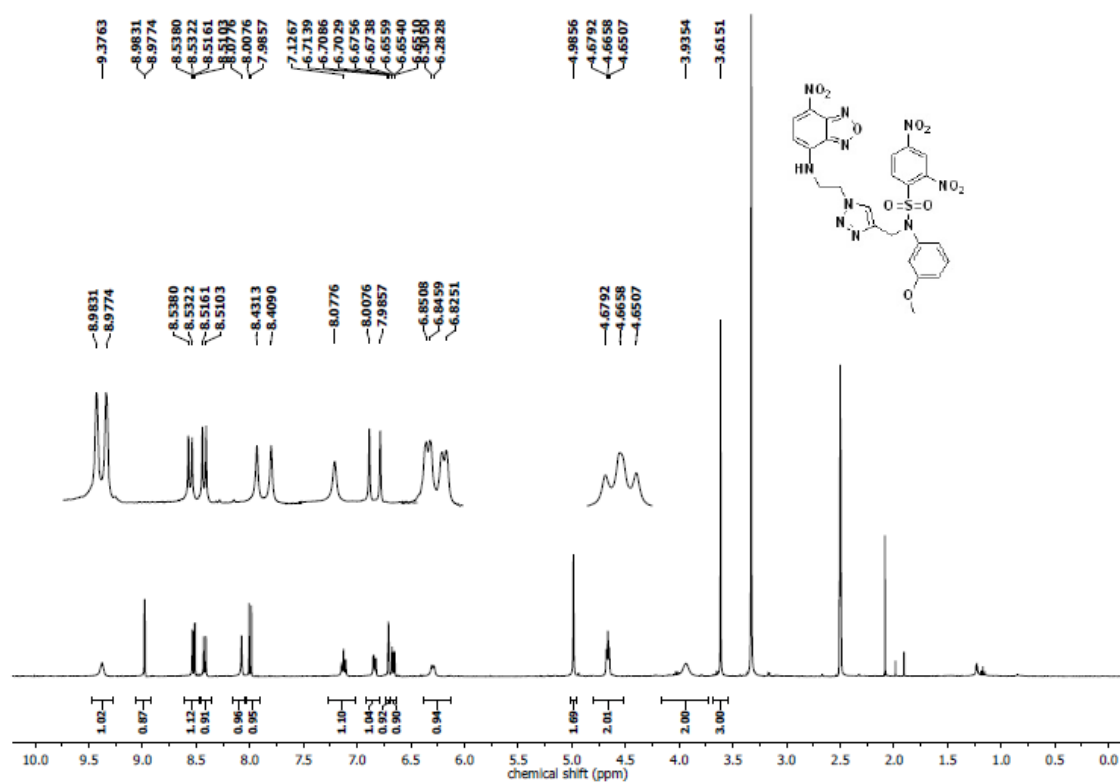¹³C NMR Spectrum (100 MHz, DMSO-d₆) of **9a**
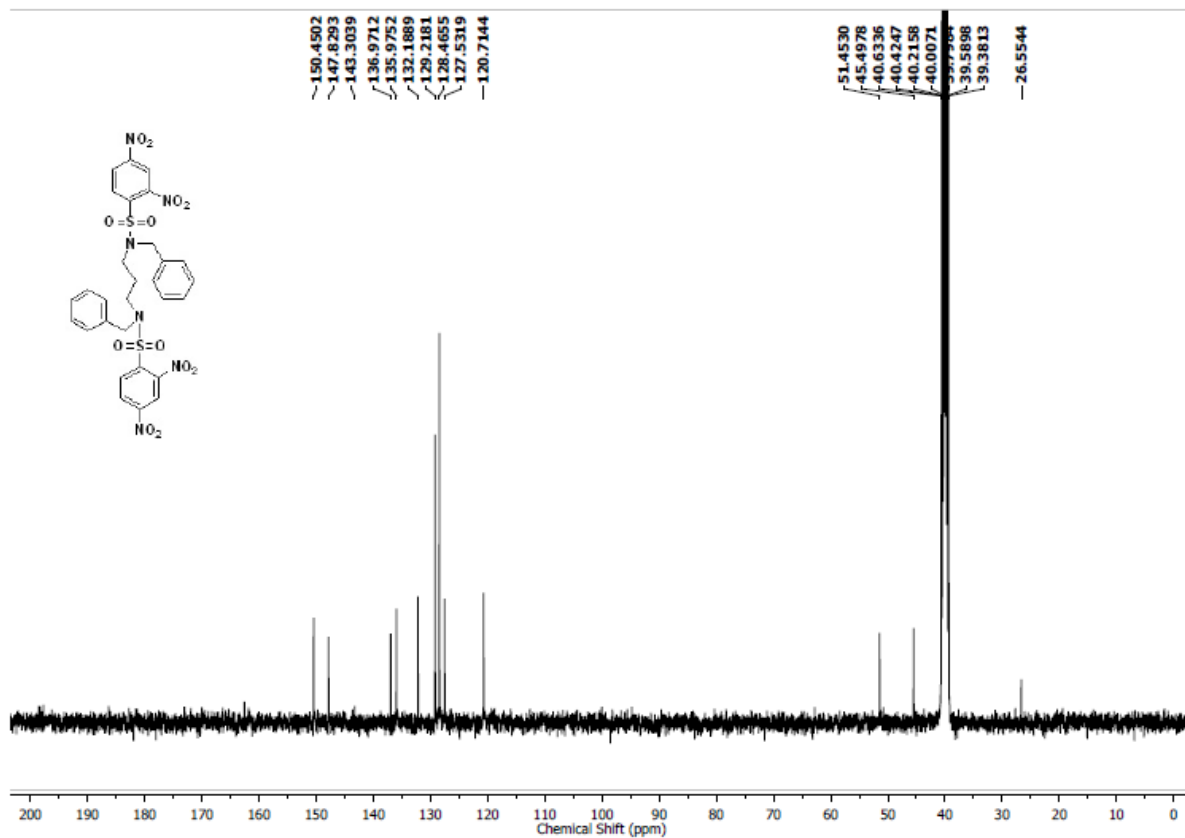
^{1}H NMR Spectrum (400 MHz, CDCl$_3$) of **9b**
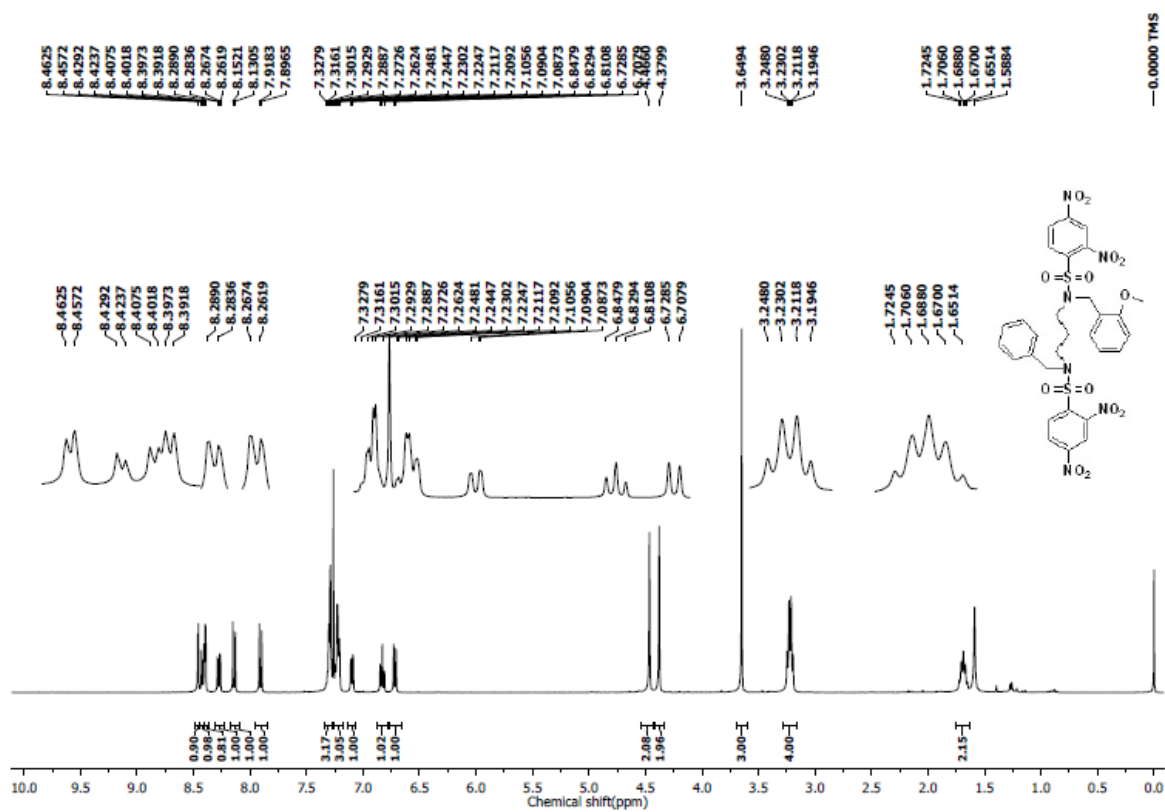
^{13}C NMR Spectrum (100 MHz, CDCl$_3$) of **9b**
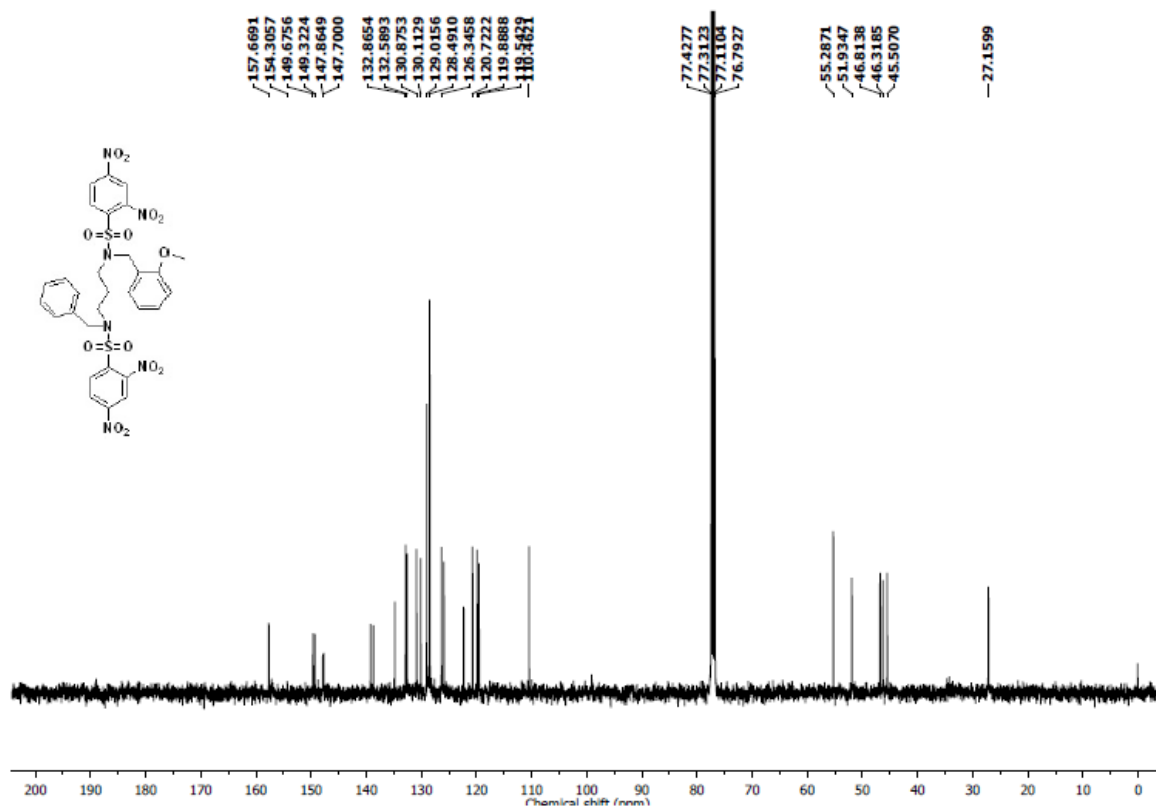
^{1}H NMR Spectrum (400 MHz, CDCl$_3$) of **9c**
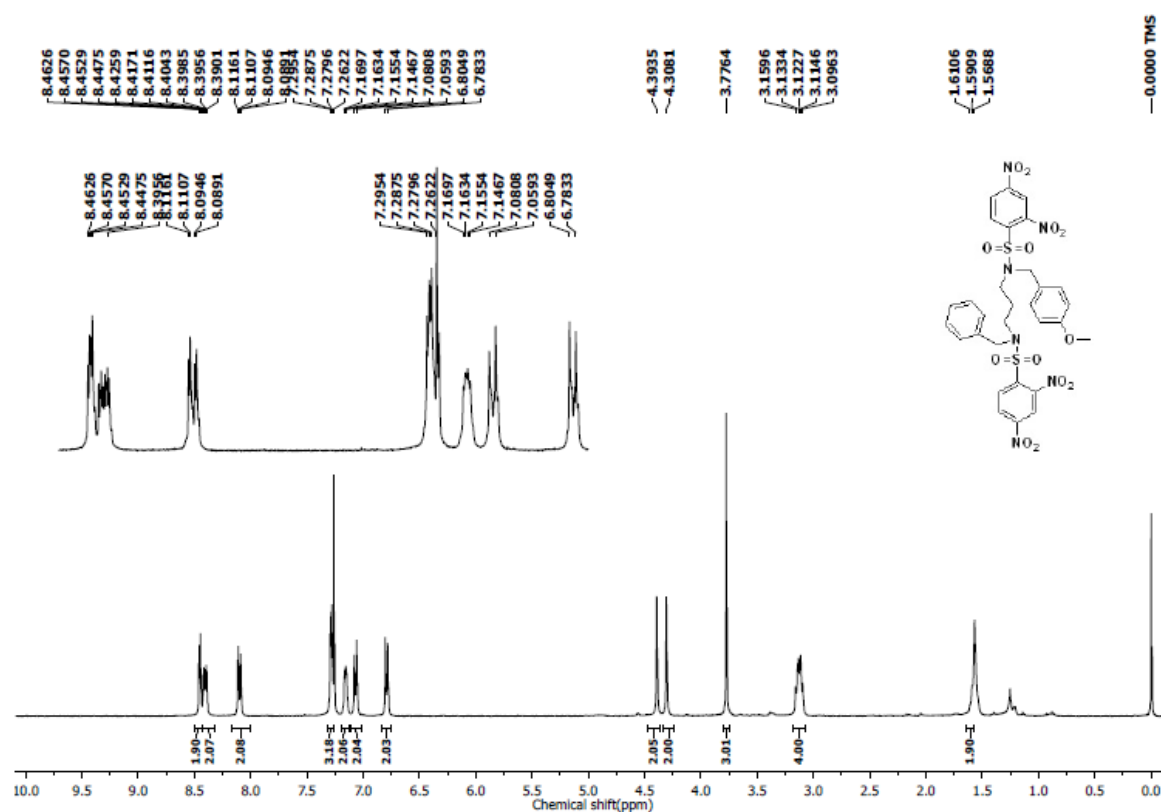
^{13}C NMR Spectrum (100 MHz, CDCl$_3$) of **9c**
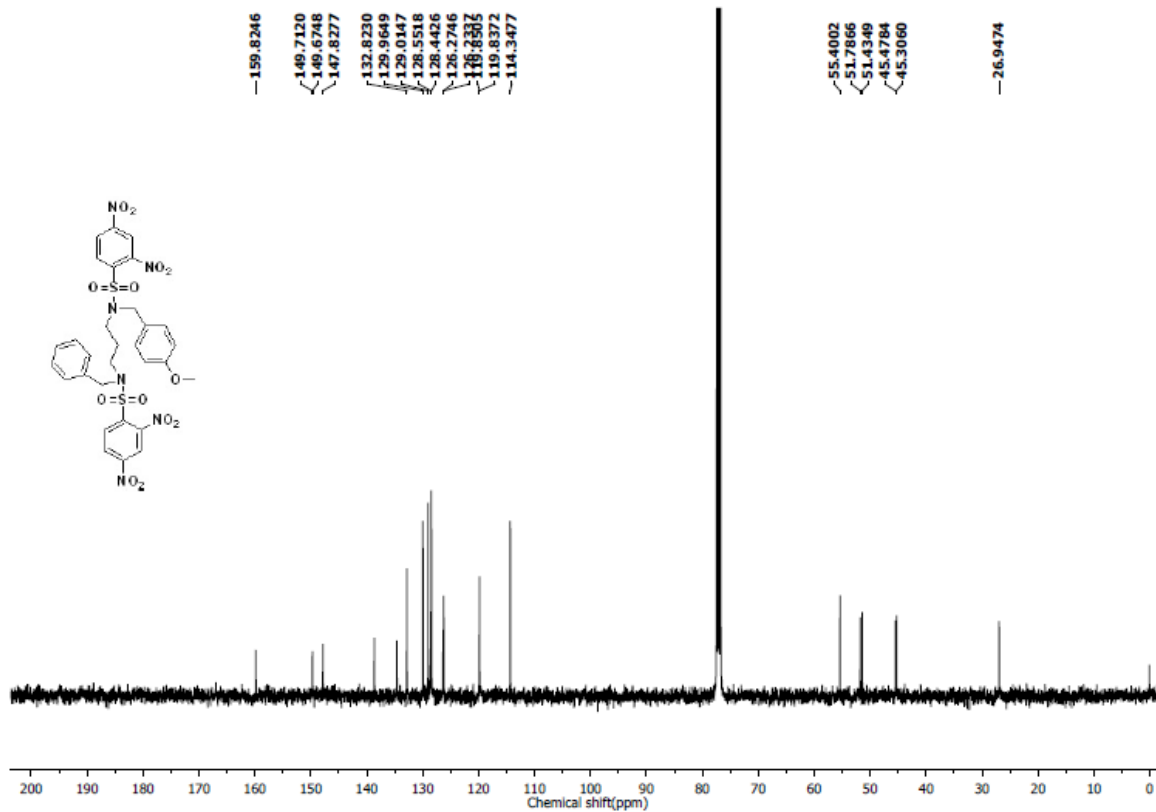
^{1}H NMR Spectrum (400 MHz, CDCl$_3$) of **9d**
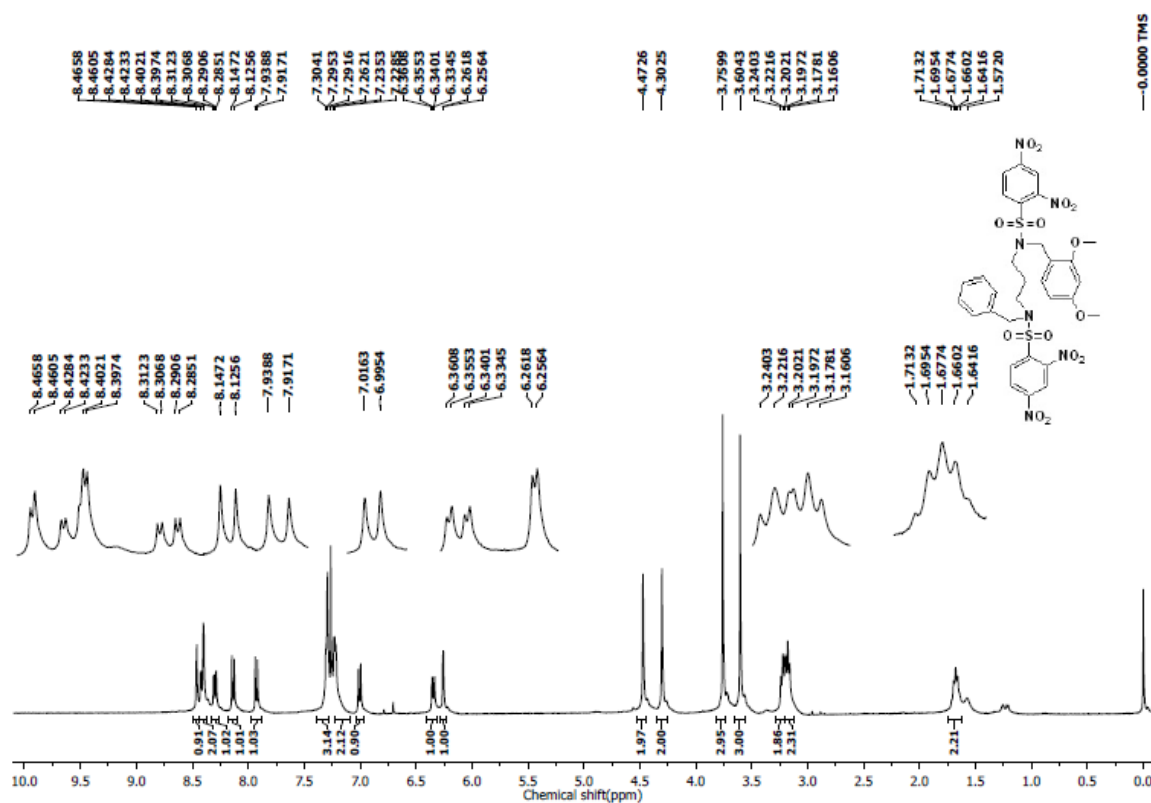
^{13}C NMR Spectrum (100 MHz, CDCl$_3$) of **9d**
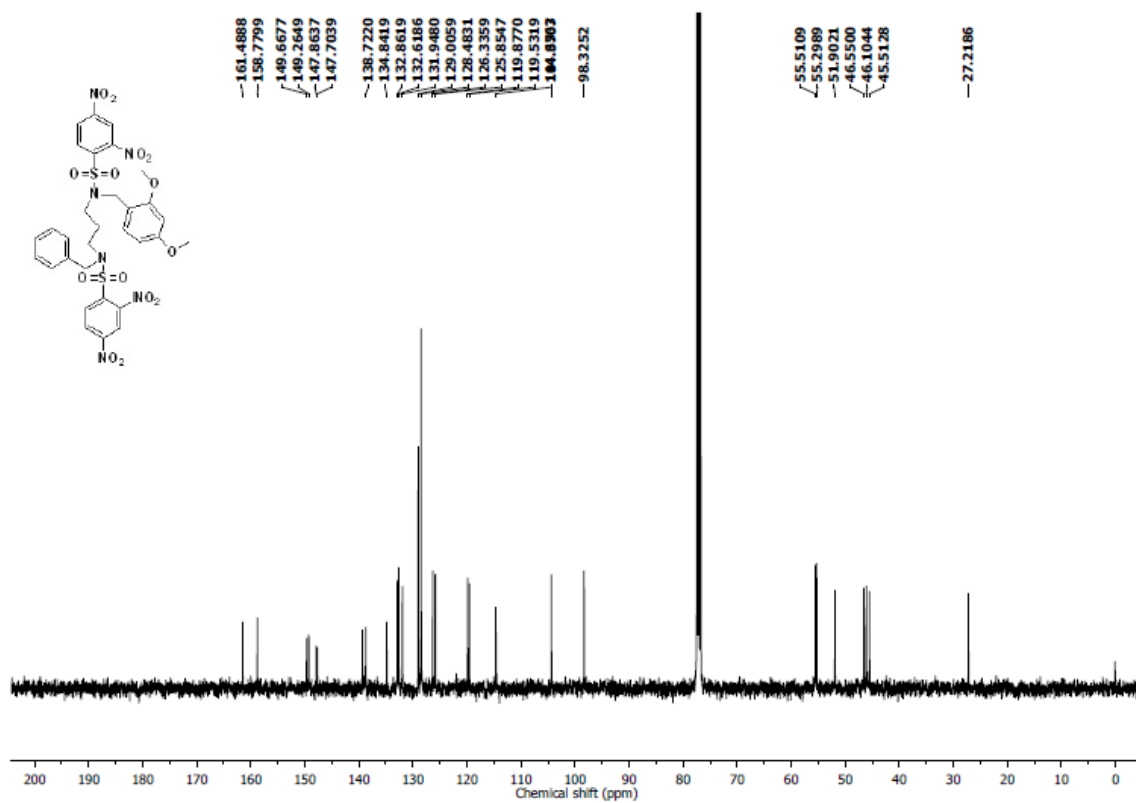
¹H NMR Spectrum (400 MHz, CDCl₃) of **9e**
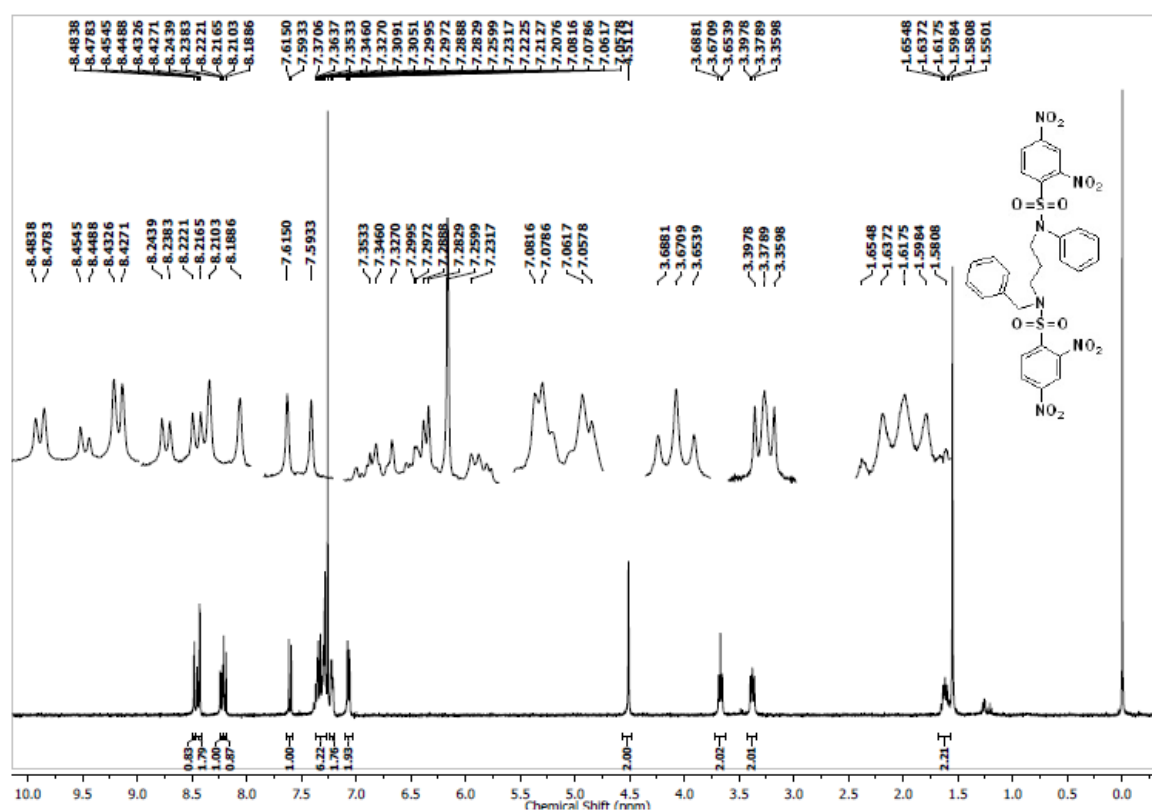
¹³C NMR Spectrum (100 MHz, CDCl₃) of **9e**
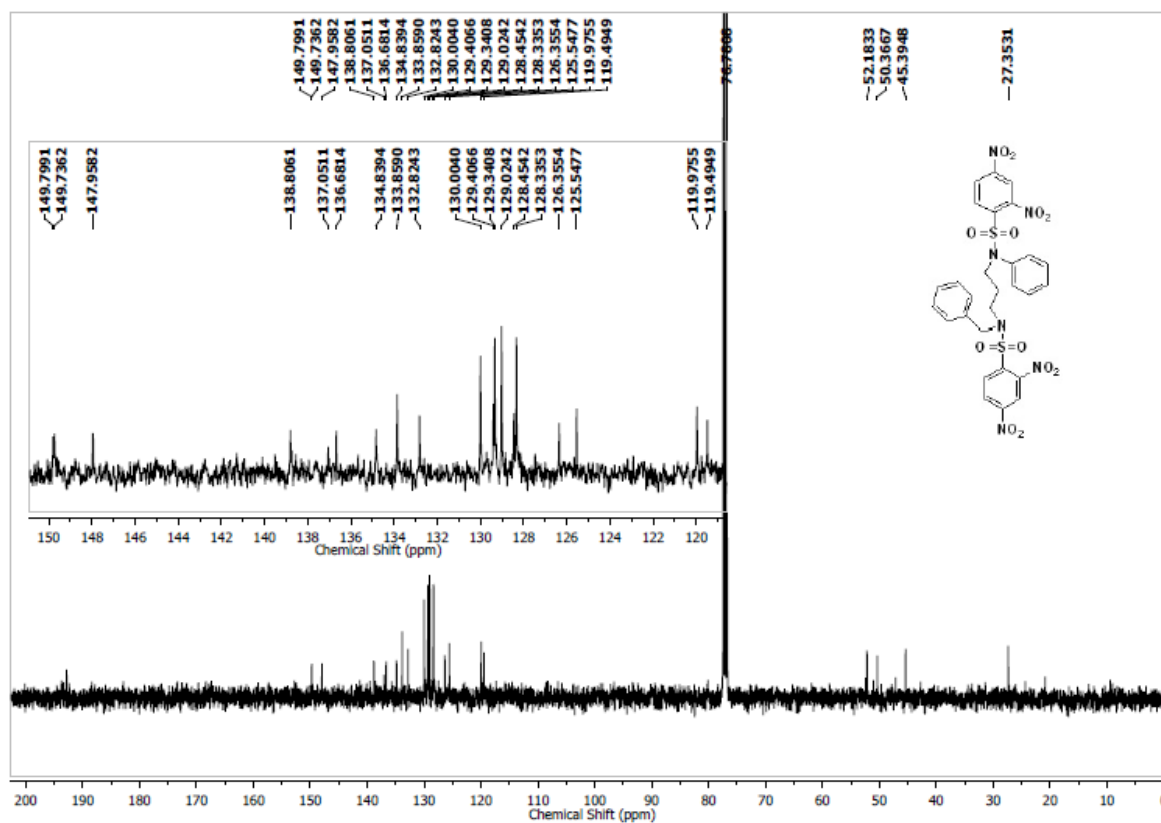
^{1}H NMR Spectrum (400 MHz, DMSO-d$_6$) of **9f**
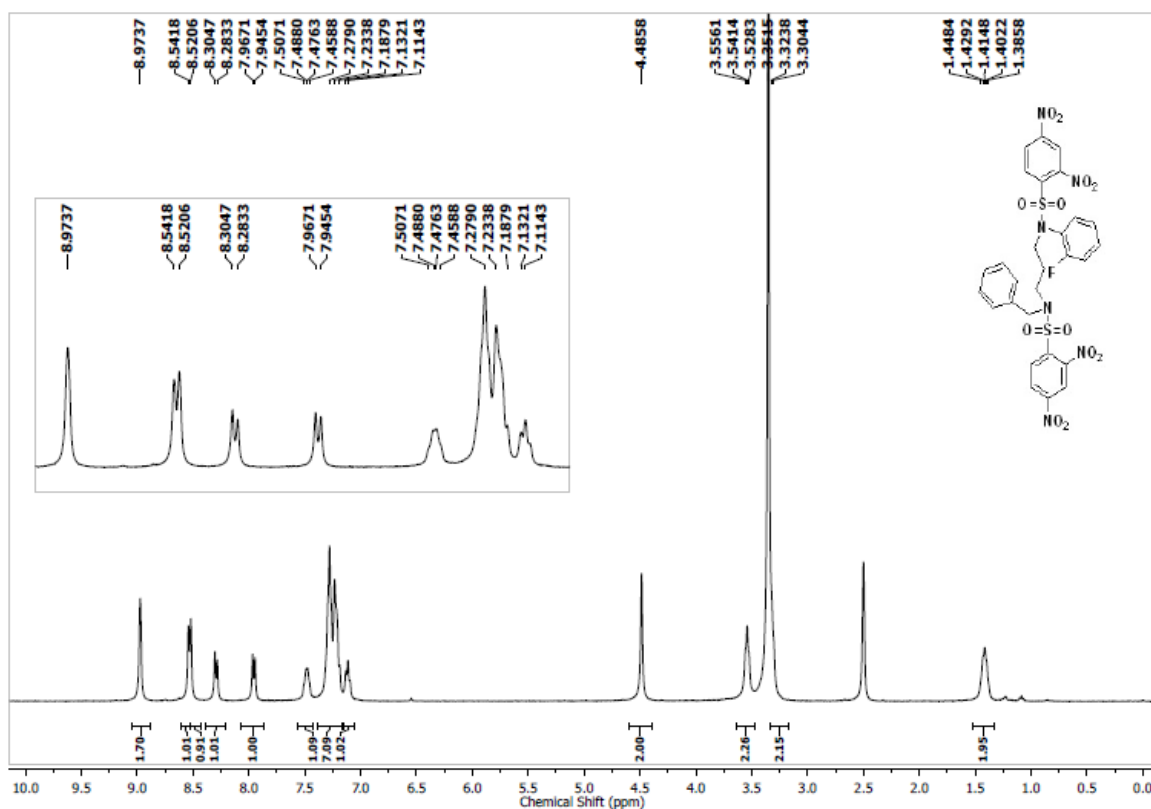
^{13}C NMR Spectrum (100 MHz, DMSO-d$_6$) of **9f**
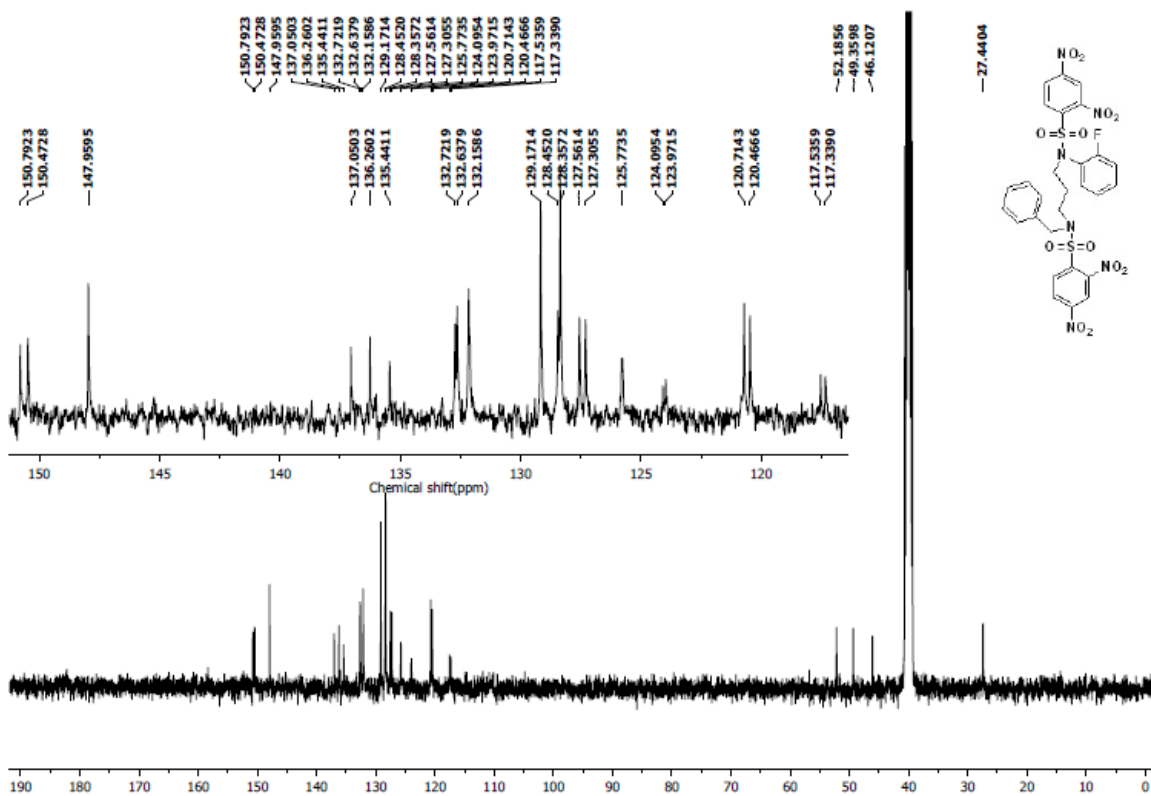
^{1}H NMR Spectrum (400 MHz, CDCl$_3$) of **9g**
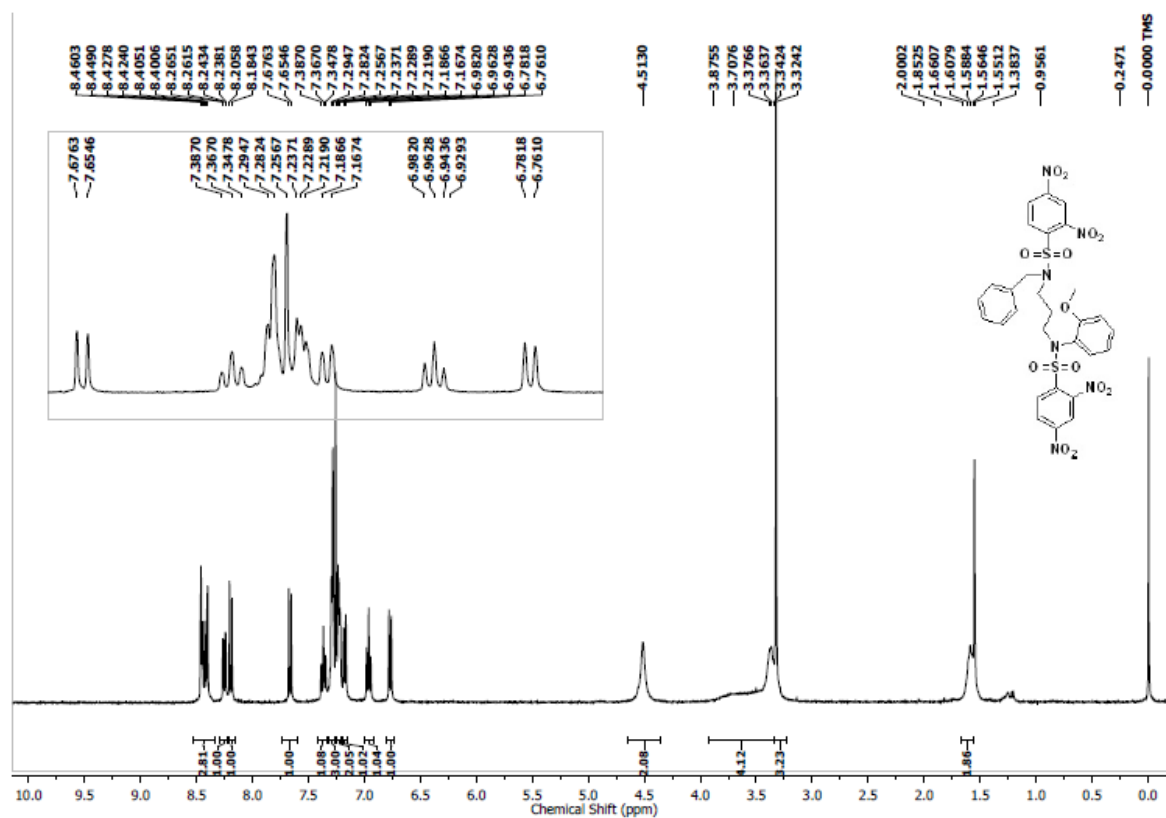
^{13}C NMR Spectrum (100 MHz, CDCl$_3$) of **9g**
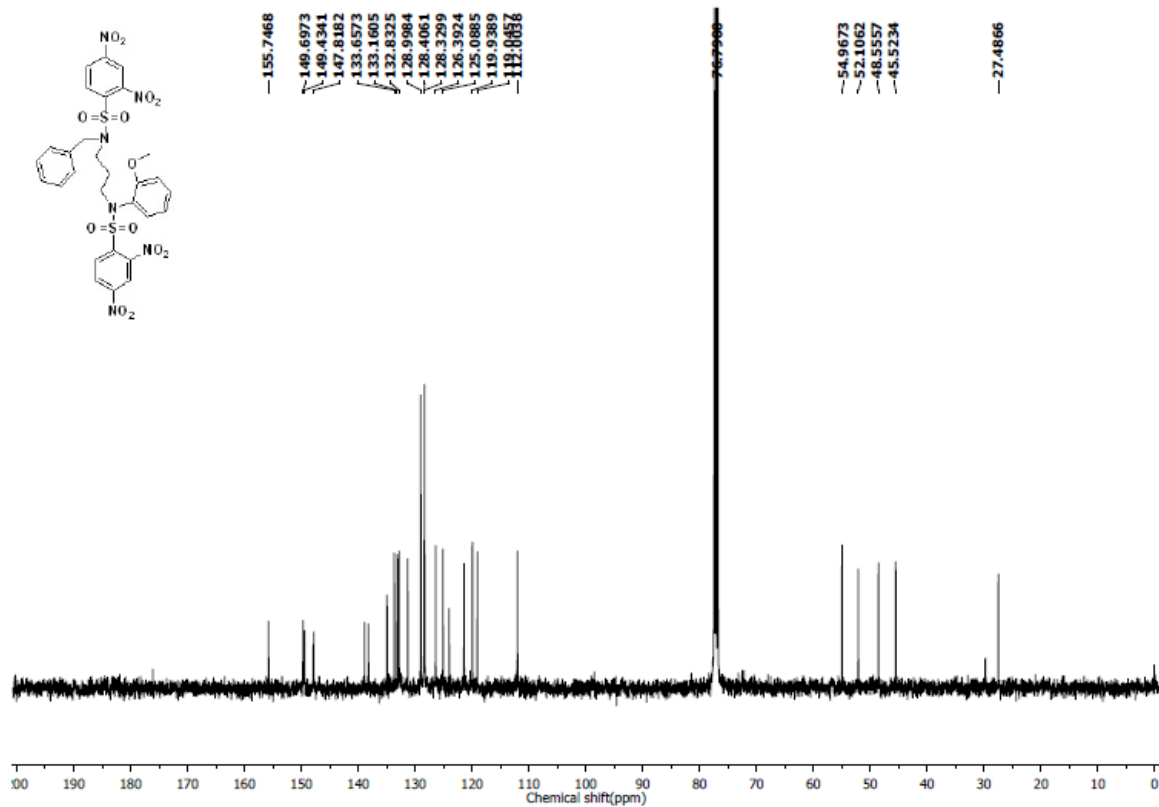
^{1}H NMR Spectrum (400 MHz, DMSO-d$_6$) of **9h**
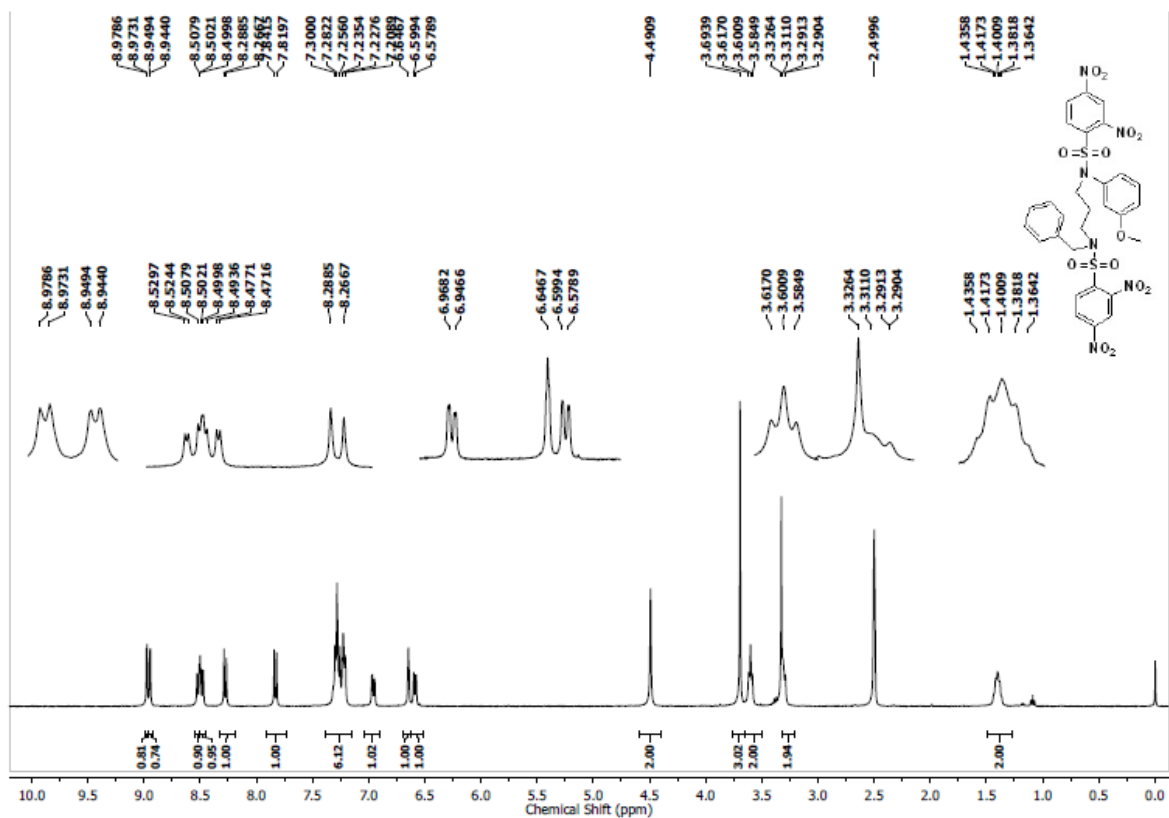
^{13}C NMR Spectrum (100 MHz, DMSO-d$_6$) of **9h**
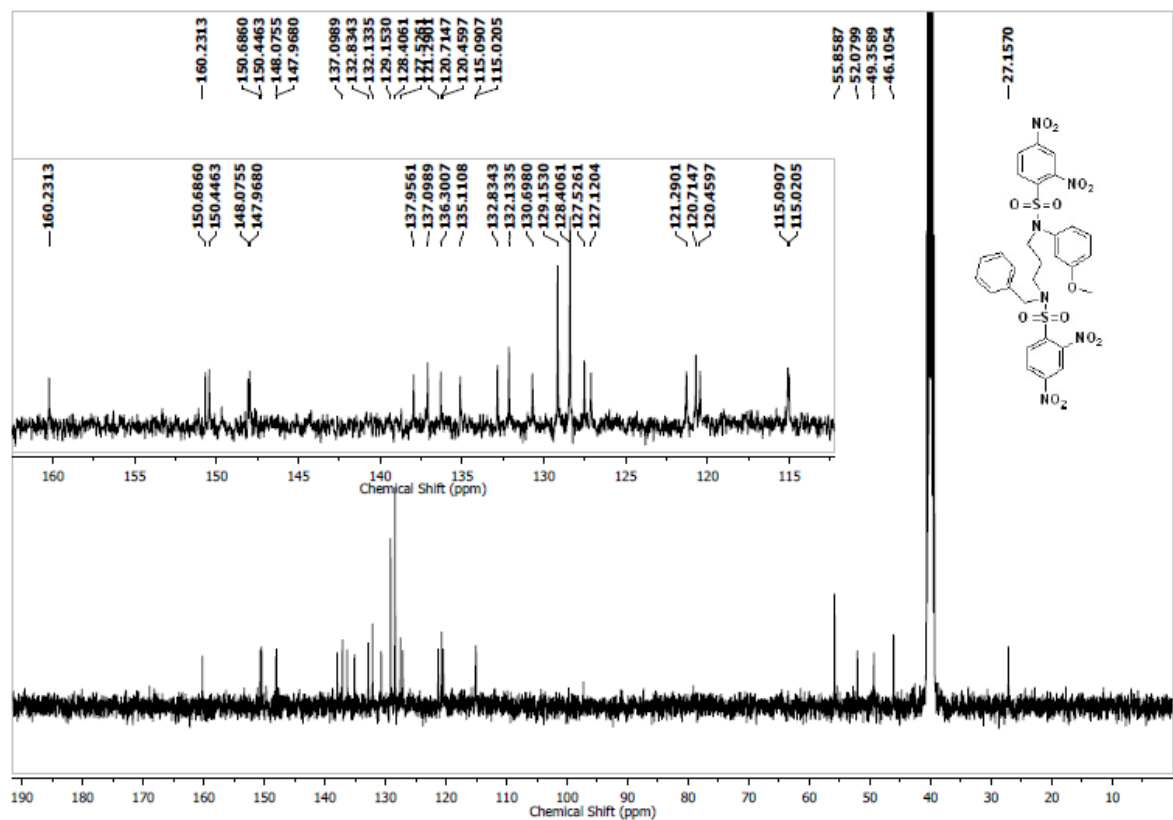
^{1}H NMR Spectrum (400 MHz, DMSO-d_6) of **9i**

^{13}C NMR Spectrum (100 MHz, DMSO-d_6) of **9i**

^{1}H NMR Spectrum (400 MHz, DMSO-d$_6$) of **9j**

^{13}C NMR Spectrum (100 MHz, DMSO-d$_6$) of **9j**

^{1}H NMR Spectrum (400 MHz, CDCl$_3$) of **9k**

^{13}C NMR Spectrum (100 MHz, DMSO-d$_6$) of **9k**

¹H NMR Spectrum (400 MHz, DMSO-d₆) of **9l**

¹³C NMR Spectrum (100 MHz, DMSO-d₆) of **9l**

^{1}H NMR Spectrum (400 MHz, CDCl$_3$) of **10a**
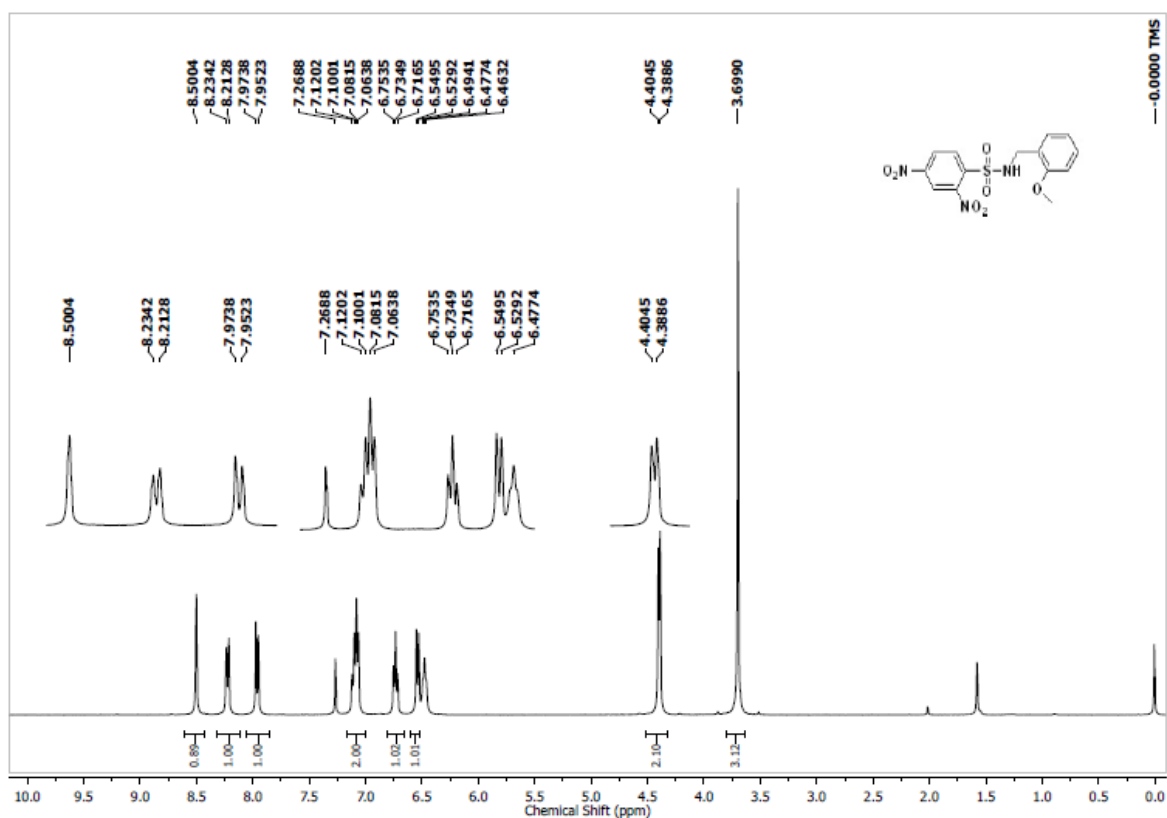
^{13}C NMR Spectrum (100 MHz, CDCl$_3$) of **10a**

¹H NMR Spectrum (400 MHz, DMSO-d₆) of **10b**
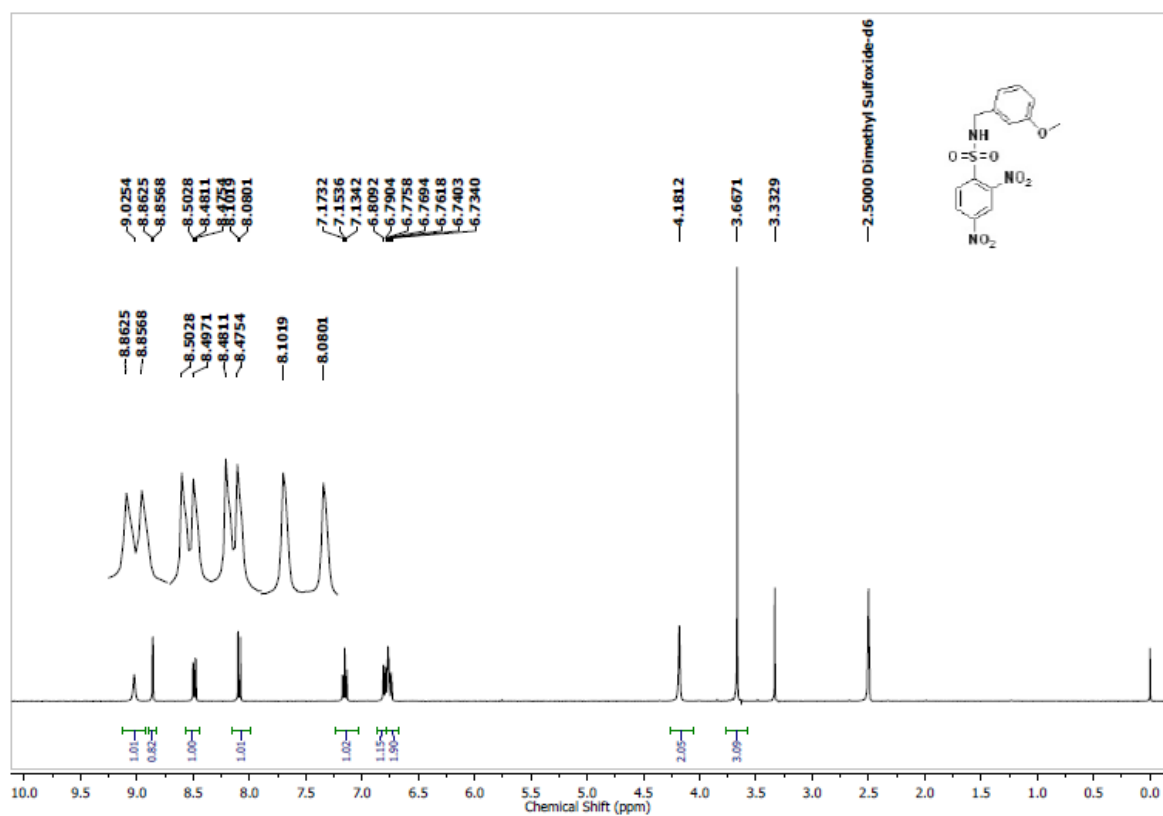
¹³C NMR Spectrum (100 MHz, DMSO-d₆) of **10b**
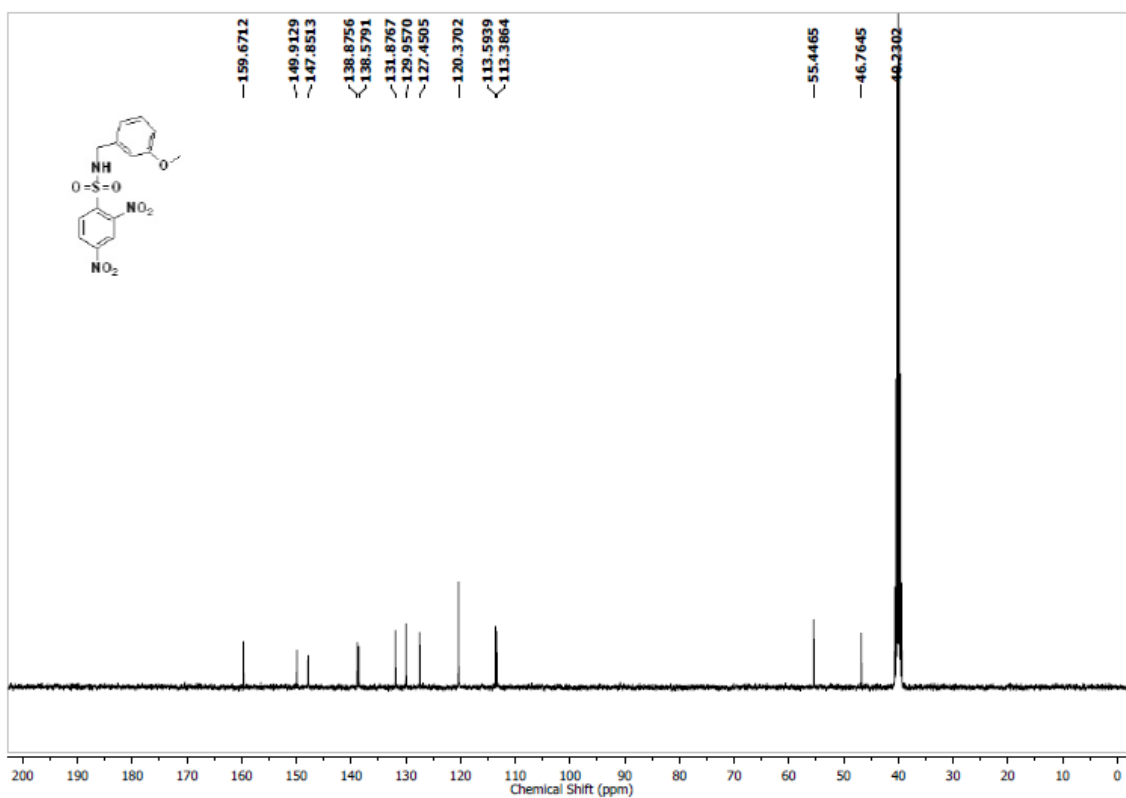
^{1}H NMR Spectrum (400 MHz, CDCl$_3$) of **11a**
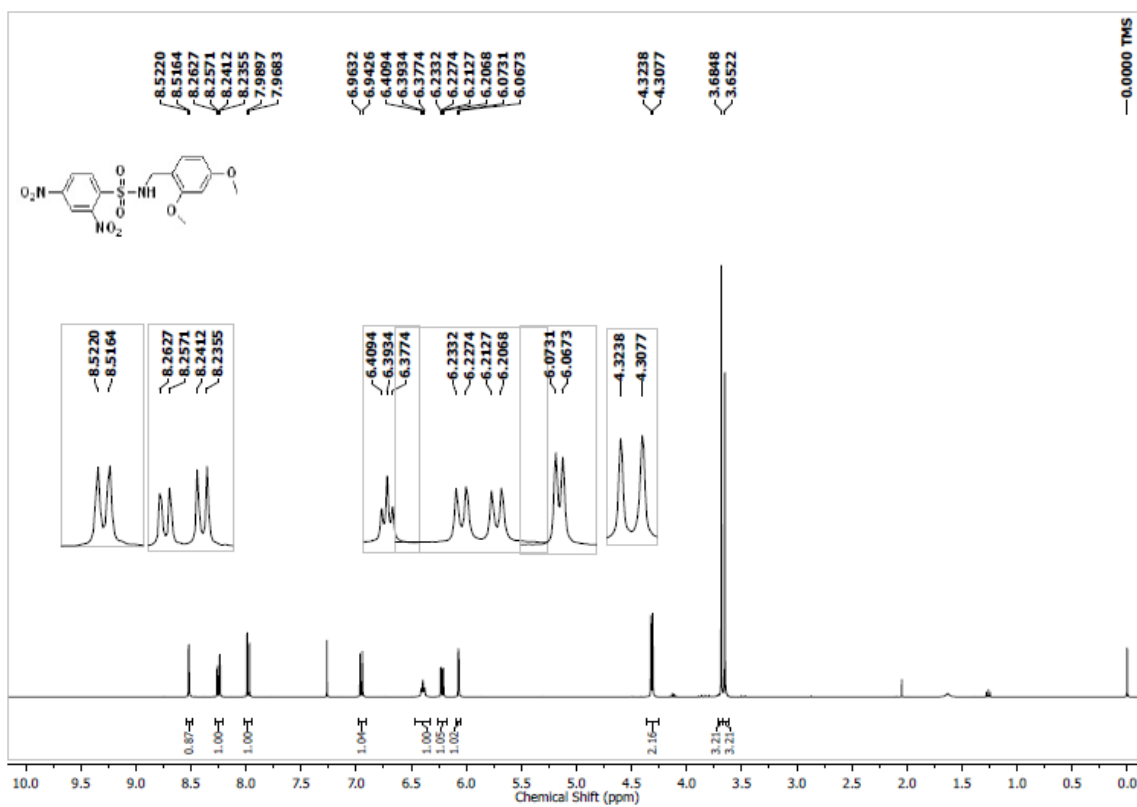
^{13}C NMR Spectrum (100 MHz, CDCl$_3$) of **11a**
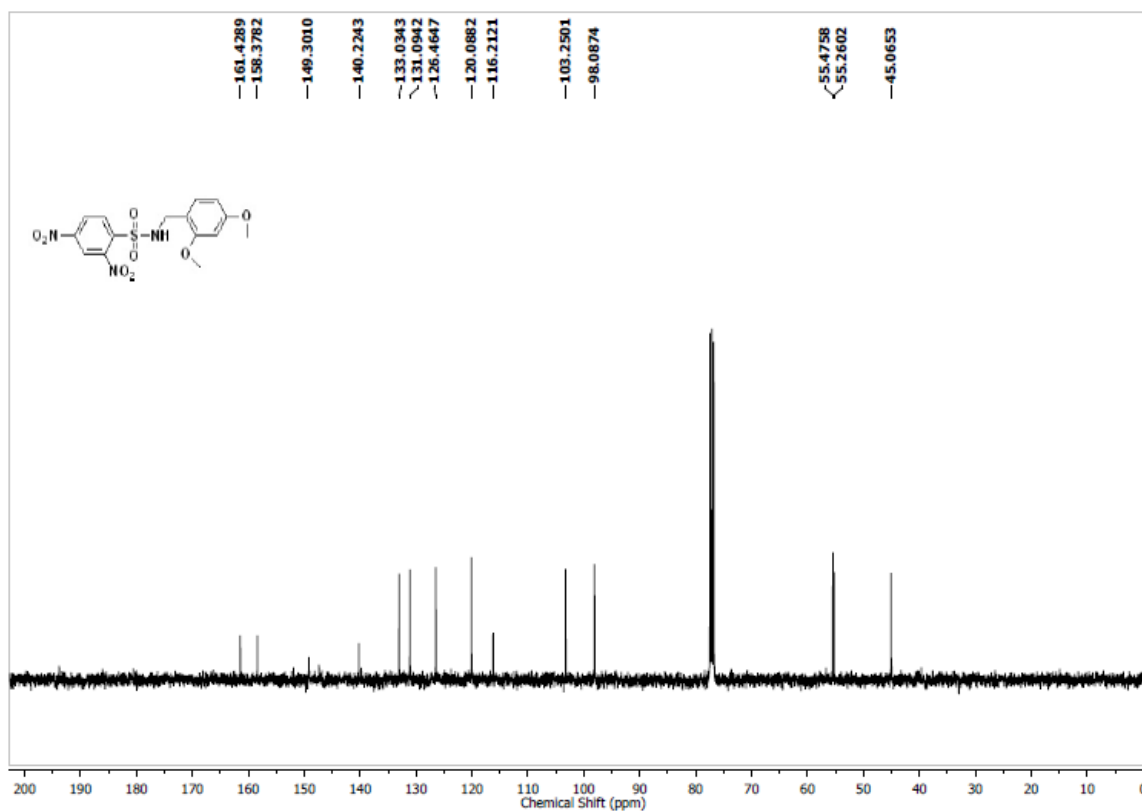
¹H NMR Spectrum (400 MHz, DMSO-*d*₆) of **15**

¹³C NMR Spectrum (100 MHz, DMSO-*d*₆) of **15**
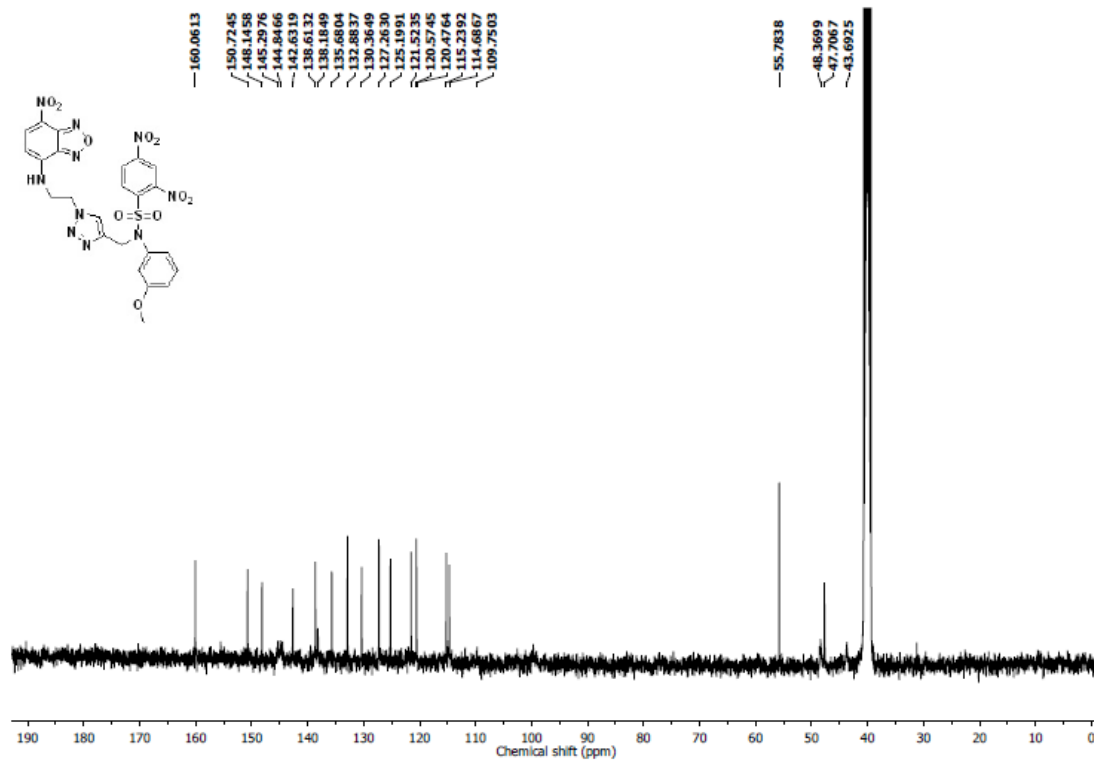
2.4.8. References

1   S. R. Malwal, D. Sriram, P. Yogeeswari, V. B. Konkimalla and H. Chakrapani, *J. Med. Chem.*, 2012, **55**, 553–557.

2   G. L. Newton, R. C. Fahey and M. Rawat, *Microbiology*, 2012, **158**, 1117–1126.

3   G. L. Newton, K. Arnold, M. S. Price, C. Sherrill, S. B. Delcardayre, Y. Aharonowitz, G. Cohen, J. Davies, R. C. Fahey and C. Davis, *J. Bacteriol.*, 1996, **178**, 1990–1995.

4   R. G. M. Moreno, M. H. G. Medeiros and N. Coichev, *Dalt. Trans.*, 2005, **0**, 1101–1107.

5   M. V. Alipázaga, R. G. M. Moreno, E. Linares, M. H. G. Medeiros and N. Coichev, *Dalt. Trans.*, 2008, **0**, 5636–5644.

6   A. T. Dharmaraja, T. K. Dash, V. B. Konkimalla and H. Chakrapani, *Medchemcomm*, 2012, **3**, 219–224.

7   S. R. Malwal, M. Gudem, A. Hazra and H. Chakrapani, *Org. Lett.*, 2013, **15**, 1116–1119.

8   A. T. Dharmaraja, M. Alvala, D. Sriram, P. Yogeeswari and H. Chakrapani, *Chem. Commun.*, 2012, **48**, 10325–10327.

9   N. Pool, U. Cell, J. J. Foti, B. Devadoss, J. a Winkler, J. J. Collins and G. C. Walker, 2012, **336**, 315–319.

10 M. C. Becerra, S. H. Mangoli, N. Jawali, M. a Kohanski, B. Hayete, J. J. Collins, D. J. Dwyer, C. a Lawrence, J. Wierzbowski, G. Cottarel, J. a Imlay, W. Park, B. Devadoss, J. a Winkler, G. C. Walker, X. Zhao, M. Malik, K. Drlica, B. B. Kaufmann, N. S. Chand, N. Haseley, D. T. Hung, T. Mashino, I. Fridovich, S. Mobashery, J. P. Mueller, P. F. Miller, a S. Arrow, X. You, M. Zheng, J. Beckwith, G. Storz, Y. Urano, K. Kakinuma, H. J. Majima, T. Nagano, P. Neta, C. K. Vanderpool and S. Gottesman, *Science*, 2013, 1213–1216.

11 Y. Liu and J. A. Imlay, *Science (80-.).*, 2013, **339**, 1210–1213.

12 B. Ezraty, A. Vergnes, M. Banzhaf, Y. Duverger, A. Huguenot, A. R. Brochado, S. Su, L. Espinosa, L. Loiseau, B. Py, A. Typas and F. Barras, *Science*, 2013, **340**, 1583–1588.

13 V. S. Khodade, A. T. Dharmaraja and H. Chakrapani, *Bioorganic Med. Chem. Lett.*, 2012, **22**, 3766–3769.

14 V. S. Khodade, M. Sharath Chandra, A. Banerjee, S. Lahiri, M. Pulipeta, R. Rangarajan and H. Chakrapani, *ACS Med. Chem. Lett.*, 2014, **5**, 777–781.

15 B. J. Privett, S. M. Deupree, C. J. Backlund, K. S. Rao, C. B. Johnson, P. N. Coneski

and M. H. Schoenfisch, *Mol. Pharm.*, 2010, **7**, 2289–2296.

16   B. Sun, D. L. Slomberg, S. L. Chudasama, Y. Lu and M. H. Schoenfisch, *Biomacromolecules*, 2012, **13**, 3343–3354.

17   Y. Lu, D. L. Slomberg, A. Shah and M. H. Schoenfisch, *Biomacromolecules*, 2013, **14**, 3589–3598.

18   J. K. Lithgow, E. J. Hayhurst, G. Cohen, S. J. Foster and Y. Aharonowitz, *Society*, 2004, **186**, 1579–1590.

19   A. Nakashio, N. Fujita, S. Rokudai, S. Sato and T. Tsuruo, *Cancer Res.*, 2000, **60**, 5303–5309.

20   S. R. Malwal, D. Sriram, P. Yogeeswari and H. Chakrapani, *Bioorg. Med. Chem. Lett.*, 2012, **22**, 3603–3606.

21   A. Ramunno, S. Cosconati, S. Sartini, V. Maglio, S. Angiuoli, V. La Pietra, S. Di Maro, M. Giustiniano, C. La Motta, F. Da Settimo, L. Marinelli and E. Novellino, *Eur. J. Med. Chem.*, 2012, **51**, 216–226.

22   C. Li, E. Henry, N. K. Mani, J. Tang, J. C. Brochon, E. Deprez and J. Xie, *European J. Org. Chem.*, 2010, 2395–2405.

23   T. Fukuyama, C. K. Jow and M. Cheung, *Tetrahedron Lett.*, 1995, **36**, 6373–6374.

24   T. Fukuyama, M. Cheung, C. K. Jow, Y. Hidai and T. Kan, *Tetrahedron Lett.*, 1997, **38**, 5831–5834.

Chapter 3. Esterase Sensitive Self-Immolative Sulfur Dioxide Donors

3.1. Introduction

As described in the previous chapter, thiol-activated SO_2 donors are a type of a bio-activatable donor. They are found to be very good *MRSA* inhibitors but their consumption of endogenous thiol (which is a vital part of the protein and antioxidant systems) means that the observed antibacterial activity is based on not just SO_2-release. It may also have a component based on the raised levels of reactive species (ROS, RSS *etc.*), which is a consequence of thiol depletion. Therefore, to study the physiological roles of SO_2 precisely, it would be desirable to have a new SO_2 donor that can be activated by a non-redox metabolic trigger. Also, the byproducts generated after SO_2 generation should be well tolerated by cells.

3.2. Results and discussion

3.2.1. Synthesis

As a prototype for our proposed SO_2-donor, compound **16b,** a carbonate, was synthesized from compound **19** (Scheme 3.1). It was also derivatized with umbelliferone *via* a reported procedure, in order to afford a negative control **16a**. The cyclopropyl carboxylic ester moiety was chosen due to the improved hydrolytic stability of such esters (in comparison with other aliphatic esters).[1,2] Pivaloyloxymethyl, as a protective group, offers good hydrolytic stability but was not considered as it generates formaldehyde upon hydrolysis. Since sulfite is known to react with formaldehyde, this may complicate interpretation of data for such a donor.[3]
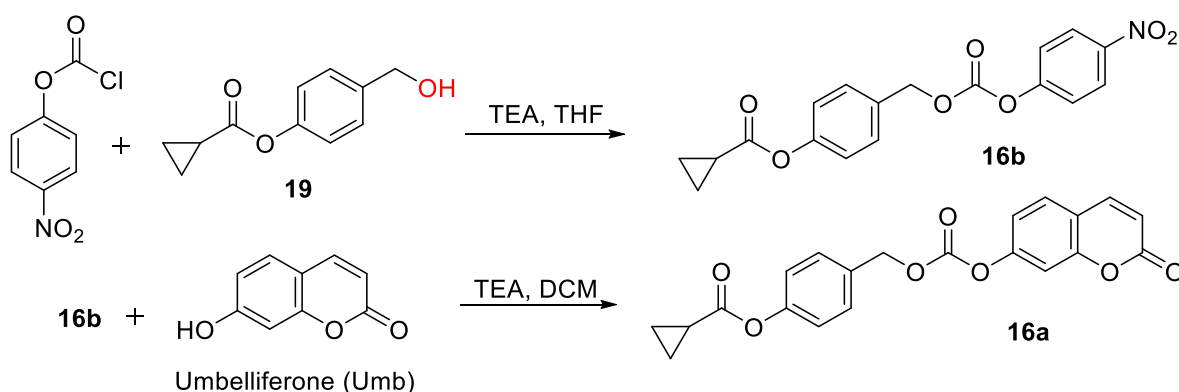
Scheme 3.1. Synthesis of control compound **16a**

In order to synthesize the sulfonate **17a**, the aldehyde **18** was synthesized from 4-hydroxybenzaldehyde. Reduction of **18** with sodium borohydride gave **19**, which was then converted to the thioacetate **20** in two steps. The thioacetate was treated with *N*-chlorosuccinimide to afford the sulfonyl chloride **21**.[4] Treatment of **21** with umbelliferone

(denoted, here, by ROH) yielded **17a** (Table 3.1). The structure of **17a** was confirmed by the X-ray diffraction method (Figure 3.2). Next, we proceeded to study the effect of the leaving group in this sulfonyl scaffold. A series of phenols and aliphatic alcohols were independently reacted with **21** to produce the corresponding sulfonates **17b-17k** (Table 3.1), in moderate to good yields.
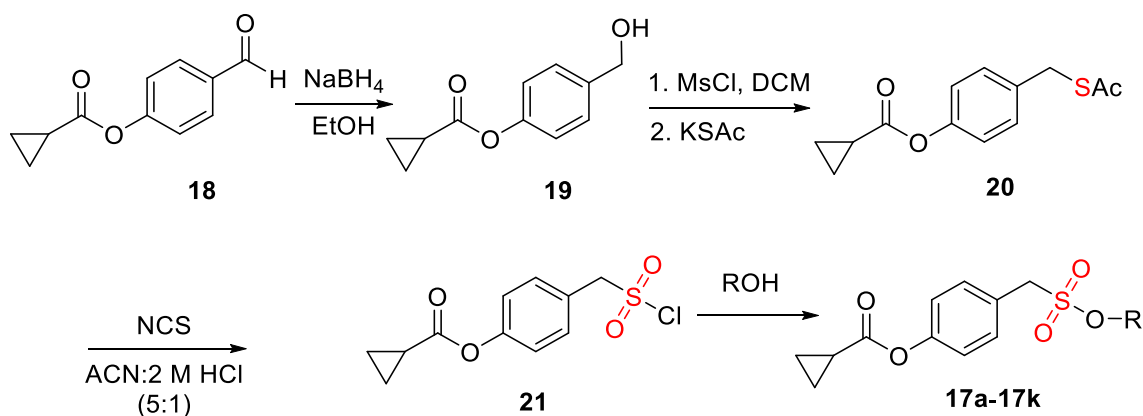
Scheme 3.2. Synthesis of sulfonates **17a-17k**

Table 3.1. Synthesis of **17a-17k**

Entry	R	pK_a of ROH*	Product	Yield, %**
1	Umbelliferone	7.7	**17a**	50
2	Ph	9.9	**17b**	75
3	4-OMePh	10.2	**17c**	65
4	4-NO$_2$Ph	7.1	**17d**	70
5	(2-*tert*-Butyl-4-Me)Ph	10.2	**17e**	65
6	(3,5-dimethyl-4-Cl)Ph	9.4	**17f**	72
7	Bn	15.4	**17g**	23
8	Allyl	15.5	**17h**	27
9	Propargyl	13.6	**17i**	24
10	*n*-Butyl	16.0	**17j**	53
11	iPr	17.0	**17k**	44

*pK_a values are either for the compound itself or analogs with similar structures[5–8]
**Percentage yield of the compounds represents the yield for the final step
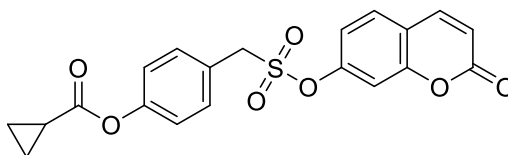
Figure 3.1 Compound **17a** that is expected to produce SO$_2$ and umbelliferone upon esterase activation
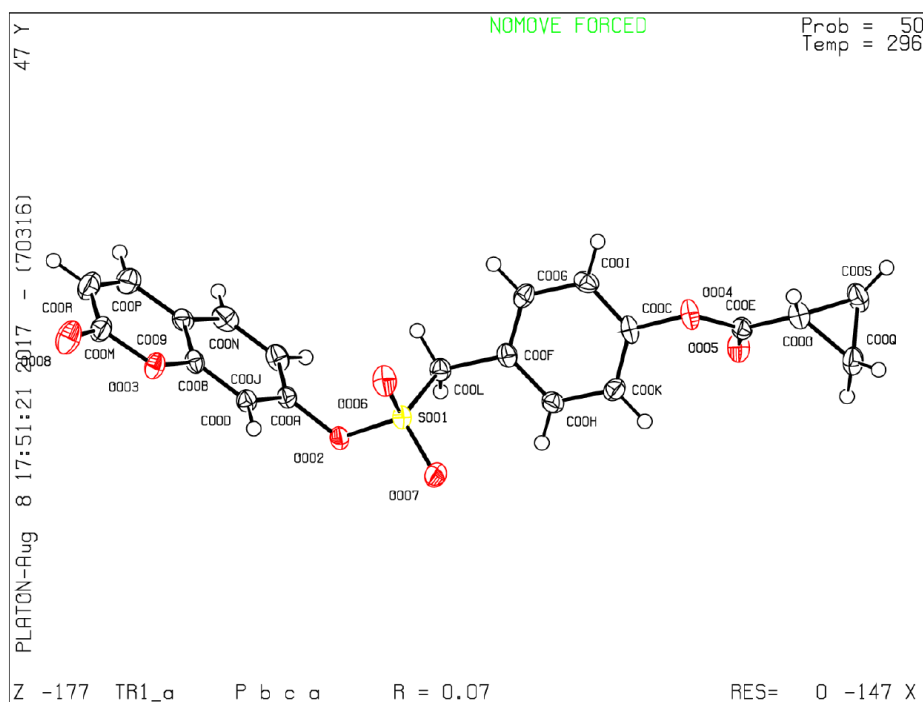
Figure 3.2 ORTEP diagram for **17a**. $R = 0.062$

3.2.2. Stability and decomposition studies

To evaluate the hypothesis that our synthesized compounds undergo self-immolation to generate umbelliferone (Umb), the control compound **16a** and sulfonate **17a** were independently treated with porcine liver esterase under physiological conditions and aliquots were monitored independently at different time intervals by HPLC.[3,9] HPLC analysis of the reaction mixture after 10 min revealed the complete disappearance of **16a** (Figure 3.3a). The rate constant for the disappearance of **16a** was found to be 0.54 ± 0.08 min^{-1}, with a half-life of 5 min. Similarly, the disappearance of **17a** (Figure 3.3b) was comparable with that of **16a**. The rate constant for the disappearance of **17a** was found to be 0.13 ± 0.01 min^{-1}. Also, the rate constant was comparable with that of the formation of umbelliferone, *i.e.*, 0.18 min^{-1}, which had been monitored similarly (Figure 3.3b). The yield of formation of Umb was found to be 80%, suggesting an efficient conversion of **17a** upon esterase activation to form Umb.
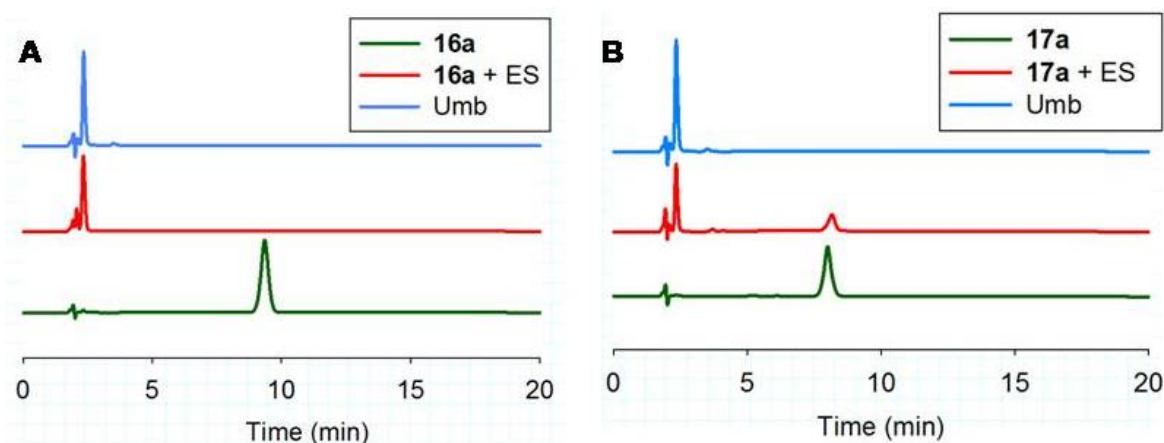
Figure 3.3. Monitoring the release of Umbelliferone (Umb) by HPLC in PBS (pH 7.4, 10 mM) upon esterase activation (1 U/mL) (a) Decomposition of **16a** (50 µM) after 10 min (b) Decomposition of **17a** (50 µM) after 10 min. Absorbance was monitored at 280 nm.
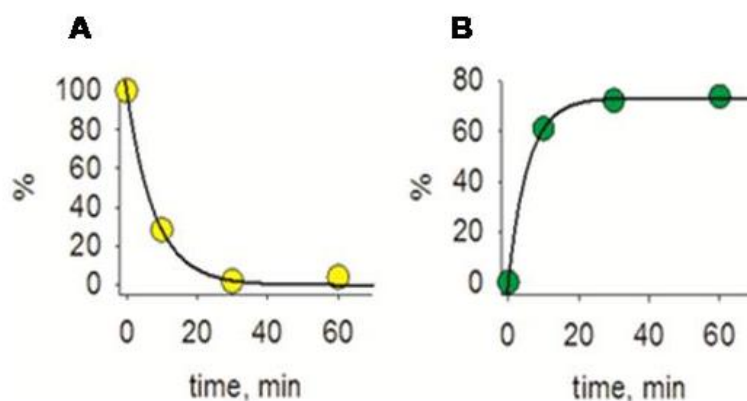
Figure 3.4. HPLC analysis of **17a** (a) **17a** (50 µM) was incubated in PBS (pH 7.4, 10 mM) at 37 ℃ in the presence of esterase; the disappearance of **17a** is readily apparent. The rate constant for this disappearance was found to be 0.13 ± 0.01 min^{-1}; (b) HPLC analysis of the reaction mixture for Umb. The rate constant for the appearance of Umb was found to be 0.18 ± 0.006 min^{-1}.

3.2.3. Evaluation of buffer stability for the sulfonate functional group

In the previous section, we validated that **17a** undergoes self-immolation to produce Umb; from this, the production of SO_2 can also be inferred. Next, we proposed to study, the stability of the sulfonate functional group in different pHs by measuring fluorescence readouts for umbelliferone release, in order to check for its broad range pH applicability. In the absence of esterase, no significant decomposition of **16a** or **17a** was observed (Figure 3.5) at physiological pH, suggesting that the cyclopropyl ester was not susceptible to hydrolysis. However, compound **16a** was found to be unstable at pH 9.2, suggesting the instability of the carbonate group in basic conditions.
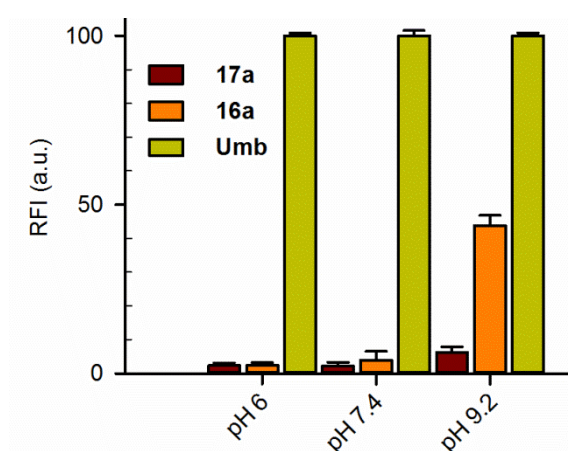
Figure 3.5. pH stability of the sulfonate functional group. Compounds **16a** and **17a** (50μM) were incubated in different buffers for 30 min. Fluorescence measurement for the formation of Umb (λ_{ex} = 350 nm and λ_{em} = 450 nm) was monitored, with authentic umbelliferone used as a control. Umb formation is an indicator of the stability of the compounds. Compound **16a** was found to be unstable in basic sodium borate buffer (pH 9.2, 50 mM)

3.2.4. Compiled data for stability and selectivity of the sulfonate functional group towards esterase, in the presence of biological nucleophiles and esterase inhibitor

In order to study the reactivity of the sulfonate functional group towards esterase, control compound **23** (without the cyclopropyl carboxylic ester) was synthesized. No significant fluorescence signal corresponding to Umb formation was recorded from compound **23** upon treatment with esterase, suggesting that the sulfonate functional group was stable towards esterase. However, a significant decrease in the fluorescence signal corresponding to Umb formation was recorded when **17a** was pre-treated with an esterase inhibitor (phenylmethanesulfonyl fluoride, PMSF)[10,11] and subsequently exposed to ES a diminished

signal for Umb was observed, as shown (Figure 3.6, orange bars). Preincubation of ES with PMSF and subsequent addition of **17a** showed a dose-dependent decrease in fluorescence, again supporting the idea that catalysis by esterase is necessary for activation of **17a** (Figure 3.6, inset). In the presence of common biological nucleophiles, **17a** was found to be stable (Figure 3.6, pink bars). Sulfonate stability was assessed by monitoring the fluorescence associated with the formation of Umb (λ_{ex} = 350 nm and λ_{em} = 450 nm).

This enhanced stability of sulfonate at different pHs and against common biological nucleophiles may present opportunities for delivering SO_2-based hybrid drugs.
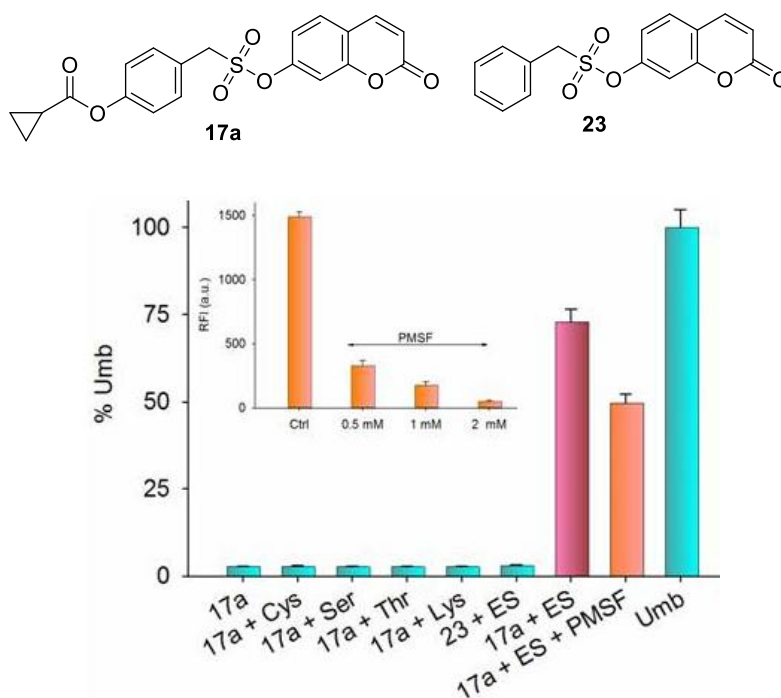
Figure 3.6. Compiled data for stability and selectivity of SO_2-donors and their sulfonate functional group**.** Compounds **17a** (25 µM) and **23** (25 µM) were incubated independently in the presence of esterase, ES (1 U/mL) for 30 min. Similarly, **17a** (25 µM) was incubated with 250 µM of various biological nucleophiles Cys, Ser, Thr and Lys independently for 1h. For the esterase inhibitor experiment, **17a** (25 µM) was incubated with PMSF (250 µM) and esterase (1 U/mL) for 30 min. The inset figure represents the data for the preincubation of esterase with PMSF in a dose-dependent manner. All the experiments were conducted in PBS (pH 7.4, 10 mM) at 37 °C.

3.2.5. Stability of the sulfonate functional group in mammalian cellular conditions

In order to study the stability of the sulfonate functional group, the control compound **23** was treated with esterases, and we did not observe any significant fluorescence signal corresponding to Umb formation, unlike in the case of **17a** (Figure 3.6). A similar result was observed when **23** was incubated within human cervical cancer HeLa cell lysate for 1 h, suggesting that the sulfonate group is stable under mammalian cellular conditions (Figure 3.7). Incubation of **17a**, as expected, produced a fluorescence signal, confirming the production of Umb. Taken together, our data support that mammalian cellular esterases selectively cleave the cyclopropyl carboxyl ester moiety in **17a** and it can also be inferred from this data that the sulfonate group has a broad range stability towards mammalian cellular nucleophiles.
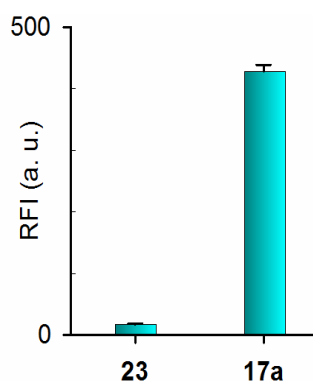
Figure 3.7. Monitoring the stability of the sulfonate functional group in a mammalian cellular environment by measuring the fluorescence readout for Umb from **17a** (25 µM) and from the control compound **23** (25 µM) in PBS (1X) at 37 °C for 1 h. The absence of a significant fluorescence signal from **23** suggests sulfonate functional group stability in a mammalian cellular environment. **17a** shows a significant fluorescence signal for Umb (λ_{ex} = 350 nm and λ_{em} = 450 nm) as the cyclopropyl carboxyl moiety of **17a** gets hydrolyzed in mammalian cellular conditions by esterases

3.2.6. Colorimetry based sulfite detection of 17a

Incubation of **17a** with esterases generates SO_2 so that it gets converted into the sulfite/bisulfite mixture, under physiological conditions. Therefore, for the detection of SO_2 from **17a** by colorimetry, the coumarin-hemicyanine dye **22** was synthesized (Scheme 3.3).[12] Also, this probe has been found to be a useful fluorimetry based detector of sulfite *in vitro* and also, for cellular-based studies.
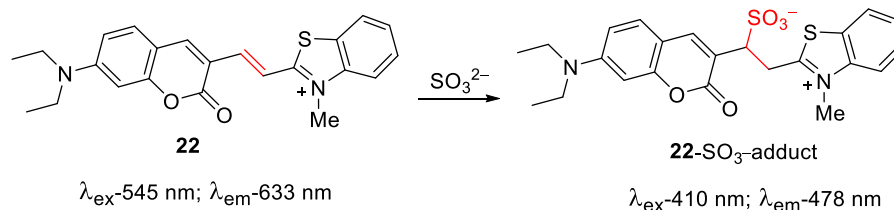
Scheme 3.3. The sulfite dye, **22**, and the formation of its sulfite adduct

The dye **22** reacts selectively with sulfite to produce a covalent adduct (Scheme 3.3). This results in the characteristic decrease of the absorbance signal at 545 nm, with a concomitant increase in the absorbance signal at 410 nm. In this experiment, NaHSO$_3$ (sodium bisulfite) has been used as a positive control. Sodium bisulfite was incubated with **22** and we observed spectra (Figure 3.8a, sky blue line) similar to the ones reported in the literature. Similarly, when **17a** was analyzed for sulfite along with sulfite dye **22** and esterase, a decrease in absorbance at 545 nm was observed (Figure 3.8b, sky blue line). However, due to the significant absorbance of Umb at 410 nm, the use of **22** to accurately detect sulfite was not possible for **17a**. Based on the diminution of the absorbance at 545 nm, the generation of sulfite during the decomposition of **17a** in the presence of the esterases was inferred (Figure 3.8b, sky blue line). In addition, as a control experiment, the mixture of authentic Umb, NaHSO$_3$ and **22** together showed a spectrum similar to that of **17a** upon esterase activation (Figure 3.8b, blue line).
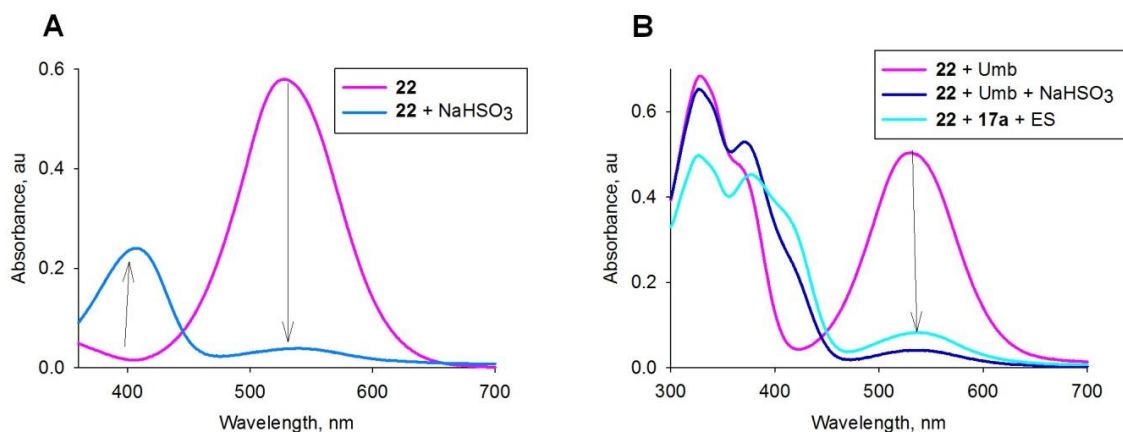
Figure 3.8. (a) Absorbance profiles of **22** upon the addition of NaHSO$_3$ show a decrease in the absorbance signal at 545 nm and an increase in the same at 410 nm (b) A similar absorbance decrease was observed for **22** at 545 nm, for the reaction mixture of (**22** + **17a** + ES)

3.2.7 Colorimetric analysis for other SO₂-donors, 17b-17k

Having established that **17a** was capable of undergoing self-immolation in the presence of esterase to generate SO_2, the effect of the leaving group in this process was studied. A series of phenols and aliphatic alcohols were independently reacted with **21** to produce the corresponding sulfonates **17b**-**17k** (Table 3.1). Again, the sulfite-sensitive dye, **22**, was used to assess the capability of these compounds to generate SO_2. Next, these compounds were exposed to porcine liver esterase along with the sulfite dye, **22**. The ratio of absorbance at 410 nm (A_{410}) to the absorbance at 545 nm (A_{545}) provides an estimate of the ability of the compound to produce SO_2. No sulfite generation was observed, in the absence of esterases (Figure 3.9a). A representative example of SO_2 generation, upon esterase activation, showed for compound 17c (figure 3.9b). All the SO_2 donors derived from substituted phenols (**17b-17f**) were able to generate sulfite (figure 3.10). However, SO_2 donors derived from aliphatic alcohols except **17i** were found to be poor donors of SO_2.
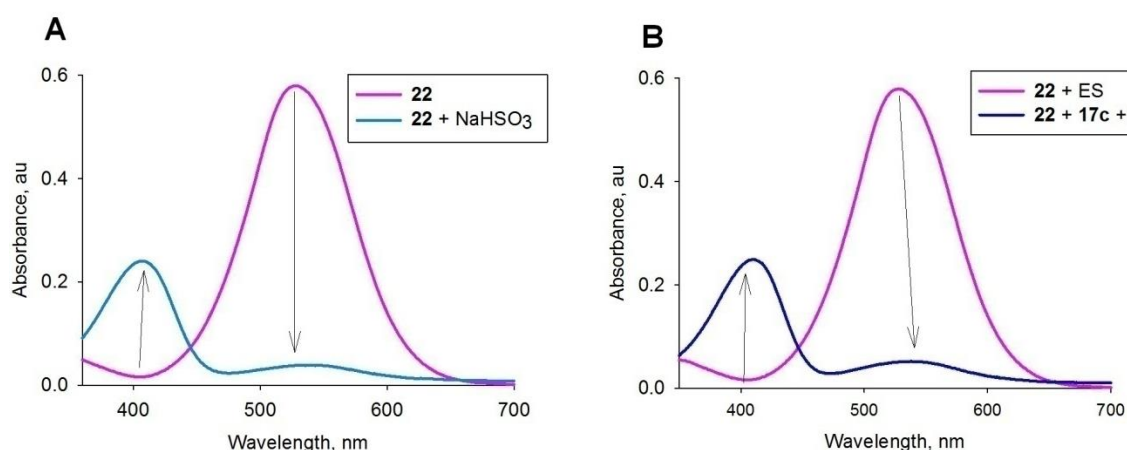
Figure 3.9. Representative absorbance spectra (A) Incubation of **22** (10 µM) in the presence of NaHSO₃ (50 µM) for 15 min shows a decrease in absorbance at 545 nm and a corresponding increase in absorbance at 410 nm. (B) Incubation of **17c** (50 µM) and **22** (10 µM) in the presence of ES for 15 min. The disappearance of the 545 nm signal was observed and is indicative of sulfite formation. The absorbance profile was similar to that with NaHSO₃. All experiments were conducted in PBS (pH 7.4, 10 mM) at 37 °C.
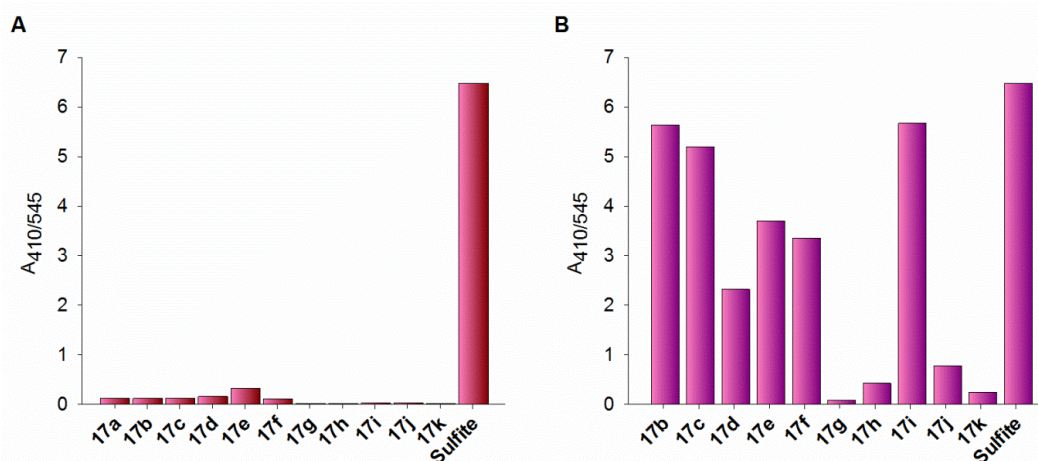
Figure 3.10. (A) The ratio of absorbance intensity (A_{410}/A_{545}) when SO_2 donors **17a-17k** (50 µM) and the sulfite dye, **22**, were incubated for 15 min in the absence of esterase. No significant increase in absorption intensity ratio was observed (B) Ratio of absorbance intensity (A_{410}/A_{545}) when SO_2 donors **17b-17k** (50 µM) and the sulfite dye, **22**, were incubated for 15 min in the presence of esterase, ES (1 U/mL). A distinct decrease in absorbance at 545 nm for the sulfite dye and a corresponding increase in absorbance at 410 nm for the sulfite adduct was observed, thus, yielding a significant increase in absorption intensity ratio.

3.2.8 Further study of SO_2 donors derived from an aliphatic alcohol

Compounds **17g-17k**, which are derived from aliphatic alcohol, were subjected to SO_2 analysis in the presence of esterase; among these, **17g**, **17h,** and **17k** did not show a significant shift in the absorbance profile and accordingly, the ratio of A_{410}/A_{545} was diminished (Figure 3.10b). This data suggested that these compounds were poor donors of SO_2 when compared with their counterparts. Prolonged incubation of these reaction mixtures in a buffer also did not produce significant levels of sulfite. We hypothesized that there could be two major pathways by which these compounds dissociated. First, the formation of intermediate I, which undergoes self-immolation to produce an alkoxide and a quinone methide (Scheme 3.4). Being aliphatic alcohols, their leaving group ability is significantly lower than that of phenols (see Table 3.1 for pK_a values). Secondly, there may be a propensity for a different sort of hydrolysis (in the buffer) to produce II, which does not generate SO_2. Either or both of these pathways would result in a diminished yield of sulfite. In order to study whether hydrolysis occurred, compounds **17g-17k** were independently incubated in pH 7.4 buffer and we found that all compounds except for the benzyl and allyl compounds were stable towards hydrolysis (of the second kind) (Figure 3.11). When the benzyl derivative was

103

incubated in the buffer, we found nearly complete disappearance in 30 min, while partial hydrolysis was observed in the case of the allyl derivative. These data suggested that only certain sulfonates were susceptible to hydrolysis. Thus, among aliphatic alcohol-derived sulfonates, SO_2 generation after activation by esterase is possible, provided the sulfonate is not susceptible to hydrolysis and if the alcohol is a good leaving group (such as propargyl alcohol).
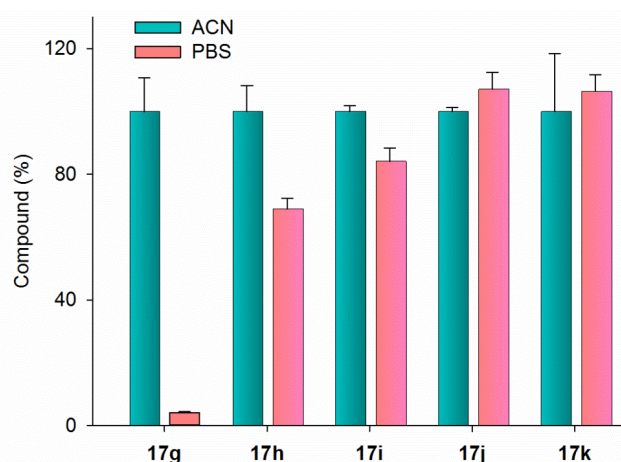
Figure 3.11. Decomposition study of aliphatic SO_2 donors (**17g-17k**) in the buffer. Compounds **17g-17k** (500 µM) were incubated for 30 min 50% PBS: ACN at 37 ºC and injected in an HPLC instrument. Due to the competitive pathways of hydrolysis, certain compounds decomposed in the buffer. However, a majority of the compounds tested were stable in the buffer.

3.3.9. Proposed mechanism for generation of SO_2 from sulfonates

For sulfonates derived from phenols, SO_2 generation is dominant. Certain sulfonates derived from aliphatic alcohols were susceptible to hydrolysis (through intermediate II) and were poor SO_2 donors or are possibly trapped as intermediate I.
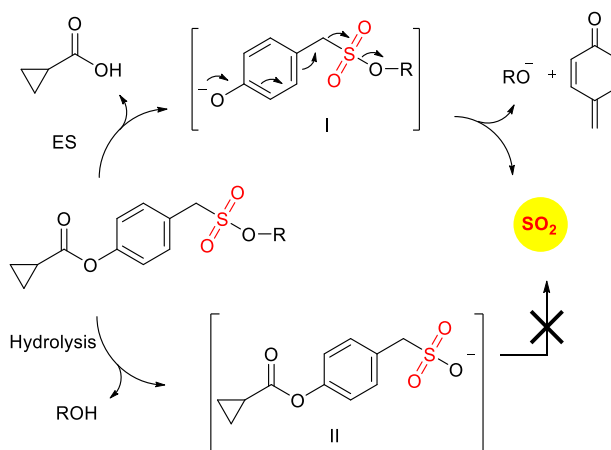
Scheme 3.4. Proposed mechanism for the generation of SO_2 from sulfonates

3.2.10. Compiled data for sulfite generation in the presence of biological nucleophiles and esterase inhibitor

As discussed in the previous section, a majority of SO_2-donors derived from aliphatic alcohols were poor SO_2 donors, unlike their aromatic counterparts. Therefore, we proceeded to study the effects of biological nucleophiles and the esterase inhibitor, PMSF, on SO_2 generation, with the SO_2-donors derived from phenols. When we incubated one of the SO_2-donors, namely, **17c**, with biological nucleophiles, there was no significant generation of sulfite, suggesting the absence of hydrolysis in the presence of only biological nucleophiles (Figure 3.12). Sulfite generation was somewhat diminished with PMSF, in comparison with the positive control ((**17c** + ES), Figure 3.12). Thus, this experiment further validated the specificity of these SO_2 donors for esterase.
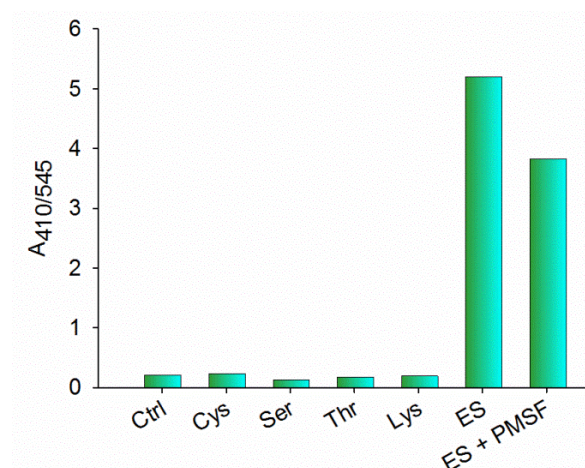
Figure 3.12. Sulfite analysis of compound **17c** with sulfite dye **22**, in the presence of esterase (ES), biological nucleophiles and esterase inhibitor, PMSF. **17c** (50 µM), and sulfite dye **22** (10 µM) were incubated in the presence of esterase (1 U/mL) for 15 min. Similarly, **2c** (50 µM) and **22** (10 µM) were incubated with 1 mM biological nucleophiles Cys, Ser, Thr and Lys independently for 15 min. In the esterase inhibitor experiment, compounds **17c** (50 µM), **7** (10 µM) and esterase, ES (1 U/mL) were incubated in the presence of PMSF (1 mM) and for 15 min. All experiments were conducted at 37 °C for 15 min in PBS (pH 7.4, 10 mM) on Eppendorf thermomixer comfort (800 rpm), followed by absorption measurement in Shimadzu UV-2600. Sulfite was assessed by calculating the ratio of the absorbance of the

sulfite adduct to that of the sulfite dye **22** (A_{410}/A_{545}). That compound **17c** did not generate any sulfite in the presence of biological nucleophiles further established the stability of the sulfonate group.

3.2.11. Fluorescence Spectroscopy for Sulfite Detection

The sulfite dye, **22**, is also used as a sulfite-sensitive fluorescence probe: the free probe displayed a red emission with the maximum at 633 nm (excitation at 545 nm). In the presence of sulfite, the fluorescence signal at this wavelength is diminished with a concomitant increase in a new blue emission peak at 478 nm (excitation at 410 nm). I_{478}/I_{633} is hence a measure of SO_2 donating capability. The fluorescence data corroborated the absorbance data that we obtained from the donors.
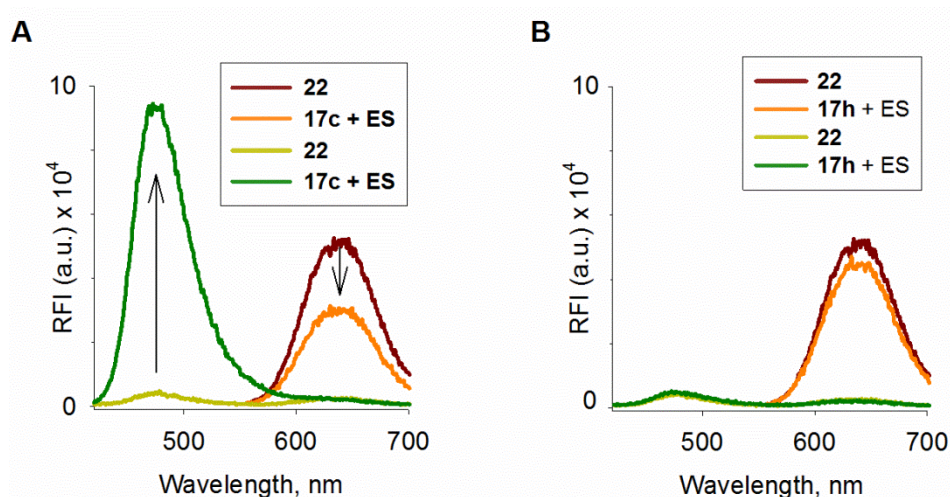
Figure 3.13. Representative fluorescence emission spectra for (a) **17c** (10µM) and (b) **17h** (10µM) incubated with **22** (10 µM) and esterase, ES (1 U/mL) in PBS (pH 7.4, 10 mM) for 30 min
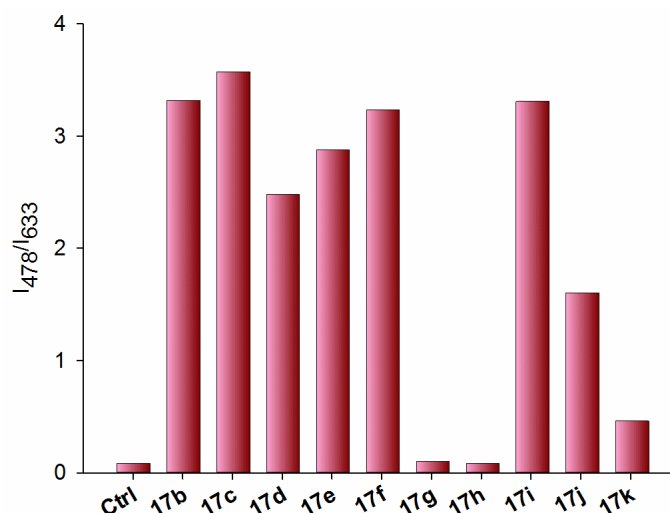
Figure 3.14. Fluorescence intensity ratio of sulfite adduct to sulfite dye (I_{478}/I_{633}) for compounds **17b-17k** (10 µM) incubated with sulfite dye **22** (10 µM) in the presence of esterase, ES (1 U/mL) in PBS (pH 7.4, 10 mM) for 30 min

3.2.12. Cell permeability of SO₂ donors

Next, we investigated the capability of the SO₂ donors to permeate cells and generate SO₂. Accordingly, we used the dye **22** and A549 lung carcinoma cells. In the presence of a sulfite (200 µM), a distinct increase in the signal in the blue channel with a concomitant decrease in signal in the red channel was observed (Figure 3.15). Coumarin dye with the SO₂ donor **17c** was similarly found to fluoresce in the blue channel but at a much lower concentration (25 µM) suggesting their superior capability to generate sulfite within cells. Compounds **17g** and **17h**, which were poor SO₂ donors when exposed to esterase, were similarly found to be incapable of generating SO₂ within cells (Figure 3.16). Lastly, we estimated the cytotoxicity of these compounds using two different cell lines and we found that a majority of these compounds were not significantly cytotoxic (Figure 3.17). The likely byproducts that were produced during the decomposition of SO₂ donors **17c** and **17i** were not cytotoxic either (Figure 3.18). Thus, the SO₂ donors prepared in this study are cell-permeable and appear to be well tolerated by cells and should facilitate a better understanding of the biology of this gas.
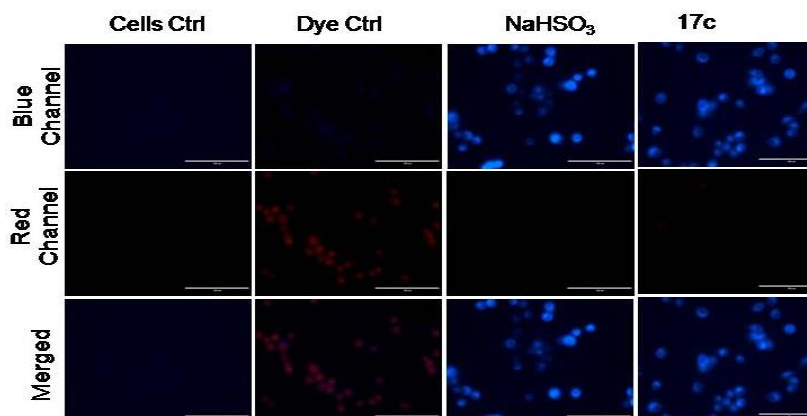
Figure 3.15. Fluorescence microscopy images of A549 cells treated with dye for 30 min and followed by treatment of the compound for 30 min at 37 °C. Fluorescence signal was monitored in the red channel (**22**) and the blue channel (**22-SO₃** adduct). The final concentration of dye **22** was 10 μM; NaHSO₃, 200 μM; SO₂ donors, 25 μM. Scale bar = 200 μM
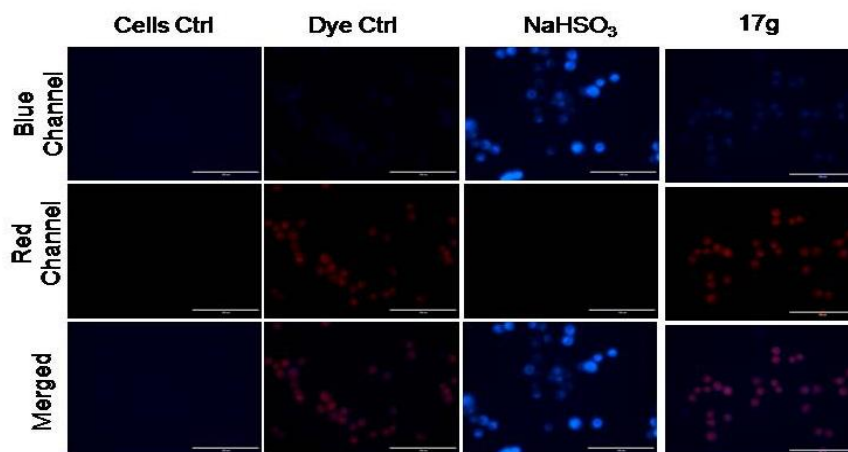
Figure 3.16. Fluorescence microscopy images of A549 cells treated with the dye and aliphatic SO₂ donors with the similar protocol (Figure 3.15)

Fluorescence microscopy data was provided by Govindan Ravikumar, IISER Pune.
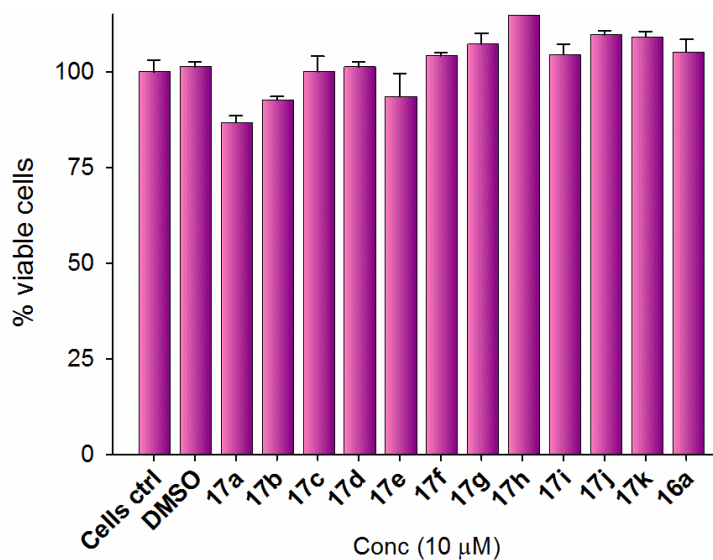
Figure 3.17.1. Cell viability assay with HeLa cells (10 µM)

Cell viability data was provided by Govindan Ravikumar, IISER Pune.
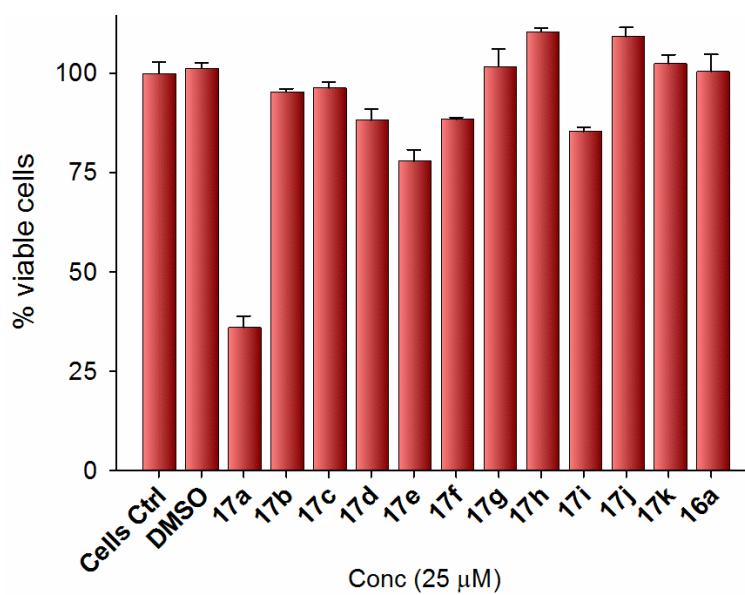
Figure 3.17.2. Cell viability assay with HeLa cells (25 µM)
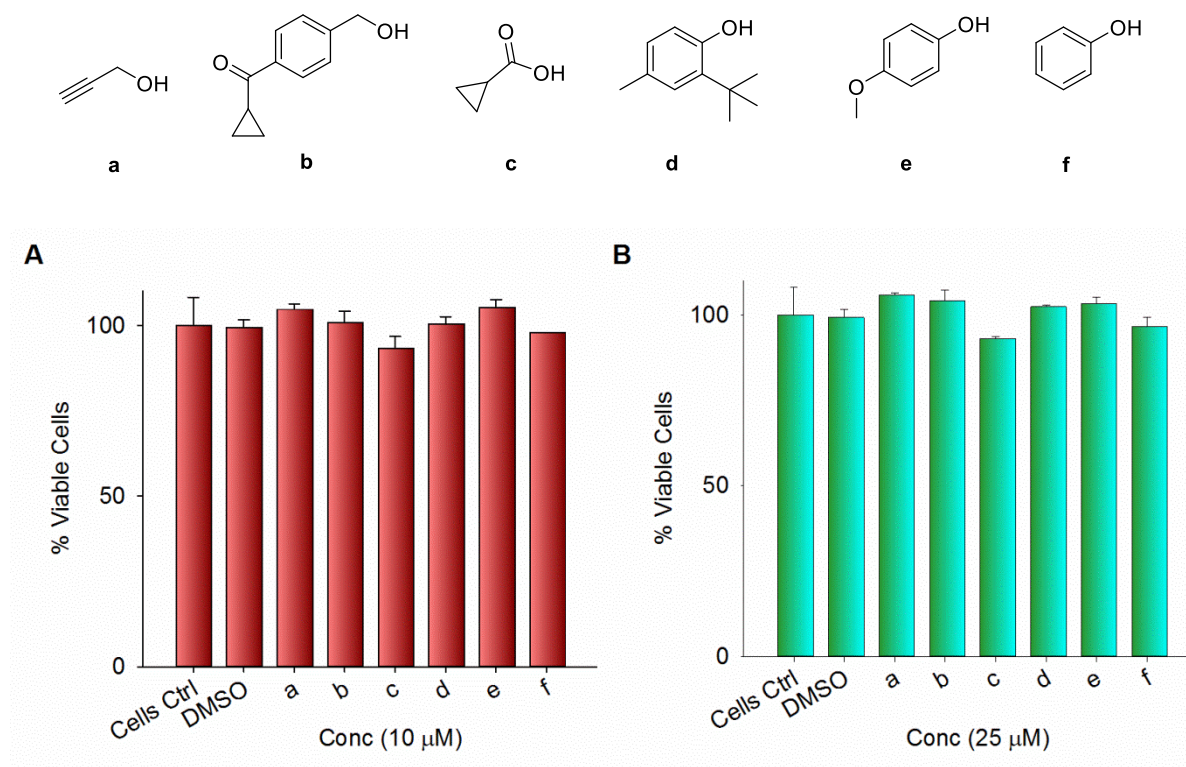
Figure 3.18. Cell viability assay for byproducts with Hela cells. Byproducts did not show any significant toxicity (25 µM and 10 µM)

Cell viability data was provided by Govindan Ravikumar, IISER Pune.

3.3 Summary

Here, in chapter 3, we synthesized a new class of esterase sensitive SO_2 donors. All the SO_2 donors derived from phenols were able to generate SO_2 when exposed to esterase. Sulfur dioxide generation was independently inferred by colorimetry and fluorimetry. These SO_2 donors found to be cell-permeable: SO_2 inside cells was detected by sulfite dye at lower concentration when compared with $NaHSO_3$. These SO_2 donors appear to be tolerated well by the cells and this class of donors should facilitate a better understanding of the biology of this gas. In addition, improved hydrolytic of cyclopropyl ester as well as sulfonate stability may present an opportunity for the new class of SO_2 based prodrug strategy and may serve as a better substitute for carbonate class of prodrugs.

3.4 Experimental section

3.4.1 Synthesis and characterization

4-(((((2-oxo-2H-chromen-7-yl)oxy)carbonyl)oxy)methyl)phenyl

cyclopropanecarboxylate (16a): Umbelliferone (168 mg, 0.44 mmol) and TEA (154 µL, 1.11 mmol) was dissolved in DCM (30mL). To this solution, **16b** (132 mg, 0.37 mmol) in DCM (1 mL) was added dropwise at 0 °C under nitrogen atmosphere. The resulting mixture was stirred at rt for 3 h.The solvent was evaporated under reduced pressure and the residue was purified over silica gel column (hexane/EtOAc) to obtain **16a** (63 mg, 49%) as a colorless solid; ^{1}H NMR (400 MHz, CDCl$_3$): δ = 7.68 (d, J = 9.6 Hz, 1H), 7.48 (d, J = 8.5 Hz, 1H), 7.45 (d, J = 8.5 Hz, 2H), 7.22 (d, J = 2.2 Hz, 1H), 7.15-7.11 (m, 3H), 6.40 (d, J = 9.6 Hz, 1H), 5.27 (s, 2H), 1.88-1.82 (m, 1H), 1.18-1.15 (m, 2H), 1.06-1.02 (m, 2H); ^{13}C NMR (100 MHz, CDCl$_3$): δ = 173.5, 160.3, 154.7, 153.4, 152.8, 151.4, 142.9, 131.8, 130.1, 128.8, 122.1, 117.8, 116.9, 116.4, 110.0, 70.3, 13.1, 9.5; FTIR (ν_{max}, cm[-1]): 1133, 1219, 1380, 1508, 1617, 1734; HRMS (ESI) calcd for C$_{21}$H$_{16}$O$_7$ [M + H]$^+$: 381.0974; Found: 381.0974.
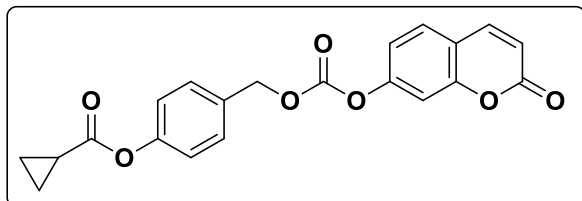
4-((((4-nitrophenoxy)carbonyl)oxy)methyl)phenyl cyclopropanecarboxylate(16b):

Solution of 4-nitrophenyl chloroformate (495 mg, 2.46 mmol) in THF (1mL) was added drop wise to a solution of **19** (315 mg, 1.64 mmol) in THF(30 mL) at 0 °C under nitrogen atmosphere. To this TEA (573 µL, 4.10 mmol) was added and the resulting mixture was stirred at rt for 2 h. The solvent was evaporated and the residue was purified over silica gel column (hexane/EtOAc) to obtain **16b** (387 mg, 66%) as a colorless solid;^{1}H NMR (400 MHz, CDCl$_3$): δ = 8.27 (d, J = 9.1 Hz, 2H), 7.46 (d, J = 8.5 Hz, 2H), 7.38 (d, J = 9.2 Hz, 2H), 7.14 (d, J = 8.6 Hz, 2H), 5.28 (s, 2H), 1.88-1.82 (m, 1H), 1.20-1.16 (m, 2H), 1.06-1.01 (m, 2H); ^{13}C NMR (100 MHz, CDCl$_3$): δ = 173.5, 155.6, 152.5, 151.5, 145.6, 131.7, 130.1, 125.4, 122.2, 121.9, 70.4, 13.1, 9.5; FTIR (ν_{max}, cm[-1]): 1135, 1160, 1205, 1347, 1380, 1521, 1746; HRMS (ESI) calcd for C$_{18}$H$_{15}$NO$_7$ [M + K]$^+$: 396.0536; Found: 396.0532.
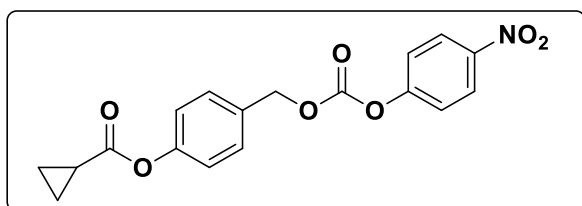
3.4.2 General Procedure for the synthesis of 17b-17k. To a solution of aromatic/aliphatic hydroxyl compound and TEA (3eq.) in DCM (25mL), a solution of **21** in DCM (1mL) was added drop wise at 0 °C under nitrogen atmosphere. The resulting mixture was stirred for 1 h (in case of aliphatic compounds the mixture was stirred for 2 h). Reaction mixture was further diluted with dI water (100mL) and the aqueous layer was extracted with DCM (3 × 30 mL). The combined organic layers were dried over Na_2SO_4 and evaporated under reduced pressure. The residue was purified over silica gel column chromatography for compounds **17b-17f**, using hexane/EtOAc as the mobile phase. Prep HPLC was used for purification of compounds **17g-17k** using H_2O/ACN as mobile phase**.**

4-((((2-oxo-2H-chromen-7-yl)oxy)sulfonyl)methyl)phenyl   cyclopropanecarboxylate
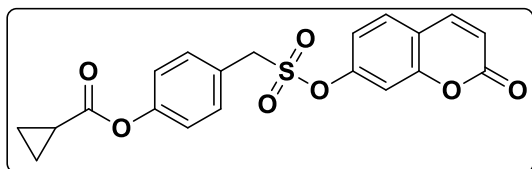
(17a): To a solution of umbelliferone (106 mg, 0.65 mmol), and TEA (166 mg, 1.64 mmol), in DCM (25 mL), a solution of **21** (150 mg, 0.55 mmol) in DCM (1 mL) was added drop wise at 0 °C under nitrogen atmosphere. The resulting mixture was stirred for 1 h. Reaction mixture was further diluted with dI water (100 mL) and the aqueous layer was extracted with DCM (3 × 30 mL). The combined organic layers were dried over Na_2SO_4 and evaporated under reduced pressure. The residue was purified over silica gel column chromatography, using hexane/EtOAc as the mobile phase. **17a** (110 mg, 50%) was isolated as a colorless solid; ^{1}H NMR (400 MHz, $CDCl_3$): δ = 7.67 (d, *J* = 9.6 Hz, 1H), 7.47-7.45 (m, 3H), 7.17 (d, *J* = 2.2 Hz, 2H), 7.08 (d, *J* = 2.2 Hz, 1H), 6.99 (dd, *J* = 8.5, 2.2 Hz, 1H), 6.41(d, *J* = 9.6 Hz, 1H), 4.57 (s, 2H), 1.88-1.82 (m, 1H), 1.20-1.16 (m, 2H), 1.07-1.02 (m, 2H); ^{13}C NMR (100 MHz, $CDCl_3$): δ = 173.3, 159.9, 154.7, 152.0, 151.2, 142.6, 132.1, 129.2, 124.2, 122.6, 118.6, 117.8, 117.0, 110.9, 57.0, 13.2, 9.6; FTIR (v_{max}, cm[-1]): 1107, 1139, 1170, 1213, 1374, 1504, 1612, 1737; HRMS (ESI) calcd for $C_{20}H_{16}O_7S$ [M + H][+]: 401.0695; Found: 401.0695.

4-((phenoxysulfonyl)methyl)phenyl cyclopropanecarboxylate (17b): Starting from phenol
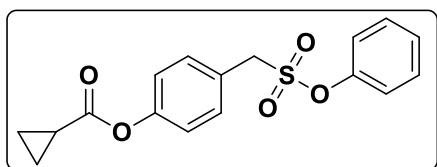
(62 mg, 0.65 mmol), TEA (229 µL, 1.64 mmol), and **21** (150 mg, 0.55 mmol), **17b** (136 mg, 75%) was isolated as a colorless solid; ^{1}H NMR (400 MHz, $CDCl_3$): δ = 7.46 (d, *J* = 8.6 Hz, 2H), 7.39-7.34 (m, 2H), 7.31-7.27 (m, 1H), 7.16 (d, *J* = 8.6 Hz, 2H), 7.14-7.11 (m, 2H), 4.50 (s, 2H), 1.88-1.82 (m, 1H), 1.20-1.16 (m, 2H), 1.07-1.02 (m, 2H); ^{13}C NMR (100 MHz, $CDCl_3$): δ = 173.4, 151.7, 149.3, 132.1,

130.1, 127.4, 124.7, 122.4, 122.1, 56.2, 13.1, 9.6; FTIR (ν_{max}, cm^{-1}): 1146, 1215, 1340, 1380, 1487, 1736; HRMS (ESI) calcd for C$_{17}$H$_{16}$O$_5$S [M + Na]$^+$:355.0603; Found: 355.0603.

4-(((4-methoxyphenoxy)sulfonyl)methyl)phenyl cyclopropanecarboxylate(17c): Starting from 4-methoxyphenol (81 mg, 0.65 mmol), TEA (229 μL, 1.64 mmol)and **21** (150 mg, 0.55 mmol), **17c** (128 mg, 65%) was isolated as a colorless solid; ^{1}H NMR (400 MHz, CDCl$_3$): δ = 7.46 (d, J = 8.5 Hz, 2H), 7.15 (d, J = 8.6 Hz, 2H), 7.04 (d, J = 9.1 Hz, 2H), 6.86 (d, J = 9.1 Hz, 2H), 4.47 (s, 2H), 3.79 (s, 3H) 1.88-1.82 (m, 1H), 1.20-1.16 (m, 2H), 1.06-1.03 (m, 2H); ^{13}C NMR (100 MHz, CDCl$_3$): δ = 173.4, 158.4, 151.7, 142.6, 132.1, 124.8, 123.2, 122.4, 114.9, 55.9, 55.8, 13.1, 9.6; FTIR (ν_{max}, cm^{-1}): 1140, 1212, 1261, 1372, 1502, 1745; HRMS (ESI) calcd for C$_{18}$H$_{18}$O$_6$S [M +Na]$^+$: 385.0721; Found: 385.0726.
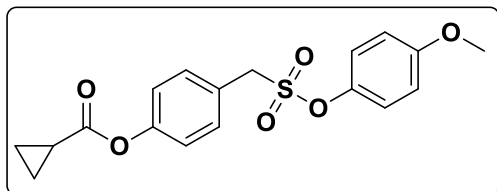
4-(((4-nitrophenoxy)sulfonyl)methyl)phenyl cyclopropanecarboxylate (17d): Starting from 4-nitrophenol (91 mg, 0.65 mmol), TEA (229 μL, 1.64 mmol) and **21** (150 mg, 0.55 mmol), **17d** (144 mg, 70%) was isolated as a colorless solid;^{1}H NMR (400 MHz, CDCl$_3$): δ = 8.21 (d, J = 9.3 Hz, 2H), 7.47 (d, J = 8.6 Hz, 2H), 7.18-7.14 (m, 4H), 4.60 (s, 2H), 1.90-1.83 (m, 1H), 1.20-1.17 (m, 2H), 1.08-1.04 (m, 2H); ^{13}C NMR (100 MHz, CDCl$_3$): δ = 173.4, 153.5, 152.0, 146.2, 132.1, 125.7, 124.1, 122.8, 122.7, 57.2, 13.1, 9.7; FTIR(ν_{max}, cm^{-1}): 1142, 1212, 1351, 1377, 1526, 1590, 1744; HRMS (ESI) calcd for C$_{17}$H$_{15}$NO$_7$S [M + Na]$^+$: 400.0466; Found: 400.0467.
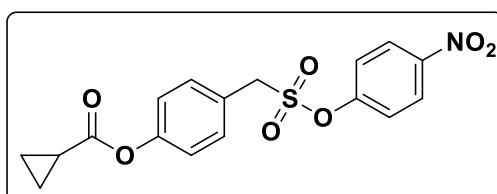
4-(((2-(*t*-butyl)-4-methylphenoxy)sulfonyl)methyl)phenyl cyclopropanecarboxylate (17e): Starting from 2-(*t*-butyl)-4-methylphenol (52 mg, 0.35 mmol), TEA (122 μL, 0.87 mmol), and **21** (80 mg, 0.29 mmol), **17e** (76 mg, 65%) was isolated as a colorless solid; ^{1}H NMR (400 MHz, CDCl$_3$): δ = 7.48 (d, J = 8.5 Hz, 2H), 7.18-7.14 (m, 4H), 6.97 (dd, J = 8.4, 1.9 Hz, 1H), 4.58 (s, 2H), 2.31 (s, 3H), 1.86-1.83 (m, 1H), 1.34 (d, J = 0.8 Hz, 9H), 1.19-1.17 (m, 2H), 1.06-1.02 (m, 2H); ^{13}C NMR (100 MHz, CDCl$_3$): δ= 173.3, 151.7, 146.9, 140.6, 135.9, 132.2, 128.8, 127.8, 124.6, 122.4, 120.9, 57.7, 34.7, 30.6, 21.2, 13.1, 9.5; FTIR (ν_{max}, cm^{-1}): 1141, 1211, 1359, 1501, 1747; HRMS (ESI) calcd for C$_{22}$H$_{26}$O$_5$S [M +Na]$^+$: 425.1398; Found: 425.1404.
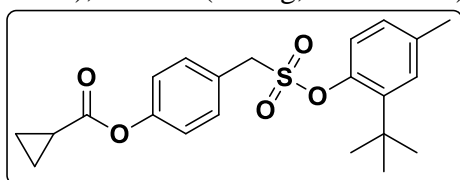
4-(((4-chloro-3,5-dimethylphenoxy)sulfonyl)methyl)phenylcyclopropanecarboxylate

(17f): Starting from 4-chloro-3,5-dimethylphenol (31 mg, 0.20 mmol), TEA (76 µL, 0.55 mmol), and **21** (50 mg, 0.18 mmol), **17f** (52 mg, 72%) was isolated as a colorless solid; ^{1}H NMR (400 MHz,CDCl$_3$): δ = 7.46 (d, J = 8.6 Hz, 2H), 7.17 (d, J = 8.6 Hz, 2H), 6.83 (s, 2H), 4.49 (s, 2H), 2.34 (s, 6H), 1.88-1.83 (m, 1H), 1.19-1.15 (m, 2H), 1.07-1.03 (m, 2H); ^{13}C NMR (100 MHz, CDCl$_3$): δ = 173.3, 151.8, 146.6, 138.3, 133.4, 132.1, 124.6, 122.4, 121.8, 56.3, 21.0, 13.1, 9.6; FTIR (v_{max}, cm^{-1}): 1136, 1212, 1375, 1464, 1746; HRMS (ESI) calcd for C$_{19}$H$_{19}$ClO$_5$S [M +Na]$^+$:417.0539; Found: 417.0539.
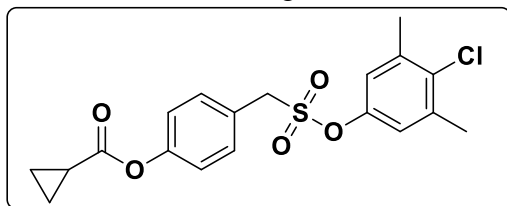
4-(((benzyloxy)sulfonyl)methyl)phenyl cyclopropanecarboxylate (17g): Starting from benzyl alcohol (91 µL, 0.87 mmol), TEA (254 µL, 1.82 mmol), and **21** (200 mg, 0.73 mmol), **17g** (57 mg, 23%) was isolated as a colorless solid; ^{1}H NMR (400 MHz, CDCl$_3$): δ = 7.39-7.26 (m, 7H), 7.10 (d, J = 8.5 Hz, 2H), 5.08 (s, 2H), 4.26 (s, 2H), 1.88-1.81 (m, 1H), 1.19-1.15 (m, 2H), 1.06-1.02 (m, 2H); ^{13}C NMR (100 MHz, CDCl$_3$): δ = 173.3, 151.6, 133.5, 131.9, 129.5, 129.1, 129.0, 125.2, 122.3, 72.8, 57.0, 13.1, 9.5; FTIR (v_{max}, cm^{-1}): 1167, 1216, 1265, 1379, 1735; HRMS (ESI) calcd for C$_{18}$H$_{18}$O$_5$S[M + H]$^+$: 347.0953; Found: 347.0952.
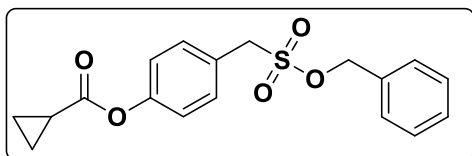
4-(((allyloxy)sulfonyl)methyl)phenyl cyclopropanecarboxylate (17h): Starting from allyl alcohol (59 µL, 0.87 mmol), TEA (304 µL, 2.18 mmol), and **21** (200 mg, 0.73 mmol), **17h** (58 mg, 27%) was isolated as a colorless solid; ^{1}H NMR (400 MHz, CDCl$_3$): δ = 7.41 (d, J = 8.7 Hz, 2H), 7.14 (d, J = 8.7 Hz, 2H), 5.88-5.78 (m, 1H), 5.37-5.29 (m, 2H), 4.52-4.51 (m, 2H), 4.34 (s, 2H), 1.87-1.81 (m, 1H), 1.18-1.15 (m, 2H), 1.06-1.02 (m, 2H); ^{13}C NMR (100 MHz, CDCl$_3$): δ = 173.4, 151.6, 131.9, 130.5, 125.3, 122.3,121.0, 71.7, 56.7, 13.1, 9.5; FTIR (υ cm^{-1}): 1166, 1266, 1350, 1426, 1510, 1738; HRMS (ESI) calcd for C$_{14}$H$_{16}$O$_5$S [M + H]$^+$: 297.0796; Found: 297.0796.
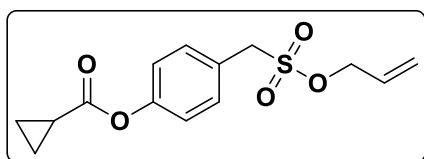
4-(((prop-2-yn-1-yloxy)sulfonyl)methyl)phenyl cyclopropanecarboxylate (17i): Starting from propargyl alcohol (63 µL, 0.87 mmol), TEA (304 µL, 2.18 mmol), and **21** (200 mg, 0.73 mmol), **17i** (52 mg, 24%) was isolated as a colorless solid; ^{1}H NMR (400
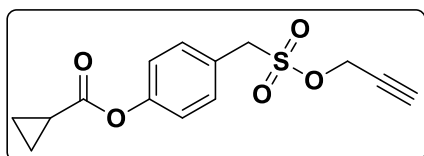
MHz, CDCl$_3$): δ = 7.45 (d, J = 8.7 Hz, 2H), 7.14 (d, J = 8.6 Hz, 2H), 4.72 (d, J = 2.4 Hz, 2H), 4.43 (s, 2H), 2.69 (t, J = 2.4 Hz, 1H), 1.86-1.82 (m, 1H), 1.18-1.15 (m, 2H), 1.06-1.02 (m, 2H); ^{13}C NMR (100 MHz, CDCl$_3$): δ = 173.4, 151.7, 132.0, 124.9, 122.4, 78.1, 75.9, 58.2, 57.4, 13.1, 9.5; FTIR (ν_{max}, cm^{-1}): 933, 980, 1098, 1142, 1169, 1263, 1368, 1511, 1743; HRMS (ESI) calcd for C$_{14}$H$_{14}$O$_5$S [M + Na]$^+$: 317.0459; Found: 317.0457.

4-((butoxysulfonyl)methyl)phenyl cyclopropanecarboxylate (17j):Starting from *n*-butyl
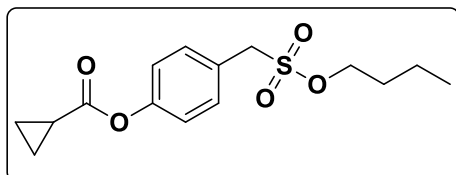
alcohol (73 µL, 0.80 mmol),TEA (304 µL, 2.18 mmol) and **21** (200 mg, 0.73 mmol), **17j** (120 mg, 53 %) was isolated as a colorless solid; ^{1}H NMR (400 MHz, CDCl$_3$): δ 7.41 (d, J = 8.6 Hz, 2H), 7.13 (d, J = 8.6 Hz, 2H), 4.32 (s, 2H), 4.07 (t, J = 6.5 Hz, 2H), 1.85-1.82 (m, 1H), 1.64-1.58 (m, 2H), 1.38-1.32 (m, 2H), 1.18-1.15 (m, 2H), 1.06-1.02 (m, 2H), 0.90(t,J = 7.4 Hz, 3H); ^{13}C NMR (100 MHz, CDCl$_3$): δ = 173.3, 151.5, 131.8, 125.5, 122.3, 71.2, 56.2, 31.3, 18.7, 13.6, 13.1, 9.5; FTIR (ν_{max}, cm^{-1}): 1168, 1217, 1349, 1383, 1511, 1735; HRMS (ESI) calcd for C$_{15}$H$_{20}$O$_5$S [M + Na] $^+$:335.0928; Found: 335.0934.

4-((isopropoxysulfonyl)methyl)phenyl cyclopropanecarboxylate (17k): Starting from *i*-

propyl alcohol (73 µL, 0.73 mmol), TEA (304 µL, 2.18 mmol), and **21** (200 mg, 0.73 mmol), **17k** (95 mg, 44%) was isolated as a colorless solid; ^{1}H NMR (400 MHz, CDCl$_3$): δ = 7.42 (d, J = 8.5 Hz, 2H), 7.13 (d, J = 8.6 Hz, 2H), 4.82-4.72 (m, 1H), 4.30 (s, 2H), 1.88-1.81 (m, 1H), 1.30 (d, J = 6.3 Hz, 6H), 1.18-1.16 (m, 2H), 1.05-1.03 (m, 2H); ^{13}C NMR (100 MHz, CDCl$_3$): δ = 173.4, 151.5, 131.9, 125.7, 122.2, 78.1, 57.0, 23.2, 13.1, 9.5; FTIR (ν_{max}, cm^{-1}): 1167, 1215, 1265, 1343, 1380, 1738; HRMS (ESI) calcd for C$_{14}$H$_{18}$O$_5$S [M + Na]$^+$: 321.0772; Found: 321.0760.
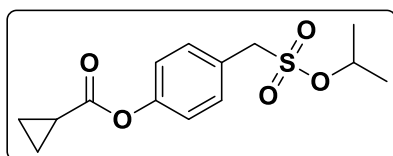
4-formylphenyl cyclopropanecarboxylate (18): 4-hydroxy benzaldehyde (8.41 g, 68.88
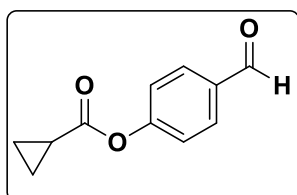
mmol) and TEA (17.60 mL, 126.28 mmol) were dissolved in DCM (100 mL). To this solution of cyclopropyl carbonyl chloride (5.22 mL, 57.40 mmol) in DCM (10 mL) was added dropwise at 0 °C under nitrogen atmosphere. The resulting mixture was stirred for 1 h and was further diluted with dI water (100 mL) and sat. NaCl (25 mL). The aqueous layer was extracted with DCM (3 × 50 mL). The combined organic layers were collected, dried over Na$_2$SO$_4$ and evaporated under reduced pressure. The residue was purified over silica gel

column (hexane/EtOAc) to afford the colorless solid compound **18** (10.43 g, 96%); ^{1}H NMR (400 MHz, CDCl$_3$): δ = 9.98 (s, 1H), 7.91 (d, J = 8.6 Hz, 2H), 7.28 (d, J = 8.6 Hz, 2H), 1.90-1.83 (m, 1H), 1.21-1.18 (m, 2H), 1.09-1.04 (m, 2H); ^{13}C NMR (100 MHz, CDCl$_3$): δ = 191.1, 172.9, 155.6, 134.0, 131.3, 122.5, 13.1, 9.7; FTIR (ν_{max}, cm^{-1}): 1133, 1210, 1748, 1699; MALDI-TOF-TOF calcd for C$_{11}$H$_{10}$O$_3$ [M + K]$^+$: 229.062; Found 228.970.

4-(hydroxymethyl)phenylcyclopropanecarboxylate(19): To a solution of **18** (5.00 g, 26.29 mmol) in EtOH (100 mL), NaBH$_4$ (2.00 g, 52.58 mmol) was added at 0°Cunder nitrogen atmosphere. The resulting mixture was stirred at rt for 1 h, acidified with 2N HCl dropwise until the effervescence stopped followed by filtration through celite and the organic fraction collected was evaporated under reduced pressure. The crude product obtained was further diluted with dI water (100 mL) and sat. NaCl (25 mL). The aqueous layer was extracted with EtOAc (3 × 50 mL), the combined organic layers were collected, dried over Na$_2$SO$_4$ and evaporated under reduced pressure. The residue was purified over silica gel column (hexane/EtOAc) to afford compound **19** (4.48 g, 89 %) as a colorless liquid; ^{1}H NMR (400 MHz, CDCl$_3$): δ = 7.34 (d, J = 8.3 Hz, 2H), 7.06 (d, J = 8.4 Hz, 2H), 4.64 (s, 2H), 2.04 (br, 1H), 1.87-1.80 (m, 1H), 1.17-1.15 (m, 2H), 1.04-1.01 (m, 2H); ^{13}C NMR (100 MHz, CDCl$_3$): δ = 173.8, 150.2, 138.5, 128.1, 121.8, 64.8, 13.1, 9.4; FTIR (ν_{max}, cm^{-1}): 1141, 1212, 1383, 1507, 1740; HRMS (ESI) calcd for C$_{11}$H$_{12}$O$_3$ [M + K]$^+$: 231.0423; Found: 231.0341.
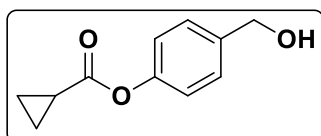
4-((acetylthio) methyl) phenyl cyclopropanecarboxylate (20): Methane sulfonyl chloride (4.77 g, 41.62 mmol) was added to a solution of **19** (4.00 g, 20.81 mmol) in DCM (80 mL) at 0 °C under nitrogen atmosphere. To this pyridine (6.32 g, 62.43 mmol) was added and the resulting mixture was stirred at rt for 5 h. The reaction mixturewas acidified with 10 mL 2M HCl, and was further diluted with dI water (100 mL) and sat. NaCl (25 mL). The aqueous layer was extracted with DCM (3 × 30 mL). The combined organic layers were dried over Na$_2$SO$_4$, and evaporated under reduced pressure. The colorless solid product was directly taken for the next step without further purification. To this solution of mesylated compound (3.40 g, 12.58 mmol) in ACN (50 mL),was added potassium thioacetate (1.72 g, 15.10 mmol) and the reaction mixture was stirred for 1 h. ACN was evaporated, and reaction mass was further diluted with 100 mL dI Water. The aqueous layer was extracted with EtOAc (3 × 25 mL). The combined organic layers were dried over
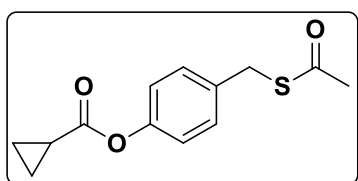
Na$_2$SO$_4$ and evaporated under reduced pressure. The residue was purified over silica gel column (hexane/EtOAc) to afford desired product. Compound **20** (3.00 g, 95 %) was isolated as a colorless solid; ^{1}H NMR (400 MHz, CDCl$_3$): δ = 7.28 (d, *J* = 8.5 Hz, 2H), 7.01 (d, *J* = 8.5 Hz, 2H), 4.10 (s, 2H), 2.34 (s, 3H), 1.84-1.80 (m, 1H), 1.16-1.14 (m, 2H), 1.03-1.00 (m, 2H); ^{13}C NMR (100 MHz, CDCl$_3$): δ = 195.2, 173.6, 150.0, 135.2, 130.0, 121.9, 33.0, 30.5, 13.1, 9.4; FTIR (ν$_{max}$, cm^{-1}): 1133, 1250, 1381, 1506, 1689, 1744; HRMS (ESI) calcd for C$_{13}$H$_{14}$O$_3$S [M + Na]$^+$: 273.0561; Found: 273.0564.

4-((chlorosulfonyl)methyl)phenyl cyclopropanecarboxylate(21): *N*-chlorosuccinimide
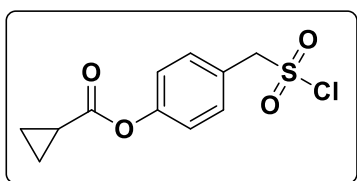
(2.99 g, 22.37 mmol) was added to a 35 mL mixture of 2M HCl:ACN (1:5) and cooled in ice water. Solution of **20** (1.40 g, 5.59 mmol) in 5 mL ACN was added drop wise to the mixture. The resulting solution was stirred for 30 min. The temperature of the ice water bath was maintained below 10 °C. On completion, the reaction mixture was further diluted with 20mL dI water. ACN was evaporated under reduced pressure while maintaining the water bath at 20 °C. The mixture was extracted with *i*-propyl ether (2 × 30 mL). The combined organic layers were dried over Na$_2$SO$_4$ and evaporated under reduced pressure. The colorless solid product was used in next step without further purification. **21** (3.00 g, 91%); ^{1}H NMR (400 MHz, CDCl$_3$): δ = 7.49 (d, *J* = 8.7 Hz, 2H), 7.20 (d, *J* = 8.6 Hz, 2H), 4.85 (s, 2H), 1.88-1.82 (m, 1H), 1.20-1.16 (m, 2H), 1.07-1.04 (m, 2H); ^{13}C NMR (100 MHz, CDCl$_3$): δ 173.1, 152.5, 132.7, 123.5, 122.7, 70.3, 13.2, 9.7; FTIR (ν$_{max}$, cm^{-1}): 1097, 1152, 1211, 1373, 1509, 1730; MALDI-TOF-TOF calcd for C$_{11}$H$_{11}$ClO$_4$S [M + K]$^+$: 312.9704; Found: 312.9000.

2-oxo-2H-chromen-7-yl phenylmethanesulfonate (23): To a solution of umbelliferone (210
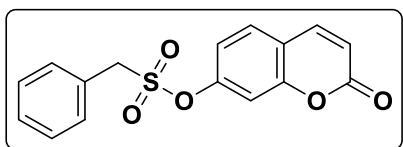
mg, 1.30 mmol), and TEA (361 μL, 2.59 mmol), in DCM (25 mL), a solution of benzylsulfonyl chloride (370 mg, 1.94 mmol) in DCM (1 mL) was added drop wise at 0 °C under nitrogen atmosphere. The resulting mixture was stirred for 1 h. Reaction mixture was further diluted with dI water (100 mL) and the aqueous layer was extracted with DCM (3 × 30 mL). The combined organic layers were dried over Na$_2$SO$_4$ and evaporated under reduced pressure. The residue was purified over silica gel column chromatography using hexane/EtOAc as the mobile phase. **23** (330 mg, 81 %) was isolated as a colorless solid; ^{1}H NMR (400 MHz, CDCl$_3$): δ = 8.09 (d, *J* = 9.6 Hz, 1H), 7.82 (d, *J* = 8.5 Hz, 1H), 7.53-7.42

(m, 5H), 7.30 (d, J = 2.3 Hz, 1H), 7.24 (dd, J = 8.5, 2.3 Hz, 1H), 6.53 (d, J = 9.6Hz, 1H), 5.08 (s, 2H); ^{13}C NMR (100 MHz, CDCl$_3$): δ = 159.5, 154.1, 150.9, 143.6, 131.1, 129.9, 129.0, 128.7, 127.8, 118.6, 117.8, 116.3, 110.2, 56.2; FTIR (v_{max}, cm^{-1}): 1113, 1264, 1357, 1616, 1728; HRMS (ESI) calcd for C$_{16}$H$_{12}$O$_5$S [M + H]$^+$: 317.0483; Found: 317.0484.

3.4.3. Decomposition study of 16a and 17a by HPLC on esterase activation: A stock solution of porcine liver esterase, ES (1 U/10 µL) was prepared in PBS (pH 7.4, 10 mM). 5 mM stock solution of compounds **16** and **17a** were independently prepared in DMSO. In a typical reaction, compound **16a** (10 µL, final conc. 50 µM) or **17a** (10 µL, final conc. 50 µM) and esterase, ES (10 µL, final conc. 1 U/mL) were added to 980 µL of PBS (pH 7.4, 10 mM). The reaction mixture was incubated at 37 ℃ for 30 min on Eppendorf thermomixer comfort (800 rpm). Aliquots were taken periodically and injected (50 µL) in an HPLC attached with a diode-array detector (detection wavelength was 280 nm). The stationary phase used was C-18 reversed phase column (4.6 mm × 100 mm, 5 µm). The mobile phase used was 0.1 % TFA in H$_2$O: ACN (70:30 → 0-5 min, 60:40 → 5-10 min, 50:50→ 10-15 min, 45:55 → 15-20 min 70:30).HPLC run time was 20 min with a flow rate of 1 mL/min.

3.4.4. Stability Assay for Sulfonate Functional Group

3.4.4.1 Buffer stability of sulfonate functional group: Stock solutions of **16a** and **17a** (10 mM) were independently prepared in DMSO. **16a** and **17a** (5 µL, final conc. 50 µM), were independently added to 495 µL of buffers PBS (pH 6.0, 10 mM), PBS (pH 7.4, 10 mM) and sodium borate buffer (pH 9.2, 50 mM).It was incubated at 37 ℃ on an Eppendorf thermomixer comfort (800 rpm) for 30 min. Aliquots were analyzed by fluorimetry for Umb (λ_{ex} = 350 nm and λ_{em} = 450 nm) using a Thermo Scientific Varioskanmicrotiter plate reader.

3.4.4.2. Stability and selectivity of SO$_2$ donor and sulfonate functional group with esterase, in the presence of biological nucleophiles and esterase inhibitor: Stock solution of compounds **23** and **17a** (2.5 mM) were independently prepared in ACN, a stock solution of porcine liver esterase, ES (1 U/10 µL) was prepared in PBS (pH 7.4, 10 mM), 25 mM stock solutions of biological nucleophiles Cys (Cysteine), Ser (Serine), Thr (Threonine), and Lys (Lysine) were prepared in Milli-Q water independently. 25 mM stock solution of phenylmethanesulfonyl fluoride (PMSF) was prepared in isopropanol. In a typical reaction for esterase stability, compounds **23** (5 µL, final conc. 25 µM), and **17a** (5 µL, final conc. 25 µM) were independently added to 485 µL of PBS (pH 7.4, 10 mM) and incubated with esterase, ES (10 µL, final conc. 1 U/mL)for 30 min at 37 ℃ on Eppendorf thermomixer

comfort (800 rpm). Aliquots were analyzed for Umb(λ_{ex} = 350 nm and λ_{em} = 450 nm), using a Thermo Scientific Varioskanmicrotiter plate reader. Following same protocol, the reaction of compound **17a** (5 µL, final conc. 25 µM), in absence of esterase with biological nucleophiles (5 µL, final conc. 250 µM), and 490 µL PBS (pH 7.4, 10 mM) was conducted for 1h. For the esterase inhibition experiment, compound **17a** (5 µL, final conc. 25 µM), PMSF (5 µL, final conc. 250 µM). Also for dose-dependent assay concentrations of compound used accordingly, and esterase (10 µL, final conc. 1U/mL) were added to PBS (pH 7.4, 10 mM) to make total volume of the reaction 500 µL and incubated for 30 min.

3.4.4.3. Stability of sulfonate functional group in the cellular environment: HeLa cells were grown in culture flask in Dulbecco's modified Eagle's medium (DMEM) media supplemented with 10% FBS and 1% antibiotic solution in an atmosphere of 5% CO_2 at 37°C. After 70% of confluencies, old media was removed and the cells were washed with PBS (1X) buffer. Cells were detached by trypsinization and resuspended with PBS (1X).Cells suspension was transformed microcentrifuge tube and cells were lysed by sonication using (130 Watt ultrasonic processor, VX 130W) Stepped Microtip for 2 minutes (with 5s ON and 10 s OFF pulse, 60% amplitude) under ice-cold condition. Whole cell lysate in PBS was treated with compound **22** (25 µM) and **17a** (25 µM) independently at 37 °C for 1 h and fluorescence was recorded using a Thermo Scientific Varioskan Flash microwell plate reader (λ_{ex} = 350 nm and λ_{em} = 450 nm).

3.4.5. Colorimetry Assays for Sulfite Detection

3.4.5.1 Detection of sulfite by SO$_2$ donors (17a-17k) with sulfite dye 22 on esterase activation

Stock solutions of SO$_2$ donors **17a-17k** (5 mM) and sulfite dye **22** (1 mM) were prepared in ACN independently. A stock solution of porcine liver esterase, ES (1 U/10 µL) was prepared in PBS (pH 7.4, 10 mM). In a typical reaction, SO$_2$ donors **17a-17k** (10 µL, final conc. 50 µM), **7** (10 µL, final conc. 10 µM) and esterase, ES (10 µL, final conc. 1 U/mL) were added to 970 µL PBS. The reaction mixture was incubated at 37 ℃ for 15 min on Eppendorf thermomixer comforts (800 rpm), transferred into quartz absorbance cell (Hellma, path length 1.0 cm), and the absorption spectra were recorded on Shimadzu UV-2600.

3.4.5.2. Detection of sulfite from 17c with sulfite dye 22 on esterase activation in the presence of biological nucleophiles and esterase inhibitor PMSF by spectrophotometry:

Stock solutions of **17c** (5 mM) and **22** (1 mM) were independently prepared in ACN, a stock solution of porcine liver esterase, ES (1 U/10 µL) was prepared in PBS (pH 7.4, 10 mM), 100 mM stock solutions of biological nucleophiles Cys (Cysteine), Ser (Serine), Thr (Threonine), and Lys (Lysine) were prepared in Milli-Q water independently. 100 mM stock solution of phenylmethanesulfonyl fluoride (PMSF) was prepared in isopropanol. In a typical reaction for sulfite detection, compound **17c** (10 µL, final conc. 50 µM), **22** (10 µL, final conc. 10 µM) and esterase, ES (10 µL, final conc. 1U/mL) were added to a 470 µL of PBS (pH 7.4, 10 mM). The reaction mixture incubated at 37 ℃ for 15 min on Eppendorf thermomixer comforts (800 rpm), then transferred into quartz absorbance cell (Hellma, path length 1.0 cm), and the absorption spectra were recorded on Shimadzu UV-2600. Following same protocol experiment was conducted for sulfite detection in the presence of biological nucleophiles without esterase. For the esterase inhibitor experiment, compound **17c** (10 µL, final conc. 50 µM), and **22** (10 µL, final conc. 10 µM) were added to a 460 µL of PBS (pH 7.4, 10 mM) and incubated with esterase (10 µL, final conc. 1 U/mL) and PMSF (10 µL, final conc. 1 mM).

3.4.6. HPLC based evaluation of SO₂ donors derived from aliphatic alcohols (17g-17k)

Compounds **17g-17k** did not produce sulfite significantly as compared to aromatic analogs. To evaluate these compounds, HPLC study was conducted. 5 mM stock solution of compounds (**17g-17k**) and **17c** were independently prepared in ACN. These compounds showed poor UV absorptivity, thus HPLC was conducted at 500 µM and monitored at 200 nm. Compounds **17g-17k** (500 µM) and **17c** (500 µM) were incubated independently in 100 % ACN and 50 % PBS: ACN at 37 ℃ on Eppendorf thermomixer comfort (800 rpm) for 30 min and injected (50 µL) in the HPLC attached with a diode-array detector (detection wavelength was 200 nm). The chromatogram was visible with the more sensitive stationary phase of Phenomenex Luna C-18 reversed phase column (4.6 mm × 250 mm, 5 µm). The mobile phase used was 0.1 % TFA in H₂O: ACN (50:50 → 0-5 min, 40:60 → 5-10 min, 30:70→ 10-15 min, 25:75 → 15-20 min 50:50).HPLC run time was 20 min with a flow rate of 1 mL/min.

3.4.7. Sulfite detection from SO₂ donors (17a-17k) with sulfite dye 22 on esterase activation by fluorimetry: 1 mM stock solutions of the SO₂ donors (**17a-17k**) and sulfite dye **22** were prepared in DMSO independently. In a typical reaction mixture SO₂ donors **17a-17k** (10µL, final conc. 10 µM), **22** (10µL, final conc. 10 µM) and ES (10 µL, final conc.

1U/mL) were added independently to 970 µL PBS (pH 7.4, 10 mM) and was incubated at 37 ºC on Eppendorf thermomixer comfort (800 rpm) for 30 min. The reaction mixture was transferred into a quartz fluorescence cell (Hellma, path length 1.0 cm) and fluorescence measurements were carried out using a HORIBA Jobin Yvon, Fluorolog fluorescence spectrophotometer. Excitation wavelength corresponded to the absorption maxima (545 nm and 410 nm) with an excitation slit width of 1 nm and emission slit width of 1 nm. The emission profile was recorded.

3.4.8 Cellular Imaging: A549 cells in DMEM supplemented with foetal bovine serum (FBS, 10%) and antibiotic solution (1%) were seeded (2×10^5 cells per well) in 12 well plate and incubated overnight in an atmosphere of 5% CO_2 at 37 °C. After incubation, old medium was removed, and the cells were washed with PBS (1X). Then 1 mL of fresh PBS was added along with SO_2 sensitive dye **22** (10 µM), and the cells were incubated for 30 min at 37 °C. After 30 minutes, PBS was removed and cells were washed twice with PBS. Fresh PBS was added along with **17c-17h** (25 µM) and cells were incubated for 30 minutes. After 30 min, cells were imaged by EVOS fluorescence microscopy with 40X. Fluorescence of SO_2 dye **7** was monitored in TxRed channel and the formation of sulfite adduct with **22** was monitored in DAPI channel. $NaHSO_3$ (200 µM) was used as a positive control.

3.4.9. Cell viability Assay: HeLa cells in DMEM supplemented with foetal bovine serum (FBS, 10%) and antibiotic solution (1%) were seeded at a concentration of 1×10^3 cells/well overnight in a 96-well plate in DMEM. Cells were exposed to the test compounds prepared as a DMSO stock solution so that the maximum concentration of DMSO did not exceed 0.5%. The cells were incubated for 24 h at 37 °C. A stock solution of 3-(4, 5-dimethylthiazol-2-yl)-2, 5-diphenyl tetrazolium bromide (MTT) was prepared (3.5 mg in 700 µL DMEM). This stock was diluted with 6.3 mL DMEM and 100 µL of the resulting solution was added to each well. After 4h incubation, the media was removed carefully and 100 µL of DMSO was added. Spectrophotometric analysis of each well using a microplate reader (Thermo Scientific Varioscan) at 570 nm was carried out to estimate cell viability.

3.5. Spectral data

^{1}H NMR Spectrum (400 MHz, CDCl$_3$) of **16a**
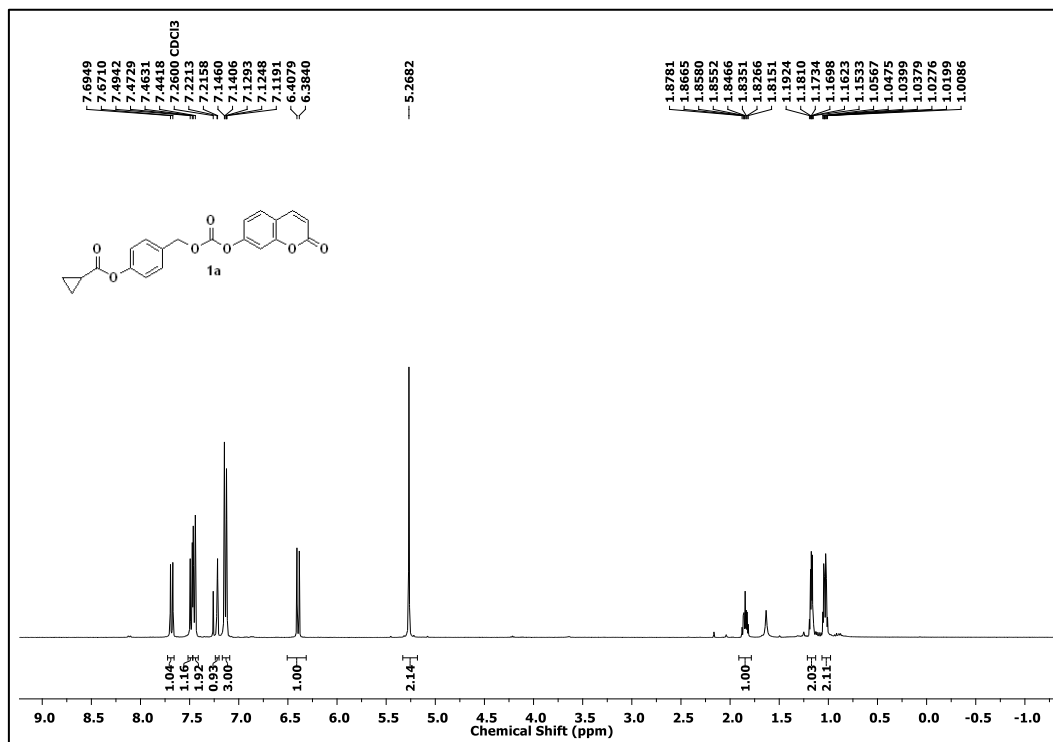
^{1}H NMR Spectrum (400 MHz, CDCl$_3$) of **16a**
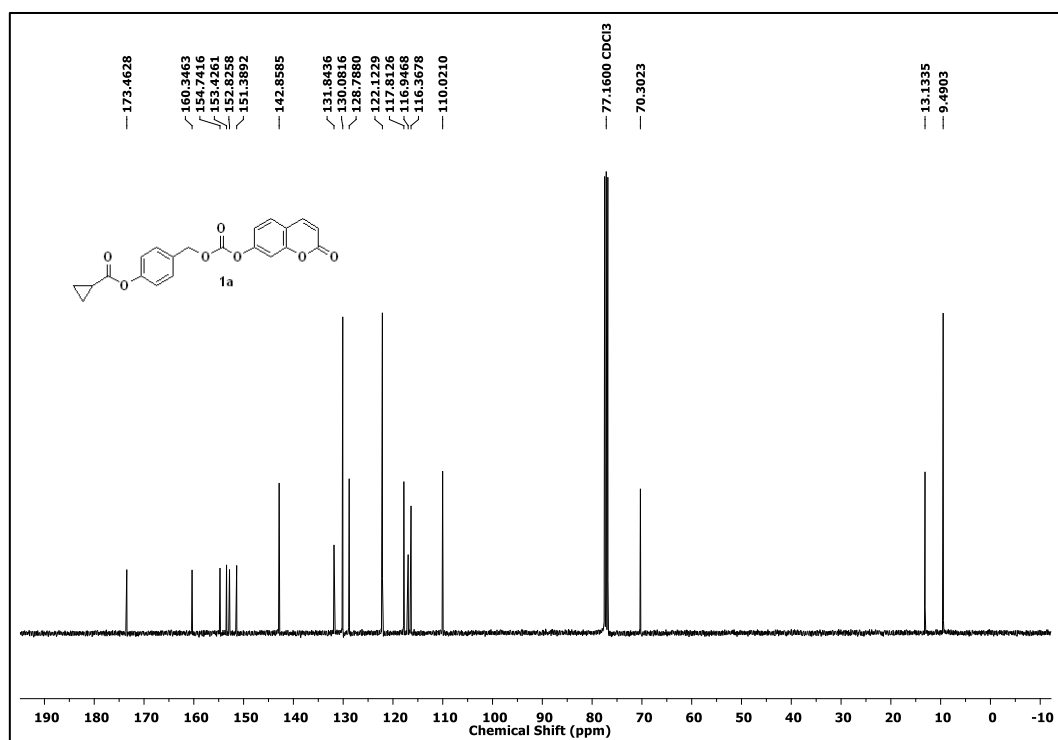
^{1}H NMR Spectrum (400 MHz, CDCl$_3$) of **16b**
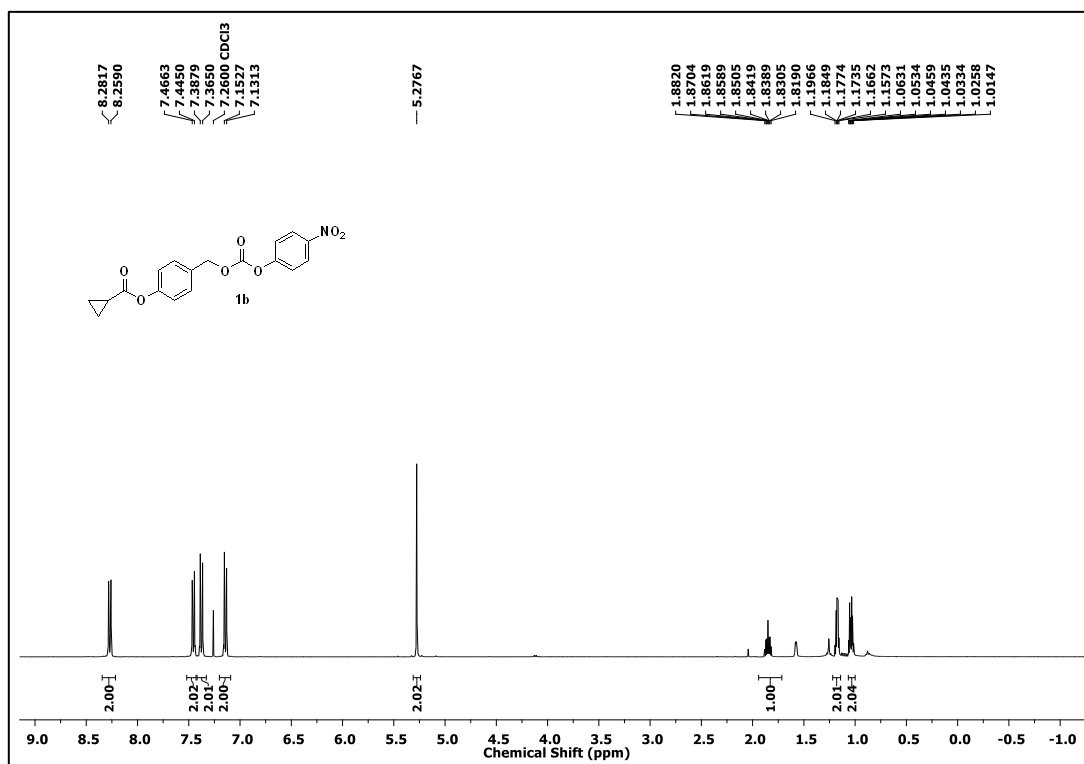
^{13}C NMR Spectrum (100 MHz, CDCl$_3$) of **16b**
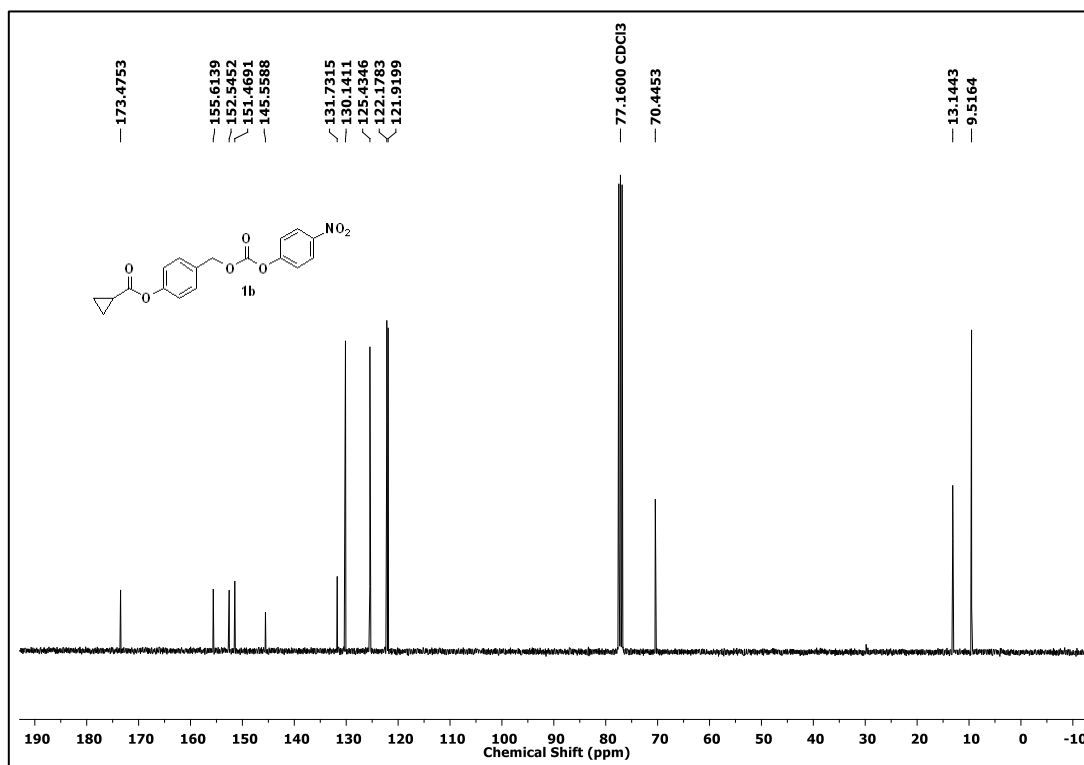
¹H NMR Spectrum (400 MHz, CDCl₃) of **17a**
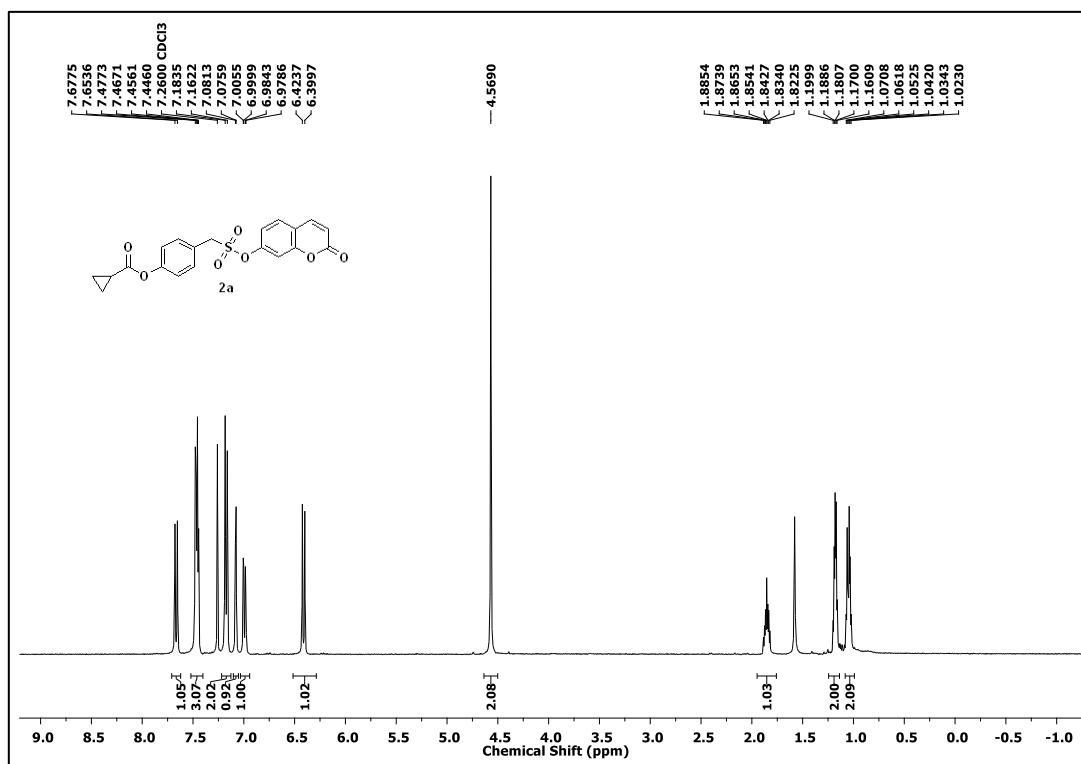
¹³C NMR Spectrum (100 MHz, CDCl₃) of **17a**
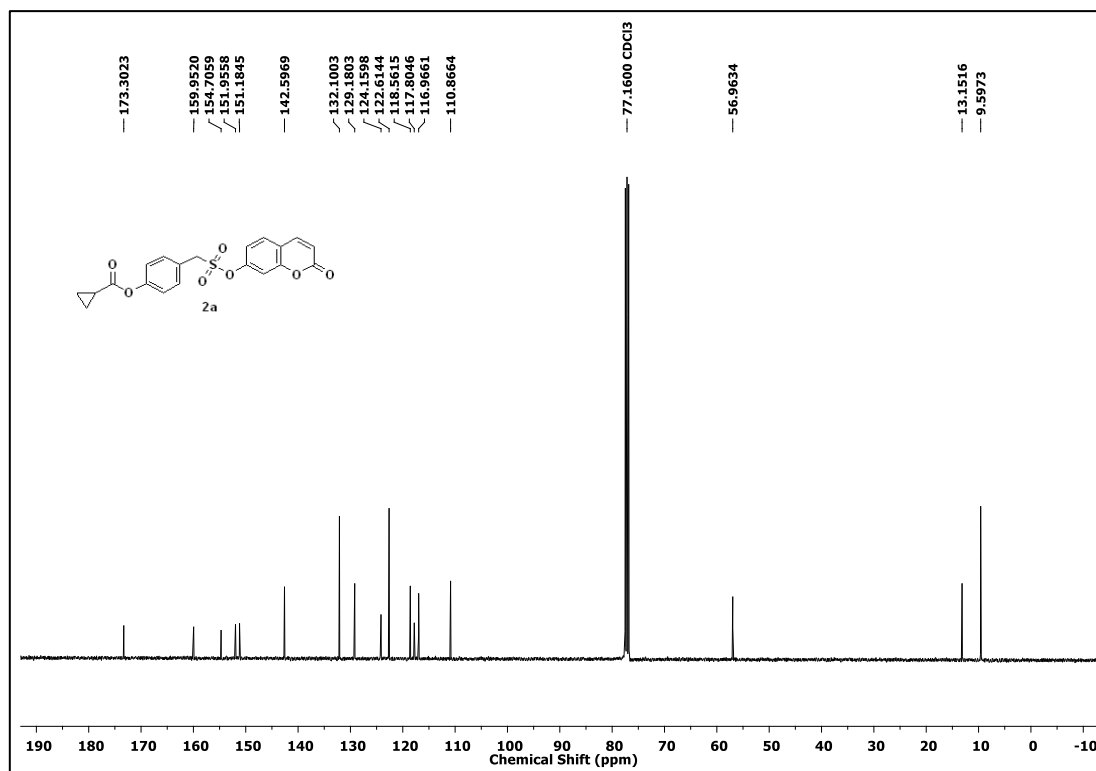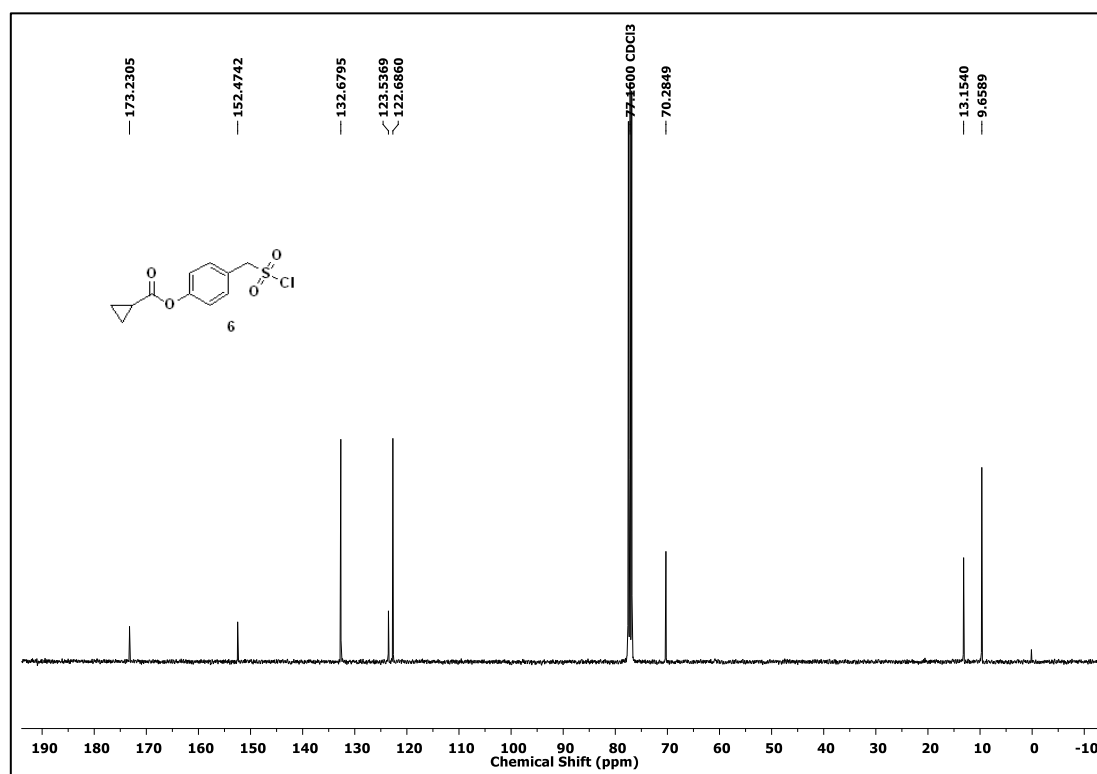
^{1}H NMR Spectrum (400 MHz, CDCl$_3$) of **17b**
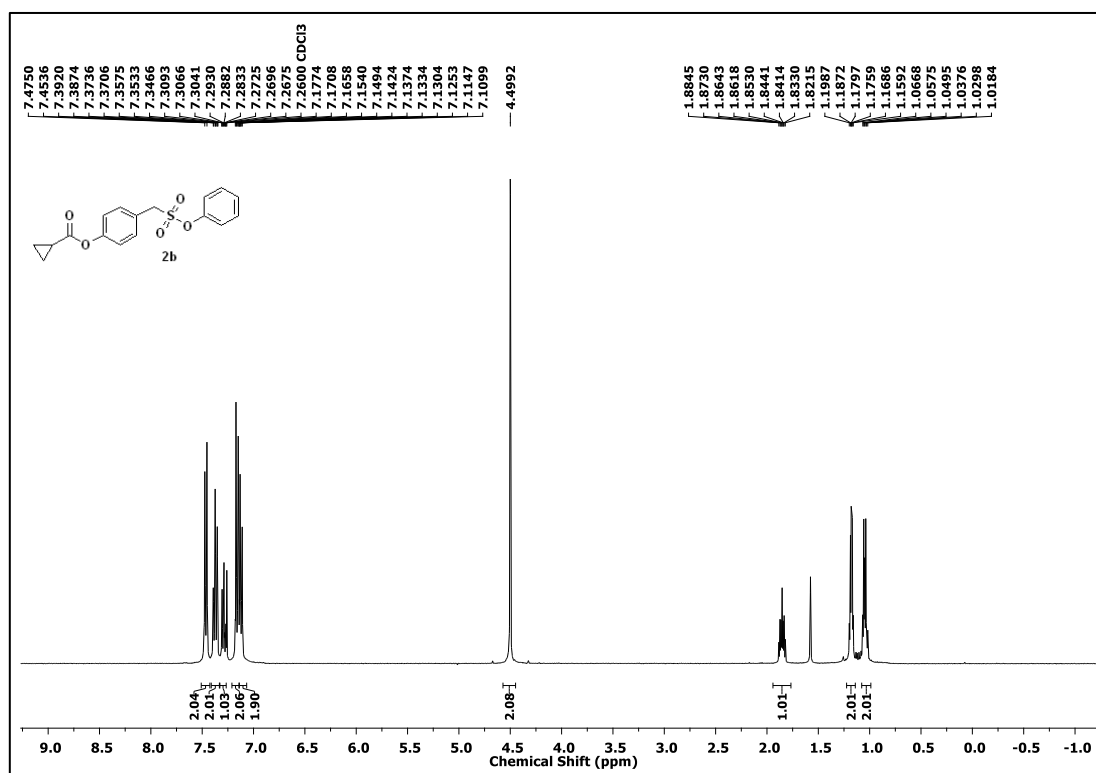
^{13}C NMR Spectrum (100 MHz, CDCl$_3$) of **17b**
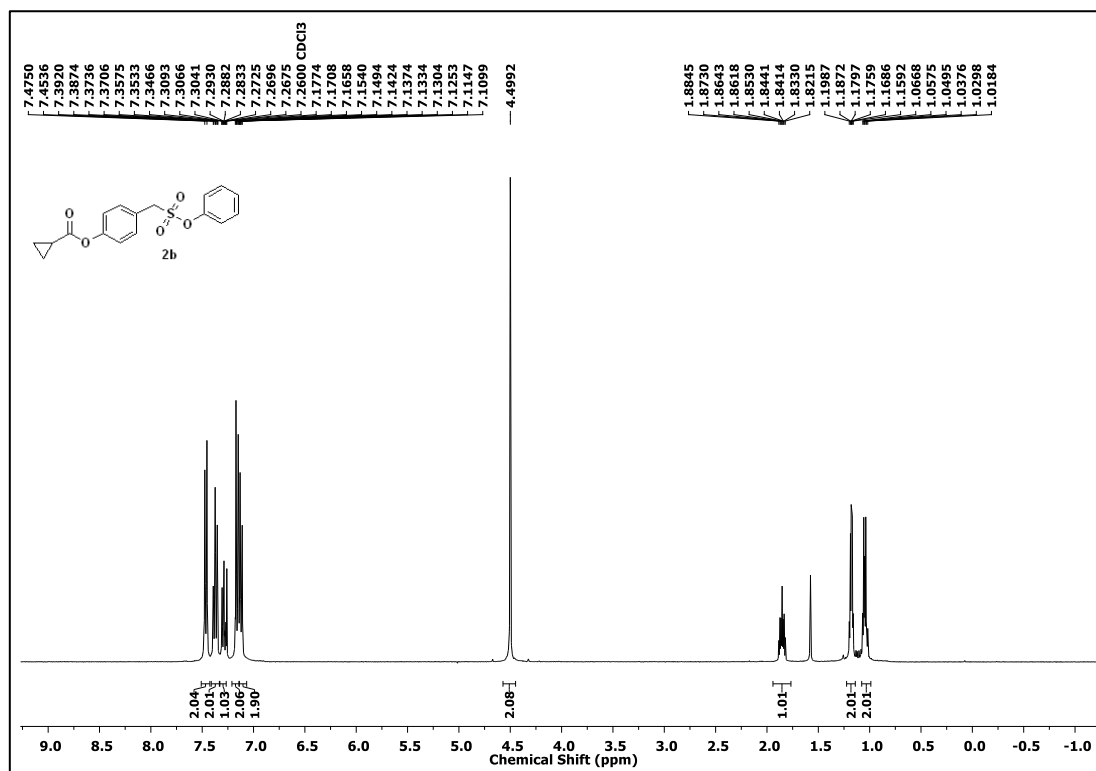
^{1}H NMR Spectrum (400 MHz, CDCl$_3$) of **17c**
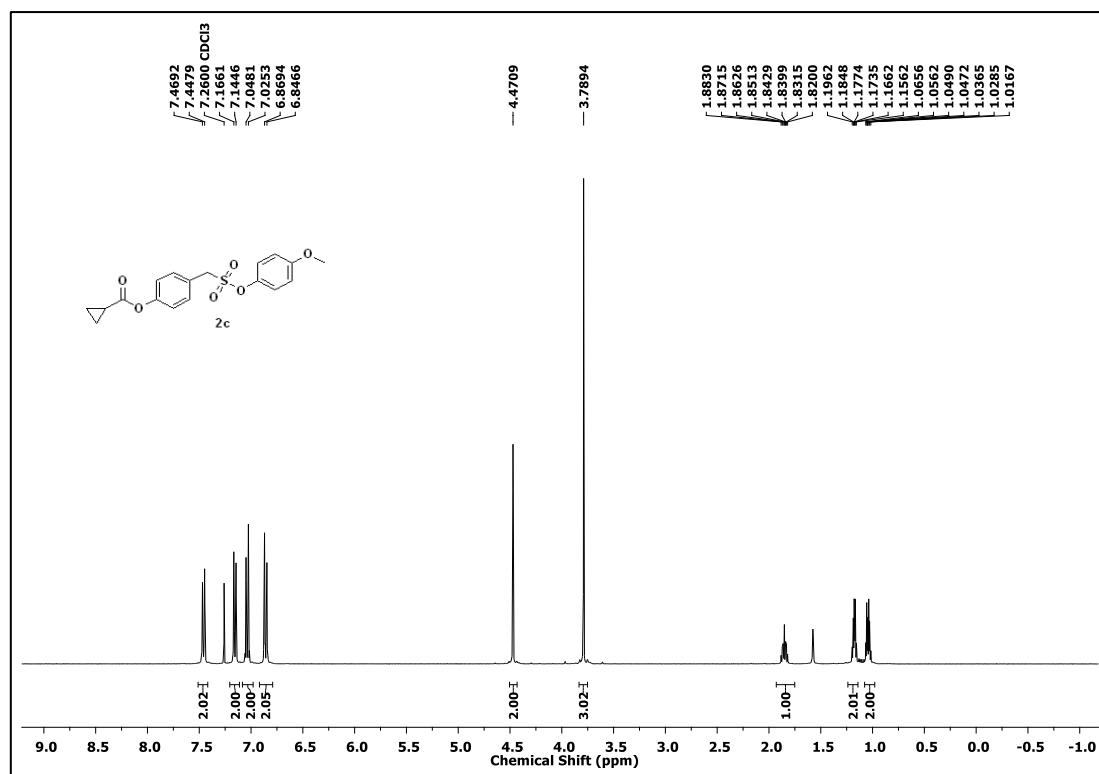
¹³C NMR Spectrum (100 MHz, CDCl₃) of **17c**
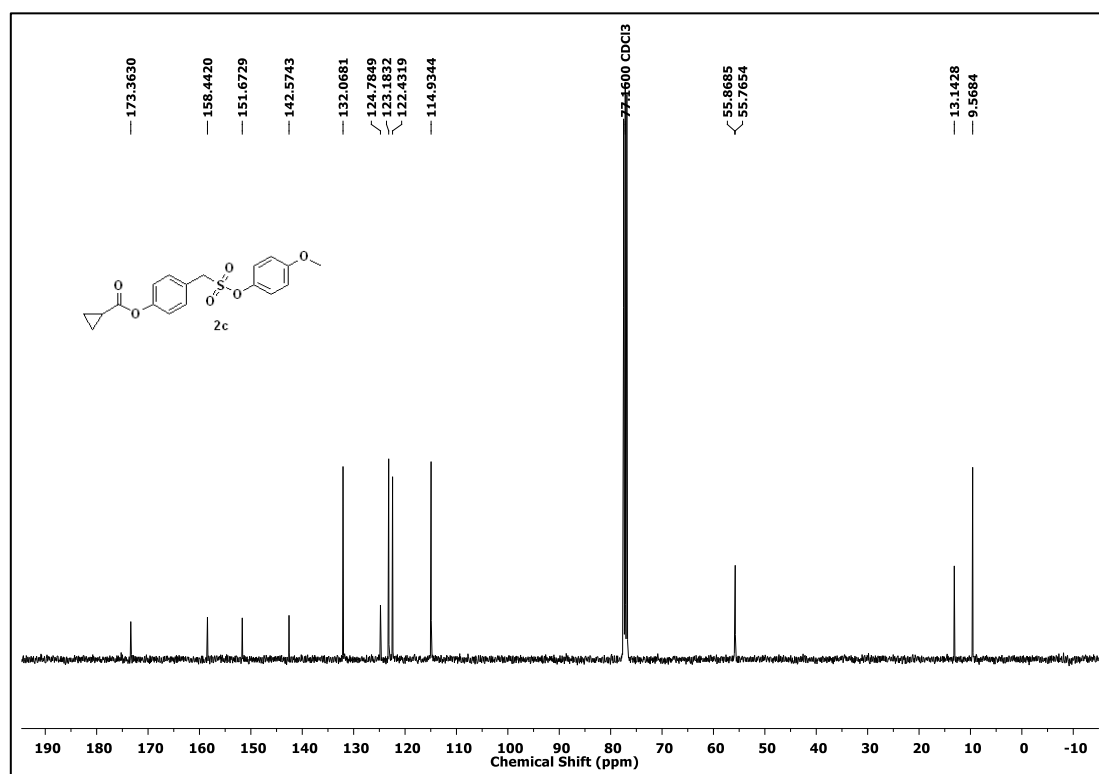
¹H NMR Spectrum (400 MHz, CDCl₃) of **17d**
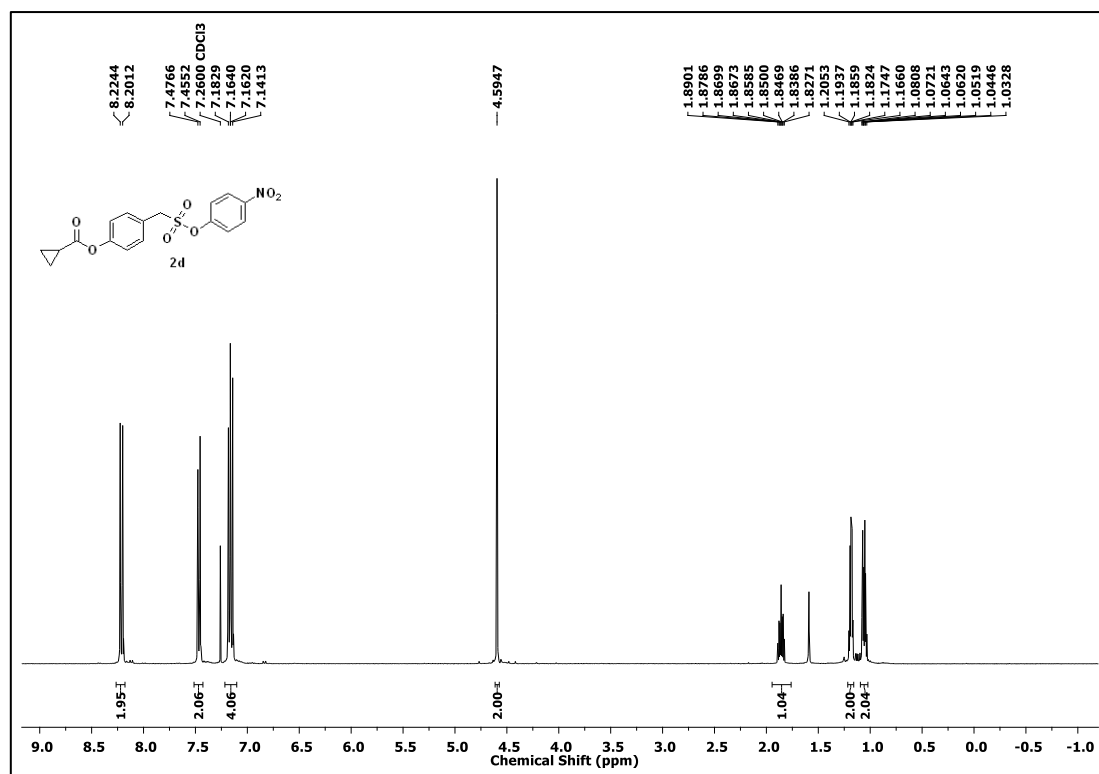
^{13}C NMR Spectrum (100 MHz, CDCl$_3$) of **17d**
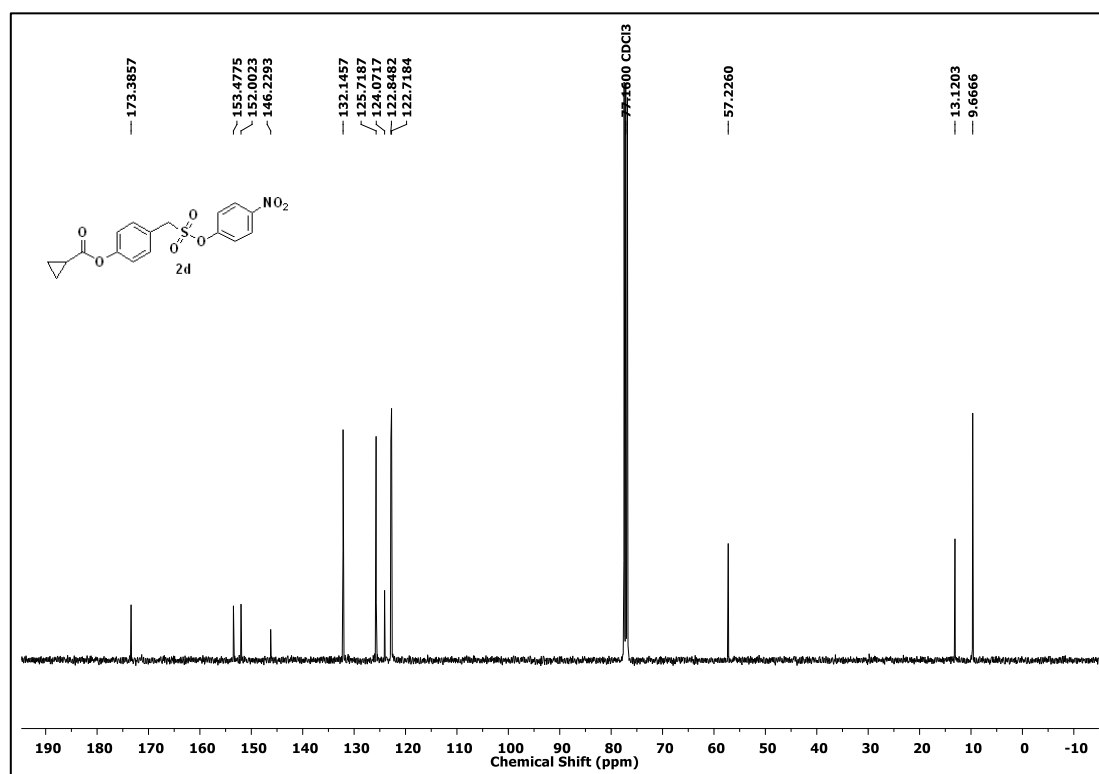
^{13}C NMR Spectrum (100 MHz, CDCl$_3$) of **17e**
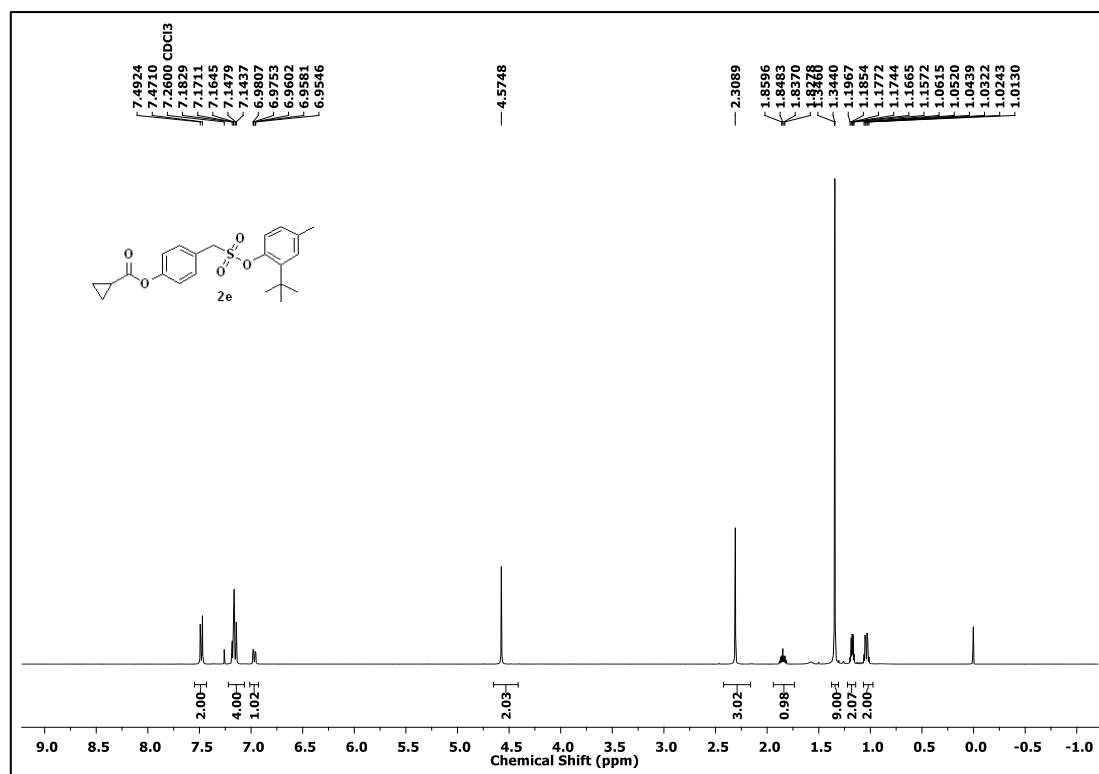
¹³C NMR Spectrum (100 MHz, CDCl₃) of **17e**
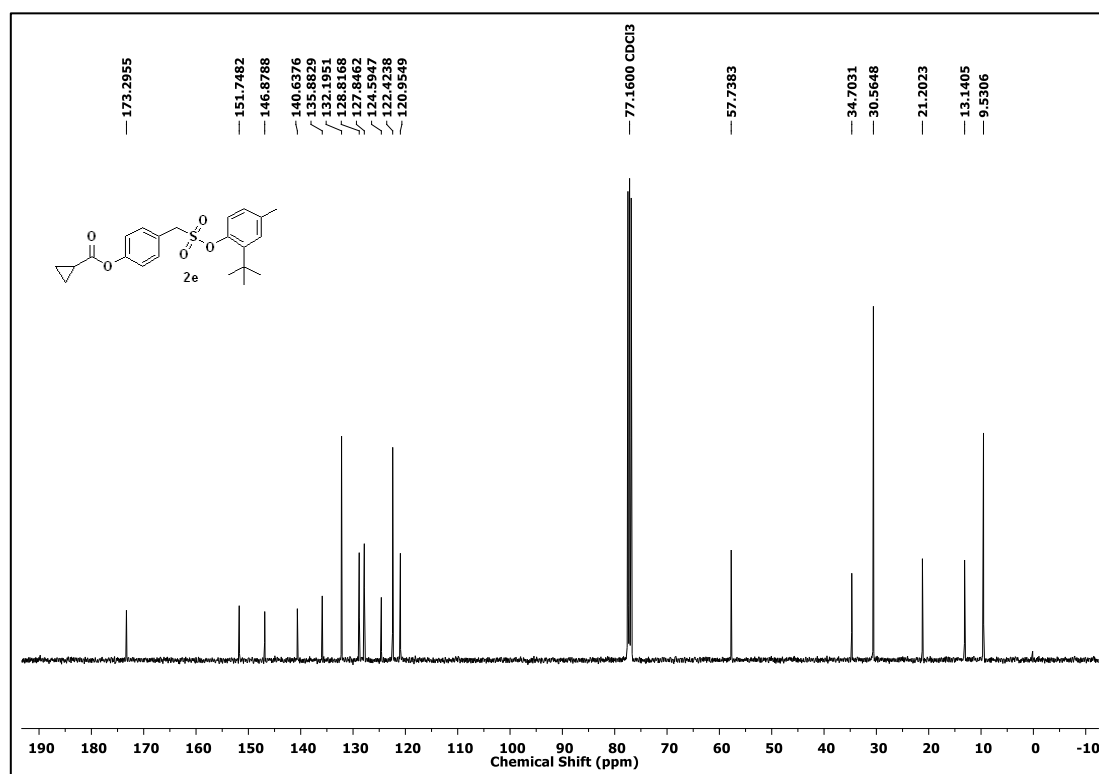
¹H NMR Spectrum (400 MHz, CDCl₃) of **17f**
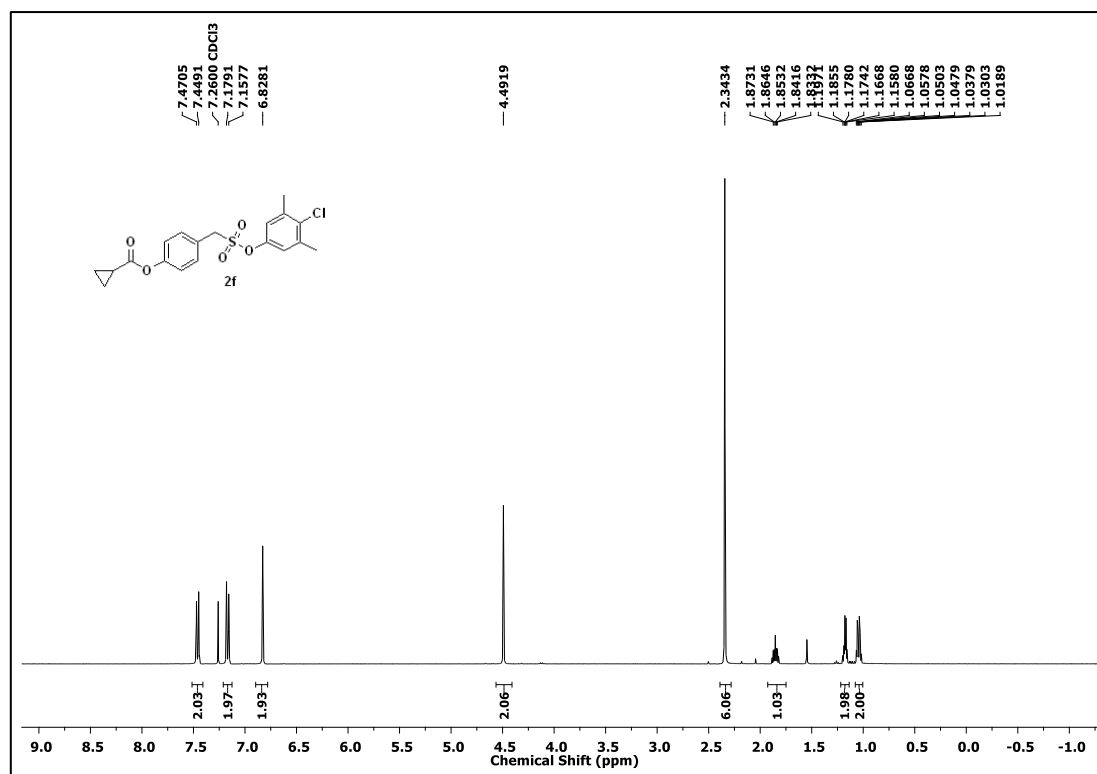
^{13}C NMR Spectrum (100 MHz, CDCl$_3$) of **17f**
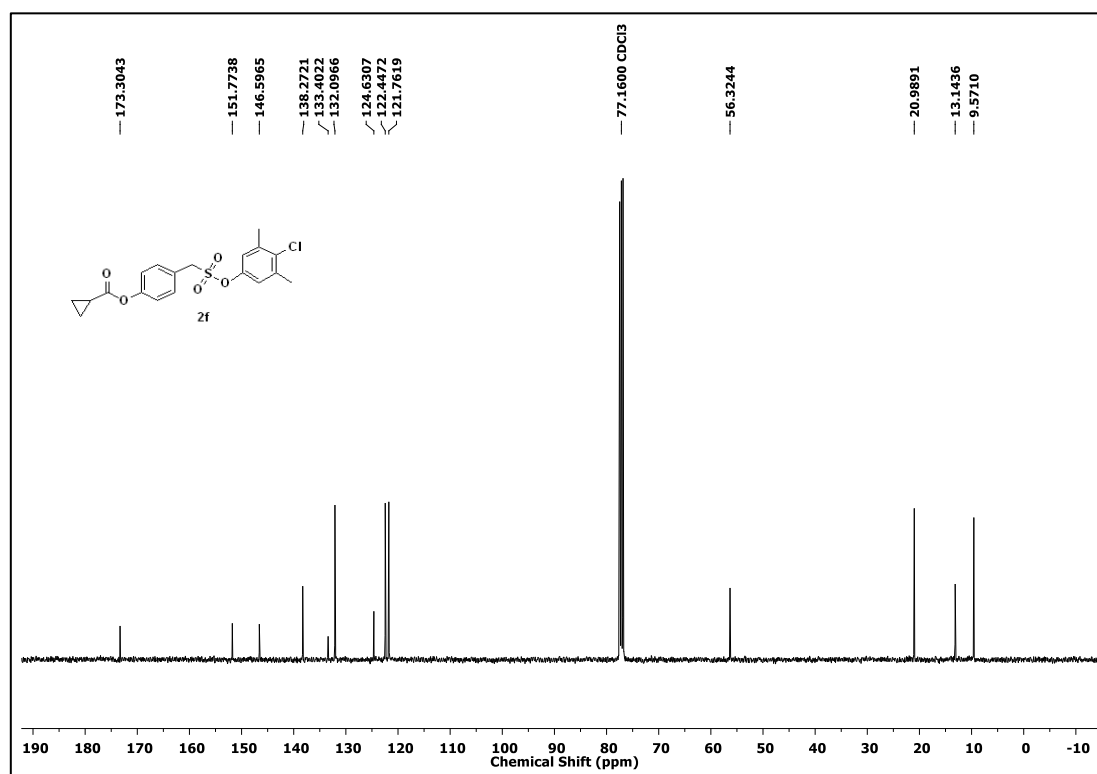
^{1}H NMR Spectrum (400 MHz, CDCl$_3$) of **17g**
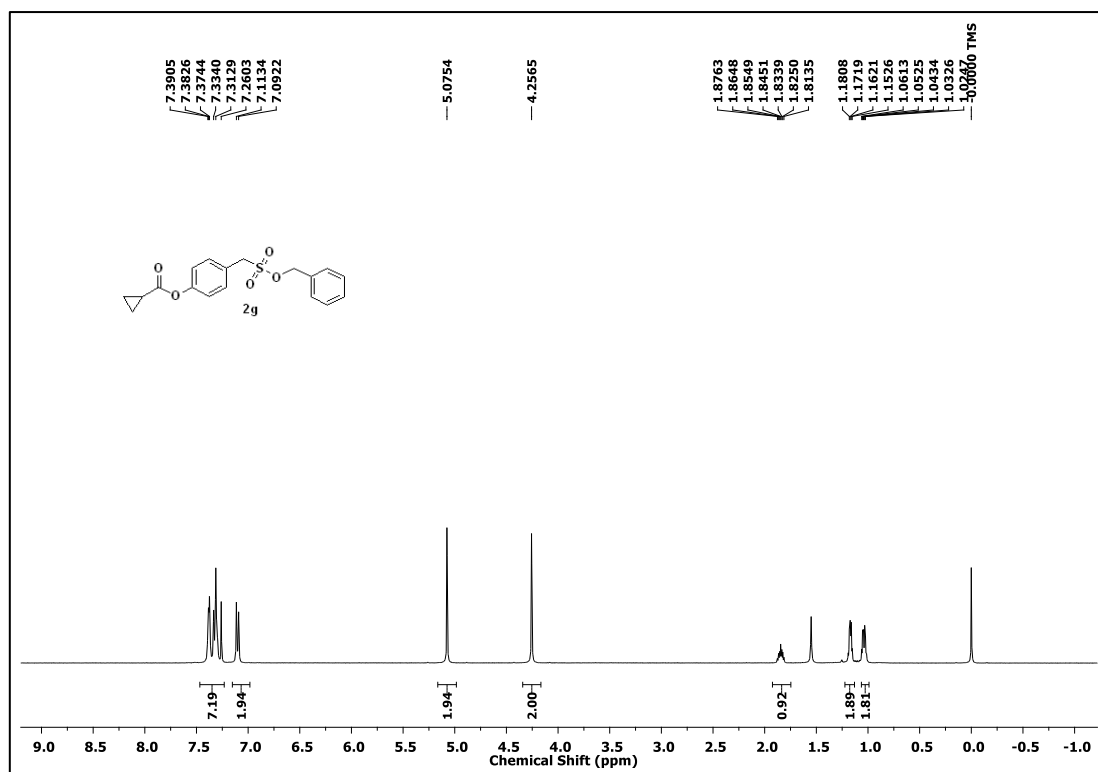
^{13}C NMR Spectrum (100 MHz, CDCl$_3$) of **17g**
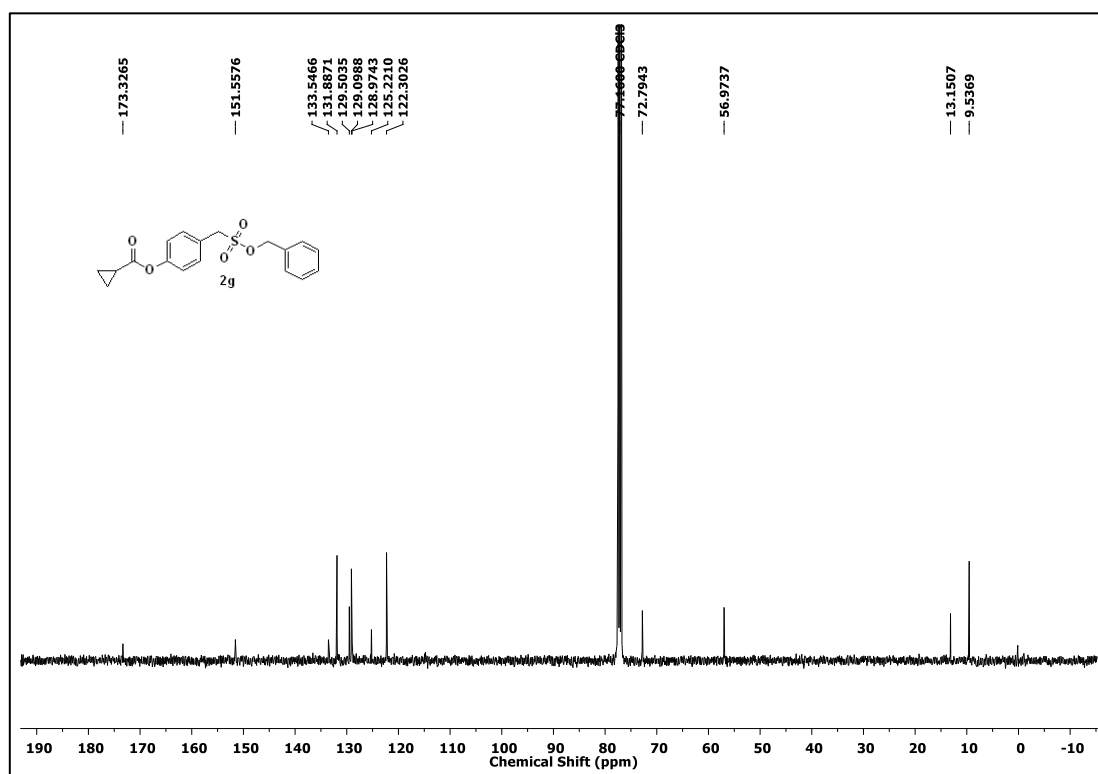
^{1}H NMR Spectrum (400 MHz, CDCl$_3$) of **17h**
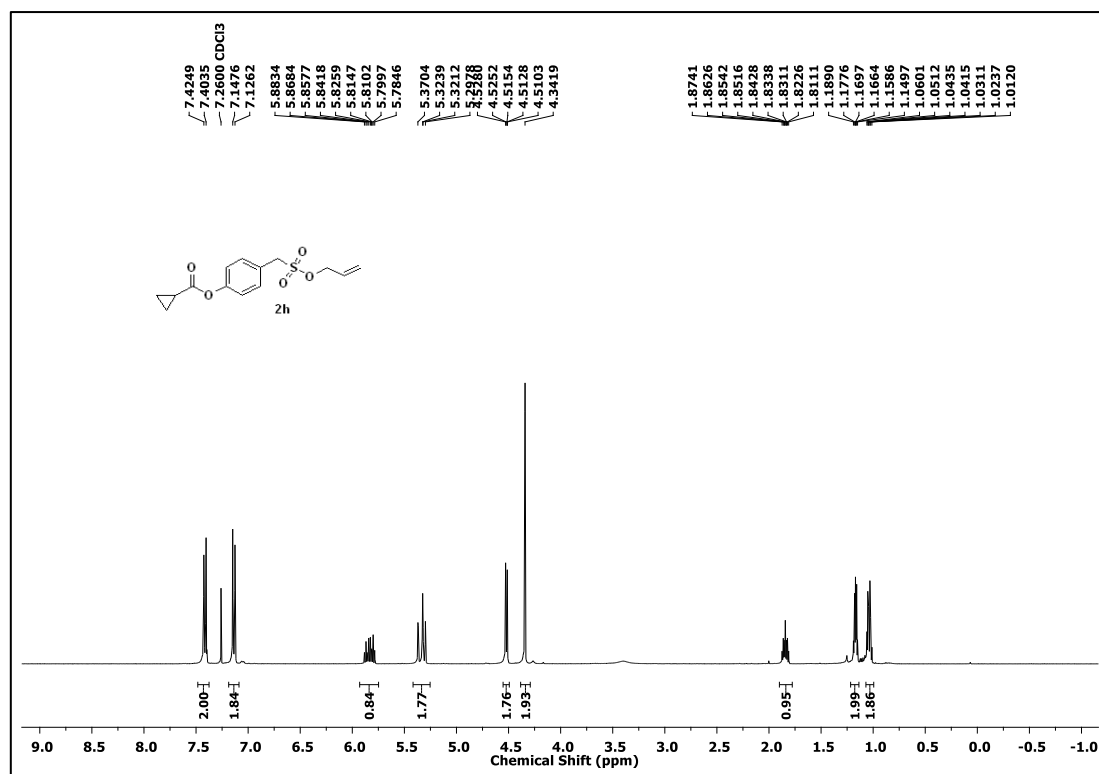
^{13}C NMR Spectrum (100 MHz, CDCl$_3$) of **17h**
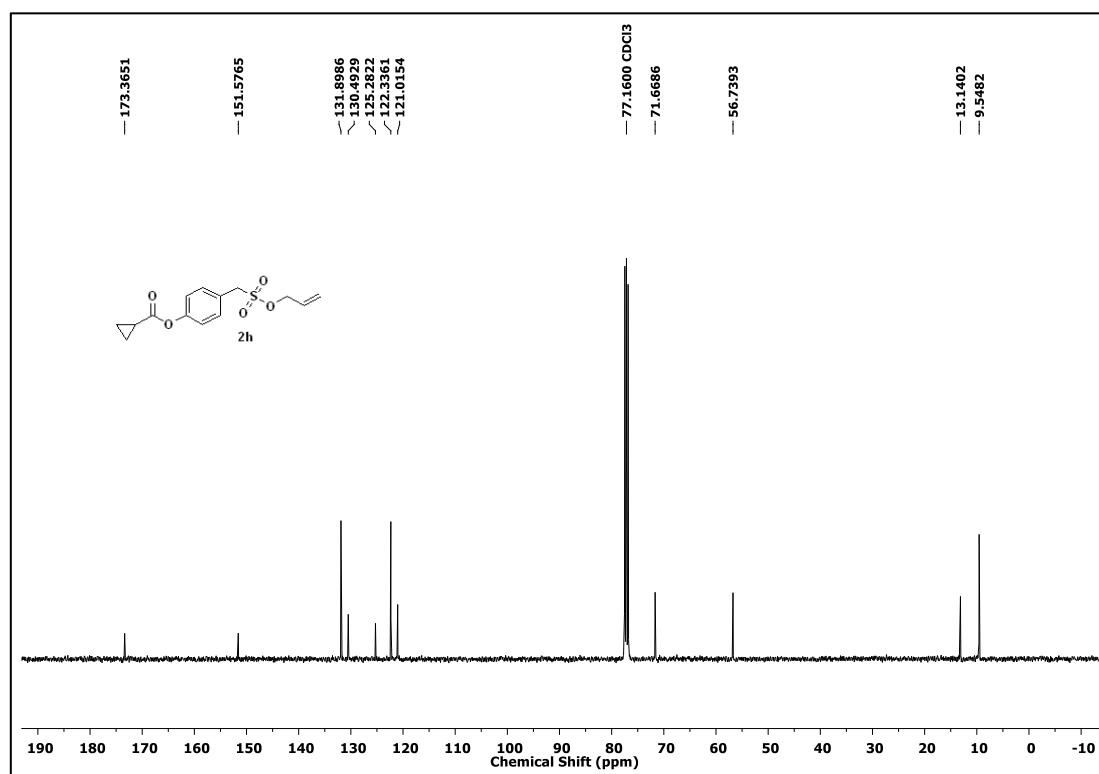
^{1}H NMR Spectrum (400 MHz, CDCl$_3$) of **17i**
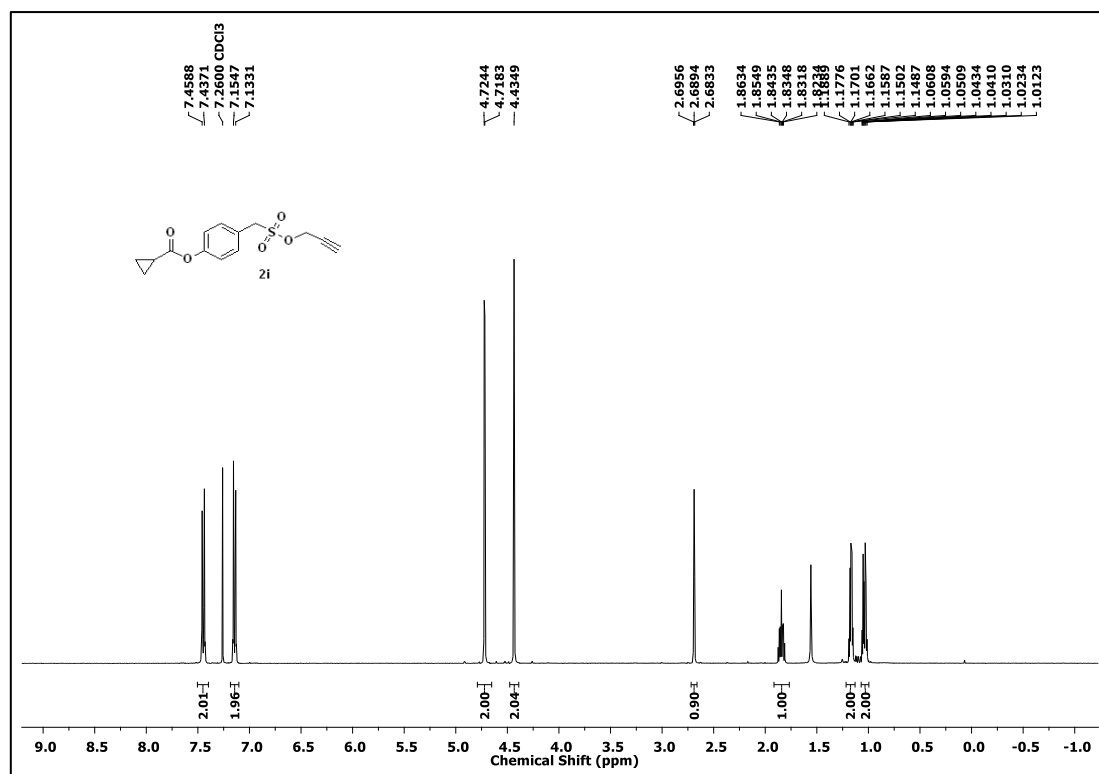
^{13}C NMR Spectrum (100 MHz, CDCl$_3$) of **17i**
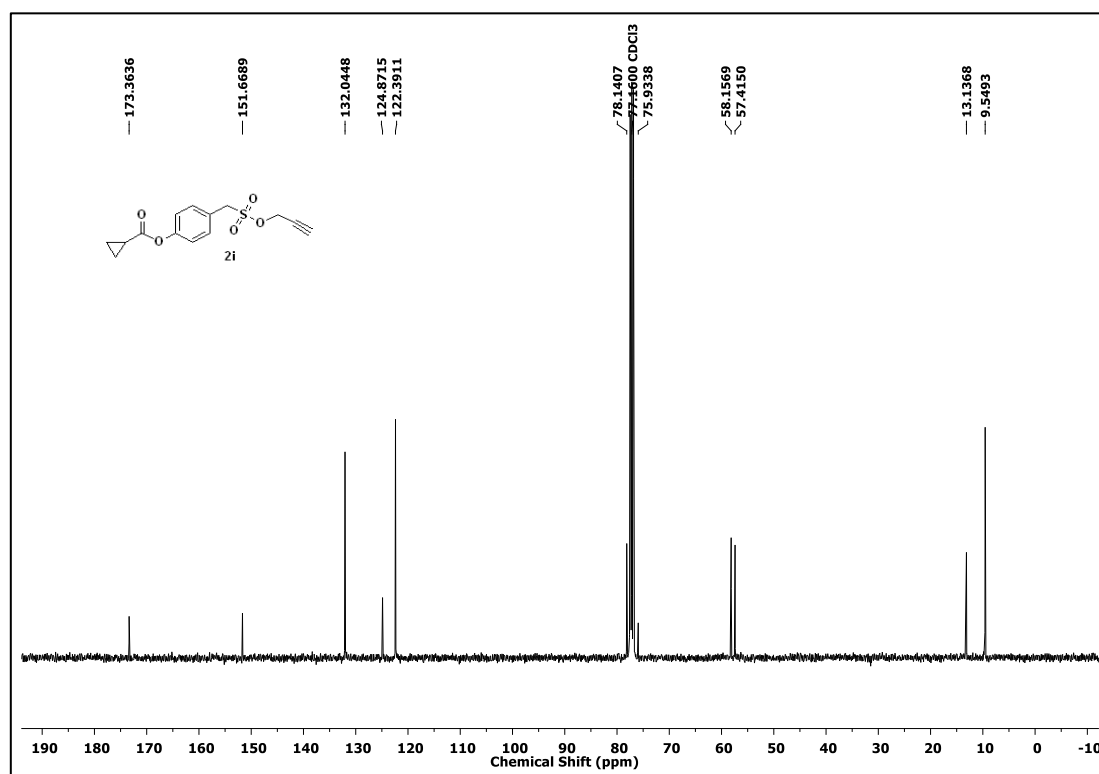
^{1}H NMR Spectrum (400 MHz, CDCl$_3$) of **17j**
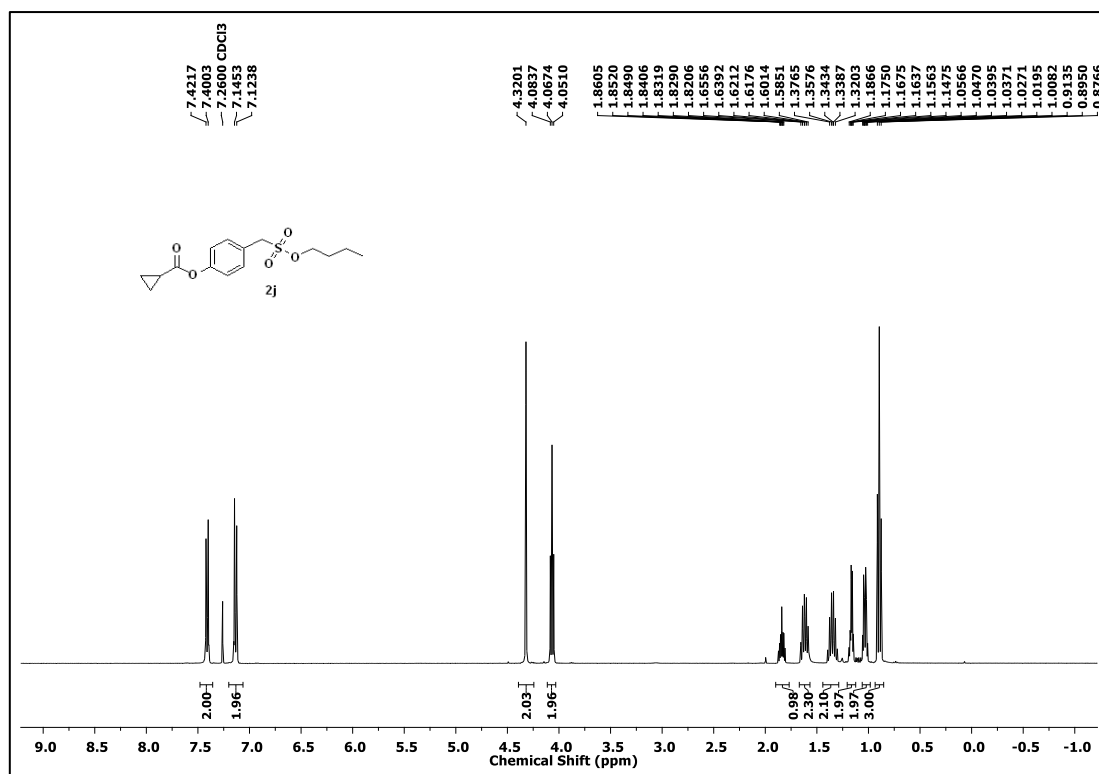
^{13}C NMR Spectrum (100 MHz, CDCl$_3$) of **17j**
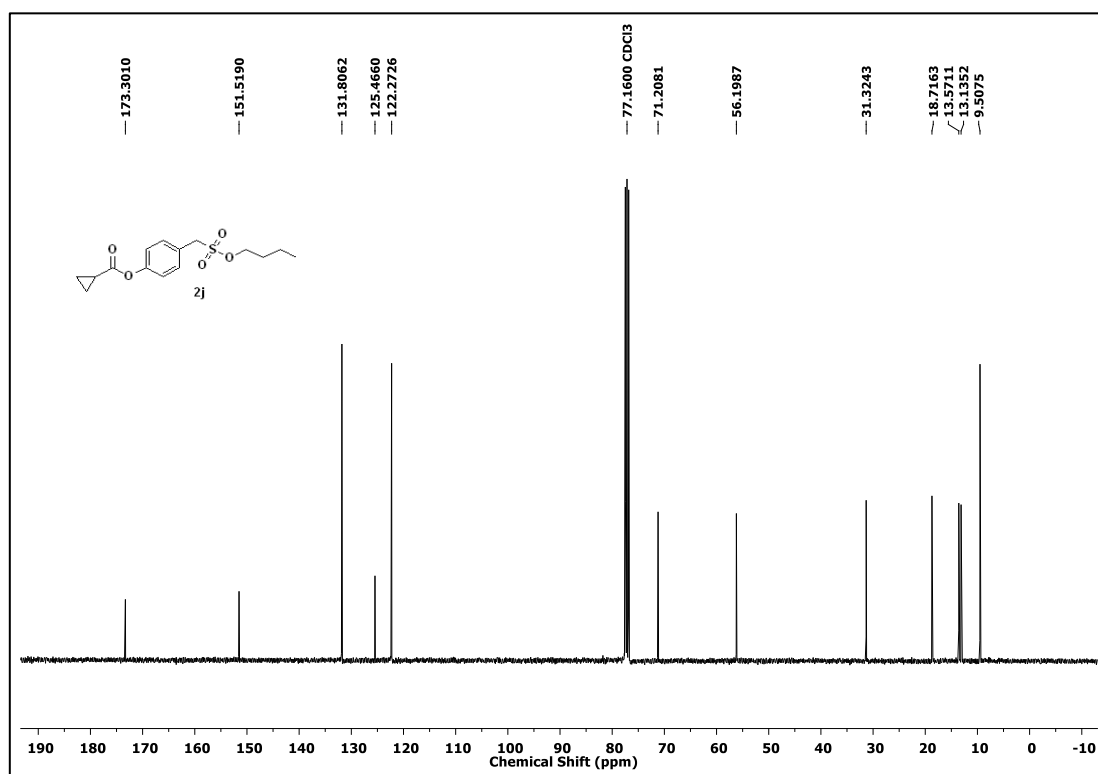
^{1}H NMR Spectrum (400 MHz, CDCl$_3$) of **17k**
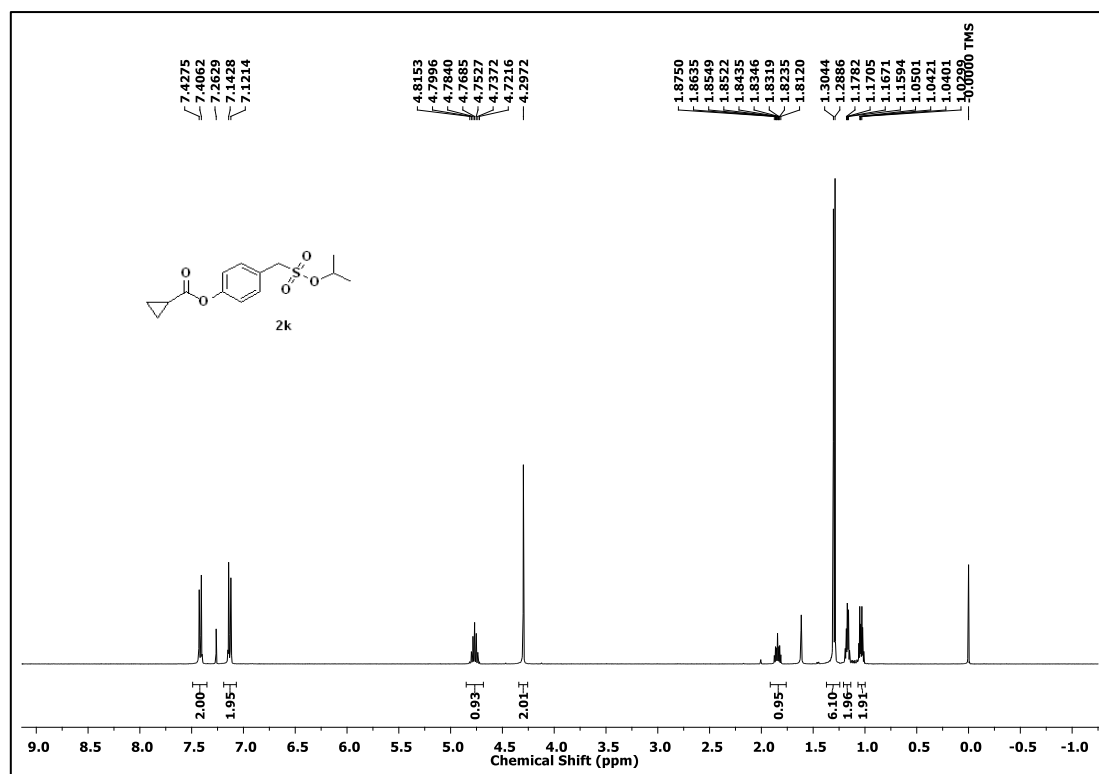
^{13}C NMR Spectrum (100 MHz, CDCl$_3$) of **17k**
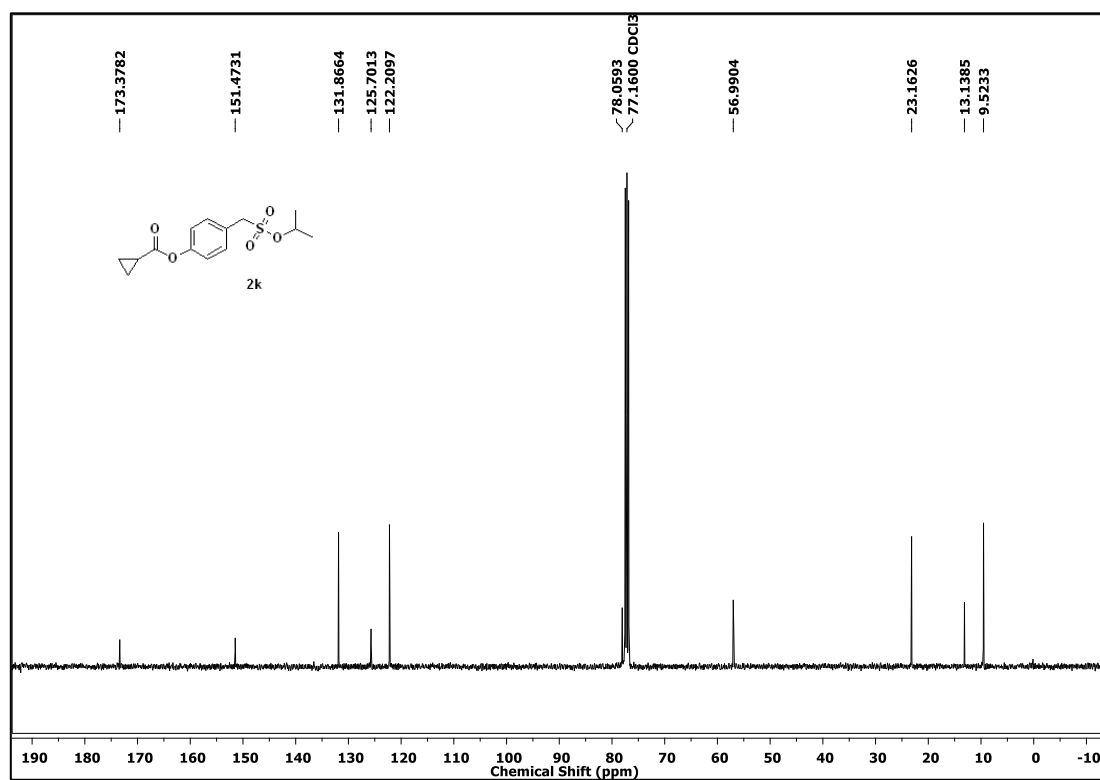
^{1}H NMR Spectrum (400 MHz, CDCl$_3$) of **18**
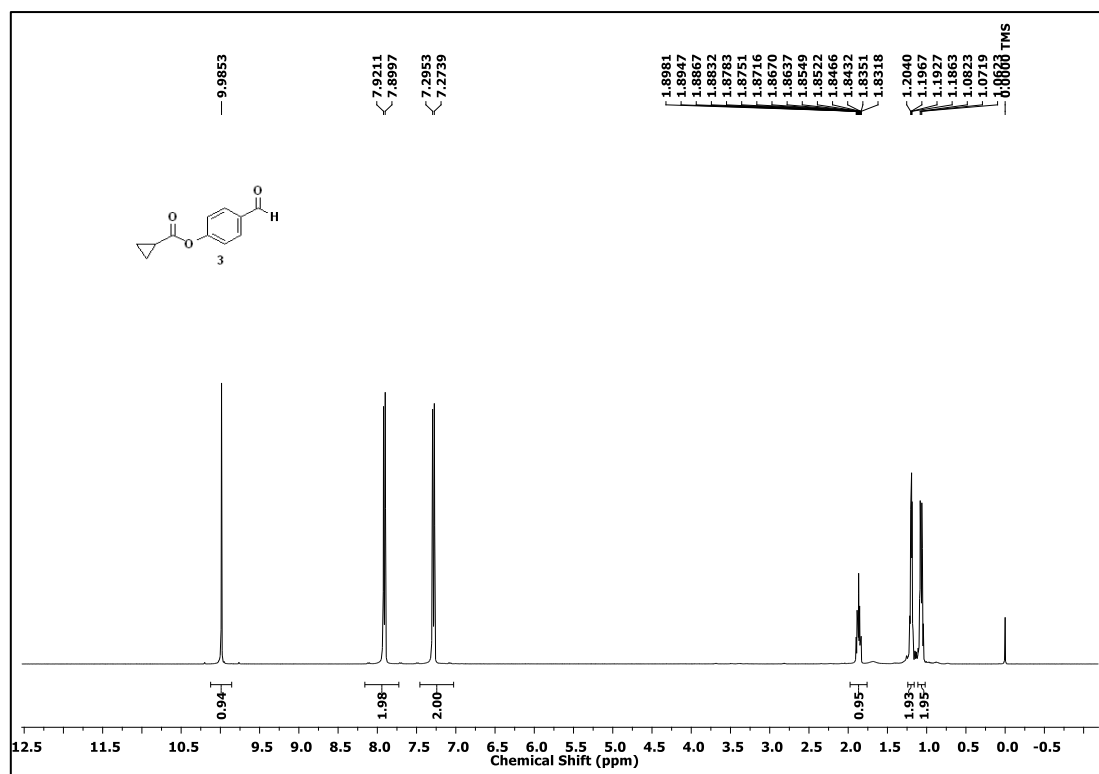
^{13}C NMR Spectrum (100 MHz, CDCl$_3$) of **18**
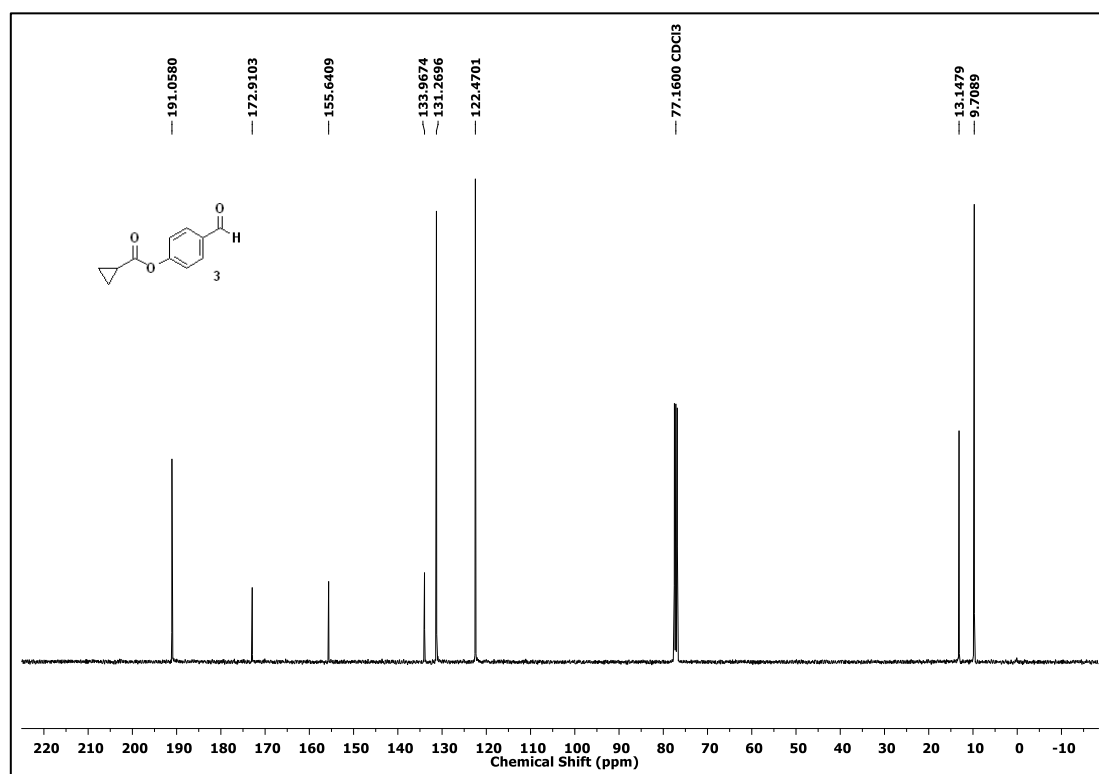
^{1}H NMR Spectrum (400 MHz, CDCl$_3$) of **19**
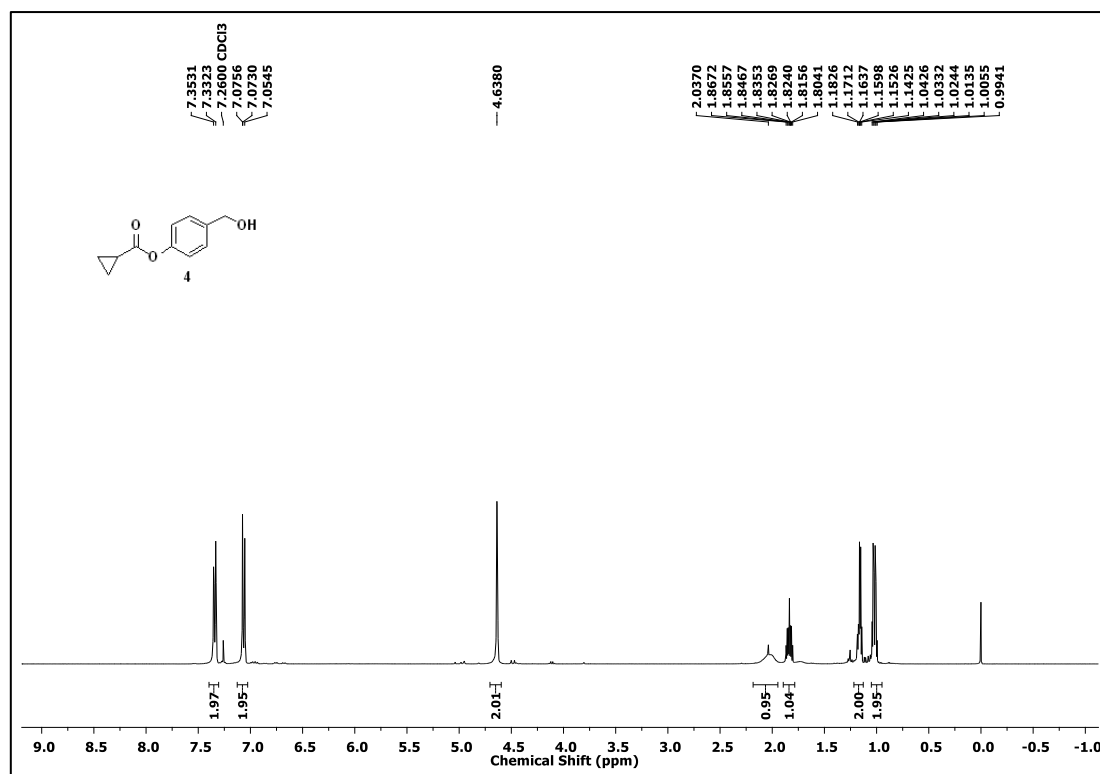
^{13}C NMR Spectrum (100 MHz, CDCl$_3$) of **19**
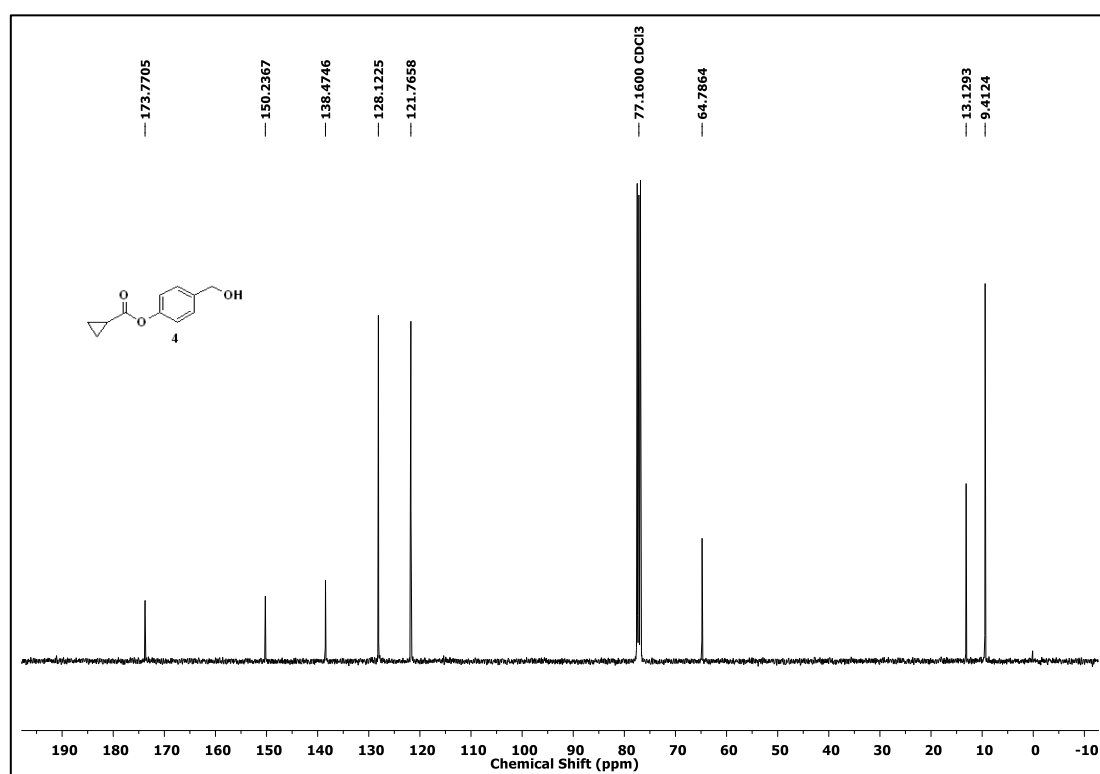
^{1}H NMR Spectrum (400 MHz, CDCl$_3$) of **20**

7.2906
7.2693
7.2600 CDCl3
7.0223
7.0010

4.0956

2.3443

1.8433
1.8349
1.8234
1.8117
1.1931
1.1617
1.1540
1.1504
1.1428
1.1338
1.0338
1.0251
1.0172
1.0152
1.0049
0.9974
0.9859

1.90
1.94

2.07

3.07

1.04

2.10
2.00

Chemical Shift (ppm)

^{13}C NMR Spectrum (100 MHz, CDCl$_3$) of **20**

195.2100

173.5946

150.0169

135.1782
129.9837

121.8601

77.0000 CDCl3

32.9719
30.4804

13.1337
9.4193

Chemical Shift (ppm)
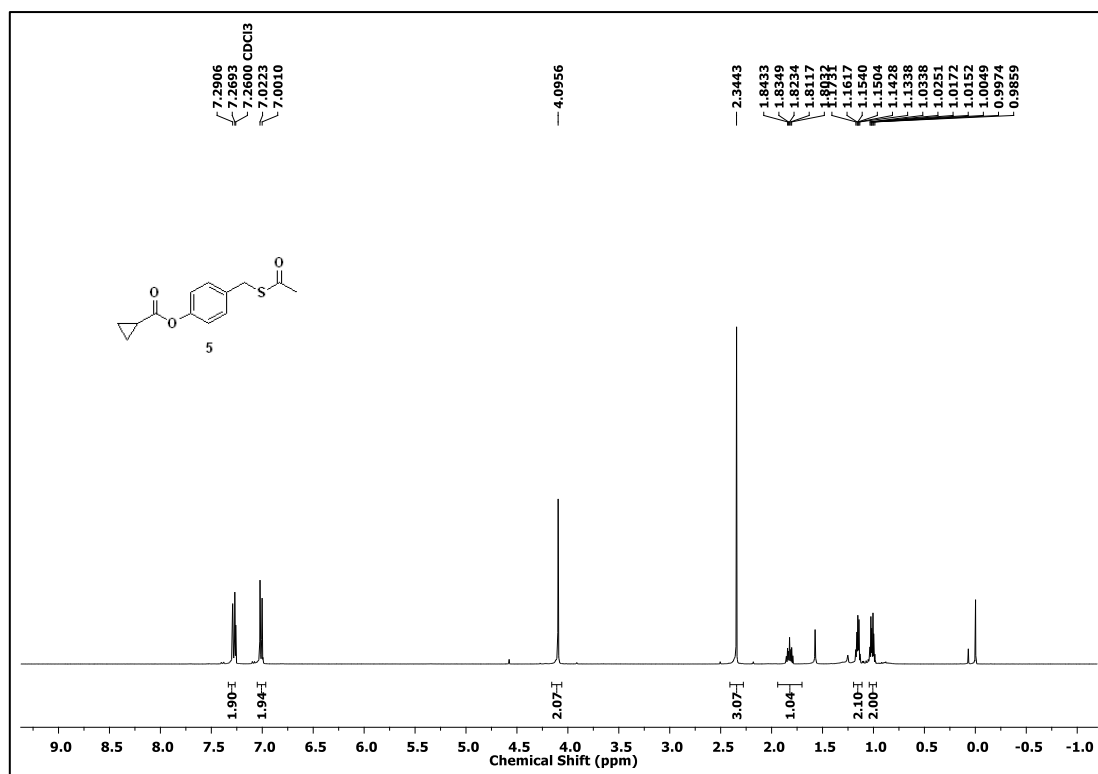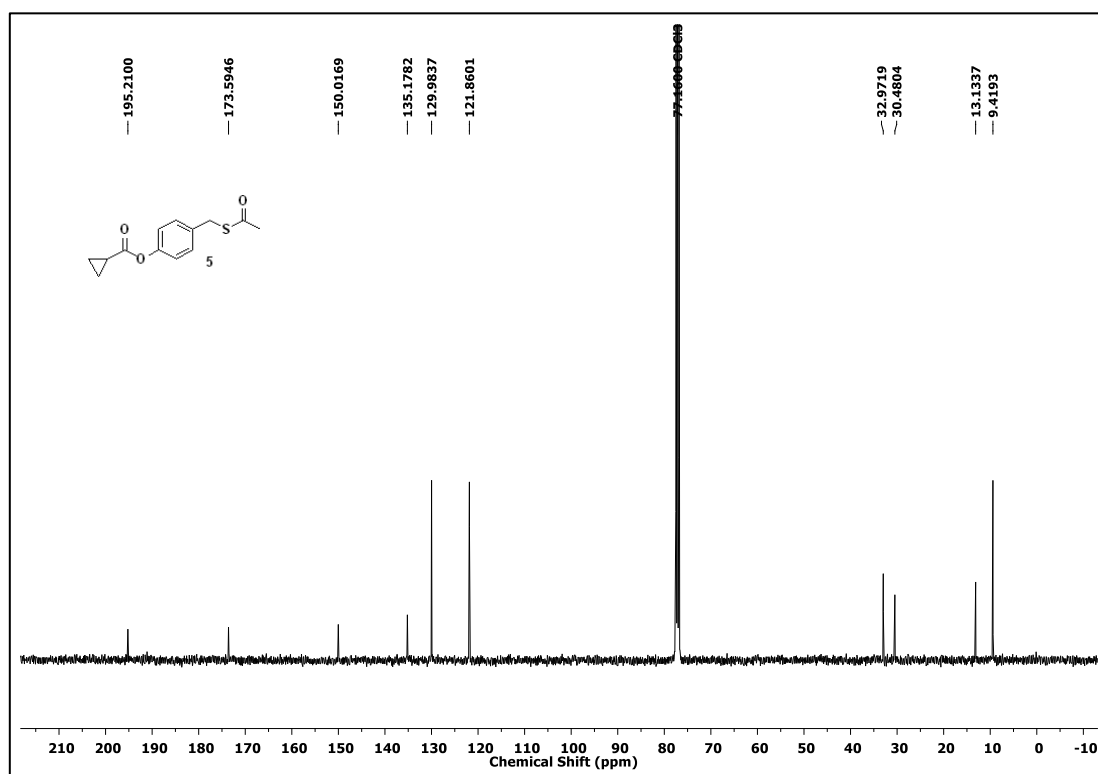
^{1}H NMR Spectrum (400 MHz, CDCl$_3$) of **21**
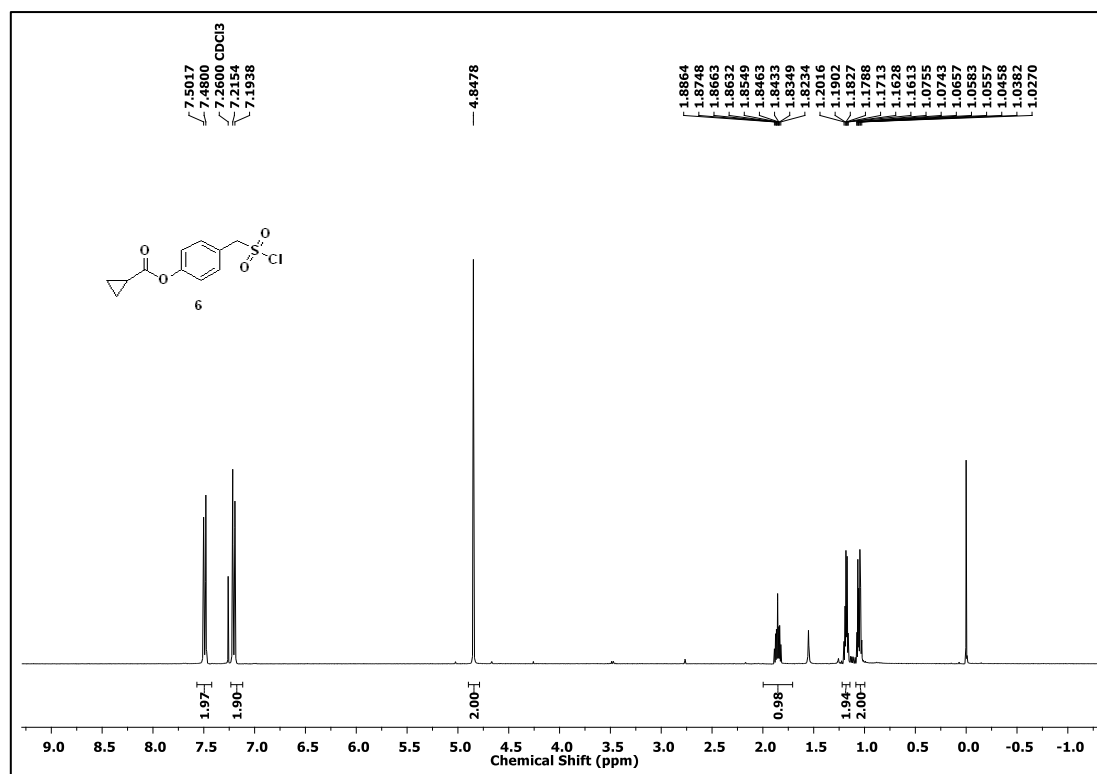
^{13}C NMR Spectrum (100 MHz, CDCl$_3$) of **21**

^{1}H NMR Spectrum (400 MHz, DMSO-d$_6$) of **22**
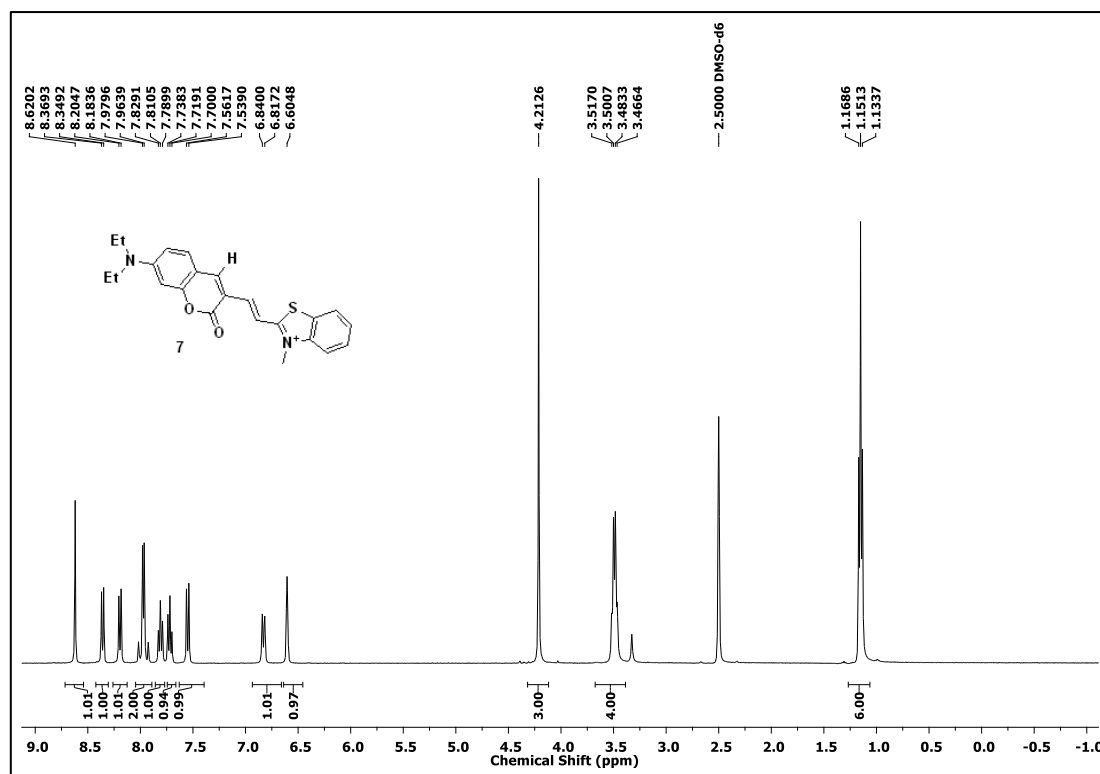
^{1}H NMR Spectrum (400 MHz, DMSO-d$_6$) of **23h**
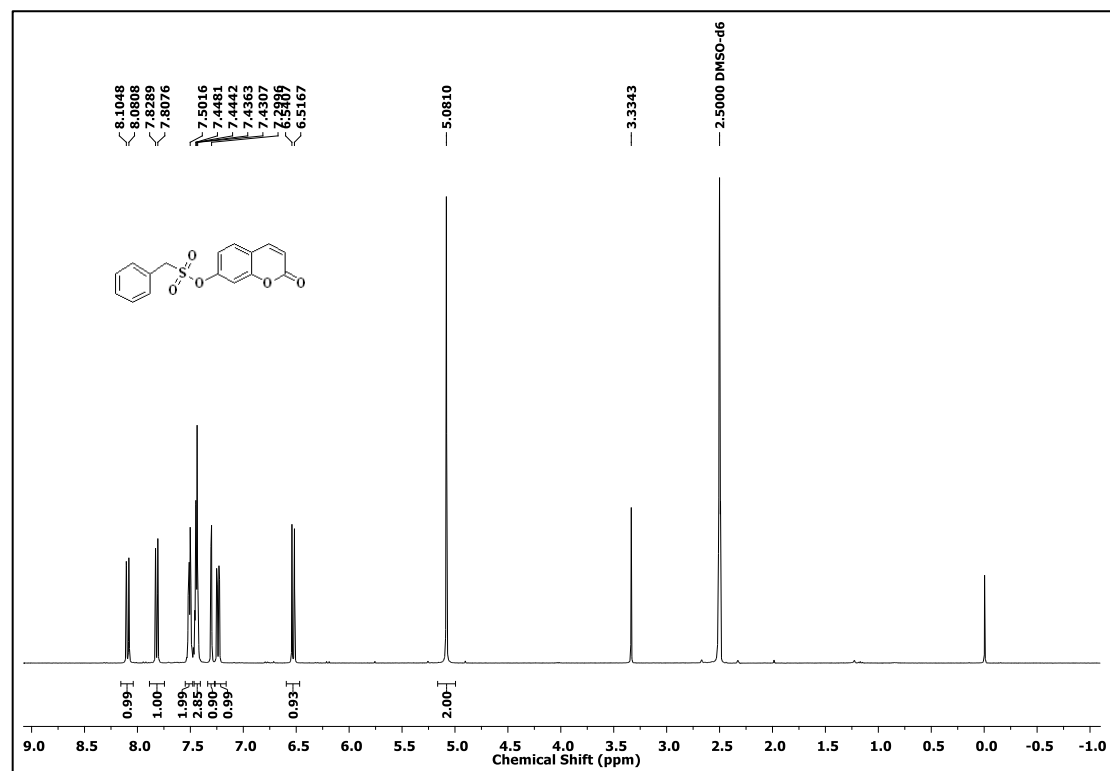
^{13}C NMR Spectrum (100 MHz, DMSO-d$_6$) of **23**
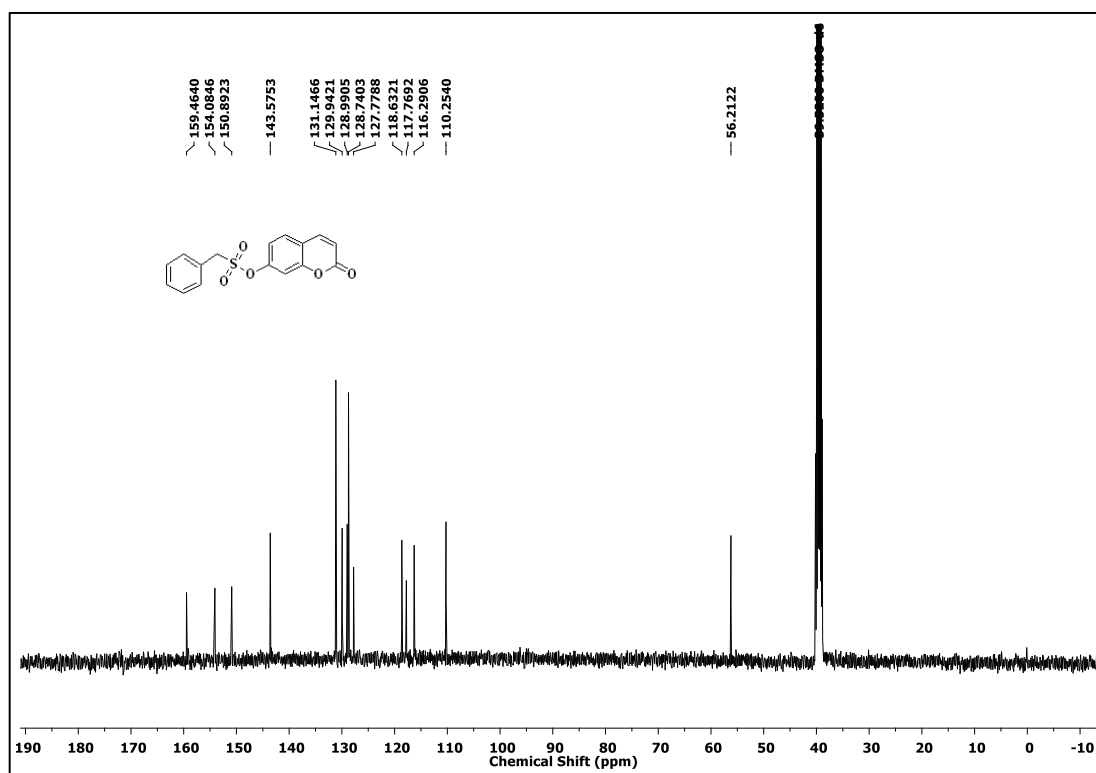
3.6. References

1   E. Leroy, N. Bensel and J. Reymond, 2003, **13**, 2105–2108.

2   Y. Zheng, B. Yu, K. Ji, Z. Pan, V. Chittavong and B. Wang, *Angew. Chem. Int. Ed.*, 2016, **55**, 4514–4518.

3   K. Kovacs, R. Mcilwaine, K. Gannon, A. F. Taylor and S. K. Scott, *J. Phys. Chem. A*, 2005, **109**, 283–288.

4   S. Chlorides, K. Maeda and S. Miki, *Synthesis (Stuttg).*, 2006, **24**, 4131–4134.

5   A. Albert and E. P. Serjeant, *The Determination of Ionization Constants*, 3rd edn., 1984.

6   Y. Nakagawa, K. Uehara and N. Mizuno, 2005, **44**, 2004–2006.

7   D. D. Perrin and G. B. Barlin, *Quaterly Rev.*, 1965, 75–101.

8   D. D. Perrin, B. Dempsey and E. P. Serjeant, *pK a Prediction for Organic Acids and Bases*, Springer, Dordrecht, 1981.

9   P. Chauhan, P. Bora, G. Ravikumar, S. Jos and H. Chakrapani, *Org. Lett.*, 2017, **19**, 62–65.

10   G. T. James, *Anal. Biochem.*, 1978, **86**, 574–579.

11   P. C. Smith, a F. McDonagh and L. Z. Benet, *J. Pharmacol. Exp. Ther.*, 1990, **252**, 218–24.

12   Y.-Q. Sun, J. Liu, J. Zhang, T. Yang and W. Guo, *Chem. Commun.*, 2013, **49**, 2637.

Chapter 4. Nitroreductase Activated, Specific Theranostic Prodrug Therapy for Bacteria

Introduction 4.1. As demonstrated in Chapter 3, the sulfonate functional group is stable in buffers of different pH, as well as in the presence of biological nucleophiles. This presents an opportunity to develop SO_2-based prodrugs for drug delivery as an alternative for widely used carbonate prodrug strategies.[1,2] Since SO_2 is a widely used food preservative and an antibacterial agent,[3] it is likely that such compounds will be well tolerated by cells. Here, we proposed to develop an SO_2-conjugated theranostic prodrug molecule to deliver an antibiotic and fluorophore, such that the prodrug can be specifically activated by bacterial enzymes. This approach may help us exploit the unique antibacterial property of SO_2. For activation of the drug in a specific mode, we considered specific stimuli such as nitroreductase (NTR). Nitroreductases are enzymes from the flavoenzyme family, widely distributed among bacterial species to a lesser extent, in mitochondria. Reduction of the nitro group has been exploited for activation of drugs under hypoxic conditions, which are commonly encountered in solid tumours. Nitroreductases are divided into two major classes: oxygen insensitive nitroreductases (perform $2e^-$ reduction) and oxygen sensitive nitroreductases (perform $1e^-$ reduction). They are used in several prodrugs or drug delivery strategies.[4–7] Outlined below are some representative examples of NTR activated prodrugs or drugs that are dependent on the reduction of the nitroaryl functional group.

4.1.1. Application of nitroreductases in anticancer strategies

Nitroreductases have been used in several anticancer strategies as a trigger to deliver a cytotoxic drug.[8] For example, phosphoramide mustard, in the presence of NTR with NADH/NADPH as cofactor, which reduces a nitro group to form a hydroxylamine or amine derivative.[9]
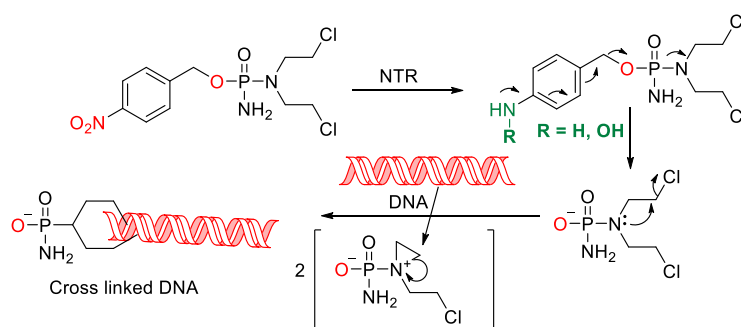
Scheme 4.1.1. NTR activated phosphoramide mustard

Thus, the compound gets converted from an electron-deficient nitroaromatic molecule to an electron rich aniline molecule, upon NTR activation. Further, it follows a cascade to release a substituted constrained aziridinium by the release of a chloride ion. Sequential nucleophilic attacks by bases of two strands of DNA on the three-member ring finally result in crosslinking and thus, are responsible for cytotoxicity.

4.1.2 Nitroreductase activated nitroaromatic compounds as anti-parasitic and antimicrobial agents

Nitrofurantoin, Nifurtimox, and benznidazole are nitro-heterocyclic compounds, primarily used for their antiparasitic potency. They also exhibit marked antibacterial activity, particularly against anaerobic bacteria, due to the activity of nitroreductases in a hypoxic environment.[10,11]
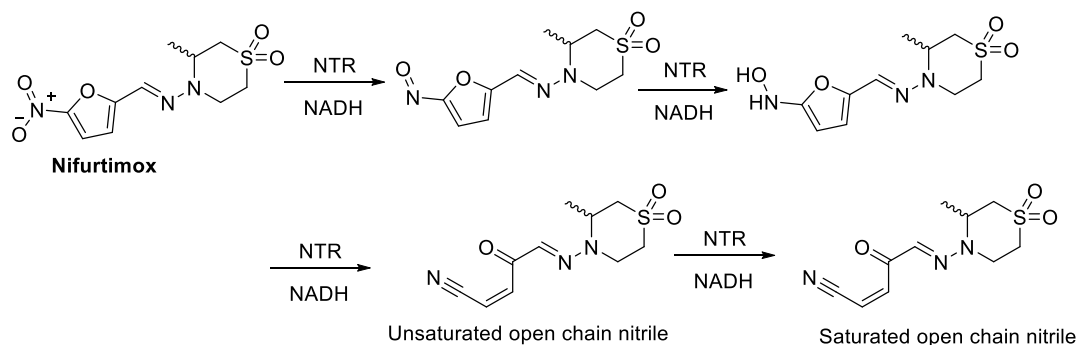
Scheme 4.1.2. NTR-mediated bio-activation of Nifurtimox and subsequent ring opening to give a toxic unsaturated open-chain nitrile
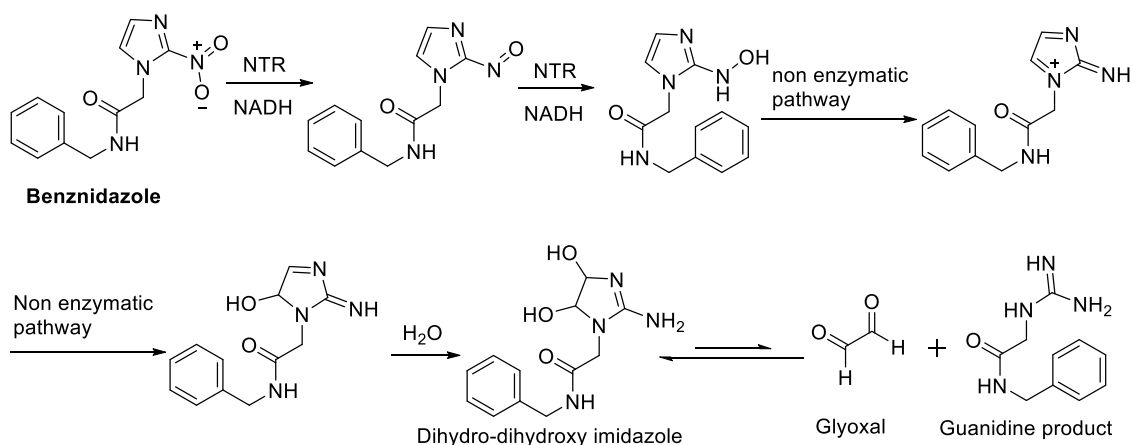
Scheme 4.1.3. NTR-mediated bio-activation of benznidazole to give a hydroxylamine, followed by a series of nonenzymatic transformations that lead to the formation of the toxic glyoxal

4.1.3 Activation of PA-824 by NTR

PA-824, which exhibits marked antimycobacterial activity, uses an *Mtb* Ddn [deazaflavin (F420)-dependent nitroreductase (Ddn)]. The mechanism of reduction of the nitro group by Ddn for PA-824 in *Mtb* is different. The first step involves the reduction of a C2–C3 bond of the five-member ring in PA-824, which subsequently gets protonated to undergo a des-nitrification and generates des-nitro-PA-824, with concomitant generation of nitrous acid. This finally produces NO (nitric oxide) and other nitrogen species that may contribute to an antimycobacterial property in *Mtb* by PA-824.[12]
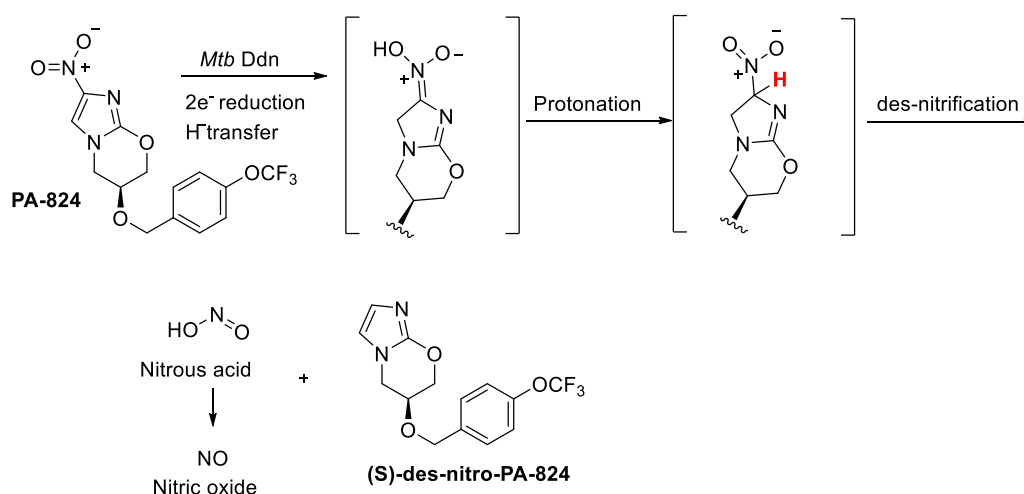
Scheme 4.1.4. Deazaflavin-dependent nitroreductase catalyzes the reduction of PA-824 in *Mycobacterium tuberculosis*

The aforementioned examples of compounds and their NTR-mediated activation suggest the utility of nitroreductases in bacteria and provide a potential opportunity for the use of a nitroaromatic compound as a stable SO_2-donor based prodrug.

4.1.4. Hypothesis

In the previous chapter, we have developed a new strategy to generate SO_2 upon esterase activation. Similarly, we hypothesized that with specific activation by NTR, we should be able to generate SO_2 specifically in bacteria and this may present a better opportunity to make a new stable class of SO_2-based prodrugs, for several bacterial species (See Figure 4.1).
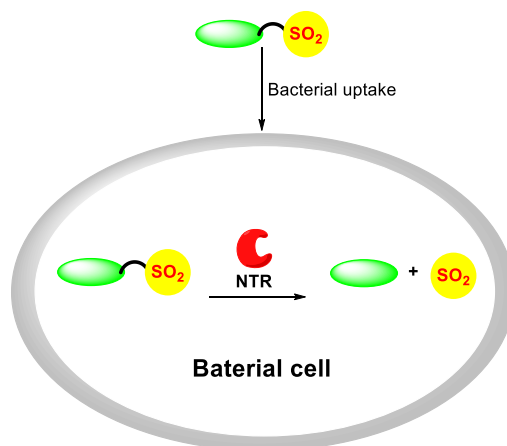
Figure. 4.1. Proposed activation of the SO$_2$ donor in bacteria by its indigenous nitroreductase (NTR)

4.2. Results and discussion

4.2.2. Synthesis

In order to test our hypothesis, we derivatized 4-nitro-α-toluenesulfonyl chloride with Umbelliferone (Umb), the fluorophore, for its wide applications to afford **24** in a good synthetic yield. Similarly, we derivatized 4-nitrobenzyl bromide to make the sulfone-deficient control compound **25** in a good yield.
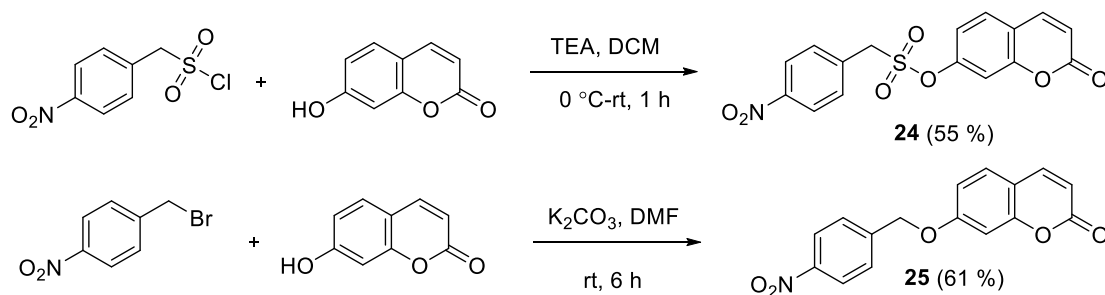
Scheme 4.2. Syntheses of the NTR activated sulfonate and control compound

4.2.3. Chemoreduction

To evaluate the hypothesis that **24** undergoes self-immolation on the reduction of the nitro group to generate Umb, compound **24** was activated by chemoreduction by the reported protocol using Zn-ammonium formate in methanol: H$_2$O (1:1, v/v) system.[13] Aliquots from the reaction mixture were analyzed using HPLC. Analysis of the reaction mixture after 30

min revealed complete disappearance of the compound **24** with the concomitant formation of Umb. The yield of Umb was found to be quantitative suggesting an efficient self-immolation of **24** upon chemoreduction.
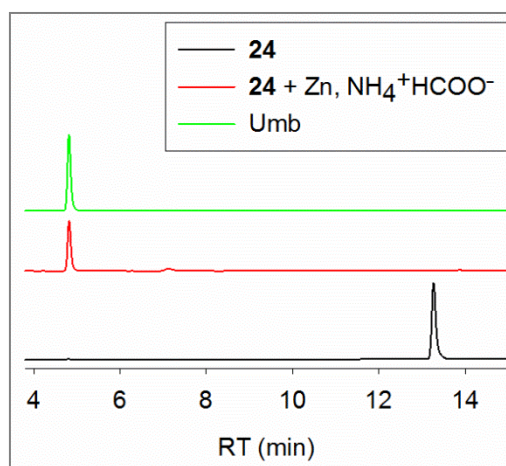
Figure 4.2. Monitoring the release of Umb by HPLC traces; the reaction mixture of **24** (25 µM) with Zn-ammonium formate in MeOH: H_2O (1:1, v/v), after 30 min, generated Umb in a quantitative yield. Absorbance at 320 nm was monitored.

4.2.4. NTR reduction

After we confirmed that **24** undergoes self-immolation to generate Umb upon chemoreduction, we proposed to assess its potential to undergo enzymatic (NTR) reduction, under physiological conditions. In order to test that, the compounds **24** (25 µM) and **25** (25 µM) were independently reacted with NTR (20 µg/mL) along with the cofactor NADH (75 µM) in PBS. Aliquots from the reaction mixture were monitored by HPLC over a period of time. HPLC analysis of the reaction mixture after 30 min revealed the complete disappearance of the compound **24** with the concomitant generation of Umb. The yield of Umb generation was found to be 82%, suggesting an efficient self-immolation of **24** on NTR reduction. Similarly, sulfone-deficient control **25** was found to generate Umb less efficiently under similar conditions. It generated 52% of Umb over a prolonged duration. These results revealed the importance of generation of thermodynamically stable gaseous species, SO_2, for efficient self-immolation.
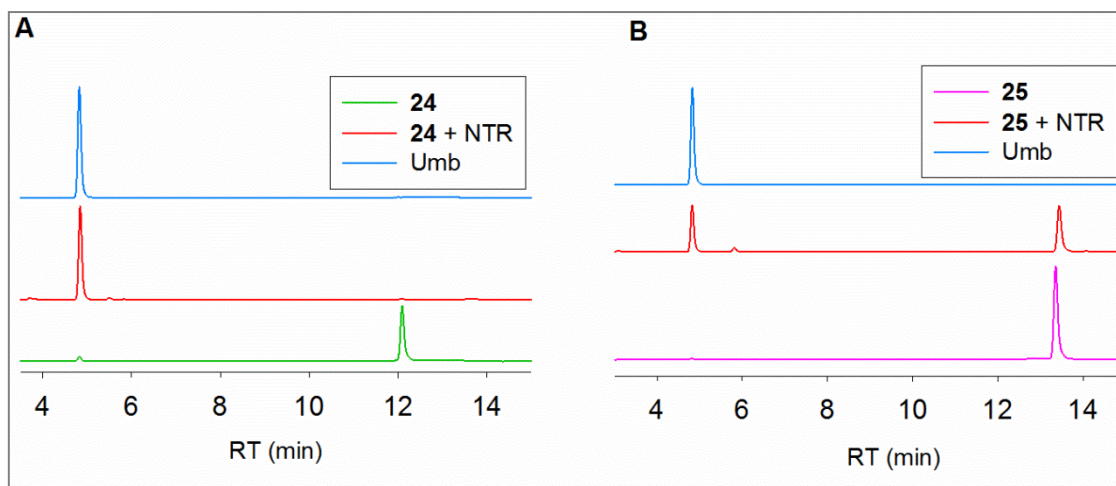
Figure 4.3. Monitoring the release of Umb from a compound by HPLC upon NTR activation (20 µg/mL) along with the NADH (75 µM) in PBS (pH 7.4, 10 mM) (a) Decomposition of **24** (25 µM) after 30 min and complete disappearance of **24** to generate 82% Umb (b) Incomplete decomposition of **25** (25 µM) after 30 min to generate 52% Umb. Absorbance at 320 nm was monitored.

4.2.5. Sulfite detection

From the HPLC analysis, we found evidence for self-immolation of **24** upon NTR activation. to generate Umb in excellent yield. Similarly, during this cascade, SO_2 generated as one of the product. In aqueous media, SO_2 is converted into its hydrated form sulfite/bisulfite under physiological conditions. Next, we proposed to detect sulfite on NTR activation with sulfite dye **22**. However, due to the interference of Umb absorbance with sulfite dye **22**, we derivatized 4-nitrobenzylsulfonyl chloride with 1-naphthol to afford **26** in good yield. Subsequently, we synthesized negative control **27**, which has a carbonate moiety, in moderate synthetic yield. Next, when we compared these compounds for their SO_2 analysis with sulfite dye **22**,[14] as expected, compound **26** generated sulfite upon NTR activation (Figure 4.4a). We found no evidence of the generation of sulfite from control compound **27**. (Figure 4.4b).
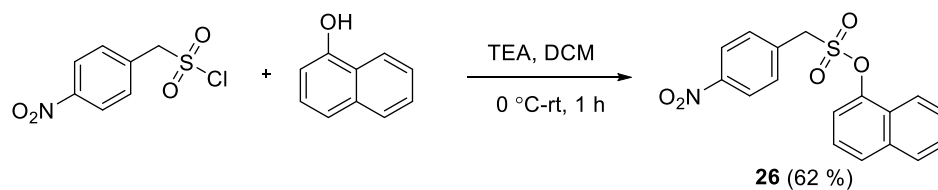
Scheme 4.2.1 Synthesis of a sulfonate for sulfite detection analysis
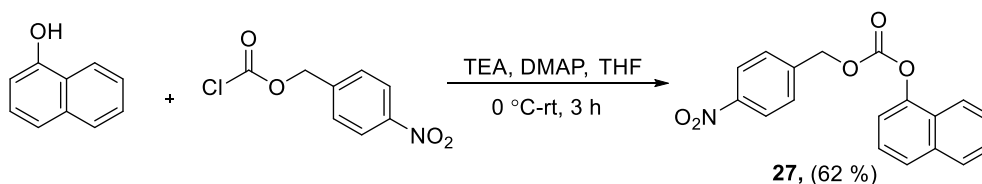
Scheme 4.2.2 Synthesis of control carbonate for sulfite detection analysis
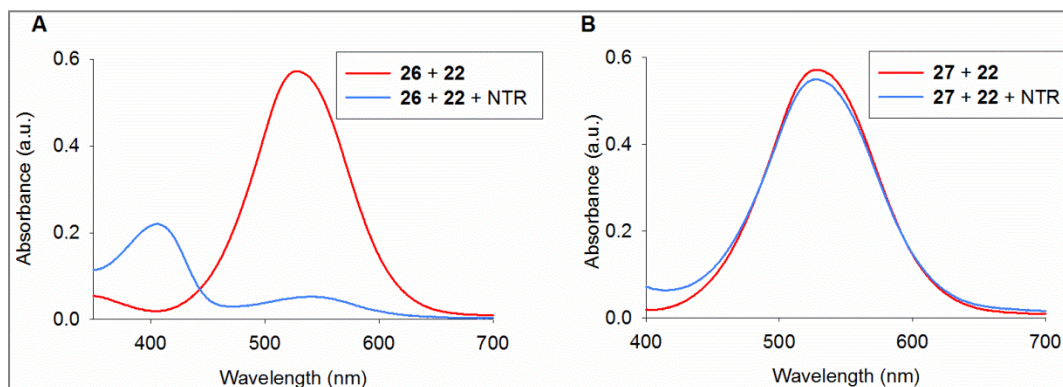
Figure 4.4. Compounds **26** (50 µM) and **27** independently incubated with **22** (10 µM) in the presence of NTR (20 µg/mL) and NADH (75 µM) for 15 min: (a) Disappearance of the signal at 545 nm of **22** and appearance of a new signal at 410 nm for sulfite adduct with dye **22** indicated the sulfite formation (b) The signal at 545 nm signal corresponding to **22** nearly remained unchanged, indicating that sulfite was not produced in the presence of **27**, also indicating no interference from side products of **27** in the absorbance signal of **22** upon NTR activation. All the experiments were conducted in PBS (pH 7.4, 10 mM) at 37 °C.

4.2.6. Activation of compounds in *E. coli* cell lysate

NTR is present in several bacterial species and nitroaromatic compounds are a well-known substrate for NTR. Thus, in order to test the potential of **24** and **25** for activation with a bacterial source of NTR to release Umb, we chose *E. coli,* a Gram negative bacteria. In the assay, *E. coli* was grown overnight and its OD was adjusted to 1.0. Cells were lysed by sonication and compounds (25 µM) were independently exposed to the whole cell lysate in PBS for 1 h. Fluorescence for Umb at λ_{ex}: 350 nm and λ_{em}: 450 nm, was monitored with **17a** as a reference compound. Compounds **24** and **25** were able to generate Umb (Figure 4.5) in a bacterial cellular environment suggesting the reduction of the nitro group and subsequent self-immolation. Again, **24** was found to be more efficient in undergoing self-immolation, compared to control compound **25**. This result further validated the importance of a masked

SO$_2$ donor for efficient self-immolation**. We reacted the esterase-sensitive compound **17a**, which gets activated in the bacterial cellular environment to generate Umb.
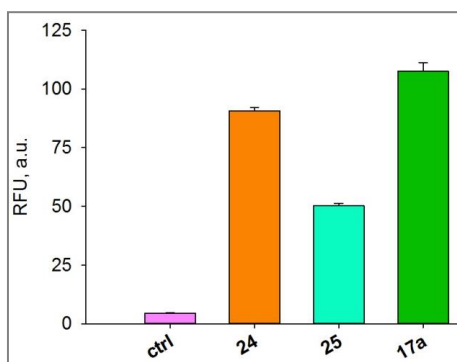
Figure 4.5. Bio-activation of **24**, **25** by *E. coli* NTR and measurement of fluorescence for Umb release

4.2.7. Nitroreductase activated, specific theranostic prodrug strategy for bacteria

There is a pressing need to design new strategies, find new antimicrobial therapeutics and rejuvenate existing available antibiotics to fight the grave threat of drug resistance. These will allow reducing the mortality and morbidity caused by infectious diseases. Unfortunately, in the past few decades, very few new drug molecules with novel mechanisms of action are in development. Thus, puts an excessive burden on the available antimicrobial therapies. In order to prolong and retain the efficacy of available drugs, they can be formulated as prodrugs, preferably with regard to the indigenous bio-activable triggers of a pathogen. Next, detection of infectious disease causing bacilli *in vivo* is a challenging task and one of the major reasons to cause fatalities. To tackle these better, sophisticated detection techniques are needed. Theranostics is a rapidly emerging field which engages both diagnostics (detection) and therapeutics together on a single platform. This field has a vast potential, with multiple folds of advantages. Theranostics helps with early detection of disease causing bacilli along with their inhibition. No secondary assays would be required in order to image the delivered drug in the bacteria. For bacteria, there are a few non-invasive theranostics reports that have emerged in the past decade which are mostly based on materials science.[15–25] Our examples of small organic SO$_2$ donors were found to undergo efficient self-immolation to produce respective products and were activated by an enzyme of bacterial origin (NTR). Therefore, we proposed to synthesize SO$_2$ donor based self-immolative theranostic agents, which could be activated by NTR (Figure 4.6).
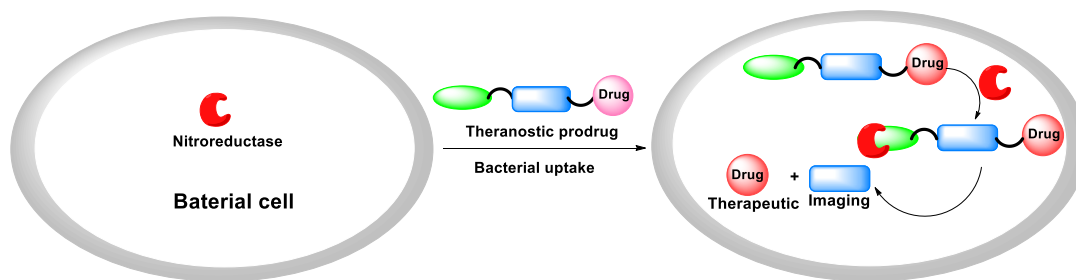
Figure 4.6. Proposed design for antibiotic conjugated, specific theranostic prodrug approach for bacteria

In order to synthesize theranostic prodrugs and to have a proof-of-concept, at the starting point, we chose to synthesize prototypic examples of antibiotic conjugated drugs.
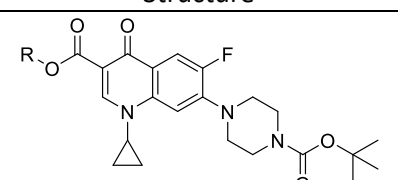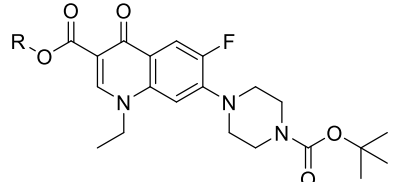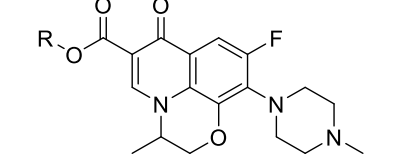
4.2.8. Synthesis of antibiotic-conjugated model compounds for theranostic strategy

To synthesize the prototypical SO_2-donor based, antibiotic conjugated prodrug, we chose to use fluoroquinolones as an antibiotic in our theranostic prodrug approach. Fluoroquinolones are quinolone-related molecules containing fluorine as one of the atoms in their core structures. They form a class of broad-spectrum antibiotics, especially active against Gram-negative bacteria, which are difficult to inhibit.[26–28] We started synthesis by derivatizing 4-nitrobenzylsulfonyl chloride with 4-hydroxybenzaldehyde to afford aldehyde **28** (Scheme 4.3.1) in excellent yield. Further, it was reduced with sodium borohydride to afford the sulfonate containing benzyl alcohol **29** (Scheme 4.3.1). Next, compound **29** was coupled by HBTU coupling with *t*-boc protected fluoroquinolones **30-31** (synthesized by a reported protocol)[29] and Levofloxacin (LevoX) to afford compounds **32-34** (Scheme 4.3.2) in good yield. Study with this compounds, would permit us to identify the most potent fluoroquinolone.
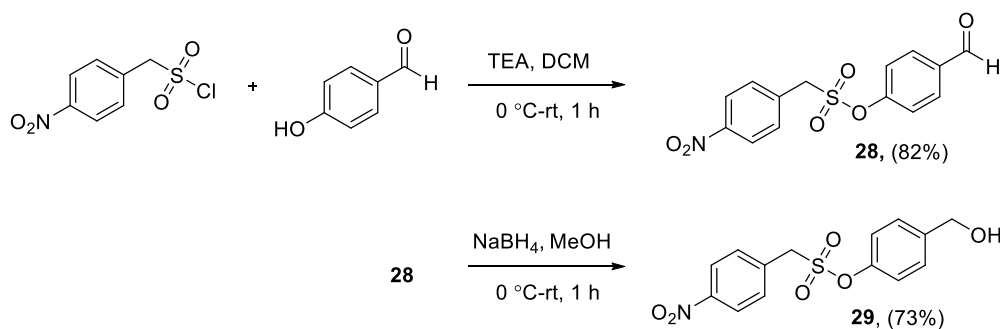
Scheme 4.3.1. Synthesis of sulfonate substituted benzyl alcohol

Scheme 4.3.2. Synthesis of drug conjugates of fluoroquinolones

R = Cyclopropyl (**35**, 93%), Et (**36**, 85%)
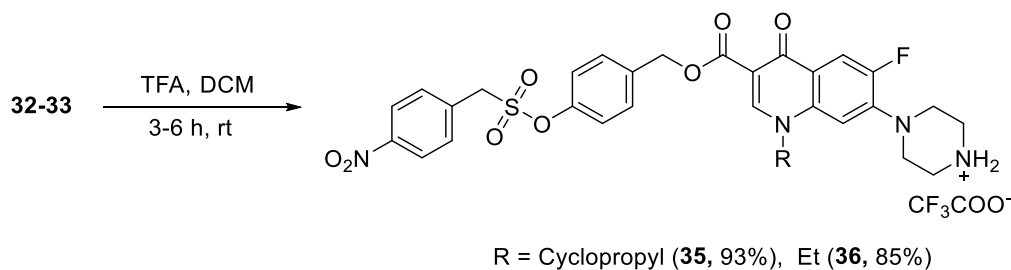
Scheme 4.3.3. Deprotection of *t*-boc protected fluoroquinolone drug conjugates

Finally, *t*-boc protected fluoroquinolones **32-33** were deprotected by TFA to afford the TFA salts of fluoroquinolone drug conjugated **35-36** in excellent yield (Scheme 4.3.3).

4.2.9 An HPLC-based evaluation of chemoreduction of fluoroquinolone drug conjugates

To evaluate our hypothesis that compounds **34-36** would undergo self-immolation upon reduction of the nitro group to generate their respective fluoroquinolones, these compounds were independently treated with Zn-ammonium formate in methanol: H_2O (1:1, v/v). Aliquots from these reaction mixtures were analyzed using HPLC. After 1 h, a nearly complete disappearance of the compounds, with the concomitant formation of their respective

fluoroquinolones, was observed. The yield of formation of levofloxacin (LevoX) was found to be 73% from **34**, 63% of ciprofloxacin (CipX) from **35** and 69% of norfloxacin (NorX) from **36** suggesting an efficient self-immolation of compounds **34-36** upon chemoreduction, to subsequently generate fluoroquinolones.
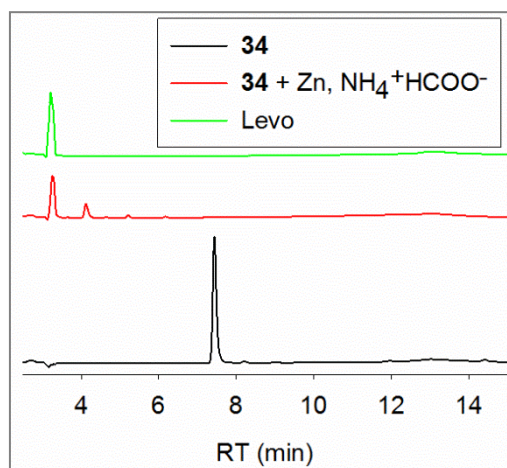
Figure 4.7. Monitoring the release of Levofloxacin (LevoX) by HPLC. Traces are from the reaction mixture of **34** (25 µM) with Zn-ammonium formate in MeOH: H_2O (1:1, v/v) after 1 h. Absorbance at 280 nm was monitored.
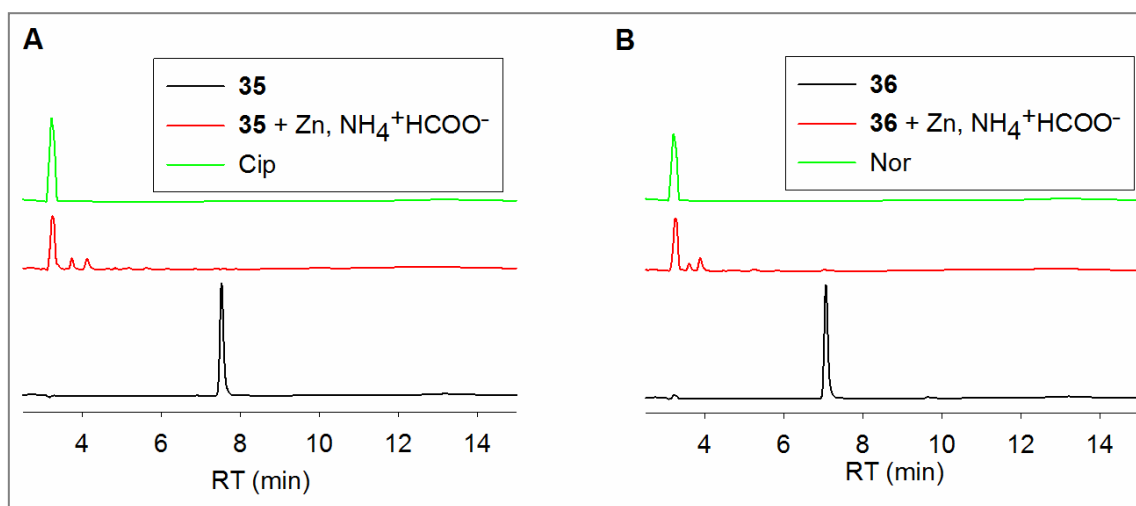
Figure 4.8. Monitoring the release of fluoroquinolones by HPLC. Traces are from the reaction mixtures of **35** (25 µM) and **36** (25 µM), when independently treated with Zn-ammonium formate in MeOH: H_2O (1:1, v/v) after 1 h. Absorbance at 280 nm was monitored. (a) The release of Ciprofloxacin (CipX) (b) Release of norfloxacin (NorX)

4.2.10.1 Antibacterial activity for NTR activated, fluoroquinolone conjugated prodrug

Upon validating the generation of their respective fluoroquinolones from fluoroquinolone conjugated prodrugs **34-36**, these compounds were tested for their antibacterial activity. Compounds were found to have a good inhibitory activity against Gram-negative *E. coli*, as well as Gram-positive *S. aureus.* The observed antibacterial activity of these conjugated prodrugs was diminished in comparison with their unconjugated counterparts. However, the antibacterial activity that we obtained for this new class of antibiotic conjugated drugs was in accordance with our hypothesis of initial activation of the drug inside bacteria (with NTR), followed by bacterial growth inhibition.

Table 4.1 Antibacterial activity of nitroreductase-specific, fluoroquinolone conjugated prodrugs

Compds	*E.coli* ATCC 25922	*S.aureus* ATCC 29213	*K.pneumoniae* BAA 1705	*A.baumannii* BAA 1605
32	>64	>64	>64	>64
34	8	32	>64	>64
35	2	64	>64	>64
36	4	32	>64	>64
Levofloxacin	<0.03	0.125	0.125	8

Antibacterial activities are in µg/mL and are provided by Dr. Sidharth Chopra from Central Drug Research Institute (CDRI), Lucknow

4.2.10.2 Time-kill curve of NTR activated ciprofloxacin drug conjugate

Time-kill curve is performed to assess bacterial growth over a period of time at different concentrations of a drug. We obtained a time-kill curve for *E. coli* using compound **35** at three different concentrations (1X, 4X, and 10X of MIC) with ciprofloxacin as a standard reference compound. The results that we obtained were similar at 1X and 10X concentrations and were moderately similar to 4X concentration. This data clearly revealed that the ciprofloxacin conjugated prodrug had retained activity similar to ciprofloxacin, *i.e.*, bactericidal activity.
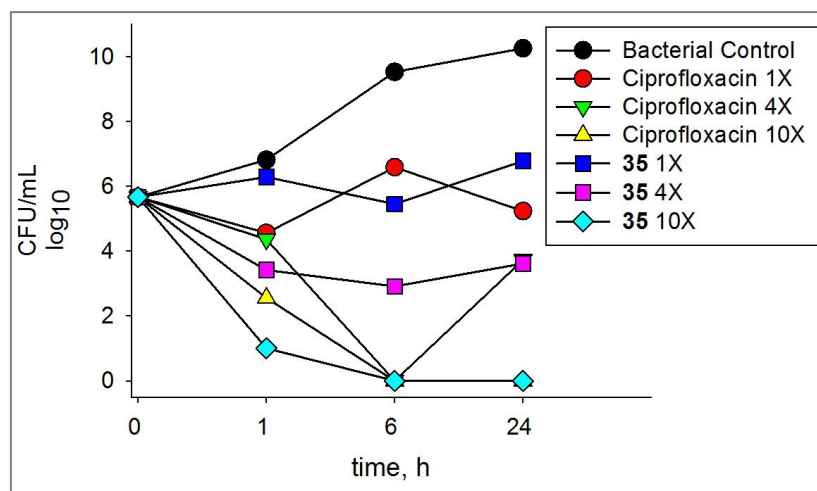
Figure 4.9. Time-kill curve for compound **35** for *E. coli*. Data provided by Dr. Sidharth Chopra from CDRI, Lucknow

4.2.11.1 NTR activated, specific theranostic prodrug approach for fluoroquinolones

Based on our antibacterial data for the aforementioned model compounds, we chose to modify ciprofloxacin into a therapeutic and fluorophore-containing prodrug for imaging in the proposed theranostic strategy (see proposed design, Figure 4.10). In order to synthesize the coumarin-based derivative, we started synthesis based on a report from Doron Shabat and co-workers.[25]
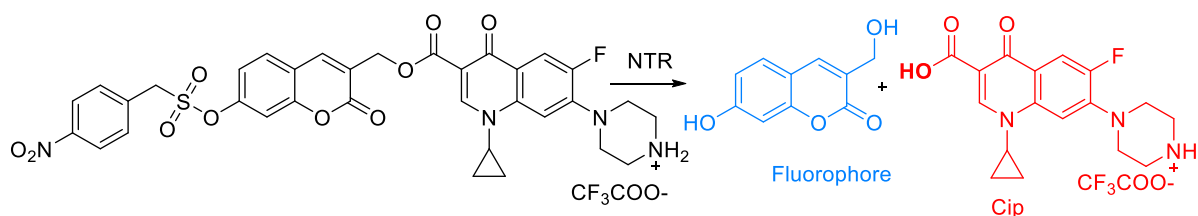
Figure 4.10. Proposed design for NTR specific theranostic prodrug

4.2.11.2 Synthesis of nitroreductase-specific, ciprofloxacin conjugated theranostic prodrug

In order to synthesize coumarin fluorophore intermediates, we synthesized molecules **37a**, **37b**, and **37c**, by reported protocols (Scheme 4.4.1).[17]

154
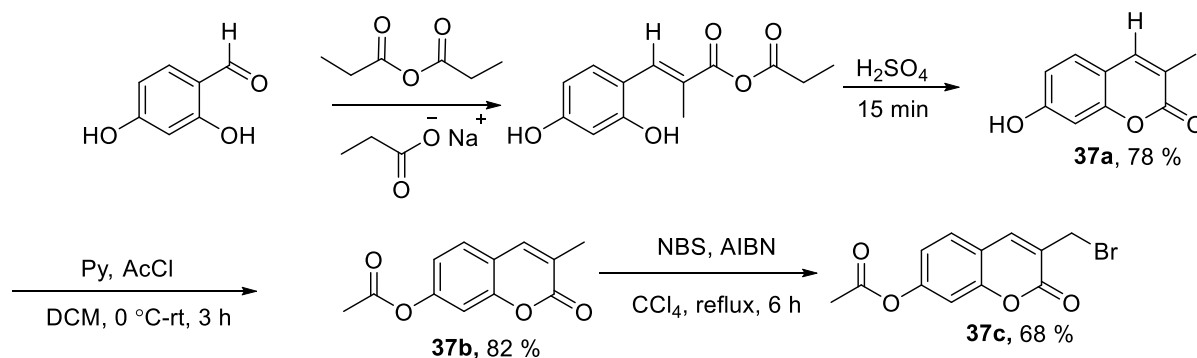
Scheme 4.4.1 Synthesis of 3-(bromomethyl)-2-oxo-2H-chromen-7-yl acetate **37c**

When we attempted to synthesize 7-hydroxy-3-(hydroxymethyl)-2H-chromen-2-one (UmbOH) from the hydrolysis reaction of **37c** with CaCO₃, we obtained unexpectedly **37d** as the major product (Scheme 4.4.2) in moderate yield. Next, we continued synthesis and utilized **37d** to our advantage with orthogonal protection and deprotection chemistry. **37d** was subjected to orthogonal protection with DHP to give the THP protected compound **37e** in good yield. The acetyl group of **37e** was deprotected with K₂CO₃ to afford **37f** in good yield. **37f** was further derivatized with a 4-nitrobenzyl sulfonyl chloride to give **37g** in a good yield. Finally, the THP-deprotection of **37g** was catalyzed by pyridinium *p*-toluene sulfonate (PPTS) in a protic solvent, to afford the final alcohol **38** (Scheme 4.4.2) in a good yield.
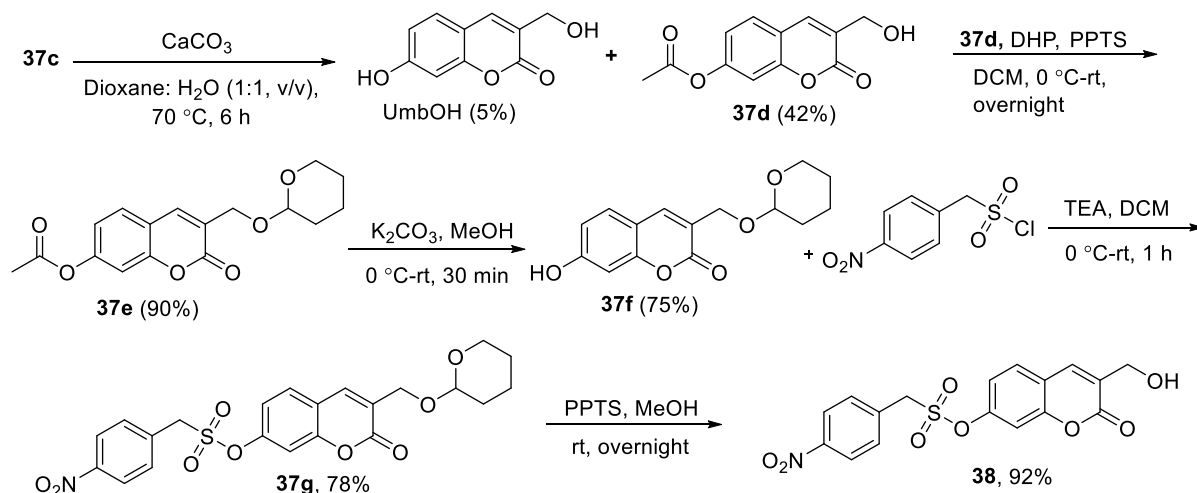
Scheme 4.4.2. Synthesis of coumarin alcohol (**38**)

The alcohol **38**, masked with a coumarin fluorophore, was derivatized with *t*-boc ciprofloxacin to give **39** (Scheme 4.4.3) in a good yield. Subsequent deprotection of **39** with TFA gave the final desired theranostic product **40** (Scheme 4.4.3).
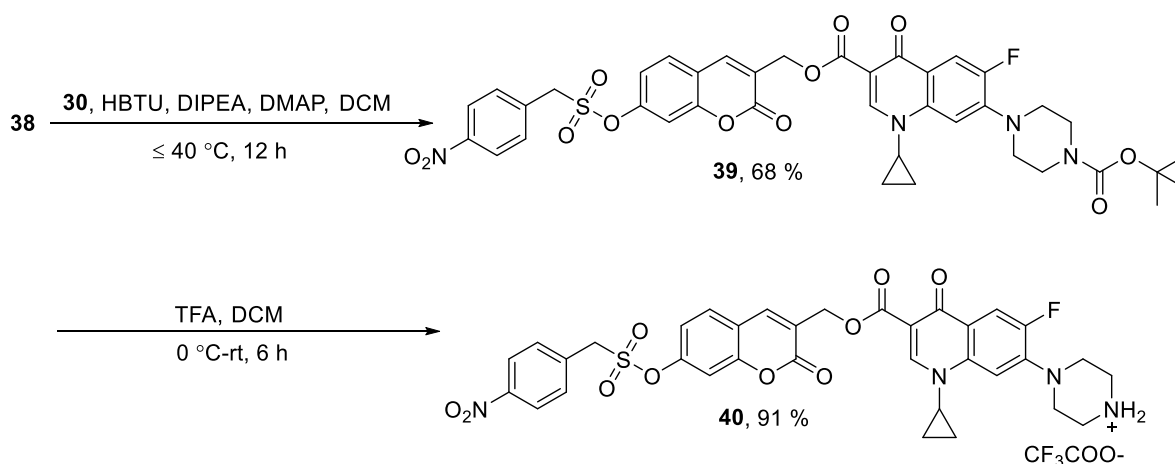
Scheme 4.4.3 Synthesis of nitroreductase-specific, ciprofloxacin conjugated theranostic agent.

4.2.12. Fluorescence measurement of compound 40

To evaluate the hypothesis that our synthesized theranostic agent **40** undergoes self-immolation on the reduction of the nitro group with NTR to generate a fluorophore, we proposed to assess the fluorescence of UmbOH from **40**, *via* fluorimetry. Compound **40** (10 µM) was reacted with NTR (10 µg/mL) along with NADH (30 µM) in PBS. The reaction mixture was monitored by fluorimetry after 30 min. which indicated the generation of UmbOH in a 42% yield.
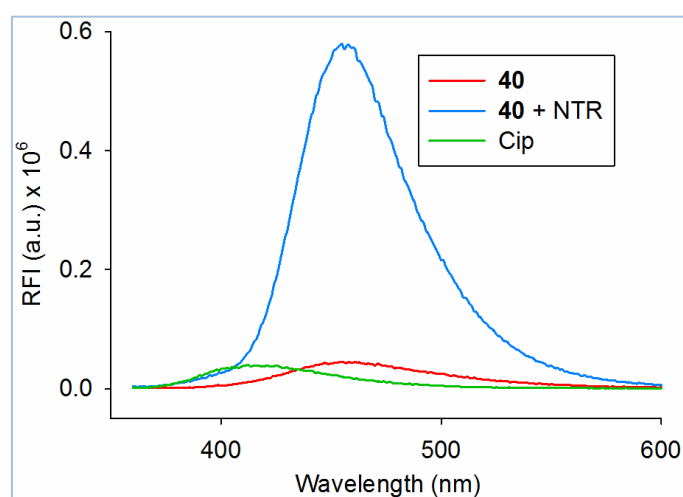
Figure 4.11. Monitoring the release of UmbOH by fluorimetry upon NTR activation of **40** (10 µg/mL) along with NADH (30 µM) in PBS (pH 7.4, 10 mM). Decomposition of **40** (10 µM) generated UmbOH in a 42% yield.

4.2.13. NTR reduction

Since we confirmed that our synthesized theranostic compound **40** undergoes self-immolation on the reduction of the nitro group with NTR to generate a fluorophore, we also proposed to assess both UmbOH and ciprofloxacin simultaneously. In order to evaluate that, compound **40** (25 µM) was reacted with NTR (20 µg/mL) along with NADH (75 µM) in PBS. Aliquots from the reaction mixture were monitored by HPLC. Analysis of the reaction mixture after 60 min revealed that 37% of compound **40** remained, with the concomitant formation of ciprofloxacin (53%) and the fluorophore UmbOH (30%). The yield of the compounds remained unchanged over prolonged incubation periods. We assume that for efficient activation of a prodrug, the aqueous solubility of the compound and catalytic efficiency of NTR would play an important role. Since NTR is widely distributed among several bacterial species, this may find wide applications across a spectrum of bacteria.
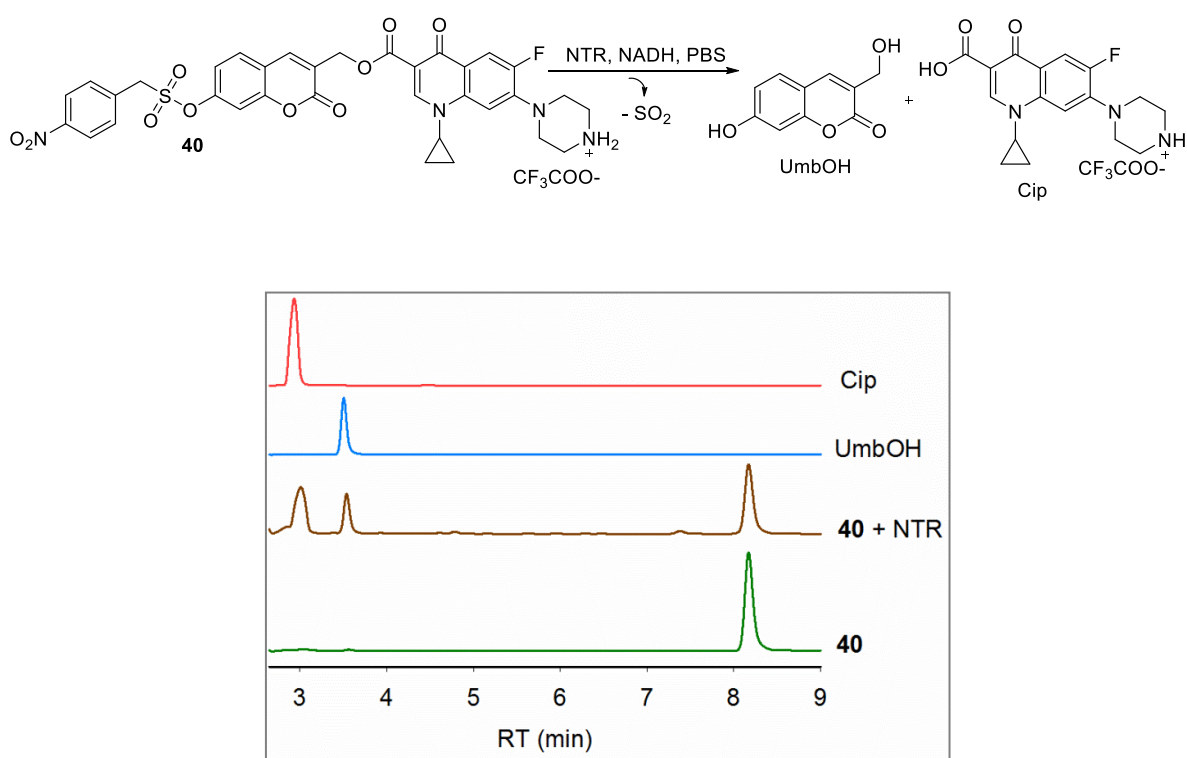
Figure 4.12. Monitoring the release of ciprofloxacin and UmbOH from **40** by HPLC on NTR (20 µg/mL) activation, along with NADH (75 µM) in PBS (pH 7.4, 10mM). Decomposition of **40** (25 µM) generated 53% ciprofloxacin and 30% UmbOH. Absorbance at 320 nm was monitored.

4.2.14. Stability of compounds in mammalian cell lysate

In order to test the stability of our nitroreductase-specific, fluoroquinolone-conjugated compounds in mammalian cellular conditions and for their nonspecific activation, Hela cell lysates were exposed to the fluorophore-conjugated compounds **24**, **35**, and **40**, with our esterase activated SO_2 donor **17a** as a reference compound (Figure 4.13). We found no significant fluorescence signal corresponding to fluorophore formation during 30 min. As nitroreductases are not normally present in mammalian cells, it is understandable that reduction of the nitro group is not efficient and does not generate the fluorophore. Taken together, our data support the selectivity, specificity and broad-range stability of a nitroreductase activated prodrug.
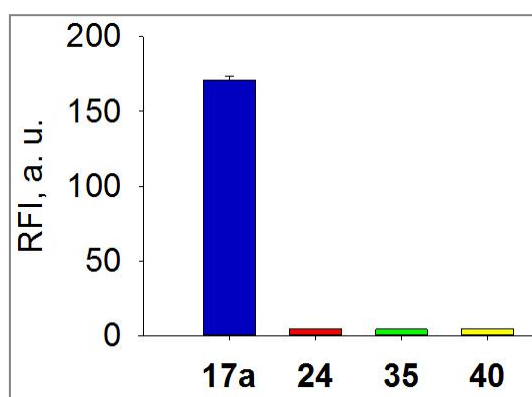
Figure 4.13. Monitoring the release of Umb and UmbOH fluorophores from differemt compounds (25 µM) in Hela cell lysate

4.2.15. Cell imaging of *E. coli* on the treatment of antibiotic conjugated prodrugs

In order to check the theranostic property of our compound **40** for undergoing activation in *E. coli* and to generate fluorophore-antibiotic inside bacteria, we incubated compound **40** with *E. coli* for 30 min. Imaging in the DAPI channel by confocal microscopy revealed significant fluorescence (Figure 4.2.15). This observation supports the ability of **40** to penetrate bacterial cells and to generate a fluorophore and an antibiotic. Similarly, treatment of compound **35** did not show any evidence of fluorescence, due to the absence of a fluorophore.
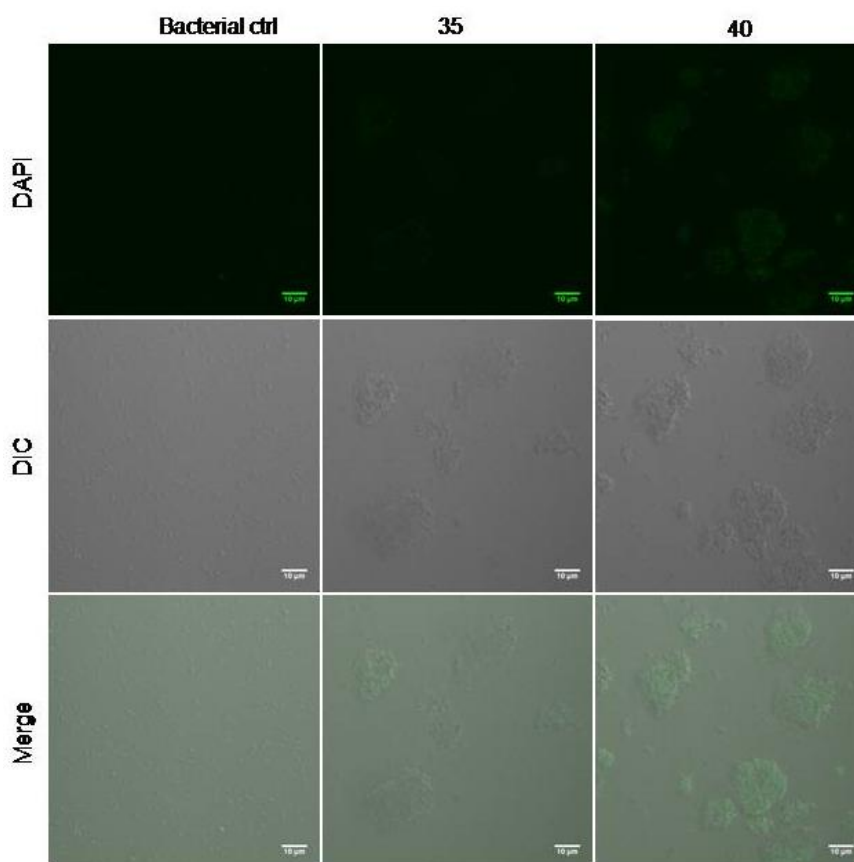
Figure 4.14. Confocal microscopy images of compound **40** (25 µM) when incubated for 30 min with *E. coli.*
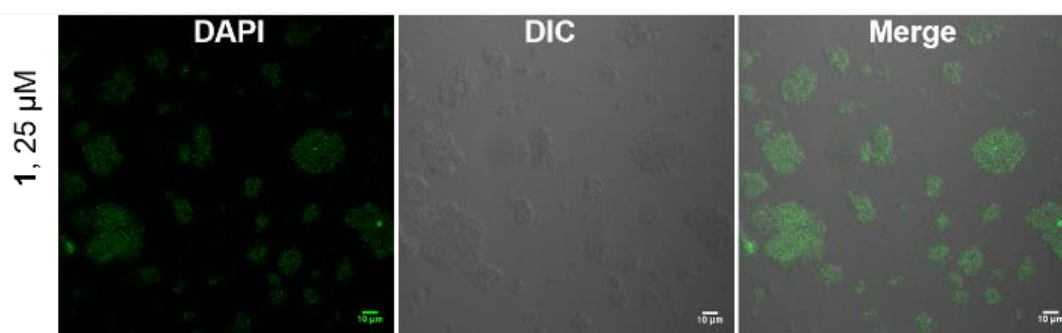
Figure 4.15. Magnified confocal microscopy images of compound **40** (25 µM) when incubated for 30 min with *E. coli* (reprocessed image)

Confocal images were provided by Govindan Ravikumar, IISER Pune.

4.2.15. Antibacterial activity of ciprofloxacin-conjugated theranostic drug

Having demonstrated the generation of ciprofloxacin and fluorophore together on NTR-specific activation, we proposed to check for antibacterial activity. Compound **38** as a control, and compound **40,** were tested for their antibacterial activity. Compounds **40** was found to be an excellent antibacterial agent against Gram-negative *E. coli* and *P. aeruginosa* bacteria (Table 4.2). Compound **38** was found to be inactive. The results were in accordance with our hypothesis of NTR-activation of the drug inside bacteria, which would lead its killing by the released antibiotic.

Table 4.2 Antibacterial activity of nitroreductase specific, ciprofloxacin conjugated theranostic prodrug

Compd	*E. coli* ATCC 25922	*S.aureus* ATCC 29213	*K.pneumoniae* BAA 1705	*A.baumannii* BAA 1605	*P. areginosa*
40	0.0625	4	>64	>64	4
38	>64	>64	>64	>64	>64
Levo	<0.03	0.125	64	8	0.5

Antibacterial activities are in µg/mL; data provided by Dr. Sidharth Chopra, from CDRI, Lucknow

4.2.17. Cytotoxicity

In order to estimate the toxicity of our theranostic compound **40**, we tested it against Vero cell line (a kidney epithelial cell line); we found no significant killing even at 40 fold concentration of the MIC value. This result indicates that compound **40** was well tolerated in mammalian cells.

4.3. Summary

In this chapter, we presented the design and synthesis of a novel class of nitroreductase stimulus-specific, fluoroquinolone conjugated prodrugs. In this approach, we synthesized theranostic prodrugs of ciprofloxacin as therapeutic coumarin-based fluorophores, to allow for real-time monitoring of drug release. Upon nitro reduction, the prodrugs undergo self-

immolation to produce the corresponding fluorophore and fluoroquinolones. Compound **40** was found to penetrate Gram-negative *E. coli* and was activated by NTR to generate a fluorophore and ciprofloxacin. We found excellent antibacterial activity for compound **40** when tested against *E. coli* (0.0625 µg/mL) and *P. aeruginosa* (4 µg/mL), which are difficult to treat. Compound **40** appeared to be well tolerated in mammalian cells when tested for cytotoxicity. Prototypical fluoroquinolones were also found to be good inhibitors of bacteria when tested against Gram-negative *E. coli* as well as Gram-positive *S. aureus*. These small molecule prodrugs, when tested for their stability and specificity to get activated in mammalian, *i.e.*, Hela cells, gave no evidence of decomposition, due to the absence of NTR in mammalian cells. This method is advantageous as it offers a completely new class of prodrug molecules, with the stability of sulfonate linkers and the specificity of NTR as an enzymatic trigger. The theranostic approach allows real time monitoring of drug release.

4.4. Experimental section

4.4.1 Synthesis and characterization

Compounds **30**, **31**, **37a**, **37b**, **37c** have been previously reported and analytical data that we have collected were consistent with reported values.

2-oxo-2H-chromen-7-yl (4-nitrophenyl)methanesulfonate (24)
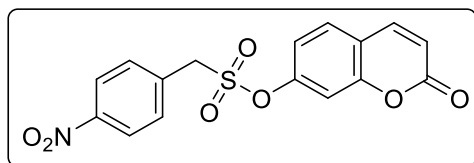
Umbelliferone (82 mg, 0.51 mmol) and pyridine (66 µL, 0.84 mmol) were dissolved in DCM (25 mL). To this, a solution of 4-nitrobenzyl sulfonyl chloride (100 mg, 0.42 mmol) in DCM (1 mL) was added dropwise at 0 °C under nitrogen atmosphere. The resulting reaction mixture was stirred for 1 h at rt and was further diluted with dI water (100 mL). The aqueous layer was extracted with DCM (3 × 25 mL). The combined organic layers were collected, dried over Na_2SO_4 and evaporated under reduced pressure. The residue was purified over silica gel column (hexane/EtOAc). The compound **24** (90 mg, 55%) was isolated as a colorless solid; ^{1}H NMR (400 MHz, DMSO-d_6): δ 8.31 (d, *J* = 8.8 Hz, 2H), 8.10 (d, *J* = 9.6 Hz, 1H), 7.84 (d, *J* = 8.6 Hz, 1H), 7.80 (d, *J* = 8.8 Hz, 2H), 7.41 (d, *J* = 2.3 Hz, 1H), 7.27 (dd, *J* = 8.8, 2.4 Hz, 1H), 6.54 (d, *J* = 9.6 Hz, 1H), 5.33 (s, 2H); ^{13}C NMR (100 MHz, DMSO-d_6): δ 159.5, 154.1, 150.6, 147.9, 143.6, 135.4, 132.5, 130.0, 123.8, 118.6, 117.9, 116.4, 110.3, 55.3; FTIR (v_{max}, cm^{-1}): 1109, 1345, 1513, 1603, 1728; HRMS (ESI) calcd for $C_{16}H_{11}NO_7S$ [M+H]$^+$: 362.0334; found: 362.0336.

7-((4-nitrobenzyl)oxy)-2H-chromen-2-one (25)
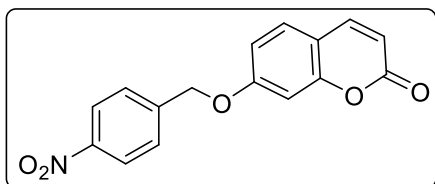
K_2CO_3 (767 mg, 5.55 mmol) was added to a solution of Umbelliferone (300 mg, 1.85 mmol) in dry DMF and stirred for 10 min under a nitrogen atmosphere at rt. To this, solution 4-ntrobenzyl bromide (600 mg, 2.78 mmol) was added and was stirred for 6 h. The reaction mixture was diluted with dI water (100 mL). The aqueous layer was extracted with EtOAc (3×35 mL). The combined organic layers were collected, dried over Na_2SO_4 and evaporated under reduced pressure. The residue was purified over silica gel column (hexane/EtOAc). The compound **25** (337 mg, 61%) was isolated as a colorless solid; ^{1}H NMR (400 MHz, DMSO-d_6): δ 8.27 (d, J = 8.6 Hz, 2H), 7.99 (d, J = 9.4 Hz, 1H), 7.74 (d, J = 8.6 Hz, 2H), 7.66 (d, J = 8.5 Hz, 1H), 7.10 (d, J = 2.1 Hz, 1H), 7.06 (dd, J = 8.6, 2.3 Hz, 1H), 6.31 (d, J = 9.4 Hz, 1H), 5.40 (s, 2H); ^{13}C (100 MHz, DMSO-d_6): δ 161.0, 160.2, 155.3, 147.1, 144.2, 144.1, 129.6, 128.4, 123.7, 112.9, 112.9, 112.8, 101.8, 68.6; FT-IR (ν_{max}, cm^{-1}): 1728, 1614, 1516, 1346, 1127; HRMS (ESI) calcd for $C_{16}H_{11}NO_5$ [M+H]$^+$: 298.0715; found: 298.0685.

naphthalen-1-yl (4-nitrophenyl)methanesulfonate (26)
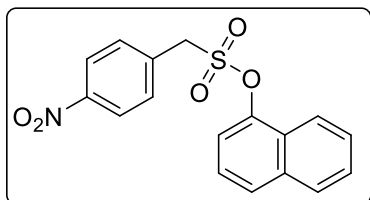
1-naphthol (92 mg, 0.64 mmol) and pyridine (50 µL, 0.64 mmol) were dissolved in DCM (25 mL). To this, a solution of 4-nitrobenzyl sulfonyl chloride (125 mg, 0.53 mmol) in DCM (1 mL) was added dropwise at 0 °C under nitrogen atmosphere. The resulting reaction mixture was stirred for 1 h at rt and was further diluted with dI water (100 mL). The aqueous layer was extracted with DCM (3×25 mL). The combined organic layers were collected, dried over Na_2SO_4 and evaporated under reduced pressure. The residue was purified over silica gel column (hexane/EtOAc). Compound **26** (113 mg, 62%) was isolated as a colorless solid; ^{1}H NMR (400 MHz, DMSO-d_6): δ 8.34 (d, J = 8.8 Hz, 2H), 8.03-8.01 (m, 1H), 7.95-7.92 (m, 2H), 7.88 (d, J = 8.8 Hz, 2H), 7.64-7.54 (m, 3H), 7.44 (dd, J = 7.6, 0.9 Hz, 1H), 5.45 (s, 2H); ^{13}C NMR (100 MHz, DMSO-d_6): 147.8, 144.4, 135.7, 134.3, 132.5, 127.9, 127.22, 127.17, 127.0, 126.8, 125.7, 123.7, 121.3, 118.5, 55.5; FTIR (ν_{max}, cm^{-1}): 1168, 1214, 1337, 1518; HRMS (ESI) calcd for $C_{17}H_{13}NO_5S$ [M+Na]$^+$: 366.0411; found: 366.0410.

naphthalen-1-yl (4-nitrobenzyl) carbonate (27)
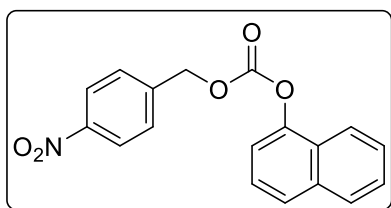
A solution of 4-nitrobenzyl chloroformate (300 mg, 1.40 mmol) in THF (1mL) was added dropwise to a solution of 1-naphthol (240 mg, 1.67 mmol), TEA (232 µL, 1.67 mmol) and DMAP (17 mg, 0.14 mmol) in THF (25 mL) at 0 °C under nitrogen atmosphere. The resulting reaction mixture was stirred at rt for 3 h. Solvent was evaporated from reaction mixture at < 10 °C and the residue obtained was purified over silica gel column (hexane/EtOAc). Compound **27** (110 mg, 25%) was isolated as colorless solid; ^{1}H NMR (CDCl$_3$): δ 8.28 (d, J = 8.7 Hz, 2H), 7.95-7.87 (m, 2H), 7.78 (d, J = 8.3 Hz, 1H), 7.63 (d, J = 8.8 Hz, 2H), 7.56-7.52 (m, 2H), 7.50-7.46 (m, 1H), 7.36-7.34 (m, 1H), 5.42 (s, 2H); ^{13}C NMR (100 MHz, CDCl$_3$): 153.6, 148.2, 146.9, 141.9, 134.8, 128.8, 128.2, 126.9, 126.8, 126.7, 126.6, 125.5, 124.1, 120.9, 117.6, 68.9; FTIR (ν_{max}, cm^{-1}):1217, 1516, 1744; HRMS (ESI) calcd for C$_{18}$H$_{13}$NO$_5$ [M+Na]$^+$: 346.0692; found: 346.0692.

4-formylphenyl (4-nitrophenyl)methanesulfonate (28)
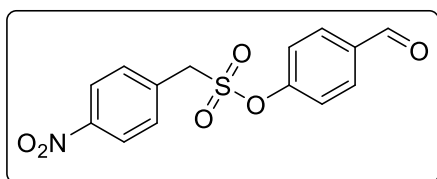
4-hydroxy benzaldehyde (1.14 g, 9.34 mmol) and TEA (2.96 mL, 21.22 mmol) were dissolved in DCM (50 mL). To this, a solution of 4-nitrobenzyl sulfonyl chloride (2.00 g, 8.49 mmol) in DCM (5 mL) was added dropwise at 0 °C under nitrogen atmosphere and was stirred for 1 h at rt. The reaction mixture was diluted with dI water (100 mL) and sat. NaCl (25 mL). The aqueous layer was extracted with DCM (3 × 50 mL). The combined organic layers were collected, dried over Na$_2$SO$_4$ and evaporated under reduced pressure. The residue was purified over silica gel column (hexane/EtOAc). Compound **28** (2.24 g, 82%) was isolated as a colorless solid; ^{1}H NMR (400 MHz, CDCl$_3$): δ 10.01 (s, 1H), 8.31 (d, J = 8.7 Hz, 2H), 7.93 (d, J = 8.8 Hz, 2H), 7.68 (d, J = 8.8 Hz, 2H), 7.33 (d, J = 8.6 Hz, 2H), 4.68 (s, 2H);^{13}C NMR (100 MHz, CDCl$_3$): δ 190.4, 153.0, 148.8, 135.3, 134.0, 132.0, 131.7, 124.3, 122.6, 56.7; FTIR (ν_{max}, cm^{-1}): 1145, 1203, 1352, 1523, 1596, 1702; HRMS (ESI) calcd for C$_{14}$H$_{11}$NO$_6$S [M + H]$^+$: 322.0385; found: 322.0359.

4-(hydroxymethyl)phenyl (4-nitrophenyl)methanesulfonate (29)
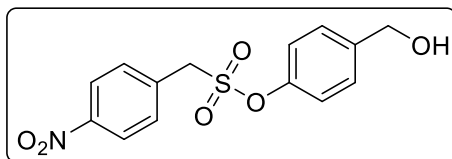
Sodium borohydride (377 mg, 9.96 mmol) was added in portions to an ice-cold solution of **28** (1.60 g, 4.98 mmol) in methanol (50 mL) and stirred for 1 h at rt. The reaction mixture was quenched by careful addition of sat. aq. NH$_4$Cl (30 mL). Methanol was removed under reduced pressure from the reaction mixture. The resulting aqueous solution was extracted with EtOAc (3 x 30 mL) and the combined organic layers were washed with brine (25 mL), dried over Na$_2$SO$_4$, filtered and concentrated under reduced pressure. The residue was purified over silica gel column (hexane/EtOAc). Compound **29** (1.17 g, 73%) was isolated as a colorless solid; ^{1}H NMR (400 MHz, CDCl$_3$): δ 8.28 (d, J = 8.6 Hz, 2H), 7.65 (d, J = 8.6 Hz, 2H), 7.39 (d, J = 8.4 Hz, 2H), 7.15 (d, J = 8.5 Hz, 2H), 4.70 (s, 2H), 4.60 (s, 2H), 1.86 (s, 1H); ^{13}C NMR (100 MHz, CDCl$_3$): δ 148.6, 148.1, 140.5, 134.4, 132.0, 128.6, 124.2, 122.0, 64.4, 56.0; FTIR (ν$_{max}$, cm^{-1}):1144, 1202, 1351, 1520, 1604; HRMS (ESI) calcd for C$_{14}$H$_{13}$NO$_6$S [M + Na]$^+$:346.0361; found: 346.0343.

4-(((4-nitrobenzyl)sulfonyl)oxy)benzyl7-(4-(tert-butoxycarbonyl)piperazin-1-yl)-1-cyclo cyclopropyl-6-fluoro-4-oxo-1,4-dihydroquinoline-3-carboxylate (32)
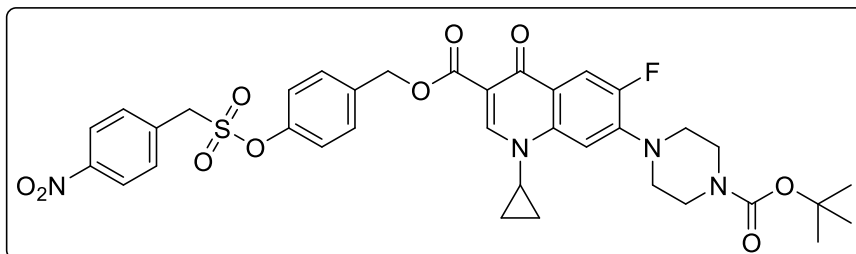
Compound **30** (300 mg, 0.70 mmol), HBTU (1056 mg, 2.78 mmol) and DMAP (34 mg, 0.28 mmol) was dissolved in 100 mL dry DCM before addition of DIPEA (485 µL, 2.78 mmol) and stirred at rt under nitrogen atmosphere for 30 min. To the reaction mixture, alcohol **29** (150 mg, 0.46 mmol) was added and stirred at < 40 °C for 12 h. Further, an aqueous work up was performed by adding dI water (100 mL) and DCM (2 x 30 mL). Collected organic layers were dried over Na$_2$SO$_4$, concentrated under vacuum. Prep HPLC was performed for purification of the compound using H$_2$O/ACN as the mobile phase to obtain **32** (263 mg, 84%) as a pale yellow solid; ^{1}H NMR (400 MHz, CDCl$_3$): δ 8.54 (s, 1H), 8.27 (d, J = 8.4 Hz, 2H), 8.06 (d, J = 13.0 Hz, 1H), 7.65 (d, J = 8.6 Hz, 2H), 7.58 (d, J = 8.4 Hz, 2H), 7.28 (br, 1H), 7.19 (d, J = 8.5 Hz, 2H), 5.38 (s, 2H), 4.59 (s, 2H), 3.65 (t, J = 4.4 Hz, 4H), 3.45-3.40 (m, 1H), 3.22 (t, J = 4.5 Hz, 4H), 1.50 (s, 9H), 1.35-1.30 (m, 2H), 1.15-1.10 (m, 2H); ^{13}C NMR (100 MHz, CDCl$_3$):δ 173.1, 165.8, 154.7, 152.3, 148.7, 148.4, 144.6 (d), 138.1, 136.2, 134.4, 132.0, 129.7, 124.2,

123.4 (d), 122.0, 113.5 (d), 109.9, 105.2 (d), 80.3, 77.4, 65.4, 55.8, 50.0, 34.7, 28.5, 8.3; FTIR (ν_{max}, cm^{-1}): 1164, 1249, 1356, 1495, 1622, 1695; HRMS (ESI) calcd for $C_{36}H_{37}FN_4O_{10}S$ [M+H]$^+$: 737.2292; found: 737.2275.

4-(((4-nitrobenzyl)sulfonyl)oxy)benzyl7-(4-(tert-butoxycarbonyl)piperazin-1-yl)-1-ethyl-6-fluoro-4-oxo-1,4-dihydroquinoline-3-carboxylate (33)
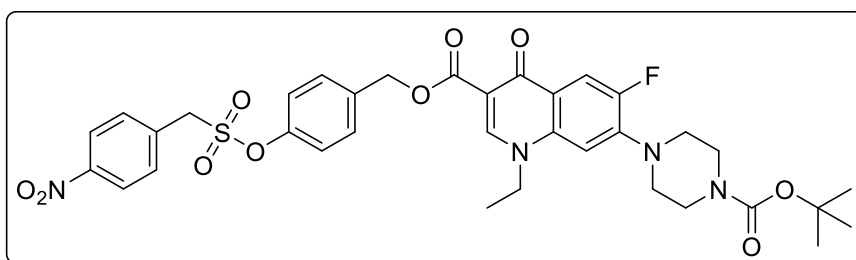
Compound **31** (292 mg, 0.70 mmol), HBTU (1056 mg, 2.78 mmol) and DMAP (34 mg, 0.28 mmol) was dissolved in 100 mL dry DCM before addition of DIPEA (485 µL, 2.78 mmol) and stirred at rt under nitrogen atmosphere for 30 min. To the reaction mixture, alcohol **29** (150 mg, 0.46 mmol) was added and stirred at < 40 °C for 12 h. Further, an aqueous work up was performed by adding DCM (2 x 30 mL). Collected organic layers were dried over Na$_2$SO$_4$, concentrated under vacuum. Prep HPLC was used for purification of compound using H$_2$O/ACN as the mobile phase to obtain **33** (254 mg, 76%) as a pale yellow solid; ^{1}H NMR (400 MHz, CDCl$_3$): δ 8.44 (s, 1H), 8.28 (d, *J* = 8.6 Hz, 2H), 8.10 (dd, *J* = 13.1, 1.8 Hz, 1H), 7.65 (d, *J* = 8.6 Hz, 2H), 7.59 (d, *J* = 8.5 Hz, 2H), 7.19 (d, *J* = 8.6 Hz, 2H), 6.75 (d, *J* = 6.8 Hz, 1H), 5.38 (s, 2H), 4.60 (s, 2H), 4.20 (qt, *J* = 7.2 Hz, 2H), 3.65 (t, *J* = 4.8 Hz, 4H), 3.20 (t, *J* = 4.8 Hz, 4H), 1.54 (t, *J* = 7.2 Hz, 3H), 1.49 (s, 9H); ^{13}C NMR (100 MHz, CDCl$_3$): δ 173.0 (d), 165.8, 154.6, 154.5, 152.0, 148.5 (d), 148.4, 144.8 (d), 136.13, 136.09 (d), 134.3, 131.9, 129.6, 124.1, 121.9, 114.0 (d), 110.0, 104.1 (d), 80.2, 77.2, 65.3, 55.8, 50.0, 49.1, 28.4, 14.4; FTIR (ν_{max}, cm^{-1}): 1216, 1370, 1498, 1528, 1738; HRMS (ESI) calcd for $C_{35}H_{37}FN_4O_{10}S$ [M+H]$^+$: 725.2292; found: 725.2294.

4-(((4-nitrobenzyl)sulfonyl)oxy)benzyl 9-fluoro-3-methyl-10-(4-methylpiperazin-1-yl)-7-oxo-2,3-dihydro-7H-[1,4]oxazino[2,3,4-ij]quinoline-6-carboxylate (34)

Compound Levo (251 mg, 0.70 mmol), HBTU (1056 mg, 2.78 mmol) and DMAP (34 mg,
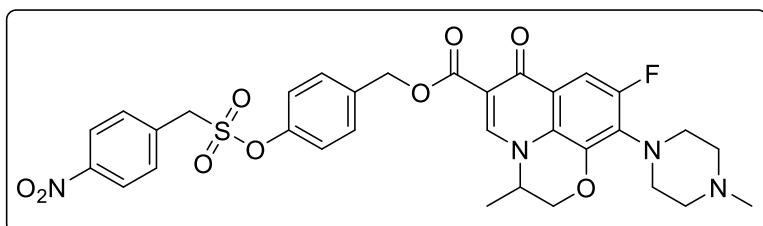
0.28 mmol) were dissolved in 100 mL dry DCM before addition of DIPEA (485 µL, 2.78 mmol) and stirred at rt

under nitrogen atmosphere for 30 min. To the reaction mixture, alcohol **29** (150 mg, 0.46 mmol) was added and stirred at < 40 °C for 12 h. Further, an aqueous work up was performed by adding DCM (2 x 30 mL). Collected organic layers were dried over Na_2SO_4, concentrated under vacuum. Prep HPLC was used for purification of compound using H_2O/ACN as the mobile phase to obtain **34** (120 mg, 39%) as a pale yellow solid; ^1H NMR (400 MHz, $CDCl_3$): δ 8.22 (d, J = 8.8 Hz, 2H), 8.17 (s, 1H), 7.62 (d, J = 8.7 Hz, 2H), 7.52 (d, J = 8.6 Hz, 2H), 7.45 (d, J = 12.5 Hz, 1H), 7.15 (d, J = 8.6 Hz, 2H), 5.29 (d, J = 0.8 Hz, 2H), 4.59 (s, 2H), 4.39-4.28 (m, 2H), 4.19 (qt, J = 6.8 Hz, 2H), 3.36-3.27 (m, 4H), 2.53 (br, 4H), 2.34 (s, 3H), 1.44 (d, J = 6.8 Hz, 3H); ^{13}C NMR (100 MHz, $CDCl_3$): δ 172.7 (d), 165.5, 156.9, 154.5, 148.4, 145.5, 139.6 (d), 136.1, 134.3, 132.0, 131.8 (d), 129.8, 124.1, 123.7, 123.3 (d), 122.1, 109.0, 105.4 (d), 68.1, 65.3, 55.9, 55.7, 54.9, 50.5 (d), 46.4, 18.2; FTIR (v_{max}, cm^{-1}): 1213, 1370, 1448, 1535, 1736; HRMS (ESI) calcd for $C_{32}H_{31}FN_4O_9S$ $[M+H]^+$: 667.1874; found: 667.1869.

TFA salt of 4-(((4-nitrobenzyl)sulfonyl)oxy)benzyl 1-cyclopropyl-6-fluoro-4-oxo-7-(4l4-piperazin-1-yl)-1,4-dihydroquinoline-3-carboxylate (35)
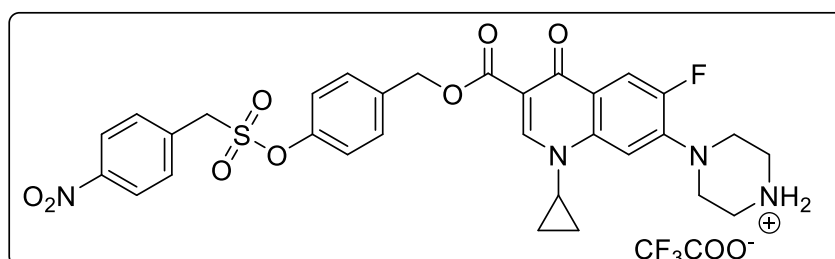
TFA (2.00 mL, 27.15 mmol) was added dropwise to a solution of **32** (100 mg, 0.14 mmol) dissolved in DCM (20 mL) at 0 °C under nitrogen atmosphere. The resulting reaction mixture was stirred for 6 h at rt. After complete disappearance of starting material by TLC (6 h) the solvent was removed under vacuum at < 20 °C. The product was precipitated by diethyl ether on sonication. The obtained white solid was washed by adding diethyl ether and its careful decantation, finally dried under vaccum. The compound **35** (95 mg, 93%) was isolated as a colorless solid; ^1H NMR (500 MHz, DMSO-d_6): δ 8.99 (s, 2H), 8.50 (s, 1H), 8.30 (d, J = 8.7 Hz, 2H), 7.84-7.79 (m, 3H), 7.60 (d, J = 8.5 Hz, 2H), 7.49 (d, J = 7.3 Hz, 1H), 7.29 (d, J = 8.5 Hz, 2H), 5.30 (s, 2H), 5.24 (s, 2H), 3.71-3.66 (m, 1H), 3.46 (br, 4H), 3.35 (br, 4H), 1.28-1.24 (m, 2H), 1.11(br, 2H); ^{13}C NMR (100 MHz, DMSO-d_6): δ 171.6 (d), 164.5, 153.7, 151.3, 148.7, 148.2, 147.7, 142.8 (d), 138.0, 136.0, 135.7, 132.4, 129.3, 123.7, 122.6 (d), 122.0, 111.9 (d), 108.8, 106.8

(d), 64.5, 55.1, 46.6, 42.7, 34.9, 7.6; FTIR (ν_{max}, cm^{-1}): 1147, 1181, 1268, 1354, 1497, 1623, 1721; HRMS (ESI) calcd for $C_{31}H_{32}FN_4O_8S$ [M]$^+$: 639.1919; found: 639.1829.

TFA salt of 4-((((4-nitrobenzyl)sulfonyl)oxy)benzyl 1-ethyl-6-fluoro-4-oxo-7-(4l4-piperazin-1-yl)-1,4-dihydroquinoline-3-carboxylate (36)
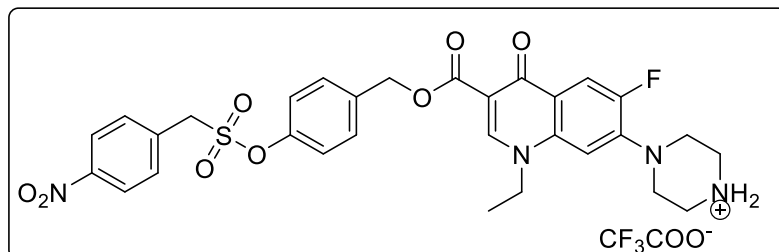
TFA (2.11 mL, 27.60 mmol) was added dropwise to a solution of **33** (100 mg, 0.14 mmol) dissolved in DCM (20 mL) at 0 °C under nitrogen atmosphere. The resulting reaction mixture was stirred for 6 h at rt. After complete disappearance of starting material by TLC (6 h) the solvent was removed under vacuum at < 20 °C. The product was precipitated by diethyl ether on sonication. The obtained white solid was washed by adding diethyl ether and careful decantation, finally dried under vaccum. Compound **36** (87 mg, 85%) was isolated as a colorless solid; ^{1}H NMR (400 MHz, DMSO-d_6): δ = 8.91 (s, 2H), 8.71 (s, 1H), 8.31 (d, J = 8.8 Hz, 2H), 7.87 (d, J = 13.2 Hz, 1H), 7.80 (d, J = 8.7 Hz, 2H), 7.61 (d, J = 8.6 Hz, 2H), 7.29 (d, J = 8.6 Hz, 2H), 7.14 (d, J = 7.2 Hz, 1H), 5.30 (s, 2H), 5.24 (s, 2H), 4.46 (qt, J = 6.9 Hz, 2H), 3.46 (br, 4H), 3.32 (br, 4H), 1.38 (t, J = 7.1 Hz, 3H); ^{13}C NMR (100 MHz, DMSO-d_6): δ = 171.7, 164.8, 153.7, 151.2, 149.8, 148.3, 147.9, 143.2 (d), 136.3, 136.1, 135.8, 132.5, 129.5, 123.8, 123.4, 122.1, 112.3 (d), 109.1, 106.5, 64.5, 55.2, 48.3, 46.8, 42.9, 14.4; FTIR (ν_{max}, cm^{-1}): 1144, 1179, 1266, 1354, 1494, 1620, 1716; HRMS (ESI) calcd for $C_{30}H_{30}FN_4O_8S$ [M]$^+$: 625.1763; found: 625.1763.

3-(hydroxymethyl)-2-oxo-2H-chromen-7-yl acetate (37d)
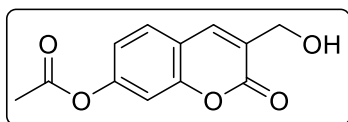
CaCO$_3$ (2.43 g, 24.23 mmol) was added to a solution of **37c** (1.20 g, 4.04 mmol) in 100 mL of water: dioxane (1:1, v/v) system and was heated at 70 °C for 6 h. Dioxane was evaporated from the resulting reaction mixture. The aqueous layer was extracted with EtOAc (3 × 50 mL) washed with sat. NaCl (25 mL). The collected organic layers were combined, dried over Na$_2$SO$_4$ and evaporated under reduced pressure. The residue was purified over silica gel column (hexane/EtOAc). The compound **37d** (0.39 g, 42%) was isolated as a pale yellow solid; ^{1}H NMR (400 MHz, CDCl$_3$): δ 7.74 (s, 1H), 7.50 (d, J = 8.4 Hz, 1H), 7.13 (d, J = 2.0 Hz, 1H), 7.06 (dd, J = 8.4, 2.0 Hz, 1H), 4.61 (s, 2H), 2.51 (br, 1H), 2.34 (s, 3H); ^{13}C

NMR (100 MHz, CDCl$_3$): δ 168.9, 161.0, 153.8, 152.8, 138.1, 128.7, 127.5, 118.8, 117.0, 110.3, 61.0, 21.3; FTIR (ν$_{max}$, cm^{-1}): 1207, 1373, 1439, 1541, 1652, 1717; HRMS (ESI) calcd for C$_{12}$H$_{10}$O$_5$ [M+Na]$^+$: 257.0420; found: 257.0424

2-oxo-3-(((tetrahydro-2H-pyran-2-yl)oxy)methyl)-2H-chromen-7-yl acetate (37e)
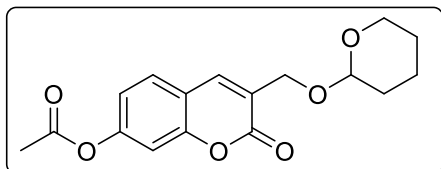
37d (300 mg, 1.28 mmol) and PPTS (97 mg, 0.32 mmol) were dissolved in DCM (30 mL). 3,4-Dihydro-2H-pyran (326 µL, 3.84 mmol) was added and the reaction mixture was stirred overnight at rt under nitrogen atmosphere. The reaction mixture was diluted with dI water (50 mL) and the aqueous layer was extracted with DCM (3 × 25 mL). The collected organic layers were combined, dried over Na$_2$SO$_4$ and evaporated under reduced pressure. The residue was purified over silica gel column (hexane/EtOAc). The compound **37e** (367 mg, 90%) was isolated as a colorless solid; ^{1}H NMR (400 MHz, CDCl$_3$): δ 7.79 (s, 1H), 7.51 (d, J = 8.4 Hz, 1H), 7.12 (d, J = 2.0 Hz, 1H), 7.05 (dd, J = 8.4, 2.0 Hz, 1H), 4.77 (t, J = 3.5 Hz, 1H), 4.74-4.70 (m, 1H), 4.48-4.44 (m, 1H), 3.93-3.87 (m, 1H), 3.59-3.54 (m, 1H), 2.33 (s, 3H), 1.95-1.51 (m, 6H); ^{13}C NMR (100 MHz, CDCl$_3$): 168.9, 160.2, 153.8, 152.6, 137.9, 128.5, 125.9, 118.5, 117.2, 110.2, 99.1, 64.0, 62.7, 30.6, 25.4, 21.3, 19.7; FTIR (ν$_{max}$, cm^{-1}): 1026, 1132, 1205, 1714, 1754; HRMS (ESI) calcd for C$_{17}$H$_{18}$O$_6$ [M + Na]$^+$: 341.1001; found: 341.1001.

7-hydroxy-3-(((tetrahydro-2H-pyran-2-yl)oxy)methyl)-2H-chromen-2-one (37f)
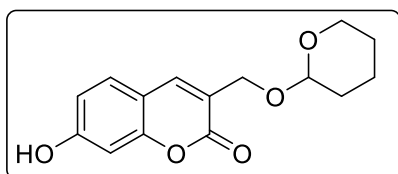
To a solution of **37f** (350 mg, 1.10 mmol) in MeOH (30 mL), K$_2$CO$_3$ (380 mg, 2.75 mmol) was added at 0 °C under nitrogen atmosphere and stirred for 30 min at rt. MeOH was evaporated under reduced pressure from the reaction mixture and was diluted with dI water (30 mL). The aqueous layer was extracted with DCM (3 × 50 mL) and washed with sat. NaCl (30 mL). The combined organic layers were collected, dried over Na$_2$SO$_4$ and evaporated under reduced pressure. It was used in next step without further purification. The compound **37f** (290 mg, 95%) was isolated as a colorless solid; ^{1}H NMR (400 MHz, CDCl$_3$): δ 10.51 (s, 1H), 7.89 (s, 1H), 7.57 (d, J = 8.5 Hz, 1H), 7.05 (dd, J = 8.5, 2.3 Hz, 1H), 6.72 (d, J = 2.2 Hz, 1H), 4.72 (t, J = 3.6 Hz, 1H), 4.47 (dd, J = 13.6, 1.1 Hz, 1H), 4.28 (dd, J = 13.6, 1.0 Hz, 1H); 3.82-3.76 (m, 1H), 3.50-3.44 (m, 1H), 1.81-1.43 (m, 6H); ^{13}C NMR (100 MHz, CDCl$_3$): 160.9, 160.2, 154.7, 140.1, 129.6, 120.5, 113.2, 111.3,

101.9, 97.7, 63.4, 61.3, 30.1, 25.0, 18.9; FTIR (ν_{max}, cm^{-1}): 1217, 1373, 1444, 1541, 1738; HRMS (ESI) calcd for $C_{16}H_{15}O_5$ [M + H]$^+$: 277.1076; found: 277.1079.

3-(hydroxymethyl)-2-oxo-2H-chromen-7-yl (4-nitrophenyl)methanesulfonate (38)
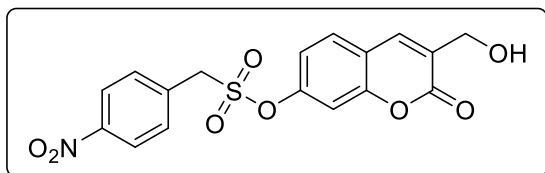
37f (250 mg, 0.90 mmol) and TEA (315 µL, 2.26 mmol) were dissolved in DCM (50 mL). To this solution of 4-nitrobenzyl sulfonyl chloride (256 mg, 1.09 mmol) in DCM (1 mL) was added dropwise at 0 °C under nitrogen atmosphere. The resulting reaction mixture was stirred for 1 h at rt and was further diluted with dI water (50 mL). The aqueous layer was extracted with DCM (3 × 30 mL) and washed with sat. NaCl (25 mL). The combined organic layers were collected, dried over Na$_2$SO$_4$ and evaporated under reduced pressure. It was used in next step without further purification. The product obtained was pale yellow solid THP protected intermediate, **37g** (337 mg, 78%). THP protected intermediate (300 mg, 0.63 mmol) and PPTS (40 mg, 0.16 mmol) were dissolved in MeOH (20 mL) and the reaction mixture was stirred overnight at rt. Methanol was evaporated under reduced pressure and the reaction mixture was diluted with dI water (50 mL). The aqueous layer was extracted with DCM (3 × 50 mL). The combined organic layers were collected, dried over Na$_2$SO$_4$ and evaporated under reduced pressure. It was used in next step without further purification. The compound **38** (227 mg, 92%) was isolated as a colorless solid; ^{1}H NMR (400 MHz, CDCl$_3$): δ 8.32 (d, J = 8.8 Hz, 2H), 8.01 (s, 1H), 7.90 (d, J = 8.6 Hz, 1H), 7.81 (d, J = 8.8 Hz, 2H), 7.41 (d, J = 2.3 Hz, 1H), 7.27 (dd, J = 8.5, 2.3 Hz, 1H), 5.53 (t, J = 5.5 Hz, 1H), 5.33 (s, 2H), 4.38 (dd, J = 5.4, 1.5 Hz, 2H); ^{13}C NMR (100 MHz, CDCl$_3$): δ 159.2, 152.8, 149.9, 147.9, 136.3, 135.4, 132.5, 129.6, 129.5, 123.8, 118.6, 118.3, 110.0, 58.2, 55.3; FTIR (ν_{max}, cm^{-1}): 1443, 1520, 1734; HRMS (ESI) calcd for $C_{17}H_{13}NO_8S$ [M + H]$^+$: 392.0440; found: 392.0444.

(7-(((4-nitrobenzyl)sulfonyl)oxy)-2-oxo-2H-chromen-3-yl)methyl 7-(4-(tert-butoxycarbonyl)piperazin-1-yl)-1-cyclopropyl-6-fluoro-4-oxo-1,4-dihydroquinoline-3-carboxylate (39)
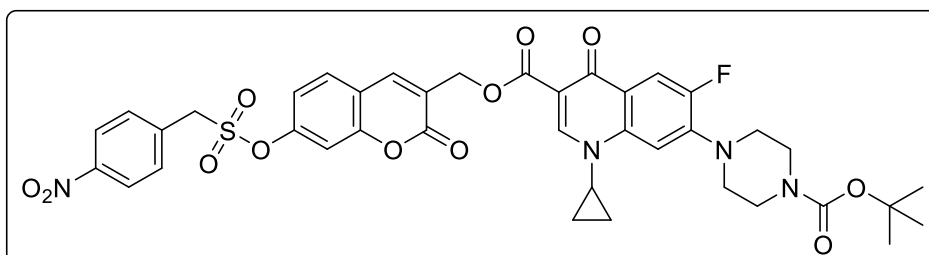
30 (165 mg, 0.38 mmol), HBTU (581 mg, 1.53 mmol) and DMAP

(19 mg, 0.15 mmol) was dissolved in 100 mL dry DCM before addition of DIPEA (267 µL, 1.53 mmol) and stirred at rt under nitrogen atmosphere for 30 min. To the reaction mixture, the alcohol **38** (100 mg, 0.26 mmol) was added and the reaction was stirred at < 40 °C for 12 h. 50 mL DCM was added, and an aqueous work up was performed. The organic phase was dried over Na_2SO_4, concentrated under vacuum. Prep HPLC was used for purification of compound using H_2O/ACN as the mobile phase. The compound **39** (129 mg, 68%) was isolated as a pale yellow solid; ^{1}H NMR (400 MHz, CDCl$_3$): δ 8.61(s, 1H), 8.33-8.29 (m, 3H), 8.07 (d, J = 13.1 Hz, 1H), 7.70- 7.65 (m, 3H), 7.30 (d, J = 7.0 Hz, 1H), 7.18 (d, J = 1.8 Hz, 1H), 7.11 (dd, J = 8.5, 2.1 Hz, 1H), 5.30 (s, 2H), 4.68 (s, 2H), 3.66 (t, J = 4.6 Hz, 4H), 3.47-3.43 (m, 1H), 3.24 (t, J = 4.8 Hz, 4H), 1.50 (s, 9H), 1.38-1.33 (m, 2H), 1.19-1.15 (m, 2H); ^{13}C NMR (100 MHz, CDCl$_3$): δ 173.3, 165.5, 159.5, 154.7, 154.3, 153.8, 153.7, 152.4, 150.3, 149.0, 148.7, 144.8, 139.3, 138.2, 133.9, 132.0, 129.9, 124.6, 124.3, 123.4, 118.5, 118.4, 113.6, 113.4, 110.4, 109.7, 105.2, 80.4, 77.4, 61.4, 56.5, 50.0, 34.7, 28.5, 8.4; FTIR (ν_{max}, cm^{-1}): 1045, 1243, 1373, 1620, 1737; HRMS (ESI) calcd for $C_{39}H_{37}FN_4O_{12}S$ [M+H]$^+$: 805.2191; found: 805.2172.

TFA salt of 4-(1-cyclopropyl-6-fluoro-3-(((7-(((4-nitrobenzyl)sulfonyl)oxy)-2-oxo-2H-chromen-3-yl)methoxy)carbonyl)-4-oxo-1,4-dihydroquinolin-7-yl)piperazin-1-ium (40)
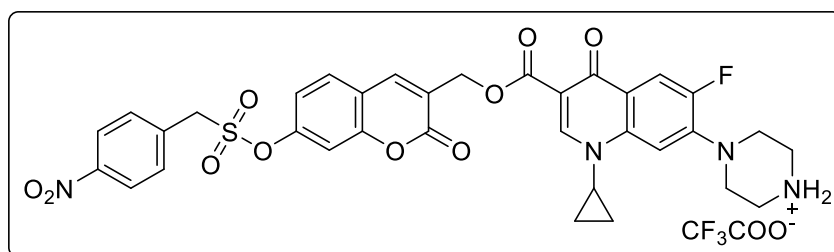
TFA (2.09 mL, 27.34 mmol) was added dropwise to a solution of **39** (110 mg, 0.14 mmol) dissolved in DCM (20 mL) at 0 °C under nitrogen atmosphere. The resulting reaction mixture was stirred for 6 h at rt. After complete disappearance of starting material by TLC, the solvent was removed under vacuum at < 20 °C. The product was precipitated by diethyl ether on sonication. The obtained white solid was washed by adding diethyl ether and its careful decantation, finally dried under vaccum. The compound **40** (102 mg, 91%) was isolated as a colorless solid; ^{1}H NMR (400 MHz, DMSO-d_6): δ 8.94 (s, 2H), 8.55 (s, 1H), 8.33-8.29 (m, 3H), 7.87 (d, J = 4.0 Hz, 1H), 7.84-7.80 (m, 3H), 7.50 (d, J = 7.4 Hz, 1H), 7.46 (d, J = 2.3 Hz, 1H), 7.30 (dd, J = 8.5, 2.4 Hz, 1H), 5.34 (s, 2H), 5.14 (s, 2H), 3.74-3.68 (m, 1H), 3.47-3.45 (m, 4H), 3.34 (br, 4H), 1.30-1.25 (m, 2H), 1.15-1.11 (m, 2H); ^{13}C NMR (100 MHz, DMSO-d_6): δ 171.5 (d), 163.9, 158.9, 153.6, 153.2, 151.2, 150.3, 148.8, 147.7, 142.7 (d), 139.4, 137.9, 135.2, 132.4, 129.9, 123.8, 123.7, 122.5 (d), 118.7, 117.7, 111.8 (d), 110.0, 108.4, 106.7, 60.6, 55.3, 46.4, 42.6,

34.9, 7.5; FTIR (ν_{max}, cm^{-1}): 1176, 1263, 1349, 1512, 1621, 1695; HRMS (ESI) calcd for C$_{34}$H$_{30}$FN$_4$O$_{10}$S [M]$^+$: 705.1661; found [M]$^+$: 705.1661.

4.4.2. General procedure for chemoreduction of compounds (24, 34, 35, 36) and monitoring of reactions by HPLC

5 mM Stock solutions of compounds **24**, **34**, **35** and **36** were prepared independently in DMSO. 15 mM stock solution of ammonium formate was prepared in water. Compounds to be analyzed (among **24**, or **34-36**) was added (5 µL, 25 µM) to the (1:1, v/v) Methanol: Water system (990 µL), to that ammonium formate (5 µL, 75 µM) and Zn (20 mg) were added. Reaction mixtures were incubated at 37 ºC on Eppendorf thermomixer comfort (800 rpm). Aliquots were taken periodically, centrifuged and injected (50 µL) in an HPLC attached with a diode-array detector (detection wavelength was 320 nm for **24** and 280 nm for **34-36**). The stationary phase used was C-18 reversed phase column (4.6 mm × 100 mm, 5 µm). The mobile phase used was 0.1% TFA in H$_2$O: ACN HPLC run time was 15 min with flow rate of 1 mL/min starting with 60:40 → 0-5 min, 50:50 → 5-10 min, 30:70→ 10-15 min, 60:40 and the reduction of the test compounds were analyzed using HPLC by monitoring disappearance of the peak for the test compound. It was observed that all the compounds were completely reduced within 30-60 min.

4.4.3. Detection of sulfite by from sulfonate 26, and control carbonate 27 with sulfite dye 22 on NTR activation by photometry

Stock solutions of compound **26** (5 mM)**, 27** (5 mM) and sulfite dye **22** (1 mM) were prepared in ACN independently. A stock solution of *E. Coli* nitroreductase, NTR (1 µg /1 µL) was prepared in PBS (pH 7.0, 10mM). In a typical reaction, compounds **26** or **27** (10µL, final conc. 50 µM), **22** (10µL, final conc. 10 µM) and NTR (10 µL, final conc. 10 µg /mL) were added to 970 µL PBS. The reaction mixture was incubated at 37 ºC for 15 min on Eppendorf thermomixer comfort (800 rpm), transferred into quartz absorbance cell (Hellma, path length 1.0 cm), and the absorption spectra were recorded on Shimadzu UV-2600.

4.4.4. General procedure for nitroreductase activated decomposition of compounds (24, 25, 40) and monitoring of reaction by HPLC

Stock solutions of compounds **24** (5 mM), **25** (5 mM), Umb (5 mM), Umb OH (5 mM), CipX (5 mM), and **40** (5 mM) were prepared in DMSO independently. A stock solution of *E. Coli* nitroreductase, NTR (1 µg /1 µL) and NADH (7.5 mM) were prepared in PBS (pH 7.0, 10

mM). In a typical reaction, respective compounds to be analyzed (5µL, final conc. 25 µM), NADH (10µL, final conc. 75 µM) and NTR (20 µL, final conc. 20 µg /mL) were added to 965 µL PBS. Reaction mixtures were incubated at 37 ºC on Eppendorf thermomixer comfort (800 rpm). Aliquots were taken periodically and injected (50 µL) in an HPLC attached with a diode-array detector (detection wavelength was 320 nm). The stationary phase used was C-18 reversed phase column (4.6 mm × 100 mm, 5 µm). The mobile phase used was 0.1% TFA in H_2O: ACN HPLC run time was 15 min with flow rate of 1 mL/min starting with 60:40 → 0-5 min, 50:50 → 5-10 min, 30:70→ 10-15 min, 60:40 and the reduction of the test compounds were analyzed using HPLC by monitoring disappearance of the peak for the test compound.

4.4.5. Nitroreductase activated decomposition theranostic agent 40 and monitoring of its fluorescence by fluorimetry

Stock solutions of compound **40** (1 mM), CipX (1 mM) and Umb OH (1 mM) were prepared in DMSO independently. A stock solution of *E. Coli* nitroreductase, NTR (1 µg /1 µL) was prepared and NADH (3 mM) in PBS (pH 7.0, 10 mM). In a reaction compound **40** (10 µL, final conc. 10 µM), NADH (10µL, final conc. 30 µM) and NTR (10 µL, final conc. 10 µg /mL) was added to 970 µL PBS. The reaction mixture was incubated at 37 ºC for 30 min on Eppendorf thermomixer comfort (800 rpm). The reaction mixture was transferred into a quartz fluorescence cell (Hellma, path length 1.0 cm) and fluorescence measurements were carried out using a HORIBA Jobin Yvon, Fluorolog fluorescence spectrophotometer. Fluorescence was monitored for Umb OH (λ_{ex} = 350 nm and λ_{em} = 450 nm) with an excitation slit width of 1 nm and emission slit width of 1 nm. The emission profile was recorded.

4.4.6. Activation of the nitro group in a group in the cellular environment: HeLa cells were grown in culture flask in DMEM media supplemented with 10% FBS and 1% antibiotic solution in an atmosphere of 5% CO_2 at 37°C. After 70% of confluency, old media was removed and the cells were washed with PBS (1X) buffer.Cells were detached by trypsinization and resuspended with PBS (1X).Cells suspension was transformed microcentrifuge tube and cells were lysed by sonication using (130 Watt ultrasonic processor, VX 130W) Stepped Microtip for 2 minutes (with 5s ON and 10 s OFF pulse, 60% amplitude) under ice-cold condition. Whole cell lysate in PBS was treated with compound **24** (25 µM), **35** (25 µM), **40** and **17a** (25 µM) incubated independently at 37 °C for 30 min. Fluorescence

was recorded using a Thermo Scientific Varioskan Flash microwell plate reader (λ_{ex} = 350 nm and λ_{em} = 450 nm).

4.4.7. *E. coli* imaging on the treatment of theranostic compound 40

E. coli were grown overnight in LB media. These cells were centrifuged for 10 min at 4,000 rpm, 4 °C. The resulting bacterial pellet was washed twice with PBS and resuspended in fresh PBS (pH 7.4, 10 mM). *E. coli* culture (1 mL, OD$_{600}$ of 0.5) was incubated independently with compound **35** (25 µM) and compound **40** (25 µM) for 30 min at 37 °C. The cell suspension was then centrifuged at 10,000 rpm at 4 °C for 5 min and the pellet was washed twice with PBS to remove excess of compounds. Fluorescence from compounds was monitored in DAPI channel by confocal fluorescence microscopy with 40X.

4.5. Spectral data

^{1}H NMR Spectrum (400 MHz, DMSO-d_6) of **24**
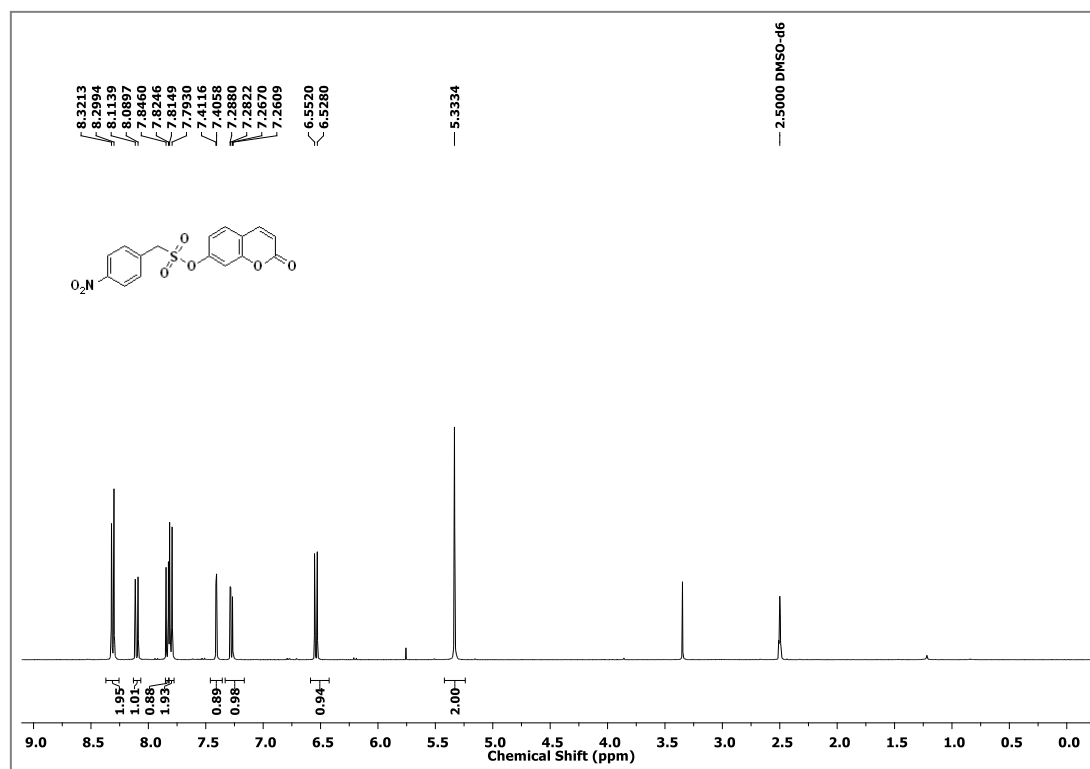
^{13}C NMR Spectrum (100 MHz, DMSO-d_6) of **24**
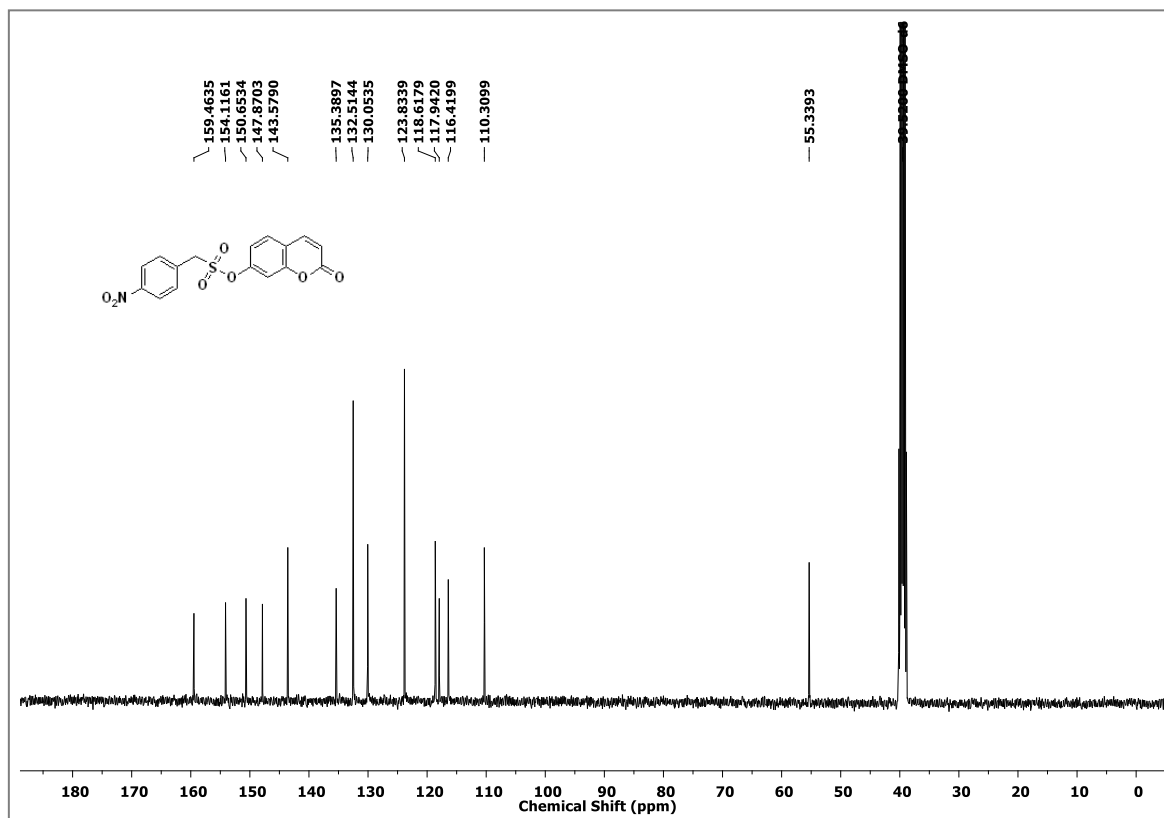
^{1}H NMR Spectrum (400 MHz, DMSO-d_6) of **25**
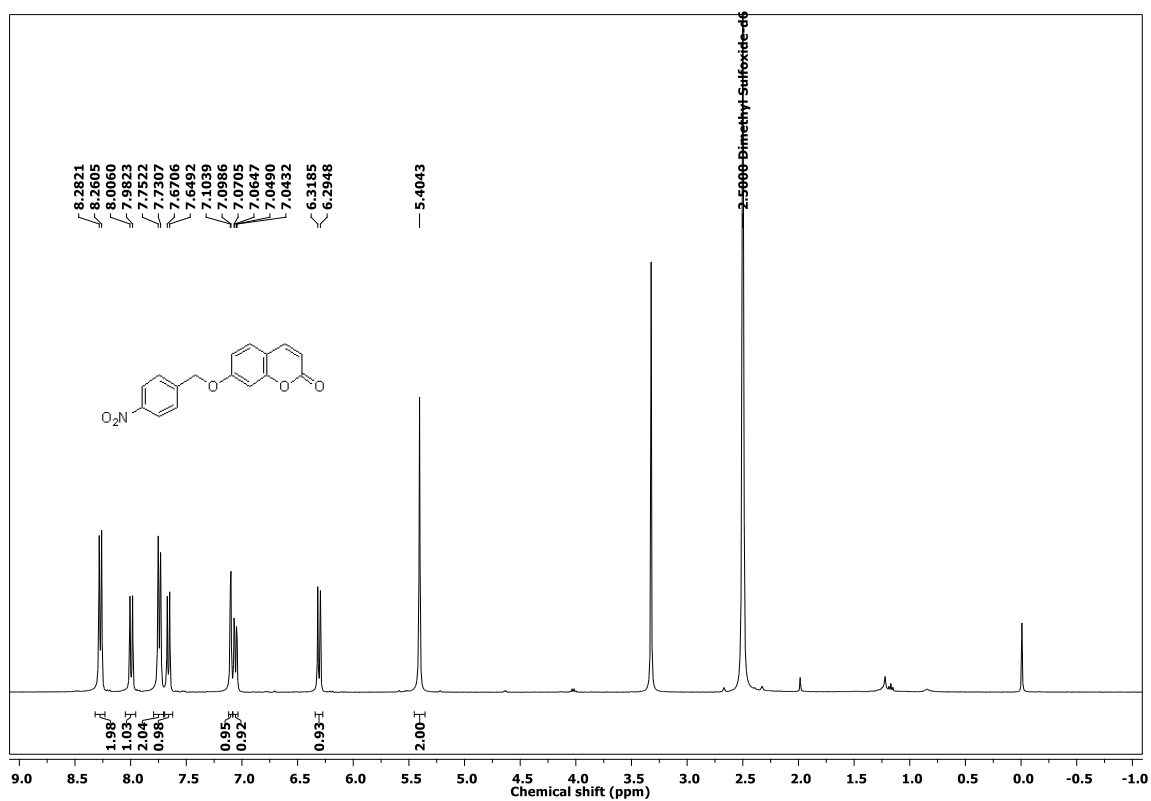
^{13}C NMR Spectrum (100 MHz, DMSO-d_6) of **25**
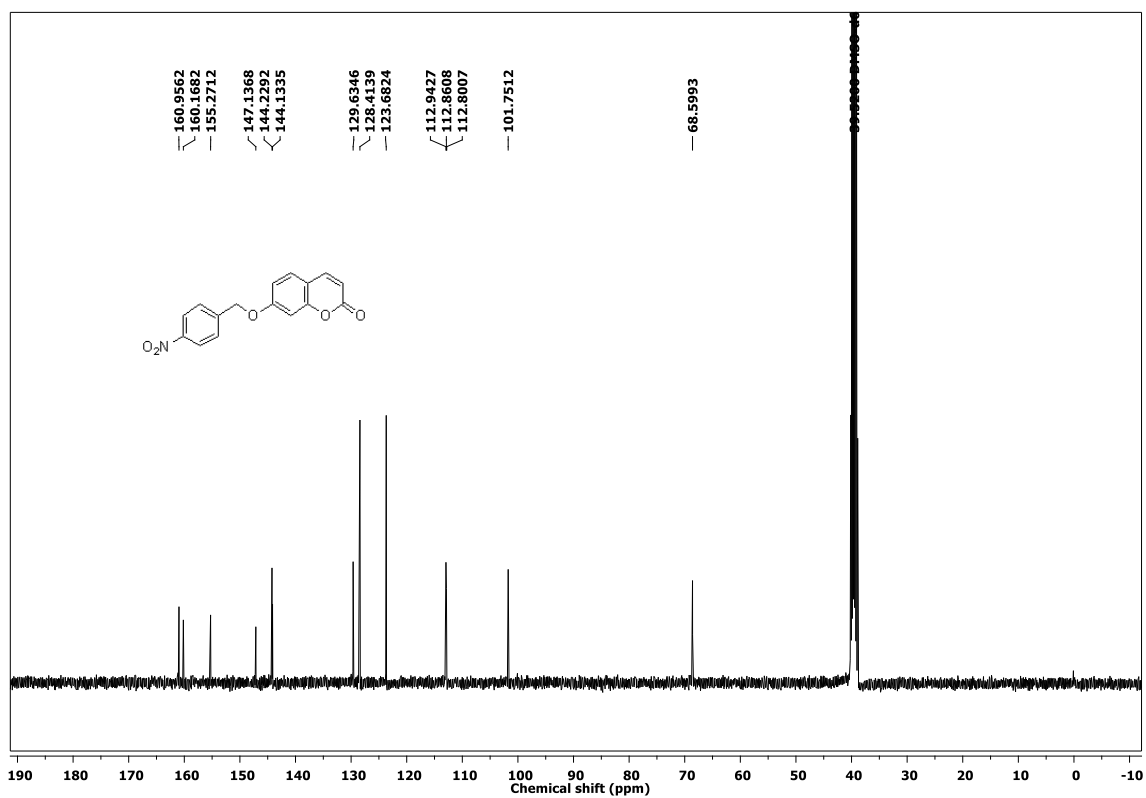
^{1}H NMR Spectrum (400 MHz, DMSO-d_6) of **26**
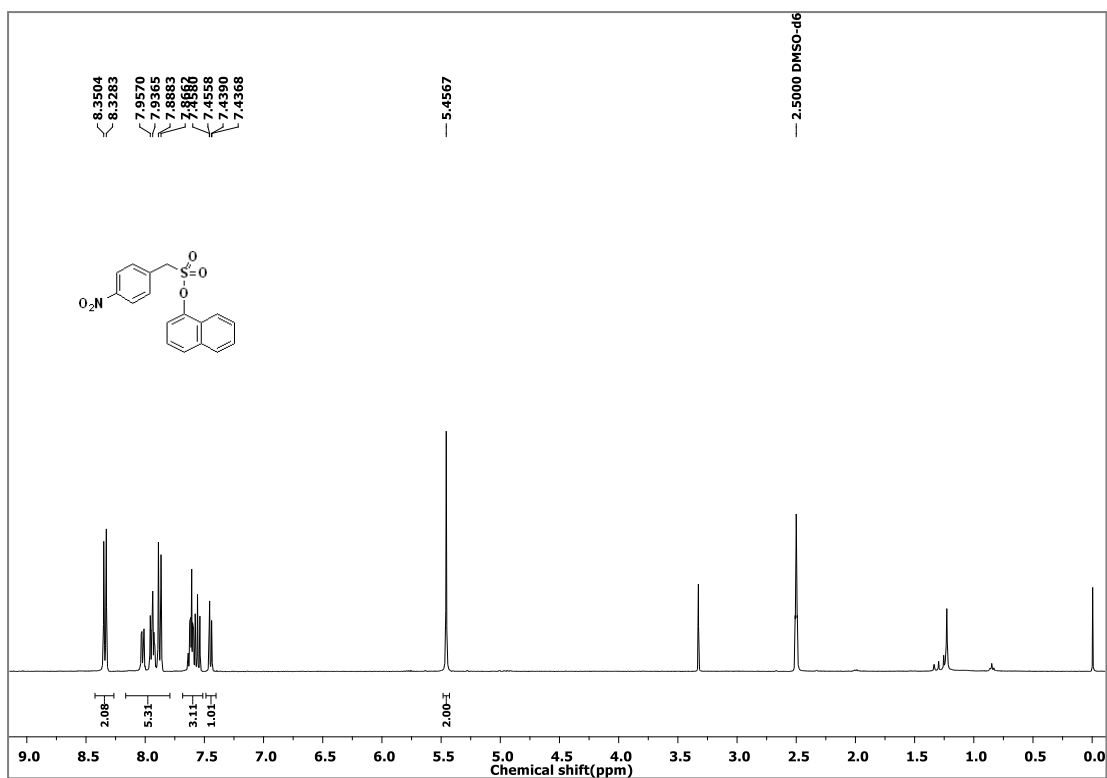
^{13}C NMR Spectrum (100 MHz, DMSO-d_6) of **26**
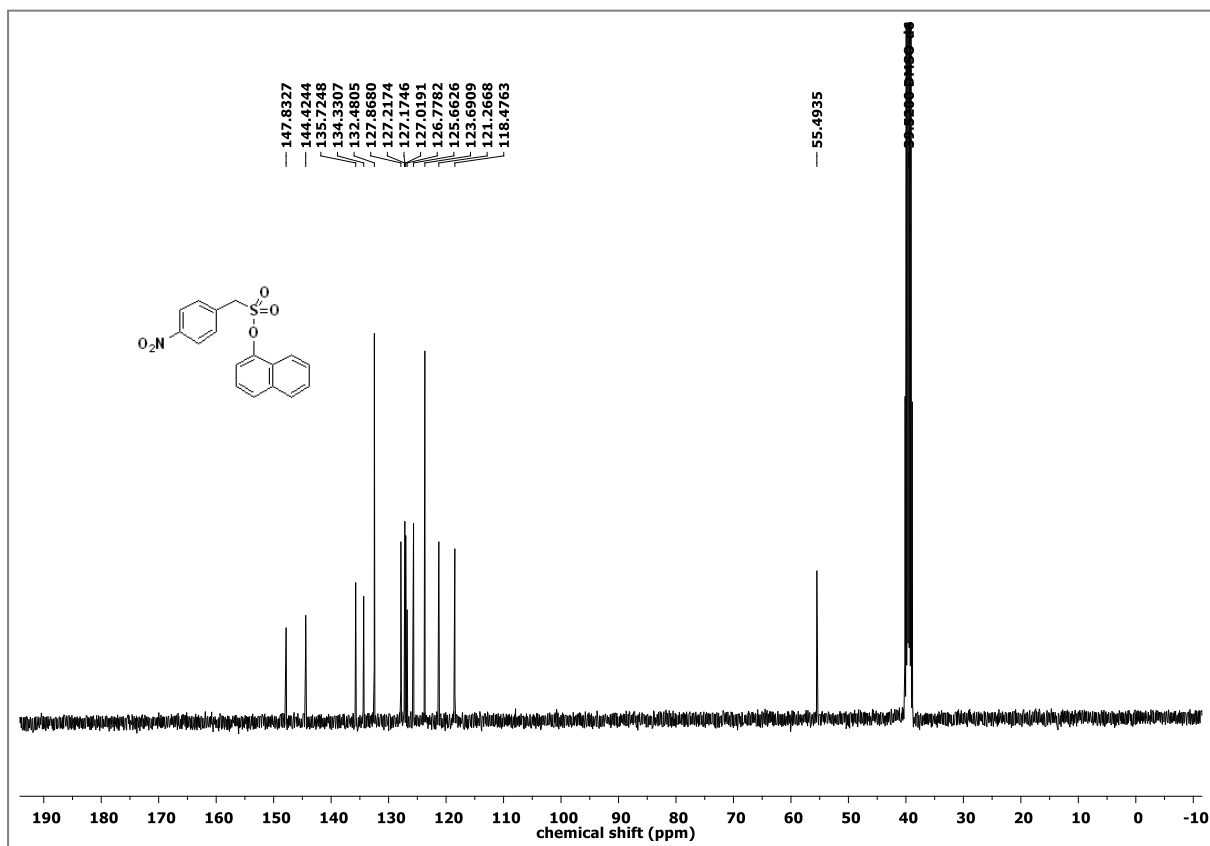
^{1}H NMR Spectrum (400 MHz, CDCl$_3$) of **27**
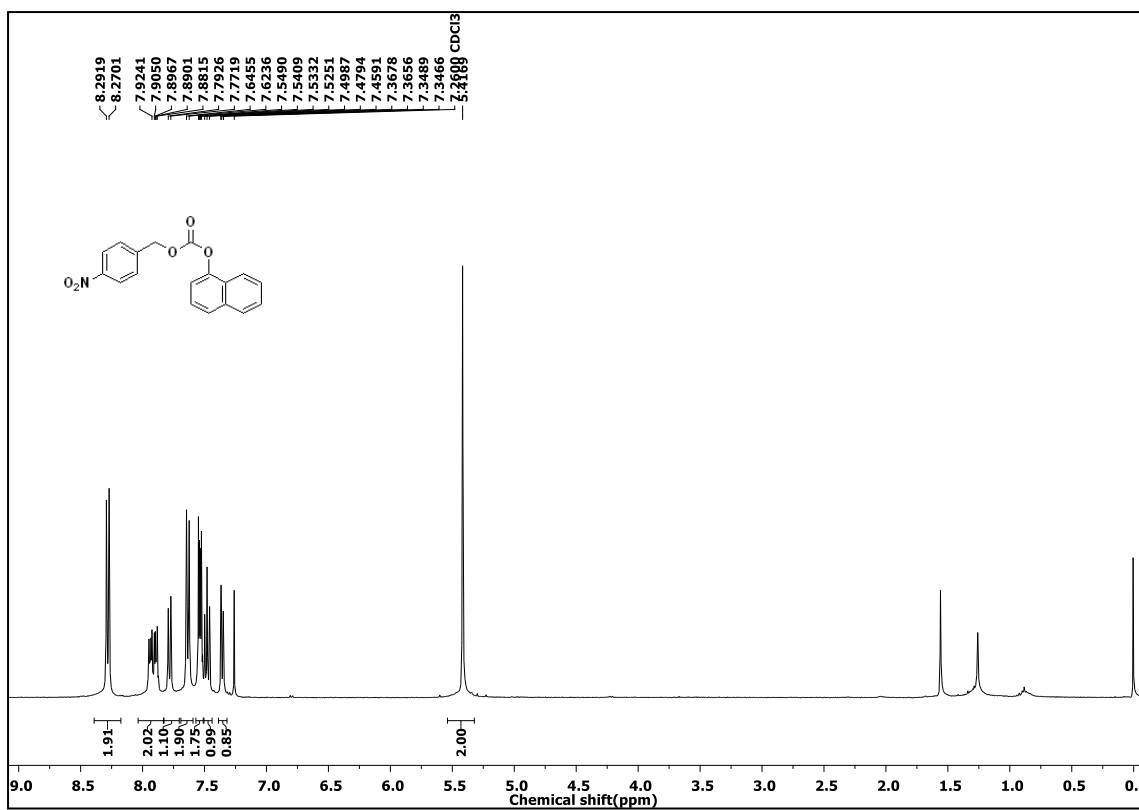
^{13}C NMR Spectrum (100 MHz, CDCl$_3$) of **27**
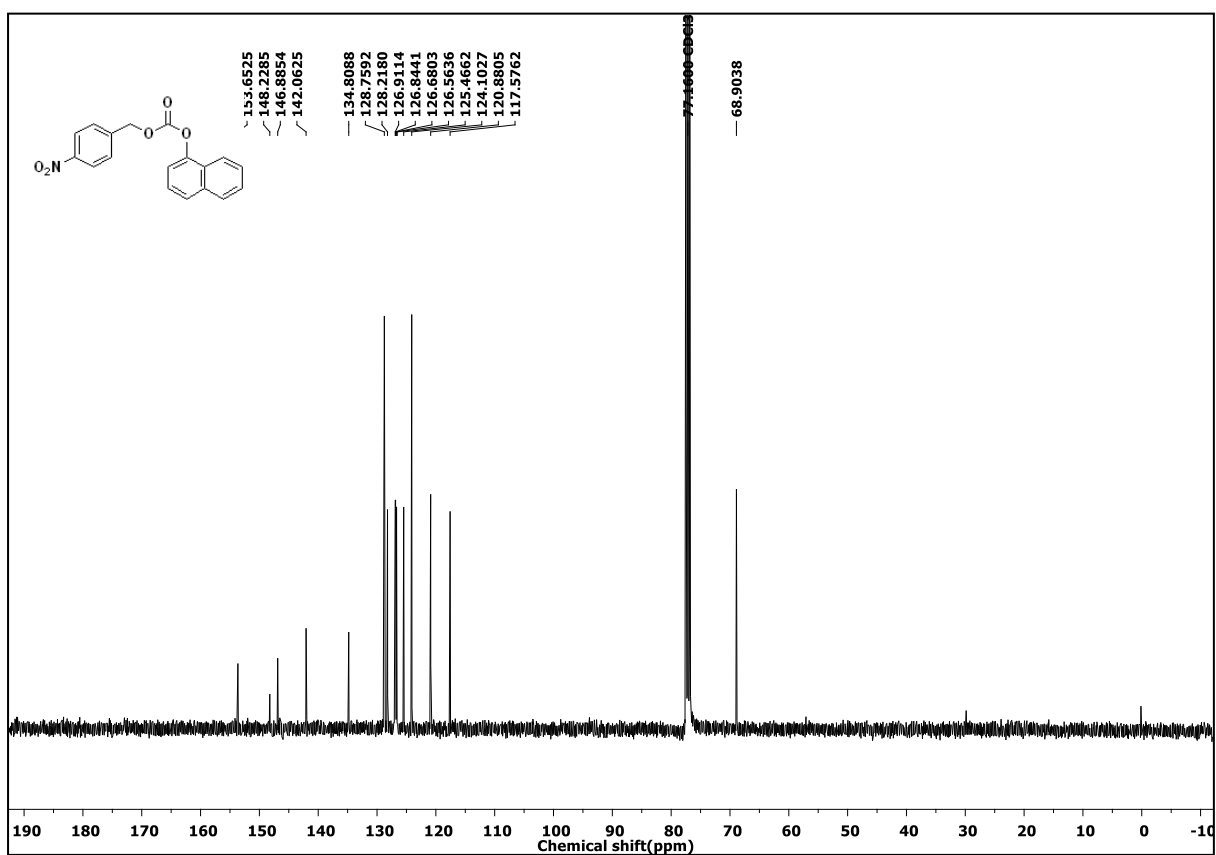
^{1}H NMR Spectrum (400 MHz, CDCl$_3$) of **28**
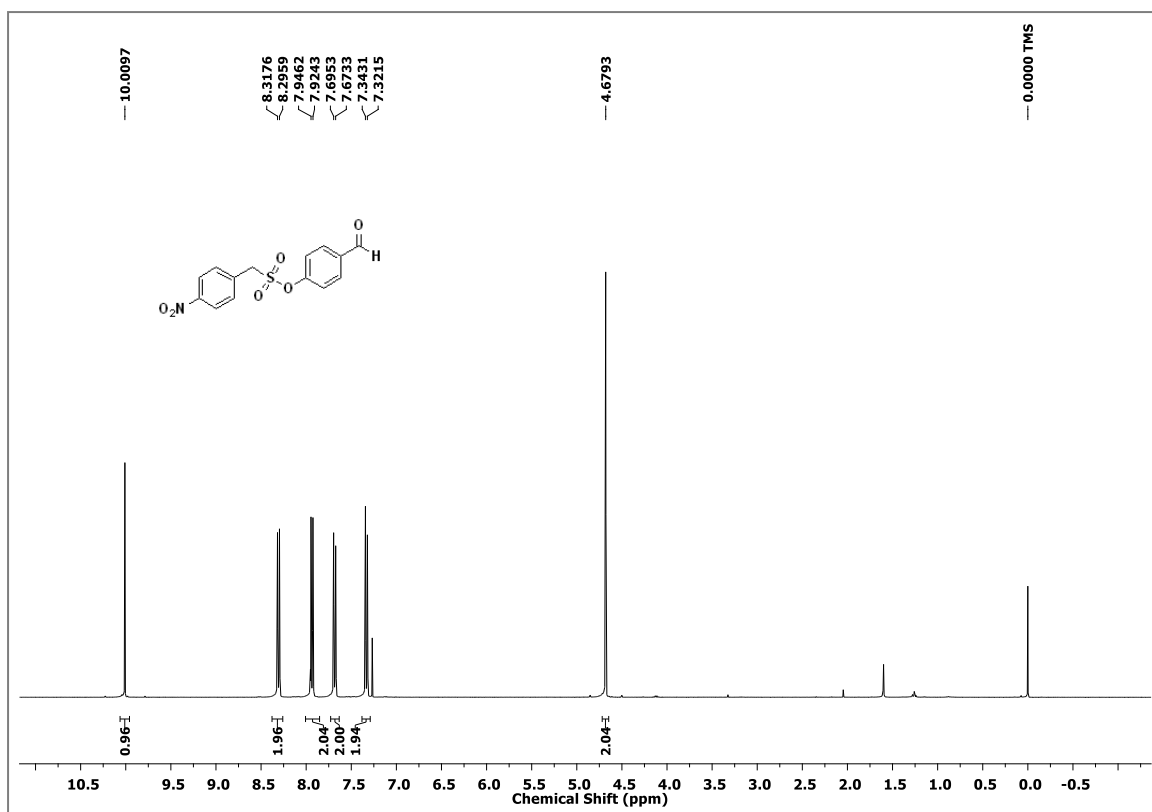
^{13}C NMR Spectrum (100 MHz, CDCl$_3$) of **28**
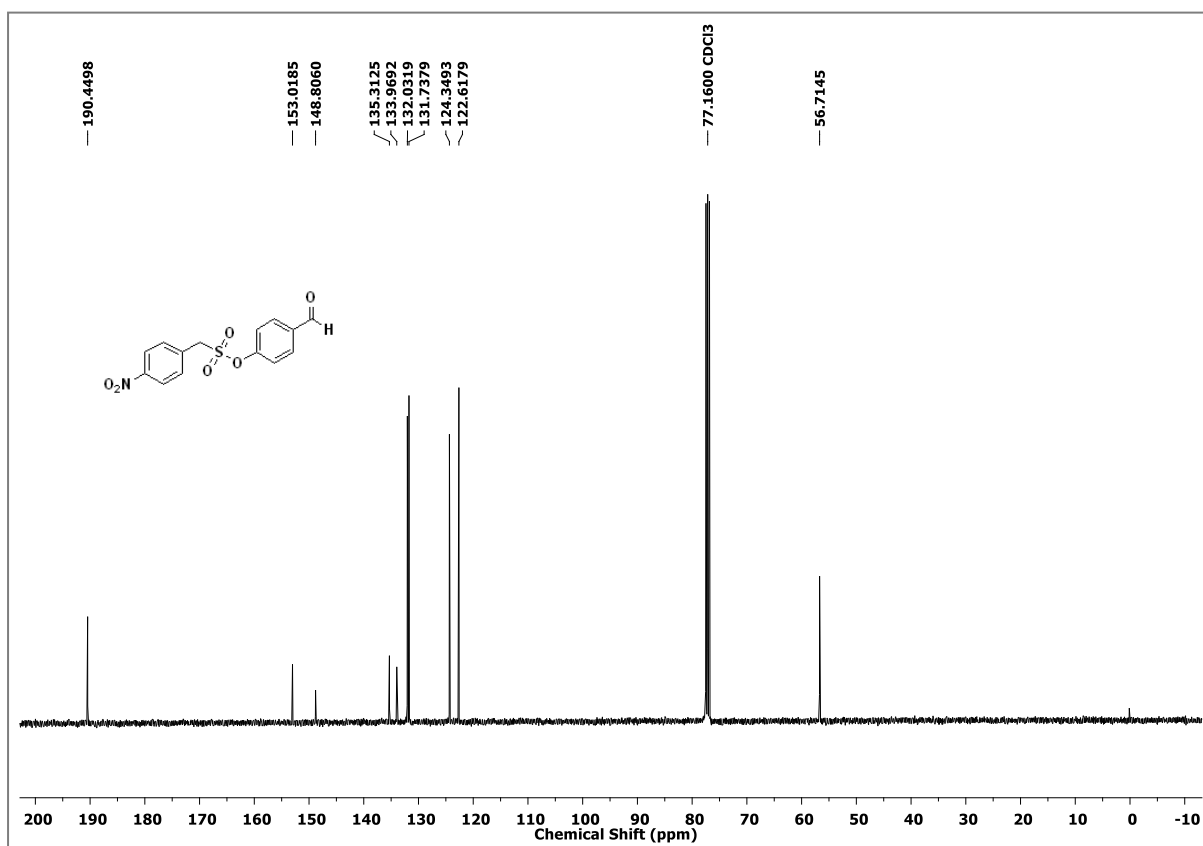
^{1}H NMR Spectrum (400 MHz, CDCl$_3$) of **29**

178
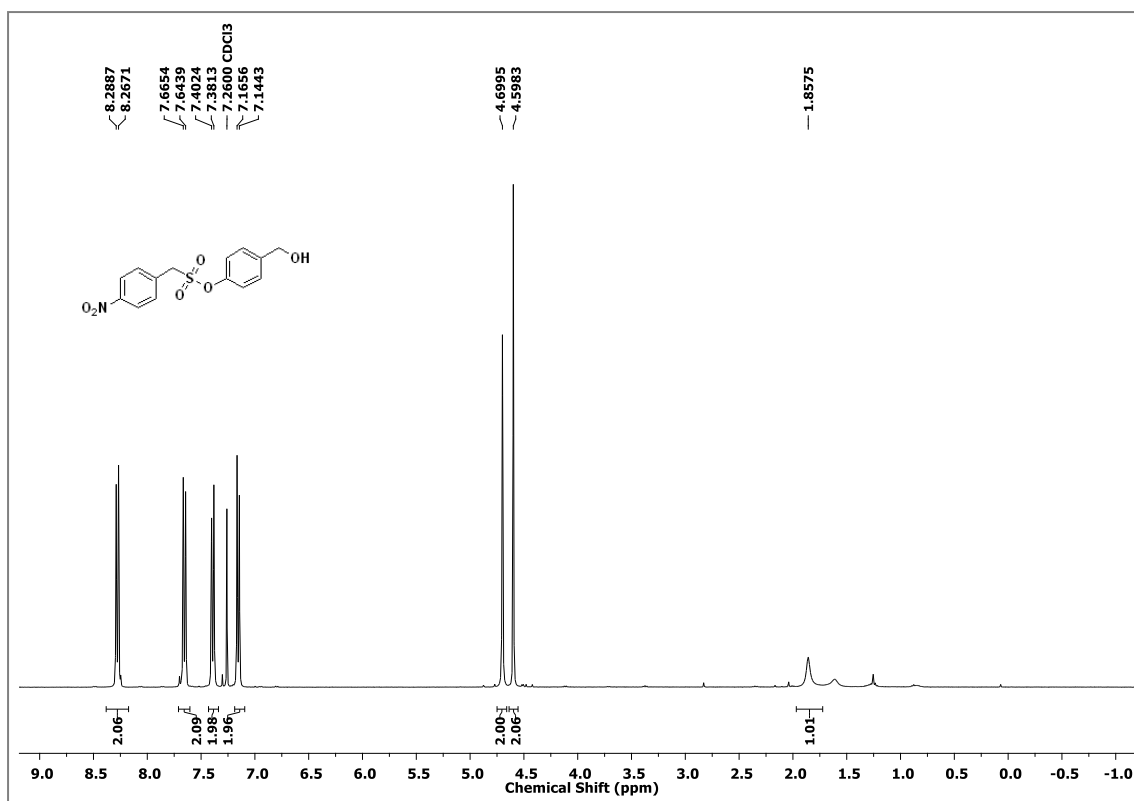
^{13}C NMR Spectrum (100 MHz, CDCl$_3$) of **29**
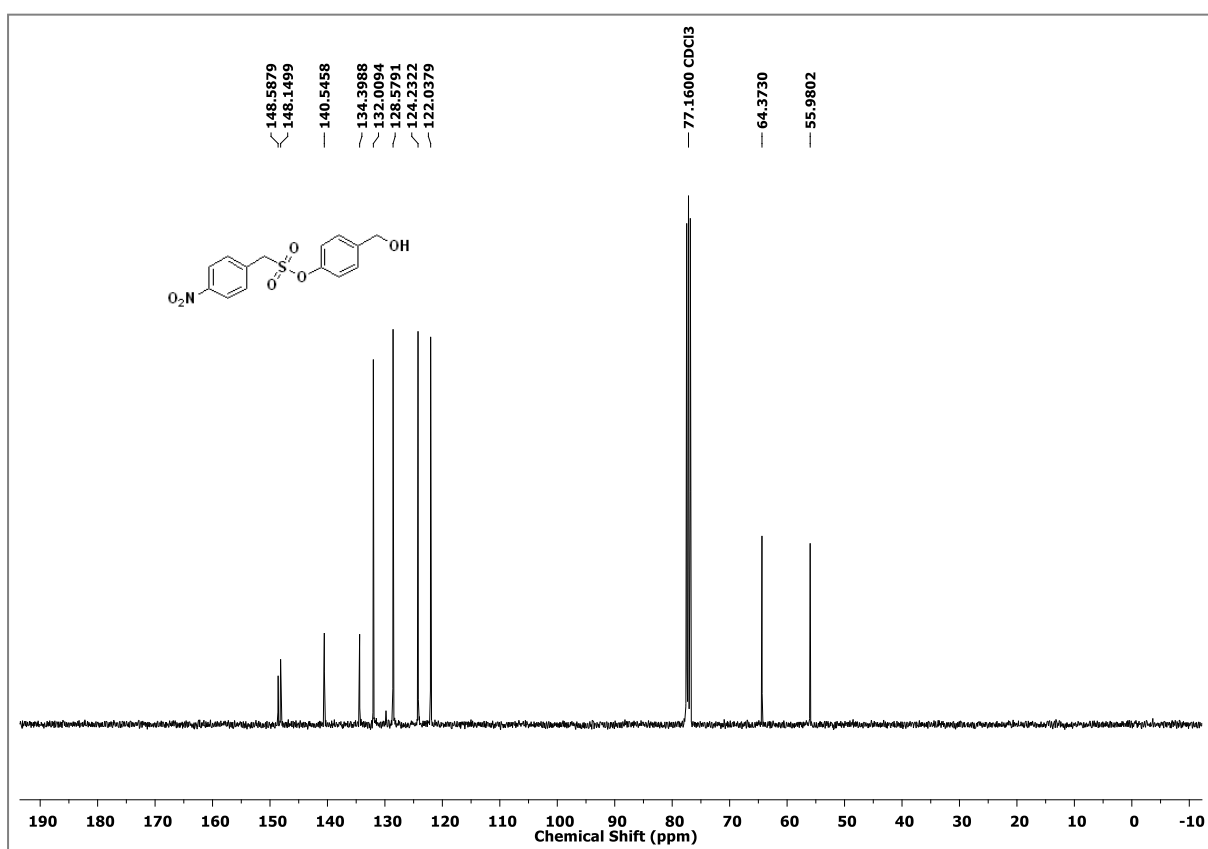
¹H NMR Spectrum (400 MHz, CDCl₃) of **30**
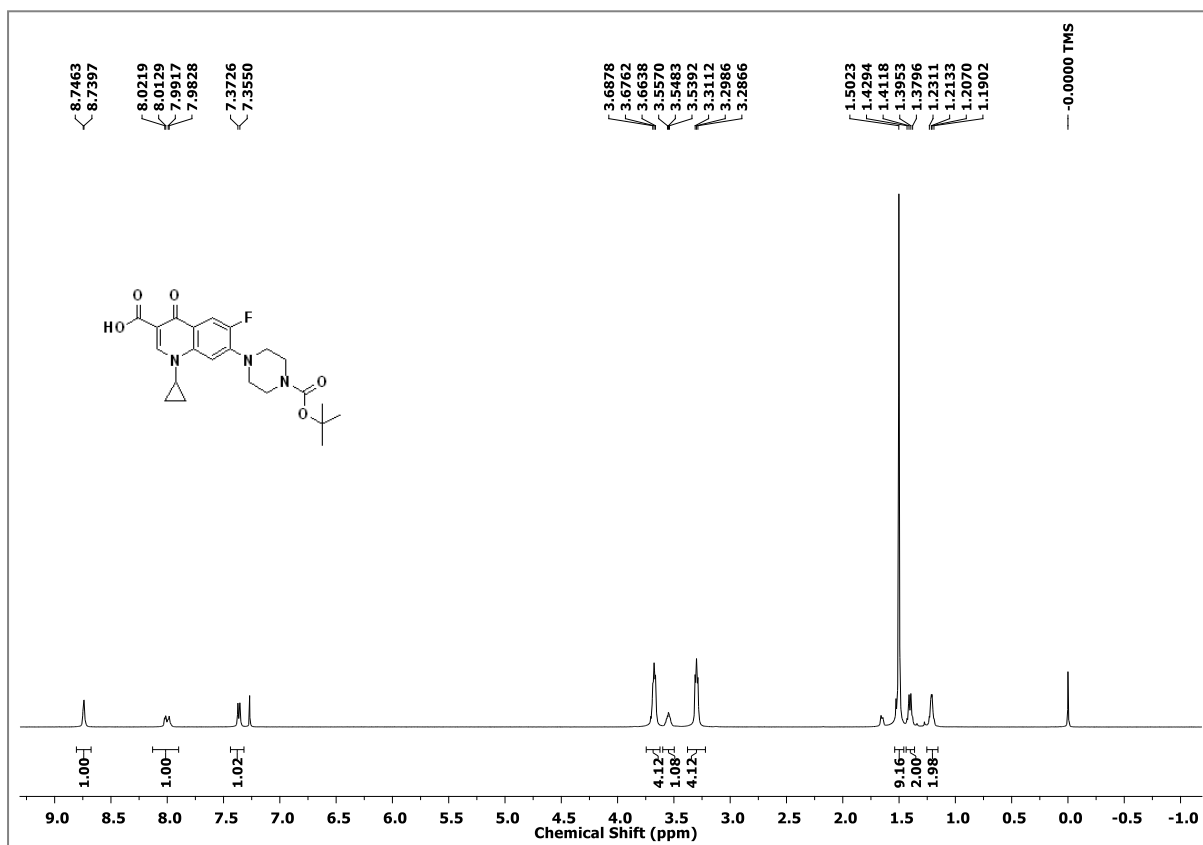
¹H NMR Spectrum (400 MHz, CDCl₃) of **31**
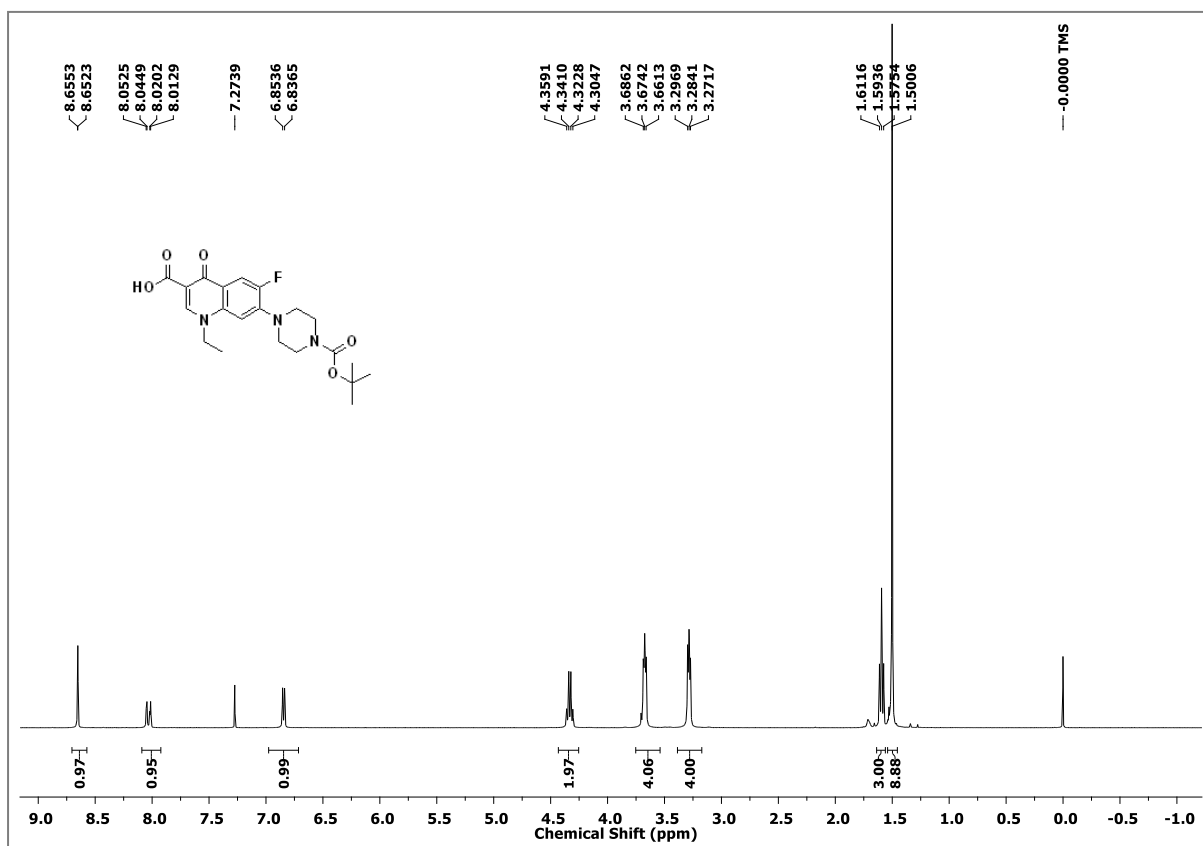
^{1}H NMR Spectrum (400 MHz, CDCl$_3$) of **32**
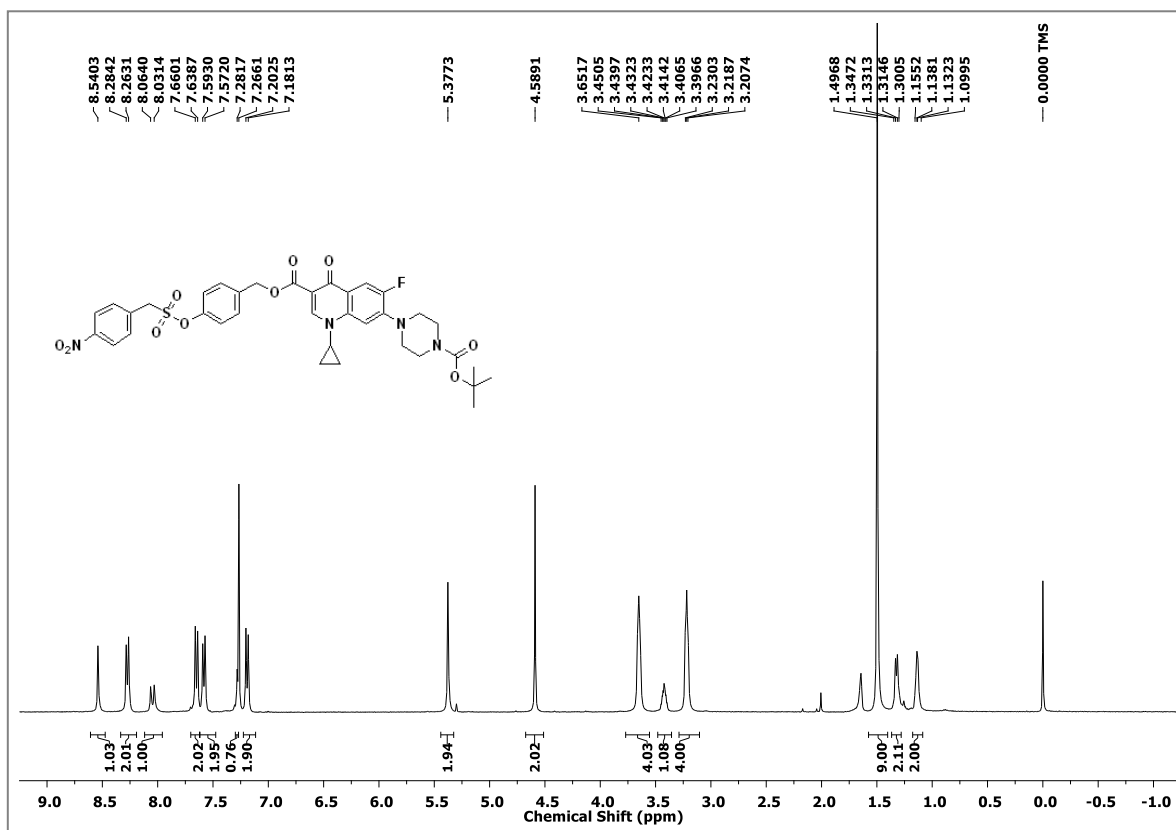
^{13}C NMR Spectrum (100 MHz, CDCl$_3$) of **32**
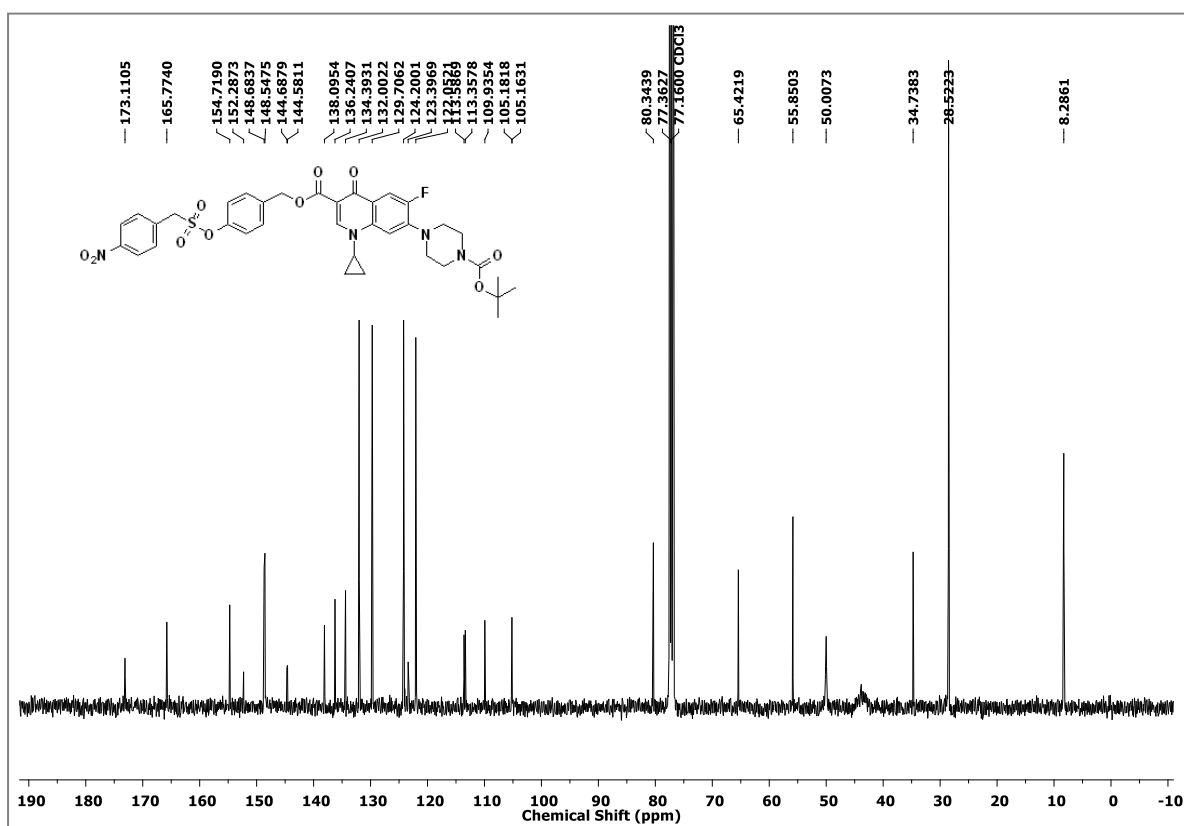
^{1}H NMR Spectrum (400 MHz, CDCl$_3$) of **33**
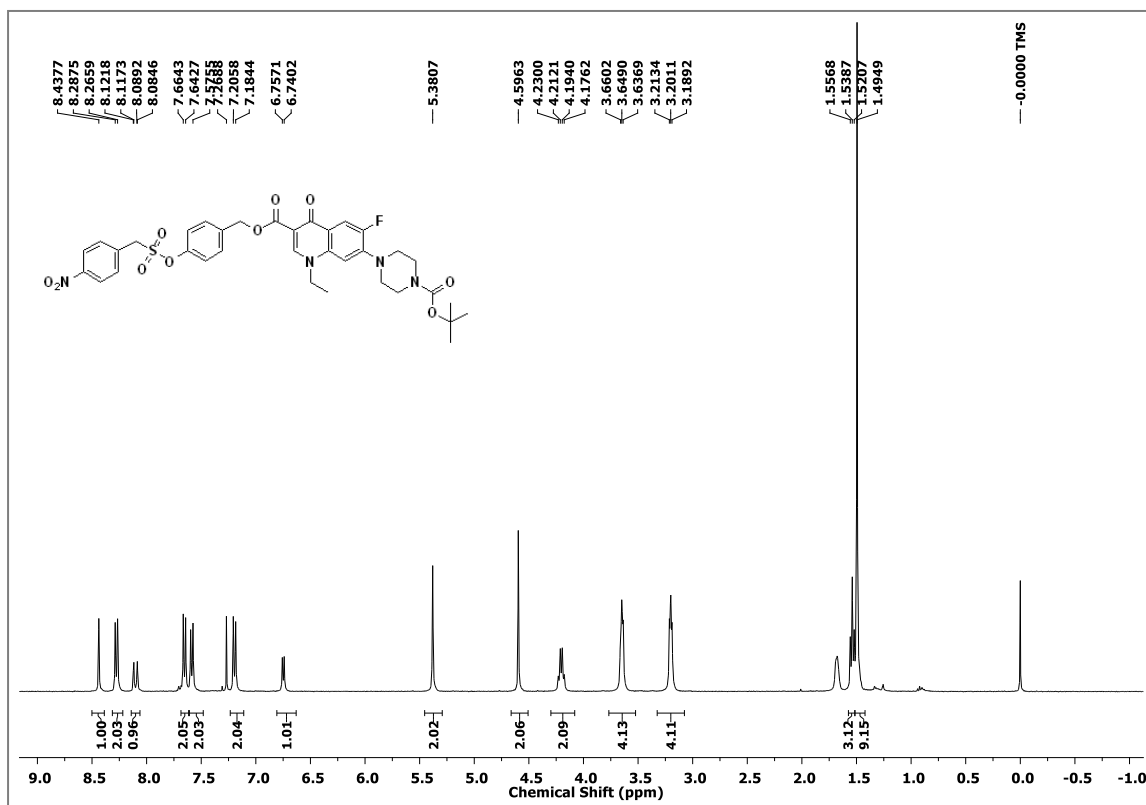
^{13}C NMR Spectrum (100 MHz, CDCl$_3$) of **33**
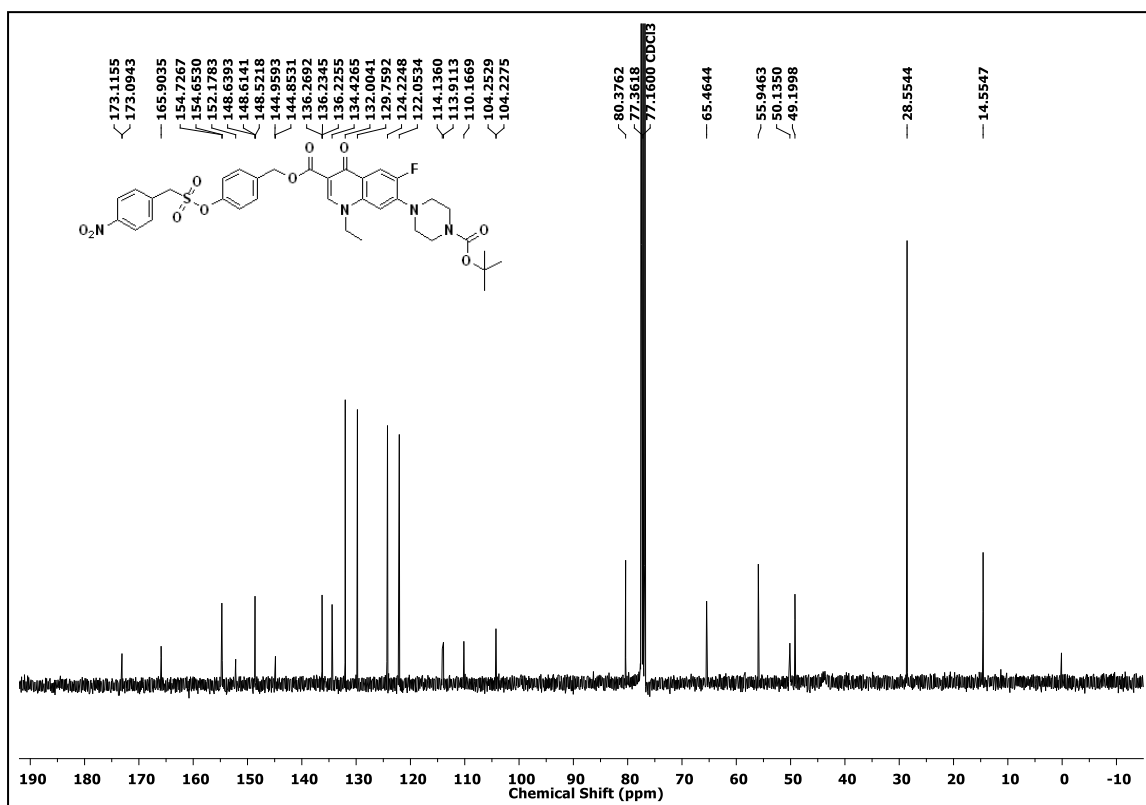
¹H NMR Spectrum (400 MHz, CDCl₃) of **34**
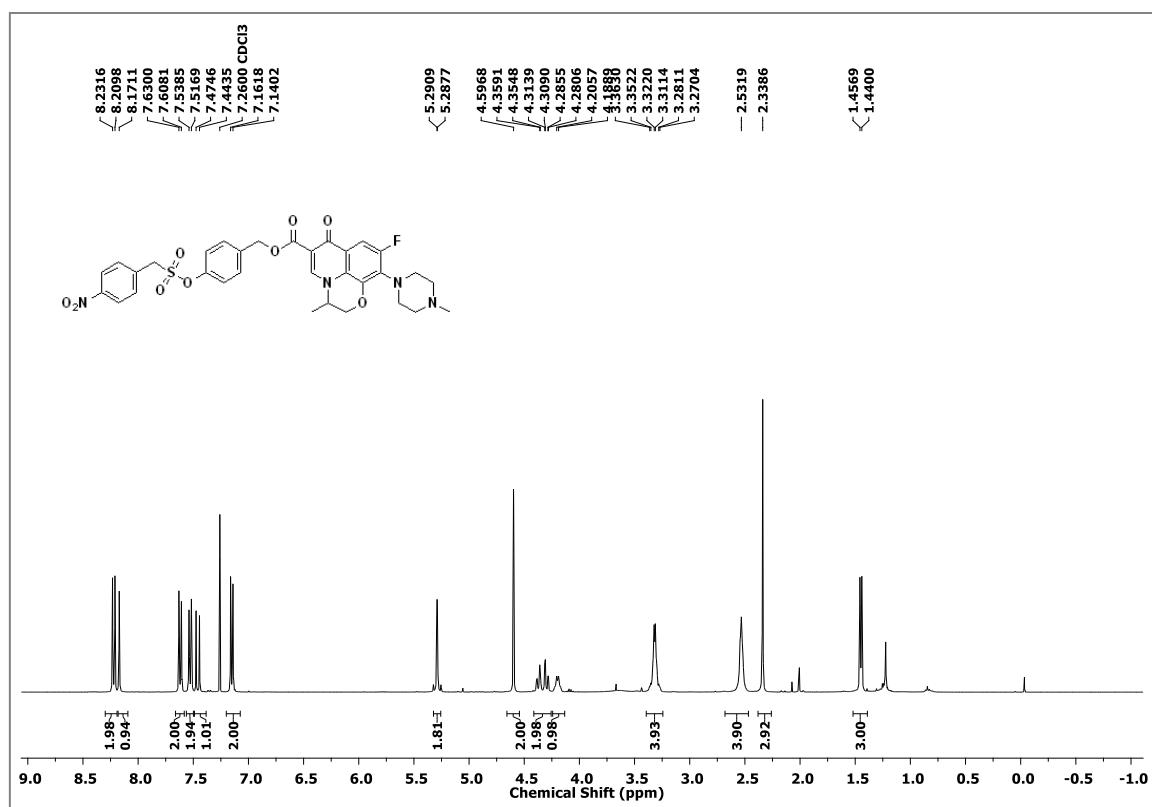
¹³C NMR Spectrum (100 MHz, CDCl₃) of **34**
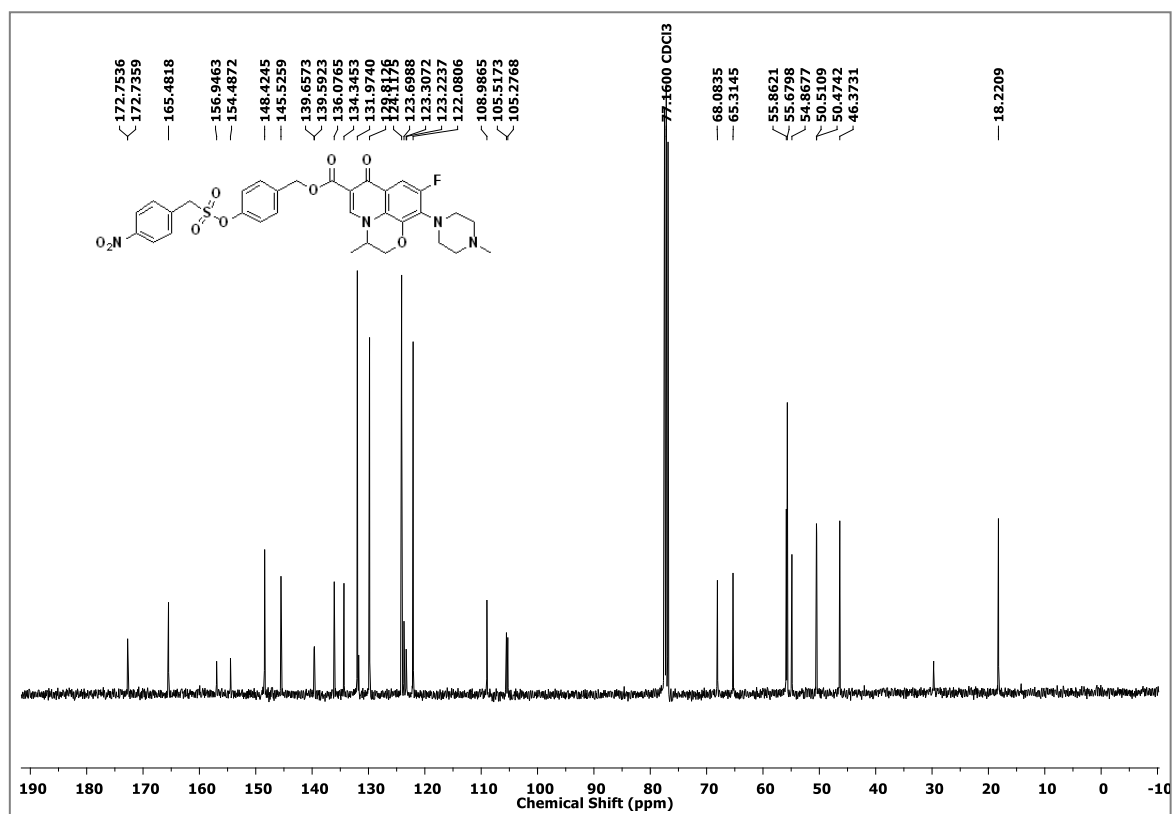
^{1}H NMR Spectrum (400 MHz, DMSO-d_6) of **35**
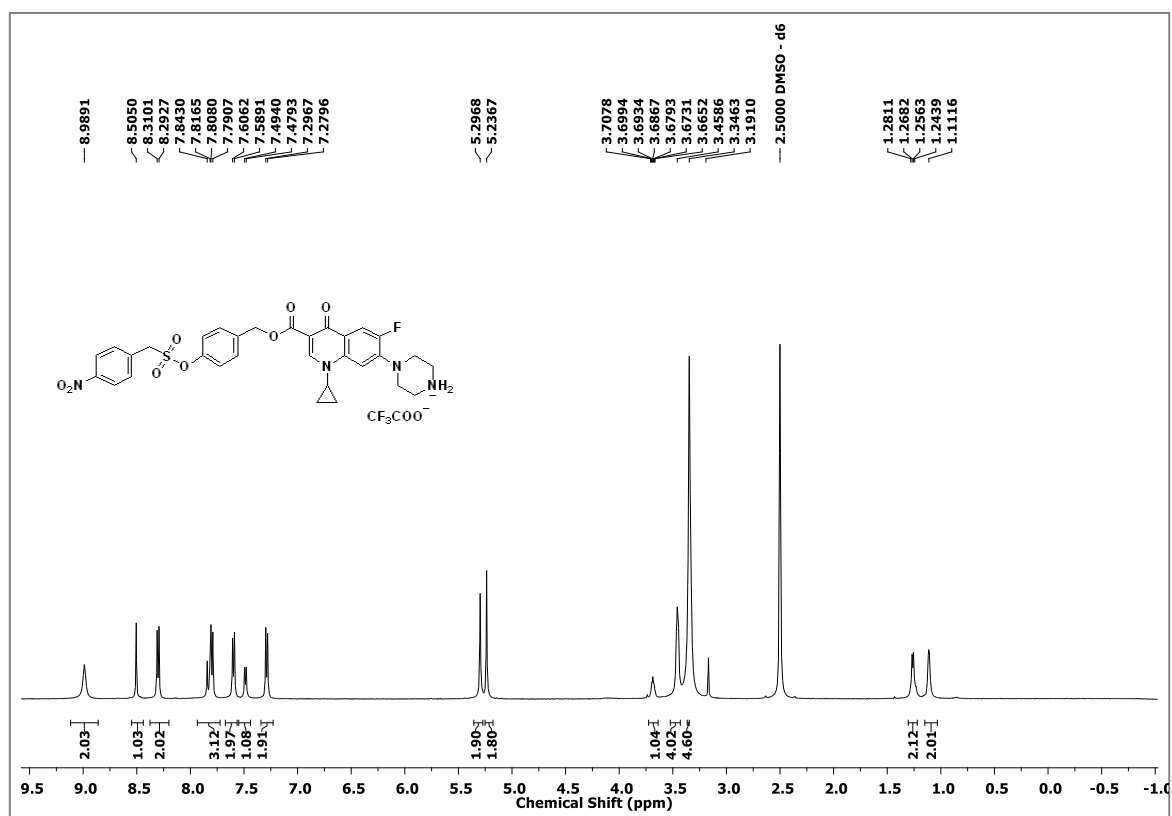
^{13}C NMR Spectrum (100 MHz, DMSO-d_6) of **35**
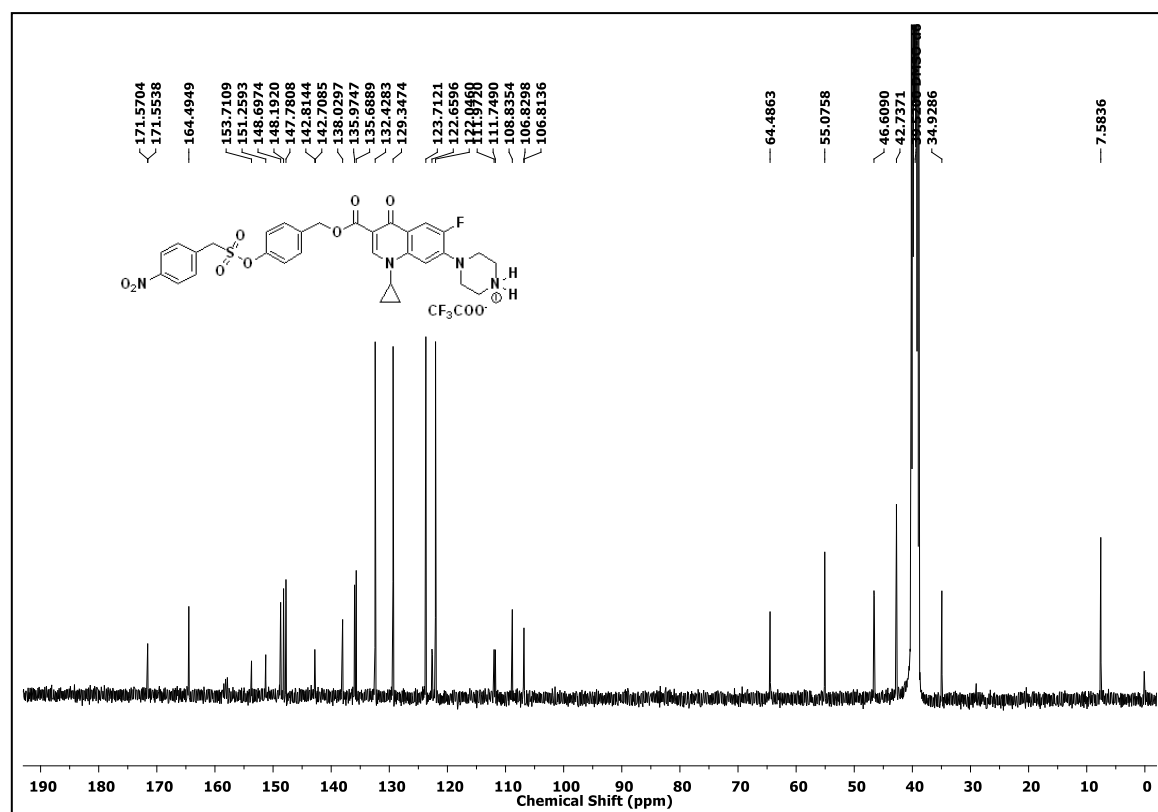
^{1}H NMR Spectrum (400 MHz, DMSO-d_6) of **36**
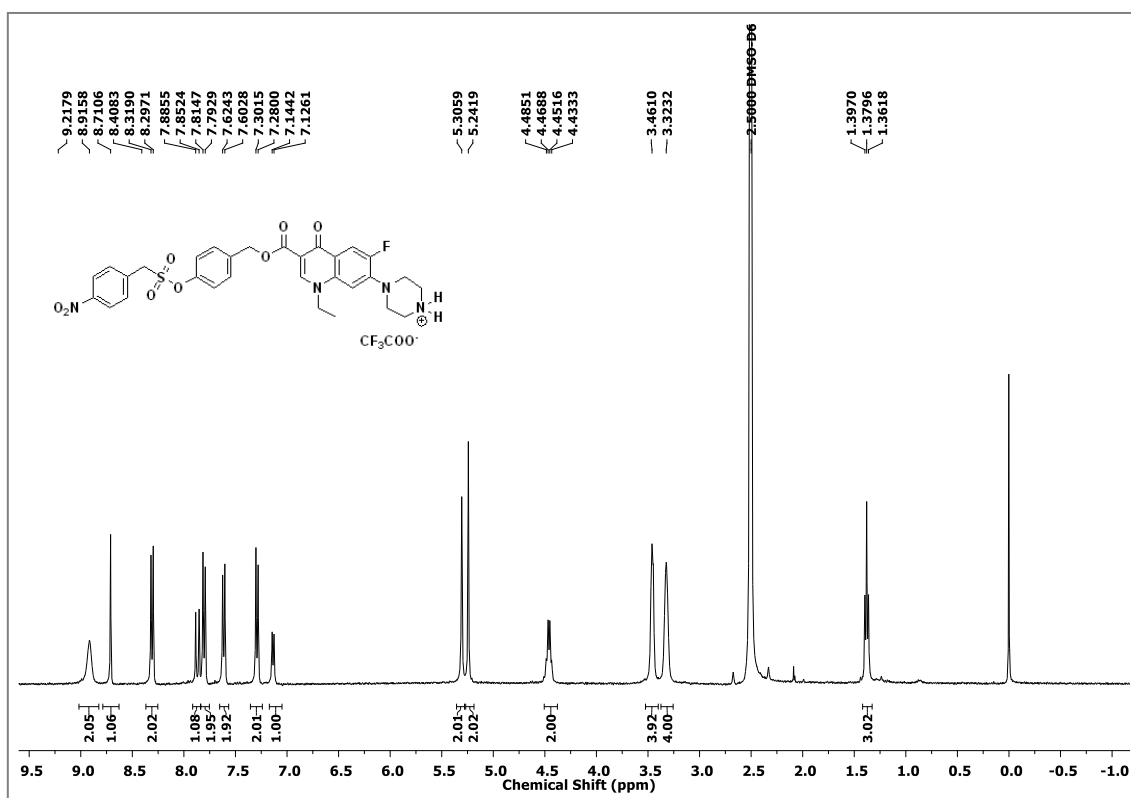
^{13}C NMR Spectrum (100 MHz, DMSO-d_6) of **36**
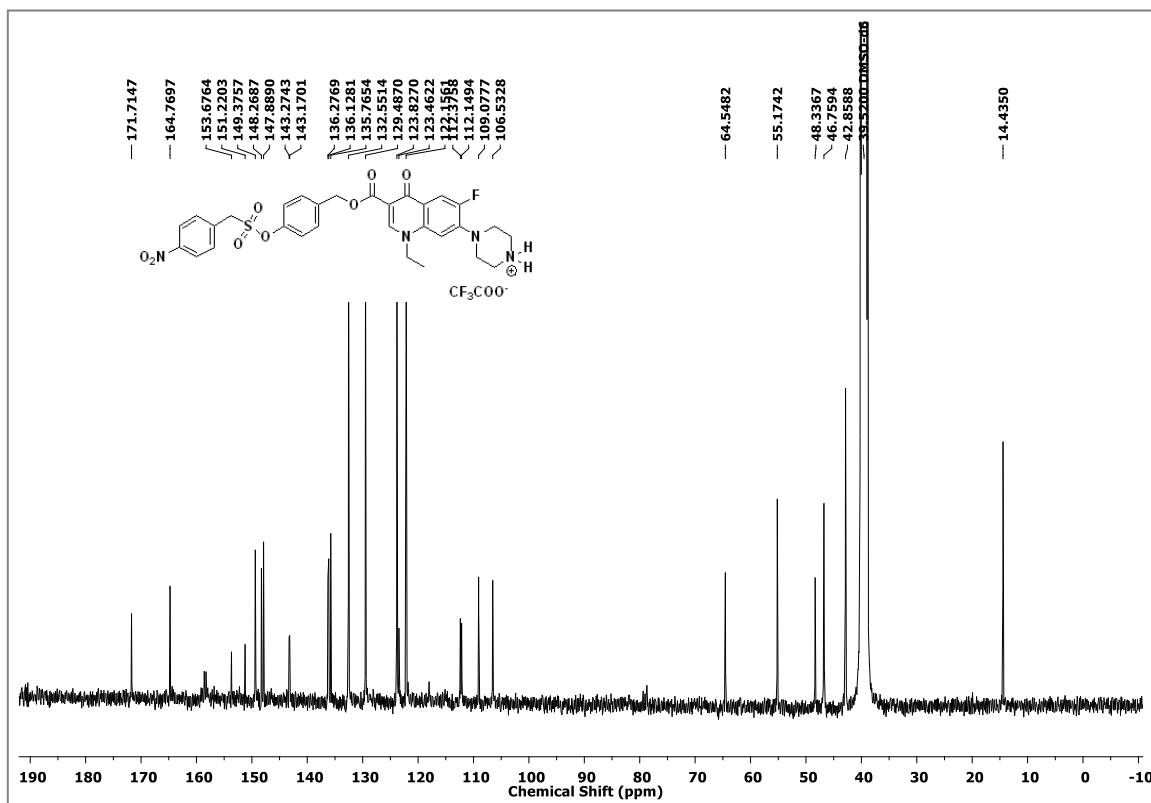
^{1}H NMR Spectrum (400 MHz, CDCl$_3$) of **37d**
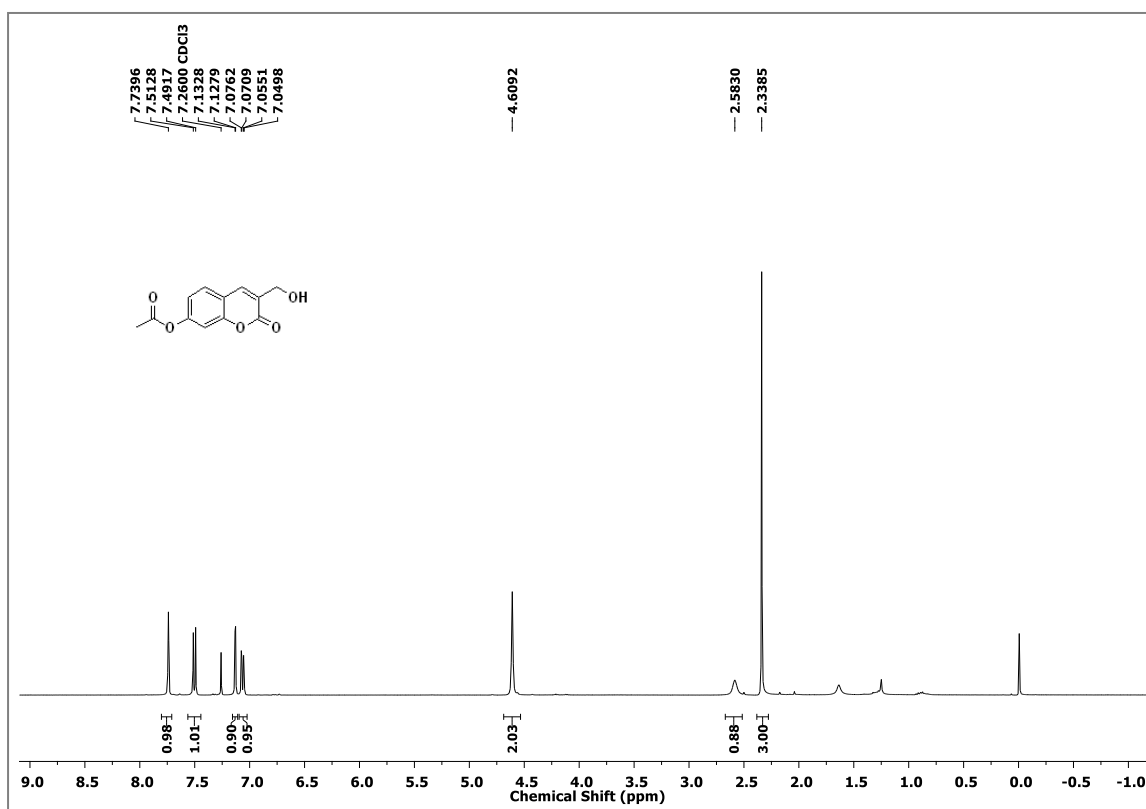
^{13}C NMR Spectrum (100 MHz, CDCl$_3$) of **37d**
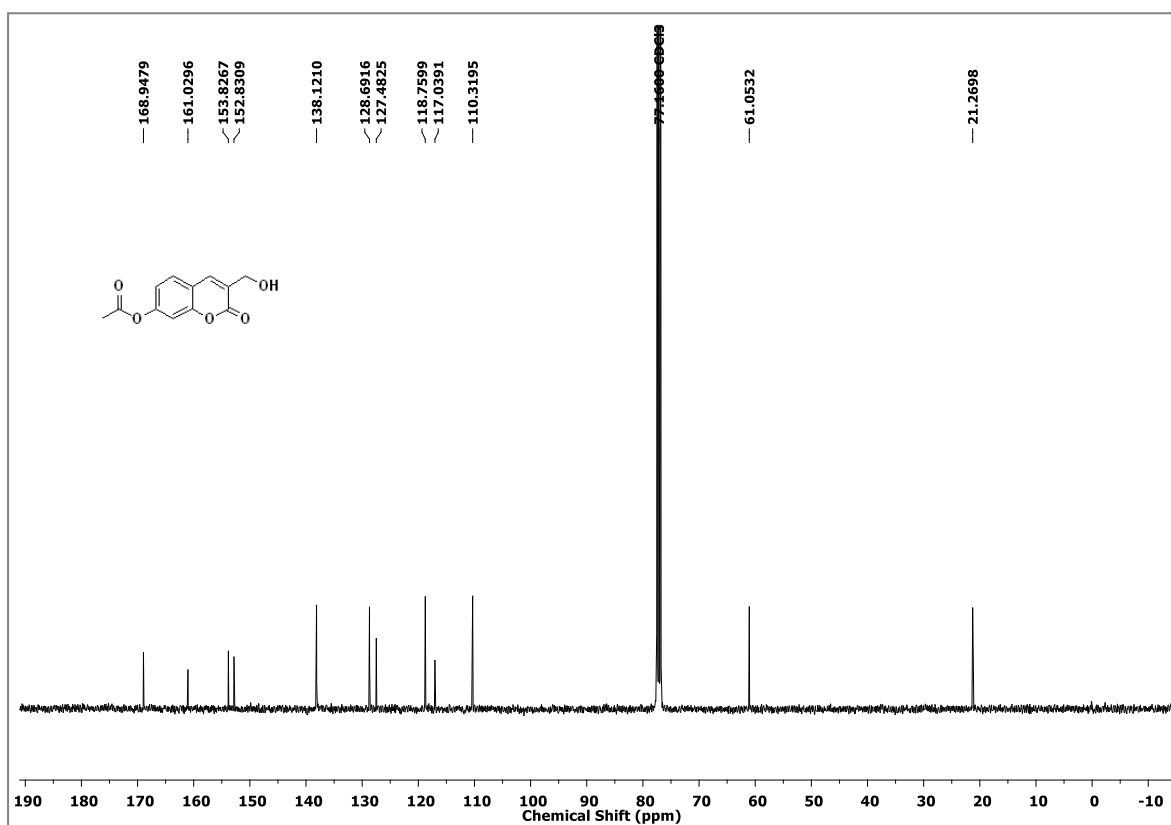
^{1}H NMR Spectrum (400 MHz, CDCl$_3$) of **37e**
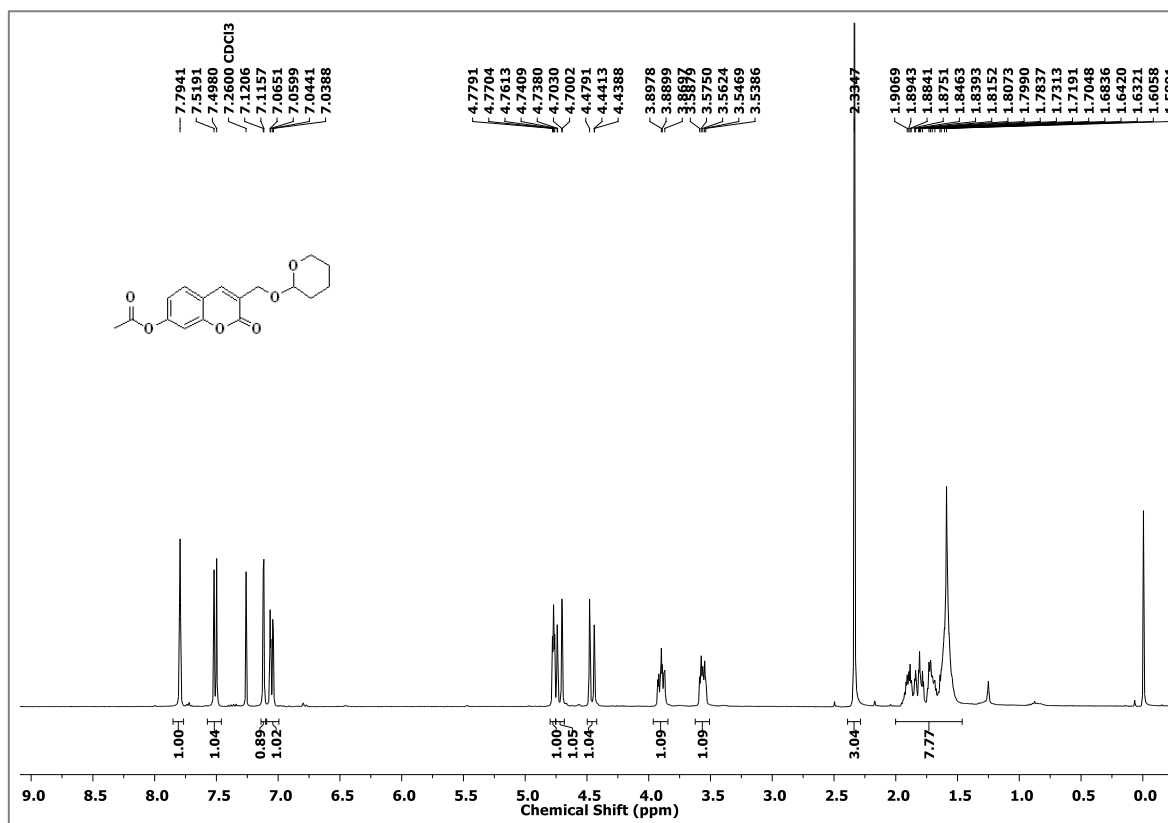
^{13}C NMR Spectrum (100 MHz, CDCl$_3$) of **37e**
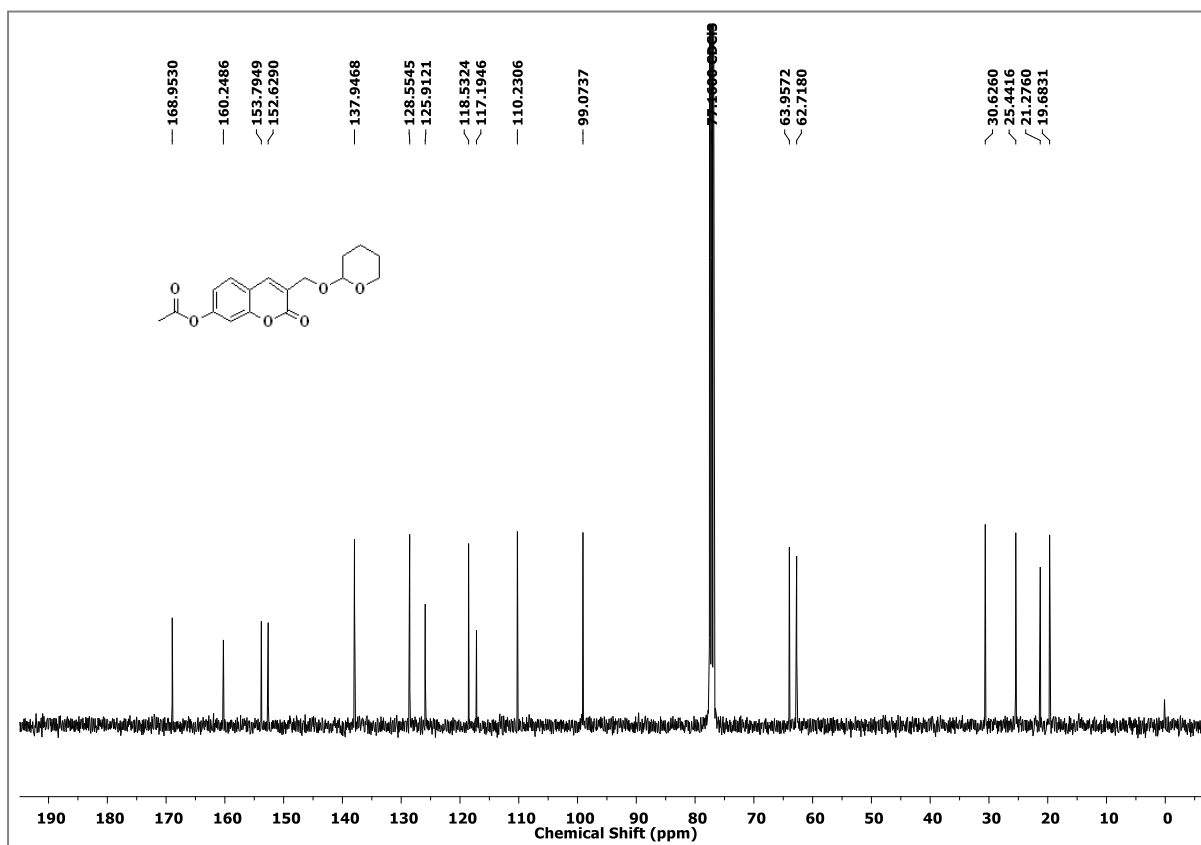
^{1}H NMR Spectrum (400 MHz, CDCl$_3$) of **37f**
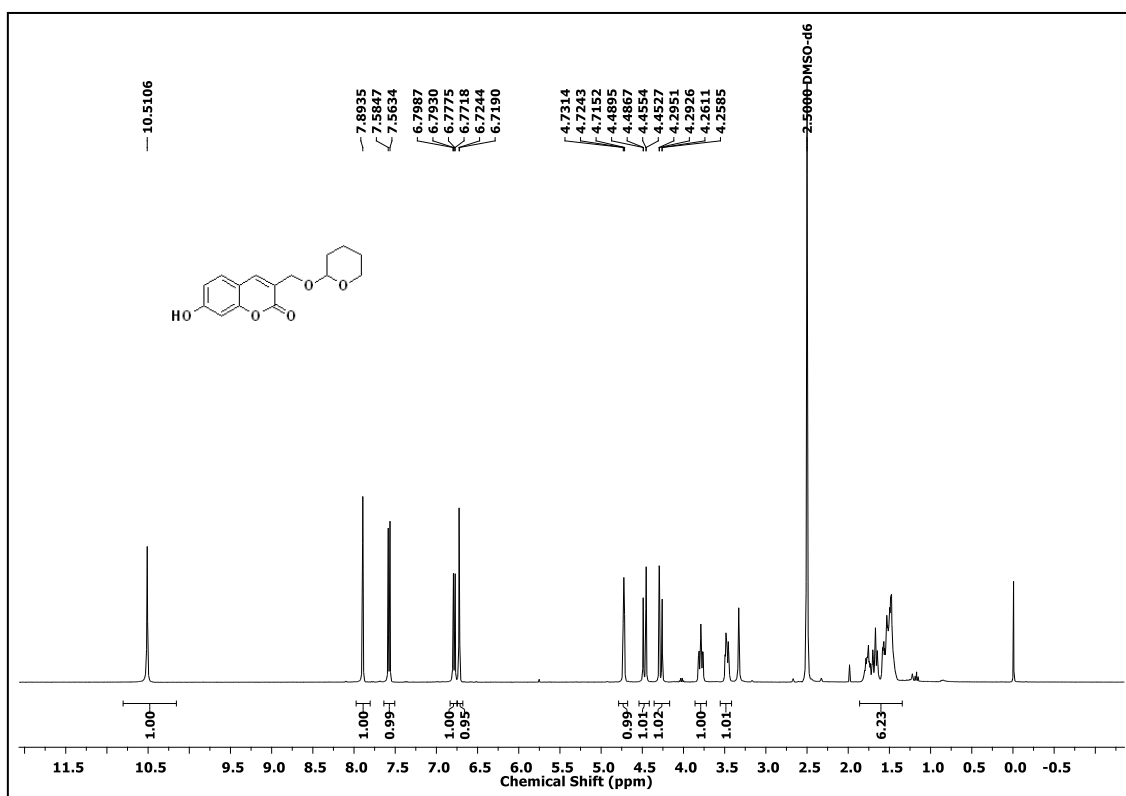
^{13}C NMR Spectrum (100 MHz, CDCl$_3$) of **37f**
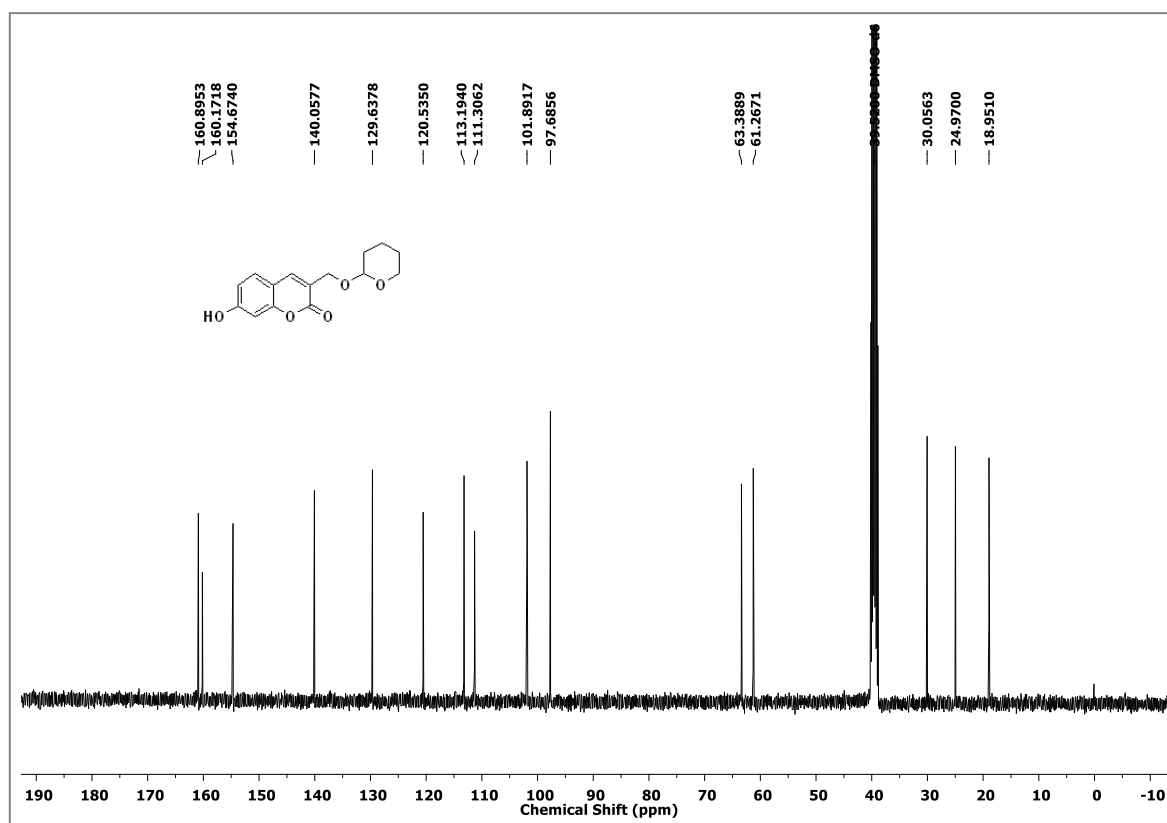
^{1}H NMR Spectrum (400 MHz, DMSO-d_6) of **38**
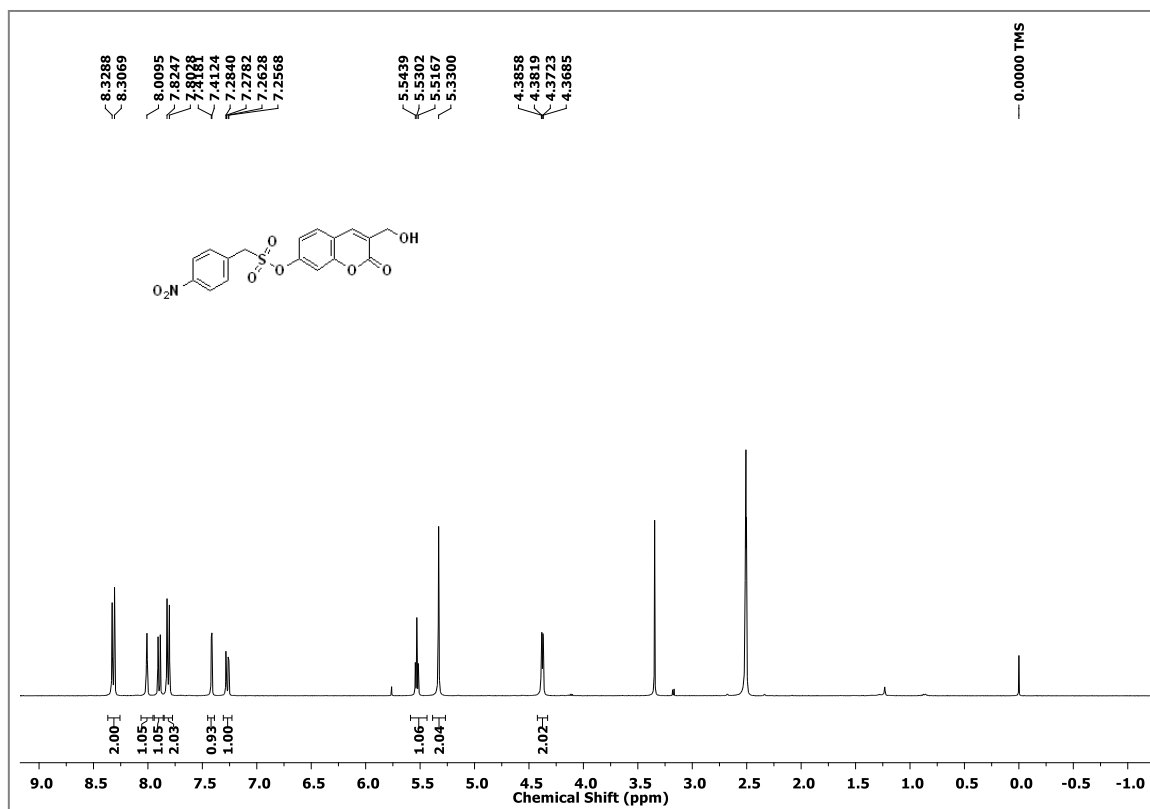
^{13}C NMR Spectrum (100 MHz, DMSO-d_6) of **38**
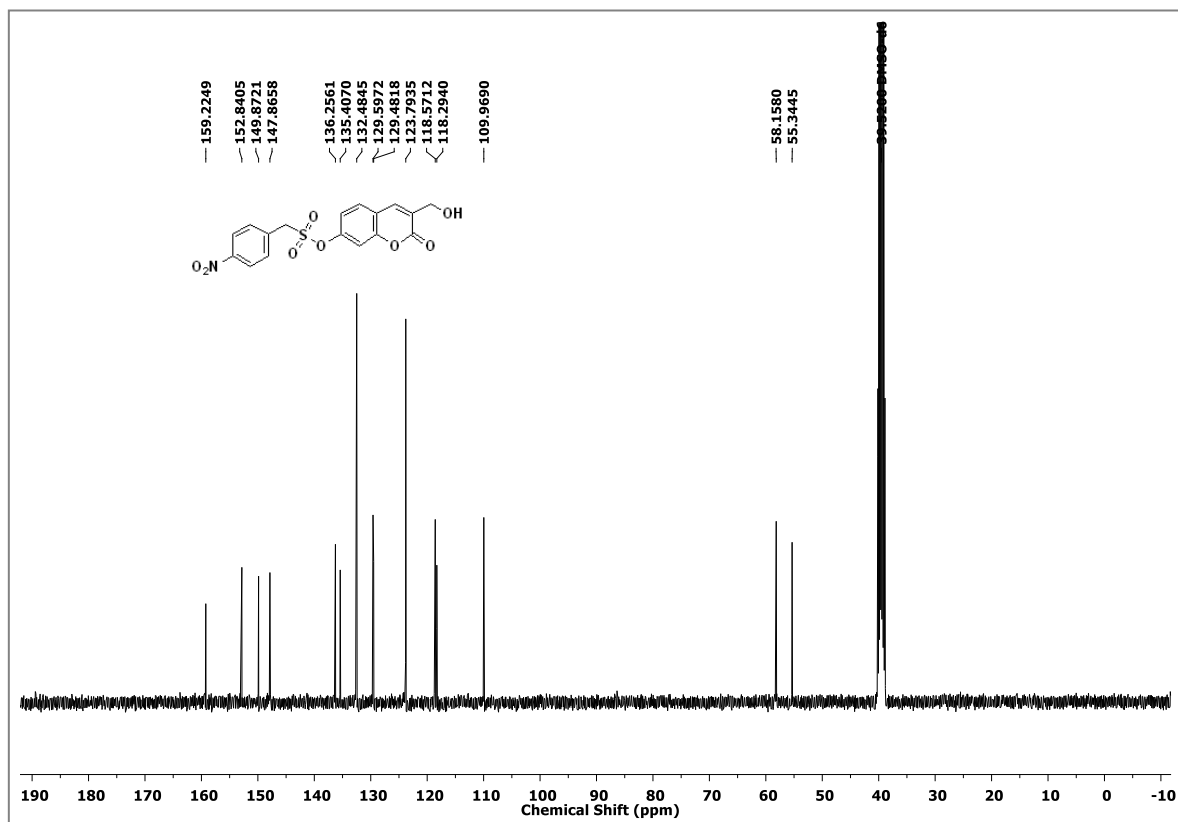
^{1}H NMR Spectrum (400 MHz, CDCl$_3$) of **39**
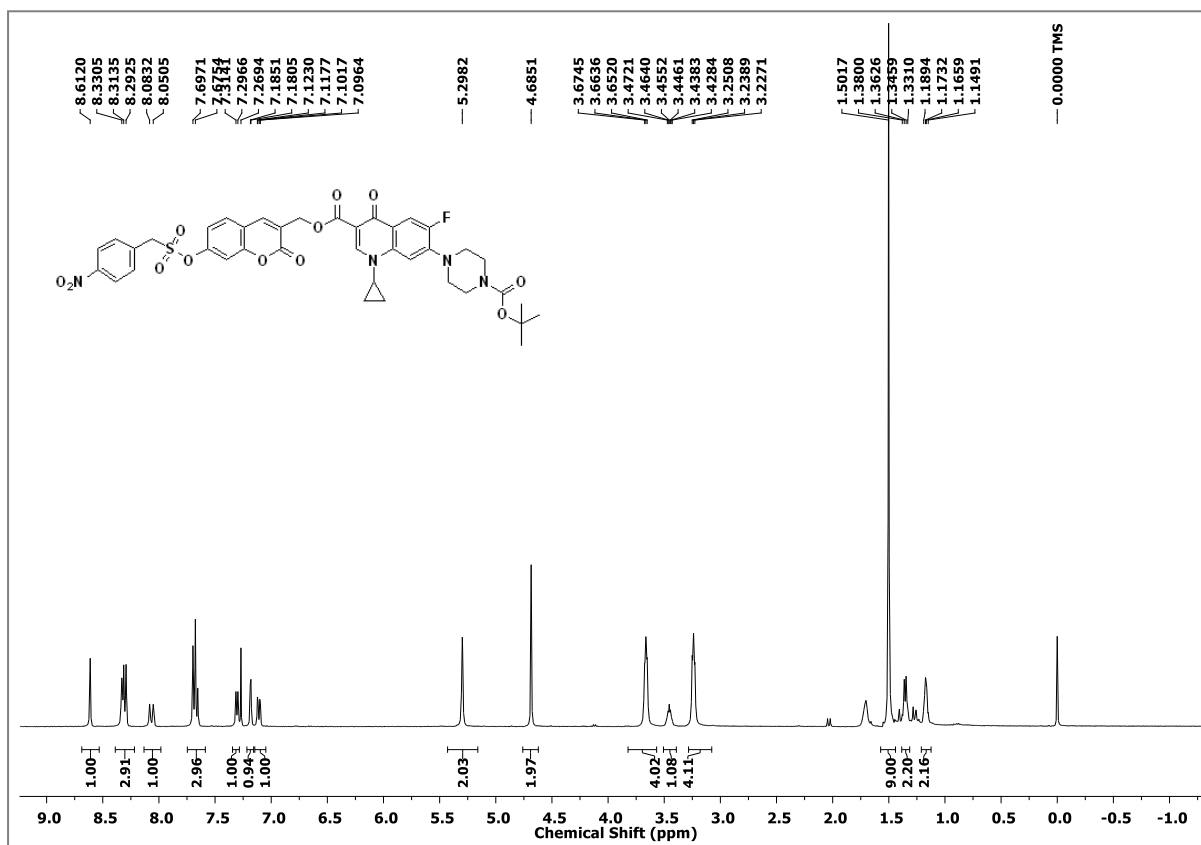
^{13}C NMR Spectrum (100 MHz, CDCl$_3$) of **39**
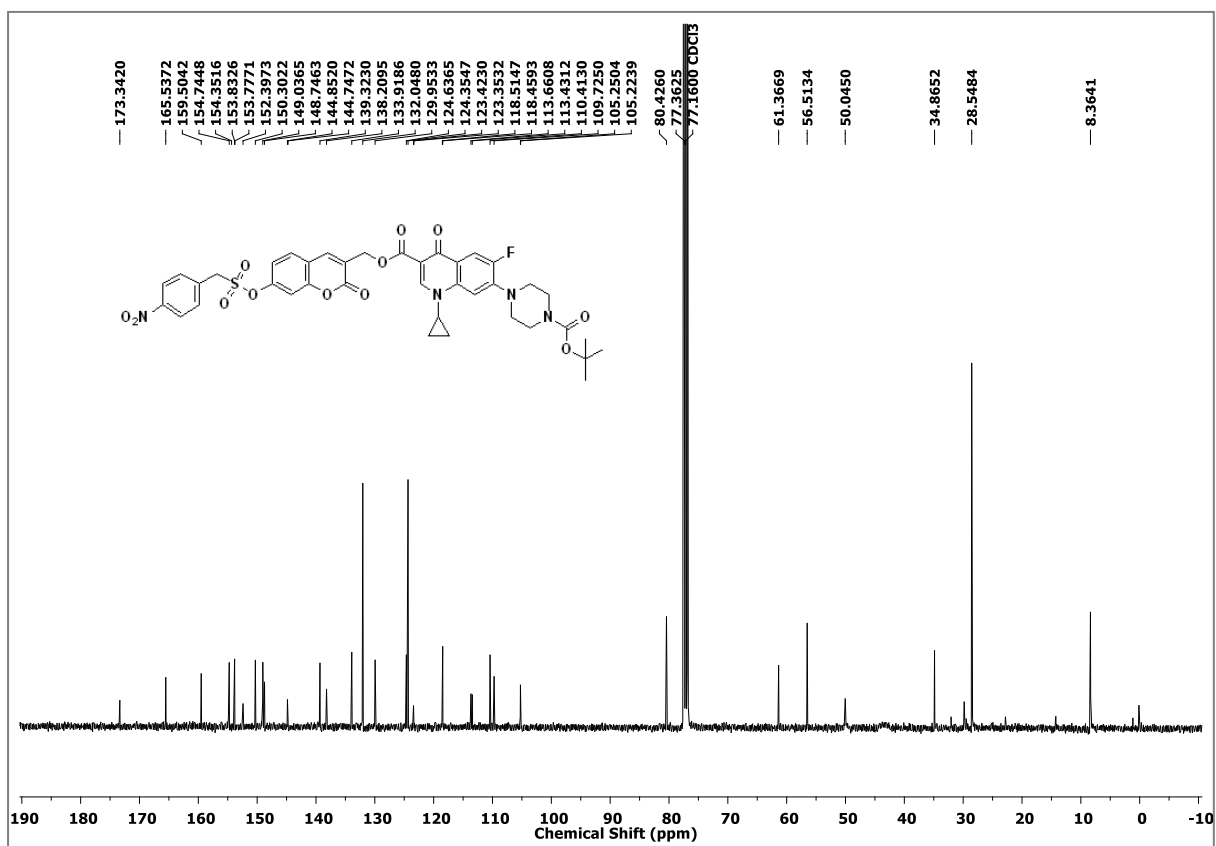
^{1}H NMR Spectrum (400 MHz, DMSO-d_6) of **40**
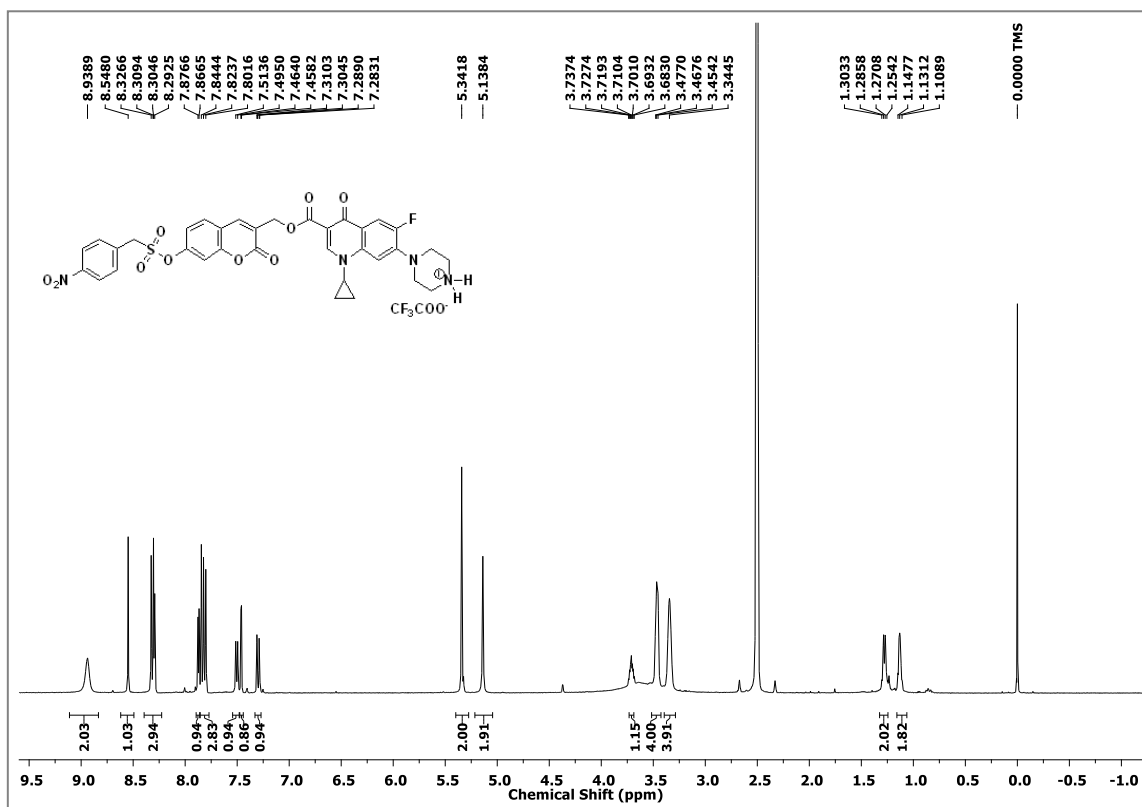
^{13}C NMR Spectrum (100 MHz, DMSO-d_6) of **40**
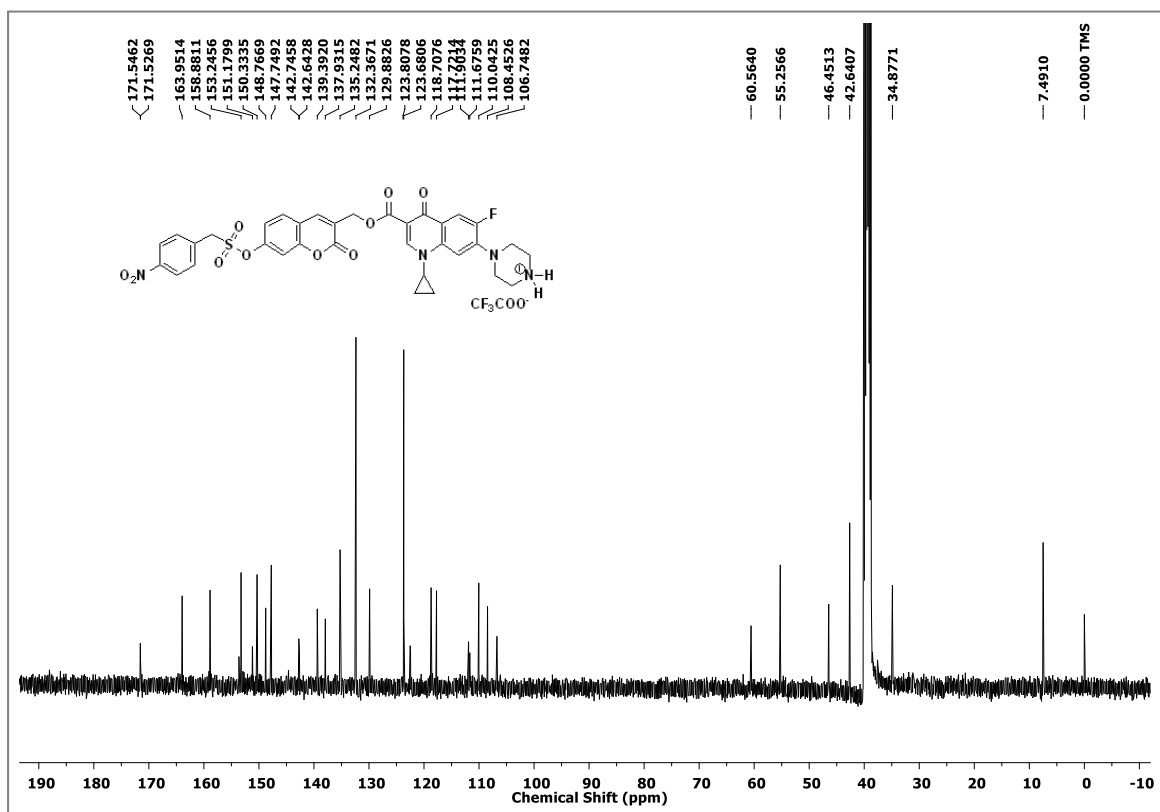
References

(1)   Pardeshi, K. A.; Ravikumar, G.; Chakrapani, H. Esterase Sensitive Self-Immolative Sulfur Dioxide Donors. *Org. Lett.* **2018**, *20* (1), 4–7.

(2)   Rautio, J.; Kumpulainen, H.; Heimbach, T.; Oliyai, R.; Oh, D.; Järvinen, T.; Savolainen, J. Prodrugs: Design and Clinical Applications. *Nat. Rev. Drug Discov.* **2008**, *7* (3), 255–270.

(3)   Malwal, S. R.; Sriram, D.; Yogeeswari, P.; Konkimalla, V. B.; Chakrapani, H. Design, Synthesis, and Evaluation of Thiol-Activated Sources of Sulfur Dioxide (SO 2) as Antimycobacterial Agents. *J. Med. Chem.* **2012**, *55* (1), 553–557.

(4)   Çelik, A.; Yetiş, G. An Unusually Cold Active Nitroreductase for Prodrug Activations. *Bioorganic Med. Chem.* **2012**, *20* (11), 3540–3550.

(5)   Pitsawong, W.; Hoben, J. P.; Miller, A. F. Understanding the Broad Substrate Repertoire of Nitroreductase Based on Its Kinetic Mechanism. *J. Biol. Chem.* **2014**, *289* (22), 15203–15214.

(6)   Roldán, M. D.; Pérez-Reinado, E.; Castillo, F.; Moreno-Vivián, C. Reduction of Polynitroaromatic Compounds: The Bacterial Nitroreductases. *FEMS Microbiol. Rev.* **2008**, *32* (3), 474–500.

(7)   Williams, E. M.; Little, R. F.; Mowday, A. M.; Rich, M. H.; Chan-Hyams, J. V. E.; Copp, J. N.; Smaill, J. B.; Patterson, A. V.; Ackerley, D. F. Nitroreductase Gene-Directed Enzyme Prodrug Therapy: Insights and Advances toward Clinical Utility. *Biochem. J.* **2015**, *471* (2), 131–153.

(8)   Walther, R.; Rautio, J.; Zelikin, A. N. Prodrugs in Medicinal Chemistry and Enzyme Prodrug Therapies. *Adv. Drug Deliv. Rev.* **2017**, *118*, 65–77.

(9)   Hu, L.; Wu, X.; Han, J.; Chen, L.; Vass, S. O.; Browne, P.; Hall, B. S.; Bot, C.; Gobalakrishnapillai, V.; Searle, P. F.; et al. Synthesis and Structure-Activity Relationships of Nitrobenzyl Phosphoramide Mustards as Nitroreductase-Activated Prodrugs. *Bioorganic Med. Chem. Lett.* **2011**, *21* (13), 3986–3991.

(10)   Patterson, S.; Wyllie, S. Nitro Drugs for the Treatment of Trypanosomatid Diseases: Past, Present, and Future Prospects. *Trends Parasitol.* **2014**, *30* (6), 289–298.

(11)   Hof, H. Antibacterial Activities of the Antiparasitic Drugs Nifurtimox and Benznidazole. *Antimicrob. Agents Chemother.* **1989**, *33* (3), 404–405.

(12)   Singh, R.; Manjunatha, U.; Boshoff, H.; Ha, Y.; Niyomrattanakit, P.; Ledwidge, R.; Dowd, C.; Lee, I.; Kim, P.; Zhang, L.; et al. PA-824 Kills Nonreplicating. *Science (80-.).* **2008**, *322* (November), 1392–1395.

(13)   Sykes, B. M.; Hay, M. P.; Bohinc-Herceg, D.; Helsby, N. A.; O'Connor, C. J.; Denny, W. A. Leaving Group Effects in Reductively Triggered Fragmentation of 4-Nitrobenzyl Carbamates. *J. Chem. Soc. Perkin Trans. 1* **2000**, No. 10, 1601–1608.

(14)   Sun, Y. Q.; Liu, J.; Zhang, J.; Yang, T.; Guo, W. Fluorescent Probe for Biological Gas SO2derivatives Bisulfite and Sulfite. *Chem. Commun.* **2013**, *49* (26), 2637–2639.

(15)   Wolfbeis, O. S. An Overview of Nanoparticles Commonly Used in Fluorescent Bioimaging. *Chem. Soc. Rev.* **2015**, *44* (14), 4743–4768.

(16)   Zhao, Z.; Yan, R.; Yi, X.; Li, J.; Rao, J.; Guo, Z.; Yang, Y.; Li, W.; Li, Y. Q.; Chen, C. Bacteria-Activated Theranostic Nanoprobes against Methicillin-Resistant Staphylococcus Aureus Infection. *ACS Nano* **2017**, *11* (5), 4428–4438.

(17)   Hou, J. T.; Li, K.; Liu, B. Y.; Liao, Y. X.; Yu, X. Q. The First Ratiometric Probe for Lysine in Water. *Tetrahedron* **2013**, *69* (9), 2118–2123.

(18)   Wang, Y.; Shim, M. S.; Levinson, N. S.; Sung, H. W.; Xia, Y. Stimuli-Responsive Materials for Controlled Release of Theranostic Agents. *Adv. Funct. Mater.* **2014**, *24* (27), 4206–4220.

(19)   Van Oosten, M.; Schäfer, T.; Gazendam, J. A. C.; Ohlsen, K.; Tsompanidou, E.; De Goffau, M. C.; Harmsen, H. J. M.; Crane, L. M. A.; Lim, E.; Francis, K. P.; et al. Real-Time in Vivo Imaging of Invasive- and Biomaterial-Associated Bacterial Infections Using Fluorescently Labelled Vancomycin. *Nat. Commun.* **2013**, *4*.

(20)   Wang, T.; Wang, C.; Zhou, S.; Xu, J.; Jiang, W.; Tan, L.; Fu, J. Nanovalves-Based Bacteria-Triggered, Self-Defensive Antibacterial Coating: Using Combination Therapy, Dual Stimuli-Responsiveness, and Multiple Release Modes for Treatment of Implant-Associated Infections. *Chem. Mater.* **2017**, *29* (19), 8325–8337.

(21)   Zhang, Z.; Taylor, M.; Collins, C.; Haworth, S.; Shi, Z.; Yuan, Z.; He, X.; Cao, Z.;

Park, Y. C. Light-Activatable Theranostic Agents for Image-Monitored Controlled Drug Delivery. *ACS Appl. Mater. Interfaces* **2018**, *10* (2), 1534–1543.

(22)   Panizzi, P.; Nahrendorf, M.; Figueiredo, J. L.; Panizzi, J.; Marinelli, B.; Iwamoto, Y.; Keliher, E.; Maddur, A. A.; Waterman, P.; Kroh, H. K.; et al. In Vivo Detection of Staphylococcus Aureus Endocarditis by Targeting Pathogen-Specific Prothrombin Activation. *Nat. Med.* **2011**, *17* (9), 1142–1147.

(23)   Thakur, M.; Pandey, S.; Mewada, A.; Patil, V.; Khade, M.; Goshi, E.; Sharon, M. Antibiotic Conjugated Fluorescent Carbon Dots as a Theranostic Agent for Controlled Drug Release, Bioimaging, and Enhanced Antimicrobial Activity. *J. Drug Deliv.* **2014**, *2014*, 282193.

(24)   Gopinath, P. M.; Ranjani, A.; Dhanasekaran, D.; Thajuddin, N.; Archunan, G.; Akbarsha, M. A.; Gulyás, B.; Padmanabhan, P. Multi-Functional Nano Silver: A Novel Disruptive and Theranostic Agent for Pathogenic Organisms in Real-Time. *Sci. Rep.* **2016**, *6* (September), 1–16.

(25)   Weinstain, R.; Segal, E.; Satchi-Fainaro, R.; Shabat, D. Real-Time Monitoring of Drug Release. *Chem. Commun.* **2010**, *46* (4), 553–555.

(26)   Redgrave, L. S.; Sutton, S. B.; Webber, M. A.; Piddock, L. J. V. Fluoroquinolone Resistance: Mechanisms, Impact on Bacteria, and Role in Evolutionary Success. *Trends Microbiol.* **2014**, *22* (8), 438–445.

(27)   Scheld, W. M. Maintaining Fluoroquinolone Class Efficacy: Review of Influencing Factors. *Emerg. Infect. Dis.* **2003**, *9* (1), 1–9.

(28)   Sharma, P. C.; Jain, A.; Jain, S. Fluoroquinolone Antibacterials: A Review on Chemistry, Microbiology and Therapeutic Prospects. *Acta Pol. Pharm. - Drug Res.* **2009**, *66* (6), 587–604.

(29)   Tehler, U.; Fagerberg, J. H.; Svensson, R.; Larhed, M.; Artursson, P.; Bergström, C. A. S. Optimizing Solubility and Permeability of a Biopharmaceutics Classification System (BCS) Class 4 Antibiotic Drug Using Lipophilic Fragments Disturbing the Crystal Lattice. *J. Med. Chem.* **2013**, *56* (6), 2690–2694.

Chapter 1: Introduction

Reactive Species

Reactive species are N, O and S centered small reactive molecules. These species are broadly classified into three major classes namely reactive oxygen species (ROS), reactive nitrogen species (RNS) and reactive sulfur species (RSS). These species are produced endogenously and are freely diffusible across the cell membranes. At elevated concentrations, the reactive species are hazardous to cells and can cause cell death by damaging macromolecules such as DNA, proteins and lipids. However, at moderate concentration, they have a profound effect in a vast array of cellular processes such as cell signaling, metabolism, redox homeostasis. and these species are the primary immune response to counter various infectious diseases.[1-7]
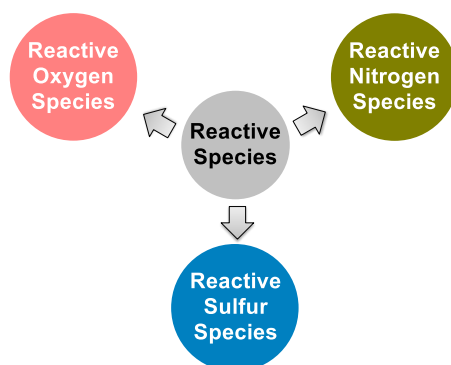
Figure 1. Reactive species in the biological system

Chemical biology of endogenous SO$_2$

Nitric oxide (NO), carbon monoxide (CO) and hydrogensulfide (H$_2$S) are gaseous environmental pollutant but are also synthesized endogenously and have been shown to perform diverse physiological and pathophysiological functions inside the cell. These gaseous molecules are classified as cell signaling molecules or gasotransmitters. The major role performed by all these three gases is to regulate the vascular homeostasis and central nervous system functions.[8] Sulfur dioxide (SO$_2$) a reactive sulfur species is also found to be generated endogenously and performs similar functions as to that of cell signaling molecules. SO$_2$ could be the potential fourth gaseous molecule in the family gasotransmitters. SO$_2$ has found to show significant vasodilatory effects. As SO$_2$ is being looked upon a potential entrant in gasotransmitter family multiple reports suggesting its participation in diverse physiological and pathophysiological function are surfaced in past few years.[9-14]

Thus looking at all different reports on SO_2, it deserves an extensive attention. All the reports need to be further validated to fully understand SO_2 biology and to establish SO_2 as the fourth gasotransmitter in the family.

Controlled generation of SO_2

To understand the chemical biology of SO_2 within cells, promising SO_2 donors needed to be cell permeable. Also, the generation of SO_2 in a controlled manner with endogenous activation is highly desirable. Usually, to study chemical biology of SO_2, it is either employed in gaseous form or predominantly in the form of inorganic salts (sulfinating agents) as a surrogate for SO_2. These salts have poor bioavailability being a charged molecular species and required at higher concentration to elicit a response in physiological and pathophysiological processes and this may compromise the final interpretations regarding SO_2.[13,15] Therefore, new and efficient SO_2 donors are highly anticipated to study the precise role of SO_2 in chemical biology and to assess its unique therapeutic potential. Few existing organic donors of SO_2 have been shown to produce SO_2 under biologically relevant conditions with certain limitations.

Thiol activated SO_2 donors as antimycobacterial agents

The first report of sulfur dioxide donors in the literature describing the anti-bacterial effects was from our laboratory in 2012. The authors used a 2,4-dinitrophenylsulfonamide as the major functional group for generating sulfur dioxide. This functional group has been used as a protective group in organic synthesis previously and is deprotected by thiols. Since cellular thiols occur in large concentrations, Malwal and co-workers demonstrated the suitability of this series of compounds as sources of sulfur dioxide. They find that the rate of sulfur dioxide generation was dependent on the nature of the amine. The more basic the amine was, the faster was the sulfur dioxide generation. Thus, simple structural modifications that affected the basicity of the amine formed the basis for modulating SO_2 release rates.[16-18]

2,4 dinitrosulfonyl group (DNs)   Amine
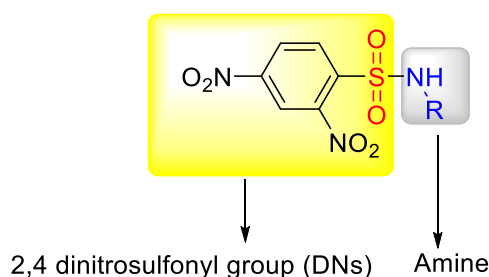
Figure 2. DNs protected scaffold for SO_2 generation
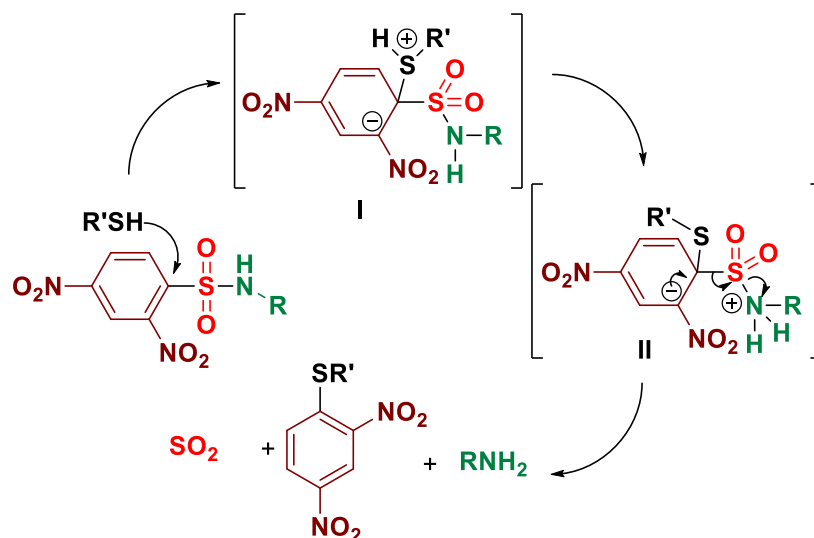
Scheme 1. Thiol activated SO$_2$ generation

The authors evaluated the potential for these compounds to inhibit bacterial growth and they found that, among closely related compounds, the propensity to inhibit mycobacterial growth was dependent on the rate of sulfur dioxide generation. The lead compound was found to have low micromolar inhibitory potency against *Mycobacterium tuberculosis*, the causative agent of tuberculosis, a disease that affects millions each year. A recent study on the effects of sulfur dioxide on tuberculosis occurrence in human populations was conducted. The authors found protective effects of this gas when patients were exposed to low-level ambient sulfur dioxide against TB.[19]

Chapter 2. Thiol activated SO$_2$ donors as MRSA inhibitors

Benzylamine lead derivative, which had potent anti-mycobacterial activity evaluated for the broad-spectrum antibacterial activity and found to be inactive against other gram-positive as well as gram-negative bacteria.

Next, starting with thiol activated SO$_2$ donors to target the other strains of bacteria. We did a series of structural modifications on thiol activated sulfur dioxide donors that led to improved anti-bacterial properties. These SO$_2$ donors were found to be potent inhibitors of *MSSA*. Also, these donors were found to be excellent inhibitors infectious bacteria like *MRSA* and *E. feacalis*. Antibacterial activity of lead compound was found to be comparable with clinically used antibiotics against patient-derived strains of *MRSA* (Table 1).
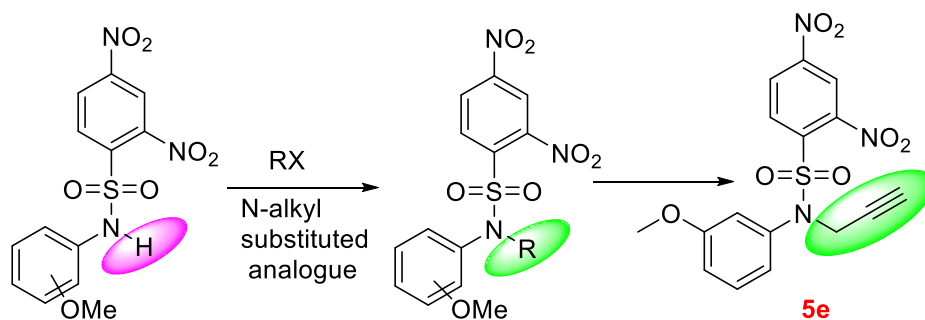
Figure 3. Selected synthesis of thiol activated SO_2 donors

Table 1. Inhibitory data of **5e** against clinical isolates of *MRSA*

Comp	*MRSA* 7419	B19506	*MRSA* K-1	*MRSA* 7425	*MRSA* 7386
5e	4	2	4	2	2
Vancomycin	1	1	1	1	2
Linezolid	2	4	2	4	2
Ciprofoxacin	>4	32	0.5	>4	>4
Meropenem	16	1	0.5	4	>32
Tobramycin	>32	>32	8	1	>32

Next, we estimated of intracellular generation of oxidative species using DCFH2-DA assay. Thiol attack at 2,4 dinitrosulfony group to generate SO_2 and oxidative reactive species (RS) resulting in biomacromolecular damage.[20-23] We tested the ability of **5e** to produce oxidative species intracellularly using 7-dichlorodihydrofluorescein-diacetate (DCFH2-DA) assay.[24,25] We found increased fluorescence levels intracellularly in *S. aureus* upon incubation with **5e** (Figure 5). This result was indicative of production of oxidative species and perhaps, induction of oxidative stress was the mechanism of action.
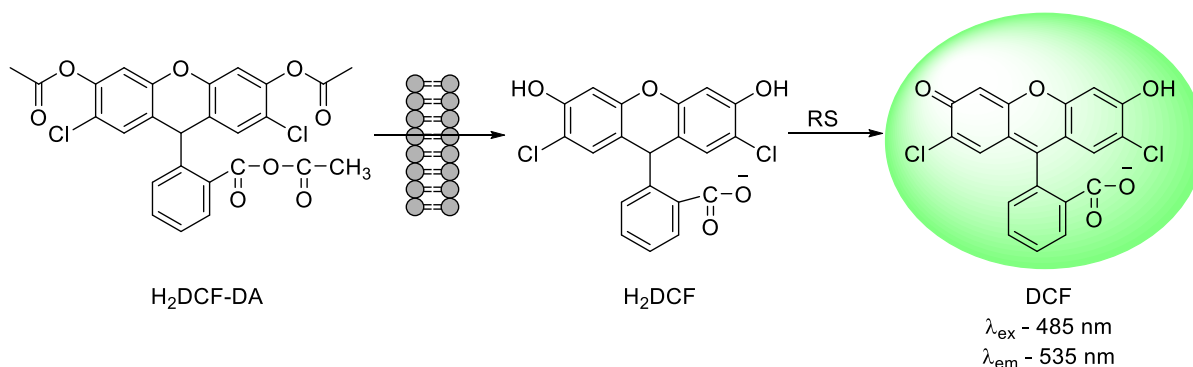
Figure 4. Oxidation of non-fluorescent H2DCF-DA by RS to fluorescent dye, DCF
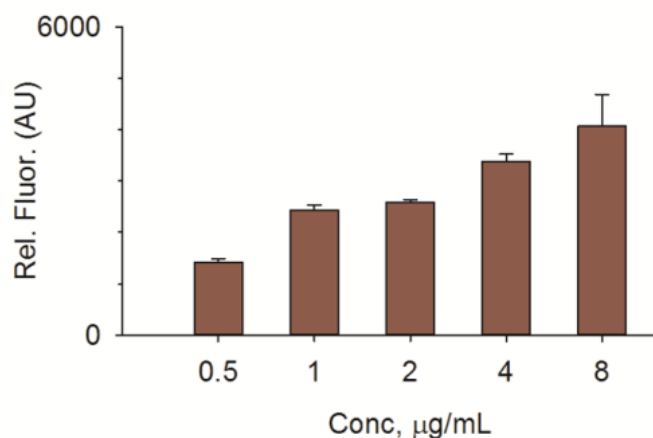
Figure 5. Dose dependent increase in fluorescence upon treatment of **5e** against *MSSA* indicative of formation of reactive sulfur species (DCF assay)

Next, we synthesized series of double SO_2 donors. Sulfur dioxide donors reported showed significant antibacterial activity. To explore it further we reasoned the possibility of enhancement in the efficacy of existing thiol activated sulfur dioxide donors on the increment of SO_2 payload. Therefore to test further the effect of increased payload of SO_2, we synthesized double SO_2 donors (Figure 6). They were all found to be inactive.
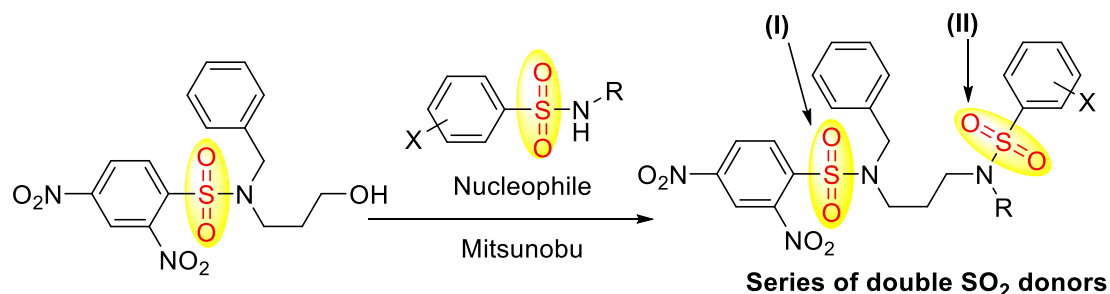
Figure 6. Synthesis of thiol activated double SO_2 donors

Next, we performed thiol depletion assay. Our hypothesis was the antibacterial activity of SO_2 prodrugs is mediated by compound's entry into cells followed by thiol attack at 2,4-dinitrosulfony group to generate SO_2 intracellularly. Therefore, intracellular generation of oxidative reactive sulfur species. Depletion of free thiols might thus occur as a response to enhanced oxidative species as well. A monobromobimane (mBBr) protocol was used to assess levels of free thiols within cells. The weakly fluorescent mBBr reacts with thiols and is converted to a highly fluorescent adduct.[26] Hence, increased fluorescence response in this assay is an indicator of free thiol levels inside cells and vice versa.
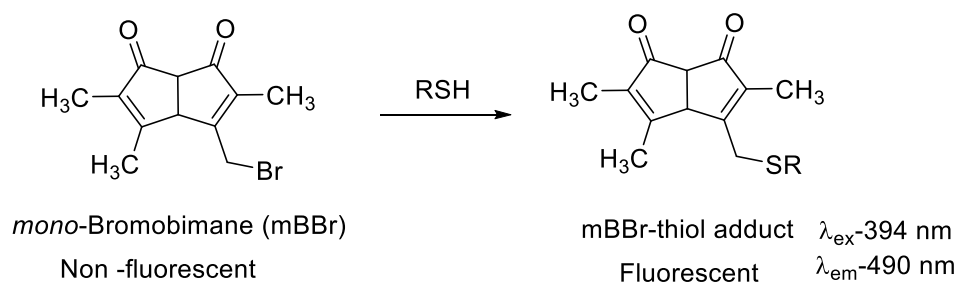
Figure 7. Thiol depletion assay for 2,4-Dinitrobenzenesulfonamide based SO_2 donors

Double SO_2 donor **9d** and compound **8b** with poor inhibitory activity against *MRSA* showed an enhanced fluorescence signal indicating their diminished capacity to deplete thiols (Figure 8). Whereas, **5e** depleted thiol significantly. In this experiment, we used a known thiol-reactive compound *N*-ethylmaleimide (NEM) as the positive control and we found a diminished fluorescence that is consistent with decreased thiol levels. These data indicated that the capacity of the compound to permeate cells to deplete free thiols played a significant role in the observed inhibitory potency.
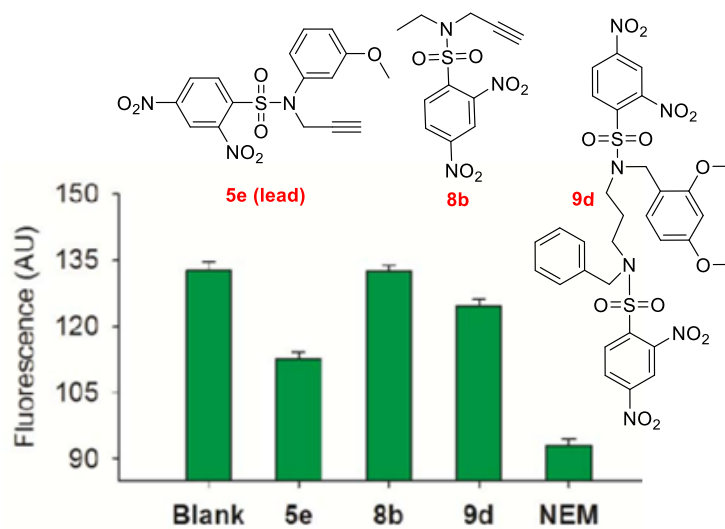
Figure 8. Intracellular thiol depletion in *S. aureus* upon treatment with the compounds

Chapter 3 Esterase sensitive Self–Immolative SO₂ Donors

The existing organic donors of SO_2 have either have sulfone or sulfinate moiety in their chemical scaffold (Scheme 2).
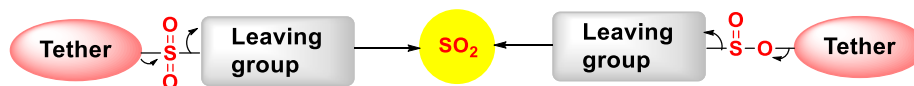
Scheme 2. General sulfone and sulfinate based methods of SO_2 donors

In our new proposed design, we considered the chemistry associated with decomposition of carbonates, which has been extensively used for drug delivery. Similarly, in case of sulfonate C-S Bond dissociation energy (BDE) is comparable with that of C-O of carbonate (Scheme 3, shown by arrow).[27] Therefore, based on the carbonate model, we have reported a sulfonate ester that undergoes self-immolation in the presence of esterase to produce sulfur dioxide and an alcohol (Scheme 3). A large majority of the sulfonates evaluated were found to generate sulfur dioxide. Certain donors which are derived from aliphatic alcohols were found to hydrolyze even in the absence of esterase without generation sulfur dioxide.
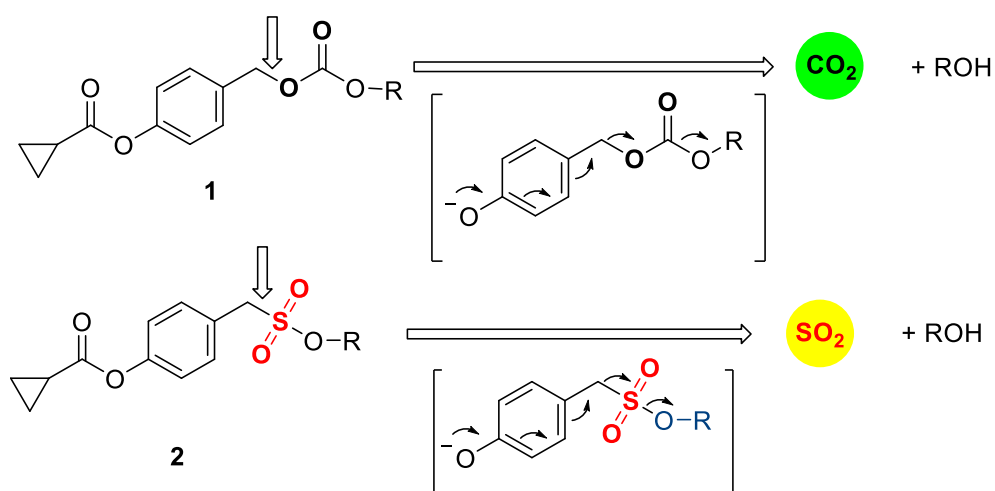
Scheme 3. Esterase activated SO_2 donors

Next, we synthesized **17a** and monitored the self-immolation reaction of it by HPLC. When incubated with esterase, was found to undergo self-immolation efficiently to generate umbelliferone (Umb).
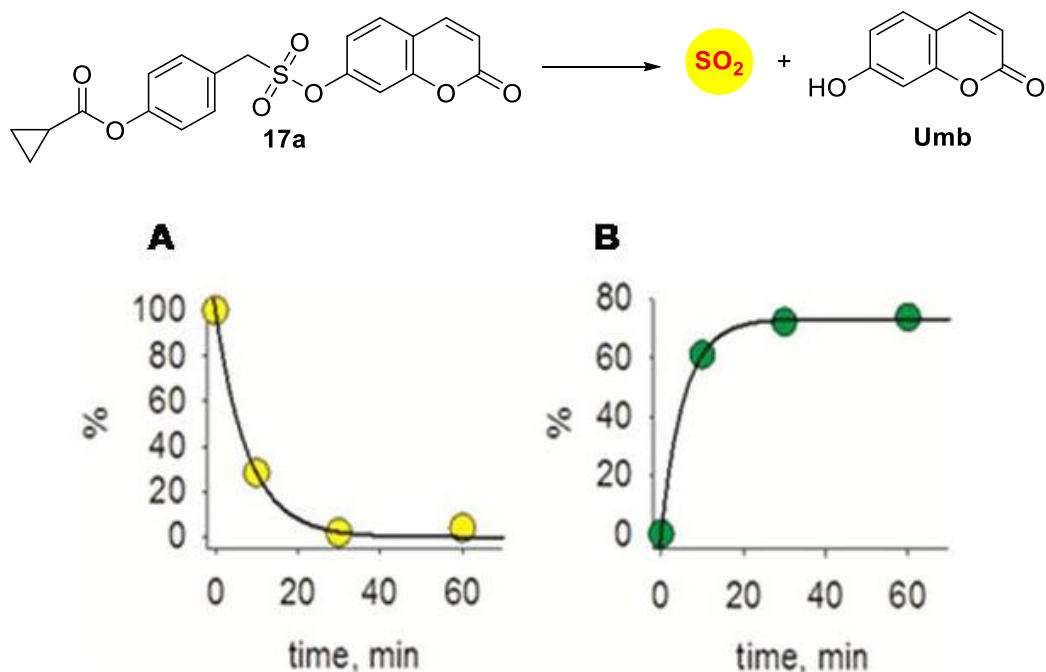
Figure 9. HPLC analysis of **17a** (A) Disappearance of **17a** (50 µM) upon incubation with esterase, in PBS (pH 7.4, 10 mM) at 37 ºC disappeared (B) Concomitant appearance of Umb

λ$_{ex}$ - 545 nm; λ$_{em}$ - 633 nm λ$_{ex}$ - 410 nm; λ$_{em}$ - 478 nm
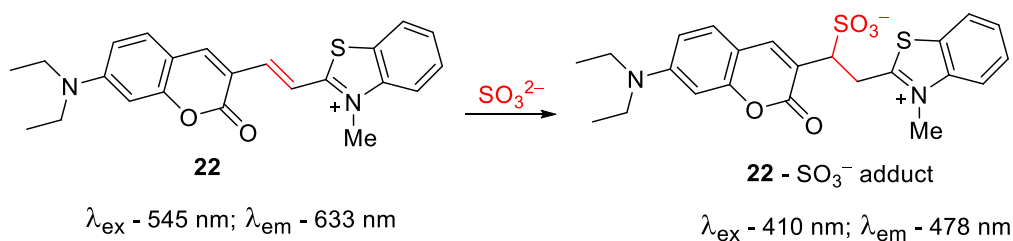
Scheme 4. Calorimetric and fluorimetric probe for detection of SO$_2$

Next, SO$_2$ was also expected to be formed during the self-immolation. SO$_2$ gets converted to its hydrated form (sulfite/bisulfite) in physiological condition. For the detection of sulfite generated from **17a**, coumarin−hemicyanine dye **22** was used for colorimetric detection of sulfite (Scheme 4). However, it was not possible detect sulfite accurately due to interference of Umb in absorption signal upon self-immolation of **17a**. The other compounds in the series

found to generate SO_2 without any interference (Figure 10, please see representative example of **17c**). Also, The probe **22** has been found to be the useful in fluorimetric based detection of sulfite *in vitro* and for cellular-based studies (Figure 11). This series of compounds will be potentially useful for studying the chemical biology of sulfur dioxide.[5]
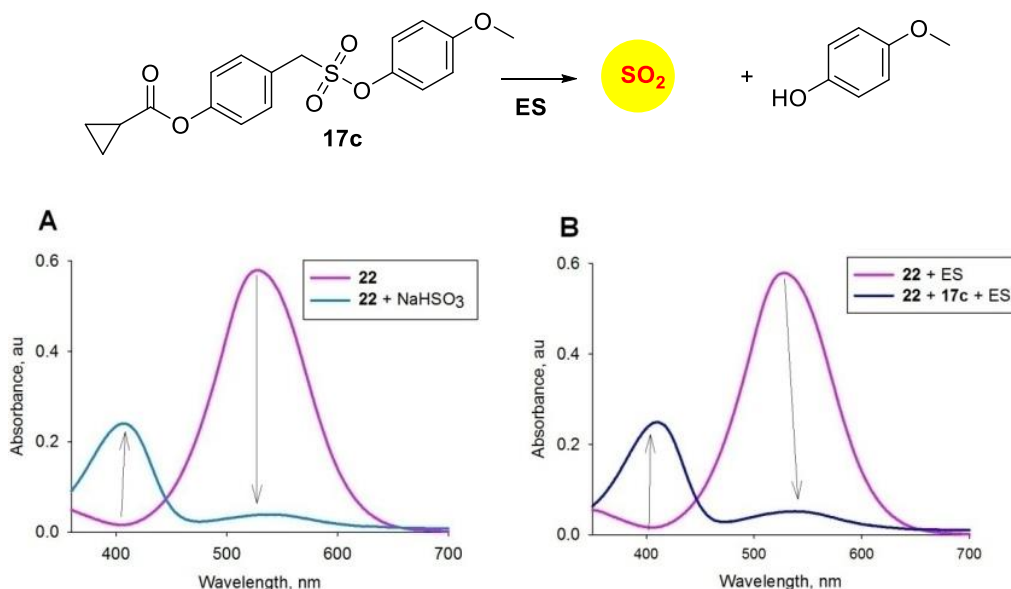
Figure 10. Representative absorbance spectra (A) Incubation of **22** (10 µM) in the presence of positive control $NaHSO_3$ (50 µM) shows a decrease in absorbance at 545 nm and a corresponding increase in absorbance at 410 nm. (B) Similar profile was observed with Incubation of our SO_2 donor **17c** (50 µM) and **22** (10 µM) in the presence of ES. This result was indicative of sulfite generation
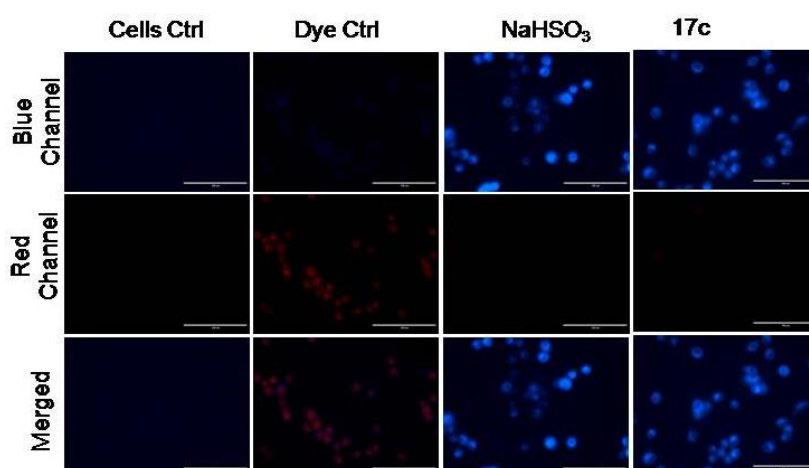
Figure 11. Fluorescence microscopy images of A549 cells treated with **22** and independently incubated with positive control $NaHSO_3$ and **17c**. Thus the SO_2 donors were found to permeate cells to generate sulfite.

Chapter3.

Theranostics

Esterase sensitive self-immolative sulfonates were found to be stable in different pHs and in the presence of biological nucleophiles.Therefore it presented an opportunity to develop SO_2 based prodrugs for drug delivery. Since SO_2 is a widely used food preservative and an antibacterial agent, we developed a SO_2 donor-conjugated theranostic prodrug molecule to deliver clinically used antibiotic and fluorophore that can be specifically activated by bacterial enzymes.
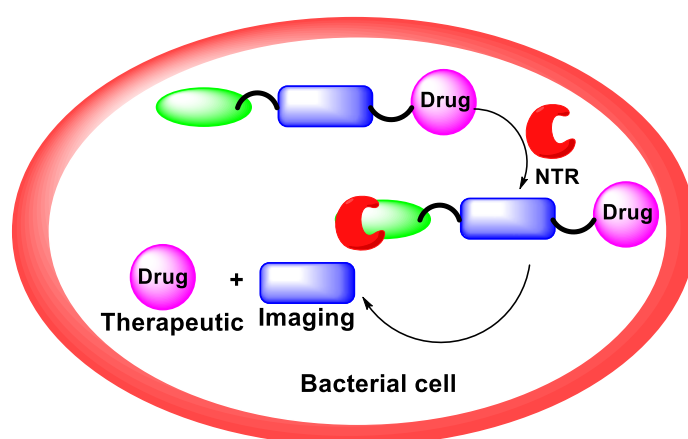
Figure 12. Nitroreductase activated, theranostic prodrug approach for bacteria

Theranostics is rapidly emerging field with vast potential due to its therapeutic and diagnostic application in a single platform. Diagnostics in any infectious disease is an important aspect to cure the disease at an early stage of infection by which morbidity and mortality will be greatly reduced. No secondary assays are required in order to image delivered drug. However, limited numbers of reports are available for small molecule theranostics in bacteria.[28-34] For activation of the drug in a specific mode, we considered specific stimulus such as nitroreductase (NTR). Nitroreductasesare from flavoenzyme family widely distributed among the numerous bacterial species and to a lesser extent in mammalian hypoxic tissues and mitochondria. Nitroreductases are used in several prodrug or drugs delivery strategies. Initially a set of prototypic compounds were synthesized and evaluated for their antibacterial activity. Modelled on these compounds, a theranostic prodrug (**40**) was synthesized, for delivery of clinically used drug along with fluorophore for real-time imaging in bacteria.

When **40** was incubated with NTR, it was found to undergo self-immolation to generate fluorescence (Figure 13) and also in *E. coli* monitored by cellular imaging. Similarly when reaction was monitored by HPLC, compound **40** found to generate corresponding fluorophore and drug (Figure 14)
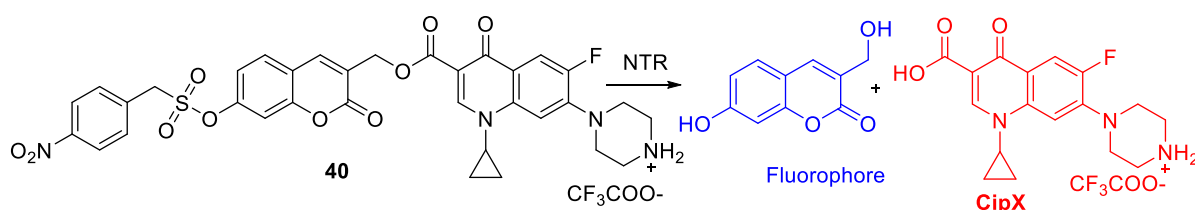
Scheme 5. NTR activation and generation of Fluorophore and Ciprofloxcin simultaneously upon self-immolation
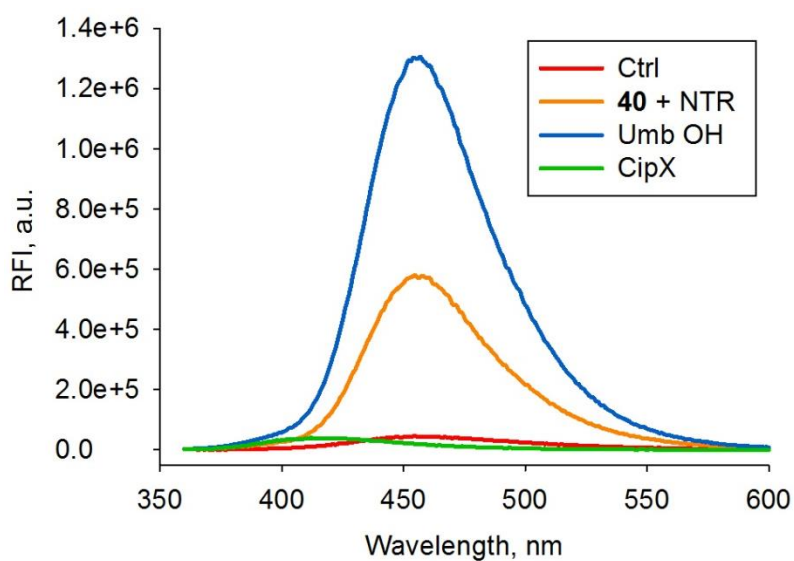
Figure 13. Monitoring the release of fluorophore from **40** upon NTR activation (10 µg/mL) along with the NADH (30 µM) in PBS (pH 7.4, 10mM)
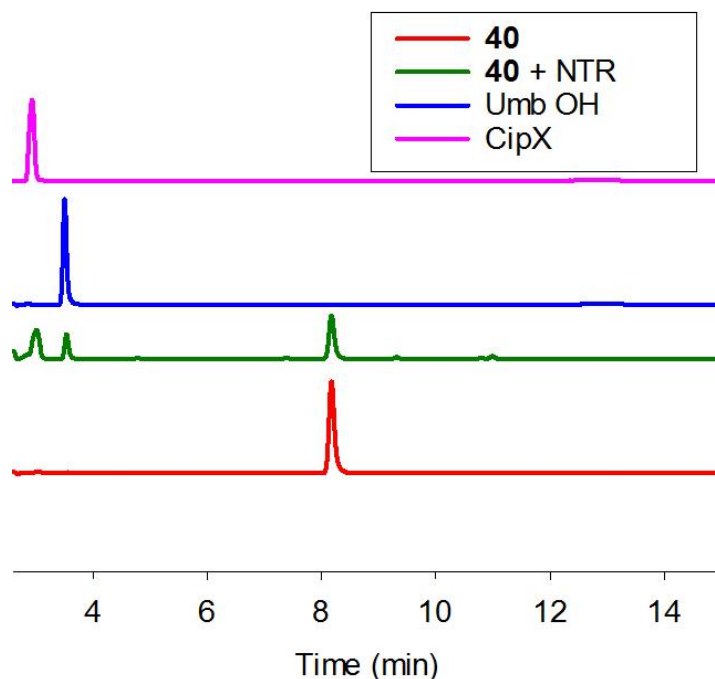
Figure 14. Monitoring the release drug and fluorophore from **40** (Theranostic prodrug) by an HPLC upon activation with NTR (20 µg/mL) and NADH (75 µM) in PBS (pH 7.4, 10mM)

Next, in order to test the stability of our nitroreductase specific fluoroquinolones conjugated compounds in mammalian cellular condition and for its nonspecific activation, Hela cell lysates were exposed to the fluorophore-conjugated compounds **24**, **35**, and **40** in with our esterase activated SO_2 donor **17a** as a reference compound (Figure 15). We found no significant fluorescence signal corresponding to fluorophore formation. As nitroreductases are not normally present in mammalian cells, it is understandable that reduction of the nitro group is not efficient and does not generate the fluorophore. Taken together, our data support the selectivity, specificity and broad-range stability of nitroreductase activated prodrug.
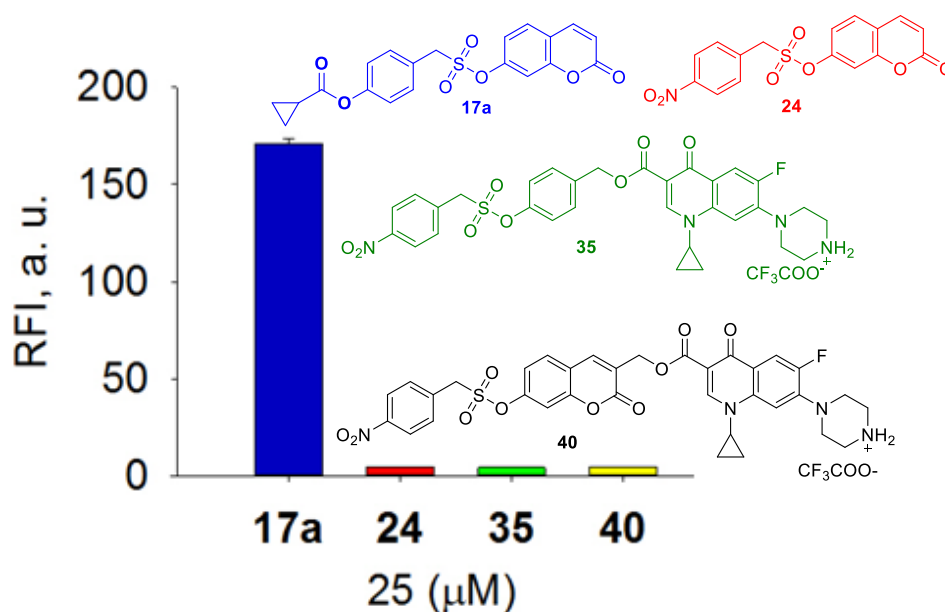
Figure 15. Monitoring the release of Umb and Umb OH fluorophores from compounds (25 µM) in Hela cell lysate

Next, we found excellent antibacterial activity for compound **40** against *E. Coli* (0.0625 µg/mL) and a superbug *P. aeruginosa* (4 µg/mL) which are difficult to treat.Compound **40** appeared to be well tolerated in mammalian cells when tested for cytotoxicity. According to our knowledge, this is the first report of the small molecule theranostic prodrug approach to bacteria with NTR as a specific stimulus. This method is advantageous as it offers a completely new class of prodrug molecules, with stability of sulfonate linker and specificity of NTR as enzymatic trigger. The theranostic approach takes it to completely different level with a unique offering of real-time monitoring of drug release in bacteria.

1.10. References

(1)   Halliwell, B. Reactive Species, and Antioxidants. Redox Biology Is a Fundamental Theme of Aerobic Life. *Plant Physiol.***2006**, *141* (2), 312–322.

(2)   Winterbourn, C. C.; Kettle, A. J.; Hampton, M. B. Reactive Oxygen Species, and Neutrophil Function. *Annu. Rev. Biochem.***2016**, *85* (1), 765–792.

(3)   Sharma, P.; Jha, A. B.; Dubey, R. S.; Pessarakli, M. Reactive Oxygen Species, Oxidative Damage, and Antioxidative Defense Mechanism in Plants under Stressful Conditions. *J. Bot.***2012**, *2012*, 1–26.

(4)   Giles, G.; Nasim, M.; Ali, W.; Jacob, C. The Reactive Sulfur Species Concept: 15 Years On. *Antioxidants* **2017**, *6* (2), 38.

(5)   Chaki, M.; Valderrama, R.; Fernández-Ocaña, A. M.; Carreras, A.; Gómez-Rodríguez, M. V.; Pedrajas, J. R.; Begara-Morales, J. C.; Sánchez-Calvo, B.; Luque, F.; Leterrier, M.; et al. Mechanical Wounding Induces a Nitrosative Stress by down-Regulation of GSNO Reductase and an Increase in S-Nitrosothiols in Sunflower (Helianthus Annuus) Seedlings. *J. Exp. Bot.* **2011**, *62* (6), 1803–1813.

(6)   Stipanuk, M. H. SULFUR AMINO ACID METABOLISM: Pathways for Production and Removal of Homocysteine and Cysteine. *Annu. Rev. Nutr.* **2004**, *24* (1), 539–577.

(7)   Wang, X. B.; Jin, H. F.; Tang, C. S.; Du, J. B. Significance of Endogenous Sulphur-Containing Gases in the Cardiovascular System: Frontiers in Research Review: The Pathophysiological Significance of Sulphur-Containing Gases. *Clin. Exp. Pharmacol. Physiol.* **2010**, *37* (7), 745–752.

(8)   Li, L.; Moore, P. K. An Overview of the Biological Significance of Endogenous Gases: New Roles for Old Molecules. *Biochem. Soc. Trans.* **2007**, *35* (5), 1138–1141.

(9)   Meng, Z.; Geng, H.; Bai, J.; Yan, G. Blood Pressure of Rats Lowered by Sulfur Dioxide and Its Derivatives, Inhalation Toxicology. *Inhal. Toxicol.* **2008**, *15* (9), 951–959.

(10)   Lu, W.; Sun, Y.; Tang, C.; Ochs, T.; Qi, J.; Du, J.; Jin, H. Sulfur Dioxide Derivatives Improve the Vasorelaxation in the Spontaneously Hypertensive Rat by Enhancing the Vasorelaxant Response to Nitric Oxide. *Exp. Biol. Med.* **2012**, *237* (7), 867–872.

(11)   Day, J. J.; Yang, Z.; Chen, W.; Pacheco, A.; Xian, M. Benzothiazole Sulfinate: A Water-Soluble and Slow-Releasing Sulfur Dioxide Donor. *ACS Chem. Biol.* **2016**, *11* (6), 1647–1651.

(12)   Wang, L.-S.; Wang, L.; Wang, L.; Wang, G.; Li, Z.-H.; Wang, J.-J. Effect of 1-Butyl-3-Methylimidazolium Tetrafluoroborate on the Wheat (Triticum Aestivum L.) Seedlings. *Environ. Toxicol.* **2009**, *24* (3), 296–303.

(13)   Yao, Q.; Huang, Y.; Liu, A. D.; Zhu, M.; Liu, J.; Yan, H.; Zhang, Q.; Geng, B.; Gao, Y.; Du, S.; et al. The Vasodilatory Effect of Sulfur Dioxide via SGC/cGMP/PKG

Pathway in Association with Sulfhydryl-Dependent Dimerization. *Am. J. Physiol. - Regul. Integr. Comp. Physiol.***2016**, *310* (11), R1073–R1080.

(14) Zhang, H.; Huang, Y.; Bu, D.; Chen, S.; Tang, C.; Wang, G.; Du, J.; Jin, H. Endogenous Sulfur Dioxide Is a Novel Adipocyte-Derived Inflammatory Inhibitor. *Sci. Rep.***2016**, *6*, 1–10.

(15) Belén García-Alonso, M.; Pena-Egido, J.; García-Moreno, C. S-Sulfonate Determination and Formation in Meat Products. *J. Agric. Food Chem.***2001**, *49* (1), 423–429.

(16) Malwal, S. R.; Chakrapani, H. Benzosulfones as Photochemically Activated Sulfur Dioxide (SO$_2$) Donors. *Org. Biomol. Chem.***2015**, *13* (8), 2399–2406.

(17) Malwal, S. R.; Sriram, D.; Yogeeswari, P.; Chakrapani, H. Synthesis and Antimycobacterial Activity of Prodrugs of Sulfur Dioxide (SO$_2$). *Bioorg. Med. Chem. Lett.***2012**, *22* (11), 3603–3606.

(18) Malwal, S. R.; Sriram, D.; Yogeeswari, P.; Konkimalla, V. B.; Chakrapani, H. Design, Synthesis, and Evaluation of Thiol-Activated Sources of Sulfur Dioxide (SO 2) as Antimycobacterial Agents. *J. Med. Chem.***2012**, *55* (1), 553–557.

(19) Ge, E.; Fan, M.; Qiu, H.; Hu, H.; Tian, L.; Wang, X.; Xu, G.; Wei, X.; *Environ.pollt.,* **2017***, 228,* 408-415.

(20) Moreno, R. G. M.; Alipazaga, M. V.; Medeiros, M. H. G.; Coichev, N. *Dalton Trans.* **2005**, *0*, 1101.

(21) Malwal, S. R.; Gudem, M.; Hazra, A.; Chakrapani, H. *Org. Lett.* **2013**, *15*, 1116.

(22) Dharmaraja, A. T.; Dash, T. K.; Konkimalla, V. B.; Chakrapani, H. *Med. Chem. Comm.* **2012**, *3*, 219.

(23) Alipazaga, M. V.; Moreno, R. G. M.; Linares, E.; Medeiros, M. H. G.; Coichev, N. *Dalton Trans.* **2008**, 5636.

(24) Dharmaraja, A. T.; Alvala, M.; Sriram, D.; Yogeeswari, P.; Chakrapani, H. *Chem. Commun.* **2012**, *48*, 10325.

(25) Dharmaraja, A. T.; Chakrapani, H. *Org. Lett.* **2014**, *16*, 398.

(26) Newton, G. L.; Fahey, R. C.; Rawat, M. *Microbiol.* **2012**, *158*, 1117.

(27) Yu, H.-Z.; Fu, F.; Zhang, L.; Fu, Y.; Dang, Z.-M.; Shi, J. *Phys.Chem.Chem. Phys* .**2014,** *16*, 20964-2070

(28) Wolfbeis, O. S. An Overview of Nanoparticles Commonly Used in Fluorescent Bioimaging. *Chem. Soc. Rev.***2015**, *44* (14), 4743–4768.

(29) Thakur, M.; Pandey, S.; Mewada, A.; Patil, V.; Khade, M.; Goshi, E.; Sharon, M. Antibiotic Conjugated Fluorescent Carbon Dots as a Theranostic Agent for Controlled Drug Release, Bioimaging, and Enhanced Antimicrobial Activity. *J. Drug Deliv.***2014**, *2014*, 282193.

(30) Zhao, Z.; Yan, R.; Yi, X.; Li, J.; Rao, J.; Guo, Z.; Yang, Y.; Li, W.; Li, Y. Q.; Chen, C. Bacteria-Activated Theranostic Nanoprobes against Methicillin-Resistant Staphylococcus Aureus Infection. *ACS Nano***2017**, *11* (5), 4428–4438.

(31) Kong, Y.; Yao, H.; Ren, H.; Subbian, S.; Cirillo, S.; Sacchettini, J.; Rao, J.; Cirillo, J. Imaging Tuberculosis with Endogenous B-Lactamase Reporter Enzyme Fluorescence in Live Mice. *Proceedings of the National Academy of Sciences*. 2010, pp 12239–12244.

(32) Panizzi, P.; Nahrendorf, M.; Figueiredo, J. L.; Panizzi, J.; Marinelli, B.; Iwamoto, Y.; Keliher, E.; Maddur, A. A.; Waterman, P.; Kroh, H. K.; et al. In Vivo Detection of Staphylococcus Aureus Endocarditis by Targeting Pathogen-Specific Prothrombin Activation. *Nat. Med.***2011**, *17* (9), 1142–1147.

(33) Zhang, Z.; Taylor, M.; Collins, C.; Haworth, S.; Shi, Z.; Yuan, Z.; He, X.; Cao, Z.; Park, Y. C. Light-Activatable Theranostic Agents for Image-Monitored Controlled Drug Delivery. *ACS Appl. Mater. Interfaces* **2018**, *10* (2), 1534–1543.

(34) Weinstein, R.; Segal, E.; Satchi-Fainaro, R.; Shabat, D. Real-Time Monitoring of Drug Release. *Chem. Commun.***2010**, *46* (4), 553–555.

List of Figures

List of Tables

List of Schemes

List of Publications:

(1)   **Pardeshi, K. A.**; Ravikumar, G.; Chakrapani, H. Esterase Sensitive Self-Immolative Sulfur Dioxide Donors. *Org. Lett.* **2018**, *20* (1), 4–7.

(2)   Bora, P.; Chauhan, P.; **Pardeshi, K. A.**; Chakrapani, H. Small Molecule Generators of Biologically Reactive Sulfur Species. *RSC Adv.* **2018**, *8* (48), 27359–27374.

(3)   **Pardeshi, K. A.**; Malwal, S. R.; Banerjee, A.; Lahiri, S.; Rangarajan, R.; Chakrapani, H. Thiol Activated Prodrugs of Sulfur Dioxide (SO2) as MRSA Inhibitors. *Bioorganic Med. Chem. Lett.* **2015**, *25* (13), 2694–2697.

(4)   **Pardeshi, K. A.**; Ravikumar, G.; Shukla, M.; Kaul, G.; Kumar, T. A.; Chopra, S.; Chakrapani, H. Targeted Antibacterial Activity Guided by Bacteria-Specific Nitroreductase Catalytic Activation to Produce Ciprofloxacin. Manuscript under preparation.